OUTLOOK
Multiple myeloma

nature

THE INTERNATIONAL WEEKLY JOURNAL OF SCIENCE

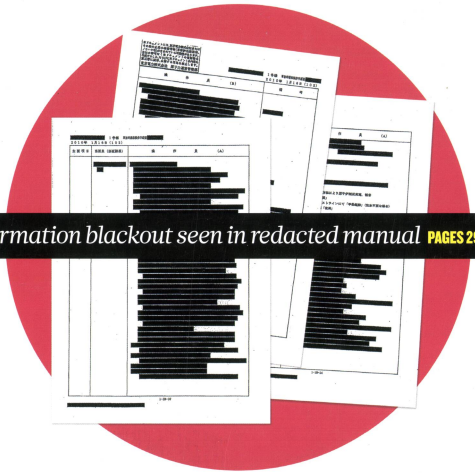

Information blackout seen in redacted manual PAGES 291 & 313

FUKUSHIMA:
THE CASE FOR NATIONALIZING THE REACTORS

BIG SCIENCE

GREEN IS BEAUTIFUL
Cutting energy costs of large-scale research
PAGE 315

HIV/AIDS

BREACHING HIV'S DEFENCES
Solving the immune avoidance puzzle
PAGES 324 & 336

MATERIALS

A STICKY JAM
How friction affects jamming in real systems
PAGES 325 & 355

NATURE.COM/NATURE
15 December 2011 £10
Vol. 480, No. 7377

New podcast with Eppendorf Award 2011 winner Suzan Rooijakkers

***Nature* is the partner for the Eppendorf Award for Young European Investigators.**
The Award acknowledges outstanding contributions to biomedical research in Europe based on methods of molecular biology, including novel analytical concepts.

New podcast with Suzan Rooijakkers

"This award is the recognition of the highly focused work of my group over the past years. For me it is the justification to further pursue bacterial pathogenesis and illustrate even more that bacteria are very clever indeed."

This year the prize was awarded to **Assistant Professor Suzan Rooijakkers, PhD**, (University Medical Center Utrecht, Department of Medical Microbiology, Utrecht, The Netherlands) for her discoveries of how the pathogen *Staphylococcus aureus* evades immune attack to survive in the human host.

Listen to Suzan Rooijakkers' podcast and learn more about her work and the impact the award has had on her career. Alternatively, you can read excerpts from the interview in a Q&A feature article online.

nature.com/nature/awards/eppendorf

eppendorf
In touch with life

In partnership with
nature

nature publishing group npg

华大基因 BGI Premier Scientific Partner

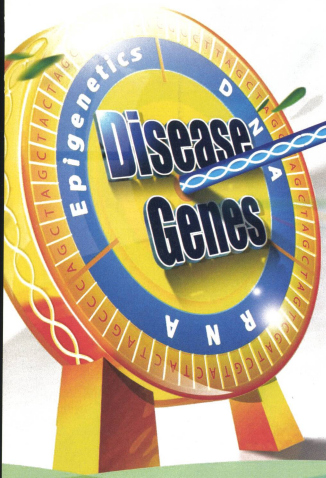

Disease Genes All Targeted

Genomics Solutions

Whole Genome Sequencing
Exome Sequencing
Target Region Sequencing
High-throughput Genotyping
Metagenomics

RNA-Seq (Transcriptome/Quantification)
Small RNA Sequencing
Non-coding RNA Sequencing
Degradome Sequencing

ChIP Sequencing
Reduced Representation Bisulfite Sequencing
Whole Genome Bisulfite Sequencing
MeDIP Sequencing

Targets

Causative Genes
Gene Expression

Common & Rare Variants
Epigenetic Regulation

Driver Mutations
Metagenome

tech@genomics.cn www.genomics.cn

nature EDUCATION

ANNOUNCING

Principles of Biology

An interactive textbook solution by Nature Education

A learning solution designed to bridge students from the classroom to the lab.

200 customizable mini-chapters created by dozens of scientists, instructors, and editors	200+ online interactive exercises to give students a hands-on way to apply their knowledge	50 Science Techniques units cultivating real scientific skills, including data analysis	3000+ assessment questions integrated into lessons
Synopses and links to milestone research papers from *Nature* and other journals	Affordably priced for all students	Optional color print companion	Access on all devices:

Learn more at **www.nature.com/principles**

nature publishing group npg

MERCK MILLIPORE

One filter. One spin. One chance to get your sample right.

Amicon® Ultra Filters – engineered for peace of mind.

Concentrate your most dilute sample with Amicon® Ultra filters in as little as 10 minutes to consistently achieve > 90% recovery. Merck Millipore's design innovations combined with years of experience in membrane technology make Amicon® Ultra filters the easy choice for your sample concentration and buffer exchange.

Get it right the first time.
www.millipore.com/Amicon1

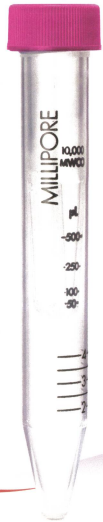

Merck Millipore is a division of MERCK

Merck Millipore and the M logo are trademarks of Merck KGaA, Darmstadt, Germany. Amicon is a trademark of Millipore Corporation. © 2011 Millipore Corporation. All rights reserved.

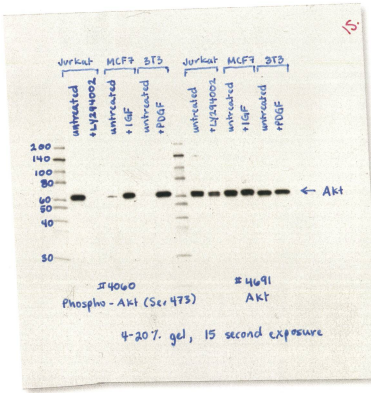

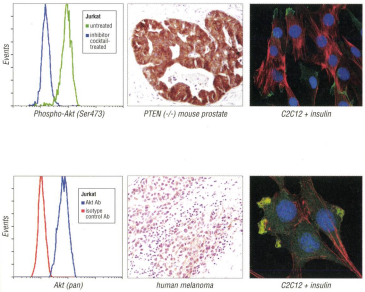

Phospho-Akt (Ser473) (D9E) XP® Rabbit mAb #4060 *(upper) and* ***Akt (pan) (C67E7) Rabbit mAb #4691*** *(lower).*
For full validation details see www.cellsignal.com

The Highest Quality
Akt Antibodies
are from Cell Signaling Technology

Over 45 thoroughly validated Akt Antibodies available

Cell Signaling Technology offers the widest range of phospho and total protein Akt antibodies. These reagents are the most thoroughly validated, widely used, and highly cited Akt antibodies available.

:: CST™ phospho and total protein Akt antibodies offer **unsurpassed specificity, sensitivity, and performance**.

:: **Extensive in-house validation** in a wide range of applications means that optimization is not left up to you, the user.

:: **Technical support is provided by scientists** who produce the products and know them best.

Unparalleled product quality, validation, and technical support

for quality products you can trust...

www.cellsignal.com

Cell Signaling TECHNOLOGY®

Orders (toll-free) 1-877-616-2355 | **Technical Support** (toll-free) 1-877-678-8324 support@cellsignal.com | **Inquiries** info@cellsignal.com | **Environmental Commitment** eco.cellsignal.com

CONTENTS

15 December 2011 / Vol 480 / Issue No 7377

THIS WEEK

EDITORIALS

291 JAPAN
Critical mass
Events in Japan over the past year underscore the need for a science adviser to the government

291 PATENTS
Error of judgment
European court has caused needless confusion with its pronouncements on stem-cell patents

292 CLIMATE CHANGE
The mask slips
Durban meeting highlights divide between science and policy

WORLD VIEW

293 **Watching the players at the climate poker table**
Frank McDonald
The changing face of climate negotiations

RESEARCH HIGHLIGHTS

294 SELECTIONS FROM THE SCIENTIFIC LITERATURE
Cell manipulation / Lifeless oceans / Minimal wasps / Ultra-sensitive infrared astronomy / The brain's nutrient sensor / Pollution from biofuels

SEVEN DAYS

296 THE NEWS IN BRIEF
More signs of water on Mars / Success for gene therapy to treat haemophilia / EPA slams fracking chemicals / Brazil backs forest code

CAREERS

401 RESEARCH
Radical rethink
Trainee researchers should be given freedom to experiment

403 TURNING POINT
Religion, science and marketing do mix, says Jimmy Lin

403 CAREER BRIEFS

NEWS IN FOCUS

299 POLICY
Frantic negotiations score last-minute climate deal in Durban

301 PARTICLE PHYSICS
LHC results hint at Higgs particle

302 ASTROPHYSICS
Kepler's cornucopia challenges model of planet formation

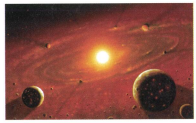

303 IMAGING
Questions raised over whether imaging technique can enter the third dimension

305 POLICY
Anne Glover named as Europe's first chief science adviser

305 POLICY
Hungary overhauls its research system

FEATURES

310 STEM CELLS
The cell division
Oliver Brüstle's struggle to secure patent rights on stem cells

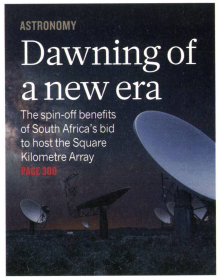

COMMENT

ON THE COVER

Power play

Incidents such as the redaction of an operator's manual have convinced Tomoyuki Taira and Yukio Hatoyama that Fukushima Daiichi should be nationalized PAGE 313

315 HIGH-ENERGY PHYSICS
Cutting science's electricity bill
Thomas Parker
Major research facilities can be green

BOOKS & ARTS

317 MOLECULAR BIOLOGY
Seed of revolution
Michael A Goldman

318 PHILOSOPHY
Life emergent
Evan Thompson

319 GEOLOGY
High on Antarctica
Gabrielle Walker

320 MATHEMATICS
Drowning by numbers
Stefan Michalowski & Georgia Smith

CORRESPONDENCE

321 Farming emissions / Europe's network needs / Lemaître's universe / GM in India / Human variance

OBITUARY

322 **Har Gobind Khorana (1922–2011)**
Uttam L RajBhandary

FUTURES

406 **Extremes**
Rachel Swirsky

- A unique Collection of 200,000 extracts of marine organisms collected Worldwide
- PharmaMar sells the right to carry out first screening of those extracts in any therapeutic indication (2nd if cytotoxicity or Alzheimer´s)
- Optional assistance in structure elucidation and chemical synthesis of marine compounds

PharmaMar

Grupo Zeltia

BDL PharmaMar
bdl@pharmamar.com
Pharmamar USA 1-212-201-6770
Pharmamar Spain 34-91-823-4518

R&D PharmaMar
ccuevas@pharmamar.com
PharmaMar Spain 34-91-823-4536

www.pharmamar.com

CONTENTS

15 December 2011 / Vol 480 / Issue No 7377

RESEARCH

NEW ONLINE

323 Papers published this week at nature.com

NEWS & VEWS

324 VACCINOLOGY
A sweet cleft in HIV's armour
Structure of the PG9 antibody bound to a minimal antigenic mimic
Quentin J Sattentau SEE ARTICLE P.336

325 SOFT MATERIALS
Marginal matters
Probing the nonlinear physics of soft materials
Vincenzo Vitelli & Martin van Hecke
SEE LETTER P.355

326 SUPRAMOLECULAR CHEMISTRY
Molecular wires get connected
Self-assembly of tubular nanowire junctions
Dario M Bassani

328 ASTROPHYSICS
Cosmic explosions under scrutiny
The progenitor of type Ia supernova SN 2011fe
Mario Hamuy SEE LETTERS P.344 & P.348

329 CANCER
A drug-resistant duo
Oncoprotein dimerization and drug resistance in melanoma
Hugo Lavoie & Marc Therrien
SEE LETTER P.387

ASTRONOMY

SN 2011fe

Archival images throw old light on an important new supernova. PAGES 340

MICROBIOLOGY

On the nose

The pathogen that has hit bat populations in North America. PAGE 376

ARTICLES

331 NEUROSCIENCE **A disinhibitory microcircuit for associative fear learning in the auditory cortex**
J J Letzkus et al.

336 IMMUNOLOGY **Structure of HIV-1 gp120 V1/V2 domain with broadly neutralizing antibody PG9**
J S McLellan et al. SEE N&V P.324

LETTERS

344 ASTRONOMY **Supernova SN 2011fe from an exploding carbon–oxygen white dwarf star**
P E Nugent et al. SEE N&V P.328

348 ASTRONOMY **Exclusion of a luminous red giant as a companion star to the progenitor of supernova SN 2011fe**
W Li et al. SEE N&V P.328

351 PHYSICS **Microwave amplification with nanomechanical resonators**
F Massel et al.

355 PHYSICS **Jamming by shear**
D Bi, J Zhang, B Chakraborty & R P Behringer SEE N&V P.325

359 EARTH SCIENCE **Messinian salinity crisis regulated by competing tectonics and erosion at the Gibraltar arc**
D García-Castellanos & A Villaseñor

364 EVOLUTION **Resolving the evolutionary relationships of molluscs with phylogenomic tools**
S A Smith et al.

368 MICROBIOLOGY **Metagenomic analysis of a permafrost microbial community reveals a rapid response to thaw**
R Mackelprang et al.

372 NEUROSCIENCE **Sustained axon regeneration induced by co-deletion of PTEN and SOCS3**
F Sun et al.

376 MICROBIOLOGY **Experimental infection of bats with *Geomyces destructans* causes white-nose syndrome**
J M Lorch et al.

379 STRUCTURAL BIOLOGY **HIV-1 restriction factor SAMHD1 is a deoxynucleoside triphosphate triphosphohydrolase**
D C Goldstone et al.

383 EVOLUTION **Regulatory evolution through divergence of a phosphoswitch in the transcription factor CEBPB**
V J Lynch, G May & G P Wagner

387 CANCER **RAF inhibitor resistance is mediated by dimerization of aberrantly spliced BRAF (V600E)**
P I Poulikakos et al. SEE N&V P.329

391 MOLECULAR BIOLOGY **Chromatin-associated RNA interference components contribute to transcriptional regulation in *Drosophila***
F M Cernilogar et al.

396 STRUCTURAL BIOLOGY **Structure of full-length *Drosophila* cryptochrome**
B D Zoltowski et al.

IMMUNOLOGY

Anti-HIV

Antibody PG9 targets a gp120 immune avoidance device. PAGE 336

PERMAFROST: SUBRAMAIS (DAVID BLILEHET ET AL.)

Let the literature find you.

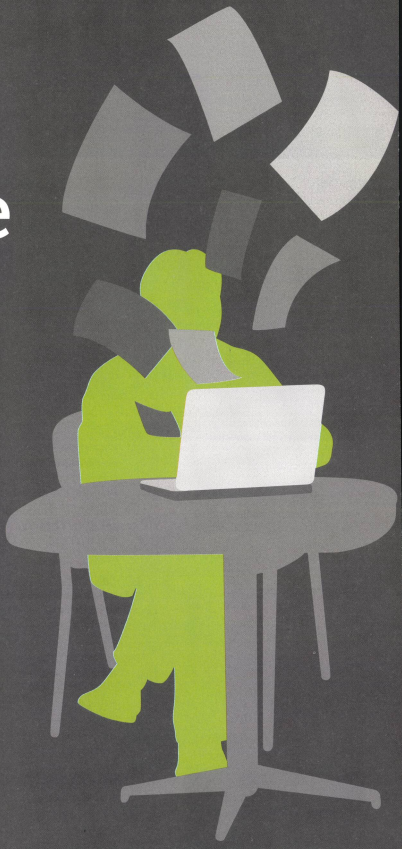

readcube instantly **organizes your research literature** for you, and makes **daily article recommendations** based on the PDFs already in your library.

Download now – it's free!

readcube.com

In association with nature.com

OUTLOOK

Supplement to 15 December 2011 / Vol 480 / Issue No. 7377

MULTIPLE MYELOMA

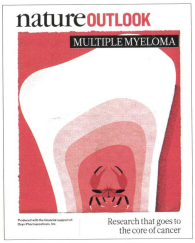

Turn to page 322

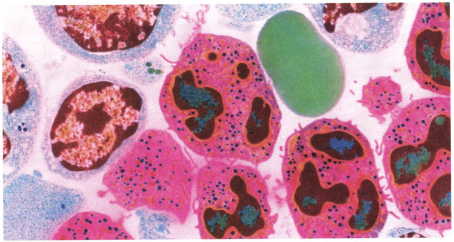

Research on this plasma cell malignancy yields insights into cancer more generally.

S34 OVERVIEW
Multiple lines of attack
Understanding multiple myeloma can help deliver the best treatments for individual patients

S36 DIAGNOSTICS
The early bird
Identifying the patients most likely to develop full-blown multiple myeloma can enable prompt treatment

S38 ANIMAL MODELS
Towards a myeloma mouse
Giving the disease to immune-deficient mice is boosting efforts to find better treatments

S40 DRUGS
More shots on target
Several promising drugs to treat myeloma are coming through clinical trials

S43 TUMORIGENESIS
Testing ground for cancer stem cells
A controversial theory about cancer biology might hold the key to finding a cure

S46 STEM CELLS
Transplants on trial
Stem-cell transplants seem to be effective, but when is the best time to give them?

S48 MICROENVIRONMENT
Neighbourhood watch
Studying molecules in the bone marrow can shed light on the growth of myeloma cells

S50 GENETICS
Profiling a shape-shifter
Understanding changes in the genes could lead to better treatments for multiple myeloma

S52 IMAGING
Seeing is believing
New imaging techniques can provide a clearer picture of multiple myeloma

S54 AETIOLOGY
The path to disease
Researchers are starting to unravel how a benign condition becomes a deadly cancer

S56 ORTHOPAEDICS
Structural support
Finding treatments for myeloma has boosted our understanding of a range of bone problems

S58 PERSPECTIVE
A model disease
Research into multiple myeloma has helped efforts to treat other cancers, says William Matsui

MORE ONLINE

LATEST RESEARCH

- For some of the latest research on the multiple myeloma tumour microenvironment: go.nature.com/balynj
- *Leukemia* looks at the possibility of using monoclonal antibodies as a new treatment for multiple myeloma: go.nature.com/ziptw2

COLLECTION

- Visit the online edition of *Nature Outlook Multiple Myeloma*, which includes an exclusive collection of the latest research and opinion: go.nature.com/mlsbuc

nature

15 December 2011 / Vol 480 / Issue No. 7377

EDITORIAL

LONDON, MUNICH, WASHINGTON DC, NEW YORK, BOSTON, PARIS, SAN FRANCISCO, TOKYO nature@nature.com

EDITOR-IN-CHIEF: Philip Campbell
MANAGING EDITOR: Nick Campbell
PUBLISHING EXECUTIVE EDITOR: Maxine Clarke **EXECUTIVE EDITOR:** Véronique Kiermer
CHIEF MAGAZINE EDITOR: Tim Appenzeller
THIS WEEK/NEWS/FEATURES: Alison Abbott, David Adam, Ananyo Bhattacharya, Geoff Brumfiel, Declan Butler, Ewen Callaway, Erika Check Hayden, Daniel Cressey, David Cyranoski, Natasha Gilbert, Eric Hand, Heidi Ledford, Corie Lok, Brendan Maher, Emma Marris, Richard Monastersky, Brian Owens, Helen Pearson, Mark Peplow, Eugenie Samuel Reich, Ivan Semeniuk, Quirin Schiermeier, Jeff Tollefson, Richard Van Noorden, Meredith Wadman, M Mitchell Waldrop **COMMENT:** Sara Abdulla, Joanne Baker, Rosalind Cotter, Barbara Kiser, Alison McCook, Lucy Odling-Smee, Sarah Tomlin **NATURE PODCAST/VIDEO:** Adam Rutherford, Eric Olson, Kerri Smith, Charlotte Stoddart **NEWS AND VIEWS:** Sadaf Shadan, Ana Lopes, Andrew Mitchinson, Cesar Sanchez **RESEARCH:** Ritu Dhand, Karl Ziemelis, Francesca Cesari, I-han Chou, Tanguy Chouard, Rosamund Daw, Alex Eccleston, Angela Eggleston, Joshua Finkelstein, Henry Gee, Patrick Goymer, Noah Gray, Marie-Thérèse Heemels, Magdalena Helmer, Karen Howell, Claudia Lupp, Barbara Marte, Andrew Mitchinson, Alberto Moscatelli, Juliane Mössinger, Deepa Nath, Leslie Sage, Magdalena Skipper, Clare Thomas, John VanDecar, Liesbeth Venema, Ursula Weiss, Michael White **INSIGHTS/REVIEWS/PERSPECTIVES:** Ursula Weiss **CAREERS:** Gene Russo, Karen Kaplan **TECHNOLOGY FEATURES:** Monya Baker **FUTURES:** Henry Gee **SUPPLEMENTS:** Herb Brody, Michelle Grayson, Tony Scully **SUBEDITORS:** Colin Sullivan, Sarah Archibald, Nicola Bailey, Anne Blewett, Nicolas Fargues, Isobel Flanagan, Paul Fletcher, Ahsanh Gray, Dinah Loon, Anna Novitzky, Yukie Ozawa, Katherine Perry, David Payne, Jenny Rooke, Chris Simms, David Winters, Anna York **PRODUCTION:** Jenny Henderson, Gemma Carder, Leonora Dawson-Bowling, Dan Foley, Stewart Fraser, Susan Gray, Simon Gribbin, James McQuat, Emilia Orviss, Yvonne Strong, Robert Sullivan, Roberta Tarran, Charles Wenz **ART AND DESIGN:** Kelly Buckheit Krause, Wesley Fernandes, Madeline Hutchinson, Barbara Izbebska, Paul Jackman, Annthea Lewis, Nik Spencer, Claire Welsh, Mark Wood **JAPAN EDITION:** Mika Nakano, Akemi Tanaka, Mitsuyo Utsugi **PRESS OFFICE:** Ruth Francis, Neda Afsarmanesh, Lisa Boucher, Rachel Twinn, Rebecca Walton **ADMINISTRATION:** Paul Sng, Helen Anthony, Liz Bankes, Roseann Campbell, Faye Fornasier, Amy Inwrnizzi, Diane Kempinski, Hazel Mayhew, Katie McGoldrick, Jenny Meyer, Rina Nozawa, Kenneth Simpson, Claire Smith, Tanya Szwarnowska

PUBLISHING

LONDON feedback@nature.com

MANAGING DIRECTOR & PUBLISHER: Steven Inchcoombe
ASSISTANT PUBLISHER: Arash Hejazi
PUBLISHING PROJECT MANAGER: Christian Manco
PROJECT MANAGER: Helen Anthony

TOKYO feedback@natureasia.com

PUBLISHING DIRECTOR — ASIA-PACIFIC: David Swinbanks
ASSOCIATE DIRECTOR — ASIA-PACIFIC: Antoine E Bocquet

DISPLAY ADVERTISING, SPONSORSHIP & NATUREJOBS

GLOBAL HEAD: Andrew Douglas a.douglas@nature.com

DISPLAY ADVERTISING AND SPONSORSHIP
GLOBAL HEAD: Gerard Preston g.preston@nature.com
ASSISTANT SPONSORSHIP MANAGER: Reya Silao Tel: +44 (0)20 7843 4977 (r.silao@nature.com)

EUROPE/REST OF WORLD display@nature.com Tel: +44 (0)20 7843 4960
GERMANY/SWITZERLAND/AUSTRIA: Sabine Hugi-Fürst Tel: +41 52761 3386
UK/IRELAND/SCANDINAVIA/SPAIN/PORTUGAL: Evelina Rubio Hakansson Tel: +44 (0)20 7843 4079
FRANCE/BELGIUM/THE NETHERLANDS/LUXEMBOURG/ITALY/OTHER EUROPE: Nicola Wright Tel: +44 (0)20 7843 4959

NORTH AMERICA display@natureny.com
NEW ENGLAND/ EASTERN CANADA: Sheila Reardon Tel: +1 617 494 4900
NEW YORK/MID-ATLANTIC/SOUTHEAST: Jim Breault Tel: +1 212 726 9334
MIDWEST: Mike Rossi Tel: +1 212 726 9255
WEST COAST/ WESTERN CANADA: George Lui Tel: +1 415 781 3804
WEST COAST NORTH: Kayla McCutchan Tel: +1 415 403 9038

ASIA-PACIFIC display@natureasia.com
ASIA-PACIFIC HEAD: Kate Yoneyama
JAPAN: Ken Mikami Tel: +81 3 3267 8765
GREATER CHINA/SINGAPORE: Gloria To Tel: +852 2811 7191
INDIA: Vikas Chawla Tel: +91 124 288 1057

SPONSORSHIP
BUSINESS DEVELOPMENT MANAGER: David Bagshaw Tel: +1 212 726 9215 **BUSINESS DEVELOPMENT MANAGER:** Patrick Murphy Tel: +1 617 475 9216

NATUREJOBS naturejobs@nature.com
EUROPEAN HEAD OFFICE, LONDON: Tel: +44 (0)20 7843 4961
EUROPEAN SALES MANAGER: Nils Moeller (n.moeller@nature.com) **BUSINESS DEVELOPMENT MANAGER, MIDDLE EAST:** Jon Giuliani (j.giuliani@nature.com) **ADVERTISING PRODUCTION MANAGER:** Stephen Russell **NATUREJOBS ONLINE PRODUCTION:** Dennis Chu
US HEAD OFFICE, NEW YORK: naturejobs@natureny.com **US SALES MANAGER:** Ken Finnegan
JAPAN HEAD OFFICE, TOKYO: Tel: +81 3 3267 8765 **ASIA-PACIFIC HEAD:** Kate Yoneyama
ASIA-PACIFIC SALES & BUSINESS DEVELOPMENT MANAGER: Yuki Fujiwara **BUSINESS DEVELOPMENT MANAGER, GREATER CHINA, SINGAPORE:** Gloria To Tel: +852 2811 7191
INDIA: Vikas Chawla Tel: +91 1242881057 (v.chawla@nature.com)

MARKETING & SUBSCRIPTIONS

USA/CANADA/LATIN AMERICA subscriptions@us.nature.com
Tel: (USA/Canada)+1 866 363 7860; (outside USA/Canada) +1 212 726 9223
MARKETING: Sara Girard **FULFILMENT:** Karen Dawson

JAPAN/CHINA/KOREA subscriptions@natureasia.com
Tel: +81 3 3267 8751 **MARKETING/PRODUCTION:** Keiko Ikeda, Takesh Murakami

EUROPE/REST OF WORLD subscriptions@nature.com
Tel: +44 (0)1256 329242
MARKETING: Elena Woodstock, Marcus Parker, Hannah Phipps **FULFILMENT:** Jean Burrows

INDIA npgindia@nature.com
Tel: +91 124 2881053/54
HEAD OF BUSINESS DEVELOPMENT, INDIA: Debashish Brahmachari **MARKETING:** Harpal Singh Gill

ANNUAL SUBSCRIPTIONS (UK/Europe, including post and packing)
FULL RATE: £1,400
PERSONAL RATES: UK £135; Europe €209; Rest of World £210
STUDENT RATES: UK £79; Europe €122; Rest of World £125
Individual rates apply to payments by personal cheque or credit card. Back issues: £20.00.

ANNUAL SUBSCRIPTIONS (USA, including post and packing)
INSTITUTIONAL/CORPORATE RATE: $2,730 ; **PERSONAL RATE:** $199; **STUDENT RATE:** $99;
POSTDOC RATE: $119
Printed in USA. Individual rates available only to subscribers paying by personal check or credit card. Orders for student/postdoc subscriptions must be accompanied by a copy of student ID. Rates apply to USA, Canada, Mexico/Central & South America. Add 7% GST tax in Canada (Canadian GST number 123011595). **BACK ISSUES:** US$20.00.

ANNUAL SUBSCRIPTIONS (Asia, including post and packing)
JAPAN: 年間購読料金： *Nature* のみ 437,800 円 +21,890 円(消費税)=459,690 円(合計)
Nature + *Nature Digest* 466,550 円 +23,328 円(消費税)=489,878 (合計)
お問い合わせ 日本出版貿易株式会社 (国内営業 1 部
〒101-0064 東京都千代田区猿楽町1-2-1 Tel: 03-3292-3767 Fax: 03-3292-8766
個人/学生購読について
NPG ネイチャー ジャパン フィックス フルフィルメント & カスタマーサービス
〒162-0843 東京都新宿区市谷田町2-37 千代田ビル Tel: 03-3267-8759Fax: 03-3267-8752
CHINA: www.natureasia.com/ch/subscribe; **KOREA:** www.natureasia.com/korea/subscribe

NATURE ONLINE WWW.NATURE.COM/NATURE

CHIEF TECHNOLOGY OFFICER: Howard Ratner **ASSOCIATE DIRECTOR, NATURE.COM:** Daniel Pollock
PLATFORM DEVELOPMENT: Jeremy Macdonald **WEB PRODUCTION:** Alexander Thurrell, Deborah Anthony **WEB DESIGN:** Juan-Carlos Sobrino, Luke Stavenhagen **PLATFORM INTERFACES:** Amanda Ward

SITE LICENCES, FULFILMENT & CUSTOMER SERVICES

SITE LICENCES: npg.nature.com/libraries feedback@nature.com
CHIEF OPERATIONS OFFICER: John Carroll **ASSOCIATE DIRECTOR OF OPERATIONS:** Dominic Pettit
CUSTOMER SERVICE: Gerald Coppin **ORDER PROCESSING OPERATIONS:** Steve Poulter

NATURE PUBLISHING GROUP OFFICES

LONDON: The Macmillan Building, 4 Crinan Street, London N1 9XW Tel: +44 (0)20 7833 4000 Fax: +44 (0)20 7843 4596/7

BASINGSTOKE: Nature Publishing Group, Subscriptions, Brunel Road, Basingstoke, Hants RG21 6XS, UK Tel: +44 (0)1256 329242

WASHINGTON DC: 968 National Press Building, 529 14th St NW, Washington DC 20045-1938 Tel: +1 202 737 2355

NEW YORK: 75 Varick St, 9th Floor, New York, NY 10013-1917 Tel: +1 212 726 9200

BOSTON: 25 First Street, Suite 104, Cambridge, MA 02141 Tel: +1 617 475 9275

SAN FRANCISCO: 225 Bush Street, Suite 1453, San Francisco, CA 94104 Tel: +1 415 403 9027

MUNICH: Nymphenburger Strasse 14, D-80335 München Tel: +49 89 549057-13

PARIS: Moulin de Malicorne, Sainte Maure de Touraine, Paris 37800 Tel: +33 2 47 35 72 15

TOKYO: Chiyoda Building, 2-37 Ichigaya Tamachi, Shinjuku-ku, Tokyo 162-0843 Tel: +81 3 3267 8751

INDIA: Nature Publishing Group, 3A, 4th Floor, DLF Corporate Park, Gurgaon 122002 Tel: +91 124 2881053/54

Nature® (ISSN 0028-0836) is published by Nature Publishing Group, a division of Macmillan Publishers Ltd (The Macmillan Building, 4 Crinan Street, London N1 9XW). Registered as a newspaper at the British Post Office. North and South American orders to subscriptions@natureny.com (Tel: +1 866 363 7860). Other orders to subscriptions@nature.com (Tel. +44 (0)1256 329242; Fax +44 (0)1256 812358). Authorization to photocopy material for internal or personal use, or internal or personal use of specific clients, is granted by *Nature* to libraries and others registered with the Copyright Clearance Center (CCC) Transactional Reporting Service, provided the relevant copyright fee is paid direct to CCC, 222 Rosewood Drive, Danvers MA 01923, USA. Identification code for *Nature*: 0028-0836/03. CPC PUB AGREEMENT #40032744. In the US, *Nature* (ISSN 0028-0836) is published weekly on Thursday, except the last week in December by Nature Publishing Group, 75 Varick St, 9th Fl, New York NY 10013-1917, USA. US Periodicals postage paid at New York NY, and additional mailing post offices. US POSTMASTER: send address changes to *Nature*, Subscription Dept, 75 Varick St, 9th Fl, New York NY 10013-1917, USA. Published in Japan by NPG Nature Asia-Pacific, Chiyoda Building, 2-37 Ichigayatamachi, Shinjuku-ku, Tokyo 162-0843, Japan. ©

2011 Macmillan Publishers Limited. All rights reserved.

SCIENTIFIC AMERICAN™

Publishing the latest in science and technology for more than 165 years

A site license provides online access to *Scientific American*, *Scientific American Mind* and Special Issues

Recommend site license access to your library today:

www.nature.com/libraries/scientificamerican

nature publishing group npg

© Scientific American, Inc.

Better inside.

MiSeq™

Inside you'll find a fully integrated sequencing solution with automated amplification, sequencing, and analysis—all on one instrument. MiSeq delivers >85% Q30 bases and workflow times as fast as 8 hours from sample to data.

www.illumina.com/MiSeq

illumina®

a nature conference

The University of Miami, Nature Publishing Group and Scripps Florida present:

Miami 2012 Winter Symposium: Nanotechnology in Biomedicine

Three decades following the initial report of scanning tunneling and atomic force microscopies and the first description of carbon nanotubes, novel nanomaterials are opening up new opportunities in imaging, sensor design and other applications in biology and biomedicine. The 45th Miami Winter Symposium will bring together leaders in the field to discuss breakthroughs in new nanomaterials and the challenges in translating these materials into products for the clinic and laboratory.

February 26-29, 2012
JW Marriott Marquis Miami
Miami, FL, USA

SYMPOSIUM AWARDEES

Feodor Lynen Lectures
Robert Langer (Massachusetts Institute of Technology, USA)
George Whitesides (Harvard University, USA)

Distinguished Service Award
Sumio Iijima (Meijo University, Japan / Nagoya University, Japan)

Bill Whelan Lifetime Achievement Award
Christoph Gerber (University of Basel, Switzerland)

Special Achievement Awards
Paul Alivisatos (University of California, Berkeley, USA)
Shuming Nie (Emory University, USA / Georgia Institute of Technology, USA)

CONFIRMED SESSION SPEAKERS

Mark Akeson
James Baker
Richard Cote
Hongjie Dai
Mark E. Davis
Jonas Korlach
Yamuna Krishnan
Iseult Lynch
Scott Manalis
Nicholas Peppas
Michael Rhodes
Samuel Stupp
Roger Tsien
David R. Walt
Jackie Ying
Shuguang Zhang
Xioawei Zhang

For more information and to register, visit:
www.nature.com/natureconferences/miami/mws2012

Abstract submission deadline extended to **November 30, 2011.**

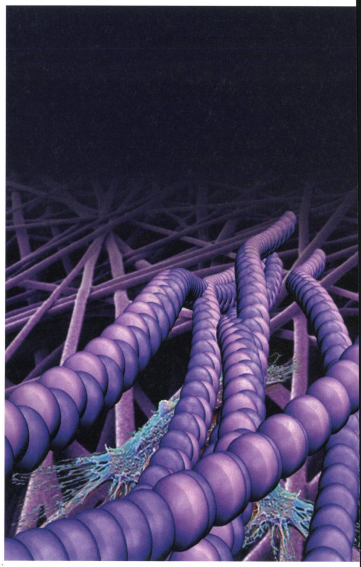

Artwork by: Bozhi Tian (Massachusetts Institute of Technology, USA)

UNIVERSITY OF MIAMI
MILLER SCHOOL of MEDICINE

SCRIPPS FLORIDA
THE SCRIPPS RESEARCH INSTITUTE

nature publishing group npg

nature climate change

SUBMIT ONLINE NOW!

Chief Editor: Rory Howlett, *PhD*

Nature Climate Change aims to be the world's leading research journal for documenting new scientific discoveries about how we will experience and respond to the challenges of a changing climate.

The Editorial team accepts submissions of original research articles from both the natural and social science communities. Central to the journal's mission, and to addressing climate change, is reaching beyond traditional academic boundaries, and bringing together diverse expertise and perspectives. As such, *Nature Climate Change* especially encourages the submission of interdisciplinary climate research. In addition, the journal welcomes disciplinary research from psychology to sociology, from policy to atmospheric physics.

Further details can be found in our Guide to Authors:
http://www.nature.com/nclimate/authors/gta/index.html

Presubmission enquiries should be sent via our online submission system designating them as presubmission enquiries as requested on the form:http://mts-nclim.nature.com/cgi-bin/main.plex

Submissions: manuscripts should be submitted through our online submission system at: http://mts-nclim.nature.com/cgi-bin/main.plex

General editorial inquiries and correspondence: should be addressed to the Editor at: nclimate@nature.com

Submit today! We welcome your contributions.

www.nature.com/natureclimatechange

nature publishing group

Better outside.

MiSeq™

Outside you'll find a streamlined user experience, with load-and-go sequencing reagents and single-tube library preparation in just 1.5 hours. Data management is made simple with onboard informatics apps and BaseSpace™, our new cloud-based analysis environment.

www.illumina.com/MiSeq

illumina®

REDISCOVER *your* nature

Print Online Mobile

ENJOY AN EXCLUSIVE

50%

DISCOUNT THIS HOLIDAY SEASON!

Celebrate with *Nature* this Holiday season and enjoy 51 weekly issues in print, online and via the nature.com app for iPhone®, iPad®, and iPod touch®. Each issue contains world class scientific research and award winning news, which you don't want to miss!

This offer is open to personal subscriptions only and is not available in Japan, China, Taiwan and South Korea – for regional offers please see www.natureasia.com

Subscribe online: nature.com/holiday11

nature chemistry

All the right **elements**

First Impact Factor: **17.927***

Number **1** primary research journal in chemistry

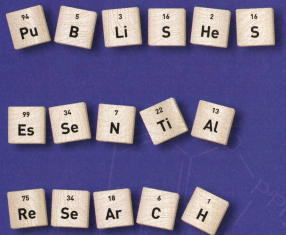

Visit: **www.nature.com/naturechemistry**

*2010 *Journal Citation Reports*® (Thomson Reuters, 2011)

nature publishing group npg

Better upside.

MiSeq™

The upside is what you can do with it. With the broadest application base and a global community of sequencing insight behind it, MiSeq took the best in next-generation sequencing and made it better.

Go to www.illumina.com/MiSeq

illumina®

NEW ENGLAND BioLabs Inc.
enabling technologies in the life sciences

Built for efficiency.

Competent Cells from New England Biolabs.

Ensure successful transformations with NEB cloning strains and take advantage of:

- High transformation efficiencies
- Value pricing and no dry ice charges
- Convenient product formats, including single-use tubes

NEB Competent *E. coli* – building a strong foundation for your cloning experiments.

Benefit from high transformation efficiencies with NEB 5-alpha.

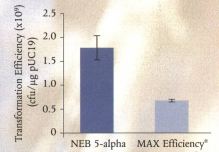

The transformation efficiencies of NEB 5-alpha and MAX Efficiency DH5α-T1R were compared using manufacturers' recommended protocols. Values shown are the average of triplicate experiments.

FREE SHIPPING OFFER

For the month of December, receive FREE SHIPPING on cloning competent cell purchases.

Visit www.neb5alpha.com for more information and a list of the competent cells included in this offer.

Valid in the US only.

MAX Efficiency® is a registered trademark of Invitrogen.
DH5α™ is a trademark of Invitrogen.

THIS WEEK

EDITORIALS

WORLD VIEW Hope and hypocrisy at two decades of climate talks **p.293**

RAT TRAP Rodents rescue imprisoned colleagues without reward **p.294**

POLLUTION EPA weighs in on gas fracking row with water warning **p.297**

Critical mass

Even Japan's political leaders struggle to get answers regarding the Fukushima disaster. It is just the latest example of the government's lack of independent scientific advice.

More than nine months after the nuclear-reactor disaster at Fukushima, fundamental questions about what happened remain unanswered. Without answers to these questions, Japan, and the rest of the world, is in the dark on what went wrong, what must be done now, and how to avoid similar accidents in future.

A Comment in this week's issue summarizes these concerns (see page 313). For the Japanese public, one of the most troubling things about the article should be the identity of its authors: two ruling party politicians, including a former prime minister. Surely they should be able to get some answers?

Following the accident, the Tokyo Electric Power Company, which operated the Fukushima plant, initially released only a heavily redacted nuclear-reactor manual. When finally released in an undoctored format in late October, the manual revealed just how lacking the company was in terms of contingency measures. This concealment gives some idea of why even senior political figures struggled for answers in the wake of the disaster, and why they have now chosen to pose their questions in this very public way.

This all points to a problem in Japan that predates Fukushima and seems to afflict every Japanese regime: the absence of a strong and independent scientific voice to advise the government. In this case, such a voice — be it from a chief scientist appointed by the government or from a truly independent nuclear regulator — could have helped to direct evacuations, medical relief, screening for radiation and decontamination efforts. It also would have helped to lead the studies needed to find answers to the questions mentioned above.

Many times in Japan's recent history, the government has handed responsibility for dealing with issues involving tricky scientific concepts to bureaucrats or politicians. All too often, these officials, not understanding the issues, do what governments shouldn't do — hide the problem and hope it will go away. In the meantime, politicians fumble for answers, while ill-informed government spokespeople tell confused stories that can make them look foolish, irresponsible or deceitful.

This is how the government handled Minamata disease caused by industrial mercury poisoning in the 1950s and 60s, the HIV-tainted blood products problem in the 1980s, and the BSE scare of a decade ago. And now it is how it has handled Fukushima. Fear of spreading panic, for example, prevented warnings being issued on the dangers of radiation predicted by simulations. As a result, more residents than necessary were exposed.

The government's main sources for scientific information for Fukushima were the industry ministry's Nuclear and Industrial Safety Agency and the Nuclear Safety Commission. Although these bodies might have expertise in nuclear-reactor physics, they also have ties to the nuclear industry that create a conflict of interest. And they were not an effective and prompt source for quick decisions on decontamination or health risks. The government recognized this by shifting nuclear monitoring and safety regulation functions to a new, as yet unproven, nuclear-energy agency under the environment ministry. It has also promised to produce its own independent report on the accident, but its workings are far from transparent.

Japan should go further and open broader and more permanent channels for scientific advice. Fukushima should be the incident that finally forces the government to put in place a structure that could bring fast and decisive action on critical situations in the future.

"Politicians fumble for answers, while spokespeople tell confused stories."

Japan could start by following the example of countries such as the United States and the United Kingdom, and take on a science adviser. Five years ago, Japan did claim to establish such a system, installing a scientist as a special adviser to the cabinet (see *Nature* **443,** 734–735; 2006). But that was based more on hopes of encouraging innovation than dealing with the broad range of scientific issues that a proper science adviser takes on — and the experiment lasted only two years. Now there is no science adviser. Efforts to give the Science Council of Japan a more influential role, akin to the US National Academy of Sciences, have also come up short (see *Nature* **428,** 357; 2004).

Scientists can help to understand what is known and, critically, what cannot be known about a situation. In the absence of certainty, they can help to understand the risks involved. They can help to explain this cogently and clearly to people at large. They can do this from an unbiased and apolitical perspective, so that even if circumstances change they can change their assessment with less risk of being criticized for political motives. And they give the politicians both cover for unpopular decisions and, in the case of a political appointee such as an adviser, a trusted personal relationship.

Japan can do better. The Japanese people deserve better. ■

Error of judgment

The European Court of Justice was wrong to weigh in on the definition of a human embryo.

The question of when a formless clump of developing cells can truly be said to become a human will never have a clear answer. It depends on whom you ask: biologists, theologians, and pro-life and pro-choice campaigners have all wrestled with the concept for years. Regulations that cover the relevant scientific fields and issues should take all these conflicting views into account. Not everybody will be happy with the outcome, but, by definition, not everybody can be.

In October, the European Court of Justice (ECJ) took on the

question. And rather than tip-toeing around the sensitivities, the judges of the court — the highest in Europe — trampled right through them. The ECJ had been asked by the German Supreme Court to clarify ambiguous wording in the European Union (EU) directive on the Legal Protection of Biotechnological Inventions, which bans patents on procedures that use human embryos. The ECJ responded with a clumsy ruling that outlaws patents involving stem cells derived from such embryos and, some critics say, raises questions about future research into regenerative medicine (see page 310). In doing so, the court effectively stepped over the line that separates the interpretation of law, which is its responsibility, from the creation of law, which is the job of parliaments and governments.

For the most part, the ECJ does a faultless job. This time, however, it exceeded its competence. In the case under consideration, Greenpeace had claimed that the existing directive should outlaw a patent relying on human embryonic stem cells that had been taken out by Oliver Brüstle, director of the Institute of Reconstructive Neurobiology in Bonn, Germany. But are human embryonic stem cells equivalent to human embryos in this context? The German Supreme Court, which was handling the Greenpeace complaint, passed the question up to the ECJ.

Unfortunately, the ECJ chose not to confine its analysis to the patent context, but took it upon itself to define the term 'human embryo' generally (and in the broadest possible way), and to assess the surrounding moral environment. A human embryo, it said, comprises an ovum activated to divide by fertilization or any artificial means. Moreover, it added, any research involving human embryonic stem-cell lines is immoral, because such cell lines are originally derived from fertilized eggs.

The ruling left many scientists, judges and legal experts in Germany and other EU member states fuming. Not only because the court had issued a de facto legal definition of a human embryo, but because it had done so with shoddy reasoning and without appropriate legal references. In the case of ambiguous law, a court should go back and ponder the intention of the law-makers. From its brief justification in *Brüstle* v. *Greenpeace*, the ECJ seems not to have done that.

"The ruling left many scientists, judges and legal experts in EU member states fuming."

The ECJ is made up of judges from each EU member state, and critics argue that it simply does not have the technical expertise to deal with issues such as patenting, or stem cells. Yet the court is not held to account by any external watchdog, and its decisions cannot be appealed.

Last week, an alliance of ten major German research organizations, including the German Research Foundation (DFG, the country's national granting agency), the University Rectors Conference and the Max Planck Society, put out a statement condemning the decision. But the damage has been done. Battle lines have already been drawn in the European Parliament, with those opposed to research with human embryonic stem cells calling for funds to be frozen.

The only obvious route out of the confusion created by the ECJ is for the real law-makers — the European Parliament and the Council of the European Union — to amend the ambiguous EU directive that caused all the trouble. They should tighten its loose language on the legal definition of a human embryo in terms of patenting, so that the law reflects what the lawmakers originally intended. This will take courage (and time — the original directive was a decade in the works) but, as the ECJ ruling shows, for all its sensitivities, this is not a subject on which it pays to be vague. ■

The mask slips

The Durban meeting shows that climate policy and climate science inhabit parallel worlds.

It says a lot about the outcome of the UN climate talks in South Africa at the weekend that most of the immediate reports focused on the wrangling that led to an agreement of sorts, rather than the contents and implications of the agreement itself. Late-night talks, later-night arguments and early-morning pacts between battling negotiators with the apparent fate of the world resting on their shoulders give the process a melodrama that is hard to resist, particularly for those who experienced it first hand in the chaos of the Durban meeting (see page 299).

Such late finishes are becoming the norm at these summits. Only as nations abandon their original negotiating positions and reveal their true demands — throwing international differences into stark relief — does a sense of urgency develop and serious negotiation take place. Combined with the consensus nature of the talks, which demands that everyone agrees to everything, the result is usually a cobbled-together compromise that allows as many countries as possible to claim victory and, most importantly, provides them with a mandate to reconvene in 12 months' time.

So it was this time. In the search for a successor to the Kyoto Protocol, we now have the Durban Platform, which comes on the heels of the Bali Road Map and the Copenhagen Accord.

It takes a certain kind of optimism — or an outbreak of collective Stockholm syndrome — to see the Durban outcome as a significant breakthrough on global warming, as many are claiming. Outside Europe — which has set itself binding emissions goals over the short and long term beyond what it will inherit under its stated plan to carry on with unilateral cuts under an extended Kyoto — there will be no obligation for any nation to reduce soaring greenhouse-gas emissions much before the end of the decade. And that is assuming that all flows smoothly in future UN talks, and that a global deal with binding commitments proves easier to find in talks due to start in 2015 than it has so far.

The Durban deal may mark a success in the political process to tackle climate change, but for the climate itself, it is an unqualified disaster. It is clear that the science of climate change and the politics of climate change, which claims to represent it, now inhabit parallel worlds.

This has always been true up to a point, but surely the mask of political rhetoric has now slipped so far, to reveal the ugly political reality underneath, that it can never be replaced. How can politicians talk now with a straight face of limiting global warming to 2 °C? How will campaigners frame this result as leaving yet another 'last chance' to save the planet?

That does not make the political process redundant — far from it. Introducing policies to curb emissions was never about saving the planet or not, or stopping global warming or not. It is about damage limitation — the 3 °C or 4 °C of average warming the planet could experience in the long term, according to some analyses of the Durban outcome doing the rounds, is clearly much worse than the 2 °C used as shorthand for dangerous at present. But it is preferable to the 5 °C or 6 °C that science suggests is possible if emissions continue to rise unabated.

To prevent that outcome will be just as difficult politically as was the now abandoned attempt to find a global successor in time to follow Kyoto. But it remains possible — and there were at least encouraging signs in Durban that previously obstinate countries recognize that it is necessary, even if it is delayed. Those, including this journal, who have long argued the scientific case for the need to control greenhouse-gas emissions should back this new political mood to the hilt. But as the Durban Platform crowds with politicians, the climate train they wait for has left the station. ■

➲ **NATURE.COM**
To comment online, click on Editorials at:
go.nature.com/xhunqv

NimbleGen

Discover More, Sequence Less

SeqCap EZ Exome Library v3.0

Discover the power of 2.1 million empirically rebalanced DNA probes for highly optimized performance and uniform coverage across the exome. Sequence more exomes per lane while simultaneously targeting the most inclusive coding region capture design available.

- **Achieve the most comprehensive coverage of coding regions**
- **Experience the highest target enrichment efficiency***
- **Maximize variant discovery while minimizing sequencing costs**

* Clark M, *et al. Nat. Biotech.* 2011; doi:10.1038/nbt.1975

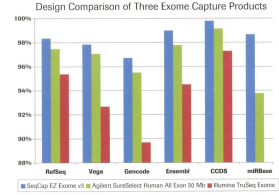

Comparison of SeqCap EZ Exome Library v3.0 design with two other products. For the databases shown, SeqCap EZ Exome v3.0 targets more exons and miRNAs compared to both Agilent and Illumina products

Discover more

www.nimblegen.com/exomev3

For life science research only.
Not for use in diagnostic procedures.

Roche NimbleGen, Inc
Madison, WI USA

Roche

NIMBLEGEN and SEQCAP are trademarks of Roche.
All other product names and trademarks are the property of their respective owners.
© 2011 Roche NimbleGen, Inc. All rights reserved.

nature café REPORT

Ageing and the brain

Swedish medical university Karolinska Institutet — in collaboration with *Nature* and the Swedish Embassy in Berlin — presents a discussion on the latest research into ageing, the brain and dementia

How does the brain change with age? Is dementia inevitable? These were among questions discussed at the latest Nature Café forum, held at the Swedish Embassy in Berlin on 18 November 2011. Nature Café is a unique meeting where *Nature* subscribers can interact with scientific experts and Nature editors to discuss hot scientific topics in a relaxed and informal atmosphere. This Nature Café was the second to be held in collaboration with the internationally renowned Karolinska Institutet, but the first to take place in Europe. The distinguished panel included two speakers from Karolinska Institutet and one from Berlin-based Charité University Medicine. The Café was moderated by Michelle Grayson, associate editor of the *Nature Outlook* supplements.

The Café opened with an address from Staffan Carlsson, the Swedish ambassador to Germany, who spoke about the need for the two countries to focus on shared challenges such as an ageing population. Following him, Dr Clara Hellner Gumpert — dean of doctoral education and vice provost of international affairs at Karolinska Institutet — added that it was important for everyone to understand more about the implications of an ageing global population.

The old-age brain

The first scientific speaker, Lars Bäckman, a professor of the psychology of ageing at the Aging Research Center at Karolinska Institutet, gave an overview of the changes seen in an ageing brain. His talk, *'Normal Cognitive Ageing: Brain Correlates and Plasticity'*, revealed that contrary to common belief, normal cognitive ageing does not affect all brain functions equally: for example, episodic memory, speed and attention decline, whereas other functions — including short-term memory and semantic memory — remain fairly well preserved.

Why is there any type of decline with age? One reason is physical: grey and white matter — the two main components of the brain — are lost from multiple regions. Levels of the neurotransmitter dopamine also decrease with age. These changes are linked to age-related cognitive losses, and they "occur at multiple levels in the central nervous system," said Bäckman.

Furthermore, although changes generally begin in a person's late 50s, the age at which someone drops below a certain level of cognitive ability varies widely. "Both the initial level of functioning as well as the rate of decline will determine your level of cognition at age 75," explained Bäckman. Initial cognitive capabilities are affected by demographic, lifestyle, biological and genetic factors — and these factors can interact. "Cultural activity could very nicely compensate for the negative effects of a low level of education," he explained. In conclusion, "the older we get, the more different we will be cognitively," said Bäckman.

Diverse dementia

The second speaker was Dr Michael Rapp, the director of the Geriatric Psychiatry Center at Charité, who discussed the diverse characteristics and causes of dementia. Speaking on the topic of *'Ageing and Mental Health'*, Rapp said that many people take dementia to mean Alzheimer's disease. However, although it accounts for the largest share of dementias, it is not the sole cause; vascular dementia is also very common. Furthermore, there is overlap between the dementia subtypes, and even within Alzheimer's disease there are discrepancies between patients' neurophysiology and their mental acuity. "Only 37% of the variance in cognitive decline in Alzheimer's disease is explained by the presence of plaques and tangles that are characteristic of Alzheimer's disease," explained Rapp.

Dementia occurs in tandem with other diseases, which could give a clue to its underlying biology. "The incidence of cardiovascular disease follows a similar pattern to the incidence of dementia in old age," said Rapp. "How these two are related is a significant question." There is one obvious link: the *APOE4* gene that regulates cholesterol levels is also a significant risk factor for developing Alzheimer's disease. Evidence suggests that exercise can mitigate or delay the onset of both Alzheimer's disease and cardiovascular disease.

A dementia-free future?

The final speaker, Professor Laura Fratiglioni from the Aging Research Center at Karolinska Institutet, expanded on the theme of how to avoid dementia. In her talk, *'Protecting the human brain and reducing the risk of dementia'*, Fratiglioni pointed out that only 50% of people who reach the age of 95 develop the condition. "It is possible to escape dementia," she observed. If scientists can find out what factors are protective, "we can develop strategies to help people who do not have these characteristics," she said.

Fratiglioni, a professor of geriatric epidemiology, presented new data from a longitudinal study of cognitively normal older patients. Researchers collected lifestyle data including levels of mental, physical and social activity, and tracked which of the patients went on to develop dementia. Subjects who were more active in all aspects were less likely to develop dementia during the nine years of the study period. The study also showed that a healthy lifestyle can help counteract a genetic predisposition for dementia.

Fratiglioni concluded by highlighting some ongoing intervention studies that are testing whether changes to lifestyle could reduce dementia risk, but cautioned that these studies are too limited to show definitive results. As with cardiovascular disease, large-scale, international intervention trials are crucial to provide answers.

Discussion highlights

Following the talks, the Nature Café audience asked the speakers about different aspects of mental health and the possibility of avoiding dementia. A popular topic was on ways to improve prospects for patients once they are diagnosed with dementia. "Once you're diagnosed very few of the risk factors affect progression," said Bäckman. Rapp agreed: "The largest share in the amount of variance in behaviour, quality of life and depression in patients with dementia is linked to their environment." As a result, Rapp said that psychosocial interventions have more impact than drug therapy. Fratiglioni added that it is not just the physical nature of interventions that benefits patients — such activities also include social and mental stimulation. When it comes to reducing the impact of dementia, "my advice is always to go dancing", she concluded. ■

Karolinska Institutet
http://ki.se

Karolinska Institutet

EMBASSY OF SWEDEN

ADVERTISEMENT FEATURE

ADVERTISER RETAINS SOLE RESPONSIBILITY FOR CONTENT

Watching the players at the climate poker table

In two decades of covering climate-change negotiations, **Frank McDonald**, *has seen youthful hope fight dark forces, and a distant threat become a reality.*

Nearly 20 years ago, as I wandered as a newspaper reporter from tent to tent at the Global Forum in Rio de Janeiro's Flamingo Park, with young, idealistic environmental activists milling about, I couldn't help thinking of Dale Arden's line from the film *Flash Gordon*, a decade before: "Flash, Flash, I love you, but we only have 14 hours to save the Earth!"

Brazil's 1992 Earth Summit was in full swing, and when it closed it even seemed that we would manage to save the world from global warming, and species extinction too. After all, delegates at the United Nations Conference on Environment and Development — as it was officially known — had just adopted two conventions to stave off these threats.

Little did I realize that the newly formed UN Framework Convention on Climate Change (UNFCCC) would become my ticket to see the world, via its annual Conference of Parties (COP). On Monday morning, I arrived home in Dublin from covering yet another frenetic COP meeting, this time in Durban, South Africa, where it was held in the International Convention Centre, surrounded by a continuous concrete barrier with steel fencing on top.

It was the latest gig in the UNFCCC travelling circus. We queued in Copenhagen in 2009 and boiled in Bali in December 2007 — after nearly freezing in Montreal two years earlier. I didn't get to Buenos Aires (1998), Marrakech (2001) or Delhi (2002), but I've been at all the rest — in exotic locations, and in Poznań, Poland.

What's striking is how the climate issue has become more pressing with each passing year, and how difficult it has proved to resolve. Back in Berlin at the first COP in 1995, climate change seemed like a distant threat — something for our grandchildren to worry about. But as the scientific evidence has hardened since then, so has the reality on the ground. Anyone who has travelled in sub-Saharan Africa (as I have) with his eyes open will have met smallholders who relate their personal experiences of how the climate is changing, and how difficult it is to survive as a result.

There have been dark forces at work over the years too, led in the 1990s by the benignly named Global Climate Coalition — the fossil-fuel lobby in disguise — and the likes of Washington lawyer Don Pearlman, who was crowned by environmentalists and frustrated delegates as King of the Carbon Club. Pearlman, who died in 2005, was such an expert on the process that the Saudi Arabian delegates, long-running obstructionists, took their orders from him.

Still, Pearlman met his match in Angela Merkel, who chaired that first COP in Berlin when she was Germany's environment minister. As the deadline for agreement loomed, she simply overlooked the Saudi delegate's objections and, despite his screeched protests, and the UN rules that demand unanimous decisions, gavelled through the mandate that led us to the Kyoto Protocol two years later.

The current crop of COP delegates are a diverse bunch, from the hawkish Todd Stern, the US climate-change envoy, who seems to be entirely devoid of emotion, to the more engaging Connie Hedegaard, who survived the shambles of Copenhagen to become the European Union (EU) Climate Action Commissioner, and burly Xie Zhenhua, China's rising star in this bewildering game of climate poker.

The latest big player is India's environment minister, Jayanthi Natarajan. She played with high stakes in Durban, in a showdown with Hedegaard over an EU road map on future action (see page 299). In response, the EU forged an impressive coalition with delegates representing people much more vulnerable and equally blameless — the Alliance of Small Island States, which fear global warming could wipe them off the map, and the impoverished group of least developed countries, which are mainly in Africa. And as Durban had been dubbed 'the African COP', the moral power of this alliance heaped pressure on the three biggest emitters — China, the United States and India.

What we got, after two all-night sessions and nearly two days of 'injury time' was hailed by insiders as a breakthrough, comparable to that first COP in Berlin, in giving a mandate for negotiations and a 2015 deadline to conclude them.

But it is improbable that this will save the world. Except in Europe, bigger countries still seem unwilling to take the steps required to respond to the science. One wonders if this will ever change, even after the UN's Intergovernmental Panel on Climate Change produces its Fifth Assessment, due by 2014.

EXCEPT IN EUROPE, BIGGER COUNTRIES STILL SEEM UNWILLING TO TAKE THE STEPS REQUIRED TO RESPOND TO THE SCIENCE.

In 2009, US President Barack Obama pledged to "lead the world" on climate change, but there has been no evidence of any such leadership. And with a US presidential election next year, there's even less chance that Obama will give any hostages to his sceptical and hostile Republican Party opponents.

As for China, the advantage of having a totalitarian regime is that once it decides that wind turbines or high-speed trains are good things, they start to happen very quickly — but not fast enough to ensure that its now-prodigious carbon emissions, or those of the United States, will peak any time soon. And as each is fearful of the other gaining any advantage, the game of climate poker will run and run. ■

➲ **NATURE.COM**
Discuss this article online at:
go.nature.com/NGxnCl

Frank McDonald *is environment editor of the* Irish Times, *author of several books and was recently elected as an honorary fellow of the Royal Institute of British Architects.*
e-mail: fmcd@eircom.net

RESEARCH HIGHLIGHTS

Selections from the scientific literature

NANOTECHNOLOGY

Swirls move tiny objects

Individual cells can be manipulated by tiny vortices generated in fluids, rather than by the potentially harmful lasers or electric fields typically used. The concept is the brainchild of Li Zhang and his colleagues at the Swiss Federal Institute of Technology in Zurich, who used the vortices to control the movement of microscopic objects.

The team placed a tank of water in a rotating magnetic field, which triggered nickel nanowires in the tank to rotate in turn, generating microvortices. The vortices trapped polystyrene microbeads in the water. By controlling the movement of the nanowires, the authors could tightly control the movement of the beads.

They also successfully manipulated *Escherichia coli* bacteria using a pair of microspheres in place of the nanowires.

Nano Lett. **http://dx.doi.org/10.1021/nl2032487 (2011)**

ANIMAL BEHAVIOUR

Rats rescue others in distress

Primates show signs of empathy, but can other mammals sense and respond to emotional distress in another individual? Yes, say Peggy Mason and her co-workers at the University of Chicago in Illinois, who report that rats will liberate a trapped individual even when they do not receive a reward for doing so.

In the experiments, one rat was trapped inside a container within a larger arena in which another rat roamed free. By day six or seven, on average, the roaming rat learned to free the trapped one. When a container holding chocolate was added to the arena, the liberators took roughly the same amount of time to free a trapped rat as to access the treat.

Distressed rats typically freeze in response to another distressed rat. The fact that the creatures can control such urges to help another shows that empathy can motivate behaviour in animals other than primates, the authors suggest.

Science 334, **1427–1430 (2011)**

For a longer story on this research, see go.nature.com/87bk8y

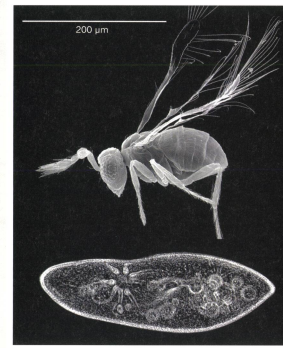

NEURODEVELOPMENT

Wasp neurons lack nuclei

A tiny parasitic wasp that is smaller than some single-cell organisms (such as *Paramecium*, pictured bottom) has the fewest neurons of any insect studied so far. The bulk of the cells even lose their nuclei when the insects become adults.

Alexey Polilov of Lomonosov Moscow State University sectioned pupae and adults of the wasp (*Megaphragma mymaripenne*, pictured top) and examined their central nervous systems with light and electron microscopy. The wasp's brain contained around 4,600 neurons — orders of magnitude fewer than house flies (340,000 neurons), bees (850,000) or even closely related parasitic wasps (37,000).

During metamorphosis to an adult, more than 95% of *M. mymaripenne*'s neurons lost their nuclei and cell bodies — the bulbous part of the neuron that contains the nucleus. As a result, the creature's brain shrank by almost 50%. The neurons seem to function without nuclei, because the wasps were still able to fly, eat and find hosts for eggs.

Arthropod Struct. Dev. 41, **29–34 (2012)**

CLIMATE CHANGE

The growth of dying seas

Oxygen-deprived dead zones in coastal waters around the world have expanded exponentially since the 1960s and are likely to increase further in a warming climate.

Markus Meier of the Swedish Meteorological and Hydrological Institute in Norrköping and his colleagues used a group of physical–biogeochemical models, driven by data from regional climate models, to project the effects of climate change and changes in nutrient cycles on oxygen conditions in the Baltic Sea.

Most scenarios suggested that oxygen-depleted zones at the bottom of the sea would expand by the end of the century. Driving factors include rising nutrient input from river runoff; reduced oxygen flux from the atmosphere to the ocean; and increased oxygen consumption by surface-level organisms that are fed by the boost in nutrients. Similar changes can be expected for coastal oceans worldwide, the authors say.

Geophys. Res. Lett. **http://dx.doi.org/10.1029/2011GL049929 (2011)**

ASTRONOMY

A filter for the night sky

Infrared signals from distant stars that formed soon after the Universe itself could one day be discerned from Earth, thanks to a specially

ELSEVIER

designed filter. Such signals are normally drowned out by a blaze of infrared emissions of wavelength 1,000–1,800 nanometres coming from hydroxyl chemicals in Earth's upper atmosphere.

The filter, developed by Joss Bland-Hawthorn at the University of Sydney, Australia, and his colleagues, combines two technologies: Bragg gratings, which are fibre-optic cables with unevenly spaced notches that suppress and reflect up to 400 hydroxyl spectral lines; and a converter that funnels the light from the sky into the grating as a single ray.

Tests at an observatory over three evenings showed that the filter blocked out most of the brightest emissions with wavelengths between 1,440 and 1,630 nanometres. Although a still a prototype, the device could be used with 8-metre and future 30-metre telescopes, the authors say.

Nature Commun. 2, **581 (2011)**

BIOELECTRONICS

Recharge through the skin

Replacing the batteries of implanted medical devices such as pacemakers usually requires surgery. An invention (**pictured**) by Eijiro Miyako at the National Institute of Advanced Industrial Science and Technology in Ikeda, Japan, and his colleagues could, in theory, provide a noninvasive way to recharge such devices. The authors have built an implantable converter that generates electric current when hit with laser light that is beamed through the skin.

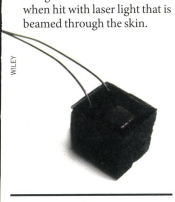

WILEY

1 cm

The device consists of carbon nanotubes — which heat up when exposed to laser light — wrapped in a polymer and dispersed in silicone. The heat warms one side of the converter more than the other, and the flow of heat to the cooler side generates an electric voltage.

The researchers show that, when irradiated with laser light, their device can electrically stimulate a zebrafish heart, and can generate a voltage while implanted in a rat.

Angew. Chem. Int. Edn **http://dx.doi.org/10.1002/anie.201106136 (2011)**

EVOLUTION AND DEVELOPMENT

How the brain became human

Humans' evolution of big brains and unique cognitive abilities may be down to key regulators that control gene expression during development.

Philipp Khaitovich and Svante Pääbo at the Max Planck Institute for Evolutionary Anthropology in Leipzig, Germany, and their colleagues compared gene-expression patterns in the brains of dozens of humans, chimpanzees and rhesus macaques of different ages. Relative to those of chimps and macaques, human brains showed many more differences in gene-expression patterns as newborns developed into adults, particularly in a region involved in cognition called the prefrontal cortex (PFC). Genes that encode microRNAs, which regulate the activity of many other genes, were among those whose developmental expression patterns varied most between the PFCs of humans and other primates.

The authors suggest that a small number of microRNAs and proteins controlling brain development could have driven the evolution of the human brain.

PLoS Biol. 9, **e1001214 (2011)**

COMMUNITY CHOICE

The most viewed papers in science

NEUROSCIENCE

The brain's nutrient sensor

HIGHLY READ on www.cell.com in November

Certain brain cells can respond not only to changing glucose levels, but also to mixtures of amino acids — the building blocks of proteins. This suggests that the brain can sense the body's nutrient status in addition to its energy needs.

Denis Burdakov at the University of Cambridge, UK, and his colleagues looked at cells in the brain's hypothalamus called orexin/hypocretin neurons, which regulate energy balance and feeding. Working with mice, they found that these cells were activated both *in vitro* and *in vivo* when exposed to nutritionally relevant amino-acid mixtures.

Glucose normally suppresses the activity of these neurons, but when the researchers exposed the cells to both glucose and amino acids, the amino acids excited the neurons and blocked the effect of glucose. The authors suggest that this boosts the signal from amino acids, which are typically at lower concentrations in the brain than glucose.

Neuron 72, **616–629 (2011)**

OCEAN/CORBIS

ENERGY

Sugar-cane biofuel fouls air

Brazil has rapidly become the world's biggest producer of ethanol — an alternative to petroleum-based fuel — from sugar cane. The greenhouse-gas emissions created during sugar-cane ethanol production are lower than those associated with the creation of other biofuels, but a study shows that the process generates up to seven times more air pollutants than previously estimated from remote-sensing data.

Elliott Campbell at the University of California, Merced, and his colleagues used agricultural survey data from Brazil to calculate emissions of various air pollutants, such as sulphur dioxide and black carbon, from the entire production cycle of sugar-cane ethanol in 2000–08. A major source of emissions is the burning of sugar-cane fields before harvest (**pictured**). The authors' estimates of emissions from just this burning phase were 1.5–7.3 times higher than those from satellite-based methods. Altogether, the production of sugar-cane ethanol generated more pollutants than petrol or diesel production.

The authors say that even in regions where burning has been scaled back, pollutant emissions continue to grow because of the increase in sugar-cane production in Brazil.

Nature Climate Change **http://dx.doi.org/10.1038/nclimate1325 (2011)**

NATURE.COM
For the latest research published by *Nature* visit:
www.nature.com/latestresearch

SEVEN DAYS *The news in brief*

RESEARCH

Higgs hunt

Physicists at the Large Hadron Collider at CERN, near Geneva, Switzerland, announced on 13 December that the collider has seen signals consistent with the possible existence of the Higgs boson with a mass of about 125 gigaelectronvolts. But the evidence isn't strong enough to rule out the particle's absence. See page 301 for more.

Gene-therapy boost

A gene-therapy treatment for patients with the blood-clotting disorder haemophilia B has scored its first unequivocal success, scientists at University College London reported at the American Society of Hematology meeting in San Diego, California, on 11 December (A. C. Nathwani *et al. N. Engl. J. Med.* http://doi.org/g8n; 2011). Haemophilia B is caused by mutations in the gene that codes for the factor IX protein; the treatment uses viruses to deliver a healthy version of the gene to patients' liver cells. In a previous trial, protein production dropped below therapeutic levels after two months (C. S. Manno *et al. Nature Med.* **12**, 342–347; 2006). But in the latest trial, four out of six patients were still making the protein up to 18 months after one treatment, and did not need injections of blood-clotting factors.

NASA/JPL-CALTECH/CORNELL/ASU

Fresh clue to ancient Mars water

NASA's Opportunity rover has discovered veins of hydrothermally deposited minerals at the edge of Endeavour crater on Mars. The bright, stick-like veins (pictured), apparently comprised of gypsum, show that hot, mineral-rich water once pulsed through fractures in the volcanic rock. Gypsum deposits can form in water that is much less acidic than required by the water-altered sulphate minerals previously discovered on Mars — meaning that the site could have been more habitable than others explored by the rover. Principal investigator Steve Squyres, of Cornell University in Ithaca, New York, told a meeting of the American Geophysical Union in San Francisco, California, on 8 December that the discovery is the most "bullet-proof" support yet for ancient water. See go.nature.com/nmsldl for more.

MENTOR AWARDS

The annual *Nature* Awards for Mentoring in Science (go.nature.com/qithms), which this year recognized mentors in France, were presented on 12 December in Paris. Two Paris-based researchers shared the €10,000 (US$13,200) lifetime-achievement award: Moshe Yaniv, a geneticist at the Pasteur Institute, and Jean Rossier, a neurobiologist at ESPCI ParisTech. The €10,000 mid-career award went to Barbara Demeneix, a developmental endocrinologist at the National Museum of Natural History in Paris.

Targeting cancer

Efforts to create cancer therapies tailored to a patient's genetic make-up were boosted by promising clinical-trial results reported on 7 December (J. Baselga *et al. N. Engl. J. Med.* http://doi.org/g8m; 2011). The trial was conducted on women with advanced forms of breast cancer that involved mutations in the *HER2* gene, which drives about 20% of breast-cancer cases. Those given the experimental monoclonal antibody pertuzumab and the widely used drug trastuzumab (Herceptin), together with chemotherapy, gained an extra 6-month lull in disease progression compared with women receiving only chemotherapy and trastuzumab. Both antibodies target the protein affected by *HER2* mutations. See go.nature.com/hwxlbd for more.

POLICY

Durban deal

After negotiations that ran into the early morning, tired politicians at the climate talks in Durban, South Africa, agreed that by 2015, the world would negotiate a new climate treaty, which would require all nations to meet as-yet-unspecified emissions targets and would come into force from 2020. The Kyoto Protocol will be extended by at least 5 years. Emotions were mixed after the deal on 11 December, which brought in previously recalcitrant countries, but also deferred action for a decade. See pages 292 and 299 for more.

Forest threat

Brazil's Senate has approved a new 'forest code', which scientists fear will weaken strict rules on tree-clearing that have reduced deforestation in the Amazon. All landowners there have had to maintain forest on 80% of their land, but the new bill creates exemptions for small landowners and pardons those who deforested illegally before 2008. This could "unleash a wave of impunity", to wipe out forests and woodlands, says

Daniel Nepstad, an ecologist who works with the Amazon Environmental Research Institute in Brasília. President Dilma Rouseff has pledged to veto the legislation. See go.nature.com/rutitm for more.

Stem-cell appeal

A lawsuit seeking to halt US federal funding for research on human embryonic stem cells is not quite dead — although it was thrown out in July by a District of Columbia judge (see *Nature* **476,** 14–15; 2011). On 7 December, the Court of Appeals for the District of Columbia circuit (one level below the Supreme Court) set a date of 23 April 2012 to hear an appeal from the plaintiffs in the case, James Sherley, of the Boston Biomedical Research Institute in Massachusetts, and Theresa Deisher, who runs AVM Biotechnology in Seattle, Washington. Both work on adult stem cells.

Fracking worry

The US Environmental Protection Agency (EPA) has said that chemicals associated with fracking, a controversial technique that involves pumping high-pressure fluids into shale to force out natural gas, probably polluted water supplies in central Wyoming. Shale-gas companies have maintained that complaints of methane and other

F. ROBERTS/ALAMY

chemicals in groundwater can't definitely be linked to fracking, despite the many public protests against the practice (**pictured**). The EPA's draft report was released on 8 December and has yet to be peer-reviewed; the agency is also working on a national study on fracking's impacts, to be released in 2012.

Pill politics

In a surprise move, the US Secretary of Health and Human Services, Kathleen Sebelius, has overruled the Food and Drug Administration (FDA) and denied girls under 17 access to the emergency contraceptive levonorgestrel — known as the morning-after pill, or Plan B — unless it is prescribed by a physician. Drug-makers Teva had asked that the pill be made available over the counter to girls, and FDA research had found it to be safe and effective. But Sebelius said on 7 December that she did not believe the pill could be used safely by the youngest girls of reproductive age. See go.nature.com/w3343o for more.

Fisheries push

The United Nations has stepped up a push to encourage sustainable fisheries. Its general assembly on 6 December adopted a draft resolution that urges nations to reduce or eliminate by-catch and to increase efforts to deal with the impact of climate change on stocks. With many fish stocks being harvested at unsustainable levels — and many suffering from a lack of data on actual catch levels — the resolution also encouraged states to "increase their reliance on scientific advice" to manage fisheries.

Name and shame

Funding agencies in Canada will no longer keep secret the identities of researchers they support who commit misconduct. The change — called for in a *Nature* Editorial in September (see *Nature* **477,** 509–510; 2011) — came as part of a new policy on responsible conduct of research, released on 5 December. See go.nature.com/aj2zq6 for more.

NOAA integrity

It was more than 2 years in the making, but the US National Oceanic and Atmospheric Administration (NOAA) finally released its scientific integrity policy on 7 December. The policy, which applies to thousands of NOAA employees conducting research on climate, oil spills, marine mammals and other sometimes controversial topics, prohibits agency employees from distorting science and protects the rights of NOAA scientists to speak openly about their work and to report wrongdoing. See go.nature.com/ihfjbv for more.

COMING UP

16 DECEMBER
The Japanese government is expected to announce that the Fukushima Daiichi nuclear plant has reached cold shutdown — a declaration that the stricken reactors have reached stable, low temperatures and the immediate crisis is over.

17 DECEMBER
The deadline for US science agencies to send final policies on scientific integrity to the White House.

PEOPLE

US integrity head

After a 22-month search, the US Department of Health and Human Services' Office of Research Integrity (ORI) named David Wright as its permanent director on 5 December. Wright is a historian of US science and technology who previously served as a research-integrity administrator at Michigan State University in East Lansing. He has also worked as a consultant to the ORI. He replaces Don Wright, who has served as acting director since the retirement of Chris Pascal in 2009.

TREND WATCH

The US National Human Genome Research Institute (NHGRI) announced a four-year plan on 6 December that focuses heavily on the use of genome sequences in the clinic. The institute's funding of programmes for large-scale sequencing has actually shrunk in recent years (see chart), but because the per-base cost of sequencing has dropped so much, the hope is that patients will routinely undergo sequencing for medical purposes. See go.nature.com/jhjz2l for more details of the NHGRI programme.

SOURCE: NHGRI

MEGABASE BOOM

Despite falling funds, US agencies can support more DNA base sequencing — thanks to next-generation technologies.

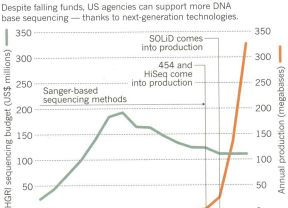

NATURE.COM
For daily news updates see:
www.nature.com/news

MACMILLAN
SCIENTIFIC COMMUNICATIONS

Scientific ***Editing***

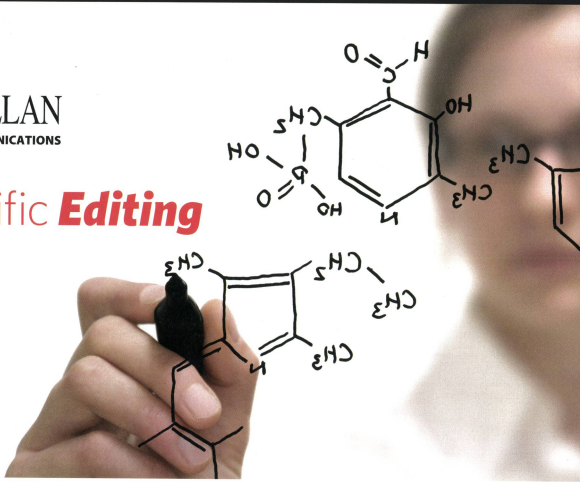

Publishing help now available

Give yourself the best chance of publishing in high-ranked international journals by using Macmillan Scientific Communication's premier Scientific Editing service. MSC goes far beyond regular language editing and provides:

- in-depth **developmental editing** by ***Nature*-standard editors**
- **feedback** and suggestions on your manuscript's content, organisation and presentation by an expert in your field
- **advice on suitable journals** for your manuscript
- **language editing** by Nature Publishing Group Language Editing

Maximize the impact of your research. **Submit** your manuscript today!

www.mscediting.com

[1]Nature Publishing Group editorial and publishing decisions are independent of MSC services.

Exclusive partner of Nature Publishing Group, publisher of Nature *and* Scientific American

MACMILLAN
SCIENTIFIC COMMUNICATIONS

NEWS IN FOCUS

PHYSICS LHC confirms long-rumoured glimmer of the Higgs particle **p.301**

EXOPLANETS Trove of super-Earths confounds the theorists **p.302**

EUROPE An independent voice for science in Brussels **p.305**

ASTRONOMY South Africa's hopes ride a mega-telescope **p.308**

A. FILAK/REUTERS

Europe's climate commissioner, Connie Hedegaard (seated left), negotiates with India's environment minister, Jayanthi Natarajan (seated mid-right), in the early hours of 11 December in Durban, South Africa.

POLICY

Durban maps path to climate treaty

Marathon talks enable Europe to break deadlock over global-warming deal with major greenhouse-gas emitters.

BY JEFF TOLLEFSON IN DURBAN

In the darkest hours of the international climate-change negotiations in Durban, South Africa, last week, there was talk of postponing a decision altogether. But one question always came up: would more time really make a difference? After all, the issues facing negotiators have not changed in years, and the scientific evidence for the potential impacts of anthropogenic climate change just keeps getting stronger.

The first round of greenhouse-gas reduction commitments under the Kyoto Protocol will expire at the end of 2012, adding to the pressure on policy-makers to tackle the problem and leaving Durban as the last, best chance to establish a fresh road map to curb greenhouse-gas emissions. Agreed in 1997, the Kyoto Protocol is still the only global treaty that sets out legally binding goals for countries to reduce greenhouse-gas emissions. However, developing nations were exempt, and the United States refused to sign up, weakening the treaty's impact.

With tensions high, long-simmering disputes between rich and poor countries erupted time and again in Durban — but the febrile atmosphere gave European negotiators enough leverage to broker a historic global deal. Through a blend of clever politicking and sheer fatigue, the deal was thrashed out in impromptu huddles that formed in the main conference hall during the small hours of 11 December, in plain sight of anyone who was willing to push their way into the crowd — this reporter included.

Known as the Durban Platform, the deal commits the world to negotiating a new climate treaty by 2015. Crucially, that treaty would legally require all nations — including the two biggest emitters, China and the United States — to meet as-yet-unspecified emissions targets. It also extends the Kyoto Protocol by a period of between five and eight years, with the final term to be decided at the next annual conference of the United Nations Framework Convention on Climate Change in Doha, Qatar, at the end of 2012. The European Union (EU) has already promised to register its existing emissions pledges under the extended protocol, as has a handful of other countries. Canada, however, has been unable to meet its Kyoto commitments, and announced on 12 December that it would formally withdraw from the protocol.

Many observers had expected the conference to continue down the path towards voluntary climate commitments that was paved at the climate summit in Copenhagen two years ago (see *Nature* **479**, 291–292; 2011). Instead, the Durban Platform shifts countries towards a legally binding agreement, which would come into force in 2020. "These really were very high-stakes negotiations over competing visions of the world," says Alden Meyer, who heads climate policy for the Union of Concerned Scientists in Washington DC.

Despite the celebratory atmosphere, the platform represents an exercise in legalese that does little or nothing ▶

NATURE.COM
Read more analysis from the summit at: go.nature.com/dw9pu2

THE GIGATONNE GAP

By the time a new treaty to limit emissions comes into force in 2020, the world will have diverged further from the path needed to limit warming to 2 °C by 2100, according to an analysis by Climate Action Tracker.

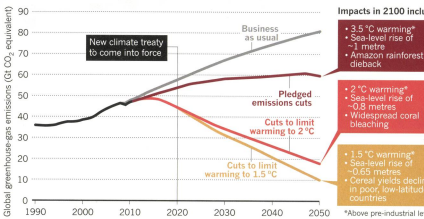

SOURCE: CLIMATEACTIONTRACKER.ORG

to reduce emissions, and defers action for almost a decade. The stated goal of the talks was to limit global warming to 2 °C, although many developing nations and small-island states have advocated a target of 1.5 °C. But the latest analysis of current pledges from climate scientists advising delegates in Durban suggests that the world is on course to see 3.5 °C of warming this century (see 'The gigatonne gap').

Countries such as Venezuela protested against the proposed deal, noting that past emissions by the United States and Europe will drive much of this warming. They argued that rich countries have refused to reduce their own emissions, and are now demanding that poor countries sacrifice economic development to make carbon cuts. But other developing countries, acknowledging that most future emissions growth will come from once-poor nations, were willing to sign up. Early in the summit, Brazil and South Africa said that they would accept binding commitments under a new treaty. As the final negotiations over wording began, observers said that China and the United States also acquiesced. By the morning of 11 December, India was the main holdout.

India's environment and forests minister, Jayanthi Natarajan, gave an impassioned speech invoking the original 1992 Framework Convention on Climate Change, which stated that countries have "common but differentiated responsibilities" for tackling global warming — language that was not part of the new proposal. "Does climate change mean you give up equity?" Natarajan asked. "India will never be intimidated by threats or any kind of pressure like this."

After objecting to stronger wording, India finally agreed to pursue talks towards a "protocol, legal instrument or an agreed outcome with legal force". Connie Hedegaard, the EU commissioner for climate change, who was instrumental in pushing for a road map to a legally binding treaty, said the outcome was a "good and strong result". Luiz Alberto Figueiredo Machado, Brazil's lead negotiator, called the agreement a significant step. "I am relieved that we have what we came here to get," he said.

"There is going to be some tough bargaining ahead."

Island states threatened by rising seas, such as Grenada and Papua New Guinea, had hoped for more immediate, aggressive steps. Kevin Conrad, the representative for Papua New Guinea in the negotiations, lays part of the blame for inaction on the ongoing global financial crisis. Economic woes have certainly diverted attention from the climate threat and, in the United States, emboldened right-wing politicians who have blocked President Barack Obama's climate agenda. The political situation may be no more favourable when treaty negotiations culminate in 2015, but "we need to start somewhere and then begin a process to ramp things up", says Conrad. Fearing that the Durban agreement could lock in weak commitments until 2020, some countries plan to use a formal scientific review built into the process to push for additional, early emissions cuts.

Negotiators did, however, make some progress in establishing a Green Climate Fund designed to help developing countries cope with global warming, although the talks failed to identify any sources of new funding. Industrialized nations had agreed at previous meetings to boost funding for developing countries to US$100 billion annually by 2020; now they need to begin allocating the money.

The talks also moved closer to establishing a system that would allow payments to countries that reduce carbon emissions by preventing deforestation, which accounts for roughly 15% of global emissions. Negotiators settled some technical details about how nations will calculate their emissions, and launched a process to explore how the funding system will work.

The agreement also modified the Clean Development Mechanism, by which countries can sell carbon credits for projects that lower greenhouse-gas emissions, such as renewable energy. The mechanism, negotiated in Kyoto, allows developing countries to build up their green infrastructure, and sell the resulting credits to more developed nations. In Durban, negotiators extended the mechanism to include projects that capture and store carbon emissions from power plants, allowing Western countries to finance these plants more cheaply in India or China. The agreement also requires industrialized countries to accept long-term liability for the projects, with 5% of the carbon credits being set aside to account for any leakage of stored greenhouse gases in the 20 years after they are buried.

And in answer to growing demands to consider agriculture as a separate sector within the UN climate framework (see *Nature* **479**, 279; 2011), the agreement establishes a technical body to investigate the issue and report back at the next meeting in Doha.

That meeting will be the first test of whether the Durban Platform really can work as a global road map for climate-change action. "There is going to be some tough bargaining ahead," says Meyer. "But I'm a lot more hopeful now than I was a couple of days ago." ■ SEE EDITORIAL P.292

MORE ONLINE

SPL

TOP STORY

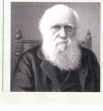

Shipping timetables debunk Darwin plagiarism accusations
go.nature.com/xoqp2p

MORE NEWS

- Lukewarm reception for UK government's life-sciences investment go.nature.com/oexfz4
- Method predicts size of fracking earthquakes go.nature.com/rk7luf
- Mammoth femur yields first ancient proteome go.nature.com/hvblo

AUDIO

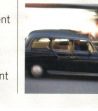

How having 'the Knowledge' enlarges your brain
go.nature.com/pbtsge

M. NOSKOWSKI/GETTY

© MARCELLON/CERN

ATLAS at the Large Hadron Collider is one of two experiments focused on finding the Higgs particle.

PARTICLE PHYSICS

Detectors home in on Higgs boson

Hunt gathers momentum as range narrows and hints of a possible signal emerge.

BY EUGENIE SAMUEL REICH

The result is not definitive evidence of the long-sought Higgs boson — yet. But it is the closest so far to come out of the US$6.5-billion Large Hadron Collider (LHC) at CERN, Europe's high-energy physics laboratory near Geneva in Switzerland. On 13 December, physicists on the LHC's two largest experiments announced signals consistent with the possible appearance of the Higgs boson, a manifestation of the force field that endows all other particles with mass. If supported by further data, the results suggest a Higgs particle with a mass of about 125 gigaelectronvolts (GeV). But members of both experiments emphasize that the latest data are also statistically consistent with the particle's absence.

"We have not collected enough evidence for a discovery. There is an excess of events compatible with the hypothesis that it could be a Higgs," says Guido Tonelli, spokesman for the Compact Muon Solenoid (CMS) experiment. His sentiment was echoed by Fabiola Gianotti, spokeswoman for the LHC's ATLAS experiment. "It could well be something intriguing, but it could be a background fluctuation," she says.

Last month, the CMS and ATLAS experiments presented a combined analysis that left little room for the Higgs to hide. If the particle exists, it must have a mass of between 114 GeV and 141 GeV. The latest results narrow the field even more: ATLAS has excluded all masses outside the range of 115–130 GeV, and the CMS team has revised the range to 117–127 GeV. Raising anticipation still further, each experiment separately reports that the LHC's high-energy collisions between protons generated an excess of particles that could be the products of Higgs particle production. The ATLAS result is consistent with a 125–126 GeV Higgs at a statistical level of at most 3.6 standard deviations, and the CMS team reports a 124-GeV signal of at most 2.6 standard deviations. In particle physics, a statistical significance of five standard deviations is considered to be proof of a particle's existence, and three standard deviations to be evidence that a particle may exist. The ATLAS and CMS results have not yet been combined, so a joint probability is not available.

The situation is further complicated by another signal seen by both experiments at around 119 GeV. It is a weaker signal and less convincing as a sign of the Higgs, particularly in the ATLAS data, but its presence has heightened researchers' caution in interpreting what is real and what is not in the new data. A sighting of the Higgs boson at either energy is consistent with the standard model of particle physics, and also with its extension, known as supersymmetry, in which known particles are associated with superheavy partners that have yet to be found.

The Higgs particle is a ripple in the Higgs field, which was proposed in 1964 by several scientists, including British physicist Peter Higgs, to explain why the W and Z bosons, which transmit the weak nuclear force, have mass, whereas the photon, which carries the electromagnetic force, does not. Tom Kibble of Imperial College London, another of the theorists to have proposed the Higgs mechanism, says that, over the years, the focus has gradually moved from the Higgs field to spotting the Higgs particle, because all other aspects of the standard model have been observed in particle accelerators. "The only thing missing is the Higgs boson," Kibble says.

Even if confirmed as an initial sighting of the Higgs particle, the 125-GeV result will leave many questions unanswered. The processes of production and decay of the Higgs particle still need to be carefully defined to help to inform theories beyond the standard model. Such theories would ideally answer long-standing questions such as why the known particles have the masses they do and why gravity is so much weaker than other forces of nature. The latter puzzle is one that supersymmetry is intended to solve.

"There is an excess of events compatible with the hypothesis that it could be a Higgs."

More data will be needed to establish the existence of the Higgs with confidence. Thus far, the ATLAS and CMS experiments have each detected the results of some 500 trillion proton–proton collisions. Spokespeople say that both experiments should have gathered four times as much data by the end of 2012. "Next year's data should answer it without question," says Bill Murray of the Rutherford Appleton Laboratory near Oxford, UK, who is leading the ATLAS search for the Higgs. Soon enough it will be clear whether this week's hints amount to a seductive mirage or a true glimmer of the LHC's quarry. ■

NATURE.COM
For more on the Large Hadron Colider see:
www.nature.com/lhc

ASTROPHYSICS

Super-Earths give theorists a super headache

An abundance of medium-sized worlds is challenging planet-formation models.

BY ERIC HAND

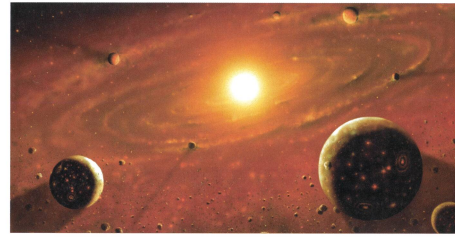

M. GARLICK/SPL

Planets coalesce out of dust swirling around their parent stars — but where super-Earths form is unclear.

By now, it's not surprising that NASA's Kepler space telescope is turning up extrasolar planets by the bushel. Last week, at the first Kepler science conference at NASA's Ames Research Center in Moffett Field, California, mission scientists announced that the space telescope has identified 2,326 candidate planets, nearly doubling its haul since February.

But what has puzzled observers and theorists so far is the high proportion of planets — roughly one-third to one-half — that are bigger than Earth but smaller than Neptune. These 'super-Earths' are emerging as a new category of planet — and they could be the most numerous of all (see 'Super-Earths rising'). Their very existence upsets conventional models of planetary formation and, furthermore, most of them are in tight orbits around their host star, precisely where the modellers say they shouldn't be.

"It poses a challenge," says Douglas Lin, a planet-formation modeller and director of the Kavli Institute for Astronomy and Astrophysics at Peking University in Beijing, China. "You can't just tweak the parameters. You need to think about the physics."

Guided by the example of our own Solar System, with its distinct sets of large and small worlds, early planet-formation models were based on the notion of 'core accretion'. Dust swirling around a star in a protoplanetary disk can aggregate into small planetesimals of rock and ice, which collide and stick together. The inner part of the disk contains too little material for these cores to grow much bigger than Earth. But farther out, they can attain ten Earth masses or more, enough to attract a vast volume of gas and become Jupiter-like.

The detection, starting in 1995, of Jupiter-sized planets with orbits as short as a few Earth days contradicted these models. The theorists revised their models to allow these 'hot Jupiters' to form far from their star and then migrate in. Yet these models predicted that anything reaching super-Earth size should either become a gas giant or be swallowed by its star, creating a 'planetary desert' in this size range. Kepler's discoveries wreck those predictions. "It's a tropical rainforest, not a desert," says Andrew Howard, an astronomer at the University of California, Berkeley. "We hope the theory is going to catch up."

Kepler measures a planet's size by detecting how much light it blocks as it passes in front of its star. For a handful of the super-Earths detected by Kepler, ground-based observations have also determined mass, by tracking the wobble of the host star induced by the planet's gravity. And some of these super-Earths seem to have very low densities — indicating that they may have small rocky cores surrounded by large gas envelopes.

Kepler astronomer Jack Lissauer, of Ames, thinks that they may have begun as small cores in the outer parts of their solar system, accreting a large amount of gas without reaching the point of runaway growth that leads to a true gas giant. Without the gravitational heft of a giant to hold in gas, such a planet would have a large, low-density atmosphere, but it could still grow to super-Earth size by a cooling process that shrinks the atmosphere and allows more gas to be drawn in, he says.

SUPER-EARTHS RISING

Ground-based telescopes have detected around 650 planets from the wobble of their parent star. A new class of planet — between the size of Earth and Neptune — has emerged precisely where modellers have said planets shouldn't exist.

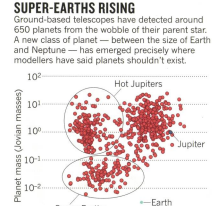

But that scenario may not explain smaller and denser super-Earths. Several such planets have already been detected, and Kepler is starting to reach the sensitivity required to spot them, says Greg Laughlin, an astronomer at the University of California, Santa Cruz. "Kepler is just seeing the tip of the iceberg."

Nor can any current theory explain how super-Earths can sit so close to their stars. Lissauer says the problem lies in the migration portion of the models. But Norm Murray, an astrophysicist at the University of Toronto, is exploring other ways of forming super-Earths. Instead of assembling them and migrating them towards the star, Murray's model first migrates rocky planetesimals and then allows them to accrete. "'Migration then assembly' is the catchphrase," he says.

In any event, Laughlin says that modellers will probably find a way to explain the current observations. "They'll scramble to fix the models," he says. But it's probably not the last time they'll have to revisit their codes, he adds. "My prediction is that they'll completely miss the next big thing, whatever that will be." ■

A SHORT CUT TO THE THIRD DIMENSION?

Ankylography promised to elucidate three-dimensional (3D) structures from data gathered on a curved, two-dimensional (2D) surface.

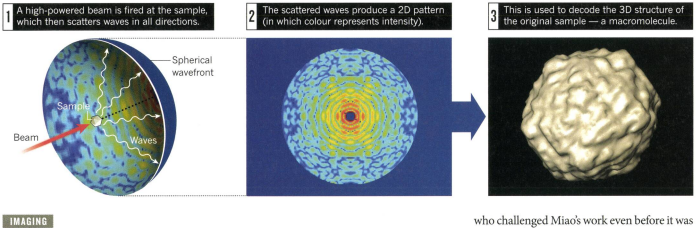
1 A high-powered beam is fired at the sample, which then scatters waves in all directions.
2 The scattered waves produce a 2D pattern (in which colour represents intensity).
3 This is used to decode the 3D structure of the original sample — a macromolecule.
Spherical wavefront
Sample
Beam
Waves

IMAGING

Three-dimensional technique on trial

Critics take a hard look at ankylography, a proposed method for revealing molecular structures from single pictures.

BY EUGENIE SAMUEL REICH

Imagine developing a detailed and accurate three-dimensional model from a single two-dimensional photograph. That is the promise of ankylography[1], a technique that, according to its creators, could reveal the structure of scientifically important subjects such as complex proteins that can be glimpsed only once before they are destroyed by the high-powered lasers used to image them.

But rather than sparking a revolution in imaging, the idea has raised objections from researchers who say that it amounts to pulling a three-dimensional rabbit out of a two-dimensional hat. Now, critics have weighed in with two technical comments[2,3], putting ankylographers on the defensive.

"The imaging principles and proposed methodology of ankylography are flawed, bringing into question its applications," one group of commenters writes[3].

Ankylography was developed by John Miao, a physicist at the University of California, Los Angeles, and his colleagues. It uses the spherical wavefront formed when radiation scatters off an object (see 'A short cut to the third dimension?'). Most current imaging technologies assume that this wavefront is roughly flat where it meets the imaging detector — a reasonable assumption for a detector that intercepts only a very small fraction of the sphere. Miao and his colleagues collected waves across a larger angle, from different depths of the object. They argued that this larger sample could be reconstructed into an accurate three-dimensional (3D) image using only very basic assumptions. They derived the name of their technique from the Greek *ankylos*, or 'curved', and *graphein*, or 'writing'.

"The claim is amazingly attractive, to take a single projection and do three-dimensional reconstruction," says Ge Wang, a biomedical imager at the Virginia Polytechnic Institute and State University in Blacksburg, and an author of one of the critical comments[3].

Ankylography seemed to be a boon for an emerging X-ray technology called diffract and destroy, which would use X-ray lasers — online or under construction at around a dozen sites worldwide — to take images of objects using a dose of radiation high enough to destroy them, forming an image from the X-rays scattered in the few dozen femtoseconds (10^{-15} seconds) before the object explodes. The ideal application would be imaging biological samples such as proteins, viruses, cells or tissue that are very sensitive to radiation. Ankylography would allow researchers to extrapolate 3D structures.

Despite the appeal of ankylography, many researchers were perplexed by what they see as a violation of the basic physical principle that you cannot get complete, 3D information from a single flat picture. In particular, the picture will provide incomplete information about the interior of a subject, and critics argue that many possible 3D structures could generate the same image. Pierre Thibault, a physicist at the Technical University of Munich in Germany, who challenged Miao's work even before it was published[4], explains that the curvature of the wave scattered from an object contains some 3D information, like the blurriness produced by a camera with a limited depth of field, but not enough to build up an accurate 3D image.

Miao is unable to comment, because a response to the criticism is still under review. However, his research group has placed all the computer code used to make his ankylographic reconstructions on a website so that others can test it (go.nature.com/gd6dvo). Miao has since made clear that the technique does not work on objects larger than $15 \times 15 \times 15$ volume pixels, a size dependent on the resolution of the imaging technology. "I can't think of any object that exists in nature that we care about that it would work for," says Stefano Marchesini, a physicist at Lawrence Berkeley National Laboratory in Berkeley, California, who has analysed ankylography.

Even if ankylography can be made to work for objects larger than the current range, it is likely that more than one image would be needed to generate a high enough signal-to-noise ratio to see fine detail, says John Spence, an expert in diffract-and-destroy imaging at Arizona State University in Tempe.

Without ankylography, X-ray lasers can still be used to take two-dimensional snapshots of a series of subjects from various angles, building up an average 3D image. This would work for identical objects such as viruses or proteins, but not for dissimilar objects such as cells.

Felipe Maia, a physicist at Lawrence Berkeley, says that the ankylography controversy has triggered a useful discussion about the limitations of 3D imaging. Wang agrees; he has been inspired to propose an alternative technique[3], in which waves of different energies are collected and used to derive some of the 3D information that a flat image lacks. "There's been some positive influence," he says. ■

1. Raines, K. S. *et al. Nature* **463,** 214–217 (2010).
2. Wei, H. *Nature* http://dx.doi.org/10.1038/nature10634 (2011).
3. Wang, G., Yu, H., Cong, W. & Katsevich, A. *Nature* http://dx.doi.org/10.1038/nature10635 (2011).
4. Thibault, P. Preprint available at http://arxiv.org/abs/0909.1643 (2009).

ONCOPOLE
TOULOUSE I FRANCE

Chief Executive Officer of the University Cancer Institute of Toulouse Midi-Pyrénées (South of France).

The innovative European campus, Oncopole Cancer Campus of Toulouse, will house over 4,000 persons on a site covering almost 2 million m², with the combined support of the European Community, the French Government, local public authorities and private investment exceeding one billion Euros. This Cancer Campus will include at its heart a large University Cancer Institute (UCI), which will feature both a 300-bed 65,000 m² hospital and the adjoining 10,000 m² Cancer Research Center of Toulouse (CRCT, which is a Inserm/CNRS/University Paul Sabatier laboratory), including a total floor space for research team (5200 m²), their administration (800 m²) and many facilities (such as 2700 m² animal facility).

The UCI is connected on site to:

- an interdisciplinary research center dedicated to innovation in biology (Centre P. Potier/ITAV)
- pharmaceutical companies (Sanofi, Pierre Fabre) and biotechs
- a large amount of technological platforms and facilities.

The UCI will also benefit from foundations (RITC/ InNaBioSanté) and a network (Oncomip) to coordinate and improve the efficiency of research exploitation and healthcare practices in Toulouse.

The University of Toulouse, acting on behalf of the co-sponsors of the Oncopole, is inviting applications for the important post of Chief Executive Officer of UCI.

The CEO will run the UCI including the Hospital and the Cancer Research Center of Toulouse. He/she will bring vision and main orientations for research and care. He/she will define in co-development with the main key stakeholders, and his/her team, the medical and scientific project. He/she will then be responsible for the implementation of the project, impacting research works, translational research, therapeutical protocols, technological platforms, innovation transfer, international partnerships... He/she will contribute to develop the UCI in 5 years as one of the most renowned international cancer centers.

Missions:

- Have the responsibility of drawing up the medical and scientific programs, budgets and reports;
- Support the implantation and the development of new clinical and research labs at the UCI (Hospital and CRCT);
- Promote the UCI at the international level;
- Favor the industrial development of UCI findings together with the Oncopole partners (pharmas, Centre Pierre Potier/ITAV, etc.);
- Coordinate the regional clinical strategy in the fields of oncology

He/she chairs a Board, with the Secretary General, the Research Director and the Hospital Director.

He/she must be a MD/PhD in an oncological discipline and have a successful track record in the management of a hospital and/or a translational research lab and/or a health or research organization

The CEO will start his/her mission at the latest on January 1st 2013.

This is a 5 year position with internationally competitive salary.

All applications will be considered by the nominating committee chaired by J. Mendelsohn (Houston).

Candidates should submit their curriculum vitae + letter of application + list of publications + letters of recommendation to the President of University of Toulouse 3, Pr. Gilles FOURTANIER
(iuc.recrutement@univ-tlse3.fr)

W217993R

To advertise here please contact — US tel. +1 800 989 7718, naturejobs@natureny.com or Europe/ROW tel. +44 20 7843 4961, naturejobs@nature.com

POLICY

Europe appoints science adviser

Scottish cell biologist Anne Glover hopes to influence EU policy-making.

BY NATASHA GILBERT IN BRUSSELS

The dearth of independent, sound scientific advice in European policy-making provokes endless complaints from science advocates, who blame it for the continent's wrangling over charged issues such as genetically modified crops and nanotechnology.

They might finally have a saviour, in the person of Anne Glover, a Scottish molecular and cell biologist, who was named last week as Europe's first chief scientific adviser.

More than two years after pledging to create the post, José Manuel Barroso, the president of the European Commission, officially announced Glover's appointment on 5 December. He also outlined her role, ending long-standing speculation about the extent of the job's remit. *Nature* first reported that Glover had won the job on 21 November (see *Nature* http://doi.org/g8k; 2011).

"I have long pressed for the creation of a high-level scientific adviser at the heart of the European Commission, which is key to ensuring that development and implementation of EU policy and legislation are underpinned by a robust evidence base," says John Beddington, the United Kingdom's chief scientific adviser.

Glover, who was not available for interview, spent most of her academic career at the University of Aberdeen, UK, studying microbial diversity and how organisms respond to stress at a cellular level. She has served as chief scientific adviser to Scotland's government since 2006, and will leave the job on 21 December before beginning her new life in Brussels in the new year.

UNIV. ABERDEEN

Anne Glover, Europe's first chief scientific adviser.

Glover will report directly to Barroso, providing him with advice on policy proposals, and guidance on interpreting uncertainty in scientific evidence. She will also have a key role in strategic planning for emergencies — such as the *Escherichia coli* outbreak that swept across Europe this year — and providing updates on scientific advances and novel technologies. Another key role will be to communicate science to the public, particularly the benefits and risks of new technologies.

Glover will have an office in the Berlaymont building in Brussels, where Barroso works, putting her at the heart of European policy-making. Her position will be at a high managerial level in the European Commission, equivalent to a director-general, which other science advisers believe will give her the independence and authority to succeed.

The Bureau of European Policy Advisers will provide Glover with administrative support. But it is still uncertain whether she will have her own team of scientists to support her. Nor is it clear what her relationship will be with other existing Brussels-based commission advisory groups, such as the European Research Area Board — which advises on research policy — and the Joint Research Centre, a collection of seven research institutes carrying out research relevant to policy.

Ultimately, Glover's success will depend on having "direct access to the relevant science policy-makers", says Robert May, a former chief scientific adviser to the UK government. "She must have the authority to speak the truth, never twisting the science to suit political expedience, but also recognize that policy needs will sometimes override what you think as a scientist." ■

POLICY

Rhapsody for Hungarian science

Major reforms and extra funding will help free country's researchers from communist legacy.

BY QUIRIN SCHIERMEIER

With a shake-up of its national academy and a major boost in research funding next year, Hungary hopes to regain its long-lost status as a scientific powerhouse in central Europe.

The Hungarian Academy of Sciences dominates the country's research scene. Like most of its counterparts in the formerly communist countries in central and eastern Europe, it is a cross between a distinguished learned society and an operational research organization, supporting research at universities and employing around 2,800 scientists at 40 research units.

The country has an eminent scientific past, boasting a string of Hungarian-born Nobel prizewinners in the twentieth century. But today its funding and scientific output lag behind those of many other European nations.

"Many of our present institutes have a mundane office air about them when they should be inspiring academic hubs," says József Pálinkás, the academy's president, who has campaigned vigorously for the changes since his re-election in May. "Without more pronounced teamwork and competition we will lose our foothold in the world's scientific community."

At a special general assembly held last week in Budapest, three-quarters of members with voting rights approved a plan to reorganize the academy into ten large multidisciplinary research centres. These will have revised research agendas, modernized management structures and international advisory boards that regularly review operations. Five remaining institutes, including the prestigious Institute of Experimental Medicine in Budapest, will remain separate and keep their existing remits.

Scientists formerly working in isolated institutes will be brought together to pursue more collaborative research at the new centres, which will cover disciplines including photonics and particle physics, astronomy and the Earth sciences, chemistry and materials research,

ecology, energy research, and the humanities. Two vacated buildings will be sold and the revenues invested in improving other institutes. On 19 December, Pálinkás will appoint interim directors of the new centres, before the positions are advertised internationally next year.

During communist times, the institutes were organized along Soviet lines — controlled by an exclusive circle of academicians and funded directly by the state, with no competitive grants or external review of research agendas. The new structure is inspired by Western research organizations such as Germany's Max Planck Society, Pálinkás says, where principal investigators vie for grants in a highly competitive system.

"There are some people here who have a strong dislike of change of any type," says Tamás Vicsek, a biophysicist at the Eötvös Loránd University in Budapest who oversees one of some 140 academy-funded university research groups. "But the new generation of Hungarian scientists is eager to see improvements in how research is operated in this country — and I totally agree with them that this is what we need."

Vicsek, who won a European Research Council advanced grant in 2008 for his work on collective cell motion, says that he is looking forward to collaborating with the academy's multidisciplinary centre for natural sciences, which will be based at his university's campus in a laboratory facility currently under construction. "I'm always in favour of putting biology next to physics," he says. "It's a big improvement and it will certainly facilitate joint research."

Science advocates have also secured the first notable increase in government funding in almost a decade. In 2012, the government will increase its funding to the academy by more than 20%, from Ft35 billion (US$152 million) to Ft43 billion. This includes a more than doubled contribution of Ft2.5 billion for a programme created in 2009 to help young scientists set up independent research groups in Hungary. Because Prime Minister Viktor Orbán is eager to break with the weak institutions of the post-communist era, insiders say that modernization of the academy was a prerequisite for the funding boost.

The extra money will enable the new centres to hire some 200 young group leaders and senior scientists next year, says Pálinkás. Moreover, Ft2.3 billion will be spent on urgently needed research equipment next year, and the budget of the Hungarian Scientific Research Fund, Hungary's main grant-giving agency for basic research, will rise from Ft5.4 billion to around Ft8 billion (see 'Growth spurt').

The changes are set to bring Hungarian science capacity closer to that of neighbouring eastern European Union member states such as Slovenia and the Czech Republic. But to capitalize on the changes, Hungary must also revamp its inefficient patent system and other bureaucratic hurdles to innovation, says Balázs Gulyás, a Hungarian neurobiologist at the Karolinska Institute in Stockholm, who is also executive director of the World Science Forum, a biannual science policy conference held in Budapest. "The academy changes were absolutely necessary, but they are only a first step," Gulyás says. ■

NATURE.COM
For more on the progress of science in eastern Europe see:
go.nature.com/kyvipv

GROWTH SPURT

The Hungarian Scientific Research Fund, the country's main research granting agency, expects a budget increase of more than 40% next year.

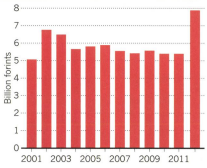

SIGMA-ALDRICH
SIGMA Life Science Where bio begins™

Bioflexible.

Unleash superior performance with custom oligos from Sigma®.

Flexible manufacturing, guaranteed quality and fastest delivery make Sigma Life Science a reliable partner for today's leading researchers. Choose Sigma custom DNA and RNA oligos, and get the performance you need from the name you trust.

sigma.com/oligos

bionucleics

©2011 Sigma-Aldrich Co. LLC. All rights reserved. SIGMA and SIGMA-ALDRICH are trademarks of Sigma-Aldrich Co. LLC, registered in the US and other countries. Where bio begins is a trademark of Sigma-Aldrich Co. LLC.

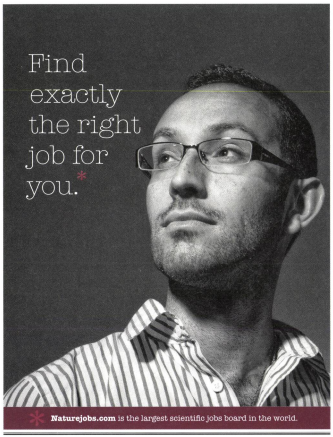

naturejobs

nature publishing group npg

ProMab BIOTECHNOLOGIES, INC.

Custom Recombinant Protein

Transient transfection or stable cell line

HEK293, CHO, Baculovirus
Recombinant antibody, scFv, Fab
0.5 to 500 liters scale

1-866-339-0871

www.ProMab.com info@ProMab.com
5221 Central Avenue, Suite 200, Richmond, CA 94804

The Klein Bottle Opener

Stylish, ergonomic, built to last in stainless steel, it's the perfect touch for any math fan's kitchen. $72 at www.bathsheba.com

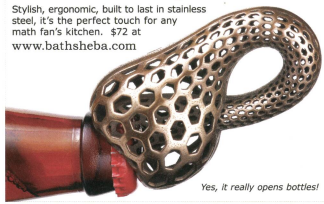

Yes, it really opens bottles!

REDISCOVER *your* nature

timely
convenient
Relevant
TOPICAL.

NEWS FROM *NATURE* IN THE PALM OF YOUR HAND.

Now you can have in-depth analysis of the most important science policy, business, community and breaking news wherever you are. The nature.com Reader apps for iPhone® or iPad® give you free access to all news content from *Nature*.

Download the apps for free – search for 'nature.com' on the App Store.

Apple, the Apple logo, iPhone, iPad and iPod touch are trademarks of Apple Inc., registered in the U.S. and other countries.

Available on the App Store

nature.com/mobileapps

THE LONG SHOT

BY MICHAEL CHERRY

The MeerKAT telescope in South Africa, seen here in an artist's impression, will be a prototype for the vast Square Kilometre Array.

SKA SOUTH AFRICA

The 90-kilometre drive starts in the sheep-ranching town of Carnarvon in western South Africa, and runs northwest through the semi-desert plains of the Karoo, where the only sign of human settlement is an occasional sheep farm. But as the road begins to pass north of the flat hills of the Losberg mountains, it suddenly comes upon seven huge white radio dishes.

This is the Karoo Array Telescope (KAT-7), a government-funded facility sheltered by distance and the Losberg from human-generated radio interference. Commissioned just this year, KAT-7 is both an operational radio telescope and a prototype for the much more ambitious MeerKAT project, a 64-antenna array that will be the largest radio-astronomy facility in the Southern Hemisphere when it is completed at this site in 2018. But KAT-7 also symbolizes an even bigger ambition: South Africa hopes that by 2024, this remote expanse will be the centre of a radio facility spanning the continent.

The Square Kilometre Array (SKA) — named after the total collecting area of its 3,000 or so antennas — would be by far the largest radio telescope ever built (see 'The biggest array'), and would need international funding to cover its estimated US$2.1-billion cost. It would allow astronomers to see how primordial gas formed the first stars and galaxies; how mysterious 'dark energy' has shaped galactic clusters; and how

SOUTH AFRICA IS VYING FIERCELY WITH AUSTRALIA TO HOST A GIANT RADIO TELESCOPE THAT MAY NEVER BE BUILT — BUT THE COMPETITION ITSELF IS CHANGING THE COUNTRY'S SCIENCE LANDSCAPE.

Earth-like planets form around young stars. It might even allow researchers to eavesdrop on the faint radio emissions of extraterrestrial life.

Or maybe not: South Africa's quest faces long odds. The most immediate hurdle is a fierce competition with Australia to host the facility. The two nations submitted their sealed bids in September to the international SKA Program Development Office at the University of Manchester, UK, and a decision is expected by March 2012.

REAL BIG DISH

A more serious question is whether the SKA will be built at all. Getting cash-strapped governments to invest in radio astronomy is a daunting prospect in the current economic climate. And even more daunting is the computational challenge: the number of calculations required to correlate the antennas' radio signals and forge them into a single image increases massively with the number of dishes. The full-scale SKA would need thousands of times more processing power than is currently available in the fastest supercomputers — a big reason why US researchers didn't rank the SKA when drawing up astronomy priorities last year[1].

"It is not clear that the technology for the required correlators is in hand, or even over the horizon," says Adam Burrows, vice-chairman of the US National Research Council's space-studies board. "It just may require another decade to establish a credible financial and technological plan for such a massive undertaking."

But the SKA's proponents in South Africa are undeterred. The act of competing has given the country's astronomy programme a major boost and, they argue, could do the same for science and technology across the board. "By giving the country a major opportunity to raise its level, and to inspire and train a new generation, the SKA could represent a new dawn for science in Africa," says Roy Maartens, a cosmologist at the University of the Western Cape in Cape Town.

The prospect of an astronomy renaissance was a big draw for Bernard Fanaroff, the director of South Africa's SKA effort. A radio astronomer by training, Fanaroff left academia in the 1970s to pursue racial and economic justice in South Africa — first with the country's nascent trade-union movement, and then as a senior civil servant in the reconstruction and development programme of the first post-apartheid government. After leaving government in

the early 2000s, Fanaroff seized on the SKA's potential for inspiration as yet another way to pursue change.

International planning had been under way for a decade by that point. But the country still had a fighting chance. All of the site-selection criteria, starting with the need for a good view of the centre of our Galaxy, favoured the Southern Hemisphere.

Fanaroff soon found an ally in Rob Adam, then director-general of the South Africa Department of Science and Technology. Adam wanted to address the chronic lack of maths and science skills in the black majority of the country's population — a legacy of both apartheid and a stagnant education system. And he believed that high-profile science projects such as the SKA were the best way to excite young people and draw them into research[2].

BIDDING WAR

With Adam's backing, Fanaroff prepared a bid for the SKA and submitted it in 2004. Bids also came in from Australia, China and Argentina. But only when the field was narrowed to South Africa and Australia in 2006 did the race really begin. Ever since, the two countries have chased the SKA with as much fervour as they strive against each other in cricket and rugby.

In 2007, for example, Australia vowed to build the Australian SKA Pathfinder (ASKAP) at its proposed site near Murchison, in the arid west of the country. The 36-dish facility would demonstrate antenna designs and other technologies, and together with associated infrastructure and human-capacity development would cost an estimated US$490 million (ref. 3). In 2008, despite the global recession, South Africa countered with a commitment to its own pathfinder, MeerKAT. (The name refers to *meer*, Afrikaans for 'more,' as well as to a famously photogenic mammal found in the Karoo.)

The $275-million estimated cost of the South African scheme represents the country's largest-ever investment in a pure-science project — and a source of major irritation for researchers in more tightly funded disciplines[4]. But officials say that the project is good for economic development: not only were MeerKAT's antennas designed by Land Systems Dynamics, a subsidiary of British Aerospace Engineering based in Pretoria, but they will be manufactured and assembled mainly in South Africa.

The ruling government, which was elected in 2009, is determined to protect the bid. This year, when oil company Shell applied to drill for natural gas just south of the MeerKAT site, for example, Naledi Pandor, the science and technology minister, made it clear that she would invoke the country's Astronomy Geographic Advantage Act to block interference with the array, whether it came from radio activity or seismic disturbances[5].

Pandor has also moved to resolve a major embarrassment: last year's suspension and subsequent exoneration of Phil Charles, then director of the South African Astronomical Observatory in Cape Town, who had tangled with his bosses in the National Research Foundation for reasons that are still unclear[6]. The incident left many South African astronomers mistrustful of the foundation. In October, Pandor announced that control of the country's astronomical facilities would eventually be taken from the agency and vested in a new organization.

The South African and Australian bids for the SKA are being evaluated this month by a site advisory committee. The committee's recommendation will be sent to the directors of the SKA organization before its final decision.

DOWN TO THE WIRE

It could be a close call. Radio interference is minimal at both sites, and other observing conditions are equivalent, so the SKA directors will have to look at other criteria, such as antenna design. The technical differences boil down to a trade-off, says Tony Foley, head of science operations at MeerKAT. "The Australians can catch a larger patch of sky" at any one time, he says, "whereas we are operating at higher sensitivity" — meaning that the South African antennas will look farther into the Universe with a shorter observation time.

Another factor will be the strength of the host country's astronomy community. Australia has a longer and stronger tradition of radio astronomy, but South Africa has poured money into closing the gap. The country's roster of radio astronomers currently numbers about 65, many of whom have moved from elsewhere during the past decade.

Then there is what some see as the moral imperative. "There is a need for the first world to help the third world build up science," says George Ellis, a cosmologist at the University of Cape Town. "This is an ideal opportunity."

How the international SKA organization will weigh these factors is hard to predict. But astronomy isn't rugby; it could be that both sides will win. In July, recognizing the bleak prospects for international funding and the computational challenges, European astronomers proposed a cheaper alternative: fund modest expansions of both ASKAP and MeerKAT, then combine their signals as if they were a single instrument. The combined array wouldn't have nearly the same sensitivity to very faint signals as the full-scale SKA. But it may well be the most realistic option.

Win, lose or draw, the competition has already given South Africa a symbol of national unity. From government officials to cab drivers, everyone there seems to know about the SKA. The Department of Science and Technology sponsors a monthly performing-arts festival in support of the bid. And South Africa's financial daily, *Business Day*, often runs front-page advertisements sponsored by the SKA project, featuring a full-colour photo of the KAT-7 antennas with the boastful headline: "South Africa is ready to host the SKA." ■

THE BIGGEST ARRAY
South Africa's plan for the Square Kilometre Array (SKA) calls for some 3,000 antennas spaced over half the continent.
The outer antennas will form a rough spiral pattern designed to maximize the fidelity of the array's combined image.
NAMIBIA
SOUTH AFRICA
SKA core site
Cape Town
Most of the antennas would be clustered in the Karoo, around the SKA core, where the prototype KAT-7 is almost complete.

Michael Cherry *is* Nature's *contributing correspondent in South Africa.*

1. *Nature* **466,** 910 (2010).
2. Adam, R. *Nature* **464,** 30 (2010).
3. *Nature* **476,** 241–242 (2011).
4. *Nature* **463,** 726–728 (2010).
5. *Nature* http://www.nature.com/doifinder/10.1038/news.2011.174 (2011).
6. *Nature* http://doi.org/g2k (2010).

The cell division

LIFE & BRAIN CENTER

Oliver Brüstle fought for more than a decade to pursue and patent human embryonic stem-cell research in Germany. Now his efforts have backfired.

BY ALISON ABBOTT

It was overcast and unseasonably sultry in Luxembourg, home to the European Court of Justice, on the morning of 18 October 2011. But German neuroscientist Oliver Brüstle wasn't sweating when the 13 judges entered the court room in their flowing crimson robes. Not, that is, until they delivered their verdict, which spelt the end of his lengthy fight to defend his patent on human embryonic stem (ES) cells from attack by Greenpeace.

It took barely two minutes for the court's president to summarize aloud the four pages of the judgment. The ruling, which cannot be appealed, upheld Greenpeace's position. It declared that any patent depending even indirectly on human ES-cell lines is outlawed on moral grounds throughout the European Union (EU). Unexpectedly, it added that any research using such cell lines was similarly immoral.

For a few moments Brüstle was so shocked he could barely draw breath. Outside, the clouds burst and rain poured down. "What hurt most personally was the accusation that scientists who work on human ES-cell lines are somehow immoral," says Brüstle, who says he never doubted that he would win the case. "But now I accept it's the end of the road."

That road has been a long and twisted one for Brüstle, one of Europe's leading stem-cell researchers, based at the University of Bonn in Germany. Germany is a scientific powerhouse, but it has always been slow to accept any form of new genetic technology. Long before the patent battle, Brüstle was fighting to pursue research using human ES cells — which can differentiate into many types of mature cell — while the German government vacillated about its legitimacy.

The latest dispute centred on the ethics of patenting discoveries that stem from the use of human embryos. Brüstle argued that patenting was crucial because, without it, industry would not be interested in pursuing what he saw as potentially life-saving therapies. And whereas some people charge that patenting could actually impede research, Brüstle argues that patents held by academics are normally free for other researchers to use. Brüstle admits his battles were lonely, and took their toll on him and his family, who at one time even found themselves under police protection. Yet he says that he never once considered pulling out. "I just didn't think it right that an environmental organization, rather than a government, should define research agendas," he says.

Brüstle's single-mindedness is not a reflection of an aggressive personality: his aura is calm, not domineering. "I think he's just been driven — rightly — by strong scientific convictions," says stem-cell biologist Elena Cattaneo at the University of Milan, Italy, who has worked with him as part of scientific networks funded by the European Commission. "Oliver has been an important figure in the ethical debate and he deserves a lot of credit," adds Ronald McKay, a stem-cell researcher at the Lieber Institute for Brain Development in Baltimore, Maryland, and a former mentor of Brüstle's.

The reality, however, is that although those convictions have helped to further human ES-cell work in Germany a little, only a handful of research groups have ever tried to work with such cell lines. And Brüstle's patent fight may now have backfired, because the new ruling could hinder researchers working on human ES cells throughout Europe. By declaring such research to be immoral, many fear, the court ruling could prompt funding agencies to stop funding it — and it certainly means that no patent, foreign or home-grown, that involves human ES cells can be defended in Europe. Even Christoph Then, an equally driven one-man crusader against biopatenting who spearheaded Greenpeace's campaign, expressed surprise at the court's wide-reaching condemnation of human ES-cell research. "I don't think anyone has the moral right to patent any sort of life, so this is a happy victory for us," he says. "But our intention was never to stop basic research in the area."

"It's easy, in hindsight, to question if I was right to take the patent fight so far," Brüstle says now, "and I'm sorry that there has been collateral damage for my colleagues in other countries." But, he adds, he would do exactly the same if he had his time again.

NATURE.COM
To listen to *Nature*'s podcast on the patent debate, visit:
go.nature.com/hx7pmt

PLANBROCZENIT/GREENPEACE

After Oliver Brüstle was granted a patent for his work on human embryonic stem cells, Greenpeace pushed to 'stop the patenting of life'.

"No one could have predicted that what started with a goal to have more liberal rules in Germany would have made Europe ultra-restrictive."

As a medical student at the University of Ulm in southern Germany, Brüstle fell in love with the brain. He set a career trajectory to become a neurosurgeon, but in the early months of his residency at the University of Erlangen, he felt the irresistible draw of research. "I wanted to do more than just remove brain tumours," he says. "I wanted to find out how brain disease could be avoided."

He interrupted his residency in 1993 for a research break in McKay's lab at the National Institute for Neurological Disorders and Stroke in Bethesda, Maryland. There he studied how human fetal brain cells behaved after they were grafted into the brains of embryonic rats[1]. "We joked in the lab that we wanted to see if it would be the American way of adapting to a new environment or the European way of not adapting," he recalls. The cells adapted.

When, in the mid-1990s, several research groups developed procedures for turning mouse ES cells into heart cells using a cocktail of growth factors, Brüstle adapted the method to generate neural cells[2]. "Suddenly, stem-cell biology was at a point where reconstructive therapy was not just a pipe dream," he says. Brüstle wanted to be part of the global research effort that would realize it.

Like his stem cells, Brüstle had adapted well to his new home, but he began thinking about returning to Germany to establish an independent scientific career. He was drawn by the newly dynamized research environment, where scientists were being strongly encouraged by universities and the government to think about how their basic research could be commercialized or otherwise put to use for the public good. Patenting in particular was being encouraged. "Newspaper articles had been saying that German scientists were too stupid to patent, unlike American scientists who were helping the US economy — it was a constant lament," Brüstle recalls.

He returned to Bonn in September 1997, and shortly thereafter submitted his fateful patent on procedures for generating neural precursors from ES cells to the German Patent Office. It was based on his mouse work, but its claims covered most species, including primates, both non-human and human. He thought that a method to derive endless neural precursors would be bound to prove useful in medicine. "I wasn't thinking in concrete terms about commercialization," he says. "I just had an idea that a company might want to license it at some point and that would help translation to the clinic." The patent was granted in 1999.

The year before, James Thomson, then at the University of Wisconsin–Madison, reported his team's success in generating the first stem-cell lines from human embryos[3]. Like many scientists, Brüstle was keen to get hold of the cell lines and translate his animal work to humans. Knowing that Thomson had been swamped with requests for collaboration, he simply booked a flight to Madison. "I told Jamie I would just stay in the hotel until he had time to meet me and talk about research we could do together." They met, and hatched a plan to work together on ways to generate neural precursor cells from Thomson's new cell lines.

For Brüstle, this decision also marked the start of his fight for acceptance of human ES-cell work in Germany. He put together a grant application to work on the methods he had devised with Thomson, and in August 2000 submitted it to the DFG, Germany's main university granting agency. "I had a gut feeling though that its passage may not be smooth," says Brüstle. "It just wasn't clear whether the DFG would be allowed to fund such work." The country's 1990 Embryo Protection Act forbids research on human embryos but does not refer to research on established ES-cell lines, which didn't exist when it was written. In 1999, the DFG stated that a 'societal debate' was needed on the issue and in the meantime it would fund just adult stem-cell research. Brüstle's application was a direct challenge to this stance.

Brüstle, who is a practising Catholic, had thought hard about his own moral position. He disagrees with the creation of human embryos specifically for research. But almost all human ES-cell lines have been derived from embryos leftover from fertility treatment that would otherwise

have been destroyed. Brüstle maintains that using them for biomedical research rather than discarding them is the moral imperative.

Ernst-Ludwig Winnacker, a biochemist and then-president of the DFG, decided that Brüstle's application should be peer reviewed. It was highly rated. In May 2001, the DFG opined that human ES-cell research on imported cell lines was legal, morally justified and scientifically necessary. It was ready to fund Brüstle. This was a point of explosion.

Within days the government intervened, asking the DFG to defer giving Brüstle his grant to allow more societal debate. That debate, which grew progressively hotter, took the form of local and national panel discussions, newspaper articles and parliamentary hearings. Some sections of the media, the churches and other groups attacked Brüstle — and, in turn, Brüstle appeared in newspapers and television shows to state his case. His four children had to deal with remarks from schoolmates. "It was a very stressful time," he says.

Elsewhere, other countries were devising their own solutions, amid similarly polarized debates. Some conservative governments, such as Ireland's, do not allow any human ES-cell research. Bolder ones have been more permissive: in the United Kingdom, for example, the government decided to allow new human ES-cell lines to be derived from spare embryos, and in some cases to allow human embryos to be created for research purposes. In the end, the German government fudged the decision. On 30 January 2002, it passed a law that forbade projects involving newly derived lines but allowed research on cell lines that existed before a specific date. That same year, Brüstle finally got his grant.

"HOW CAN A EUROPEAN COURT RULE IMMORAL WHAT NATIONAL GOVERNMENTS HAVE ALLOWED?"

MORAL CHALLENGES

The small victory didn't stop the debate. Some groups argued vehemently that the use of any human ES-cell lines was wrong. Brüstle became such a target of vitriol that undercover police officers had to mingle with the audience at his talks.

Given the climate, Brüstle was not particularly surprised when Greenpeace challenged his patent in 2005. The organization invoked the 'ordre public' clause in the EU's Directive on the Legal Protection of Biotechnological Inventions, to which all national patent law must defer. The directive states that inventions whose commercial use could lead to a breach of morality cannot be patented, and uses the commercialization of the human embryo as an example.

A year later, Brüstle arrived at the Federal Patent Court in Munich in an armoured limousine with three police escorts. The judge found in favour of Greenpeace and ordered claims for human ES-cell lines to be removed from his patent. Still, Brüstle was certain that he would be able to overturn the decision on appeal.

What actually ensued, however, was a series of court setbacks and delays. When the Federal Patent Court ruled against Brüstle on appeal, he took the case to the country's Supreme Court. At a hearing in November 2009, the Supreme Court seemed to accept Brüstle's arguments, but, before making its final ruling, decided to refer the case to the European Court of Justice to clarify ambiguous points of patent law regarding the definition and potential commercial use of human embryos and stem cells derived from them. At that stage, even Greenpeace's Christoph Then told the press that he thought his case was lost.

It wasn't. In March 2011, Judge Yves Bot, who was responsible for working the case, delivered his preliminary opinion for the European court. He argued that an invention that had involved destruction of an embryo would be immoral.

Brüstle was still confident that the Grand Chamber, which comprises all 13 judges, would rule the other way. He had read the statements provided by the European Commission and many of the EU member states. None of them — even from the most conservative of countries — asked for patents based on human ES-cell lines to be outlawed.

When the Grand Chamber ruled in October, however, there was no place for more optimism. The judges took the preliminary ruling further, making it clear that even inventions that indirectly involved destruction of an embryo were immoral and could not be patented. Brüstle walked from the courtroom into a swarm of journalists, and spent the next five hours telling them why he thought the judgment was wrong. "How can a European court rule immoral what national governments have allowed and which national research agencies have funded?" He then drove the two hours home, he says, "too exhausted to feel anything".

Elsewhere, the response to the ruling was muted. German scientific organizations remained silent — although they eventually published a joint statement condemning the judgment on 7 December. "I was quite shocked that no one spoke up after the judgment," says Winnacker, who is now head of the international Human Frontier Science Programme based in Strasbourg, France.

A handful of patent lawyers, companies and scientists in other countries pronounced that patents were not so important anyway and that clarity in the matter has its own advantages. "Industry also wanted clarity, even if that result was tough," says Johan Hyllner, chief executive of Cellartis in Gothenburg, Sweden, which derives cell lines from human ES-cell lines for drug discovery. "Now we know how to proceed and we can always choose to keep trade secrets instead of patenting."

But Brüstle and some other stem-cell scientists and legal experts view those pronouncements as an effort to play down the damage. "Many were afraid that investors or funding agencies would pull out of the area," says stem-cell researcher Christine Mummery at Leiden University Medical Centre in the Netherlands.

Since the ruling, scientists and funding agencies across Europe have been trying to analyse its impact. If academic scientists using human ES cells want to found a biotechnology start-up company, they'll now find it hard, admits Hyllner. "Venture capitalists like to see a strong patent portfolio, and this won't be possible in Europe now." And there are hints that research organizations are getting cold feet about funding the work. On 23 November, the European Parliament's official cross-party working group on bioethics urged zero funding of human ES-cell work in the next multi-billion-euro EU framework research programme, Horizon 2020, on the grounds that the work is now legally challengeable. But a week later, Europe's research commissioner Máire Geoghegan-Quinn said that she wanted to continue funding such research. Scientists expect a fight to ensue.

Through all this, Brüstle says that colleagues using human ES cells have been supportive. No one has publicly expressed regret that Brüstle pushed his case so far.

Brüstle is taking a break from battle, however. Methods for reprogramming adult cells to make stem cells capable of differentiating into many cell types look encouraging, he says, and his own lab now spends 80% of its time in this area. Last month, he published a paper[4] showing how his team reprogrammed skin cells taken from patients with Machado–Joseph disease into such 'induced pluripotent' stem cells, work that helps explain how the rare disorder attacks neurons. "But we don't yet know if those induced pluripotent cells will work as well — we still need to use human ES cells in research," he says.

On reflection, Brüstle says, the thing he just can't understand is that the tough decision on human ES-cell research and patenting has not been made through reasoned debate by law- and policy-makers, as it has in many other countries. "It's been made instead by a struggle between a single researcher and an environmental organization: was that quite right?" ■ SEE EDITORIAL P. 291

Alison Abbott *is* Nature's *senior European correspondent.*

1. Brüstle, O. *et al. Nature Biotechnol.* **16,** 1040–1044 (1998).
2. Brüstle, O. *et al. Science* **285,** 754–756 (1999).
3. Thomson, J. A. *et al. Science* **282,** 1145–1147 (1998).
4. Koch, P. *et al. Nature* http://dx.doi.org/10.1038/nature10671 (2011).

COMMENT

PHYSICS Large science facilities should shrink their electricity load **p.315**

MOLECULAR BIOLOGY The field's covert origins in a Berlin apartment **p.317**

EXHIBITION Mathematics meets theatrical effects in a Paris show **p.320**

OBITUARY Har Gobind Khorana rose from humble origins to fathom the genetic code **p.322**

ARTWORK BUF

DIGITALGLOBE/GETTY

Exactly how much damage the Fukushima Daiichi nuclear plant sustained as a result of the 11 March earthquake and tsunami remains to be determined.

Nationalize the Fukushima Daiichi atomic plant

Only by bringing the nuclear power station into government hands can scientists find out what really happened, say **Tomoyuki Taira** and **Yukio Hatoyama**.

Events at the Fukushima Daiichi nuclear plant following the 11 March 2011 earthquake and tsunami are of crucial importance for the future of atomic energy — in Japan and globally. To respond adequately to the accident, we have to know precisely what happened then and what is continuing to happen now.

To establish the facts, all the evidence and counter-evidence for what might have taken place must be gathered and made public. Only then will the world be able to have faith in the containment plan developed by the Tokyo Electric Power Company (TEPCO), or be able to judge how it should be modified.

Particularly important is finding out whether the 'worst-case' scenario occurred: that is, whether self-sustaining nuclear reactions were re-ignited in the core ('re-criticality'), creating more fission products and heat damage; whether the explosions that rocked the plant days after the earthquake were nuclear in origin, releasing radioactive metals from damaged fuel rods; and whether molten fuel has broken through the reactor's base, threatening environmental contamination.

➲ NATURE.COM
For more on Fukushima, see:
go.nature.com/ulsz2n

A group of representatives from the Japanese Diet (called the 'B-team'; in relation to the government's 'A-team') was formed on 24 March to develop a response plan for the worst-case scenario. Set up by one of us (Y.H., former prime minister) and including us both, the B-team's other members are Yukihisa Fujita (now a senior vice-minister of finance) and Hiroshi Kawauchi (now chairman of the Deliberative Council on ▶

▶ Political Ethics). The team's recommendations — to be released in a future report — will be independent from those of Japan's government, the Nuclear and Industrial Safety Agency (NISA) and TEPCO.

Our investigation has already shown that key pieces of evidence remain incomplete. We do not yet know whether the worst-case scenario happened. To find out, we believe that independent scientists must be given access to the nuclear plant, and that the plant should be brought into national ownership.

RE-CRITICALITY

If nuclear reactions are ongoing within the core, they will continue to create fission products, and the heat generated is likely to damage the cooling and decontamination systems. Proof that re-criticality has occurred hinges on the detection of certain isotopes. The radionuclide chlorine-38, for example, has a short half-life of about 37 minutes and can be generated only if neutrons are available. Its presence would therefore indicate current nuclear activity.

Reports of such a detection have been mixed. On 26 March, NISA reported that TEPCO had found ^{38}Cl in a water sample drawn two days earlier, after sea water (which includes sodium chloride) had been injected into the basement of unit 1. On 1 April, NISA questioned TEPCO's analysis, and said that radioactive sodium-24 should also have been present in the sample. However, some scientists claim that ^{38}Cl can be detected even if ^{24}Na is not. On 20 April, TEPCO negated its earlier report, asserting that ^{38}Cl was not seen in the sea water, and neither was ^{24}Na. It did not, however, publish the data from its analysis. Through NISA, we obtained and reanalysed TEPCO's data, which were measured with a germanium semiconductor detector. We concluded that ^{38}Cl was indeed present, and at a level close to that initially reported (1.6 million becquerels per millilitre). In our view, NISA's and TEPCO's questioning of this detection were therefore unfounded.

Another indicator is xenon-135, which is made when uranium or plutonium undergoes fission; it has a half-life of 9 hours. On 1 November, TEPCO detected ^{135}Xe in unit 2. But, because the concentration was low, NISA concluded that the nuclide could have been produced by spontaneous fission of the dormant fuel, so was not necessarily caused by continuing nuclear reactions. The evidence for re-criticality is therefore still inconclusive.

NUCLEAR EXPLOSIONS

Another question that must be answered is what caused the explosions at the site. They were initially reported as being caused by the ignition of hydrogen generated by a high-temperature chemical reaction between the alloy covering the fuel rods and the vapour in the core. But, again, this has not been settled. Other possibilities include a nuclear explosion, or the ignition of other gases.

Knowing whether a nuclear explosion took place is essential for predicting how much radioactivity might have been released, what it would have consisted of and how far it would have spread, as well as the state of the spent-fuel rods stored in a pool in unit 3. Two observations suggest that this is plausible. First, some metals heavier than uranium have been detected tens of kilometres from the plant. Second, the steel frame on top of the unit-3 reactor building is twisted, apparently as a result of melting.

Japan's Ministry of Education, Culture, Sports, Science and Technology (MEXT) reported finding heavy metals such as curium-242 up to 3 kilometres from the reactor site and plutonium-238 up to 45 kilometres away. These isotopes are deadly poisons if ingested, causing internal exposure to radiation. Because ^{242}Cm has a short half-life (about 163 days), and because the concentrations of ^{238}Pu around the plant were much higher than usual, MEXT concluded that these radionuclides were not fallout from past nuclear tests in the atmosphere, so must have come from the Fukushima reactor. If so, they suggest that broken spent-fuel rods might be scattered around the site — a considerable hazard.

Such elements are too heavy to have been borne in a plume, like the lighter caesium and iodine, so they must have been blown out with great force. Whether a hydrogen explosion would have been powerful enough to scatter heavy metals that far remains unclear. And a hydrogen explosion should not have generated enough heat to melt steel. Initially, TEPCO claimed that the explosion in unit 3 generated white smoke; on re-examination, the smoke was black, and therefore unlikely to have been caused by a pure hydrogen explosion. So a nuclear explosion is a possibility. Whether other explosive gases were present on the site would be equally important to establish.

"Solutions for the Fukushima nuclear disaster must be based on the worst-case scenario."

MELT DOWN

Similarly unconfirmed is how much of the concrete base of the reactor has been breached by molten fuel. This is important because TEPCO plans to fill in the core with water to absorb the radioactivity while it extracts the fuel. If the concrete below the reactor is cracked, then radioactive materials could leak into the groundwater.

Until recently, the government did not believe that this was the case. In a 7 June report to the International Atomic Energy Agency, it reported that most of the melted fuels are being cooled in the lower portion of the reactor pressure vessel and that little fuel is thought to have leaked out into the preliminary containment vessel.

However, two weeks ago, TEPCO admitted that molten fuel may have eaten through three-quarters of the concrete under unit 1, and damaged the bases of two of the other reactors. But again, caution is required. No one has actually looked at the fuel inside the reactor core. So the extent of the leakage is yet to be established.

NATIONALIZE AND INTERVENE

Solutions for the Fukushima nuclear disaster — from how to lock up radioactive contamination for half a century to how to discard the reactor core and the molten fuel — must be based on the worst-case scenario, even if the people most involved remain optimistic that this wasn't the case. Although many facts remain to be established, in our view, two things must be done.

First, the Fukushima Daiichi nuclear power plant must be nationalized so that information can be gathered openly. Even the most troubling facts should be released to the public. Nationalization is inevitable, moreover, because the government is obliged to investigate and provide compensation for the disaster.

As an illustration of how information about the accident is being restricted, our committee struggled to obtain even a manual for the plant when we requested it in August. Initially, TEPCO refused to supply it. When a copy was eventually sent to us, a month later, many passages (including key temperatures and emergency procedures) had been blacked out. TEPCO said that it considered those parts to be its intellectual property and of possible security concern. Only after six months did TEPCO release the full manual to us. It was important that we saw the manual to learn why the company had switched part of the emergency core-cooling system off and on again after the earthquake (and before the tsunami) — to find out when the emergency systems were destroyed.

Second, a special science council should be created to help scientists from various disciplines to work together on the analyses. That should help to overcome the dangerous optimism of some of the engineers who work within the nuclear industry. Through such a council, the technologies needed for decommissioning and decontamination and for construction of a deep geological repository for radioactive waste can be developed, even for a worst-case scenario. ■ SEE EDITORIAL P. 291

Tomoyuki Taira *and* **Yukio Hatoyama** *are members of the House of Representatives in the Japanese Diet.* **Y.H.** *was also prime minister of Japan from 2009 until 2010. e-mails: g11426@shugiin.go.jp; g03629@shugiin.go.jp*

The European Spallation Source, to be built in Sweden, will be powered entirely by renewable energy.

Cutting science's electricity bill

Large-scale research facilities need to reduce their energy consumption and begin moving towards sustainability, says **Thomas Parker**.

Major research facilities such as accelerators and reactors each consume roughly as much electricity as a small town — hundreds of gigawatt hours (GWh) of energy per year or more (see 'Annual energy expenditure'). International and national labs use a total of roughly 3 terawatt hours per year in Europe and 4 terawatt hours (TWh) in the United States, adding up to about the energy consumption of countries such as Estonia or Ghana. This energy use is perhaps these facilities' greatest environmental impact, greater even than the radioactive waste that many produce. Radioactivity can be contained and handled safely; climate change cannot.

The European Spallation Source (ESS) — a neutron source to be built in Lund, Sweden, by 2019, for which I am the energy manager — aims to be the first sustainable such facility. We will use only renewable energy sources to power the accelerator and the lab. We will limit our energy use: so far in the design process we have reduced our energy requirements by more than 20%. And 70% of the energy that we consume will be recovered as usable heat.

Many of the specific solutions that we are adopting at the ESS rely on local conditions, including a liberalized energy market, a well-developed district heating system, a relatively cool climate and public and political support. But the project stands as proof of principle that big science can be sustainable science, and it challenges other facilities to live up to the same standards.

USE IT, DON'T LOSE IT

One area in which there is obvious room for improvement at big labs is the use of waste heat from lab equipment. Water at 40 °C can easily supply buildings with under-floor heating or thermal ventilation, if the right systems are in place. Waste heat of 75 °C can even be used to run cooling air conditioners. But most labs intentionally destroy this resource.

Conventionally, equipment ranging from accelerators to manufacturing machinery is cooled to run at 40 °C or lower. This is in part because early electronics operated best at lukewarm or cool temperatures, and in part to avoid harming aquatic life when the cooling water from hotter systems is discharged into natural systems such as rivers. This target has become so firmly entrenched that manufacturers were surprised two years ago when we began asking them if their modern equipment would work efficiently at higher temperatures. No one else had asked.

It turns out that many modern systems can work at much higher temperatures, allowing the heat to be saved for reuse, with or without conversion to electrical power, rather than being extracted by a heat pump, dissipated in expensive cooling towers, or dumped into the air or water. Sometimes this requires small modifications, such as using sturdier components, or adding adaptable cooling systems that can handle variable heat loads and deal with rare instances of overheating. At the ESS, we are working to design power systems for our accelerators and helium compressors for our cryogenics that can operate at 75–100 °C. One of the challenges is finding the room for extra sets of pipes: some parts of the facility will still need to be cooled to 40 °C for proper operation, so we need parallel cooling systems for parts that are cooled to different temperatures.

Few places recycle their heat. Instead, they burn fossil fuels to meet their heating and cooling needs. For example, CERN, the European high-energy physics laboratory near Geneva, generates waste heat at 40 °C before disposal. This could be used for heating, but its current system uses pressurized 120 °C water instead. Changing CERN's entire heating system retrospectively might be too costly, but new buildings could be

designed to use the 40 °C heat. Likewise, the spallation neutron source at Oak Ridge National Laboratory in Tennessee cools its equipment to about 30 °C using a cooling tower, and then uses gas-fired boilers to heat its building, with no connection between the two systems.

Rather than dumping its leftover heat into cooling towers, the ESS will plug in to the city of Lund's district heating system, which operates a network of hot-water pipes under the entire city and a neighbouring community 20 kilometres away — showing that long distances between the producers and users of heat energy aren't necessarily a problem. We estimate that the ESS will produce about 180 GWh of heat per year, of which about half will be of a suitable temperature to go straight into the district heating system; much of the rest will be warmed electrically so that it doesn't go to waste.

A handful of facilities are taking similar steps. The ESS has a neighbouring synchrotron light facility, Max IV, currently under construction, which plans to cool some of its waste streams only to 75 °C or higher, again to feed into Lund's district heating system. On the other side of the world, a team at the TRIUMF particle accelerator at the University of British Columbia in Vancouver, Canada, is investigating whether it can use its waste heat to warm residential buildings on campus.

REDUNDANT SYSTEMS

TRIUMF demonstrates the problems that such systems can face. The plumbing and heat pumps needed can be costly. And because the surrounding communities don't need heating during summer, a lab such as TRIUMF will have to install back-up cooling devices. In Lund this won't be a problem: the district heating system is being extended, so there will always be sufficient demand for hot water to use up the ESS's waste heat. Conversely, a lab might not provide heat when the community needs it, again requiring a back-up system. If redundant systems are needed on both sides, then there are no savings in investment costs, although there may still be benefits for operating costs.

It is better to be energy efficient in the first place than to recycle: an industry rule of thumb is that electricity is about 2.5 times more valuable than high-grade heat.

Research facilities by their very nature are often pushing the limits of technology and science: cooling to temperatures near absolute zero, for example, or accelerating to near light-speed. Some of these processes are staggeringly inefficient in terms of energy use. Supercooling, for example, uses about 1,000 kWh of energy for every 1 kWh of heat energy that it removes from a system, as it fights to get to ultracold temperatures.

Many labs, including the ESS and CERN, have ongoing projects to improve the efficiency of cryogenics and accelerator power systems, to name two examples. Radio-frequency accelerator power systems have to be tuned to the right frequency for a given beamline, and while that is happening, the electrical energy needs to be diverted. Often it is used to heat water, but it would be more efficient to divert the electricity to somewhere it is needed. CERN in particular is looking into this now.

The ESS has so far managed to reduce its power requirements by 22% in the design update. Nearly two-thirds of this was achieved by using superconductivity in the accelerator power system, which eliminates losses to electrical resistance. Achieving superconductivity requires cooling the equipment to close to absolute zero, with all the inefficiencies that entails. Despite this, there is still a net efficiency gain.

The ESS will build its own renewable-energy-generating facilities to cover all its power needs. This makes the lab more sustainable and hedges against future energy-price volatility. The exact power systems have yet to be decided, although wind power seems the most economical resource in this region. Part of the plan is to have some demonstration plants on site showcasing innovative energy technologies to the public.

There is a funding problem for big facilities that tends to perpetuate energy wastage: facility budgets for initial infrastructure and for ongoing operations often come from different purses, making it hard to justify an initial investment in energy-efficient systems in exchange for long-term savings. The governing bodies of such facilities need to be aware of this issue, and remember that there is more than cash at stake.

In the United States, the national labs are obliged to reduce their emissions to 28% of 2008 levels by 2020. The plans in place to achieve this goal mostly involve increasing energy efficiency or relying on renewables — heat recycling is not mentioned in the Department of Energy's Strategic Sustainability Performance Plan. Ongoing projects include biomass heat and energy co-generation at Savannah River, and biomass steam generation at Oak Ridge.

PRACTICAL VISIONARIES

At a workshop in Lund this October on energy management for large-scale research infrastructures, initiated in part by myself and co-hosted by the ESS, CERN and the European Research Forum (the organization of national laboratories in Europe), it was clear that although many heads of national labs are in favour of greening their facilities, most are in only the earliest stages of changing operations.

Some larger projects should serve as an inspiration. The DESERTEC project, for example, promotes the construction of solar power plants and wind parks in north Africa, along with transmission lines to high-usage areas in southern Europe. As part of the programme, African nations that supplied facilities with renewable resources would also be given a say in the running of these projects. This promotes not just energy sustainability, but also intellectual sustainability in emerging economies. At our meeting, Helmut Dosch, chair of the board of directors of the German accelerator complex DESY, made an impassioned call for national labs to get involved in making this programme a reality. There is a place for both visionary leadership and practical groundwork.

As the public and its representatives become increasingly aware of the need for energy efficiency, the argument for energy-intensive research becomes weaker. Big science needs to do some housekeeping. The scientists who work at these facilities, perhaps contrary to popular perception, are people with ethical concerns about the environment. They need to translate those concerns into action. ■

Thomas Parker *is the energy manager of the European Spallation Source.*
e-mail: thomas.parker@esss.se

ANNUAL ENERGY EXPENDITURE

Large physics facilities, such as CERN, use as much energy as a small town every year. Smaller ones, such as the European Spallation Source (ESS), also consume lots of electricity. All would benefit from going green.

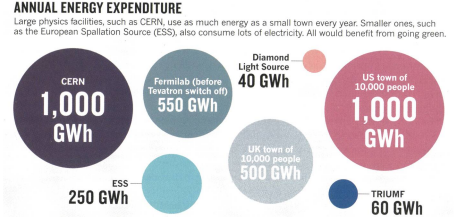

KEYSTONE-FRANCE/GAMMA-KEYSTONE/GETTY IMAGES; SCIENCE PHOTO LIBRARY; AP PHOTO/ITAR-TASS

Molecular-genetics pioneers Nikolai Timoféeff-Ressovsky, Max Delbrück and Karl Zimmer.

MOLECULAR BIOLOGY

Seed of revolution

Michael A. Goldman hails the first English translation of the three-man paper that launched molecular biology.

The spectacular achievements in our understanding of the human genome are the outcome of an era of molecular biology that dates back to the 1930s. The seed was a 1935 collaboration in Germany between a theoretical physicist, a radiation physicist and a *Drosophila* geneticist — Max Delbrück, Karl Zimmer and Nikolai Timoféeff-Ressovsky, respectively. Their 'three-man paper', which sets out the interdisciplinary basis for studying the molecular nature of the gene, was revolutionary.

But this revolution burned with a slow fuse. The paper, 'On the nature of gene mutation and gene structure' was published in an obscure journal at the University of Göttingen. The manuscript had little influence until physicist Erwin Schrödinger drew heavily on it for his popular lectures, collected in his book *What Is Life?* published in 1944.

More than 75 years after it first appeared, the groundbreaking paper appears in English for the first time in *Creating a Physical Biology*. Edited by philosophers of science Phillip Sloan and Brandon Fogel, the volume also contains commentary by historians and philosophers of biology on the paper's genesis and place in history.

As Sloan and Fogel point out, the detail of the three-man paper's findings no longer holds up. But, written at a time when DNA's role in the transmission of genetic information was not understood, the paper clearly established genes as an entity that could be studied using the rigorous methods of physical science. This molecular approach to genetics would lead to the sequencing of the human genome.

NATURE.COM
For more on early molecular genetics:
go.nature.com/qdiiby

The three authors combined their understanding of X-rays and mutation into a coherent picture of the gene. They recognized its molecular basis, stating "we view the gene as an assemblage of atoms within which a mutation can proceed as a rearrangement of atoms or dissociation of bonds".

These ideas emerged as Nazism was rising in Germany; the Jewish scientific community lived in fear of academic purges. Many key meetings between physicists and biologists took place not at universities but at Delbrück's house in Grunewald and Timoféeff-Ressovsky's apartment in Berlin. Such covert encounters had a pressure-cooker effect.

Meanwhile, quantum ideas were permeating the physical sciences, and Danish physicist Niels Bohr's interpretation of them had taken Copenhagen by storm. Bohr's 1932 lecture 'Light and life' probably prompted Delbrück, who studied theoretical physics under him, to turn to biology.

Creating a Physical Biology: The Three-Man Paper and Early Molecular Biology
EDITED BY PHILLIP R. SLOAN AND BRANDON FOGEL
Univ. Chicago Press: 2011. 320 pp. $35

Bohr thought that the wave–particle duality of light was part of a general principle of complementarity in physics, in which two phenomena arising from different experimental conditions, or parallel explanations, are needed for understanding. He felt biology was the same, sensing that the vitalistic aspect of life and its physical and chemical aspect are both key to comprehending the whole.

Delbrück took this one step farther in his search for biological complementarity — something beyond reductionism that molecular genetics could not explain. Paradoxically, he sought it by hammering away at gene replication, one of the most reductionist paradigms ever to hit mainstream biology. When it looked like everything in genetics was going to yield to physical explanation, he moved on to different turf: more complex physiological networks. His hopes for complementarity were dashed, yet his work drew the attention of dozens of physicists to the new biology.

The paper's logic and thoroughness cannot hide the (still unresolved) struggle to understand the complex nature of life. The authors stuck to genetics to avoid "methodologically questionable conclusions" from fields such as developmental physiology. They recognized that the mapping of genotype to phenotype was tenuous, a gap that has yet to be closed.

The contemporary contributions to *Creating a Physical Biology* smack of historians and philosophers of science talking to one another, and for the most part agreeing. Gino Segre's *Ordinary Geniuses* (Viking, 2011), among other books, gives more of scientists' perception of the science of the times.

Sloan and Fogel argue that Schrödinger's *What Is Life?* misrepresents the three-man paper. They note, for instance, that he misleads by saying that quantum mechanics makes possible "a complete reduction of biological to physical systems", which the paper never claims. Schrödinger also ignores its reservations about mapping genotype to phenotype. But there is little evidence that he intended to provide an authentic account.

Most scientists I asked, young and old, knew of Delbrück's role in the origins of physical biology. Not one had heard of the three-man paper. Yet the work anticipates some of today's cutting-edge science.

Interdisciplinary research remains tenuous. Delbrück wrote to Bohr that biologists have difficulty understanding "a new subtle thought". Such attitudes between disciplines have barely altered. But there is still that edge between known and unknown, the still-elusive theory of everything, and still time for paradigm shifts. This intriguing book gives us insight into how such shifts may happen. ■

Michael A. Goldman *is a geneticist at San Francisco State University, California 94132, USA. e-mail: goldman@sfsu.edu*

PHILOSOPHY

Life emergent

Evan Thompson weighs up a treatise that explores the dynamics of matter and consciousness.

How is mind — cognition and consciousness — related to biological life? Current thinking in cognitive science suggests that living and cognitive systems share basic organizational properties, such as being autonomous or self-producing and self-sustaining. Anthropologist Terrence Deacon's *Incomplete Nature* is a welcome contribution to this field.

Deacon draws on thermodynamics, complex-systems theory and biology to show how we can understand the characteristics of mind in relation to life, and those of life in relation to inanimate matter, without losing sight of their continuity. He plots the ways in which non-living physical systems can self-organize and evolve into living systems, and how living systems can evolve into cognitive systems.

Deacon takes his guiding idea from one of my favourite chapters of a classic Chinese philosophical text from the fourth century BC, the *Tao Te Ching*: "Pots are fashioned from clay/But it's the hollow that makes a pot work." Similarly, Deacon sees the 'constitutive absence' as functional, a defining property of life and mind. Living things are dynamically organized around ends, such as finding nourishment; and minds are dynamically organized around meanings, such as anticipated future events. And like the hollowed interior of the pot, these ends and meanings are both functional and absent, in the sense that they affect a system's behaviour, yet are not material parts of it.

This idea leads Deacon to offer a new twist on theories of how inanimate matter can self-organize and evolve to become living, and how living systems can evolve to become cognitive. To reflect absence, he introduces the concept of constraints in a dynamical system. For example, water molecules heated in a pan organize into rotating convection cells, with their motions constrained by the geometry of the cells. In this system, absence is the variety of alternative paths the water molecules could have taken. Yet the system, Deacon says, depends on their absence.

Applying this idea to the emergence of life, Deacon considers autocatalytic molecules. These copy themselves by catalysing their own production, and can collectively build systems that evolve to have a metabolism and reproduce. In Deacon's version, autocatalytic molecules manufacture by-products that self-assemble into a container that then houses those reactions. Again, the absence on which the system depends is the other ways in which the molecules could have been distributed.

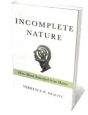

Incomplete Nature: How Mind Emerged from Matter
TERRENCE W. DEACON
W. W. Norton: 2011. 624 pp. $29.95, £19.99

Such self-generating systems, for Deacon, already have a minimal kind of self. Multicellular organisms have a more complex bodily self than these systems, and animals with brains have a cognitive self because the brain must constantly represent its own ongoing activity in relation to the body and to the outside world. As Deacon unfolds this narrative, he provides perceptive accounts of key notions, such as information and emergence — how complex systems arise from many comparatively simple interactions.

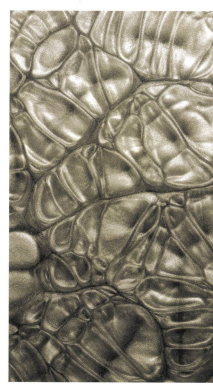

The geometry of convection cells in heated liquid.

But *Incomplete Nature* has shortcomings. Deacon doesn't discuss other theorists who have given similar accounts of life and mind, such as Alicia Juarrero in *Dynamics in Action* (MIT Press, 2002) or myself in *Mind in Life* (Harvard University Press, 2007). He also sometimes overemphasizes the differences between his views and those of the theorists he does cite.

Deacon stumbles at two crucial junctures — his explanations for the emergence of meaning and for the emergence of consciousness. The problem of meaning is the problem of how it is possible for certain physical phenomena, such as brain states, to have content or to be 'about' something beyond themselves.

Deacon's answer is not easy to decipher. Roughly, he seems to be saying that certain states of a self-generating system acquire content when they correlate reliably with features of the environment that are useful to that system. For example, a system that needs molecules from the environment in order to reproduce 'interprets' the presence of these molecules as meaning that the environment is conducive to reproduction. But this seems little more than metaphorical. As many philosophers have shown, meaning cannot be reduced to such processes.

With consciousness, Deacon says that sentience — the capacity to feel — arises from a system being self-sustaining and goal-directed. So he sees individual cells as sentient. But, as he explains, an animal's sentience is not the sum of the sentience of its individual cells: the nervous system creates its own sentience at the level of the whole animal. Yet Deacon doesn't get to grips with the hard problem of explaining why and how we and other animals have conscious experience.

Simply pointing to the neural activity associated with sentience is not enough to answer this question. What we need to know is why this activity feels pleasant or painful to the animal, instead of being an absence of feeling. In my view, Deacon's error is not that he has no answers to such questions (no one does), but that he fails to recognize them.

On the empirical side, Deacon's discussion also falls short. He doesn't explore the neuroscience literature showing how large-scale brain activity is related to consciousness, and makes no use of writings that relate these findings to how we experience emotion, time and the self.

Although incomplete in these ways, *Incomplete Nature* contains many rewarding thoughts about life and mind and their place in nature. ■

Evan Thompson *is professor of philosophy at the University of Toronto, Ontario M5R 2M8, Canada.*
e-mail: evan.thompson@utoronto.ca

S. CAMAZINE/SPL

E.STUMP

The Transantarctics, backbone of the continent, have fascinated explorers since James Cook's time.

GEOLOGY

High on Antarctica

Gabrielle Walker enjoys a historic exploration of the frozen continent's great mountain range.

Think of Antarctica and you don't immediately think of mountains. Almost all the attention given to the continent focuses either on the charismatic animals that patrol its periphery or the two vast sheets of ice that drape its interior. Geologist Edmund Stump has taken a fresh tack.

In *The Roof at the Bottom of the World*, he follows the great range of mountains known as the Transantarctics. These run through the centre of the continent: a backbone between the two ice sheets. Many of the Transantarctic peaks are fully submerged in ice, but some hold enough of it at bay to preside over rare 'dry' valleys and bare outcrops of rock.

Stump has made studying these mountains his life's work. However, in this book he relates not his own geological studies, but the history of the Transantarctics' discovery, from their earliest sighting by James Cook in the eighteenth century through the heroic age of Antarctic exploration and on to the great era of Antarctic science. Thanks to the stunning photographs — many by the author — this solid and dependable book is as beautiful as the mountains it describes.

Stump begins at the northern end of the range, the first to be sighted, and traces the history inland. This makes for some odd chronologies. We read, for example, that the exploring party of Lieutenant Victor Campbell (a member of Robert Falcon Scott's expedition) was dismayed, on returning to base in 1912, to discover Scott's terrible fate — more than a chapter before Scott himself departs on his disastrous journey to the South Pole.

➲ NATURE.COM
For more Antarctic science:
go.nature.com/9fbuuj

However, the benefit of making the mountains the focus is that it enables Stump to dwell on the unsung heroes. These were the less glamorous exploring parties that went off east and west when most eyes were on the south. They had their share of adventure, disaster and reward, but their exploits were often overshadowed. Campbell's party, for example, became stranded in Terra Nova Bay in winter with minimal rations and half-shredded tents, and ended up living through months of darkness and cold in a dismal snow cave lined with seaweed.

The Roof at the Bottom of the World: Discovering the Transantarctic Mountains
EDMUND STUMP
Yale University Press: 2011. 272 pp. $29.95, £25

Stump's telling of these tales is competent, accurate and frequently vivid, and he has a good instinct for when to quote from the diaries of the men who discovered, mapped and explored these mysterious mountains. "It falls to the lot of few men to view land not previously seen by human eyes," Ernest Shackleton wrote in his diary in 1908, "and it was with feelings of keen curiosity, not unmingled with awe, that we watched the new mountains rise from the great unknown that lay ahead of us."

And although I couldn't help but wish that Stump had included some of his own scientific findings in the book, I enjoyed the occasional sidebars in which he recounts journeys through mountains he clearly loves. He speaks of becoming aware of the silence "behind me, just at my shoulder", of his delight at exploring a hidden ice cave, of how it felt ascending (by helicopter and then snowmobile) a hitherto untouched mountain. Like Shackleton, Stump was enchanted by the prospect of seeing something no human had ever witnessed.

In the end, it is the human tales that most interest Stump. He delights in showing recent photographs alongside those taken from the same spot decades earlier. These paired pictures are marvellous, a reminder of how patient this continent is, and how little it has changed over the time that we have observed it.

Stump also writes of how, after many field seasons in the Transantarctic mountains, the thrill of being first in a spot faded, to be replaced by the thrill of knowing that he was standing exactly where members of a previous party had stood. Sometimes he even diverted a trek to find a cairn left behind by an earlier expedition, to prise out the carefully balanced stone that hid the messages left inside, extract the paper like a treasure map, read it, fold it, replace it and add a note of his own.

I have met many other scientists working in Antarctica who show a similar reverence for such traces. The artefacts' state of preservation is part of the fascination — a reminder that the age of exploration was not so very long ago, and that the bond to these first heroes is more palpable here than anywhere else on Earth. Towards the end of the book, Stump's sidebars become philosophical on this point. He describes how he was enchanted to find some rusted cans in a far-off outpost, and then disgusted when he found two more sets. Where, he asks, does history end and pollution begin?

Many of the photos and maps in the book tread a similar fine line between connection and desecration, overdrawn as they are with coloured traces showing the routes where explorers planted their feet, sledge runners and then tractors and planes on this alien landscape. Rather to my surprise, I liked this.

Stump's focus on the human diminishes neither the photographs nor the stories. Instead, it gives us a reassuring handhold when faced with overwhelming grandeur. After all, our explorations of Antarctica may have told us a great deal about the snow, ice and rocks we have found there, but they have taught us even more about ourselves. ■

Gabrielle Walker *is a writer based in London. Her book* Antarctica *will be published in March 2012 by Bloomsbury. e-mail: gw@gabriellewalker.com*

O. OUADAH

A Paris exhibition mingles mathematical concepts with work by artists including songwriter Patti Smith.

MATHEMATICS

Drowning by numbers

Stefan Michalowski and **Georgia Smith** find that a mix of unexplained equations and thunderclaps doesn't add up.

Entering the Cartier Foundation for Contemporary Art in Paris for the exhibition *Mathematics: A Beautiful Elsewhere*, you are directed to an oval room, entirely white and very noisy. A recording of singer-songwriter Patti Smith intoning *Baa, Baa, Black Sheep* in a weary voice plays over deep, rumbling sounds. In a video projected on the wall, a book crashes into view as if dropped from the sky, accompanied by a thunderclap. It is Gregor Mendel's 1865 *Experiments in Plant Hybridization*. A long quote from the book appears on the screen.

Turn around and you find yourself staring at a fireplace in which black-and-white cartoon flames flicker, numbers dancing above them. Another thunderclap. Blaise Pascal's *Of the Geometrical Spirit* drops into view on the back wall. Overhead, an animated mandala by US film-maker David Lynch grows: stones, trees, humans, continents, planets, stars and galaxies, all drawn in a childlike hand. "Yes, sir, yes, sir, three bags full," drones Smith.

What is going on here? According to the exhibition guide, the goal is to "transform the abstract thinking of mathematics into a stimulating experience for the mind and the senses, an experience accessible to everyone". In this eclectic array of maths-inspired art, it is the pieces that don't try too hard that really work.

To create the show, the foundation's director, Hervé Chandès, and astrophysicist Michel Cassé of the French Atomic Energy Commission, brought together pairs of artists and mathematicians who then collaborated to make the exhibits. Jean-Pierre Bourguignon, director of France's Institute for Advanced Scientific Study (IHES) near Paris, one of the world's leading centres of mathematical research, is co-curator. Most of the mathematicians involved have worked at the IHES. Chandès selected artists from among those who had exhibited previously at the foundation.

Mathematics: A Beautiful Elsewhere
Fondation Cartier, Paris. Until 18 March 2012.

"No format was fixed, and everything was open," says Bourguignon. "It was very difficult to predict at the beginning what would happen."

The main exhibits in the museum's quiet basement work well. Film-makers Raymond Depardon and Claudine Nougaret had the excellent idea of letting mathematicians speak for themselves: four minutes to say whatever they wanted. These mini-monologues are fascinating, accessible and beautifully shot. Cédric Villani (wearing his signature velvet butterfly bow-tie) recounts his passion for triangles. Michael Atiyah eloquently describes how maths and art are explorations of inner thoughts and visions, as well as external reality.

In another room, an elegant aluminium sculpture by Hiroshi Sugimoto embodies a surface with constant negative curvature. It tapers upwards from a round base in an asymptotic curve that, theoretically, would come to a point at infinity. There is an equation on the wall, but no explanation of its relationship to the sculpture.

Other installations border on the inexplicable. A static video feed from the control room at the Large Hadron Collider at CERN, Europe's particle-physics lab near Geneva, Switzerland, cuts to a silvery hand that draws Feynman diagrams; the accompanying voice-over is too technical for most visitors. Nearby, a video by Brazilian artist Beatriz Milhazes uses origami-like graphics to demonstrate some nicely rendered geometrical proofs that flit past too quickly to follow. Milhazes illustrates other mathematical phenomena, such as Penrose tiling and prime numbers, with beautifully apt images, and she shows some natural phenomena (iridescence, bird flight) alongside the equations that describe them. Again, unexplained images flash by and the equations become merely decorative.

In the same room, Lynch has fitted a group of robotic arms with mask-like faces. No information is volunteered, but quizzing a staff member reveals that they were created at the University of Bordeaux, France, to explore a theory of artificial curiosity that links sensing, interpreting the environment and learning. Visitors can interact with the machines using simple gestures and sounds.

The lack of information is intentional: the curators didn't want to be didactic. "That's not our role," says Chandès. "Our idea was, we'll immerse people. They can read later, at home, on the Internet."

But have the artists actually transformed abstract mathematical concepts into stimulating, accessible art? For the science-library video in the first room, IHES mathematician Misha Gromov selected a set of books that constitute a scientific canon. But all the visitor sees is covers and a few quotes, often framed off-kilter by a jittery camera. The crashing sound effects verge on self-parody, as if the oracle at Delphi (or the Wizard of Oz) were proclaiming these to be Very Important Texts. At times, the exhibition's refusal to help the visitor understand the mathematical content produces the discouraging sensation that one is being shown fancy images, but excluded from the priesthood of knowledge.

Despite what must have been serious efforts by both mathematicians and artists, most of the latter seem to have acquired relatively superficial notions of maths, physics or biology. This is a show rich in theatrical effects, but it reveals little engagement with the power and beauty of maths on a deeper artistic level. ■

Stefan Michalowski *is a former particle physicist, and executive secretary of the OECD Global Science Forum in Paris.*
Georgia Smith *is a freelance journalist based in Paris.*
e-mails: stefanm@noos.fr; georgias@noos.fr

This article does not represent the views of the OECD.

Correspondence

Relative drop for farming emissions

The depiction of farming's greenhouse-gas footprint (estimated at 30.9% of total emissions) is derived from a 2007 report that used data from 2004 (*Nature* **479,** 279; 2011). But relative estimates of emissions from different sources have altered appreciably since then, largely because fossil-fuel usage and cement production for building have both escalated.

In 2000–07, carbon dioxide emissions due to land-use changes were 1.1 petagram carbon equivalents (Pg C) per year and emissions from fossil-fuel usage and cement production accounted for 7.6 Pg C per year (Y. Pan *et al. Science* **333,** 988–993; 2011). The contribution from land-use changes was therefore 12.6% of carbon dioxide emissions over this period. Emissions of methane, nitrous oxide and fluorine-containing gases were about 3.1 Pg C per year, so land-use changes contributed less than 10% of total greenhouse-gas emissions.

Carbon dioxide emissions from fossil-fuel burning and cement production went up to about 9.1 Pg C in 2010. Assuming that the emissions from land-use changes were the same as in 2000–07 and that the carbon-equivalent contributions of methane, nitrous oxide and fluorine-containing gases were the same as in 2004, land-use changes would have accounted for only about 8% of total emissions last year.

Although the increase in emissions from fossil-fuel usage and cement production is well documented, estimates of emissions from land-use changes remain uncertain. But they are unlikely to be as high as the earlier data might indicate.

Hans Martin Seip *Center for International Climate and Environmental Research — Oslo (CICERO); University of Oslo, Norway.*
h.m.seip@kjemi.uio.no

Europe needs research networks

A new European science-policy body, ScienceEurope, was launched in October to give a stronger voice in Brussels to the major national research-funding agencies. Likely casualties of this effort include some of the most successful activities of the venerated European Science Foundation, causing major concern among many scientists.

For example, the future of the Research Networking Programmes is under threat. These have been fostering cost-effective collaborations and networking between scientists from European countries in all fields for almost 20 years.

Ninety such programmes are currently in operation. They rely on minimal bureaucracy, simple rules and very modest funding — €80,000 (US$107,000) per year and per network on average (covered by participating member organizations). This combination allows them to react swiftly to new scientific challenges.

Our Research Networking Programmes in electronic-structure theory and molecular simulation, for example, have made Europe a leader in computational materials and molecular sciences, thanks to the sustained support of the European Science Foundation.

It is not clear whether ScienceEurope, or the European Commission's Horizon 2020 programme, will make a long-term commitment to research networks. However, we consider it of utmost importance that this type of funding instrument should survive, along with its nimble and flexible administration.

Peter Dederichs* *Psi-k Research Networking Programme and Jülich Research Centre, Germany.*
p.h.dederichs@fz-juelich.de
**On behalf of 4 co-signatories (see go.nature.com/xsbeig).*

Lemaître did stake a claim on discovery

In a brilliant piece of detective work, Mario Livio clarifies the mysterious differences between Georges Lemaître's original 1927 paper, which announced the expansion of the Universe, and its 1931 translation from French into English (*Nature* **479,** 171–173; 2011). He suggests that "Lemaître was not at all obsessed with establishing priority for his original discovery". However, Lemaître's important later paper, 'L'expansion de l'Univers' (*Ann. d'Ap.* **13,** 344–345; 1950), argues otherwise.

In that paper, Lemaître writes (translated from the French): "The title of my note leaves no doubt about my intentions: a Universe of constant mass and growing radius accounts for the radial velocities of the extra-galactic nebulae."

Sidney van den Bergh *Dominion Astrophysical Observatory, Herzberg Institute of Astrophysics, Victoria, British Columbia, Canada.*
sidney.vandenbergh@nrc-cnrc.gc.ca

Overcome India's GM crops prejudice

India's agricultural productivity is not keeping pace with its population, despite its growing economy. Advances in transgenic technology could alleviate the situation, but there is strident opposition in the nation to genetically modified (GM) crops from non-governmental organizations and from spiritual gurus, in the name of tradition, biodiversity and other ill-founded concerns.

Millions of people worldwide have been consuming GM maize (known as *Bt* corn) over the past decade, and no authenticated health issues have arisen. *Bt*-transformed plants reduce pesticide application so are suitable for organic farming. GM rice that provides a balance of protein and micronutrients would vastly improve the health of millions of children.

The biodiversity argument doesn't stand up either: random transfer of engineered genes to a non-target plant is likely to be harmless if the genes are well tested, given that genes are constantly shuffled on an evolutionary scale anyway.

Embargos from the Indian government and the courts have destroyed the efforts of researchers here to improve the productivity of crops outside the agendas of multinational corporations.

No single technology can solve all the problems, but a combination of transgenic technology, organic farming, marker-assisted breeding and traditional practices would markedly improve crop yields. India cannot afford to lose even one of these technology options.

Govindarajan Padmanaban *Indian Institute of Science, Bangalore, India.*
geepee@biochem.iisc.ernet.in

Social norms depend on what is typical

I agree with Laurent Mottron that autism should be described as a variant within the human species (*Nature* **479,** 33; 2011). But it is worth pointing out that neurotypical modes of social conduct prevail only because the neurotypical population far outnumbers the autistic one.

I have friends in the high-IQ society Mensa who are also autistic: we have our own set of non-verbal communications, our own set of social rules. When we predominate in a group, we communicate in the autistic way, and (neurotypical) people who cannot communicate in this way are unable to join in. In this setting, Mottron's 'normocentrism' would put our way of communicating as the norm, and class those who are left out as socially inept.

Jasper van Haasteren *Groningen, the Netherlands.*
jasper.vanhaasteren@mensa.nl

Har Gobind Khorana

(1922–2011)

Chemical biologist who helped to establish the genetic code.

Har Gobind Khorana, who died on 9 November 2011 at the age of 89, was a pioneer and a visionary. That someone with such a humble background could rise to become an icon of molecular biology is a testament to his extraordinary drive, discipline and striving for excellence.

His background was in chemistry, but his interests lay in applying chemistry to problems in biology. By doing so, he started the field of 'chemical biology'. For his work on uncovering the genetic code, Khorana was awarded the Nobel Prize in Physiology or Medicine in 1968.

Khorana's chemical synthesis of the first gene in 1970, followed by his synthesis of a related gene and demonstration in 1979 that it was functional in a bacterium, was a landmark in genetics. This work ushered in the era of recombinant DNA and underlies the *in vitro* assembly of whole genomes from shorter DNA strands.

Khorana was born in Raipur, a small village in the Punjab province of what is now Pakistan, but was then India. His father, an agricultural taxation clerk, believed in education; and Khorana and his siblings were the only literate children in the village. Despite poor educational facilities, Khorana completed high school and went on to receive bachelor's and master's degrees in chemistry from University of the Punjab in Lahore. In 1945, Khorana moved to the University of Liverpool, UK, under a Government of India Fellowship. He was slated to study insecticides and fungicides, but because of lack of space was asked to pursue organic chemistry. It was there that he obtained a PhD in 1948 working on the chemistry of melanins with Roger Beer.

Having seen much German scientific literature, Khorana wanted to do postdoctoral research in a German-speaking country. So he went to the Swiss Federal Institute of Technology (ETH) in Zurich, where he worked for 11 months on alkaloid chemistry with Vladimir Prelog. His stay was short — he received no stipend and had to sustain himself on savings. Fortunately, in 1949, he received a fellowship to work with Alexander Todd at the University of Cambridge, UK, on peptides and nucleotides.

In 1952, Khorana moved to Vancouver to start his own research group at the British Columbia Research Council. The council's director, Gordon Shrum, had come from Canada to interview him and said: "You can have all the freedom to do what you want", but we don't have much in terms of facilities. Shrum said candidly that he wanted to hire an organic chemist because they were cheap — needing only test tubes to do research. Undaunted, Khorana accepted the offer, and established an outstanding research programme.

In 1960, he moved to the University of Wisconsin–Madison, where he worked on the genetic code and chemical synthesis of a transfer RNA gene. In 1970, he moved to the Massachusetts Institute of Technology in Cambridge, where he switched to working on membranes and signal transduction, problems on which he worked for more than 30 years until his retirement in 2007.

A DEEP THINKER

Much of Khorana's early work used a class of reagents called carbodiimides, which he had come across in Zurich while translating papers from German to English. In Vancouver, his use of these reagents led to the synthesis of nucleotide coenzymes and oligonucleotides, and brought him into contact with biochemists Arthur Kornberg, Paul Berg, Saul Roseman, Jerry Hurwitz, Fritz Lipmann, Charles Dekker and Leon Heppel, many of whom spent summers in his lab.

Khorana was a pioneer. Spanning chemistry, biology and physics, he was doing interdisciplinary research before the current trend. In 1968, he wrote about gene manipulation before individual genes from any organism had been characterized. And in 1971, he wrote about the need to amplify the synthetic gene, using a series of steps that looks eerily similar to the technique for this now known as PCR.

A deep thinker, Khorana put much thought into choosing a problem to work on. He was not influenced by its difficulty or the time needed to solve it, as long as it was of fundamental importance. He often said: "If you want to get far, you have to travel alone." Yet he was always well prepared, making "pilgrimages" to work in laboratories — ranging from Stanford University in California to the National Cancer Center of Tokyo — before undertaking new projects.

As a mentor, Khorana set high standards. He was loyal to the people who helped him and to the institutions at which he worked. He could be demanding, but he was no more so of others than he was of himself. One associate said: "He showed us what excellence in science was and we learnt to recognize it."

Gobind was modest, humble and avoided publicity. He loved music, swimming and long walks, and had a curiosity that lasted until the end. Three days before he passed away, I was by his hospital bed and we talked about glucose and the brain.

Gobind used the solitude of hiking to think about scientific problems, and always carried a pen and notecards to write down his thoughts. On the day of his Nobel prize announcement, he was among the last at the university to hear about it. As he often did, he had gone to a rented cottage by a lake outside Madison with no telephone or radio, to write papers. His wife Esther had to drive over to give him the news. At the celebration, I remember him enthusiastically explaining his latest work on the blackboard to two professors holding glasses of champagne. Gobind was at heart an experimental scientist. With him gone, we have lost an extraordinary man. ■

Uttam L. RajBhandary *is in the Department of Biology, Massachusetts Institute of Technology, Cambridge, Massachusetts 02139, USA. He joined Khorana's lab as a postdoc in 1962 and has been a close friend and colleague since. e-mail: bhandary@mit.edu*

UNIVERSITY OF WISCONSIN-MADISON LIBRARIES

nature OUTLOOK

MULTIPLE MYELOMA

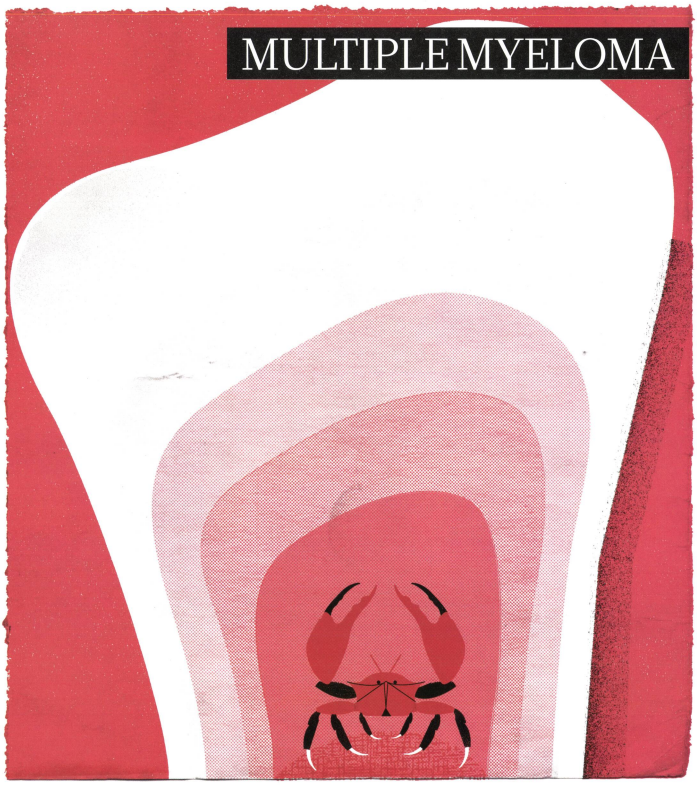

Produced with the financial support of:
Onyx Pharmaceuticals, Inc.

Research that goes to the core of cancer

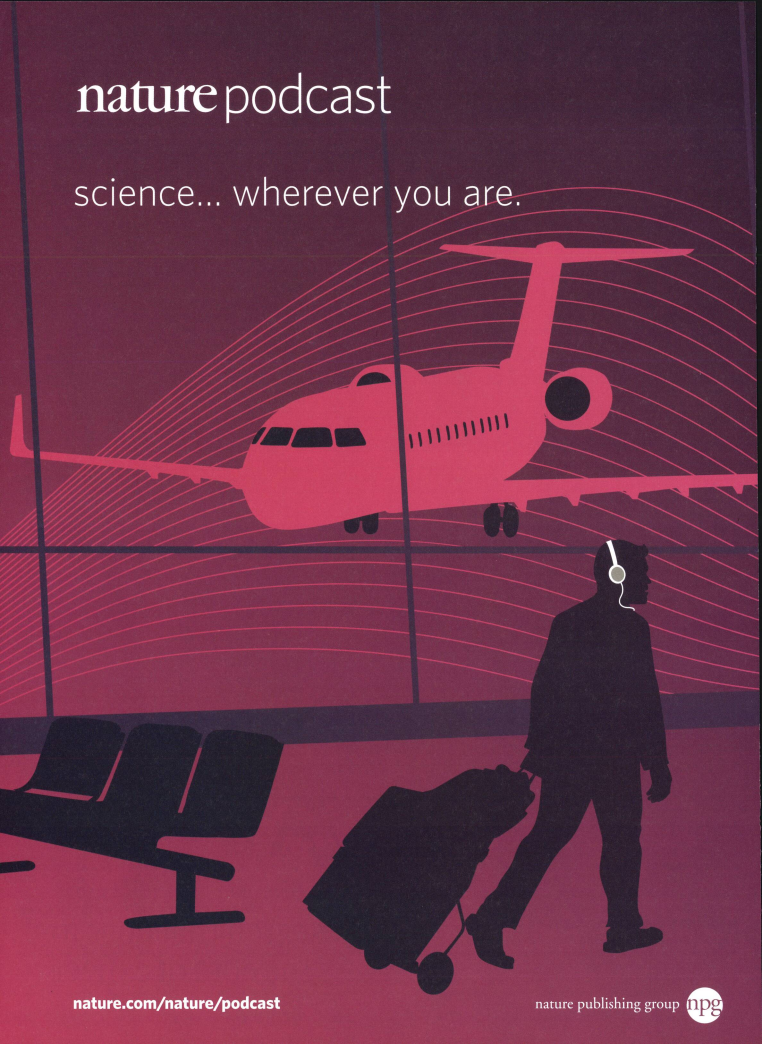
nature podcast
science... wherever you are.
nature.com/nature/podcast
nature publishing group
npg

MULTIPLE MYELOMA

15 December 2011 / Vol 480 / Issue No. 7377

COVER ART: MATTHEW HOLLISTER

Editorial
Herb Brody, Michelle Grayson, Nick Haines

Art & Design
Wes Fernandes, Alisdair MacDonald, Andrea Duffy

Production
Donald McDonald, Emilia Orviss, Leonora Dawson-Bowling, Stephen Russell

Sponsorship
Reya Silao, Yvette Smith, Gerard Preston

Marketing
Elena Woodstock, Hannah Phipps

Project Managers
Helen Anthony, Claudia Deasy

Art Director
Kelly Buckheit Krause

Magazine Editor
Tim Appenzeller

Editor-in-Chief
Philip Campbell

The bar for what constitutes good news about multiple myeloma is low. Physicians and researchers who study this deadly cancer of blood plasma cells can point to a doubling of the average survival time over the past decade or so. But make no mistake, a diagnosis of multiple myeloma is still horrible news: patients can expect to live a mere 7–8 years, during which time they'll probably find themselves hobbled as the disease damages their bones. The new classes of drugs that have extended life expectancy will inevitably lose their power as resistance develops, leaving only the option of an autologous stem-cell transplant — an arduous procedure that introduces risks of its own.

Yet through the lens of this rare form of cancer, researchers are gaining important insights into many other diseases. The progression of myeloma from a benign precursor state known as MGUS to the deadly malignancy depends on a complex of factors that are not yet fully understood. But it is clear that myeloma, with its epicentre in the bone marrow, depends strongly on the composition and behaviour of the cells and tissues around it. Studying this relationship has helped researchers learn more about the role of the tumour microenvironment in many other cancers. Similarly, multiple myeloma has provided an ideal opportunity to investigate the theory that the origin of malignancy lies in cancer stem cells that continue to produce new cancer cells even as drugs kill the old ones. And efforts to protect bones from the ravages of multiple myeloma have helped further the development of drugs that can serve those suffering from non-malignant bone disorders such as osteoporosis. Drugs and surgical techniques developed initially for multiple myeloma have revolutionized the way doctors treat other bone diseases.

We are pleased to acknowledge the financial support of Onyx Pharmaceuticals in producing this *Outlook*. As always, *Nature* takes sole responsibility for all editorial content.

Herb Brody
Supplements Editor

CONTENTS

S34 OVERVIEW
Multiple lines of attack
From basic research to treatment

S36 DIAGNOSTICS
The early bird
High-risk patients need prompt treatment

S38 ANIMAL MODELS
Towards a myeloma mouse
Can mice help us find a cure?

S40 DRUGS
More shots on target
The drugs are getting better

S43 TUMORIGENESIS
Testing ground for cancer stem cells
A controversial theory about cancer biology

S46 STEM CELLS
Transplants on trial
When should stem-cell transplants be given?

S48 MICROENVIRONMENT
Neighbourhood watch
Looking for clues in the bone marrow

S50 GENETICS
Profiling a shape-shifter
There are patterns in the genes

S52 IMAGING
Seeing is believing
Getting a clearer picture of myeloma

S54 AETIOLOGY
The path to disease
How a benign condition turns deadly

S56 ORTHOPAEDICS
Structural support
Myeloma helps researchers understand bones

S58 PERSPECTIVE
A model disease
A useful tool for cancer research

Nature Outlooks are sponsored supplements that aim to stimulate interest and debate around a subject of interest to the sponsor, while satisfying the editorial values of *Nature* and our readers' expectations. The boundaries of sponsor involvement are clearly delineated in the *Nature Outlook* editorial guidelines available at http://www.nature.com/advertising/resources/pdf/outlook_guidelines.pdf.

CITING THE OUTLOOK
Cite as a supplement to *Nature*, for example, *Nature* **Vol XXX**, No. XXXX Suppl, Sxx–Sxx (2011).

VISIT THE OUTLOOK ONLINE
The *Nature Outlook Multiple Myeloma* supplement can be found at http://www.nature.com/nature/outlook/multiple_myeloma. It features all newly commissioned content as well as a selection of relevant previously published material.

All featured articles will be freely available for 6 months.

SUBSCRIPTIONS AND CUSTOMER SERVICES
For UK/Europe (excluding Japan): Nature Publishing Group, Subscriptions, Brunel Road, Basingstoke, Hants, RG21 6XS, UK. Tel: +44 (0) 1256 329242. Subscriptions and customer services for Americas – including Canada, Latin America and the Caribbean: Nature Publishing Group, 75 Varick St, 9th floor, New York, NY 10013-1917, USA. Tel: +1 866 3637860 (US/Canada) or +1 212 726 9223 (outside US/Canada). Japan/China/Korea: Nature Publishing Group — Asia-Pacific, Chiyoda Building 5-6th Floor, 2-37 Ichigaya Tamachi, Shinjuku-ku, Tokyo, 162-0843, Japan. Tel: +81 3 3267 8751.

CUSTOMER SERVICES
Feedback@nature.com
Copyright © 2011 Nature Publishing Group

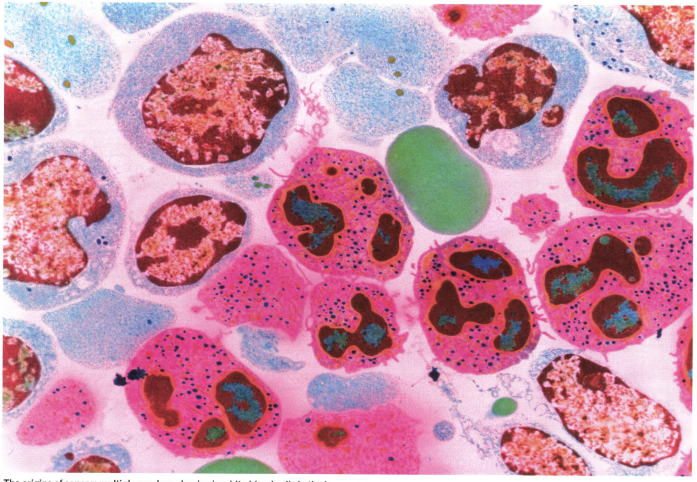

GOPAL MURTI/SCIENCE PHOTO LIBRARY

The origins of cancer: multiple myeloma begins in white blood cells in the bone marrow.

OVERVIEW

Multiple lines of attack

Researchers are developing new weapons to fight a deadly form of blood cancer.

BY DUNCAN GRAHAM-ROWE

Multiple myeloma is a cancer of the blood that is both rare and deadly. Each year in the United States alone there are around 20,000 new cases, and just over half that number die of the disease. But in the past few years, new drugs and the availability of stem-cell therapy seem to have set multiple myeloma on a different course: the survival rate from the disease has increased faster than that of any other form of cancer. For some people, multiple myeloma is changing from an imminent death sentence to a chronic disease that can be managed for many years.

Myelomas are malignant plasma cells. Normally these white blood cells play an important role in the immune system, producing antibodies that help fight off infections and disease. Plasma cells are generated in the bone marrow, and when they become cancerous their unfettered growth creates lesions within the bone. The presence of more than one lesion is known as multiple myeloma.

Once formed, these lesions often crowd out healthy plasma cells, interfering with the production of other types of blood cell as well as those involved in regenerating the bone and keeping it strong. As a result, patients often have low blood counts and develop weak bones that are easily broken. Cancerous plasma cells continue to produce antibodies, but because these immunoglobulin proteins are abnormal and monoclonal (identical copies of each other), they offer no protection against infections. Instead, these so-called M proteins can damage the kidney. The main symptoms of multiple myeloma are often referred to as CRAB, for elevated calcium (caused by the destruction of bone), renal failure, anaemia and bone lesions.

Although it is the second most common form of blood cancer (after the group of diseases lumped together as non-Hodgkins lymphoma), multiple myeloma is still rare. Global incidence ranges from just 1 in 100,000 people in China to 4 in 100,000 in developed countries. The disease is more common among men than women, and is roughly twice as prevalent in African Americans as in Caucasian Americans. But by far the biggest risk factor is age — the vast majority of patients are more than 60 years old, and only 2% are younger than 40.

Until the late 1990s, life expectancy with multiple myeloma using the best available treatments, such as melphalan and prednisone, was just three to four years. But the availability of stem-cell transplants and the introduction of lenalidomide (an analogue of thalidomide marketed as Revlimid by Celgene in Summit, New Jersey) and bortezomib (a proteasome inhibitor branded

➲ NATURE.COM
For some of the latest research on multiple myeloma:
go.nature.com/swtknk

INTERNATIONAL AGENCY FOR RESEARCH ON CANCER

MULTIPLE MYELOMA HOTSPOTS

Men and those of African ancestry are hit the hardest.

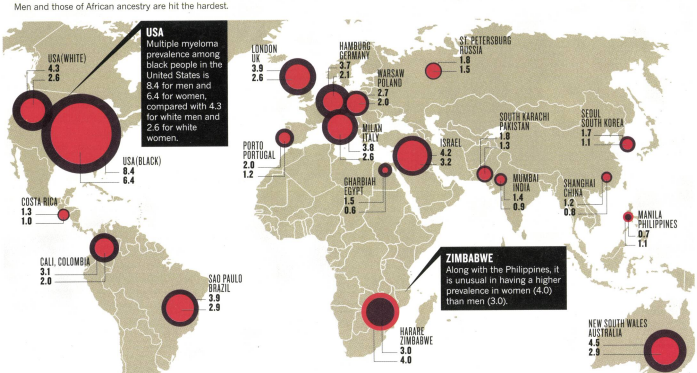
USA
Multiple myeloma prevalence among black people in the United States is 8.4 for men and 6.4 for women, compared with 4.3 for white men and 2.6 for white women.
USA (WHITE) 4.3 2.6
USA (BLACK) 8.4 6.4
COSTA RICA 1.3 1.0
CALI, COLOMBIA 3.1 2.0
SÃO PAULO BRAZIL 3.9 2.9
LONDON UK 3.9 2.6
HAMBURG GERMANY 3.7 2.1
WARSAW POLAND 2.7 2.0
MILAN ITALY 3.8 2.6
PORTO PORTUGAL 2.0 1.2
GHARBIAH EGYPT 1.5 0.6
ST. PETERSBURG RUSSIA 1.8 1.5
ISRAEL 4.2 3.2
SOUTH KARACHI PAKISTAN 1.8 1.3
MUMBAI INDIA 1.4 0.9
SHANGHAI CHINA 1.2 0.8
SEOUL SOUTH KOREA 1.7 1.1
MANILA PHILIPPINES 0.7 1.1
ZIMBABWE
Along with the Philippines, it is unusual in having a higher prevalence in women (4.0) than men (3.0).
HARARE ZIMBABWE 3.0 4.0
NEW SOUTH WALES AUSTRALIA 4.5 2.9
Men
Women
Age-standardized (world) incidence per 100,000

as Velcade by Millennium Pharmaceuticals in Cambridge, Massachusetts) has since doubled life expectancy to 7–8 years. Although the response to these new drugs is positive, studies show that once patients relapse, the cancer becomes resistant to the drugs.

TAILORED TREATMENT

Multiple myeloma follows a predictable progression. It begins as a precursor condition known as monoclonal gammopathy of undetermined significance (MGUS). Characterized by an excess of M proteins, MGUS is not normally harmful to the health — people generally don't even know they have it and exhibit no symptoms of disease. But every year 1% of MGUS patients go on to develop multiple myeloma, and every case of multiple myeloma is thought to have started as MGUS. "Currently there is no good way of identifying which patients with MGUS will develop multiple myeloma," says Louise Perkins, chief scientific officer of the Multiple Myeloma Research Foundation (MMRF) in Norwalk, Connecticut.

What is now known, however, is that specific chromosomal translocations — where parts of one chromosome break off and attach to another — occur in myeloma cells. The sequencing of 38 genomes of multiple myeloma tumours earlier this year[1] led to certain genetic mutations being shown to play a major role in the pathogenesis of myelomas. These mutations alter important genetic pathways, including one known as NF-κB, which controls the transcription of DNA.

The predictive power of genetics is limited, however. There is little overlap in the genetic signatures, says Perkins, and not everyone shares the same translocations. The translocation t(4;14), for example, which when found with other genomic aberrations is an important predictor of survival, occurs in only 15% of patients, she says. Many researchers believe that multiple myeloma is best tackled by 'personalized medicine', a much-touted approach where treatments are tailored to an individual's genetic make-up. A genomic initiative is already underway, spearheaded by the MMRF in partnership with the Broad Institute in Cambridge, Massachusetts, and the Translational Genomics Research Institute in Phoenix, Arizona.

"A fair bit of high-level genetic categorization has been done," says Perkins. But one task still facing researchers, she says, is to find molecular markers that can help predict new therapeutic drugs. A central tissue bank has already been set up, and more than US$12 million has been poured into genetic profiling and 'deep' sequencing research, and to create an open portal as a resource for researchers to use. The hope is that accelerating research into this disease will ultimately lead to personalized treatment — and much better outcomes for patients. ■

Duncan Graham-Rowe *is a science writer based in Brighton, UK.*

HOW FAR ALONG?

Multiple myeloma has three distinct stages.

MGUS	Smouldering myeloma	Symptomatic myeloma
• Serum paraprotein <30 g l^{-1} and • Clonal plasma cells <10% on bone-marrow biopsy and • No myeloma-related organ or tissue impairment.	• Serum paraprotein >30 g l^{-1} and/or • Clonal plasma cells >10% on bone-marrow biopsy and • No myeloma-related organ or tissue impairment.	• Clonal plasma cells >10% on bone-marrow biopsy or (in any quantity) in a biopsy from other tissues • A monoclonal protein (paraprotein) in either serum or urine • Evidence of end-organ damage: hypercalcemia (corrected calcium >2.75 mmol l^{-1}); renal insufficiency; anaemia (haemoglobin <10 g dl^{-1}); bone lesions (lytic lesions or osteoporosis with compression fractures).

1. Chapman, M. A. *et al. Nature* **471,** 467–472 (2011).

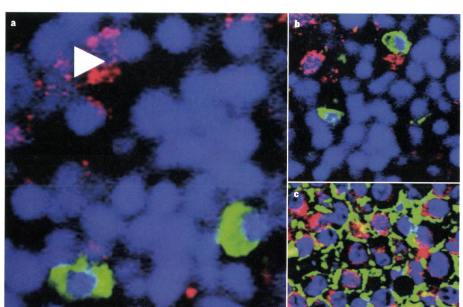

Bone-marrow cells from healthy people (a) and patients with MGUS (b) are clearly different to those from multiple myeloma patients (c) when labelled with two protein markers.

DIAGNOSTICS

The early bird

Identifying the patients most likely to progress from a precancerous condition to multiple myeloma could help doctors catch the disease early and stop it taking hold.

BY LAUREN GRAVITZ

Unlike many other forms of cancer, multiple myeloma does not lend itself to early warnings. The condition that precedes it — an accumulation of precancerous cells called 'monoclonal gammopathy of undetermined significance' (MGUS) — is remarkably common, occurring in 3% of people over 50 years of age, but it converts to cancer at a rate of just 1% a year. Predicting which individuals are most at risk is extremely difficult. But given the rapid progression and high mortality of the disease, researchers are keen to identify them and start treatment as early as possible.

This idea may seem obvious, but it's beset with problems. Myeloma exists on a spectrum, from benign MGUS to asymptomatic 'smouldering' multiple myeloma to the full-blown disease. Treating everyone with MGUS is not a viable option: many doctors worry that they could do more harm than good if they treat people on the healthy end of the spectrum, the vast majority of whom will never develop the disease.

In a 1988 study using the best drugs available, researchers concluded that treatment at the smouldering stage caused unnecessary side effects with no impact on survival time. Since that first trial, however, newer treatments with better prognoses have emerged for multiple myeloma, and many researchers believe that these therapies could work for MGUS as well and should be tested in earlier stages of disease. But, they say, this should only be done if there's a way of stratifying patients based on their risk of progression from MGUS or smouldering myeloma into the symptomatic stages of disease. And only those at the highest risk of converting to full-blown myeloma should be treated.

Studies of early treatment must be done with extreme caution. Unless a patient has smouldering disease and is deemed exceedingly likely to progress rapidly to symptomatic myeloma, the evidence suggests that it might be a mistake to start treatment. According to W. Michael Kuehl, who studies myeloma pathogenesis at the US National Cancer Institute in Bethesda, Maryland, treating MGUS too early could actually induce myeloma. "You might find that if you treat a patient you could get rid of premalignant cells, but they would come back very quickly with malignant clones that had been kept in check by MGUS," he says.

CHAIN REACTION

The definition of multiple myeloma is based on clinical signs such as anaemia or elevated blood calcium levels. This is because when pathologists examine biopsies from MGUS and multiple myeloma patients, the cells are virtually identical. "People have generally said that unless there's end-organ damage we should sit tight and watch," says Vincent Rajkumar, a haematologist and myeloma specialist at the Mayo Clinic in Rochester, Minnesota. "People like me are starting to say we have to go early and treat early if we're going to make a difference."

Currently, patients are diagnosed as having MGUS, smouldering myeloma or multiple myeloma according to three major factors. The first is the amount of protein from identical (monoclonal) antibodies in the blood. The second is the ratio of the number of genetically diverse plasma cells to the number of identical, clonal plasma cells in a bone-marrow biopsy. The third is the presence of clinical symptoms (see '–––How far along', page S35). However, more researchers and clinicians think the disease exists on a spectrum, and that they would be better able to treat and follow-up with their patients if they had a better understanding of where on the disease spectrum each patient lies.

Rajkumar has worked on some of the more promising stratification strategies to emerge in the past few years. One of the more straightforward methods is to measure the tumour burden, or the percentage of clonal plasma cells in the bone marrow. By the time that number reaches 60%, most patients already have symptoms — but if they don't, they will almost certainly develop them within the next two years and would be an ideal group of patients to start early therapy.

Another method the Mayo group found that indicates risk of progression is a blood test that measures levels of immunoglobulin free-light chains. Antibodies, or immunoglobulins, are composed of two heavy and two light protein chains that are made separately and then built up into antibodies inside plasma cells. There are two types of light chain, kappa and lambda. A skewed ratio of free kappa to free lambda light chains indicates a proliferation of clonal plasma cells and thus a higher risk of progression. In a person with MGUS, a kappa-to-lambda light-chain ratio of less than 0.65 or more than 1.65 corresponds to a tripling of the risk of progression. In a patient with smouldering multiple myeloma, a kappa-to-lambda ratio higher than 100 (or less than 0.01), Rajkumar has found, pushes the risk of progression to between 80% and 90%. The researchers are also investigating several other biomarkers. "If we can identify all of these [markers] carefully, we will be able to identify

NATURE.COM
For some of the latest research on multiple myeloma:
go.nature.com/tfsmgh

STRATIFICATION STRATEGY

There are various ways of assessing the risk of patients with early signs of multiple myeloma progressing to the full-blown disease.

Method	How it works	Potential obstacles
Molecular imaging	Contrast-enhanced positron emission tomography (PET), computed tomography (CT) and magnetic resonance imaging (MRI) scans, in combination with different molecular markers, can pick out signs of progression in the bone marrow, including blood-vessel 'leakiness' and increased blood-vessel growth (angiogenesis) characteristic of cancer.	• Whole-body imaging is expensive and difficult to justify for frequent monitoring. • There are indications that certain contrast agents may increase the risk of disease progression.
Free light-chain ratios	Immunoglobulins are composed of two heavy and two light protein chains. There is evidence that patients with a skewed ratio of kappa-to-lambda free light chains are much more at risk of progressing to full-blown multiple myeloma.	None.
Bone-marrow microenvironment	Some believe that as MGUS develops into myeloma, the tumour cells manipulate their microenvironment to their benefit. Researchers have identified inflammation signatures in the bone-marrow microenvironment — increased transcription factors and other proteins — that they believe are specific to myeloma progression.	• Researchers don't have data from enough patients to ensure they are identifying a consistent signature. • This requires bone-marrow aspiration, rather than a simple blood or urine test.
MicroRNAs	MicroRNAs (miRNAs) are involved in the suppression and silencing of gene transcription, and *in vitro* studies suggest that a combination of up- and downregulated miRNAs that creates a fingerprint specific to myeloma progression. This could be detected in a blood sample.	• So far, there are not enough data from patients to determine whether these signatures would be a reliable indication of risk.
Chromosomal mutations and deletions	Certain deletions (such as chromosome 13), chromosomal translocations (t(11;14)) and mutations (in the *RAS* genes) seem to be correlated with the transition from MGUS to myeloma.	• Each mutation is present in only a relatively small minority of patients.
Flow cytometry	Flow cytometry allows researchers to label and count plasma cells, based on immunological markers on their surface. The more abnormal cells, the higher the probability of converting to malignant disease.	• This requires a bone-marrow biopsy rather than a simple blood or urine test.
Clonal plasma levels	If a patient doesn't already have symptoms, those with a bone-marrow biopsy with more than 60% clonal plasma cells will almost certainly develop disease within the next two years.	• This needs a bone-marrow biopsy rather than a blood or urine test. • Many patients become symptomatic before their clonal plasma cell count reaches 60%.

the people who will progress in the next two years," Rajkumar says.

GO WITH THE FLOW

Another group making good headway in stratifying risk is based at the University Hospital of Salamanca in Spain. Jesús San Miguel, a haematologist with the Salamanca group, found that the percentage of plasma cells that are clonal, as determined by immunological markers on their surface, correlates with the probability of conversion to malignant disease. The cells are collected from bone-marrow biopsies and examined by a process called flow cytometry, in which thousands of cells per second stream past a laser and can be counted and examined for fluorescent markers. "We have shown that in MGUS patients with the benign form of the disease, normal plasma cells coexist with tumour plasma cells," San Miguel says. By contrast, he explains, in a person with symptomatic myeloma, nearly all the plasma cells are phenotypically aberrant or clonal. It is only through the use of flow cytometry that this intuitive result — the more abnormal cells a patient has, the more likely they are to progress — has been confirmed.

After separating out the highest-risk patients as predicted by flow cytometry, San Miguel performed the first long-term trial to see whether early intervention can prolong survival. He tested a combination of two drugs, lenalidomide and dexamethasone, on patients with smouldering myeloma and high counts of abnormal plasma cells. After five years, 98% of the treatment group survived, compared with only 87% of the untreated group. "We are seeing a trend for benefit in overall survival in these high-risk smouldering-myeloma groups," he says.

Researchers are watching both the Mayo and the Salamanca groups closely. "The better stratification you have, the more rational you can be about what to do with treatment," says Kuehl. "But a big part of cancer is just blind luck. We're never going to be able to perfectly predict what happens, but both the Mayo and Spanish stratifications are good steps in the right direction."

Several other techniques for risk stratification are making their way into labs across the United States and Europe, but progress is slow. Genetic approaches hold promise, but if researchers are to tease out high-risk genetic profiles, they must follow MGUS patients from the moment of diagnosis until they convert, which can take a decade or more. This hasn't stopped scientists at the University of Arkansas for Medical Sciences, who are monitoring about 120 MGUS patients as part of a group of trials done by SWOG, formerly the Southwest Oncology Group. "We've been watching these patients and trying to identify features associated with early progression," says John Shaughnessy, a myeloma geneticist at that university. Shaughnessy has the same difficulties as his peers. "It's been an arduous task. It's very difficult to see any signal even after ten years, because it's so rare that these people progress."

EXPRESSION OF HOPE

Most of the patients Shaughnessy is studying also undergo gene-expression studies to determine whether rapidly progressing MGUS has a unique signature of gene activity. Using a 70-gene risk model that Shaughnessy developed to pinpoint the most aggressive myeloma cases, the Arkansas researchers believe they might be able to identify increased risk of MGUS progression. They are also studying a protein made by myeloma tumour cells, called DKK1, which suppresses the differentiation of bone-forming cells. "We can show that if a patient's gene-expression profiling shows that their DKK1 expression is in the highest 25%, they are at increased risk of progression," Shaughnessy says. Half the patients in that group progressed to disease within three to four years, whereas none of those with DKK1 levels in the lowest quartile have done.

Other genes and chromosomal mutations have also yielded encouraging results. Scientists have found that the activity of the *MYC* and *KRAS* genes also seems to be different in MGUS and myeloma. "Let's say you get a patient with MGUS and monitor him closely, and find out that all of a sudden he has *MYC* rearrangements in a lot of cells," says Leif Bergsagel, a cancer geneticist at the Mayo Clinic in Scottsdale, Arizona. In this case, it may be prudent to consider treatment even if no symptoms have emerged. "We don't have the technology to do it now, but as the price of next-generation sequencing comes down, we could quantify even low levels of *MYC* rearrangements," he says. Identifying the genes responsible and their products could ultimately have implications for treatment too if drug companies could identify those most at risk and then target and eradicate just the abnormal cells to stop the full-blown disease taking hold.

For now, researchers are working on a variety of screening tools — from assessing clinical symptoms to blood tests and imaging — to create a fingerprint that could identify who is most likely to progress (see 'Seeing is believing', page S52). "It's a big challenge, but I think finding biomarkers is the easy part," Rajkumar says. "The hard part will be convincing my colleagues that we really can predict who will progress and don't have to wait for symptoms to appear." ■

Lauren Gravitz *is a science writer based in Los Angeles, California.*

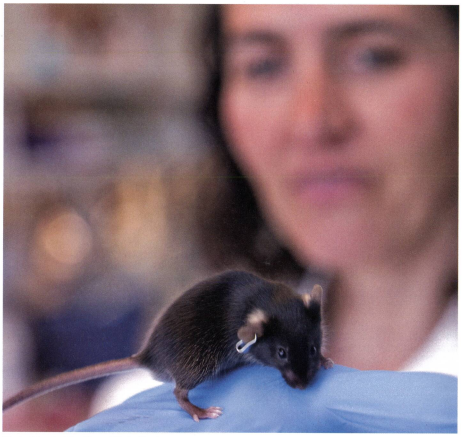

MAYO CLINIC

Marta Chesi of the Mayo Clinic displays a transgenic mouse used to model multiple myeloma.

ANIMAL MODELS

Towards a myeloma mouse

Introducing a human disease into mice is helping researchers explore its nature and find potential therapies.

BY SARAH DEWEERDT

A few years ago, two scientists from the Magna Graecia University of Catanzaro in Italy found themselves riding together on a train to Rome. By the time the train reached its destination, the pair — oncologist Pierfrancesco Tassone and bioengineer Filippo Causa — had devised a new way of studying multiple myeloma in a mouse model[1].

First, Causa would create tiny, cylindrical scaffolding made of high-tech plastic, shot through with pores of various sizes that mimic the architecture of human bone. Tassone would then inject cells from human bone marrow into the artificial bone scaffolds and implant them under the skin of immune-deficient mice. He would later inject the scaffolds with purified myeloma cells taken directly from patients with the disease.

Tassone compares the scaffolding to "an empty apartment, a house for cells". Once the apartment and its bone-marrow furnishings are in place, the myeloma cells can move in, giving scientists the ability to study the interaction between a patient's myeloma cells and his or her own bone marrow. They call the arrangement SCID-synth-hu, for the immune-deficient *SCID* mouse, synthetic bone and human bone marrow.

This might sound like a convoluted system, but that's not unusual for animal models of multiple myeloma. "The myeloma cell depends on the microenvironment of the bone marrow," says Nikhil Munshi, who studies myeloma at the Dana-Farber Cancer Institute in Boston, Massachusetts. "It requires human bone marrow to grow and survive."

This fact makes studying the disease in the laboratory rather complex. But over the past 15 years, the models that have emerged, flawed though they may be, have yielded important insights into the biology of multiple myeloma.

MAKING A MODEL

Perhaps the simplest way to study cancer in an animal model is to inject cancer cells into an immune-deficient mouse and allow them to grow into tumours. This approach, called a xenograft model, is widely used to study many types of cancer, and in myeloma it can be a quick and inexpensive way to screen possible new drugs. A molecule that doesn't affect xenograft tumours is unlikely to work in patients with multiple myeloma, for example.

But myeloma xenografts are generated from lab-grown cell lines, which don't behave much like the primary multiple myeloma cells found in patients' bone marrow. They are more like cells from the most advanced, aggressive stage of the disease, called plasma cell leukaemia. Researchers want to arrest the disease before it gets to that point, however, when it is still confined to the bone marrow and growing slowly. This is difficult to model because it is hard to grow human primary myeloma cells in mouse bones.

Even so, mice can get a form of multiple myeloma. In the late 1970s, a Dutch gerontology researcher, Jiri Radl, noticed that mice of a particular strain occasionally developed the disease late in life. When Radl isolated these myeloma cells and injected them into young mice of the same strain, the cells colonized the bone marrow and caused myeloma. Repeating this process over and over again led to a group of myeloma animal models collectively known as 5TMM mice.

Several different types of 5TMM mice exist, each bearing tumour cells from a different original 'donor' and having specific characteristics. For example, 5T2MM mice develop bone disease very similar to that of human myeloma, says Karin Vanderkerken, professor of haematology and immunology at Vrije Universiteit Brussel in Belgium. Vanderkerken has led extensive studies of 5TMM mice — primarily the 5T2MM and 5T33MM strains — in order to unravel the large variety of cells and molecules involved when myeloma cells travel to, enter and establish themselves in the bone marrow.

Vanderkerken and colleagues have found that this process, called homing, involves a high degree of redundancy. Blocking one pathway will not stop the process, she says. "But if you combine several different ones then you can block it."

More recently, Vanderkerken's studies have pointed in a new therapeutic direction. In 5T33MM mice, her team found that the bone marrow surrounding multiple myeloma cells is much lower in oxygen than the bone marrow around healthy cells[2]. Low oxygen, or hypoxia, is known to play a role in other forms of cancer, but this was the first evidence of it in multiple myeloma. Further studies showed that TH-302, a drug that is activated by hypoxia and that is

being investigated in clinical trials for other types of cancer, caused the death of multiple myeloma cells in the bone marrow of 5T33MM mice.

TRANSGENIC MICE

Vanderkerken acknowledges that using 5TMM mice has its downsides. In humans, myeloma is highly variable in terms of both genetics and tumour behaviour. Because 5T2MM mice all have myeloma cells derived from the same original donor mouse, however, they fail to capture this variability. "One of the limitations is that we work with two models [5T2MM and 5T33MM], so we have two 'patients'," Vanderkerken says. That simply isn't enough.

To explore the genetics of multiple myeloma, researchers have turned to transgenic models, in which mice are genetically engineered to have changes in myeloma-related genes. For example, one transgenic mouse model expresses abnormally high levels of XBP-1s, a protein involved in the differentiation of B cells, from which myeloma is eventually derived. Many of these mice develop a precursor condition called MGUS (monoclonal gammopathy of undetermined significance) and some of the mice develop myeloma at around one year of age[3].

In another transgenic model, researchers spliced the human *MYC* gene into mouse DNA near genes related to the production of antibodies[4]. As they ramp up antibody production, B cells undergo rapid DNA changes. In the mice, these changes can lead to the *MYC* gene being turned on and the onset of myeloma. Rearrangements, or translocations, of DNA are thought to give rise to myeloma in humans, says Leif Bergsagel, professor of medicine at the Mayo Clinic in Arizona, who led the development of the *MYC* mouse model. "This mouse reproduces that effect."

The *MYC* oncogene has a well-known role in other cancers, being involved in the rapid cell proliferation of many tumours. But because myeloma cells divide slowly, researchers had believed that *MYC* had only a minor role in the disease. "I think we give the cells just enough *MYC* to observe this oncogenic role without really becoming proliferative," says molecular biologist Marta Chesi, who is married to Bergsagel and works with him at the Mayo Clinic.

The researchers say the *MYC* model could be used to test potential myeloma drugs. Studies of existing cancer drugs have shown that "drugs that work in the clinic work in the mice, and drugs that do not work in the clinic do not work in the mice," Chesi says. "It's highly predictive."

MORE HUMAN

Transgenic mice and mice with myeloma are useful tools, but they are still mice, and some research questions need human cells. For these studies they have used a model known as SCID-hu, in which small pieces of human fetal bone are implanted under the skin of immune-deficient mice[5]. The SCID-synth-hu model developed by Tassone and colleagues is a variation on this.

The SCID-hu model was first developed in the late 1980s for studying normal blood cell formation in bone marrow. Myeloma specialist Joshua Epstein at the University of Arkansas for Medical Sciences in Little Rock soon realized that this approach might also enable him to study abnormal events in the bone marrow, such as myeloma.

Epstein's goal was to answer one of the field's most contentious questions: what kind of cell gives rise to myeloma? At the time, scientists knew that myeloma was related to B cells, but didn't know if it arose from antibody-producing plasma cells or a precursor, such as a B cell. "No other cells in the bone marrow or the blood could cause myeloma other than these mature plasma cells in our model," Epstein says (see "Testing ground for cancer stem cells', page S43). His team implanted two fetal bones in a single mouse and injected myeloma cells into just one of them. Eventually, the myeloma cells colonized the second bone — but couldn't be found anywhere else in the mouse. "So we had a model in which we could show that myeloma cells depend on the human microenvironment," Epstein says. These findings cemented the importance of the bone-marrow microenvironment in myeloma (see 'Neighbourhood watch', page S48).

Other groups also began working with SCID-hu. In one series of studies, researchers showed that the molecule DKK1, produced by myeloma cells, plays a crucial role in causing the disease's characteristic bone damage by inhibiting bone-forming cells called osteoblasts. In SCID-hu mice, an antibody to DKK1 mitigates the bone disease and inhibits myeloma cell growth[6]. "The perfect model to test this was the SCID-hu model," says Munshi, who led these studies.

But the interest in using SCID-hu led to competition for a limited supply of fetal bones. Tassone's model incorporating synthetic bone scaffolds provides a solution. When production of the synthetic bones is scaled up, Tassone says, more researchers will be able to conduct larger studies than is now possible. And because the synthetic bones are all identical, these studies will be more uniform than those based on fetal bones.

"If it all works out, this will be a great model," says Vanderkerken. But she and others caution that the SCID-synth-hu approach is still new and largely untested.

Even if the model does catch on, it will not necessarily render other animal models of multiple myeloma irrelevant. The SCID-hu model and its variations are good for studying the human microenvironment, for example, even though they can't capture the role of the immune system in responding to this form of cancer. As Epstein puts it: "Each model has its purpose." ■

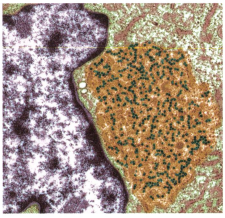

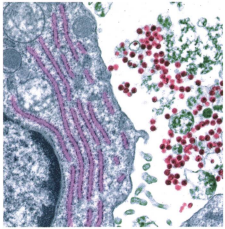

Hybridomas produced by fusing plasma cells with myeloma cells and used to test for antibodies.

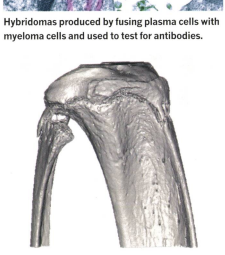

Micro-CT scans reveal bone damage from myeloma in a 5T2MM-bearing mouse.

Sarah DeWeerdt *is a science writer based in Seattle, Washington.*

1. Calimeri, T. *et al. Leukemia* **25,** 707–737 (2011).
2. Hu, J. *et al. Blood* **116,** 1524–1527 (2010).
3. Carrasco, D. R. *et al. Cancer Cell* **11,** 349–360 (2007).
4. Chesi, M. *et al. Cancer Cell* **13,** 167–180 (2008).
5. Yaccoby, S., Barlogie, B. & Epstein, J. *et al. Blood* **92,** 2908–2913 (1998).
6. Fulciniti, M. *et al. Blood* **114,** 371–379 (2009).

STEVE GSCHMEISSNER/SCIENCE PHOTO LIBRARY
PETER CIRCUCHER & KARIN VANDERKERKEN

MILLENNIUM PHARMACEUTICALS

Looking good: researchers are starting to see results in their search for improved drugs.

DRUGS

More shots on target

Drugs introduced to fight multiple myeloma in the past decade have revolutionized treatment and extended patients' lives. Are the improvements set to continue?

BY ADRIANNE APPEL

Multiple myeloma is a confounding disease to treat. More often than not, treatment seems to be effective, only for the blood malignancy to come roaring back months or years later. Most patients go through four, five or even more rounds of potent drug treatment in their struggle against mounting myeloma cells and increasing drug side effects.

But two classes of drug that became available in the past decade — proteasome inhibitors and immunomodulators — have been far more effective than any previous drugs against this form of cancer. Just three of these new drugs have so far been licensed — a proteasome inhibitor called bortezomib and two immunomodulatory drugs, thalidomide and its cousin lenalidomide — with additional drugs currently in clinical trials.

In the 1990s, the median survival time of patients whose only option was conventional chemotherapy was just three years. The new drugs extended this to five years. Furthermore, "90% of patients respond, while it used to be 65%," says haematological oncologist Keith Stewart of the Mayo Clinic in Scottsdale, Arizona. "They get immediate pain relief. They get into remission faster and they stay in remission longer." More people with multiple myeloma, especially those under 65 years of age, can expect to live 10 years or more with the disease, he says. These younger patients generally receive bortezomib intravenously, often as a first treatment in a two- or three-drug combination with a conventional chemotherapy drug, a strategy based on research showing that hitting myeloma early and hard gives a better chance of remission. Younger patients can also undergo autologous stem-cell transplants in a bid to get them into remission (see 'Transplants on trial', page S46).

Patients aged 70 and older in the United States, or 65 and older in Europe, are ineligible for stem-cell transplants and are often too fragile to tolerate intravenous drugs. Their treatments are focused on oral drugs such as thalidomide and lenalidomide, as well as conventional chemotherapy. But the myeloma nearly always returns after several months or years, requiring another round of drugs. Each time the cancer comes back, the treatment options are further narrowed, as the myeloma cells develop resistance to more of the available drugs.

PROTEASOME INHIBITORS

The development of bortezomib sprang directly from basic research on the cell and has helped build the multi-lane research highway that has now delivered several second-generation proteasome inhibitors to clinical trials.

In multiple myeloma, plasma cells reproduce furiously, creating piles of damaged proteins that must be cleared from the cell. Protein complexes called proteasomes normally remove them, aided by enzymes that slice up the amino-acid chains. But in myeloma cells, this proteasome,

known as 26S, can barely keep up with demand, suggesting a weakness that could be exploited. In 1993, Alfred Goldberg, a cell biologist at Harvard Medical School in Boston, Massachusetts, created the first proteasome inhibitor, MG132. It worked by interfering with protein clearing. Myeloma cells, which are already awash with damaged proteins, proved particularly vulnerable to MG132 and would suffocate in their own waste protein. Further refinement of MG132 led to bortezomib and the other proteasome inhibitors now in development.

Early trials of bortezomib hinted at its effectiveness, particularly against myeloma cells that were already resistant to conventional chemotherapy. The drug demonstrated "remarkable activity against myeloma in a phase I trial", recalls Kenneth Anderson, director of the haematologic neoplasias division at Harvard Medical School in Boston, Massachusetts. When his phase II trial showed bortezomib to be twice as effective as the standard therapy for multiple myeloma, he successfully petitioned the US Food and Drug Administration (FDA) in 2003 for fast-track approval to use it on patients who had exhausted other possible treatments. In 2008, bortezomib (marketed as Velcade by Millennium Pharmaceuticals of Cambridge, Massachusetts) became the standard drug to treat multiple myeloma.

But bortezomib has some serious side effects. It often causes severe nausea, and can aggravate and cause problems in the heart, lungs and kidneys. It can also induce pain or tingling in the feet and hands. More than 40% of patients are afflicted with this peripheral neuropathy, and 13% are debilitated by the symptoms. So onerous are these side effects that many patients give up on the drug before completing a full course. The neuropathy is probably associated with bortezomib's sloppy mechanism. Although it is intended to target a particular enzyme called the chymotrypsin-like protease enzyme, it can also disrupt the proteasome's two other enzymes. And as with other drugs for multiple myeloma, nearly all patients develop resistance to bortezomib.

Alternative proteasome inhibitors are already in clinical trials, and one — carfilzomib — is nearing approval. Developed by Onyx Pharmaceuticals of South San Francisco, California, carfilzomib is now in phase III trials. It works in much the same way as bortezomib, but has one clear advantage: fewer than 1% of patients experience neuropathy. Like bortezomib, carfilzomib acts on the chymotrypsin-like protease enzyme, but it is more selective than bortezomib and doesn't hit the 26S proteasome's other two enzymes. It should soon receive FDA approval for use by patients who have become resistant to bortezomib and lenalidomide, Stewart says.

NATURE.COM
For some of the latest research on multiple myeloma:
go.nature.com/9yatax

Another next-generation proteasome inhibitor — MLN9708, developed by Millennium Pharmaceuticals — also shows a low association with neuropathy, probably because it accurately targets the chymotrypsin-like enzyme. Now in phase I and phase II trials for relapsed patients and in combination with other drugs for newly diagnosed patients, MLN9708 is "very effective in overcoming bortezomib resistance", says Anderson, whose lab is investigating the drug. Unlike the other proteasome inhibitors, MLN9708 can be taken orally. Anderson's lab is also working with NPI-0052, which was developed by Nereus Pharmaceuticals in San Diego, California, and is now in phase I trials. This drug hits not just one but all three inhibitors of the 26S proteasome, and easily overcomes bortezomib resistance. But it also gives patients a powerful dose of side effects, Anderson warns.

Other promising drugs include the oral proteasome inhibitor ONX 0912, which is being tested against solid tumours in phase I trials. A phase II trial in patients with multiple myeloma and other blood cancers will begin soon, according to the drug's developer, Onyx Pharmaceuticals. Another drug, CEP-18770, developed by Cephalon in Frazer, Pennsylvania, works in a similar way to bortezomib, and has about the same efficacy against multiple myeloma — but with less toxicity.

DISRUPTING A PROTEIN DISPOSAL OPERATION

Proteasome inhibitors such as bortezomib turn off the machinery that disposes of damaged proteins, causing myeloma cells to suffocate in their own waste. The drug targets the β5 (chymotrypsin-like) enzyme but also hits the β1 and β2 enzymes, causing side effects.

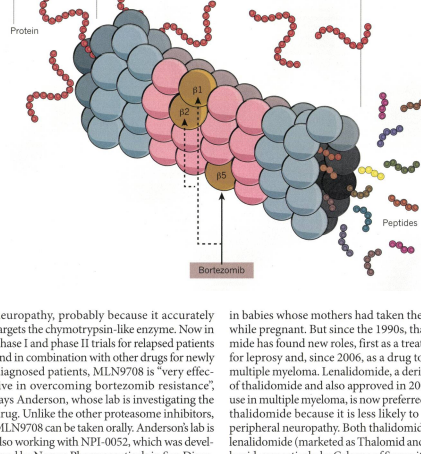

THE IMMUNOMODULATORS

From an unlikely start, a new category of drugs — the immunomodulators — has opened up fresh treatment options in multiple myeloma. The sedative thalidomide became notorious in the 1960s when it was linked to birth defects in babies whose mothers had taken the drug while pregnant. But since the 1990s, thalidomide has found new roles, first as a treatment for leprosy and, since 2006, as a drug to treat multiple myeloma. Lenalidomide, a derivative of thalidomide and also approved in 2006 for use in multiple myeloma, is now preferred over thalidomide because it is less likely to cause peripheral neuropathy. Both thalidomide and lenalidomide (marketed as Thalomid and Revlamid, respectively, by Celgene of Summit, New Jersey) fight multiple myeloma by reducing levels of cytokines, including the interleukin-6 (IL-6) protein. Because IL-6 helps malignant myeloma cells survive by inhibiting apoptosis (cell death), any drug that lowers IL-6 levels will diminish the cancer.

Thalidomide is approved for use in newly diagnosed patients, and is favoured for older patients who cope best with oral drugs. Lenalidomide is licensed for use in combination with the anti-inflammatory dexamethasone in patients who have previously been treated with other drugs, and is also used in newly diagnosed patients. For younger patients, adding bortezomib to the mix increases the benefit of lenalidomide: one 2010 study showed an almost 100% positive response to this combination by patients in an early stage of the disease, says Anderson, whose lab oversaw the trial. Even in advanced myeloma patients, 58% responded to the triple-drug therapy. Studies also are underway to test lenalidomide as a maintenance drug that relatively healthy

THE ECSTASY ALTERNATIVE

A notorious party drug aims to beat myeloma.

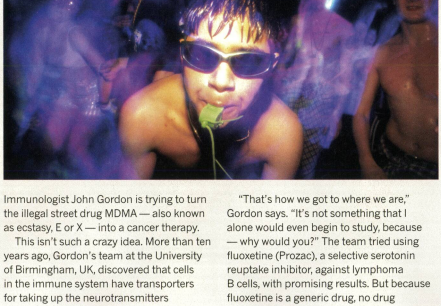

ARCLIGHT/ALAMY

Immunologist John Gordon is trying to turn the illegal street drug MDMA — also known as ecstasy, E or X — into a cancer therapy.

This isn't such a crazy idea. More than ten years ago, Gordon's team at the University of Birmingham, UK, discovered that cells in the immune system have transporters for taking up the neurotransmitters serotonin and dopamine, just like cells in the brain and central nervous system. They also found that these transporters allow some antidepressant drugs and MDMA (3,4-methylenedioxymethamphetamine) to enter.

Why can cells in the immune system do this? It's not something Gordon had considered until about ten years ago when it came up in discussions with his colleague Nicholas Barnes, a neuropharmacologist at Birmingham who studies serotonin. At the time, Gordon was investigating whether there was a relationship between brain neurochemicals and the combative attitude of cancer patients who beat their disease — a psychological state probably influenced by serotonin. Conversations between Gordon and Barnes led to a fresh line of enquiry about the immune system, brain chemicals and possible new cancer treatments.

The team knew they were on to something when they mixed serotonin in a test-tube with Burkitt's lymphoma cells, a type of B-cell cancer strongly associated with AIDS. Many of the cancer cells died: the serotonin had entered the cancerous immune cells and killed them. Gordon and Barnes speculated about the transport system for serotonin in immune-system cells, and wondered whether it could be exploited to deliver lethal levels of mood-altering drugs into cancers, particularly immune-cell cancers such as lymphoma, leukaemia and multiple myeloma.

"That's how we got to where we are," Gordon says. "It's not something that I alone would even begin to study, because — why would you?" The team tried using fluoxetine (Prozac), a selective serotonin reuptake inhibitor, against lymphoma B cells, with promising results. But because fluoxetine is a generic drug, no drug company stepped forward to further the research, Gordon says.

So Gordon switched to MDMA. Preliminary tests are encouraging, and the team, joined by pharmacologist Matthew Piggott of the University of Western Australia in Crawley, is now creating analogues to MDMA that are more potent cancer killers but are safe enough to be ingested. The idea is to limit the drug's neurotoxicity, and therefore its psychotropic activity, while increasing its anticancer action. At levels typically found in the street drug, "to kill the lymphoma you'd have to kill the patient", Gordon says.

Gordon modified the alpha-carbon site of MDMA by adding lipophilic aromatic rings, magnifying MDMA's cancer-killing potency 100-fold. This alteration also decreases MDMA's psychoactive affect, he reported in a paper published in August 2011. "As we add more aromatic rings, we see improved killing," he says. This effect suggests that the lipophilicity enhances the drug's ability to cross the cell membrane, allowing more of the drug to enter the cell.

Gordon estimates that his approach is at least five years away from preclinical testing. "We'll try a few more variants, and once we're pretty confident we have the optimal compound, that's when we'll go ahead," he says. By this point, Gordon believes, the cancer-killing MDMA analogues will have little psychoactive capacity left. **A.A.**

patients can take to keep their myeloma at bay.

But lenalidomide's future as a myeloma therapy is in question. A safety warning from the FDA in April 2011 cited studies showing an association between the drug and the later development of secondary cancers — a particular concern when treating younger patients. "It's a big problem for us," says haematologist Vincent Rajkumar of the Mayo Clinic in Rochester, Minnesota. "Secondary cancers can be devastating and we really need to know if overall survival is superior after taking lenalidomide."

The next generation of immunomodulatory drugs could mitigate these fears. Early trials at the Mayo Clinic suggested that pomalidomide was a safe and effective alternative for patients who develop resistance to lenalidomide and bortezomib. Two phase III trials of pomalidomide — being developed by Celgene as Actimid — are currently underway. The Nimbus trial will enrol 400 patients to study whether pomalidomide plus dexamethasone is more effective than dexamethasone alone in resistant patients. A sister trial will give pomalidomide alone to 85 people who failed to respond to the dexamethasone control in Nimbus. These trials will lay the groundwork for an application to the FDA to use pomalidomide in newly diagnosed patients. The drug is "enlarging treatment opportunities", says Antonio Palumbo, a haematologist at the University of Torino in Italy.

SUPPLANTING TRANSPLANTS

Some of the treatments being developed for multiple myeloma seem to be nearly as effective as stem-cell transplants, which are offered to younger patients as a highly effective but brutal treatment. Anderson says that many patients ask him if they really have to endure the gruelling procedure if today's drugs are almost as good.

The answer, Anderson says, is still yes, because most patients become resistant to medication, even though the drugs are getting better all the time. A combination of lenalidomide, bortezomib and dexamethasone was recently tested against stem-cell transplants in a 1,000-patient study in France. The trial showed equivalent response rates and better progression-free survival for the combination therapy than for the transplants, and has inspired a similar US trial, led by Anderson's lab.

The past decade's progress in developing drugs for multiple myeloma has led some to hope that this form of cancer will succumb to treatment in the not too distant future, as new proteasome inhibitors and immunomodulatory agents become available. Thanks largely to these drugs, says Stewart, "for many patients, multiple myeloma has become a chronic condition rather than a quickly fatal disease". ■

Adrianne Appel *is a science writer based in Boston, Massachusetts.*

GRAZIA LAM

TUMORIGENESIS

Testing ground for cancer stem cells

Multiple myeloma is the ideal disease to study a controversial theory about the biology of cancer — and how to cure it.

BY CATHRYN DELUDE

Why can drugs send patients with multiple myeloma into seemingly complete remission 80–90% of the time but never cure them? By all objective measures of the disease — malignant plasma cells in the bone marrow and aberrant M protein in the bloodstream — the cancer is eradicated. Yet patients nearly always relapse.

One possible explanation for this paradox comes from the compelling but controversial cancer stem-cell hypothesis. It states that the drugs kill the malignant plasma cells but leave a reservoir of cancer stem cells that continue growing and can produce more plasma cells. These cancer stem cells are largely untouched by current drugs, says oncologist William Matsui of the Sidney Kimmel Comprehensive Cancer Center at Johns Hopkins University in Baltimore, Maryland. If we had a way of killing these cells, he says, we could cure multiple myeloma.

The cancer stem-cell hypothesis contradicts the prevailing view that every cancer cell can create more cancer cells or tumours, a process known as tumorigenesis. Instead, according to the hypothesis, cancer consists of a cellular hierarchy. At the bottom, the bulk of tumour cells can cause disease symptoms but cannot maintain cancer growth or propagate new tumours, and they eventually die off. At the top, the long-lived cancer stem cells can renew themselves indefinitely and replenish bulk tumour cells, generate new tumours, and cause metastasis and relapse. Proponents of the cancer stem-cell idea say it explains why, in multiple myeloma and other cancers, drugs that can seem to miraculously and rapidly shrink tumours do not lead to long-term survival[1].

There is growing evidence that cancer stem cells exist in several cancers, says Max Wicha, a cancer biologist at the University of Michigan. But there is still no evidence that they can be targeted therapeutically, or that doing so would cure the disease or even prevent a relapse and prolong survival. These ideas can be tested, Wicha and others believe, in patients with multiple myeloma who have used existing drugs to achieve clinical remission, with all their cancerous plasma cells eradicated.

But efforts so far to identify multiple myeloma stem cells have been "loaded with controversy, emotion, scepticism and difference of opinion", says physician–researcher Constantine Mitsiades of the Dana-Farber Cancer Institute in Boston, Massachusetts, who is studying

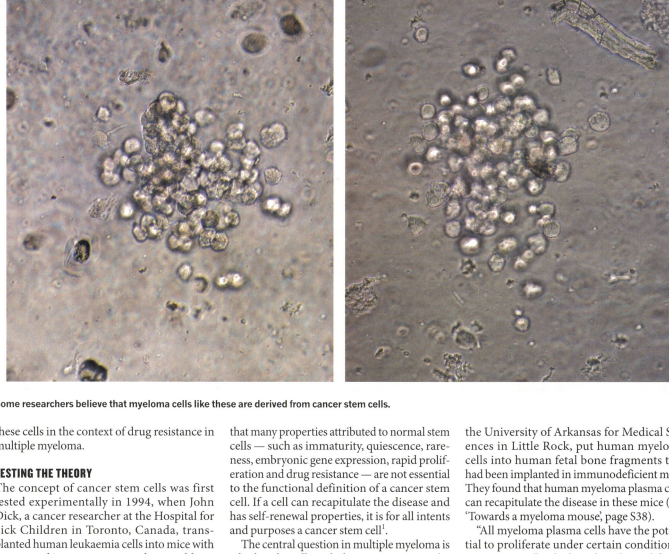

WILLIAM MATSUI

Some researchers believe that myeloma cells like these are derived from cancer stem cells.

these cells in the context of drug resistance in multiple myeloma.

TESTING THE THEORY

The concept of cancer stem cells was first tested experimentally in 1994, when John Dick, a cancer researcher at the Hospital for Sick Children in Toronto, Canada, transplanted human leukaemia cells into mice with suppressed immune systems that would not reject human cells. Only certain cells could recapitulate the original cancer, with its varied cell types, in a mouse. Harvesting these tumour cells and transplanting them into new mice again and again showed which cells could continue producing tumours without burning out. This method, called serial transplantation, is a functional assay that is still the standard for demonstrating two essential properties of cancer stem cells: the capacities to recapitulate the original tumour and to self-renew.

In the early days, Matsui explains, people thought that cancer stem cells were either normal stem cells that had turned cancerous, or primitive, undifferentiated progenitors that could give rise to many differentiated cell types, and that they must be exceedingly rare in the tumour. These assumptions led to confusion and debates about whether cells that were more differentiated, or less rare, could be considered cancer stem cells — a controversy that is particularly relevant to multiple myeloma. But researchers now generally agree that many properties attributed to normal stem cells — such as immaturity, quiescence, rareness, embryonic gene expression, rapid proliferation and drug resistance — are not essential to the functional definition of a cancer stem cell. If a cell can recapitulate the disease and has self-renewal properties, it is for all intents and purposes a cancer stem cell[1].

The central question in multiple myeloma is whether the cells with these properties — the ability to recapitulate the disease and to self-renew — are plasma cells or the B cells that give rise to plasma cells. Plasma cells are terminally differentiated cells derived from the B-cell lineage that produces our adaptive immunity as we encounter antigens. The debate has important clinical implications because it may take different kinds of drug to target plasma cells and B cells[2].

Proponents of the cancer stem-cell idea say it explains why drugs that shrink tumours do not lead to long-term survival.

By the late 1990s, several labs were using variations of the serial transplantation method on multiple myeloma. Some of the first transplant experiments refuted the notion of a subpopulation of myeloma cancer stem cells that is distinct from the plasma cells. Joshua Epstein and Shmuel Yaccoby, cancer cell biologists at the University of Arkansas for Medical Sciences in Little Rock, put human myeloma cells into human fetal bone fragments that had been implanted in immunodeficient mice. They found that human myeloma plasma cells can recapitulate the disease in these mice (see "Towards a myeloma mouse," page S38).

"All myeloma plasma cells have the potential to proliferate under certain conditions," Epstein says, "and when they do proliferate they change their phenotype to something that other people consider a stem cell." But he does not consider these cells to have self-renewal properties. Instead, he thinks they can maintain the disease and cause relapse because of the capacity of different plasma cells to temporarily acquire the ability to divide. Interestingly, the ability of cells to go in and out of various stem-cell-like states has recently been observed in other cancers.

TURNING TO B CELLS

Other researchers point to potential problems with the methodology, however. Linda Pilarski, an experimental oncologist at the University of Alberta in Edmonton, Canada, suggests that the fetal bone environment used by Epstein somehow supports the growth of myeloma plasma cells that normally live in adult bones. "The problem is, when you look in the bone marrow, plasma cells do not divide, so the cancer growth must come from an earlier cell that does divide," she says.

That earlier cell must come from a B-cell progenitor that gives rise to the plasma cells. B cells produce antibodies to a specific antigen, and one type of B cell, the memory B cell, provides long-term or even lifelong immunity to a particular antigen. It does so by continuing to give rise to new plasma cells that keep churning out the antibody to that antigen. Specifically, in response to an antigen, B cells undergo genetic mutations in which they rearrange an immunoglobulin gene in a unique sequence, conferring the 'memory' to memory B cells. The plasma cells derived from these memory B cells inherit the sequence and make antibodies specific to the antigen. In healthy people, the plasma cells produce different antibodies, but in patients with myeloma, all the plasma cells produce the same clone of an antibody: the M (monoclonal) protein. Pilarski says that this 'clonotypic' relationship between myeloma plasma cells and the precursor memory B cell could reveal the derivation of all the bulk tumour cells from a putative cancer stem cell.

In the early 2000s, Pilarski and her research partner, Andrew Belch, found that it was not the plasma cells but B-cell progenitors (although not necessarily memory B cells) that could self-renew and recapitulate new multiple myeloma tumours. Some previous research had suggested that B cells were involved in multiple myeloma, but no one had tested this idea, and Pilarski recalls that most researchers still assumed that plasma cells were the sole component of multiple myeloma.

The scepticism about her B-cell results forced her to do a more rigorous molecular analysis. In 2008, Pilarski, Belch and Julia Kirshner, then a postdoctoral fellow in Pilarski's lab, showed that a self-renewing population of B cells can give rise to myeloma plasma cells in their three-dimensional bone-marrow tissue model[1]. "We think these B-cell precursors really were cancer stem cells," she says, "and that this will be a useful therapeutic model."

Pilarski's next aim is to find a way of destroying the tumorigenic B cells. She is also investigating whether myeloma patients with higher levels of these cells relapse earlier. The preliminary evidence suggests that they do. "That tells you these early cells are very important, and very bad for the patient," she says.

In 2004, Matsui extended Pilarski's earlier findings by further defining the clonogenic myeloma cells as memory B cells. Some researchers objected to calling them stem cells because memory B cells do not give rise to a variety of differentiated cell types, a characteristic typical of other adult stem cells. However, Matsui points out, unlike other differentiated cells in the body, memory B cells have the capacity to self-renew because they can confer lifelong immunity. Also, because of the clonotypic relationship between myeloma plasma cells and earlier memory B cells, there can be no doubt that whatever the myeloma stem cell is, memory B cells are involved somehow. The uncertainty is whether the cancer stem cells started out as memory B cells and then de-differentiated to be more like the earlier B-cell progenitors, or whether they came from plasma-like cells that acquired some stem-cell-like properties but still retain the tell-tale genetic mutations of memory B cells.

NATURE.COM
For some of the latest research on multiple myeloma:
go.nature.com/za4zy7

SCRATCHING THE SURFACE

Further debate surrounds the combination of cell surface proteins, or markers, present on the putative myeloma stem cells. Researchers use these markers to sort cells for serial transplantation and other experiments, and to determine which are tumorigenic. Mature plasma cells, for example, have the CD138 marker, whereas CD20 and CD19 are the badges of a B cell. Matsui has shown that the myeloma stem cells lack CD138 but have CD20 and CD19, as well as CD27, which is found on memory B cells. However, these markers do not completely overlap with those identified by other labs.

If a cell can recapitulate the disease and has self-renewal properties, it is for all intents and purposes a cancer stem cell.

These disparate results may arise partly because different labs use different methods to investigate different stem-cell properties — they may be looking at the same phenomenon but from different angles. Researchers in other cancers have found that cancer cells can shed and acquire stem-cell markers depending on their growth cycle, and on such factors as their proximity to the microenvironment, the activity of the immune system, and exposure to drugs. This may be even more common in myeloma because there are so many distinct stages of the disease. Matsui says it is possible that markers differ not just from person to person, but also within the same person during the course of the disease.

The plasticity of cell surface markers could impede the translation of work to target cancer stem cells into the clinic. "How can clinical trials proceed without reliable markers to indicate if a therapy is targeting cancer stem cells?" asks Wicha. It is likely but not proven, he says, that in curable cancers such as testicular cancer, drugs happen to target both the bulk tumour cells and the cancer stem cells. Furthermore, autologous stem-cell replacement — the only treatment that has ever cured multiple myeloma — probably eliminates cancer stem cells. Despite achieving good results, the stem-cell procedure is generally considered a last resort, because of the risks it entails. "Everybody would greatly prefer if you could use treatments that didn't require a bone-marrow transplant," Wicha says. Many researchers are now investigating whether any drugs, or a combination of drugs, can target myeloma stem cells, or whether they are missing the target and new agents are needed.

A MEASURE OF SUCCESS

Gauging the success of a cancer stem-cell therapy poses its own problems. A clinical response to a drug is typically measured by tumour shrinkage. But the point of cancer stem-cell therapy is to prevent relapse and metastasis and to prolong survival — all outcomes that could take lengthy, large-scale clinical trials to demonstrate. It is therefore important to have an interim measure, such as reliable biomarkers to identify cancer stem cells. In this respect, multiple myeloma has another advantage: researchers can take repeat biopsies from patients' bone marrow and blood more easily than they can from a solid tumour in a lung, breast or brain. Indeed, it is common to take repeat biopsies to track the progress of the disease, and researchers can use these biopsies to track the effect of therapies on cancer stem cells. "This puts us way ahead of the curve compared to solid tumours," says Matsui, and this is one reason why some of the first trials to test the cancer stem-cell theory are in multiple myeloma.

Matsui discontinued one effort using rituximab, an antibody to CD20 that is used to treat lymphomas, after a small, 21-person phase II trial showed no improvement in progression-free survival compared with what might be expected with autologous stem-cell transplantation. Follow-up analysis showed that although the antibody targeted the putative myeloma stem cells, it did not kill them effectively. Matsui's collaborators are now analysing whether the therapy reduced the burden of circulating M protein or the number of putative myeloma stem cells in the patients' samples. Matsui and another team are separately using antibodies to CD20 linked to a radioactive molecule to make them more effective. Other monoclonal antibodies targeting other markers are also in development.

Killing myeloma stem cells will not be a replacement for therapies that target malignant plasma cells, which could kill the patient before the cancer stem-cell therapy has time to work. But targeting the cancer stem cells may turn short-term recoveries into long-term, disease-free survival. From a research standpoint, Wicha says, proving the cancer stem-cell theory in multiple myeloma is exciting because it could lead to a validation of the model for other cancers. There is increasing evidence that chasing cancer stem cells will ultimately be fruitful, he says. But the more we learn, the more we realize it is not straightforward. ■

Cathryn Delude *is a science writer based in Andover, Massachusetts.*

1. Clarke, M. F. *et al. Cancer Res.* **66,** 9339–9344 (2006).
2. Brennan, S. K. & Matsui, W. *J. Mol. Med.* **87,** 1079–1085 (2009).
3. Kirshner, J. *et al. Blood* **112,** 2935–2945 (2008).

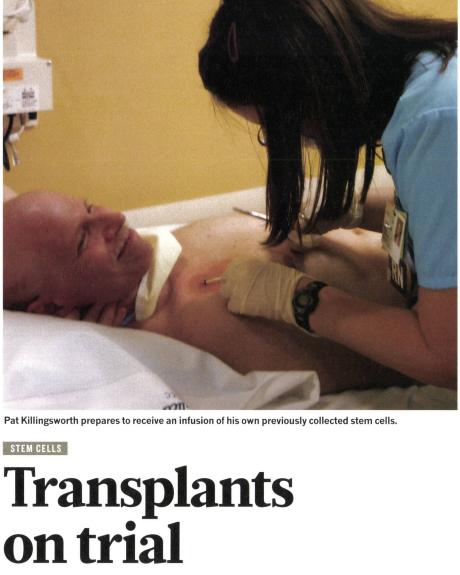

Pat Killingsworth prepares to receive an infusion of his own previously collected stem cells.

STEM CELLS

Transplants on trial

Stem-cell transplants are an important tool for treating myeloma. But with improved drug alternatives, doctors disagree about the best time to give the treatment.

BY ELIE DOLGIN

Pat Killingsworth was 51 when he learned that he had multiple myeloma. His oncologist, Steven Zeldenrust of the Mayo Clinic in Rochester, Minnesota, immediately gave him the latest combination of drugs: lenalidomide, a derivative of the immunomodulatory agent thalidomide that hit the market in 2004, and an older chemotherapy agent called dexamethasone. Four months later, the clinic harvested and banked millions of Killingsworth's blood stem cells in case he later needed a more extreme chemotherapy treatment that would destroy his bone marrow along with his cancer.

For almost three years, Killingsworth showed no signs of the disease, and his stem cells simply sat in the freezer. But in late 2010, the cancer started to creep back. Blood tests revealed rising levels of monoclonal protein — a hallmark of multiple myeloma — and X-rays exposed several lesions in the bones around his hips, sternum, ribs and head. "At that point, I said: 'It's time to get serious'," recalls Killingsworth, now semi-retired and living in Florida. "We need to transplant." This summer, he spent 16 days at the H. Lee Moffitt Cancer Center in Tampa, Florida, where he received high doses of chemotherapy with the drug melphalan to wipe out the myeloma cells, followed by a transfusion of his own banked stem cells to replace diseased or damaged bone marrow.

For weeks, he felt too nauseous to eat much or sleep through the night. But at least the stem-cell harvest itself was not much of an ordeal — doctors used to collect bone-marrow stem cells from people surgically under anaesthesia, but they now take stem cells from the blood in the same way that blood banks collect platelets. Unfortunately, the therapy didn't work, and Killingsworth's cancer levels spiked after the procedure — a rare event seen in about 2–3% of cases. "I was looking forward to years of drug-free normal living," says Killingsworth. "I did everything right, it just didn't take." In October 2011, he started a triple-drug regimen of lenalidomide, dexamethasone and the protease inhibitor bortezomib.

DIVIDED OPINION

For Killingsworth — author of the 2009 book *Living with Myeloma* and a patient's advocate for Millennium Pharmaceuticals in Cambridge, Massachusetts — waiting until he relapsed before undergoing the arduous stem-cell transplant with its concomitant high-dose chemotherapy was the right decision.

"I could have gotten it right away, but there's still no research evidence that doing so makes any difference," he says. "My cancer had over four years to become therapy-resistant, so I suppose you could argue that something like that could have happened, but you'd just be guessing." But myeloma specialists are still debating when to go ahead with such 'autologous' stem-cell transplants, so-called because they involve giving patients their own blood stem cells.

Treating people with multiple myeloma is the most common reason for autotransplants, with more than 10,000 operations performed annually in the United States alone. For younger melanoma patients — generally those under 65, although some medical centres also perform the therapy on older, medically fit individuals — transplants provide the best hope of stopping the cancer in its tracks. Some residual melanoma cells sometimes survive in the banked stem cells, so researchers are investigating whether they can use disease-free cells from healthy donors instead. But the high rates of tissue rejection associated with donor transplants have made autotransplants the standard for the field.

Even so, opinion is divided on the best treatment. Some myeloma specialists favour an aggressive treatment tactic, in which transplants are administered soon after diagnosis, when the disease is thought to be at its most vulnerable. Others opt for a milder protocol that reserves the hard-hitting transplant option — with its attendant risks of infection, bleeding and anaemia — as a last line of defence if less toxic therapies fail.

Investigations that compared early and late transplants indicated that both approaches extend people's lifespan by a comparable amount, normally one to two years on average[1,2]. But those studies were done before newer and more potent drugs, such as lenalidomide or the protease inhibitor bortezomib, were routinely

➲ NATURE.COM
For some of the latest research on multiple myeloma:
go.nature.com/z7p3ak

HEALTHSCIENCE/TIME/SPL

used (see 'More shots on target', page S40).

"Novel agents have really changed the way we think about transplant," says Kenneth Anderson, medical director of the Dana-Farber Cancer Institute's Kraft Family Blood Center in Boston, Massachusetts. "The question now is: if you have such a high extent and frequency of response to novel agents, does a transplant add value or not?"

TIMING THE TRANSPLANT

Some of the first trial data attempting to answer this question were presented in the summer of 2011 at the Congress of the European Hematology Association in London. In a study of 402 newly diagnosed patients, Antonio Palumbo, head of the myeloma unit at the University of Torino in Italy, found that 73% of people who underwent two rounds of high-dose chemotherapy and stem-cell transplantation were disease-free two years after treatment, compared with just 54% of those who received lenalidomide and conventional chemotherapy but no transplants. "Data are showing that transplant should be performed at diagnosis," says Palumbo, although he admits that long-term data are needed to see if there is any comparable effect on overall survival.

Two similar trials of 1,000 patients each are planned in the United States and Europe to compare the efficacy of stem-cell transplants with new drugs and to determine whether delaying transplants, as Killingsworth did, makes any difference to patient outcomes. Those results won't be known for many years, however. In the meantime, researchers who study multiple myeloma remain divided about when, if and how to use transplantation therapy. "The burning question is: do we need to give transplants to patients up front or [should] we use new treatments?" says Philippe Moreau, a haemotologist at the University Hospital of Nantes in France. "The novel agents are really changing the scenario."

Mayo Clinic haematologist Vincent Rajkumar argues that much of the debate boils down to a fundamental difference of opinion over the end goal of myeloma treatment. "What's happening in myeloma is really a clash of philosophies about whether this disease is curable or not," he says.

Those who believe it can be cured generally come in all guns blazing in the hopes of hitting the cancer hard and early, before secondary mutations kick in or tumours adapt to their microenvironments, which would make treatment even more difficult. They tend to use stem-cell transplants within months of diagnosis, sometimes in two back-to-back procedures, while simultaneously applying all the available therapeutic options.

According to Michele Cavo, a haematologist at the University of Bologna in Italy, this is the approach favoured by most doctors in Europe. "European physicians," he says, "prefer not to postpone transplant until the time of relapse." The aggressive tactic has some supporters in the United States too, notably Bart Barlogie, director of the Myeloma Institute for Research and Therapy at the University of Arkansas for Medical Sciences. "When you give everything up front you can have superior success," Barlogie says.

TOTAL THERAPY

Since 1990, Barlogie has advanced a provocatively titled treatment called 'total therapy', which involves a battery of chemotherapy drugs for a few months before giving patients two rounds of stem-cell transplantation. Using his procedure, he says, "we actually have been able to cure people with myeloma". Of the 231 people who received the first version of the therapy more than two decades ago — and so did not receive the recently approved drugs — around 50 are still alive, half of whom have never seen their cancer recur[1].

Over the years, Barlogie and his colleagues have updated their protocols to incorporate newer drugs, and have even found a gene signature in myeloma cells that can reliably identify who will respond well to the therapy and who will not. By focusing on only those myeloma patients expected to respond, the Arkansas team reported last year that almost 90% of the recipients of the latest incarnation of total therapy — which incorporates lenalidomide, thalidomide and dexamethasone — showed no signs of myeloma for at least four years after treatment. By using mathematical models that incorporate long-term data from previous versions of total therapy, the researchers estimate that about half of all patients will have beaten the cancer for good[1].

Researchers remain divided about when, if and how to use transplants.

"We believe this is a paradigm-shifting reality," says Arkansas molecular biologist John Shaughnessy, who with Barlogie founded a molecular diagnostics company called Myeloma Health (now a subsidiary of New York-based Signal Genetics) to commercialize the genomic profile test. "Total therapy has revealed that cure is a possibility," Shaughnessy says.

But not everyone shares this view. Survival curves in similar blood cancers, such as leukaemia and lymphoma, level out over time — the hallmark of a cure in the cancer field. This doesn't happen in patients undergoing treatment for multiple myeloma. So Rajkumar argues that some myeloma researchers are "widening the goalposts" by interpreting the word 'cure' to mean achieving in some patients a state of 'sustained complete response', defined as a long-term absence of a series of molecular markers.

For those who believe that a cure is the goal of therapy, sustained complete response is a necessary first step, and high rates of complete response generally require intensive treatment. This leads many physicians to use more aggressive therapies, including early or repeat transplants, which can produce serious side effects such as blood clots and nerve damage.

But many doctors don't accept this definition of 'cure'. And some are quick to point out that such cures have been achieved in some patients with multiple myeloma treated with protocols that are far less aggressive than total therapy. Many doctors are therefore unwilling to risk their patients' quality of life for an unproven cure, especially those who are responding well to more moderate therapies.

PATIENT CHOICE

Jean-Paul Fermand, a haematologist at the Hôpital Saint-Louis in Paris, sees another problem with the aggressive approach: the evolution of multidrug resistance. "If you use all the tools that you have at your disposal, there are risks of toxicity and of the tumour cells acquiring resistance against different classes of therapeutic agents," he says. "And then if a relapse occurs, you have no therapeutic options and the patient will die."

For this reason, clinical trials aside, many doctors use a sequential approach instead of total therapy, and emphasize the balance between treatment efficacy and the patient's quality of life. They often use the least toxic regimens first and let patients decide for themselves when to perform the transplant. "I can't look you in the eye and say I know what's going to make you live longer because those trials haven't been done," Rajkumar says. "So we're willing to allow a lot of patient autonomy in making that call."

Some doctors go even further, only using stem-cell transplants when nothing else seems to work. "I don't think transplants are worthwhile," says James Berenson, medical and scientific director of the Institute for Myeloma and Bone Cancer Research in West Hollywood, California. "You have to think long and hard about what you're doing to the patient and how [a stem-cell transplant] affects their long-term outcome."

For Dennis Dinger, a retired ceramics engineer in Clemson, South Carolina, who was diagnosed with myeloma a week after turning 60, the long-lasting side effects of stem-cell transplant are a reality of everyday life. Dinger started a protocol akin to total therapy in 2008 at St Francis Hospital in Greenville but had only one stem-cell transplant before heart problems and nerve damage cut his therapy short. Even so, Dinger, now 63 and the author of the 2010 book *My Bout with Multiple Myeloma*, has no regrets. "I can live with my fingers and toes not feeling right, and I wasn't all that active anyway, so the fact that my heart is not the equivalent of a marathon runner's is not a big deal to me," he says. "But the fact that the cancer is gone — that's the big deal."

Another big deal will come when doctors agree on guidelines for best practice. But like so much else relating to stem-cell transplants, the question is: will the consensus come sooner or later? ■

Elie Dolgin *is a news editor with* Nature Medicine.

1. Fermand, J. P. *et al. Blood* **92,** 3131–3136 (1998).
2. Barlogie, B. *et al. J. Clin. Oncol.* **24,** 929–936 (2006).
3. Barlogie, B. *et al. Br. J. Haematol.* **135,** 158–164 (2006).
4. Nair, B. *et al. Blood* **115,** 4168–4173 (2010).
5. Björkstrand, B. *et al. J. Clin. Oncol.* **29,** 3016–3022 (2011).
6. Krishnan, A. *et al. Lancet Oncol.* doi:10.1016/S1470-2045(11)70243-1 (2011).

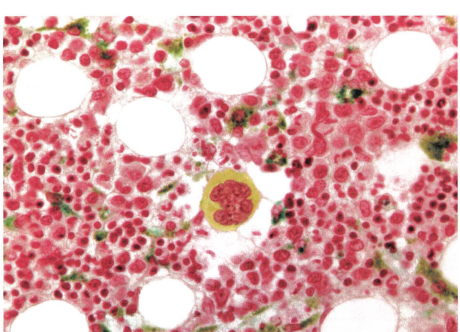

STEVE GSCHMEISSNER/SCIENCE PHOTO LIBRARY

Bone marrow contains a rich variety of cells and structures that might affect the growth of cancer.

MICROENVIRONMENT

Neighbourhood watch

In the fight against myeloma, researchers are investigating its interactions with molecular neighbours in the bone marrow.

BY VIRGINIA HUGHES

A tight budget in William Dalton's lab in the mid-1990s led to a major discovery. His group was investigating the drug resistance that inevitably occurred in patients with multiple myeloma, a cancer affecting blood plasma cells. When isolated in the lab, these cancer cells responded to treatment. So what happened in the body to make them drug resistant?

Dalton had a hunch that it was somehow connected with myeloma's home in the bone marrow, the spongy, bright-red tissue deep inside the bone that holds a motley mix of blood cells, chemicals, fats and proteins. The part he was most interested in was the extracellular matrix, a web of supportive proteins including collagen and fibronectin. "To be honest, fibronectin is cheaper than collagen, so we decided to study fibronectin," says Dalton, who is now chief executive of the Moffitt Cancer Center in Tampa, Florida. It turned out to be a good choice.

The researchers placed myeloma cells in liquid suspension, either in a clean flask or in one coated with fibronectin. Myeloma cells in the uncoated flask died when exposed to two common cancer drugs. In contrast, the cells in the coated flask attached to the fibronectin, as if they were homing into the bone marrow, and were able to survive the chemical onslaught.

This work[1], published in 1999, was a milestone in the study of myeloma's microenvironment. Until the late 1980s, myeloma researchers had studied cancer cells largely in isolation because the bone marrow's complexity is difficult to mimic in the lab. Since then, thanks to improved cellular and animal models, researchers have taken a closer look at the way myeloma exploits its many neighbours in the marrow, opening the way to new treatments.

"There's a growing recognition that cancer has no respect for its neighbourhood — it hijacks it," Dalton says. "We've got to create models that consider this microenvironment and then start looking at new drugs and targets using this more complex model."

MAKING CONTACT

The bone marrow is a colourful neighbourhood, with residents young and old, fast and slow, transient and permanent. It holds stem cells, in all stages of differentiation, and their many descendants, including blood cells and bone cells. When one particular long-lived blood cell, a plasma cell, acquires a certain combination of genetic mutations, it leads to the unchecked growth of myeloma. The cancer cells and their healthy counterparts occupy the same niche in the bone marrow, along with signalling molecules of the immune system called cytokines, supportive proteins such as fibronectin and collagen, and other blood cells.

"It appears to be a cluster of cells that for some reason are drawn together," says Kelvin Lee, chair of immunology at the Roswell Park Cancer Institute in Buffalo, New York. "You have all these things going on at the same time, in that niche, and so then that raises the question: do all those cells talk to each other?"

In the first models of myeloma's microenvironment, researchers studied a cancer cell's interaction with one neighbour at a time. This was the strategy that led Dalton to his discovery that myeloma can resist attack by sticking to fibronectin. Using a similar approach, several studies in the 1990s and early 2000s showed that when myeloma binds to various neighbours, it spurs them to produce growth factors that benefit the cancer cell. In one of the most studied examples, myeloma binds to the microenvironment's stroma (a catch-all term for many types of blood cell), causing the stroma cells to secrete interleukin-6 (IL-6), which in turn stimulates the cancer cells to proliferate[2].

More recently, with the help of genetic screening techniques, researchers have started to unravel exactly how contact with the microenvironment changes the cancer cell's genetic program. They have found, for example, that attachment to cells in the stroma can activate biochemical pathways that result in cancer proliferation and migration, blood-vessel growth, further adhesion to microenvironment cells, and the breakdown of bone. A recent study suggests that myeloma can trigger cells in the microenvironment to produce an enzyme that suppresses the activation of T cells — soldier cells of the immune system that would otherwise help the body to fight the cancer. "The myeloma cells are inducing the microenvironment to generate this immunosuppressive force field around them," says Lee, who led the study.

Intriguingly, it seems that these interactions with the microenvironment are the same in myeloma's healthy counterparts, the plasma cells. The difference is that myeloma has a mysterious way of expanding into more supportive niches, allowing it to grow unchecked. "Normal

COLOURFUL NEIGHBOURHOOD

Myeloma cells live in the bone marrow, the spongy, bright-red tissue deep inside the bone that holds a motley mix of blood cells, immune molecules, fats and proteins.

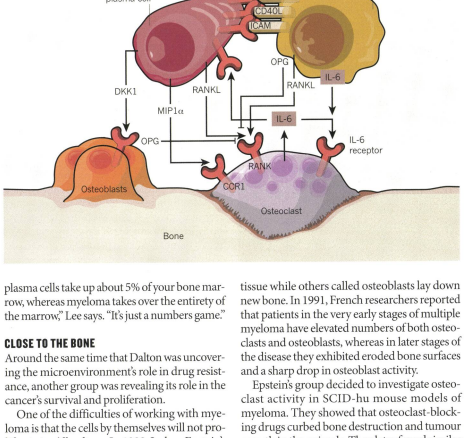

plasma cells take up about 5% of your bone marrow, whereas myeloma takes over the entirety of the marrow," Lee says. "It's just a numbers game."

CLOSE TO THE BONE

Around the same time that Dalton was uncovering the microenvironment's role in drug resistance, another group was revealing its role in the cancer's survival and proliferation.

One of the difficulties of working with myeloma is that the cells by themselves will not proliferate in cell culture. In 1998, Joshua Epstein's group at the University of Arkansas for Medical Sciences in Little Rock discovered how to make them grow inside a mouse — albeit an odd one[3].

The researchers used a newly developed mouse model called SCID-hu, in which a piece of human bone is implanted under the skin of immune-deficient mice (see 'Towards a myeloma mouse', page S38). Epstein injected these animals with fresh bone-marrow cells from patients with multiple myeloma. "Lo and behold, the bones developed myeloma," says Epstein. "It became very clear to us that the tumour cells depend on the human bone-marrow microenvironment, because they wouldn't grow anywhere else."

The SCID-hu model allowed Epstein to investigate which part of the microenvironment was helping the cells to thrive. He first focused on the cells that were already known to change with myeloma growth in patients: bone cells. Myeloma degrades bone by interfering with the crucial process of bone remodelling. Normally, cells called osteoclasts clear away old bone tissue while others called osteoblasts lay down new bone. In 1991, French researchers reported that patients in the very early stages of multiple myeloma have elevated numbers of both osteoclasts and osteoblasts, whereas in later stages of the disease they exhibited eroded bone surfaces and a sharp drop in osteoblast activity.

NATURE.COM
For some of the latest research on multiple myeloma:
go.nature.com/batynj

Epstein's group decided to investigate osteoclast activity in SCID-hu mouse models of myeloma. They showed that osteoclast-blocking drugs curbed bone destruction and tumour growth in the animals. They later found similar improvements by injecting the mice with osteoblast progenitor cells.

This research highlights what Epstein calls the "dangerous tango" of bone cells and cancer cells. "This is evidence that all the changes in bone metabolism that myeloma induces are not a simple manifestation or by-product, but rather an integral part of the disease," he says.

TREATMENT IMPLICATIONS

The growing interest in the myeloma microenvironment has led researchers to take a new approach to treatments. Rather than targeting the myeloma cells — whose genetic instability allows them to mutate quickly to evade drugs — why not go after their cellular neighbours?

Several groups of researchers are studying immune cells in the stroma called dendritic cells, for example. In 2007, Lee found that when myeloma cells encounter dendritic cells, the myeloma cells produce CD28, a signalling molecule in the immune system. CD28 then protects the myeloma from cancer drugs.

This was an exciting discovery, Lee says, because CD28 and similar molecules have long-established roles in the immune system and have already been targets of drugs used to treat rheumatoid arthritis and organ transplant rejection. "I suspect there is a whole bucketload of drugs that the rheumatologists and organ-transplant folks have been using that will be active in multiple myeloma," he says.

Kenneth Anderson, director of the Jerome Lipper Multiple Myeloma Center at the Dana-Farber Cancer Institute in Boston, Massachusetts, has taken an interest in another resident of the stroma: the plasmacytoid dendritic cell. In 2009, Anderson's team reported that in myeloma, plasmacytoid dendritic cells are immature and fail to trigger the host's immune response, allowing myeloma to thrive. Targeting these dendritic cells with pieces of synthetic DNA called CpG oligodeoxynucleotides can restore their development and dampen myeloma's ability to acquire drug resistance. The CpG oligodeoxynucleotides "don't have any direct action on the tumour itself", says Anderson. "It's a really good example of targeting only the microenvironment and having an effect on the tumour."

But because the microenvironment has so many influential characters, approaches that target only one aren't likely to have much effect. For example, after the early discoveries that IL-6 stimulates the growth of myeloma, Dalton and others tested methods of suppressing IL-6. Unfortunately, this approach "hasn't panned out to be, by itself, a very successful target therapeutically", says Ken Shain, one of Dalton's colleagues at the Moffitt Cancer Center.

So researchers have expanded the number of neighbours they study at the same time. Anderson, working with Dana-Farber colleague Constantine Mitsiades, last year published a method for screening drug candidates against myeloma cells in the presence of stromal cells. "The spectrum of potential therapeutic targets is vastly expanded by virtue of having the ability to study the tumour cell–host interaction," he says.

Dalton has also moved away from studying individual neighbours — such as fibronectin — to looking at the entire street. Dalton and Shain showed in 2009 that myeloma cells in the presence of both fibronectin and IL-6 activate a slew of pathways that are not turned on when either neighbour is there alone. They are now working with bioinformatics experts to create mathematical models that can account for multiple factors at the same time and so potentially predict how the various neighbours interact.

"It's exciting because it's starting to give us clues about how we would eventually combine therapies to interfere with the microenvironment's influence," Dalton says. "As my mathematician colleagues tell me, we've got to embrace the complexity and not run away from it." ■

Virginia Hughes *is a science writer based in Brooklyn, New York.*

1. Damiano J. S. *et al. Blood* **93,** 1658–1667 (1999).
2. Uchiyama, H. *et al. Blood* **82,** 3712–3720 (1993).
3. Yaccoby, S. *et al. Blood* **92,** 2908–2913 (1998).

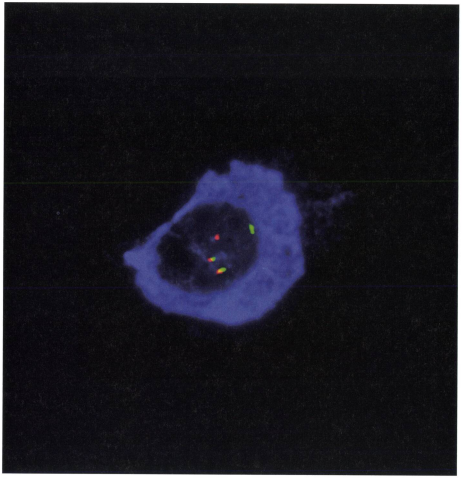

RAFAEL FONSECA

A common aberration is a switching of parts chromosomes 14 and 11 (shown here in red and green)

GENETICS

Profiling a shape-shifter

Unlocking the genetic secrets of multiple myeloma could reveal new ways to attack this killer disease.

BY COURTNEY HUMPHRIES

In the chain of events leading to multiple myeloma, two factors seem to dictate the disease process: the internal genetic alterations within cancerous plasma cells, and their external environment in the bone marrow. Nikhil Munshi, who studies myeloma at the Dana-Farber Cancer Institute in Boston, Massachusetts, says that although the cells' environment is important, "most of the tumour behaviour is predetermined by the genetic make-up". Multiple myeloma is more prevalent in African Americans, for example, and sometimes seems to be inherited in families, but even so, most of its genetic aberrations arise independently.

Understanding the nature of these genetic abnormalities has been the focus of decades of research. Tools that characterize the cancer cells at the molecular level have been useful for classifying patients, determining the severity of the disease, and guiding treatment strategies.

But multiple myeloma poses a daunting challenge for scientists. It takes many forms, and patients who have the disease can experience very different symptoms, disease courses and responses to treatments. Indeed, the variability extends to the tumours themselves. Genomics has led to fresh discoveries — and more complexity. "The more sophisticated the genomic technology becomes, the more heterogeneity we've identified," says Kenneth Anderson, head of haematologic neoplasias at the Dana-Farber Cancer Institute in Boston, Massachusetts.

LOST IN TRANSLATION

Multiple myeloma stands apart from other cancers in always being preceded by an identifiable premalignant state, called 'monoclonal gammopathy of undetermined significance' (MGUS). This window into the early stages of the disease provides an opportunity for scientists to study patients who are at risk of developing myeloma and to tease apart the genetic differences between the benign condition and the disease. These studies, along with research on patients at different stages of disease, have shown that myeloma unfolds in a stepwise progression as the genetic abnormalities accumulate.

In myeloma, antibody-producing B cells often acquire extra copies of chromosomes and genetic translocations across chromosomes. Most of the translocations involve chromosome 14, at the immunoglobulin switch region, which normally allows B cells to control which antibody, or immunoglobulin, they produce. As a result, immunoglobulin production is increased.

Leif Bergsagel, a haematological oncologist at the Mayo Clinic in Scottsdale, Arizona, explains that these early 'primary events' all activate cyclin-dependent kinases, which control the cell cycle. The aberrant activation of these kinases, he says, is "a unifying event in the pathogenesis of the disease". Further genetic abnormalities unfold as the disease progresses, including mutations that activate the *RAS* oncogene, switch on the transcription factor NF-κB, dysregulate the transcription factor Myc, or inactivate the tumour-suppressor protein p53. One of the most notable characteristics of these mutations is that none of them are common to all patients — or even most patients. This variation has made it possible to stratify patients into at least six different disease subgroups, and to separate them according to low, high or intermediate risk. More recently, gene expression profiling has also been used to identify high-risk patients, who constitute about 15% of newly diagnosed patients.

Getting a clear picture of the disease's various forms should yield better ways to classify patients, choose treatments and develop drugs. "There's a growing conviction in the cancer community that the path to better therapies for multiple myeloma is to identify the root causes of the disease," however multifactorial they are, says Todd Golub, a genomic-medicine specialist at Dana-Farber and director of the cancer programme at the Broad Institute in Cambridge, Massachusetts. "Historically, we've been doing that in a very *ad hoc* fashion."

IN SEQUENCE

Golub is one of the leaders of an ambitious effort to sequence the myeloma genome. In a paper published in *Nature* in March 2011, Golub and a consortium of researchers published the most

complete genomic analysis of myeloma to date[1]. They reported sequencing 38 cancer genomes — 23 by whole-genome sequencing and 16 by whole-exome sequencing, with one patient analysed by both. One surprising discovery was that 42% of patients had mutations in genes involved in RNA processing or protein translation. This finding suggests that flaws in protein regulation may play a major role in the disease. Golub says this is a fundamentally new idea that "was not on anyone's radar".

The analysis also confirmed previous findings, including those concerning activation of NF-κB. "Now we have a much richer view of what's going on," says Golub. Sequencing identified mutations in 11 different components of the NF-κB pathway, showing that several different mutations can lead to the gene's inactivation, and that an assortment of different factors can have the same effect.

This is a theme that Golub thinks could be important in making sense of the disease's diversity. "Individually, these mutations are rare," he says, "but collectively, as a set of mutations and a set of genes that activate a particular pathway, they're quite common." Essentially, he says, many diverse mutations funnel into a few common pathways. It may be that targeting these pathways could be a useful therapeutic strategy, rather than trying to home in on each individual mutation.

The researchers also made one discovery that could have a more immediate clinical benefit. One patient harboured a BRAF kinase mutation that was previously unseen in myeloma but known to be involved in other cancers, especially melanoma. Sequencing a further 161 patients showed that 7 had BRAF mutations. The findings indicate that a small number of myeloma patients might benefit from the BRAF inhibitors already developed to treat melanoma.

The Multiple Myeloma Research Foundation (MMRF) in Norwalk, Connecticut, which funded Golub's study, is now leading an effort to profile more patients for BRAF mutations in the hope of launching a clinical trial to test the melanoma drugs — an endeavour that the MMRF's chief scientific officer Louise Perkins admits is "an expensive and risky bet". The approach may prove fruitful for the few myeloma patients who could benefit from drugs targeted to their specific mutations but originally developed for other cancers.

The MMRF study represents the most comprehensive set of cancer genomes yet published. It brought together several academic institutions, including the Broad Institute and a long-time competitor, the Translational Genomics Research Institute based in Phoenix, Arizona. This effort was just a first step: the MMRF hopes to sequence at least 250 myeloma genomes in the near future.

MOVING TARGET

The ability to isolate multiple myeloma tumours from the blood and bone marrow has made the disease more amenable to genetic profiling than many solid tumours. But significant challenges to understanding the disease remain, particularly from the cancer's own chaotic genome. In addition to the inherent complexity in the myeloma genome, there is evidence that the cancer genome evolves over time in the same patient. "It's a moving target," says Munshi. These changes may be linked to the disease becoming more severe or developing drug resistance, and may eventually prove useful in monitoring the disease and treatment. Munshi's group has found evidence that the myeloma genome is unstable, and is investigating whether targeting this fundamental instability could be a promising therapeutic strategy.

"In addition to the complexity in the myeloma genome, there is evidence that the genome changes over time in the same patient."

As well as these genetic changes, researchers have recently found that microRNA expression correlates with different subtypes of disease and survival, providing another potential molecular tool to analyse and target disease mechanisms.

The goal now, says Anderson, is to combine these methods of molecular analysis to provide a clearer picture of the genome's heterogeneity. Because the cancer's genome changes with progression and treatment, it is important to study large groups of patients to find reproducible patterns in the way their treatments affect the cancer genome. Anderson is optimistic that such studies will make it possible to find clinically useful signatures of disease type and progression, which will aid the ultimate goal: "to get the right treatments to the right patients at the right time". ■

Courtney Humphries *is a science writer based in Boston, Massachusetts.*

1. Chapman, M. A. *et al. Nature* **471**, 467–472 (2011).

TRACKING PROGRESSION

The pattern of gene expression clearly changes as MGUS and myeloma develop.

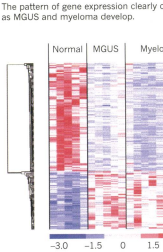

AMERICAN ASSOCIATION FOR CANCER RESEARCH

RISK ASSESSMENT

Looking for clues

Multiple myeloma is not a uniform disease. Ideally, doctors would like to treat each patient according to the distinct molecular profile of their cancer. Cytogenetic analysis makes it possible to group patients into several subclasses based on their particular genetic abnormalities. Several of these abnormalities are associated with either a higher or a lower risk: a deletion in chromosome 17 found in about 15% of patients, for instance, is associated with a short survival time and can be used to identify high-risk patients. But there is no definitive way to classify each myeloma into a molecular subtype that correlates with clinical outcome.

Over the past decade, several groups have used gene expression profiling to group patients. A team at the University of Arkansas for Medical Sciences (UAMS) in Little Rock has developed a model for predicting prognosis based on the expression profiles of 70 genes. John Shaughnessy, director of the Lambert Laboratory of Myeloma Genetics at UAMS, says the profiles show that myeloma is, genetically, "not one disease but eight different molecularly definable groups". About 20% of newly diagnosed patients, he says, have signatures indicating a high risk of the cancer returning after treatment. Shaughnessy started a company, Signal Genetics, which profiles patients using these 70 genes to aid doctors' decision-making.

As a sign of how heterogeneous the cancer is, other groups have developed their own metrics. The Intergroupe Francophone du Myelome in France, for instance, has come up with a 15-gene model. Few of the genes identified in the two models overlap. Part of the problem is that different groups of patients are given slightly different treatments; the models tend to lose predictive power when applied to other sets of patients.

So far, these techniques have identified the patients with the worst prognosis. "It tells you they're not going to do well — it doesn't tell you how they would do better," says Leif Bergsagel of the Mayo Clinic in Arizona. Identifying patients who are unlikely to benefit from current medication could help them avoid unnecessary treatment and identify candidates for new treatments. But no genetic event has been found to be linked with cure or even long-term survival — there is, as yet, no sign of success. **C.H.**

Better view: positron emission tomography can show how patients respond to treatment.

IMAGING

Seeing is believing

New technology to peer into the bones could help improve the treatment of multiple myeloma patients.

BY CASSANDRA WILLYARD

Noopur Raje first met Ben (not his real name) in 2006. Blood tests and a bone-marrow biopsy revealed that Ben had a type of multiple myeloma. But unlike most patients, who have cancerous lesions throughout their body, Ben had just one — a big one — on his rib. Raje, an oncologist at Massachusetts General Hospital in Boston, had seen cases like this before. She irradiated the cancer and began scanning Ben once a year, just in case.

The scan Raje prescribed is really two scans in one. The first identifies areas of active cancer. The second uses X-rays to create a three-dimensional image of the body's interior. Together, the scans allowed Raje to track Ben's disease.

Ben's first scan showed that the treatment had worked: the cancer was gone. But two years later, in another scan, "he lit up like a Christmas tree", Raje says. The imaging showed that Ben's rib lesion had returned, and he also had new masses around his kidneys and adrenal glands. At the time, he felt fine and his blood tests were normal. Raje put him on an aggressive treatment regimen. He experienced an almost complete remission, and today he is in good health.

Ben's case illustrates the importance of imaging technologies in the treatment of multiple myeloma. New techniques, along with refinements to existing technologies, promise to give doctors more accurate information to help them spot myeloma, predict how fast and far it will spread, and tailor treatments based on the characteristics of the individual's disease.

IMAGING IN THE CLINIC

Cancerous skeletal lesions, which resemble pits in the bone, are a hallmark of multiple myeloma. A skeletal survey using an X-ray machine has long been the gold standard for spotting these lesions, and the International Myeloma Working Group still recommends that doctors conduct such a survey once the disease is suspected. Radiography machines are inexpensive and widely available, but the process can be slow and uncomfortable for patients. To ensure that the radiologist gets images of the entire skeleton, patients must reposition themselves frequently. "You have to lie on your side and then stand up — there's a huge amount of moving around," says Ciaran Healy, a radiologist at Mater Misericordiae University Hospital in Dublin, Ireland. For patients who are frail or already in pain, the process can be agonizing. And X-rays tend to miss small lesions.

A variety of newer, more sensitive imaging technologies are now used to examine patients with multiple myeloma, but researchers are still figuring out how best to use them. Healy's team has replaced the skeletal survey with low-dose computed tomography (CT), which combines several X-ray images to create a three-dimensional picture. One benefit is that CT scans are

quicker and detect more and smaller lesions than standard X-rays; another is that the patient can lie down throughout the scan.

Many medical centres, including Mater Misericordiae, also use magnetic resonance imaging (MRI) to spot multiple myeloma. X-rays and low-dose CT scans can find lesions in the bone, but MRI is better at detecting cancer in the soft marrow inside the bones. "It can identify not only very small lesions, but lesions which spread around the spinal cord," says Homer Macapinlac, chair of the nuclear-medicine department at the M. D. Anderson Cancer Center in Houston, Texas. Spotting these lesions is particularly important because they can press against the spinal cord and cause paralysis.

Studying MRI images can also help doctors decide where to biopsy. In some patients, cancer cells are concentrated in clusters, or hotspots, in the bone marrow. If the biopsy misses those lesions, "you might miss a diagnosis", says Ronald Walker, a radiologist and nuclear-medicine physician at the Vanderbilt-Ingram Cancer Center in Nashville, Tennessee. Also, because MRI relies on radio waves and strong magnets, radiation exposure is not a concern. However, MRI is more expensive and time consuming than CT scans. And because the conventional MRI is "optimized for the marrow", Walker says, scans may not detect cancer that has spread outside the bones into the surrounding soft tissue.

HINDAM PUBLISHING CORPORATION

SEEING A RESPONSE

Imaging techniques have long been used to help diagnose patients and determine the stage of disease. They can now be used to investigate the response to treatment. New cancer is immediately evident in MRI scans, so it can catch a relapse, but the changes associated with a therapeutic response can take years to show up.

In the 1990s, oncologists working with multiple myeloma patients began combining CT with positron emission tomography (PET), which lets them visualize biological processes in the body. The radiologist injects a radioactive tracer and a scanner detects the gamma radiation it emits. The most widely used tracer, fluorodeoxyglucose (FDG), allows researchers to track the uptake of glucose. Cancer cells grow and divide faster than normal cells, so they usually use more glucose. Areas of high glucose uptake show up as bright spots on the PET image. Combining PET and CT locates these bright spots in the body. It was a PET–CT scan that alerted Raje to Ben's relapse.

Although whole-body MRI is better than PET–CT at picking up active cancer[1], PET–CT is more effective at determining whether a patient is responding to therapy. If treatment works, the cells stop proliferating, use less glucose and become dimmer on the image. The largest and most comprehensive study of the use of imaging to detect treatment response in multiple myeloma found that the number and intensity of active cancer spots on a PET–CT scan was predictive of how patients respond to therapy[2]. "The higher the number of hotspots and the greater their intensity, the poorer the outcome," says Bart Barlogie, director of the Myeloma Institute for Research and Therapy at the University of Arkansas for Medical Sciences in Little Rock. Barlogie now relies on PET–CT scans to individualize treatment. "We do the scanning sometimes on a weekly basis," he says. "And if the lights don't dim in a week, we know the drug is not active and we change course."

TRACING THE FUTURE

Researchers are working to develop imaging techniques that will make it easier to detect and treat myeloma. One approach used with MRI involves introducing a chelated form of gadolinium, which acts as a contrast agent to help

A reconstruction of the lumbar spine and pelvis reveals 'punched out' lesions caused by myeloma.

researchers quantify blood flow in the bone marrow. Jens Hillengass, a haematologist at the University of Heidelberg in Germany, has been investigating this technique — called dynamic contrast-enhanced MRI (DCE-MRI) — for more than a decade.

First, a pump intravenously injects the agent, which travels through the blood vessels. Multiple scans allow physicians to track the agent and quantify blood flow and vessel density in the bone marrow. The technique also helps doctors measure the leakiness of blood vessels, which is usually higher in areas of malignancy. This measurement could enable DCE-MRI to spot signs of progression in patients with 'smouldering myeloma' — an early form of the disease — sooner than other imaging techniques. "We are hoping that this would help to define patients at risk of going on to symptomatic myeloma," Hillengass says.

Hillengass's group is also investigating another version of MRI, called diffusion-weighted imaging (DWI), which measures the diffusion of water molecules through tissue. In regions of the body with a low density of cells, water can travel farther than in areas where cells are packed tightly together, such as malignant areas of the bone marrow. Hillengass suspects that DWI could help doctors track the progression of early stage myeloma.

Another promising direction involves new tracers to identify lesions in PET imaging. "A lot of the lesions in myeloma do not have increased glucose uptake," says Ola Landgren, head of the multiple myeloma section at the National Cancer Institute in Bethesda, Maryland. A tracer known as 18F-FLT measures the rate of DNA synthesis, rather than glucose uptake. Because cancer cells cycle more rapidly than normal cells, they synthesize more DNA. However, the rate of DNA synthesis is also high in normal bone-marrow cells, minimizing the difference between cancer cells and normal bone-marrow cells. "It's like trying to identify chocolate chips in a chocolate cupcake," Macapinlac says. "They kind of all blend in." But 18F-FLT can detect a patient's response sooner than FDG. "You don't have to wait for several cycles of therapy," he says.

Scientists are also investigating a PET tracer that is preferentially taken up by bone-forming cells. This tracer, 18F-sodium fluoride (NaF), was approved in the 1970s but was not widely adopted because for many years PET scanners were expensive and scarce. Now they are widely available, researchers are investigating how the NaF tracer can help myeloma patients. There is evidence from a South Korean PET study that NaF is better than FDG at spotting bone lesions. Doctors used to think that "once you have a hole in the bone, it's not ever going to heal", says Raje. But new therapies that promote bone formation are challenging that wisdom. And tracers such as NaF might enable physicians to observe this healing process in real time.

A machine that combines PET imaging with MRI could offer the most complete picture of multiple myeloma. The US Food and Drug Administration approved the first such system, manufactured by Siemens Medical Solutions of Malvern, Pennsylania, in June 2011. It could provide all the benefits of PET–CT without exposure to radiation. This is especially useful for younger patients, who have a greater risk of developing CT-related cancers, Macapinlac says. Researchers are working to optimize the algorithms needed to reconstruct the PET images and to make it quicker to do scans, he adds.

New imaging techniques could improve the care for myeloma patients and lead to a greater understanding of cancer biology. "One of the problems whenever people do bench work is they remove a tumour from the milieu of the human host," says Walker. Cancer cells can act differently outside the body. Imaging that allows researchers to track tumours in their natural habitat could lead to insights and drive the development of new treatments — and help patients like Ben stay cancer free. ■

Cassandra Willyard *is a freelance science writer based in Brooklyn, New York.*

1. Shortt, C. P. *et al. Am. J. Roentgenol.* **192,** 980–986 (2009).
2. Bartel, T. B. *et al. Blood* **114,** 2068–2076 (2009).

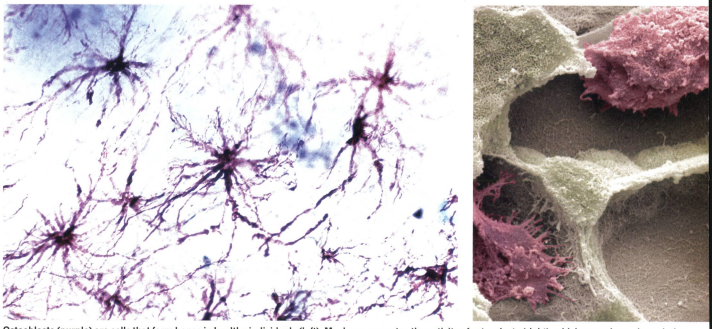

Osteoblasts (purple) are cells that form bones in healthy individuals (left). Myeloma promotes the activity of osteoclasts (right), which cause bone degradation.

AETIOLOGY

The path to disease

Multiple myeloma begins with a benign condition before progression to full-blown cancer, and work is underway to uncover the origins of both.

BY CYNTHIA GRABER

Multiple myeloma takes root years before any symptoms appear. Some plasma cells avoid the normal checks in the bone marrow and begin to clone themselves and proliferate, a condition known as 'monoclonal gammopathy of undetermined significance' (MGUS), which can persist for years or even decades. It might begin to weaken bones and cause some protein deposits on organs, but the patient typically never feels a thing. In multiple myeloma, however, these same monoclonal plasma cells explode in numbers and become malignant, causing anaemia, bone destruction and kidney failure.

Only about 1% of people with MGUS develop full-blown multiple myeloma each year. But several questions remain, with implications for early intervention and treatment. Most importantly, what causes MGUS to develop in the first place? And what is it that catapults the quiescent MGUS cells into the deadly disease of multiple myeloma?

THE ORIGINAL CAUSE

The origins of MGUS are mysterious, although researchers have been able to tease out a variety of risk factors. Men seem to be at higher risk than women. Individuals whose immune systems have been suppressed by autoimmune diseases seem to develop the disease at greater numbers, as do people over the age of 50. Some of these trends may be due to the body's heightened effort (in the case of diseases) or long-term struggle (in the case of age) to produce cells to fight infection, until finally one mutates and proliferates. "If you are older, the plasma cells are more likely to be responding to antigenic stimulation [such as an infection] all the time," explains haematologist Vincent Rajkumar, a multiple myeloma specialist at the Mayo Clinic in Rochester, Minnesota, "and at some point a mistake is going to happen."

Another likely cause is genetics. There is a greater risk of developing MGUS if an immediate family member has the disease, although it is not clear whether this is due to genetics, the environment or a combination of the two. And several studies have shown that African-Americans contract MGUS at roughly twice the rate as Caucasians, after adjusting for potential socio-economic and environmental effects.

Environmental connections are also suspected in both MGUS and multiple myeloma. A few years after the attacks on 11 September 2001, researchers tasked with evaluating the health impacts of the fires and dust from the World Trade Center alerted the public that a number of first responders had contracted multiple myeloma. A statistically significant link to the event has not held up over time, however. Despite this lack of a convincing connection, epidemiological studies have focused on whether there is a link with specific chemicals, or classes of chemicals. Some studies suggest that firefighters generally seem to contract multiple myeloma at higher rates, and farm workers may too.

According to a Mayo Clinic review published in 2010, the incidence of MGUS rises with increased pesticide exposure. Rajkumar, one of the review's authors, highlights exposure to benzene, petrochemicals and pesticides as factors that have been shown to place people at higher risk, suggesting that these chemicals may lead to DNA mutations that could convert normal plasma cells into malignant ones.

But W. Michael Kuehl, who studies the causes of multiple myeloma at the National Cancer Institute (NCI) in Bethesda, Maryland, maintains that the environmental triggers have not yet been proven. "It's very hard to make sure that the control group and the 'at risk' group are exactly the same" in epidemiological studies, he says.

Brian Durie, a myeloma specialist at the Cedars-Sinai Outpatient Cancer Center in Los Angeles, California, thinks the environmental impact may be significant, particularly for certain classes of herbicides and pesticides. "There are

➲ NATURE.COM
For some of the latest research on multiple myeloma:
go.nature.com/9dda9p

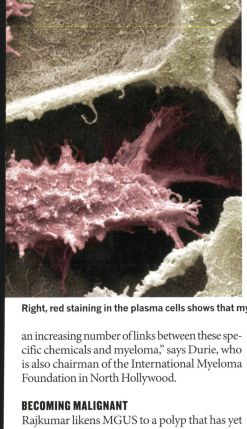

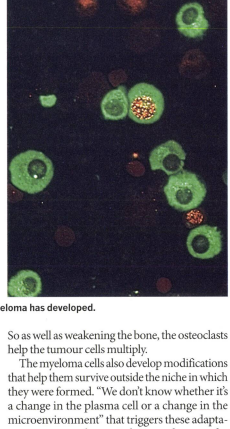

Right, red staining in the plasma cells shows that myeloma has developed.

JEAN-CLAUDE REVY, ISM/SCIENCE PHOTO LIBRARY / S. VINCENT RAJKUMAR, MAYO CLINIC / SCIENCE PHOTO LIBRARY

an increasing number of links between these specific chemicals and myeloma," says Durie, who is also chairman of the International Myeloma Foundation in North Hollywood.

BECOMING MALIGNANT

Rajkumar likens MGUS to a polyp that has yet to develop into colon cancer. "It stays quiet," he says, "unless it gets a second hit, at which point it becomes malignant colon cancer. Similarly, MGUS then becomes myeloma. That second hit — why it happens, who gets it — that's also unknown." It may be, he suggests, a combination of genetics and environmental impact.

The effects of MGUS and multiple myeloma are vastly different, but the cells look similar. Although the cells in advanced myeloma have mutations not found in MGUS cells, a researcher given a cell would be hard pressed to determine which sort it is.

Some of the differences lie in the bone marrow and the bone — the tumour's microenvironment (see 'Neighbourhood watch', page S48). This environment had previously limited the cell's ability to proliferate, but suddenly, either through changes in the cells themselves or changes in the bone and marrow, that microenvironment starts contributing to a cell's unchecked growth.

In a healthy individual, the activities of bone-creating osteoblasts and bone-absorbing osteoclasts are balanced. The signals from myeloma's plasma cells, however, inhibit the growth of osteoblasts and stimulate the growth and activity of osteoclasts (see 'Structural support', page S56). As a result, bone destruction races ahead of bone creation. David Roodman, director of the Multiple Myeloma Center at the University of Pittsburgh Cancer Institute in Pennsylvania, who has conducted extensive research on the tumour's microenvironment, says that osteoclasts also provide several growth factors for the tumour cells. So as well as weakening the bone, the osteoclasts help the tumour cells multiply.

The myeloma cells also develop modifications that help them survive outside the niche in which they were formed. "We don't know whether it's a change in the plasma cell or a change in the microenvironment" that triggers these adaptations, says Roodman. Either way, he says, the implication is that treatments to control the tumour's growth could be targeted to the microenvironment as well as the tumour.

Several different genetic mutations can lead to the same result: mutated, proliferating plasma cells. Genes in plasma cells constantly rearrange themselves so they can respond to a variety of threats by creating appropriate antibodies; the diversity of that rearrangement, and thus the diversity of the antibodies, helps us fight infections and diseases. But in multiple myeloma, this genetic rearrangement leads to one or several unwanted mutations, setting off a chain reaction that results in the cells overexpressing and creating unchecked clones.

Several different mutations can lead to the same result: mutated, proliferating plasma cells.

In addition, the *DKK1* gene may aid the destruction of osteoblasts and the proliferation of osteoclasts, although the mechanism for the activation of the gene is unknown. The DKK1 protein produced by the gene seems to trigger events that prevent bone reconstruction and drive bone destruction. This link, discovered in 2003 by researchers at the University of Arkansas for Medical Sciences (UAMS) in Little Rock, demonstrates that multiple myeloma cells produce DKK1. John Shaughnessy, director of basic research at the Myeloma Institute for Research and Therapy at UAMS, and the study's lead researcher, says there is a positive feedback loop at work: DKK1 may support the growth of more myeloma cells through increased production of osteoclasts. Indeed, Shaughnessy's group has shown that elevated levels of DKK1 expression within MGUS plasma cells are predictive of conversion to multiple myeloma. Shaughnessy is particularly excited about the development of a drug, now in phase II clinical trials, to mop up DKK1. He is optimistic that the drug will not cause serious side effects, because although DKK1 is important for embryonic development, it plays no significant role in adult biology.

ON THE MAP

Researchers have been narrowing down which aspects of MGUS make it more likely to undergo a second series of mutations to become multiple myeloma. For instance, the precancerous cells are no longer normal plasma cells, so the antibodies they create are not the same as those produced by a normal cell. The mix of 'heavy chain' proteins to 'light chain' proteins is out of proportion, with more light proteins being excreted into the blood. Understanding such changes and determining which of them are more likely to lead to myeloma will help doctors and researchers figure out which patients are most at risk.

There is still a great deal of information to be collected, says Ola Landgren, who heads multiple myeloma research at the NCI. His lab is enrolling 250 patients with either MGUS or smouldering myeloma, and plans to follow them for at least five years. Landgren says his team will be able to evaluate the differences between the end of the study and the beginning, for those who progressed to disease and those who didn't, through a variety of assays including sequencing and gene expression. It amounts to "a lot of fishing to try to build a map", he says.

Research is underway to help researchers understand the origins of the disease and home in on the specific cellular pathways involved. Epidemiological studies should help them understand who is more susceptible to MGUS in the first place. If we know why people get it, says Rajkumar, "we can try to do something about it" (see 'The early bird', page S36). Studies focusing on mutations, abnormalities, plasma cell pathways, and interactions with the tumour microenvironment, along with studies of markers to help determine who develops myeloma and who doesn't, will all provide crucial tools to support early intervention.

The research has even wider implications. Because MGUS is easy to diagnose, and is simple to track with regular, non-invasive blood tests, it is easy to follow patients and monitor their possible progression from benign to malignant disease. Information from such studies could help researchers develop a model to provide information not only to halt the disease, but to inform cancer research more broadly — and create a map of the course taken by this deadly disease. ■

Cynthia Graber *is a science writer based in Somerville, Massachusetts.*

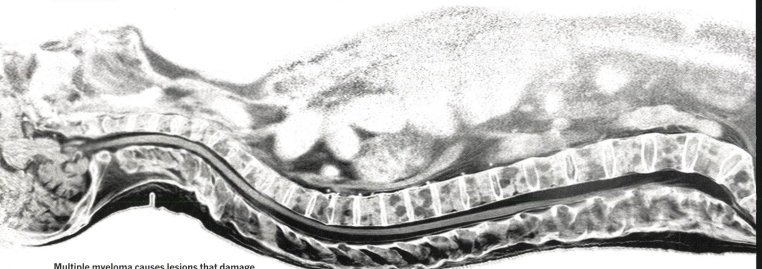

Multiple myeloma causes lesions that damage the structure of bones and leaves them weak.

ORTHOPAEDICS

Structural support

Finding a treatment for the bone destruction caused by myeloma helped researchers understand the biology of bone.

BY JENNIFER BERGLUND

In the 1960s, a remarkable substance called etidronate came into use as an effective treatment for bone problems. Etidronate is a bisphosphonate, a class of material known since the late 1800s to inhibit metal crystallization and corrosion, a feature that led to its wide usage in the oil and gas industry. More than 60 years later, researchers at Proctor & Gamble found that bisphosphonates are just as effective at preventing the destruction of bones in the human body as they are at stopping metal degradation. Proctor & Gamble began marketing etidronate as Didronel, and it soon became a standard treatment for muscle calcification, Paget's disease of bone, heterotropic ossification (in which bone is formed outside the skeleton), menopausal osteoporosis and, finally, bone degradation in multiple myeloma[1].

It was the use of bisphosphonates for multiple myeloma that led to further revelations. "The fact that these drugs were effective in myeloma led a lot of people to be interested in bone disease and what the pathophysiology was," says oncologist James Berenson, medical and scientific director for the Institute for Myeloma and Bone Cancer Research in West Hollywood, California.

➲ NATURE.COM
For some of the latest research on multiple myeloma:
go.nature.com/yyrxsS

So myeloma emerged as a model for studying bone disease. "A large part of our understanding of cancer and bone disease has come from myeloma-related work," says Nikhil Munshi, an oncologist at the Dana-Farber Cancer Institute in Boston, Massachusetts. Indeed, says Munshi, "myeloma is at the forefront" of research into bone pathology. Treatments developed primarily for multiple myeloma — including not only bisphosphonates but also proteasome inhibitors and surgical techniques — have revolutionized the way doctors treat bone diseases.

BONING UP

Myeloma cells are able to survive, differentiate and proliferate because they receive structural support from stromal cells in the bone marrow, along with soluble materials and extracellular protein. The cancer cells then release agents that suppress bone development and accelerate bone degradation. Up to 80% of multiple myeloma patients have either osteoporosis, lytic lesions or bone damage, which "tells us something important about bone biology", according to Munshi. This knowledge is applicable to most forms of cancer, because bone is one of the most common places for cancer to metastasize. For example, up to 75% of advanced prostate cancers end up in the bones, as do 30% of lung and renal cancers, says David Roodman, who leads research into multiple myeloma at the University of Pittsburgh Cancer Institute in Pennsylvania.

Cancerous cells in bone tissue trigger a destructive cascade of events that often reduces the patient's quality of life. As advances in the treatment of multiple myeloma have prolonged the lives of patients, the focus has turned to preventing the progression of bone disease and repairing damaged bone. "Myeloma has provided a good model for normal bone pathogenesis, that is, new bone formation versus bone resorption," says Kenneth Anderson, who leads multiple myeloma research at the Dana-Farber Cancer Institute. "It has also allowed us to evaluate new cancer targets as well as new target therapies to enhance bone formation and block resorption — not only in cancer, but in non-malignant diseases as well."

In healthy bone, there is a balance between the activity of cells that build up new bone tissue, called osteoblasts, and those that break it down, called osteoclasts. Myeloma cells upset this balance by promoting the activity of the destructive osteoclasts and inhibiting the work of osteoblasts, resulting in increased bone resorption. Moreover, in a vicious cycle, bone destruction releases several cell signalling molecules, or cytokines, that promote the further growth of myeloma cells. Bisphosphonates restore the balance by suppressing osteoclast activity, thereby discouraging bone resorption and suppressing tumour growth.

Bisphosphonates have "totally transformed the way we treat multiple myeloma", says Anderson, "I can't overstate how different it was when we were able to decrease the bone complications." And etidronate was only the beginning. Monthly injections of newer bisphosphonates, such as pamidronate and zoledronic acid, have become a central element of treatment for multiple myeloma. Their effectiveness in inhibiting bone resorption makes bisphosphonates effective in treating other forms of bone disease too, such as brittle bone disease (osteogenesis imperfecta), Paget's disease, postmenopausal osteoporosis and

PROTECTING THE BONE

Bisphosphonates restore the balance of bone creation and destruction by suppressing the activity of osteoclasts.

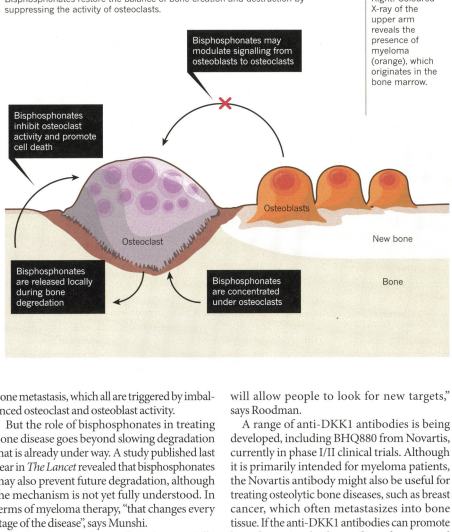
Bisphosphonates may modulate signalling from osteoblasts to osteoclasts
Bisphosphonates inhibit osteoclast activity and promote cell death
Osteoblasts
Osteoclast
New bone
Bone
Bisphosphonates are released locally during bone degredation
Bisphosphonates are concentrated under osteoclasts

Right: Coloured X-ray of the upper arm reveals the presence of myeloma (orange), which originates in the bone marrow.

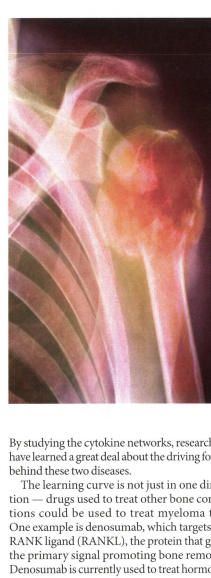

DU CANE MEDICAL IMAGING LTD/SCIENCE PHOTO LIBRARY / CNRI/SCIENCE PHOTO LIBRARY

bone metastasis, which all are triggered by imbalanced osteoclast and osteoblast activity.

But the role of bisphosphonates in treating bone disease goes beyond slowing degradation that is already under way. A study published last year in *The Lancet* revealed that bisphosphonates may also prevent future degradation, although the mechanism is not yet fully understood. In terms of myeloma therapy, "that changes every stage of the disease", says Munshi.

Bisphosphonate therapy "may be especially useful for patients who have a propensity to develop metastases", says Roodman. "If we could identify a really high-risk group, those might be the people we should treat," he adds, because some myeloma patients go on for years without developing bone damage.

DIFFERENT DISEASES

The drugs that are the gold standard in treating myeloma, proteasome inhibitors (see 'More shots on target', page S40), are also potentially beneficial in fighting bone disease. Although not currently used to treat other forms of bone disease, they have provided some interesting insight.

Over the past few years, researchers have found that the most commonly used proteasome inhibitor — bortezomib — not only inhibits osteoclast formation but also promotes bone generation in three ways. First, it stimulates the activity of osteoblasts; second, it promotes the production of the bone-building protein BMP-2; and third, it inhibits *DKK1*, the gene that encodes the DKK1 protein, which is believed to block bone growth. "These kinds of insights will allow people to look for new targets," says Roodman.

A range of anti-DKK1 antibodies is being developed, including BHQ880 from Novartis, currently in phase I/II clinical trials. Although it is primarily intended for myeloma patients, the Novartis antibody might also be useful for treating osteolytic bone diseases, such as breast cancer, which often metastasizes into bone tissue. If the anti-DKK1 antibodies can promote bone formation, leading to fewer fractures and less bone pain, they could potentially be used for other diseases, such as osteoporosis.

The similarities between myeloma and other bone diseases extend beyond pharmaceuticals. A surgical technique called kyphoplasty is routinely used to treat myeloma-related bone degradation in the spine. In this minimally invasive technique, a balloon is blown up inside the collapsed vertebra and medical cement is pumped into it. A randomized trial conducted by Berenson and his colleagues showed that kyphoplasty is extremely effective at relieving pain and reducing painkiller use, improving function, and enhancing the quality of life for myeloma patients[2].

Research into multiple myeloma also has implications for rheumatoid arthritis. The inflammation in rheumatoid arthritis is related to the activity of the cell's cytokines, which are also involved in the progression of multiple myeloma. One such cytokine, interleukin-17, causes inflammation by increasing the activity of osteoblasts and myeloma cells and thus encouraging bone degradation and tumour growth.

By studying the cytokine networks, researchers have learned a great deal about the driving forces behind these two diseases.

The learning curve is not just in one direction — drugs used to treat other bone conditions could be used to treat myeloma too. One example is denosumab, which targets the RANK ligand (RANKL), the protein that gives the primary signal promoting bone removal. Denosumab is currently used to treat hormone-induced osteoporosis in post-menopausal women[3]. In the summer of 2011, it entered clinical trials to treat multiple myeloma with bone metastases.

All these insights have their roots in the realization that a substance that stopped pipe corrosion could also help the human body build its own skeletal structure. Without bisphosphonates, multiple myeloma and other forms of bone disease may have remained a slow death sentence. But thanks to the innovations in treating bone disease for which bisphosphonates paved the way, this is no longer the case. Patients often survive for many years after being diagnosed with multiple myeloma, and the focus of research is widening from prolonging patients' lives to ensuring that those lives are more comfortable. ■

Jennifer Berglund *is a science writer based in Somerville, Massachusetts.*

1. Francis, M. D. & Valent, D. J. *J. Musculoskelet. Neuron. Interact.* **7**, 2–8 (2007).
2. Berenson, J. *et al. Lancet Oncol.* **12**, 225–235 (2011).
3. Cummings, S. R. *et al. N. Engl. J. Med.* **361**, 756–765 (2009).

PERSPECTIVE

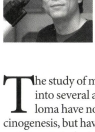

A model disease

Despite its rarity, multiple myeloma is an ideal testing ground for cancer biology, says **William Matsui**.

The study of multiple myeloma has provided exceptional insights into several areas of tumour biology. Findings in multiple myeloma have not only improved the understanding of human carcinogenesis, but have also pioneered its translation into the clinic.

Genomic techniques have dramatically improved our understanding of the pathogenesis of many human cancers, although the clinical impact of these findings has been limited in most of them. In myeloma, however, these techniques have helped to identify which patients are most at risk. Initial studies examining gross chromosomal alterations identified two subsets of patients based on the presence of unique chromosomal translocations or increased numbers of chromosomes. The development of fluorescence *in situ* hybridization subsequently enabled the evaluation of specific cytogenetic events in most patients and made it possible to further delineate specific risk categories. Treatments for other diseases also depend on risk assessments based on specific cytogenetic changes or gene mutations, but multiple myeloma has had the benefit of more global and detailed analyses — especially the pioneering work in array-based gene expression profiling (GEP), which has helped to evaluate specific biological and clinical risk[1].

As new anti-myeloma agents have emerged, GEP has also helped to identify which patients are most likely to respond to particular therapies. Moreover, by assembling large databases that combine GEP data and patient outcomes, the potential importance of the overexpression or mutation of specific genes can be clinically validated. In this way, technologies such as single-nucleotide polymorphism and comparative genomic hybridization arrays, as well as next-generation sequencing, can be used to characterize genetic changes at the single-nucleotide level. These studies are likely to influence clinical care in the future.

NEW INFORMATION ABOUT THE BASIC BIOLOGY OF MULTIPLE MYELOMA HAS LED TO MARKED IMPROVEMENTS IN PATIENT OUTCOMES.

A DEEPER UNDERSTANDING

The bone-marrow microenvironment has long been recognized as a critical factor in the pathogenesis of multiple myeloma[2]. Extracellular matrix proteins, soluble growth factors and cytokines all have a profound influence on the growth, survival and drug resistance of tumour cells. Similarly, the interaction between malignant plasma cells and a wide range of other cell types, including bone-marrow stromal cells, fibroblasts, osteoblasts, osteoclasts and endothelial cells, has been shown to mediate both tumour growth and the bone disease that commonly affects myeloma patients. The impact of the extracellular environment on tumour biology is not unique to this type of cancer, but these complex interactions have been defined at a particularly detailed level in multiple myeloma.

Cancer stem cells (CSCs) are distinguished by their ability to produce tumours that recapitulate the malignancy from which they are derived and then maintain this tumorigenic potential through the process of self-renewal. Although CSCs have been identified and characterized in many solid tumours and haematological malignancies, studies in multiple myeloma have made a significant contribution to the understanding of CSC biology[3]. For example, findings from myeloma studies were among the first to demonstrate that CSCs may be more resistant than bulk tumour cells to typical anti-cancer agents. Several processes that protect non-cancer stem cells from toxic injury are responsible for this multidrug resistance, including the increased expression of proteins that allow them to pump drugs out or convert them into inactive metabolites. The implication is that CSCs persist after treatment, mediate tumour regrowth and play a central role in disease relapse.

Given the potential role of CSCs in the pathogenesis of multiple myeloma, it is not surprising that several strategies to target them have been identified. Cellular processes regulating all kinds of stem cells are a major focus of investigation. For example, the exploration of pathways involved in normal embryonic development, such as the Hedgehog signalling pathway, have paved the way for similar findings in a broad range of tumour types. Similarly, studies of multiple myeloma identified ways of targeting CSCs by cellular processes that regulate postnatal stem-cell and tissue homeostasis, involving telomerase for example, and these are now being applied to other tumour types.

CLINICAL BENEFITS

Beyond basic research, multiple myeloma has also provided a test-bed for translating the CSC hypothesis into the clinical setting. Several clinical trials explicitly targeting CSCs in myeloma are underway. Because CSCs constitute a minority of tumour cells in many cancers, the typical means of evaluating drug efficacy, such as following changes in tumour size and bulk after treatment, are unlikely to detect whether the rare CSCs have been affected. These challenges have made it difficult to demonstrate that CSCs are clinically important. Biomarker strategies capable of serially quantifying myeloma CSCs have been developed, however, and results correlating the relative number of myeloma CSCs with clinical outcomes have provided evidence supporting the relevance of these cells[4].

The wealth of new information regarding the basic biology of multiple myeloma has led to marked improvements in the outcomes of patients that represent some of the greatest gains in clinical oncology over the past decade. It is also clear that novel findings in myeloma have made possible similar discoveries in many other cancers. In this way, multiple myeloma serves as a model to improve cancer treatment as a whole. ■

William Matsui *is an oncologist at the Sidney Kimmel Comprehensive Cancer Center at Johns Hopkins University School of Medicine in Baltimore, Maryland.*
e-mail: matsuwi@jhmi.edu

1. Munshi, N. C. *et al. Clin. Cancer Res.* **17**, 1234–1242 (2011).
2. Mitsiades, C. S. *et al. J. Cell Biochem.* **101**, 950–968 (2007).
3. Huff, C. A. *et al. J. Clin. Oncol.* **26**, 2895–2900 (2008).
4. Rasheed, Z. A. *et al. Stem Cells* **29**, 883–887 (2011).

REDISCOVER *your* nature

think.
learn.
Engage.
SUCCEED.

THIS WEEK

This Week in *Nature* is an enticing round up of timely news and research highlights. From opinionated editorials to hard hitting views by global experts, *Nature* brings you **the key science news and updates you need to know.** Sign up to receive the weekly *Nature* Alert and rediscover *Nature* today.

nature.com/register

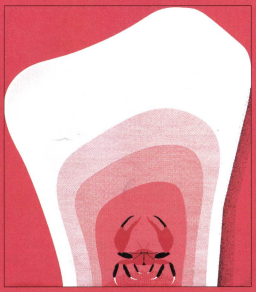

nature

www.nature.com/nature/outlook/multiple_myeloma

RESEARCH

NEW ONLINE

Papers published this week at Nature.com/nature

ARTICLE A versatile neural circuit is involved in fear-conditioning in mice **p.331**

LETTER More on what shrank the Mediterranean Sea almost six million years ago **p.359**

LETTER North American bats have a nose for trouble — it's official **p.376**

PUBLISHED 11 DECEMBER 2011

IMMUNOLOGY

Gut lymphocytes strike a balance

The gut contains a vast number of bacteria essential for the health of the organism, but it is also a rich source of lymphocytes, which eliminate infections. How do lymphocytes restrain themselves from attacking beneficial bacteria without losing their ability to combat true pathogens? This paper shows that as B cells differentiate into plasma cells in the gut, they adopt a phenotype reminiscent of innate immune cells, yet retain the ability to produce immunoglobulin A. The resultant cells in the lamina propria are the main source of the antimicrobial mediators (tumour-necrosis factor-α and inducible nitric oxide synthase) needed to maintain a balance between intestinal microbes and the immune system.

Acquisition of a multifunctional IgA$^+$ plasma cell phenotype in the gut
J H Fritz *et al.*
doi:10.1038/nature10698

CANCER

DCC protein as a tumour suppressor

As its name implies, the gene for the DCC (deleted in colorectal cancer) protein is often absent in colorectal cancers. Its role as tumour suppressor remains controversial, however, because a mouse strain lacking one copy of the gene did not develop spontaneous intestinal tumours, and because DCC deletions generally also remove the neighbouring tumour suppressor gene *Smad4*. Here, Patrick Mehlen and colleagues show that DCC does act as a tumour suppressor, by initiating tumour cell apoptosis.

DCC constrains tumour progression via its dependence receptor activity
M Castets *et al.*
doi:10.1038/nature10708

MICROBIOLOGY

Cysteine methylation disrupts ubiquitin-chain sensing in NF-κB activation
L Zhang *et al.*
doi:10.1038/nature10690

STRUCTURAL BIOLOGY

An unanticipated architecture of the 750-kDa $\alpha_6\beta_6$ holoenzyme of 3-methylcrotonyl-CoA carboxylase
C S Huang *et al.*
doi:10.1038/nature10691

PUBLISHED 14 DECEMBER 2011

CANCER

Metastasis control by microRNA

Png *et al.* show that endogenous miR-126 — a microRNA that is silenced in various human cancers — suppresses the formation of breast cancer metastases through the suppression of several new pro-angiogenic genes that help to recruit endothelial cells to support the formation of metastatic colonies. By contrast, increased expression of the genes normally regulated by miR-126 is associated with a greater probability of metastases.

A microRNA regulon that mediates endothelial recruitment and metastasis by cancer cells
K J Png *et al.*
doi:10.1038/nature10661

QUANTUM COMPUTING

A glimpse through the Toffoli gate

Quantum processors based on fragile quantum coherence are especially prone to errors due to sources of disturbance inevitable in any real system. The Toffoli gate, a logic gate that makes universal reversible classical computation possible, is a key element of universal quantum computation and error correction schemes. Its realization is challenging, requiring many single and two-qubit operations executed with high fidelity. Fedorov *et al.* have developed a Toffoli gate in a superconducting circuit, exploiting three-level qubits to simplify implementation. Its performance confirms the potential of macroscopic superconducting qubits in complex quantum operations.

Implementation of a Toffoli gate with superconducting circuits
A Fedorov *et al.*
doi:10.1038/nature10713

BIOCHEMISTRY

Glucocorticoids take their time

Mammalian metabolism follows a regular 24-hour, or circadian, pattern. The major hormonal circuits, including that of the glucocorticoids, are linked to the circadian clock, but the nature of the linkage is poorly understood. Lamia *et al.* show that two clock co-regulators, cryptochromes 1 and 2, interact with the gluco-corticoid receptor to modify gene expression and metabolic homeostasis, and thereby change the transcriptional response to glucocorticoids. Glucocorticoids are used clinically to suppress inflammation, but their nonspecific mode of action has been linked with various side effects. Altering the timing of treatment, or combining it with agents that target specific cryptochromes may help to alleviate these side effects.

Cryptochromes mediate rhythmic repression of the glucocorticoid receptor
K A Lamia *et al.*
doi:10.1038/nature10700

GENOMICS

DNA-binding factors shape the mouse methylome at distal regulatory regions
M B Stadler *et al.*
doi:10.1038/nature10716

ASTROPHYSICS

A gas cloud on its way towards the supermassive black hole at the Galactic Centre
S Gillessen *et al.*
doi:10.1038/nature10652

The final plunge
M Morris
doi:10.1038/nature10767

NATURE PODCAST

This week, the far-reaching implications of recent German and European court decisions that forbid the patenting of stem cell lines derived from human embryos. More on the supernova that is giving astrophysicists a ring-side view of a stellar explosion, and news of climate change, past, present and future.

nature.com/nature/podcast

VACCINOLOGY

A sweet cleft in HIV's armour

The structure of an antibody that potently neutralizes a wide range of HIV-1 strains, together with a minimal antigen mimic, is an advance towards the design of vaccines that may elicit protective responses. SEE ARTICLE P.336

QUENTIN J. SATTENTAU

The glycoproteins on the surface envelope of HIV-1 are essential for viral attachment to, and entry into, appropriate host cells. Antibodies that bind tightly to functional envelope glycoproteins neutralize virus infectivity and can protect against infection *in vivo*[1]. HIV-1 has, in turn, evolved various defence mechanisms against antibody neutralization, most prominent among which are amino-acid sequence variation and the masking of otherwise vulnerable regions on the envelope glycoproteins with sugars called glycans[2]. Most such immune-evasion measures have minimal effect on virus infectivity, but there are certain 'sites of vulnerability' on the envelope glycoproteins that the virus must keep relatively conserved and exposed to maintain function. In this issue, McLellan *et al.*[3] define a new site of vulnerability on the HIV-1 surface glycoprotein gp120 by solving the atomic structure of a monoclonal antibody, PG9, in complex with a minimal antigenic mimic of gp120 (see page 336).

PG9 neutralizes a broad range of HIV-1 strains with high potency[4]. Therefore, its epitope — the exact part of the gp120 antigen to which it binds — is of particular interest for vaccine design. This epitope resides within a highly variable structure called the V1/V2 domain. This domain is mostly obscured by glycans, and may form the 'cap' that brings three gp120 molecules together into a trimer. This, in turn, is associated with the trimer of a second envelope glycoprotein, gp41 (Fig. 1a).

McLellan *et al.* wanted to know where exactly in the V1/V2 domain PG9 binds. But solving the structure of PG9 in complex with its antigen was not a trivial task, because the existence of the epitope depends on the quaternary folding of gp120, to the extent that full antibody binding has been achieved only using intact, membrane-anchored envelope glycoproteins[4]. As an alternative approach, the authors used molecular modelling of V1/V2 coupled with information about PG9 binding to peptide mimics to select a molecular 'scaffold' on which V1/V2 could be restrained in the correct shape. This approach delivered an antigenic mimic of the epitope to which PG9 bound tightly. The mimic consisted of a peptide strand, flanked by two glycans, contained within a four-strand mini-domain.

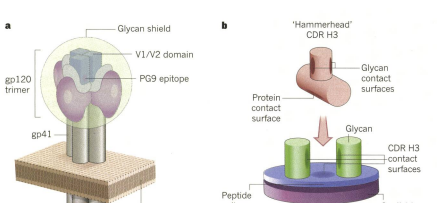

Figure 1 | Zooming in on the PG9–HIV-1 interaction. **a**, On the surface of the HIV-1 envelope, three copies of gp120 bind to three copies of gp41 to form a trimeric envelope-glycoprotein complex. The PG9 epitope is located in the V1/V2 domain of gp120, near the tip of this complex and is shrouded by a 'glycan shield'. **b**, McLellan *et al.*[3] solve the atomic structure of the PG9 antibody in complex with a scaffolded segment of the V1/V2 domain from two HIV-1 strains (see Fig. 1 of the paper[3]). To do so, the authors constructed a mimic of the antibody's minimal natural antigen. The mimic consists of a scaffold that constrains a polypeptide and two glycans such that a miniature canyon is formed. The researchers find that PG9 binds to its epitope mainly through the unusually long CDR H3 loop in its heavy chain, which forms a hammerhead-like structure. CDR H3 inserts between the glycans, contacting both, and interacts with the peptide at its tip. This allows tight binding of the antibody to these conserved antigen surfaces, accounting for its exceptional potency and breadth of HIV-1 neutralization.

Both PG9 and the closely related antibody PG16 have an unusual structure dominated by an antigen-binding site, which contains an extended region, called CDR H3, of the antibody's heavy chain. This has a unique hammerhead-like structure[5,6]. McLellan and colleagues[3] report that the hammerhead of the PG9 CDR H3 slots in neatly between the two glycans on gp120, contacting the flanking glycan surfaces and binding to the protein surface at the base of the 'mini-canyon' (Fig. 1b). PG9 overcomes variability intrinsic to the V1/V2 protein sequence by binding mainly to the atomic backbone of the protein rather than to the variable amino-acid side chains. This, along with strong evolutionary conservation of the two glycans in gp120, results in its recognizing some 80% of HIV-1 strains. Thus, PG9 is an example of the immune system turning the tables on the viral glycan defences, by binding directly to them.

Another site of vulnerability was previously identified[7] in gp120. This site, which binds the CD4 receptor on the host-cell surface, was subsequently used to isolate antibodies that neutralize a broad range of HIV-1 strains[8]. Although a valid template for vaccine design, the CD4-binding surface has intrinsic complexities that make its use for eliciting antibodies difficult. The surface is highly convoluted, and, until a couple of months ago[9], attempts to reproduce it as a polypeptide mimic were largely unsuccessful. Moreover, immunization with gp120 has so far failed to induce neutralizing antibodies of required breadth and potency, most likely because the elicited antibodies could not bind tightly to the assembled trimer of envelope glycoproteins[10].

The PG9 epitope is highly accessible on the envelope glycoprotein trimer, and so is not beset by the difficulties encountered in attempting to raise broadly neutralizing antibodies to the partly occluded CD4-binding surface on gp120. Moreover, by virtue of its

simplicity, the mini-domain V1/V2 epitope designed by McLellan *et al.* may well be a more straightforward target for re-eliciting potent neutralizing antibodies by active vaccination.

However, uncertainties remain. First, does the scaffolded V1/V2 mimic reported here accurately represent the respective molecular architecture of the actual gp120 trimer? The answer would come with the structure of the trimeric envelope glycoprotein, although the reduced affinity of PG9 for the scaffolded mimic[3] compared with that estimated for the trimeric glycoproteins suggests differences.

Second, it is not clear how common this type of interaction between antibodies and glycopeptide antigens is. But there is reason to be optimistic. McLellan *et al.* propose[3] that the epitopes of two other related, but distinct, neutralizing antibodies (CH04 and PGT145) have similar structures. Moreover, another potent neutralizing antibody, PGT128, binds a remarkably similar type of glycopeptide structure in a different region of gp120 called the V3 loop[11]. This suggests that the production of glycopeptide-reactive, broadly neutralizing antibodies may not be a particularly rare event during HIV-1 infection. The convergent evolution in antibody recognition also suggests that the immune system is rising to the challenge of generating antibodies with appropriate shapes to fit the structural constraints required to pierce the gp120 glycan shield and interact with protein surfaces beneath.

Vaccination relies on triggering the immune system's B cells to produce antibodies. Will vaccination with appropriately designed antigen mimics such as that described in this paper[3] elicit equivalent antibody responses to those seen during HIV-1 infection? This cannot be answered yet. What we do know is that B cells from some individuals infected with HIV-1 recognize this type of glycopeptide epitope after stringent selection and a substantial degree of mutational evolution to increase antibody binding strength for antigen. Whether vaccination can select the appropriate B-cell specificities and drive sufficient antibody evolution remains to be seen, but this is likely to be the major remaining hurdle on the way to an antibody-based HIV-1 vaccine. ■

Quentin J. Sattentau *is in the Sir William Dunn School of Pathology, University of Oxford, Oxford OX1 3RE, UK.*
e-mail: quentin.sattentau@path.ox.ac.uk

1. Burton, D. R. *et al. Proc. Natl Acad. Sci. USA* **108,** 11181–11186 (2011).
2. Wei, X. *et al. Nature* **422,** 307–312 (2003).
3. McLellan, J. S. *et al. Nature* **480,** 336–343 (2011).
4. Walker, L. M. *et al. Science* **326,** 285–289 (2009).
5. Pejchal, R. *et al. Proc. Natl Acad. Sci. USA* **107,** 11483–11488 (2010).
6. Pancera, M. *et al. J. Virol.* **84,** 8098–8110 (2010).
7. Zhou, T. *et al. Nature* **445,** 732–737 (2007).
8. Wu, X. *et al. Science* **329,** 856–861 (2010).
9. Azoitei, M. L. *et al. Science* **334,** 373–376 (2011).
10. Chen, L. *et al. Science* **326,** 1123–1127 (2009).
11. Pejchal, R. *et al. Science* **334,** 1097–1103 (2011).

SOFT MATERIALS

Marginal matters

Most soft materials, such as sand, can be in either a solid-like or a liquid-like state. New experiments probe the surprisingly rich nonlinear physics that can occur in between these two states. SEE LETTER P.355

VINCENZO VITELLI & MARTIN VAN HECKE

All around us, things are falling apart. The foam on our cappuccinos looks solid, but gentle stirring irreversibly changes its shape. Sand, a granular material, mimics a solid when we walk on the beach but a liquid when we pour it out of our shoes. Such examples suggest that we can think of the mechanics of soft disordered materials as either jammed (solid-like) or unjammed (freely flowing). On page 355 of this issue, however, Bi *et al.*[1] describe experiments showing that such materials come in more than just these two flavours.

The hybrid behaviour of sand and foams has fascinated physicists for decades, and lies at the heart of Liu and Nagel's jamming diagram[2] (see Fig. 1a of the paper[1]). The idea behind this diagram is that the mechanical state of a whole range of soft materials — such as granular media, pastes, foams and emulsions — is controlled by how densely their constituents (grains, bubbles or droplets) are packed. Dense packings are jammed, loose packings are unjammed, and when the constituent particles just touch, the material is said to be marginal. Think of mayonnaise, an emulsion of oil droplets in water: only when a sufficient amount of oil is added to the mixture do the oil droplets start to touch and the mayonnaise acquires its solid-like consistency.

Bi and colleagues' experiments[1] suggest that the jamming diagram should be revisited to describe a broader variety of states than the strictly jammed and unjammed ones. The authors placed a granular material consisting of small plastic discs in a box whose side walls could be moved in order to compress or shear (deform without compression) the material. The discs were photoelastic and so permitted direct visualization of the forces operating between them when the material was subjected to deformation: the more incident light that went through the material, the larger the forces[3].

The first question Bi *et al.* addressed was, what happens when such granular material is sheared? Typically, when we spread mayonnaise on a sandwich, smear foam on our skin or kick a sandcastle, we unjam these materials. By contrast, the authors[1] find that, when sheared under constant volume, collections of loose, unjammed discs build up pressure and resist further deformation — they become rigid. This phenomenon is reminiscent of Reynolds' dilatancy, in which granular materials expand when sheared under constant pressure. A familiar manifestation of this is how footprints on a wet beach tend to become dry as the deformed sand expands and sucks in water.

The second question Bi *et al.* tackled was, what is the nature of the novel states in which mechanical rigidity is generated by

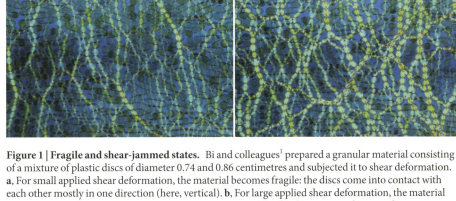

J. ZHANG & R. BEHRINGER, DUKE UNIV.

Figure 1 | Fragile and shear-jammed states. Bi and colleagues[1] prepared a granular material consisting of a mixture of plastic discs of diameter 0.74 and 0.86 centimetres and subjected it to shear deformation. **a**, For small applied shear deformation, the material becomes fragile: the discs come into contact with each other mostly in one direction (here, vertical). **b**, For large applied shear deformation, the material is said to be shear-jammed: the discs come into contact with each other in more than one direction. The intensity of light seen on each grain is proportional to the amount of force it experiences.

shearing? The authors show that these states are anisotropic, as evidenced by the patterns formed by the bright, load-bearing discs. For moderate anisotropies, the states seem to be fully jammed: they are rigid enough to resist deformation in any direction. These are shear-jammed states. However, in the case of strong anisotropy, the packings become fragile: the discs come into contact with each other mostly in one direction (Fig. 1). Such fragile packings[4] can resist deformation in some directions but not in others. These packings are thus neither fully jammed nor fully unjammed.

To account for their findings, Bi *et al.* suggest a modification to the jamming diagram: in addition to the areas describing the jammed and unjammed states, there should be an in-between region for the fragile and shear-jammed states (see Fig. 1b of the paper[1]). All of these states should meet near a point known as the marginal or jamming point, at which the rigidity vanishes.

This proposed diagram is specifically geared towards frictional granular media. But the idea of fragile states[5], which are extremely susceptible to perturbation and emerge from the marginal point, is more general. Many soft materials — including granular media, emulsions, foams and polymer networks — can be prepared in a state of vanishing rigidity and thus become marginal materials. Several examples are emerging[6–10] that show precisely how the mechanical response of such marginal materials becomes strongly nonlinear. The closer they come to the marginal point, the lower the driving force needed to access this fully nonlinear regime. At the marginal point, even the tiniest perturbation produces an extremely nonlinear mechanical response.

One example of the nonlinear behaviour of fragile matter is the mechanics of networks of randomly arranged springs. These reach a marginal state when the average number of springs equals twice the number of network nodes. Such networks are floppy if fewer springs are present and become rigid when extra springs are added, provided that they are under relatively weak stress. Between these two regimes, there is a window of extreme response: when the spring network is near its marginal state, its response becomes completely nonlinear[6].

A second example is the flow of foams and soft colloidal suspensions. Under low stress, these exhibit a liquid-like state for low densities and a solid-like state for high densities. In between these two states, an intermediate regime of nonlinear flow arises[7,8].

A third example is waves in granular media. Under large pressure, linear elastic waves occur. However, at low pressures the material approaches its marginal point, and even a gentle touch can generate strongly nonlinear shock waves[9,10].

Bi and colleagues' work[1] underscores the surprisingly rich nonlinear physics that governs marginal soft matter. The simplest manifestation of this nonlinear behaviour can be found near the marginal point. In many cases, it is unclear exactly what happens when such fragile materials are subjected to stress. But what is clear is that being marginal matters. ■

Vincenzo Vitelli *is at the Lorentz Institute, Faculty of Mathematics and Natural Sciences, and* **Martin van Hecke** *is in the Kamerlingh Onnes Laboratory, Faculty of Mathematics and Natural Sciences, Leiden University, 2300 RA Leiden, the Netherlands.*
e-mails: vitelli@lorentz.leidenuniv.nl; mvhecke@physics.leidenuniv.nl

1. Bi, D., Zhang, J., Chakraborty, B. & Behringer, R. P. *Nature* **480,** 355–358 (2011).
2. Liu, A. J. & Nagel, S. R. *Nature* **396,** 21–22 (1998).
3. Majmudar, T. S. & Behringer, R. P. *Nature* **435,** 1079–1082 (2005).
4. Cates, M. E., Wittmer, J. P., Bouchaud, J.-P. & Claudin, P. *Phys. Rev. Lett.* **81,** 1841–1844 (1998).
5. de Gennes, P.-G. & Badoz, J. *Fragile Objects: Soft Matter, Hard Science, and the Thrill of Discovery* (Springer, 1996).
6. Wyart, M. *et al. Phys. Rev. Lett.* **101,** 215501 (2008).
7. Olsson, P. & Teitel, S. *Phys. Rev. Lett.* **99,** 178001 (2007).
8. Nordstrom, K. N. *et al. Phys. Rev. Lett.* **105,** 175701 (2010).
9. Nesterenko, V. F. *Dynamics of Heterogeneous Materials* (Springer, 2011).
10. Gómez, L. R., Turner, A. M., van Hecke, M. & Vitelli, V. *Phys. Rev. Lett.* (in the press); Preprint at http://arxiv.org/abs/1108.5688 (2011).

SUPRAMOLECULAR CHEMISTRY

Molecular wires get connected

A long-standing issue in nanotechnology is how to connect molecular electronic devices. A method for splicing nanoscale wires made from different materials paves the way for a solution to this problem.

DARIO M. BASSANI

What could be easier than joining two wires together? Just about anything, if the wires in question are only 14 nanometres thick. Such nanowires are the future of miniaturization for electronics, but are so small that they cannot be handled with tweezers or through other mechanical means. Another problem is that, so far, such wires have been composed of only one type of molecule, which has limited their potential as components of future electronic devices[1]. Reporting in *Science*, Zhang *et al.*[2] now describe an approach for making nanowires in which tubular sections made from different molecular building blocks are connected together. Developing methods for joining materials that have different electronic properties is an essential step towards building nanometre-scale electronic devices such as diodes and transistors.

To achieve their aims, Zhang *et al.* built disc-shaped molecules fitted with long hydrocarbon chains on one side and a metal-binding site on the other. When the authors allowed a solution of the molecules to mix slowly with methanol, the molecules spontaneously assembled into tubes (Fig. 1). This happens because the molecules do not dissolve well in methanol — as the concentration of the methanol in the mixture increases, the disc-shaped molecules stick together to avoid being in contact with it. As they aggregate, the molecules partly overlay one another in a way that forms tubular nanowires.

Zhang *et al.* constructed the central disc of the molecules from carbon atoms with the same electronic configuration as graphene sheets[3] — that is, with atoms that form an aromatic, hexagonal network of alternating single and double bonds. This makes the molecules especially good at transporting charges when they are 'doped' (mixed with small quantities of another compound that partly ionizes the molecules) or illuminated with light. The authors also prepared similar molecules in which some of the hydrogen atoms on the periphery of the central disc were replaced by fluorine. This reduces the electron density in the disc, making the molecules better electron acceptors than the non-fluorinated analogues. Zhang *et al.* then used molecular wires made from the non-fluorinated molecules as 'seeds' that promoted the deposition of the fluorinated molecules from solution as new tubular segments at the ends of the seed wires (Fig. 1).

The authors designed their system so that the molecules in the different segments of the wires do not scramble after they are mixed. Such behaviour is highly unusual because it seems to undermine a fundamental premise of molecular self-assembly: electron-rich molecules prefer to mix with electron-poor ones to form alternating layers of each, analogous to the way that small magnets spontaneously align with their magnetic poles opposed. To understand why no scrambling occurs, we need to consider the basics of self-assembly processes.

Molecular self-assembly is driven by a

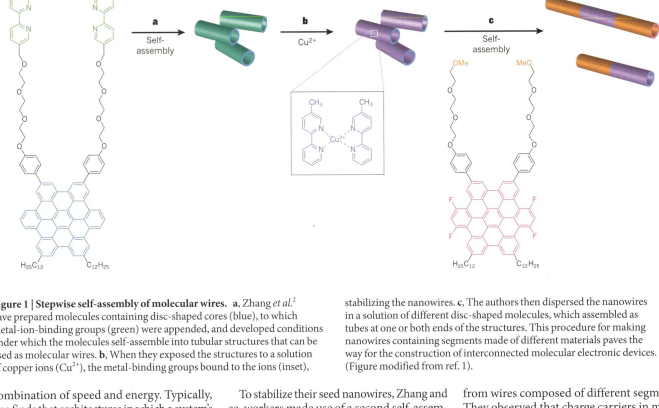

Figure 1 | Stepwise self-assembly of molecular wires. **a**, Zhang *et al.*[2] have prepared molecules containing disc-shaped cores (blue), to which metal-ion-binding groups (green) were appended, and developed conditions under which the molecules self-assemble into tubular structures that can be used as molecular wires. **b**, When they exposed the structures to a solution of copper ions (Cu^{2+}), the metal-binding groups bound to the ions (inset), stabilizing the nanowires. **c**, The authors then dispersed the nanowires in a solution of different disc-shaped molecules, which assembled as tubes at one or both ends of the structures. This procedure for making nanowires containing segments made of different materials paves the way for the construction of interconnected molecular electronic devices. (Figure modified from ref. 1).

combination of speed and energy. Typically, one finds that architectures in which a system's global energy is minimized are favoured over higher-energy ones. This is certainly the case for dynamic systems[4] in which molecules continuously assemble and disassemble, because the molecules can explore all possible structural arrangements until they find the one that has the global energy minimum. Structures that form very quickly can sometimes lock molecules into a higher-energy geometry (a process known as kinetic trapping), although this seldom gives the molecules enough time to organize themselves into ordered assemblies.

The procedure used by Zhang *et al.* to make their seed nanowires — slow diffusion of a 'poor' solvent into a solution of molecular building blocks — relies on dynamic self-assembly. At first, the molecules are well dissolved and can quickly explore many geometries as they seek an energy-minimizing structure (a tubular assembly). But as the concentration of methanol slowly increases, the forces between the molecules become stronger and they assemble faster and faster. When a critical concentration of methanol is reached, the molecules are no longer soluble and become locked into the tubular nanowire. This kind of approach is often used to make structurally robust assemblies of amphiphilic molecules (which contain both hydrophilic and hydrophobic groups). The problem with this strategy is that it frequently leads to a dead end: further growth requires the reintroduction of conditions in which molecules can dynamically exchange, at which point the assemblies rapidly fall apart.

To stabilize their seed nanowires, Zhang and co-workers made use of a second self-assembly process known as metal-ion coordination. They exposed the seed assemblies to a solution of copper ions, so that the metal-ion binding sites in the electron-rich molecules bound to the ions. This kinetically trapped the nanowires, thus preventing them from dissolving or scrambling when placed in a solution of fluorinated molecules. The fluorinated molecules could therefore assemble on the ends of the seed structures to make molecular wires composed of segments, each comprising a single type of molecule. The resulting structures contained either two or three segments, depending on whether the fluorinated molecules assembled at one or both ends of the seed wires (Fig. 1). Assuming that the electron-rich seed molecules are good conductors of positively charged particles (*p*-type materials) and that the electron-poor fluorinated molecules are better at transporting electrons (*n*-type materials), then the doubly segmented structures are analogous to the *p*–*n* junctions found in diodes, whereas the triply segmented wires are like the *p*–*n*–*p* junctions found in transistors.

When Zhang *et al.* excited the molecules in the assemblies using ultraviolet light, they found that adjoining segments communicated efficiently with each other by transferring excitation energy across the junction between the segments. The authors also used a technique known as transient microwave conductivity to determine the decay rate of charge carriers generated in wires composed of a single segment, and compared the results with those obtained from wires composed of different segments. They observed that charge carriers in multisegmented wires had the longest lifetimes, and attributed this to the presence of junctions between materials that have different conducting properties in the multi-segmented wires.

More experiments are needed to support the transient conductivity data, particularly to show that the presence of different segments can lead to desirable behaviour such as rectification (voltage-dependent modification of charge transport, typically observed in diodes). In addition, materials containing charged species (such as copper ions) are frequently viewed as a potential source of problems when incorporated into devices because they affect charge transport. A means of working around this problem might be needed to realize practical applications. Nevertheless, Zhang and colleagues' method[2] for joining nanowires of different compositions is a great stride towards overcoming one of the longest-standing problems in the field of molecule-based electronics: finding a way to connect two or more molecular devices. ■

Dario M. Bassani *is at the Institute of Molecular Sciences, University of Bordeaux 1, CNRS UMR 5255, Bâtiment A12, 351 cours de la libération, 33405 Talence Cedex, France. e-mail: d.bassani@ism.u-bordeaux1.fr*

1. Hill, J. P. *et al. Science* **304,** 1481–1483 (2004).
2. Zhang, W. *et al. Science* **334,** 340–343 (2011).
3. Novoselov, K. S. *et al. Nature* **438,** 197–200 (2005).
4. Lehn, J.-M. *Supramolecular Chemistry — Concepts and Perspectives* (Wiley, 1995).

ASTROPHYSICS

Cosmic explosions under scrutiny

Stellar explosions known as type Ia supernovae are a significant tool in cosmology, but their exact nature is unknown. Two studies bring an understanding of these cosmic blasts a step closer. SEE LETTERS P.344 & P.348

MARIO HAMUY

Type Ia supernovae are exploding stars characterized by an absence of hydrogen, the most abundant chemical element in the Universe. There is a general consensus that their progenitors are white-dwarf stars in two-star systems. But the type of star that is the companion to the white dwarf remains an open question. To date, no progenitor of a type Ia supernova has ever been directly observed before its explosion. The recently discovered[1] supernova SN 2011fe in the galaxy Messier 101, at a distance of only 6.4 million parsecs (20.9 million light years) from Earth, is the closest and brightest found in 25 years. As such, it provides a unique opportunity to search in discovery data and pre-discovery archive images for the presence of a progenitor system. Such a search is the subject of two papers in this issue, one by Nugent *et al.*[2] (page 344) and the other by Li *et al.*[3] (page 348) .

Type Ia supernovae are so powerful that they can outshine an entire galaxy such as the Milky Way, with its 200 billion stars, for several weeks. White dwarfs are the final evolutionary state of a star such as the Sun. They are Earth-sized 'diamonds' made of carbon and oxygen (one tablespoon of white dwarf weighs ten tonnes) and result from the slow but steady nuclear fusion of hydrogen and helium over millions of years. After exhausting their nuclear fuel, white dwarfs gradually emit their stored thermal energy, at a rate of 1/10,000th the luminosity of the Sun.

Under normal circumstances, white dwarfs do not explode. Instead, they slowly cool down, releasing their internal heat over billions of years. However, a dramatically different outcome can occur if a white dwarf gains weight by stealing matter from a nearby companion star. In such a case, the white dwarf contracts (the ideal diet!) and gets hotter. When the star reaches a critical mass (1.4 times the mass of the Sun), sparks of nuclear reactions begin to release heat, thereby increasing the conditions for further nuclear reactions. This is a runaway situation, and in only one second the whole white dwarf explodes as a colossal nuclear bomb (equivalent to about 10^{28} megatonnes of TNT), transforming its carbon and oxygen mainly into radioactive nickel, cobalt and iron.

According to theoretical models, there are three possible types of companion star to a white dwarf: a red giant, which is about 100 times more luminous than the Sun; a subgiant star or a main-sequence star, which are a few times more luminous than the Sun; and another white dwarf, which is 10,000 times less luminous than the Sun (Fig. 1). Because these possible companion stars span such a wide range of luminosity, examination of the explosion site on pre-discovery images of type Ia supernovae should, in principle, allow researchers to discriminate between these possibilities and ascertain the nature of the progenitor.

In their study, Li *et al.*[3] examined pre-discovery images of SN 2011fe obtained by the Hubble Space Telescope and found no evidence for an object seen before the explosion. If a red giant was the companion star, it should have been detected. This observation allowed the authors to exclude a red-giant progenitor — at least in this case. Unfortunately, the depth of the pre-discovery images was not sufficient to allow them to exclude a subgiant, main-sequence or white-dwarf companion. Nevertheless, this result represents a major advance in our understanding of the progenitor stars of type Ia supernovae.

Supernova 2011fe was discovered[1] on 24 August 2011 by the Palomar Transient Factory (PFT) project[4] with the 1.2-metre Samuel Oschin Telescope at the Palomar Observatory in California. The members of the PTF team spotted it just over 11 hours after explosion — the earliest detection ever obtained for a type Ia supernova. Their prompt reaction to the discovery allowed them to analyse the light of the object using a spectrograph mounted on the robotic Liverpool Telescope in the Canary Islands barely 16 hours after detection.

If you were to watch the explosion of a house in slow motion, the earlier you could observe the blast the clearer would be the picture you could infer of the building's initial structure, before the debris had destroyed the evidence. Likewise, at only about 28 hours after explosion, the spectrum of SN 2011fe revealed, as Nugent and colleagues[2] show, the elusive outermost layers of the exploding star before they became invisible because of the dilution caused

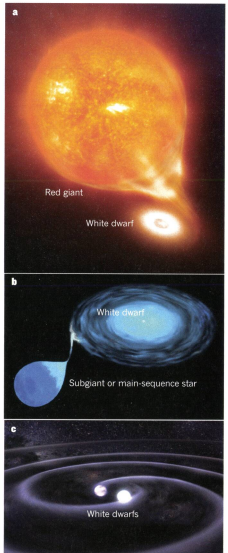

A. FEILD, G. STIRLING, NASA, C. HAYASHI/NAOJ/GSFC/D. BERRY/CHANDRA X-RAY OBSERVA...

Figure 1 | Possible progenitors of type Ia supernovae. This class of supernova is thought to originate from a white-dwarf star that accretes matter from a companion star and explodes. The companion might be: **a**, a red-giant star; **b**, a subgiant or main-sequence star; **c**, a second white dwarf. Li *et al.*[3] exclude the red-giant hypothesis for supernova 2011fe. Nugent *et al.*[2] find that the companion was probably a main-sequence star.

by their rapid expansion (7% of the speed of light). The authors' analysis[2] of the spectrum uncovers light emerging from clouds of oxygen and carbon from the surface of the supernova. This result confirms the theoretical belief that the exploding star is indeed a carbon–oxygen white dwarf, and demonstrates that a small amount of the white dwarf's outermost material managed to expand and escape the burning front coming from the centre. Although traces of carbon have been observed[5,6] in other type Ia supernovae, the detection of oxygen is unprecedented. In addition, the authors' study[2] of the supernova's early period of rising luminosity shows that the secondary star is most consistent with being a main-sequence star.

Type Ia supernovae are not only important astrophysical objects in their own right; they also provide the most precise means of measuring distances to remote galaxies. The calibration of their luminosities in the early 1990s through the Calán/Tololo project[7] allowed two groups of astronomers, headed by Brian Schmidt and Saul Perlmutter, to discover in 1998–99 that, contrary to expectation, the Universe is undergoing an accelerated expansion owing to a mysterious dark energy that constitutes 70% of the Universe's content[8,9]. This amazing discovery has been recognized with this year's Nobel Prize in Physics. Not knowing the exact nature of type Ia supernovae, which have such a crucial place in cosmology, is an embarrassing situation. Although the studies of Nugent *et al.*[2] and Li *et al.*[3] on SN 2011fe do not yet provide a definitive answer to this question, they are a reassuring step forward — one that lends support to our ideas about the nature of type Ia supernovae.

A conclusive answer to this fascinating question will have to await the discovery of other type Ia supernovae in galaxies closer to Earth than Messier 101. Because such supernovae are rare events — they occur once every two centuries in a typical galaxy such as our own[10] — and because there are only a handful of galaxies closer than Messier 101, we might have to wait 30 years for another such event. With patience and luck, we might even be rewarded in our lifetimes with a supernova in the Milky Way. ■

Mario Hamuy *is in the Department of Astronomy, Universidad de Chile, Casilla 36-D, Santiago, Chile.*
e-mail: mhamuy@das.uchile.cl

1. Nugent, P. E. *et al. Astron. Telegr.* **3581,** 1 (2011).
2. Nugent, P. E. *et al. Nature* **480,** 344–347 (2011).
3. Li, W. *et al. Nature* **480,** 348–350 (2011).
4. Rau, A. *et al. Publ. Astron. Soc. Pacif.* **121,** 1334–1351 (2009).
5. Folatelli, G. *et al.* Preprint at http://arxiv.org/abs/1110.3789 (2011).
6. Parrent, J. T. *et al. Astrophys. J.* **732,** 30 (2011).
7. Hamuy, M. *et al. Astron. J.* **112,** 2398–2407 (1996).
8. Riess, A. *et al. Astron. J.* **116,** 1009–1038 (1998).
9. Perlmutter, S. *et al. Astrophys. J.* **517,** 565–586 (1999).
10. Li, W. *et al. Mon. Not. R. Astron. Soc.* **412,** 1473–1507 (2011).

CANCER

A drug-resistant duo

The efficacy of the anticancer drug vemurafenib, which is used to treat metastatic melanoma, is plagued by acquired resistance. A picture of how such resistance develops is emerging. SEE LETTER P.387

HUGO LAVOIE & MARC THERRIEN

Vemurafenib (also known as PLX4032) is a promising drug. Newly approved by the US Food and Drug Administration, it is currently the best prospect against metastatic melanoma, the deadliest form of skin cancer[1,2]. The drug selectively inhibits an oncogenic form of B-RAF, a protein that drives cell proliferation. Unfortunately, most patients acquire resistance to vemurafenib within a year of treatment[3]. All modes of resistance discovered so far involve circumvention of this mutant B-RAF. But on page 387 of this issue, Poulikakos and colleagues[4] report a new mechanism of resistance — enhanced dimerization of the kinase domain of mutant B-RAF. Dimerization normally activates the wild-type protein.

'Gain-of-function' mutations in the *B-RAF* gene are found in about 50% of human melanomas, and its sustained expression is required for tumour-cell proliferation and survival[5]. Therefore, extensive efforts have been devoted to developing selective B-RAF inhibitors, especially those that, like vemurafenib, target its most prevalent oncogenic variant, B-RAF^{V600E}.

In normal cells, B-RAF functions in the RAS/ERK molecular signalling pathway, which has a prominent role in regulating proliferation and survival[6]. The minimum components of this pathway are a cell-membrane-associated protein, RAS, and three protein kinases — a RAF family member (such as B-RAF), MEK and ERK — which convey RAS signals along the pathway (Fig. 1a). On association with signal-activated RAS, the kinase domains of two RAF proteins form a dimer, resulting in their activation[7].

When activated by a gain-of-function mutation, B-RAF induces ERK activity independently of the normal signals, leading to the development of multiple cancers (Fig. 1b)[5]. In melanoma, inhibition of the mutant molecule B-RAF^{V600E} by vemurafenib shuts down ERK activity and rapidly leads to tumour regression[1–3]. However, acquired resistance to vemurafenib is a serious limitation, and several laboratories are hard at work investigating the underlying causes.

Previous efforts have uncovered four mechanisms that counteract vemurafenib effectiveness, all of which bypass B-RAF^{V600E}. In three cases, ERK signalling is reactivated through alternative entry points in the pathway, whereas the fourth mechanism involves

50 Years Ago

For more than one hundred years, the Royal Greenwich Observatory has been responsible for providing exact time signals for a wide variety of users both in Britain and abroad. In recent years this service has become increasingly important in various fields of scientific research where extreme accuracy is essential. In order to provide the various users with more frequent opportunities for checking the time, the present twice-daily transmissions from Rugby were increased to four as from December 1 … As long ago as 1833, the Royal Greenwich Observatory provided hourly time signals for the operation of 'time balls', which were devices consisting of a large ball secured to the top of a mast and released by a special catch at a precise time. One such ball is still in use in the grounds of the old Observatory at Greenwich.
From *Nature* 16 December 1961

100 Years Ago

In the volume on mammals in the "Fauna of British India," the late Dr. W. T. Blanford stated that the black-buck (*Antilope cervicapra*) living on a spit of sand between the Chilka Salt Lake, in Orissa, and the sea, never drank, as there is no water on the spit except in deep wells. The statement has been strongly controverted by various writers, one at least of whom has suggested that the antelopes obtain water from sheep-troughs. Of late years it has, however, been conclusively shown that giraffes, kudu, and gemsbok live for a considerable portion of the year in the Kalahari Desert without drinking, obtaining such moisture as they require from the succulent roots of certain plants … The case of the Chilka black-buck accordingly requires reinvestigation in order to ascertain whether they too may be able to obtain moisture from plants.
From *Nature* 14 December 1911

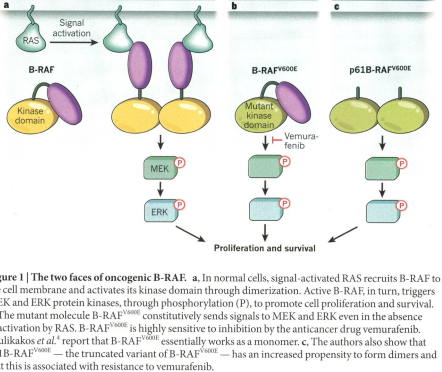

Figure 1 | The two faces of oncogenic B-RAF. **a**, In normal cells, signal-activated RAS recruits B-RAF to the cell membrane and activates its kinase domain through dimerization. Active B-RAF, in turn, triggers MEK and ERK protein kinases, through phosphorylation (P), to promote cell proliferation and survival. **b**, The mutant molecule B-RAF^{V600E} constitutively sends signals to MEK and ERK even in the absence of activation by RAS. B-RAF^{V600E} is highly sensitive to inhibition by the anticancer drug vemurafenib. Poulikakos *et al.*[4] report that B-RAF^{V600E} essentially works as a monomer. **c**, The authors also show that p61B-RAF^{V600E} — the truncated variant of B-RAF^{V600E} — has an increased propensity to form dimers and that this is associated with resistance to vemurafenib.

an ERK-independent pathway[8–10]. The prevalence of these mechanisms remains uncertain, as too few patient samples have been analysed.

To identify other processes that impart vemurafenib resistance, Poulikakos *et al.*[4] continuously exposed melanoma cells carrying B-RAF^{V600E} to the drug and derived five resistant clones. In none of these cell lines did drug resistance seem to depend on the mechanisms described previously. Instead, three lines expressed a truncated form of the B-RAF^{V600E} protein (p61B-RAF^{V600E}), which was derived from abnormal messenger RNA transcripts lacking specific exons (protein-coding sequences). The authors did not explore the molecular lesions behind this exon-skipping defect.

Two lines of evidence linked p61B-RAF^{V600E} expression to vemurafenib resistance. Selective depletion of this truncated protein resensitized the cells to vemurafenib. And its introduction in vemurafenib-sensitive B-RAF^{V600E} melanoma cells caused drug resistance.

Vemurafenib potently inhibits B-RAF^{V600E} by disrupting the activity of its kinase domain. Yet Poulikakos and co-workers report that — unlike other drug-resistant oncogenic kinases[11,12] — p61B-RAF^{V600E} contained no new mutation in its kinase domain. The authors note that the sequences missing in truncated p61B-RAF^{V600E} encompass a region that normally suppresses dimerization of the RAF kinase domain. Indeed, p61B-RAF^{V600E} exhibited increased dimerization.

To verify the potential connection between dimerization and drug resistance, the researchers introduced a mutation preventing dimer formation and compared the activity of supposedly monomeric versus dimeric variants. They made two startling observations. First, monomeric forms of full-length and truncated B-RAF^{V600E} were as active as their dimeric versions. Although it requires substantiation with further complementary evidence, this intriguing result suggests that, unlike wild-type RAF proteins, the B-RAF^{V600E} oncoprotein does not require dimerization for its activity (Fig. 1b). Second, monomeric p61B-RAF^{V600E} was as sensitive to vemurafenib as was B-RAF^{V600E}, which suggests that dimerization per se offsets the inhibitory effect of the drug. But how does this work?

RAF inhibitors, including vemurafenib, have two counter-intuitive abilities: on increased RAS activity, they promote RAF dimerization and also mediate activation, within the RAF–RAF dimer, of the drug-free RAF monomer by its drug-bound partner[13–15]. Because sequence deletions in p61B-RAF^{V600E} mimic increased RAS signalling, a similar mechanism could be involved here (Fig. 1c). If so, vemurafenib treatment should augment p61B-RAF^{V600E} dimerization and activity. Another, not mutually exclusive, possibility is that binding of the drug to one of the monomers in the p61B-RAF^{V600E} dimer inhibits drug binding to the other monomer, thereby maintaining one monomer catalytically active per dimer and so mediating drug resistance. Although this second possibility is yet to be demonstrated, crystallographic evidence[7] supports it.

Poulikakos and co-workers' findings are fascinating from a mechanistic standpoint, but are they clinically relevant? The authors report that 6 of 19 samples from patients with drug-resistant melanoma expressed B-RAF^{V600E} truncation variants similar to p61B-RAF^{V600E}. This sample number is too small to assess p61B-RAF^{V600E} prevalence. Nonetheless, the finding is impressive for suggesting that enhanced B-RAF^{V600E} dimerization significantly contributes to acquired vemurafenib resistance in patients with melanoma. In addition to analysing larger sample numbers, these observations should be corroborated in animal models.

This and related studies indicate that any event promoting RAF dimerization will lead to resistance to vemurafenib and possibly to other similar RAF inhibitors. How can we get around this problem? As Poulikakos *et al.* suggest, co-administering RAF and MEK inhibitors could be a way forward. Indeed, as p61B-RAF^{V600E}-expressing cells have been found to remain sensitive to a MEK inhibitor[4], shutting off both RAF and MEK activity might prevent the growth of resistant cells.

An attractive alternative would be to develop inhibitors of RAF dimerization for use in combination therapy with vemurafenib. The added advantage of this approach is that such inhibitors could be used to treat other RAF-dependent cancers, in particular those driven by activated RAS and for which several of the currently available RAF inhibitors are likely to be harmful, owing to their paradoxical ability to drive RAF dimerization and activation in the presence of high RAS activity[13–15].

Patient relapse following single-agent therapies is unfortunately the norm rather than the exception. Identifying the causal events, as Poulikakos *et al.* have done in this study, should assist the design of next-generation inhibitors or of combination therapy. ■

Hugo Lavoie *and* **Marc Therrien** *are at the Institute for Research in Immunology and Cancer, Université de Montréal, Montréal, Québec H3C 3J7, Canada.*
e-mail: marc.therrien@umontreal.ca

1. Bollag, G. *et al. Nature* **467,** 596–599 (2010).
2. Chapman, P. B. *et al. N. Engl. J. Med.* **364,** 2507–2516 (2011).
3. Flaherty, K. T. *et al. N. Engl. J. Med.* **363,** 809–819 (2010).
4. Poulikakos, P. I. *et al. Nature* **480,** 387–390 (2011).
5. Gray-Schopfer, V., Wellbrock, C. & Marais, R. *Nature* **445,** 851–857 (2007).
6. Wellbrock, C., Karasarides, M. & Marais, R. *Nature Rev. Mol. Cell Biol.* **5,** 875–885 (2004).
7. Udell, C. M., Rajakulendran, T., Sicheri, F. & Therrien, M. *Cell. Mol. Life Sci.* **68,** 553–565 (2011).
8. Wagle, N. *et al. J. Clin. Oncol.* **29,** 3085–3096 (2011).
9. Johannessen, C. M. *et al. Nature* **468,** 968–972 (2010).
10. Nazarian, R. *et al. Nature* **468,** 973–977 (2010).
11. Kobayashi, S. *et al. N. Engl. J. Med.* **352,** 786–792 (2005).
12. Nardi, V., Azam, M. & Daley, G. Q. *Curr. Opin. Hematol.* **11,** 35–43 (2004).
13. Poulikakos, P. I., Zhang, C., Bollag, G., Shokat, K. M. & Rosen, N. *Nature* **464,** 427–430 (2010).
14. Heidorn, S. J. *et al. Cell* **140,** 209–221 (2010).
15. Hatzivassiliou, G. *et al. Nature* **464,** 431–435 (2010).

ARTICLE

doi:10.1038/nature10674

A disinhibitory microcircuit for associative fear learning in the auditory cortex

Johannes J. Letzkus[1]*, Steffen B. E. Wolff[1,2]*, Elisabeth M. M. Meyer[1,2], Philip Tovote[1], Julien Courtin[3], Cyril Herry[3] & Andreas Lüthi[1]

Learning causes a change in how information is processed by neuronal circuits. Whereas synaptic plasticity, an important cellular mechanism, has been studied in great detail, we know much less about how learning is implemented at the level of neuronal circuits and, in particular, how interactions between distinct types of neurons within local networks contribute to the process of learning. Here we show that acquisition of associative fear memories depends on the recruitment of a disinhibitory microcircuit in the mouse auditory cortex. Fear-conditioning-associated disinhibition in auditory cortex is driven by foot-shock-mediated cholinergic activation of layer 1 interneurons, in turn generating inhibition of layer 2/3 parvalbumin-positive interneurons. Importantly, pharmacological or optogenetic block of pyramidal neuron disinhibition abolishes fear learning. Together, these data demonstrate that stimulus convergence in the auditory cortex is necessary for associative fear learning to complex tones, define the circuit elements mediating this convergence and suggest that layer-1-mediated disinhibition is an important mechanism underlying learning and information processing in neocortical circuits.

The transformation of sensory input to an appropriate behavioural output is accomplished by neuronal circuits that process information through dynamic interactions between distinct types of neurons. Learning as an adaptive change of an animal's behaviour modifies these network computations. Important cellular mechanisms underlying learning are thought to be activity-dependent synaptic plasticity[1] and subsequent structural modifications[2]. In contrast to our detailed understanding of these cellular mechanisms, the factors and circuit elements controlling neuronal activity and concomitant induction of plasticity during learning in the intact animal remain poorly understood.

Neocortical interneurons exert powerful control over circuit activity by supplying inhibition to surrounding pyramidal neurons and to other interneurons[3]. The balance of excitation and inhibition is critical to circuit function, and is maintained under most conditions including sensory stimulation, when thalamocortical input typically recruits feed-forward inhibition a few milliseconds after direct excitation[4,5]. This form of inhibition is mainly supplied by basket cells, the most abundant type of interneuron in the rodent neocortex[5]. Fast-spiking basket cells establish strong synapses with high release probability on the perisomatic region of pyramidal neurons where they control firing, and express the calcium-binding protein parvalbumin (PV)[3,6,7].

On top of the glutamatergic recruitment of inhibition by sensory input, several types of interneurons are also major targets of neuromodulation[8–11], suggesting that these systems can profoundly affect circuit computations by shifting the excitation–inhibition balance[12]. This has mainly been addressed *in vitro*, revealing a staggering complexity of effects which strongly depend on interneuron type[8–11]. Given that neuromodulation has a key role in learning[13,14], it is likely that interneurons are engaged in these processes. However, the contribution of different interneuron types to learning in the intact animal remains elusive.

Auditory fear conditioning is a form of associative learning acquired by temporal coincidence of a neutral conditioned stimulus (CS, a tone) with a mild foot shock. Fear conditioning causes prominent, long-lasting plasticity of CS responses in auditory cortex[13–15], which depends on the activity of cholinergic afferents from the basal forebrain[13,14,16]. Pairing of tones with basal forebrain stimulation can elicit similar plasticity in auditory cortex[13,14], and a recent study suggests an involvement of pyramidal neuron disinhibition in this process[17]. Here, we investigate the contribution of identified types of auditory cortex interneurons to acquisition of auditory fear memory. Our results indicate that foot shocks, via recruitment of cholinergic basal forebrain afferents, activate a disinhibitory neocortical microcircuit that is required for fear learning.

Nicotinic activation of L1 interneurons by foot shocks

Fear memory acquisition critically depends on the amygdala[18]. In contrast, the role of auditory cortex is contentious, with evidence both for[19,20] and against an essential function in auditory fear conditioning[19,21]. Based on the hypothesis that stimulus complexity determines the engagement of neocortex[18], we performed differential fear conditioning using trains of upward and downward frequency-modulated sweeps as the CS (Fig. 1a, modulation between 5 and 15 kHz). To test directly the role of auditory cortex in this paradigm, we inhibited neuronal activity during fear conditioning by local injection of the $GABA_A$ (γ-aminobutyric acid)-receptor agonist muscimol into the auditory cortex (Fig. 1a and Supplementary Fig. 1). When tested 24 h later in a drug-free state, this manipulation resulted in strongly reduced fear levels (Fig. 1b), indicating that activity in auditory cortex is required for fear learning in this paradigm.

We next focused on the circuit mechanisms underlying acquisition of fear memory in the auditory cortex (defined here as areas A1 and AuV). The role of the auditory cortex could be that of an essential relay for tone information to downstream structures like the amygdala. Alternatively, foot shocks alone might also elicit activity in the auditory cortex, and convergence of tone and foot-shock information during fear conditioning could then contribute to fear learning. To distinguish these alternatives, we used two-photon calcium imaging of neurons in

[1]Friedrich Miescher Institute for Biomedical Research, Maulbeerstrasse 66, CH-4058 Basel, Switzerland. [2]University of Basel, CH-4003 Basel, Switzerland. [3]INSERM U862, Neurocentre Magendie, 146 Rue Léo-Saignat, 33077 Bordeaux, France.
*These authors contributed equally to this work.

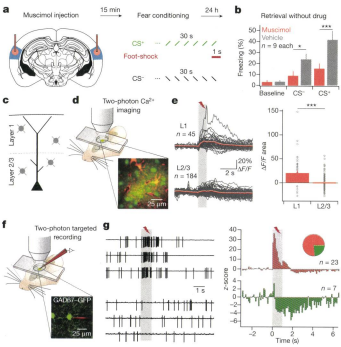

Figure 1 | Foot-shock responses in auditory cortex L1 interneurons. **a**, Left, injection of the $GABA_A$-receptor agonist muscimol (red) into the auditory cortex (blue). Right, differential fear-conditioning protocol using frequency-modulated sweeps. **b**, Drug-free freezing 1 day after conditioning in a new context. Compared to vehicle-injected mice (grey), muscimol reduced freezing to both CS^- and CS^+ (red). **c**, Cytoarchitecture of upper layers of auditory cortex (interneurons grey, pyramidal neuron black). **d**, Two-photon calcium imaging in head-fixed, anaesthetized mice using OGB-1 AM (green) and sulforhodamine 101 (red, counterstains glial cells). **e**, Left, responses in L1 and L2/3 to foot shocks in single neurons (grey) and the population average (red). Right, L1 interneurons display much stronger activation than L2/3 neurons. **f**, Two-photon targeted loose-seal cell-attached recording of L1 interneuron (green). **g**, Example traces (left) and z-scored population peri-stimulus time histograms (right) of two types of foot-shock responses in L1 interneurons. Inset, incidence of response type. Values are mean ± s.e.m. $*P < 0.05$, $***P < 0.001$. Statistical analysis in Supplementary Information.

the superficial layers of the auditory cortex in mice anaesthetized with chlorprothixene and urethane (Fig. 1c, d). Trains of frequency-modulated sweeps used as the CS strongly activated neurons in layer 2/3 (L2/3, Supplementary Fig. 2), whereas mild foot shocks applied to the hindpaws evoked little response (Fig. 1e and Supplementary Fig. 2). In marked contrast, the population of neurons located in L1 displayed strong activation by foot shocks (Fig. 1e). Layer 1 is unique in the neocortex because it contains only very few neuronal somata, almost all of which are GABAergic interneurons[22–25]. To investigate their activation in more detail, we used two-photon targeted loose-seal cell-attached recordings[26] (Fig. 1f). These experiments showed that L1 interneurons are tonically active (baseline frequency 3.2 ± 0.5 Hz, $n = 30$), and confirmed that the majority of L1 interneurons are strongly activated by foot shocks, while a minority (23%) displayed inhibition during and after foot shocks (Fig. 1g and Supplementary Fig. 3). The excitatory response was also present when foot shocks were paired with tones, whereas L1 interneurons did not show pronounced responses to tones alone (Supplementary Fig. 4). Interestingly, we observed a very similar activation of L1 interneurons by foot shocks in the primary visual cortex (Supplementary Fig. 5), indicating that the relevance of this pathway may extend beyond auditory memory acquisition.

Layer 1 is a prominent feedback pathway in the neocortex, containing both glutamatergic projections from higher cortical areas[27,28] (and from non-specific thalamic nuclei[29]) and cholinergic afferents from the basal forebrain, the major source of acetylcholine in the rodent neocortex[14,30–32]. We next sought to identify the afferent pathways mediating activation of L1 interneurons during foot shocks. Local bath-application of the glutamate receptor antagonist NBQX (1 mM) strongly reduced baseline firing frequency (Supplementary Fig. 6), but left the foot-shock response in L1 interneurons intact (Fig. 2a, b and Supplementary Fig. 6, see below). In contrast, combined application of the nicotinic acetylcholine receptor (nAChR) antagonists mecamylamine and methyllycaconitine (1 and 0.1 mM, respectively) abolished the L1 interneuron response almost completely (Fig. 2c and Supplementary Fig. 6), and drastically reduced baseline firing (Supplementary Fig. 6). In agreement with the interpretation that cholinergic basal forebrain afferents generate foot-shock responses in L1 interneurons, electrical microstimulation of the basal forebrain caused strong excitation of L1 interneurons in the absence of foot shocks (Fig. 2d and Supplementary Fig. 6). Activation of the basal forebrain by foot shocks is expected to have a longer latency than thalamocortical signalling[14]. Latency analysis showed that L1 interneuron activation was biphasic, with an early, glutamatergic peak (onset 10 to 20 ms after shock onset) which may originate from non-lemniscal thalamus[29], and a later, nicotinic peak (onset 40 to 50 ms after shock onset) that outlasted the foot shock and contained the majority of spikes (Fig. 2 insets). As previously reported[24], recordings from brain

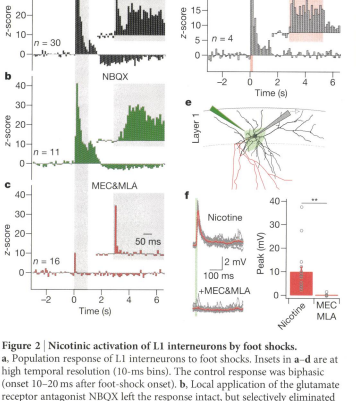

Figure 2 | Nicotinic activation of L1 interneurons by foot shocks. **a**, Population response of L1 interneurons to foot shocks. Insets in **a**–**d** are at high temporal resolution (10-ms bins). The control response was biphasic (onset 10–20 ms after foot-shock onset). **b**, Local application of the glutamate receptor antagonist NBQX left the response intact, but selectively eliminated the early peak, indicating its glutamatergic nature (inset, onset latency 40–50 ms). **c**, Local block of nAChRs by mecamylamine and methyllycaconitine (MEC&MLA) strongly reduced foot-shock responses, selectively eliminating the later, broader peak (inset). **d**, Electrical microstimulation of the basal forebrain activated L1 interneurons after 10 to 20 ms (inset, $n = 4$). **e**, Whole-cell recording of a L1 interneuron (black, soma and dendrites; red, axon) in auditory cortex slices during puff application of nicotine (100 μM, 20 ms). **f**, Left, example nicotine responses in control and after bath-application of mecamylamine (100 μM) and methyllycaconitine (0.1 μM; grey, single trials; red, average). Right, all L1 interneurons displayed nicotine responses ($n = 17$), which were blocked by the nAChR antagonists ($n = 8$). Values are mean ± s.e.m. $**P < 0.01$. Statistical analysis in Supplementary Information.

slices showed that all L1 interneurons showed responses to nicotine puffs (Fig. 2e, f) that were blocked by the same antagonists that abolished foot-shock responses *in vivo* (Fig. 2f), and could fire L1 interneurons (Supplementary Fig. 7). In summary, these results indicate that activity of cholinergic basal forebrain neurons is both necessary and sufficient to fire L1 interneurons during foot shocks, and that acetylcholine activates nAChRs on L1 interneurons. This implies that acetylcholine is released rapidly (<50 ms) after an aversive stimulus. Activation of L1 interneurons in turn is likely to have a central role in fear-conditioning-related plasticity in the cortex.

L1 interneurons inhibit L2/3 PV$^+$ interneurons

How do foot-shock responses in L1 interneurons affect processing in the local microcircuit? There is evidence that L1 interneurons can inhibit interneurons in L2/3 during nicotinic activation[24]. Fast-spiking, PV$^+$ interneurons are the most abundant type of interneuron in the neocortex[3]. We injected a conditional adeno-associated virus (AAV) expressing a fluorescent marker (venus) into auditory cortex of PV-ires-Cre mice[25] to label these cells selectively (Fig. 3a). Targeted recordings revealed that PV$^+$ interneurons in L2/3 are tonically active under baseline conditions (5.9 ± 1.2 Hz, $n = 17$), similar to fast-spiking interneurons in awake, head-fixed mice[24]. Foot shocks caused prominent, long-lasting inhibition of firing in the majority of PV$^+$ interneurons (88%, Fig. 3b and Supplementary Fig. 8), while the remaining two neurons displayed an excitatory response (Supplementary Fig. 9). Inhibition of PV$^+$ interneurons was strongly reduced by the nAChR antagonists mecamylamine and methyllycaconitine (Fig. 3b and Supplementary Fig. 8), which also blocked excitation of L1 interneurons by foot shocks (Fig. 2c). Because PV$^+$ fast-spiking interneurons lack intrinsic responses to acetylcholine[10,35], this result is consistent with direct inhibition of PV$^+$ interneurons by L1 interneurons. In line with this interpretation, we observed morphological and functional synaptic contacts between L1 interneurons and PV$^+$ interneurons (Supplementary Fig. 10). In addition, the time course of foot-shock responses in the two populations matches (Supplementary Fig. 11). Taken together, these data indicate that L2/3 fast-spiking PV$^+$ interneurons are inhibited by L1 interneurons during foot shocks.

To test whether this mechanism is also engaged in awake, freely moving animals, we implanted mice with single-unit recording electrodes in the superficial layers of the auditory cortex (Fig. 3c and Supplementary Fig. 12). Putative interneurons were distinguished from putative pyramidal neurons using unsupervised cluster analysis (Fig. 3d and Supplementary Fig. 12). Recordings during fear conditioning confirmed that a large population of putative interneurons is inhibited during and after an aversive shock (Fig. 3e and Supplementary Fig. 12). The same neurons were activated by the CS, indicating that the shock removes feed-forward inhibition in pyramidal neurons during auditory input. A similar proportion of putative interneurons displayed either excitation or no response to shocks (Supplementary Fig. 12). These data are consistent with the interpretation that excitation of L1 interneurons by aversive stimuli serves to remove both spontaneous and feed-forward inhibition provided by PV$^+$ interneurons to surrounding pyramidal neurons in behaving mice.

Disinhibition of L2/3 pyramidal neurons

PV$^+$ basket cells provide strong, perisomatic inhibition to local pyramidal neurons[3,6,7,10]. To test directly whether disinhibition is the main effect of foot shocks in auditory cortex L2/3 pyramidal cells, we used whole-cell recordings. Foot shocks elicited a depolarization from rest in all neurons tested (5 ± 1.1 mV, $n = 6$, Fig. 4a). The amplitude increased at more depolarized membrane potentials (Supplementary Fig. 13), consistent with a response mediated by strong disinhibition and weak excitation[36]. Application of nAChR antagonists converted the foot-shock response to a net inhibition (Fig. 4a), suggesting an involvement of the disinhibitory circuit described here, and perhaps indicating that its block unmasks a component of inhibition recruited by foot shocks. Finally, recordings under conditions isolating inhibitory postsynaptic currents (IPSCs)[17] revealed a drastic reduction

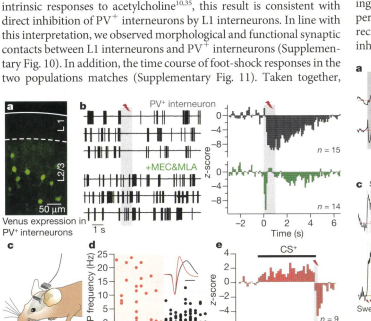

Figure 3 | Aversive shocks inhibit layer 2/3 PV$^+$ interneurons. **a**, Expression of venus in L2/3 PV$^+$ interneurons. **b**, Cell-attached recordings from PV$^+$ interneurons in control (top) show strong inhibition of spontaneous firing by foot shocks (left, example traces; right, population response). This response was strongly reduced in the presence of mecamylamine and methyllycaconitine (bottom). **c**, Single-unit recordings in the superficial layers of auditory cortex in freely behaving mice. **d**, Putative interneurons (red) were separated from putative pyramidal neurons (black) by unsupervised cluster analysis. Inset, example action potential (AP) waveforms (scale bar 400 μs). **e**, *z*-scored activity of putative interneurons showing inhibition by periorbital shocks during fear conditioning. Note recruitment by the CS$^+$ and subsequent inhibition by the shock ($n = 9$ of 24 putative interneurons, Supplementary Fig. 12).

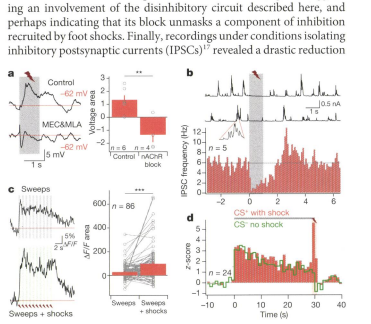

Figure 4 | Aversive shocks disinhibit L2/3 pyramidal neurons. **a**, Top left, *in vivo* whole-cell current-clamp recording of an auditory cortex pyramidal neuron during foot shocks. Bottom left, foot-shock response in the presence of mecamylamine and methyllycaconitine. Response area recorded at rest was reduced by nAChR antagonists (right). **b**, Whole-cell voltage-clamp recordings of inhibitory postsynaptic currents in pyramidal neurons show a strong reduction in IPSC frequency during and after foot shocks (top, example traces; bottom, population data, V_{hold} 0 to +20 mV). **c**, Left, example response of a L2/3 neuron to frequency-modulated sweeps (top) and sweeps paired with foot shocks (bottom) recorded with two-photon calcium imaging. Right, foot shocks caused a threefold enhancement of sweep response area in L2/3. **d**, Single-unit recordings of putative pyramidal neurons with significant response to the CS$^+$ in freely-behaving mice during fear conditioning. Note strong activation by coincidence of sweep and shock. Values are mean ± s.e.m. $^{**}P < 0.01$, $^{***}P < 0.001$. Statistical analysis in Supplementary Information.

of IPSC frequency during and after the foot shock (Fig. 4b). These results indicate that inhibition of PV^+ interneurons is a dominant influence shaping foot-shock responses in pyramidal neurons, and are in line with the observation that basal forebrain stimulation causes disinhibition of pyramidal cells[17].

Given that acetylcholine can affect many stages of neocortical information processing[8–11], we next aimed to determine how sensory input interacts with foot-shock-mediated disinhibition. We imaged calcium responses to tones in L2/3 of auditory cortex, and compared them to presentations of the same tones in conjunction with foot shocks (Fig. 4c and Supplementary Fig. 14). This experiment revealed that foot shocks cause a strong enhancement of the calcium signal integral, suggesting that tone/shock compounds elicit much greater activity than tones alone. A similar observation was made with extracellular recordings in freely moving mice, where coincidence of tone and shock excited putative pyramidal neurons much more than tone alone (Fig. 4d). This effect was highly supralinear in both experiments because shocks alone elicited almost no activity in these neurons (Supplementary Fig. 14). In summary, we provide evidence that L2/3 pyramidal neurons are disinhibited by aversive stimuli via inhibition of PV^+ interneurons.

Fear learning requires auditory cortex disinhibition

To determine whether activation of nAChRs contributes to fear learning, we applied mecamylamine and methyllycaconitine locally into the auditory cortex before fear conditioning (Fig. 5a and Supplementary Fig. 1). When tested 24 h later in drug-free state, this manipulation resulted in strongly reduced fear levels (Fig. 5b), consistent with a requirement for nicotinic activation of L1 interneurons. However, L1 interneurons are not the only circuit elements expressing nAChRs[8,9,11]. To test further whether disinhibition specifically during the foot shock contributes to fear learning, we used channelrhodopsin-2 (ChR-2)[37] expression in PV^+ interneurons (Fig. 5c and Supplementary Figs 15 and 16). Mice with chronic, bilateral optic fibre implantation (Fig. 5d) were subjected to differential fear conditioning in which optogenetic stimulation of PV^+ interneurons occurred during and for 5 s after the foot shock (Fig. 5e), the period during which we observed inhibition of these neurons (Fig. 3b). When tested 24 h later without optogenetic stimulation, these mice showed strongly reduced fear responses to the conditioned stimulus compared to sham-injected littermates (Fig. 5f). Reconditioning without optogenetic manipulation yielded normal fear learning (Fig. 5f). In addition, we ruled out the possibility that foot shock perception was perturbed by optogenetic stimulation and that laser illumination itself was perceived as a conditioned stimulus (Supplementary Fig. 17). Together, these data indicate that nicotinic disinhibition of the auditory cortex selectively during foot shock is required for associative fear learning.

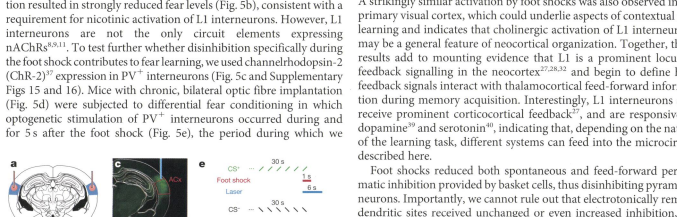

Figure 5 | Auditory cortex disinhibition is required for fear learning. **a**, Injection of mecamylamine and methyllycaconitine (red) into auditory cortex (blue) before fear conditioning. **b**, Drug-free freezing in a novel context one day after conditioning. Compared to vehicle-injected mice (grey), nAChR antagonism reduced freezing to both CS^- and CS^+ (red). **c**, Stimulation of ChR-2 expressing PV^+ interneurons (green) in auditory cortex (red) via an optic fibre (blue). **d**, Optogenetic manipulation in freely behaving mice. **e**, Differential fear conditioning protocol with optogenetic stimulation during and for 5 s after every foot shock. **f**, Freezing in a novel context without laser stimulation one day after conditioning. Compared to identically treated sham-injected littermates (black), virus-injected mice (blue) exhibit drastically reduced freezing to the CS^+. Reconditioning without optogenetic stimulation yielded strongly enhanced freezing (red) that was indistinguishable from sham. Values are mean ± s.e.m. $^{**}P < 0.01$, $^{***}P < 0.001$. Statistical analysis in Supplementary Information.

Discussion

Using targeted recordings from identified populations of auditory cortex neurons in conjunction with single-unit recordings, pharmacological and optogenetic manipulations in behaving mice, we have identified a disinhibitory microcircuit required for associative learning. Our data show that L1 interneurons play a central role in conveying information about an aversive stimulus to auditory cortex. Activity of L1 interneurons was tightly controlled by endogenous acetylcholine released from basal forebrain cholinergic projections, which determined baseline firing and acutely activated the majority of L1 interneurons during foot shocks, while a sub-set responded with inhibition. Given that all L1 interneurons express functional nAChRs[34] (Fig. 2), a likely source of this inhibition are synaptic interactions within L1 (ref. 25). Layer 1 contains several morphologically distinct subtypes of interneurons[22–25,38], and it remains to be determined whether foot-shock response type correlates with morphology. A strikingly similar activation by foot shocks was also observed in the primary visual cortex, which could underlie aspects of contextual fear learning and indicates that cholinergic activation of L1 interneurons may be a general feature of neocortical organization. Together, these results add to mounting evidence that L1 is a prominent locus of feedback signalling in the neocortex[27,28,32] and begin to define how feedback signals interact with thalamocortical feed-forward information during memory acquisition. Interestingly, L1 interneurons also receive prominent corticocortical feedback[27], and are responsive to dopamine[39] and serotonin[40], indicating that, depending on the nature of the learning task, different systems can feed into the microcircuit described here.

Foot shocks reduced both spontaneous and feed-forward perisomatic inhibition provided by basket cells, thus disinhibiting pyramidal neurons. Importantly, we cannot rule out that electrotonically remote dendritic sites received unchanged or even increased inhibition, for instance from L1 neuroglia form cells[25,38], which could serve to compartmentalize induction of synaptic plasticity. Nicotinic enhancement of inhibitory input to pyramidal neurons has been observed *in vitro*[11,41]. Therefore, the level of ongoing inhibition onto pyramidal neurons, as a prerequisite for disinhibition, may determine whether the net effect of nAChR activation is inhibitory or disinhibitory. Disinhibition is an attractive mechanism for learning because it is permissive for strong activation and concomitant plasticity induction, but not necessarily causative. Rather, the available sensory input at the time of the aversive stimulus can select the circuit elements for plasticity induction in a bottom-up fashion. In addition, other cholinergic actions like enhancement of thalamocortical transmission[11,42] and reduced GABA release from basket cell synapses[10] may have acted in synergy with the microcircuit described here to boost sensory responses.

Disinhibition of pyramidal neurons by foot shocks in turn probably gated the induction of activity-dependent plasticity in the auditory cortex[16,17] and at cortical afferents to the amygdala[18]. In parallel, cholinergic activation of L1 interneurons may also contribute to memory expression, because basal forebrain neurons acquire a conditioned response during learning[31,43]. Irrespective of the plasticity loci, our results delineate a role for the auditory cortex in fear conditioning to complex tones that goes beyond mere signalling of tone information to the amygdala[18–21]. Rather, we observe that stimulus convergence

and concomitant auditory cortex disinhibition are essential for fear learning. It is likely that the use of complex, naturalistic tones has emphasized the role of the auditory cortex[18], because fear conditioning to pure tones is often unaffected by auditory cortex lesions[19,21] (but see refs 19 and 20).

Beyond memory formation, cholinergic transmission is well known to mediate functions such as arousal and attention[30,31]. Interestingly, the transition from quiet wakefulness to active whisking is associated with a sharp drop in firing of fast-spiking interneurons in the barrel cortex[34], which is reminiscent of foot-shock responses in these neurons, and perhaps implies that cholinergic gating by inhibition of PV^+ interneurons is a general hallmark of active brain states.

METHODS SUMMARY

Male C57BL6/J mice (1.5 to 6 months old) were used. Full details of animals, materials and methods used for two-photon calcium imaging[44,45], patch-clamp[26] and single-unit recordings, pharmacological and optogenetic intervention[47] and behaviour[46] are provided in Methods.

Full Methods and any associated references are available in the online version of the paper at www.nature.com/nature.

Received 1 July; accepted 26 October 2011.
Published online 7 December 2011.

1. Martin, S. J. & Morris, R. G. New life in an old idea: the synaptic plasticity and memory hypothesis revisited. *Hippocampus* **12,** 609–636 (2002).
2. Hübener, M. & Bonhoeffer, T. Searching for engrams. *Neuron* **67,** 363–371 (2010).
3. Markram, H. *et al.* Interneurons of the neocortical inhibitory system. *Nature Rev. Neurosci.* **5,** 793–807 (2004).
4. Gabernet, L., Jadhav, S. P., Feldman, D. E., Carandini, M. & Scanziani, M. Somatosensory integration controlled by dynamic thalamocortical feed-forward inhibition. *Neuron* **48,** 315–327 (2005).
5. Wehr, M. & Zador, A. M. Balanced inhibition underlies tuning and sharpens spike timing in auditory cortex. *Nature* **426,** 442–446 (2003).
6. Freund, T. F. & Katona, I. Perisomatic inhibition. *Neuron* **56,** 33–42 (2007).
7. Kawaguchi, Y. & Kubota, Y. GABAergic cell subtypes and their synaptic connections in rat frontal cortex. *Cereb. Cortex* **7,** 476–486 (1997).
8. Lawrence, J. J. Cholinergic control of GABA release: emerging parallels between neocortex and hippocampus. *Trends Neurosci.* **31,** 317–327 (2008).
9. Bacci, A., Huguenard, J. R. & Prince, D. A. Modulation of neocortical interneurons: extrinsic influences and exercises in self-control. *Trends Neurosci.* **28,** 602–610 (2005).
10. Kruglikov, I. & Rudy, B. Perisomatic GABA release and thalamocortical integration onto neocortical excitatory cells are regulated by neuromodulators. *Neuron* **58,** 911–924 (2008).
11. Metherate, R. Nicotinic acetylcholine receptors in sensory cortex. *Learn. Mem.* **11,** 50–59 (2004).
12. Vogels, T. P. & Abbott, L. F. Gating multiple signals through detailed balance of excitation and inhibition in spiking networks. *Nature Neurosci.* **12,** 483–491 (2009).
13. Suga, N. & Ma, X. Multiparametric corticofugal modulation and plasticity in the auditory system. *Nature Rev. Neurosci.* **4,** 783–794 (2003).
14. Weinberger, N. M. Auditory associative memory and representational plasticity in the primary auditory cortex. *Hear. Res.* **229,** 54–68 (2007).
15. Quirk, G. J., Armony, J. L. & LeDoux, J. E. Fear conditioning enhances different temporal components of tone-evoked spike trains in auditory cortex and lateral amygdala. *Neuron* **19,** 613–624 (1997).
16. Ji, W., Suga, N. & Gao, E. Effects of agonists and antagonists of NMDA and ACh receptors on plasticity of bat auditory system elicited by fear conditioning. *J. Neurophysiol.* **94,** 1199–1211 (2005).
17. Froemke, R. C., Merzenich, M. M. & Schreiner, C. E. A synaptic memory trace for cortical receptive field plasticity. *Nature* **450,** 425–429 (2007).
18. LeDoux, J. E. Emotion circuits in the brain. *Annu. Rev. Neurosci.* **23,** 155–184 (2000).
19. Campeau, S. & Davis, M. Involvement of subcortical and cortical afferents to the lateral nucleus of the amygdala in fear conditioning measured with fear-potentiated startle in rats trained concurrently with auditory and visual conditioned stimuli. *J. Neurosci.* **15,** 2312–2327 (1995).
20. Boatman, J. A. & Kim, J. J. A thalamo-cortico-amygdala pathway mediates auditory fear conditioning in the intact brain. *Eur. J. Neurosci.* **24,** 894–900 (2006).
21. Romanski, L. M. & LeDoux, J. E. Bilateral destruction of neocortical and perirhinal projection targets of the acoustic thalamus does not disrupt auditory fear conditioning. *Neurosci. Lett.* **142,** 228–232 (1992).
22. Zhou, F. M. & Hablitz, J. J. Morphological properties of intracellularly labeled layer I neurons in rat neocortex. *J. Comp. Neurol.* **376,** 198–213 (1996).
23. Hestrin, S. & Armstrong, W. E. Morphology and physiology of cortical neurons in layer I. *J. Neurosci.* **16,** 5290–5300 (1996).
24. Christophe, E. *et al.* Two types of nicotinic receptors mediate an excitation of neocortical layer I interneurons. *J. Neurophysiol.* **88,** 1318–1327 (2002).
25. Chu, Z., Galarreta, M. & Hestrin, S. Synaptic interactions of late-spiking neocortical neurons in layer 1. *J. Neurosci.* **23,** 96–102 (2003).
26. Margrie, T. W. *et al.* Targeted whole-cell recordings in the mammalian brain *in vivo*. *Neuron* **39,** 911–918 (2003).
27. Gonchar, Y. & Burkhalter, A. Distinct GABAergic targets of feedforward and feedback connections between lower and higher areas of rat visual cortex. *J. Neurosci.* **23,** 10904–10912 (2003).
28. Cauller, L. J., Clancy, B. & Connors, B. W. Backward cortical projections to primary somatosensory cortex in rats extend long horizontal axons in layer I. *J. Comp. Neurol.* **390,** 297–310 (1998).
29. Rubio-Garrido, P., Perez-de-Manzo, F., Porrero, C., Galazo, M. J. & Clasca, F. Thalamic input to distal apical dendrites in neocortical layer 1 is massive and highly convergent. *Cereb. Cortex* **19,** 2380–2395 (2009).
30. Hasselmo, M. E. & Sarter, M. Modes and models of forebrain cholinergic neuromodulation of cognition. *Neuropsychopharmacology* **36,** 52–73 (2011).
31. Wenk, G. L. The nucleus basalis magnocellularis cholinergic system: one hundred years of progress. *Neurobiol. Learn. Mem.* **67,** 85–95 (1997).
32. Mechawar, N., Cozzari, C. & Descarries, L. Cholinergic innervation in adult rat cerebral cortex: a quantitative immunocytochemical description. *J. Comp. Neurol.* **428,** 305–318 (2000).
33. Hippenmeyer, S. *et al.* A developmental switch in the response of DRG neurons to ETS transcription factor signaling. *PLoS Biol.* **3,** e159 (2005).
34. Gentet, L. J., Avermann, M., Matyas, F., Staiger, J. F. & Petersen, C. C. Membrane potential dynamics of GABAergic neurons in the barrel cortex of behaving mice. *Neuron* **65,** 422–435 (2010).
35. Kawaguchi, Y. Selective cholinergic modulation of cortical GABAergic cell subtypes. *J. Neurophysiol.* **78,** 1743–1747 (1997).
36. Manookin, M. B., Beaudoin, D. L., Ernst, Z. R., Flagel, L. J. & Demb, J. B. Disinhibition combines with excitation to extend the operating range of the OFF visual pathway in daylight. *J. Neurosci.* **28,** 4136–4150 (2008).
37. Zhang, F., Aravanis, A. M., Adamantidis, A., de Lecea, L. & Deisseroth, K. Circuit-breakers: optical technologies for probing neural signals and systems. *Nature Rev. Neurosci.* **8,** 577–581 (2007).
38. Wozny, C. & Williams, S. R. Specificity of synaptic connectivity between layer 1 inhibitory interneurons and layer 2/3 pyramidal neurons in the rat neocortex. *Cereb. Cortex* **21,** 1818–1826 (2011).
39. Wu, J. & Hablitz, J. J. Cooperative activation of D1 and D2 dopamine receptors enhances a hyperpolarization-activated inward current in layer I interneurons. *J. Neurosci.* **25,** 6322–6328 (2005).
40. Foehring, R. C., van Brederode, J. F., Kinney, G. A. & Spain, W. J. Serotonergic modulation of supragranular neurons in rat sensorimotor cortex. *J. Neurosci.* **22,** 8238–8250 (2002).
41. Couey, J. J. *et al.* Distributed network actions by nicotine increase the threshold for spike-timing-dependent plasticity in prefrontal cortex. *Neuron* **54,** 73–87 (2007).
42. Gil, Z., Connors, B. W. & Amitai, Y. Differential regulation of neocortical synapses by neuromodulators and activity. *Neuron* **19,** 679–686 (1997).
43. Acquas, E., Wilson, C. & Fibiger, H. C. Conditioned and unconditioned stimuli increase frontal cortical and hippocampal acetylcholine release: effects of novelty, habituation, and fear. *J. Neurosci.* **16,** 3089–3096 (1996).
44. Stosiek, C., Garaschuk, O., Holthoff, K. & Konnerth, A. *In vivo* two-photon calcium imaging of neuronal networks. *Proc. Natl Acad. Sci. USA* **100,** 7319–7324 (2003).
45. Nimmerjahn, A., Kirchhoff, F., Kerr, J. N. & Helmchen, F. Sulforhodamine 101 as a specific marker of astroglia in the neocortex *in vivo*. *Nature Methods* **1,** 31–37 (2004).
46. Ciocchi, S. *et al.* Encoding of conditioned fear in central amygdala inhibitory circuits. *Nature* **468,** 277–282 (2010).

Supplementary Information is linked to the online version of the paper at www.nature.com/nature.

Acknowledgements We thank all members of the Lüthi laboratory for discussions and comments. We thank B. Kampa and T. Oertner for advice on two-photon imaging. R. Friedrich and J. Gründemann for comments on the manuscript. P. Argast, J. Lüdke and C. Müller for excellent technical assistance. H. Zielinska for preparation of artwork and S. Arber, Y. Yanagawa and K. Deisseroth for generously sharing materials. This work was supported by grants from the Swiss National Science Foundation (J.J.L. Ambizione; A.L.), the National Competence Center in Research (NCCR) of the Swiss Confederation on the synaptic basis of mental disorders, the French National Research Agency (C.H., ANR-2010-BLAN-1442-01), a Marie-Curie fellowship (J.J.L.), a Schering Foundation fellowship (S.B.E.W.), a Fonds AXA pour la Recherche fellowship (J.C.), the Aquitaine Regional Council (C.H.) and the Novartis Research Foundation.

Author Contributions J.J.L. initiated the project and performed most experiments and data analyses. S.B.E.W established optogenetic manipulations. S.B.E.W. and P.T. helped with optogenetic experiments. E.M.M.M. performed and analysed *in vitro* experiments. P.T. performed and analysed *in vivo* pharmacology. J.C. and C.H. performed and analysed single-unit recordings. J.J.L. and A.L. conceived the project and wrote the manuscript. All authors contributed to the experimental design and interpretation, and commented on the manuscript.

Author Information Reprints and permissions information is available at www.nature.com/reprints. The authors declare no competing financial interests. Readers are welcome to comment on the online version of this article at www.nature.com/nature. Correspondence and requests for materials should be addressed to J.J.L. (johannes.letzkus@fmi.ch) or A.L. (andreas.luthi@fmi.ch).

ARTICLE

doi:10.1038/nature10696

Structure of HIV-1 gp120 V1/V2 domain with broadly neutralizing antibody PG9

Jason S. McLellan[1]*, Marie Pancera[1]*, Chris Carrico[2], Jason Gorman[1], Jean-Philippe Julien[3], Reza Khayat[3], Robert Louder[1], Robert Pejchal[3], Mallika Sastry[1], Kaifan Dai[1], Sijy O'Dell[1], Nikita Patel[4], Syed Shahzad-ul-Hussan[1,5], Yongping Yang[1], Baoshan Zhang[1], Tongqing Zhou[1], Jiang Zhu[1], Jeffrey C. Boyington[1], Gwo-Yu Chuang[1], Devan Diwanji[3], Ivelin Georgiev[1], Young Do Kwon[1], Doyung Lee[1], Mark K. Louder[1], Stephanie Moquin[1], Stephen D. Schmidt[1], Zhi-Yong Yang[1], Mattia Bonsignori[6], John A. Crump[7,8], Saidi H. Kapiga[9], Noel E. Sam[8,9], Barton F. Haynes[6], Dennis R. Burton[10,11], Wayne C. Koff[12], Laura M. Walker[10], Sanjay Phogat[12], Richard Wyatt[13], Jared Orwenyo[14], Lai-Xi Wang[14], James Arthos[4], Carole A. Bewley[5], John R. Mascola[1], Gary J. Nabel[1], William R. Schief[2,10], Andrew B. Ward[3], Ian A. Wilson[3] & Peter D. Kwong[1]

Variable regions 1 and 2 (V1/V2) of human immunodeficiency virus-1 (HIV-1) gp120 envelope glycoprotein are critical for viral evasion of antibody neutralization, and are themselves protected by extraordinary sequence diversity and *N*-linked glycosylation. Human antibodies such as PG9 nonetheless engage V1/V2 and neutralize 80% of HIV-1 isolates. Here we report the structure of V1/V2 in complex with PG9. V1/V2 forms a four-stranded β-sheet domain, in which sequence diversity and glycosylation are largely segregated to strand-connecting loops. PG9 recognition involves electrostatic, sequence-independent and glycan interactions: the latter account for over half the interactive surface but are of sufficiently weak affinity to avoid autoreactivity. The structures of V1/V2-directed antibodies CH04 and PGT145 indicate that they share a common mode of glycan penetration by extended anionic loops. In addition to structurally defining V1/V2, the results thus identify a paradigm of antibody recognition for highly glycosylated antigens, which—with PG9—involves a site of vulnerability comprising just two glycans and a strand.

As the sole viral target of neutralizing antibodies, the HIV-1 viral spike has evolved to evade antibody-mediated neutralization (reviewed in ref. 1). V1/V2 of the gp120 component of the viral spike is critical to this evasion. Localized by electron microscopy to a membrane-distal 'cap'[2–5], which holds the spike in a neutralization-resistant conformation, V1/V2 is not essential for entry: its removal, however, renders the virus profoundly sensitive to antibody-mediated neutralization[6–9].

The ~50–90 residues that comprise V1/V2 contain two of the most variable portions of the virus, and roughly 1 in 10 residues of V1/V2 are *N*-glycosylated. Despite the diversity and glycosylation of V1/V2, a number of broadly neutralizing human antibodies have been identified that target this region, including the somatically related antibodies PG9 and PG16, which neutralize 70–80% of circulating HIV-1 isolates[10], antibodies CH01–CH04, which neutralize 40–50%[11], and antibodies PGT141–145, which neutralize 40–80%[12]. These antibodies all share specificity for an *N*-linked glycan at residue 160 in V1/V2 (HXB2 numbering) and show a preferential binding to the assembled viral spike over monomeric gp120 as well as a sensitivity to changes in V1/V2 and some V3 residues. Sera with these characteristics have been identified in a number of HIV-1 donor cohorts, and these quaternary-structure-preferring V1/V2-directed antibodies are among the most common broadly neutralizing responses in infected donors[13,14].

Despite extensive effort, V1/V2 had resisted atomic-level characterization. Here we report crystal structures of the V1/V2 domain of HIV-1 gp120 from clade C strains CAP45 and ZM109 in complexes with the antigen-binding fragment (Fab) of PG9 at 2.19- and 1.80-Å resolution, respectively. We elucidate how the V1/V2 fold accommodates sequence variation and glycosylation, provide an atomic-level description of the PG9 epitope, and analyse other members of this V1/V2-directed class of broadly neutralizing antibodies to identify conserved features that enable recognition of this key glycopeptide target.

Structure determination

Variational crystallization[15] of HIV-1 gp120 with V1/V2 was attempted following strategies that were successful for structural determination of other portions of HIV-1 gp120 (refs 15–17); this failed to produce V1/V2-containing crystals suitable for structural analysis (Supplementary Table 1). Because V1/V2 emanates from similar hairpins in core structures of HIV-1 (refs 18–21) and SIV[22] (Supplementary Fig. 1), we hypothesized that a protein scaffold that provided an appropriate hairpin might suitably incorporate and express an ectopic V1/V2 region. We identified six proteins with potentially suitable acceptor β-hairpins that ranged in size from 135 to 741 amino acids. Only the smallest of these could be expressed in

[1]Vaccine Research Center, National Institute of Allergy and Infectious Diseases, National Institutes of Health, Bethesda, Maryland 20892, USA. [2]Department of Biochemistry, University of Washington, Seattle, Washington 98195, USA. [3]Department of Molecular Biology and the Skaggs Institute for Chemical Biology, The Scripps Research Institute, La Jolla, California 92037, USA. [4]Laboratory of Immunoregulation, National Institute of Allergy and Infectious Diseases, National Institutes of Health, Bethesda, Maryland 20892, USA. [5]Laboratory of Bioorganic Chemistry, National Institute of Diabetes and Digestive and Kidney Diseases, National Institutes of Health, Bethesda, Maryland 20892, USA. [6]The Duke Human Vaccine Institute, Duke University School of Medicine, and Duke University Medical Center, Durham, North Carolina 27710, USA. [7]Division of Infectious Diseases and International Health, Department of Medicine, and Department of Pathology, Duke University Medical Center, Durham, North Carolina 27710, USA. [8]Kilimanjaro Christian Medical Centre and Kilimanjaro Christian Medical College, Tumaini University, Moshi, Tanzania. [9]Kilimanjaro Reproductive Health Programme, Moshi, Tanzania. [10]Department of Immunology and Microbial Science and IAVI Neutralizing Antibody Center, The Scripps Research Institute, La Jolla, California 92037, USA. [11]Ragon Institute of MGH, MIT, and Harvard, Cambridge, Massachusetts 02129, USA. [12]International AIDS Vaccine Initiative (IAVI), New York, New York 10004, USA. [13]IAVI Neutralizing Antibody Center at TSRI, Department of Immunology and Microbial Science, The Scripps Research Institute, La Jolla, California 92037, USA. [14]Institute of Human Virology and Department of Biochemistry & Molecular Biology, University of Maryland School of Medicine, Baltimore, Maryland 21201, USA.
*These authors contributed equally to this work.

transfected 293F cells when scaffolded with V1/V2 (Supplementary Table 2), but it behaved poorly in solution. We identified 11 smaller proteins of 36–87 amino acids in size and designed chimaeric proteins encoding V1/V2 from the YU2 strain of HIV-1 (Supplementary Fig. 2 and Supplementary Table 3). The expressed chimaeric glycoproteins from these smaller scaffolds were mostly soluble, permitting us to characterize them antigenically against a panel of six YU2-specific V1/V2 antibodies (Supplementary Tables 4 and 5). Three of the smaller scaffolded YU2 V1/V2 chimaeras showed reactivity with all six YU2-specific antibodies, and two (Protein Data Bank (PDB) accessions 1FD6 (ref. 23) and 1JO8 (ref. 24)) were also recognized by the $\alpha_4\beta_7$ integrin[25], suggesting that they retained biological integrity (Supplementary Table 5 and Supplementary Fig. 3). We next identified strains of gp120 that retained PG9 recognition in the gp120 monomer context, including clade B strain TRJO and clade C strains 16055, CAP45, ZM53 and ZM109 (Supplementary Table 6). We placed V1/V2 sequences (residues 126–196) from these strains into the 1FD6 and 1JO8 scaffolds, and assessed PG9 binding. Notably, affinities of PG9 for 1FD6-ZM109 and 1JO8-ZM109 were only 50-fold and threefold lower than wild-type ZM109 gp120, respectively (Supplementary Fig. 4). Scaffold-V1/V2 heterogeneity was apparent after expression in GnTI$^{-/-}$ cells[26] as was sulphation heterogeneity on antibody PG9 (ref. 27) (Supplementary Fig. 5). We therefore used an on-column selection procedure coupled to on-column protease cleavage of Fab to obtain homogeneous complexes of scaffold-V1/V2 with PG9 (Supplementary Fig. 6).

Two 1FD6-V1/V2 scaffolds were crystallized in complex with PG9. One scaffold contained the V1/V2 region from the gp120 of the CAP45 strain of HIV-1 with five sites of potential *N*-linked glycosylation. Crystals of this CAP45 construct with the Fab of PG9 diffracted to 2.19 Å, and the structure was refined to an R_{cryst} of 18.2% (R_{free} = 23.4%) (Fig. 1 and Supplementary Table 7). A second scaffold included the V1/V2 region from the gp120 of the ZM109 strain of HIV-1 with *N*-linked glycans at positions 160 and 173, and asparagine to alanine substitutions at four other potential *N*-linked sites. Crystals of this ZM109 construct with the Fab of PG9 diffracted to 1.80 Å, and the structure was refined to an R_{cryst} of 17.8% (R_{free} = 20.5%) (Supplementary Fig. 7 and Supplementary Table 7).

Structure of V1/V2

The V1/V2 structure, in the context of scaffold and PG9, folds as four anti-parallel β-strands (labelled A, B, C, D) arranged in (−1, −1, +3) topology[28] (Fig. 2a–d and Supplementary Table 8). Important structural elements, such as a hydrophobic core, connecting loops and disulphide bonds, cross between each of the four strands, indicating that, structurally, the V1/V2 domain should be considered a single topological entity.

Overall, the four-stranded V1/V2 sheet presents an elegant solution for maintaining a common fold while accommodating V1/V2 diversity and glycosylation. The strands contain mostly conserved residues and are welded in place by inter-strand disulphide bonds (between strand A and neighbouring strands B and D) and extensive hydrogen bonding (between strands A and D and between strands B and C). The two faces of the sheet—concave and convex—have very different characters. The concave face of the sheet is glycan-free and hydrophobic (Fig. 2e), with a cluster of aliphatic and aromatic side chains surrounding the disulphide bond that links strands A and B. This conserved hydrophobic cluster continues onto strand D at the sheet edge, to form a half-exposed hydrophobic core for this domain. The convex face of the sheet is cationic (Fig. 2f), with the main-chain atoms of the conserved strands of the sheet forming stripes on the V1/V2 surface (Fig. 2g) and the *N*-linked glycan 160 situated at its centre (Fig. 2h). In contrast, two strand-connecting loops—emanating from the same end of the sheet—are highly glycosylated and variable in sequence (Fig. 2i). We can now redefine the 'V1 loop' as the residues connecting strands A and B, and the 'V2 loop' as those residues between strands C and D (Fig. 2h, i). Of these, the V1 loop is most variable, ranging in length from ~10–30 residues. The V2 loop is less variable and contains at its start the tripeptide motif recognized by integrin $\alpha_4\beta_7$, the gut homing receptor for HIV-1 (ref. 25).

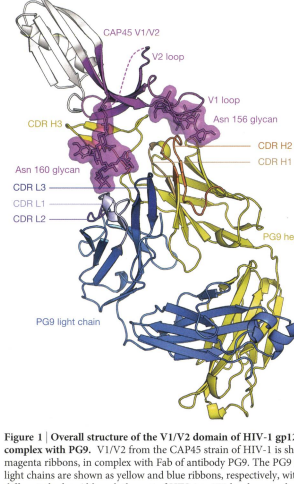

Figure 1 | Overall structure of the V1/V2 domain of HIV-1 gp120 in complex with PG9. V1/V2 from the CAP45 strain of HIV-1 is shown, in magenta ribbons, in complex with Fab of antibody PG9. The PG9 heavy and light chains are shown as yellow and blue ribbons, respectively, with CDRs in different shades. Although the rest of HIV-1 gp120 has been replaced by the 1FD6 scaffold (shown in white ribbons), the positions of V1/V2, PG9 and the scaffold are consistent with the proposal that the viral spike, and hence the viral membrane, is positioned towards the top of the page. The extended CDR H3 of PG9 is able to penetrate the glycan shield that covers the V1/V2 cap on the spike and to reach conserved elements of polypeptide, while residues in heavy- and light-chain-combining regions recognize *N*-linked glycans. The disordered region of the V2 loop is represented by a dashed line. Perpendicular views of V1/V2 are shown in Figs 2 and 6, and the structure of PG9 in complex with V1/V2 from HIV-1 strain ZM109 is shown in Supplementary Fig. 7.

PG9–V1/V2 interactions

The most prominent interaction between antibody PG9 and V1/V2 occurs with *N*-linked glycan (Fig. 3, Supplementary Fig. 8 and Supplementary Tables 9 and 10). PG9 grasps the entire ZM109 160 glycan (Fig. 3a). Its protruding third complementarity-determining region of the heavy chain (CDR H3) reaches through the glycan shield to contact the protein-proximal *N*-acetylglucosamine, burying 200 Å^2 of total surface area, with Asp 100 and Arg 100B of PG9 making four hydrogen bonds (Fig. 3b, c) (Kabat numbering[29] is used in description of antibody sequences; thus Arg 100B is two residues after Asp 100). Additional hydrogen bonds are made by the base of the CDR H3 (by Asn 100P and by the double-mannose-interacting His 100R) to terminal mannose residues, with Ser 32 and Asp 50 of the light chain contributing three additional hydrogen bonds (Fig. 3b). In sum, a total of 11 hydrogen bonds and over 1,150 Å^2 of surface area are buried in

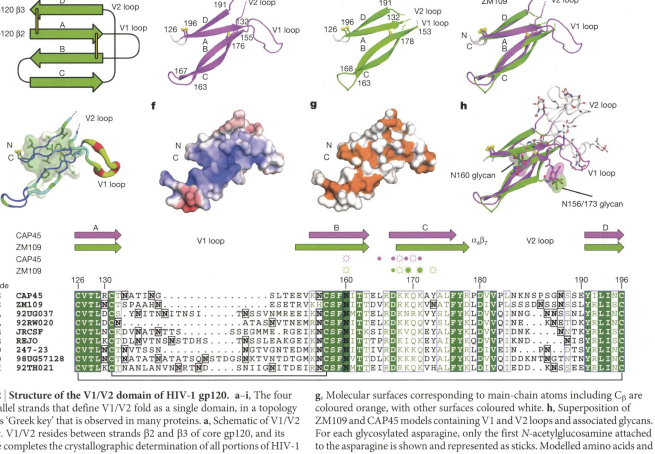

Figure 2 | Structure of the V1/V2 domain of HIV-1 gp120. **a**–**i**, The four anti-parallel strands that define V1/V2 fold as a single domain, in a topology known as 'Greek key' that is observed in many proteins. **a**, Schematic of V1/V2 topology. V1/V2 resides between strands β2 and β3 of core gp120, and its structure completes the crystallographic determination of all portions of HIV-1 gp120. Strands are depicted as arrows and disulphide bonds as yellow lines. **b**, **c**, Ribbon diagram of V1/V2 residues 126–196 from HIV-1 strains CAP45 (magenta) and ZM109 (green). Conserved disulphide bonds are represented as ball and stick, and the beginning and terminating residues of each strand are labelled. **d**, Superposition of the structures shown in **b** and **c**. **e**, Amino acid conservation of V1/V2. The backbone is shown as a tube of variable thickness, coloured as a rainbow from cold (blue) to hot (red), corresponding to conserved (thin) and to variable (thick), respectively, based on an alignment of 166 HIV-1 sequences. Aliphatic and aromatic side chains are shown as sticks with semi-transparent molecular surface, coloured by conservation as in **i**. **f**, Electrostatic surface potentials of CAP45 V1/V2 coloured blue to red, corresponding to positive and negative surface potentials (+4 to −4 kT/e), respectively. **g**, Molecular surfaces corresponding to main-chain atoms including C_β are coloured orange, with other surfaces coloured white. **h**, Superposition of ZM109 and CAP45 models containing V1 and V2 loops and associated glycans. For each glycosylated asparagine, only the first *N*-acetylglucosamine attached to the asparagine is shown and represented as sticks. Modelled amino acids and glycans that are disordered in the crystal structures are shown in grey. **i**, Sequence alignment of nine HIV-1 strains that are potently neutralized by PG9. Glycosylated asparagine residues are boxed and in bold. Identical residues have a dark green background with white characters, whereas conserved residues have white backgrounds with dark green characters. Above the alignment, β-strands are shown as arrows, coloured magenta and green for CAP45 and ZM109, respectively. Residues (including attached glycans) that make hydrogen bonds to PG9 are denoted with symbols above the alignment (side-chain hydrogen bonds are indicated by open circles with dashes, main-chain hydrogen bonds are indicated by closed circles, or main-chain and side-chain hydrogen bonds by closed circles with dashes).

the PG9–glycan–160 interface (489 $Å^2$ on PG9 and 670 $Å^2$ on glycan 160), with PG9 contacting 5 of the 7 saccharide moieties of the $Man_5GlcNAc_2$ glycan (Fig. 3c). Similar extensive interactions are observed with residue 160 of CAP45 (Supplementary Fig. 8a–c). The preference of PG9 for a $Man_5GlcNAc_2$ glycan at residue 160 is now clear: a larger glycan would clash with the antibody light chain and a shorter glycan would not stretch between tip and base of the PG9 CDR H3.

Interactions also occur between PG9 and the *N*-linked glycan at residue 156 (CAP45) or residue 173 (ZM109). With CAP45, much of the 156 glycan is ordered, stabilizing six of the seven sugars, including four of the five mannose residues (Supplementary Fig. 8). Hydrogen bonds are observed between the 156 glycan and the side chains of Asn 73 and Tyr 100K of the PG9 heavy chain, and 766 $Å^2$ of total buried surface area (337 $Å^2$ on PG9 and 429 $Å^2$ of glycan). Glycan 156 is not preserved in the ZM109 sequence, in which residue 156 is a histidine (Fig. 2i); an additional site of *N*-linked glycosylation, however, occurs in ZM109 at residue 173, in the middle of strand C. In the ZM109 structure, glycan 173 is in virtually the same spatial location as glycan 156 in the CAP45 structure (Fig. 2h). PG9 binds to the protein-proximal *N*-acetylglucosamine, with Tyr 100K making a hydrogen bond and a total of 189 $Å^2$ surface area buried (Fig. 3b). Notably, substitutions that result in changes in V1/V2 glycans indicate that glycan at 160 is critical for PG9 recognition (Supplementary Table 11), and 156/173 is important (although PG9 recognizes strains of HIV-1 lacking a 156/173 glycan; Supplementary Fig. 9). Many of the changes in the heavy and light chains that allow for glycan recognition occur during affinity maturation (Supplementary Tables 12 and 13), providing a possible explanation for the observed increase in PG9 (and PG16) breadth and affinity during affinity maturation[30].

In addition to glycan recognition, a strand in the CDR H3 of PG9 forms intermolecular parallel β-sheet-like hydrogen bonds to strand C of V1/V2 (Fig. 3d, e). Strand C is the most variable of the V1/V2 strands, and this sequence-independent means of recognition probably allows for increased recognition breadth. Specific electrostatic interactions are also made between cationic residues of strand C and acidic residues on PG9. Notably, several of these occur with sulphated tyrosines on CDR H3. Because parallel β-strand hydrogen bonding would tend to align main-chain atoms of CDR H3 and strand C, the charged tips of Lys and Arg residues would protrude beyond the standard acidic Asp and Glu side chains, whereas tyrosine sulphates provide a closer match to the side-chain length of basic Lys/Arg residues.

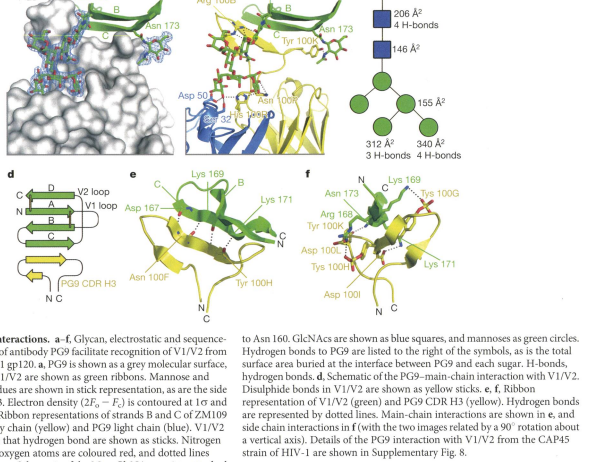

Figure 3 | PG9–V1/V2 interactions. **a**–**f**, Glycan, electrostatic and sequence-independent interactions of antibody PG9 facilitate recognition of V1/V2 from the ZM109 strain of HIV-1 gp120. **a**, PG9 is shown as a grey molecular surface, and strands B and C of V1/V2 are shown as green ribbons. Mannose and *N*-acetylglucosamine residues are shown in stick representation, as are the side chains of Asn 160 and 173. Electron density ($2F_o - F_c$) is contoured at 1σ and shown as a blue mesh. **b**, Ribbon representations of strands B and C of ZM109 V1/V2 (green), PG9 heavy chain (yellow) and PG9 light chain (blue). V1/V2 glycans and PG9 residues that hydrogen bond are shown as sticks. Nitrogen atoms are coloured blue, oxygen atoms are coloured red, and dotted lines represent hydrogen bonds. **c**, Schematic of the $Man_5GlcNAc_2$ moiety attached to Asn 160. GlcNAcs are shown as blue squares, and mannoses as green circles. Hydrogen bonds to PG9 are listed to the right of the symbols, as is the total surface area buried at the interface between PG9 and each sugar. H-bonds, hydrogen bonds. **d**, Schematic of the PG9–main-chain interaction with V1/V2. Disulphide bonds in V1/V2 are shown as yellow sticks. **e**, **f**, Ribbon representation of V1/V2 (green) and PG9 CDR H3 (yellow). Hydrogen bonds are represented by dotted lines. Main-chain interactions are shown in **e**, and side chain interactions in **f** (with the two images related by a 90° rotation about a vertical axis). Details of the PG9 interaction with V1/V2 from the CAP45 strain of HIV-1 are shown in Supplementary Fig. 8.

Overall, the structure of PG9 is consistent with published mutational data[10,14] (Supplementary Table 14). Some residues such as Phe 176 are critical because they form part of the hydrophobic core on the concave face of the V1/V2 sheet. Others form direct contacts: for example, the tyrosine sulphate at residue 100H of PG9 interacts with residue 168 when it is an Arg (strain ZM109) or Lys (strain CAP45), but would be repelled by a Glu (as in strain JR-FL); JR-FL is resistant to neutralization by PG9, but becomes sensitive if Glu 168 is changed to Lys[10].

Quaternary preferences of PG9 and PG16

PG9 and the somatically related PG16 typically recognize the assembled viral spike with higher affinity than monomeric gp120 (ref. 10). For PG9, the average monomeric gp120 affinity, as assessed by ELISA or surface plasmon resonance, was at least tenfold weaker than viral spike affinity, as assessed by neutralization; with PG16, the difference was at least 100-fold (Fig. 4a, Supplementary Tables 6 and 15–17). Such differences are probably greater as the concentration required for neutralization (half-maximum inhibitory concentration, IC_{50}) is often higher than the affinity (half-maximum effective concentration, EC_{50}, or equilibrium dissociation constant, K_d). To investigate differences between monomeric and oligomeric contexts, we acquired negatively stained electron microscopy images of PG9 in complex with monomeric gp120 (Fig. 4b, Supplementary Figs 10 and 11). To define the orientation of monomeric gp120, we used the CD4-binding-site-directed antibody T13, for which we defined the crystal structure of gp120-bound T13 Fab at 6-Å resolution (Supplementary Figs 12, 13 and Supplementary Table 18). This structure along with the V1/V2–PG9 structure allowed for the definition of six classes of relative gp120–PG9 orientations, indicating that the position of V1/V2 varies in the monomeric gp120 context. In contrast, prior cryoelectron microscopy results indicate that the position of V1/V2 in the unliganded Env trimer spike is fixed[2–5].

Additionally, we chose to map the antibody paratope by assessing neutralization with arginine mutants. We selected the PG16 paratope for characterization, as its recognition seemed to be both more quaternary-structure preferring (Fig. 4a) and more V3 dependent[10] than that of PG9. We parsed its combining site into 21 surface segments plus one in the framework as a control. Each of these was altered by the introduction of a single arginine mutation, expressed as an immunoglobulin, and assessed for neutralization on a panel of diverse HIV-1 isolates (Supplementary Fig. 14). The resultant 'arginine-scanning' mutagenesis revealed a close match to the observed V1/V2 interface for PG9 (Fig. 4c). We also measured the binding of PG9 and PG16 to monomeric gp120 in wild-type and V3-deleted contexts, and observed similar affinities, indicating that—in the context of monomeric gp120—V3 does not have a substantial role in PG9 or PG16 recognition (Supplementary Fig. 15). Lastly, accumulating data indicate that V1/V2 in the viral spike both shields and interacts with V3 (refs 6–9).

Collectively, these results suggest that the V1/V2–PG9 interaction observed in the scaffolded V1/V2–PG9 crystal structures encompasses much of the PG9/PG16 epitope, and that the structural integrity of this epitope is sensitive to appropriate assembly of the viral spike. We note parenthetically that the ability of the PG9/PG16-recognized epitope to be preferentially present in the assembled viral spike provides a useful strategy to hide this potential site of vulnerability. That is, the site may be preferentially present on the assembled viral spike, but not on shed or other monomeric forms of gp120, which are thought to be the predominant form of Env in infected individuals, and we note in this

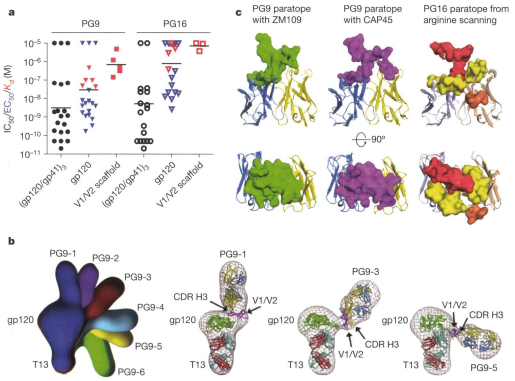

Figure 4 | PG9 and PG16 recognition of the HIV-1 viral spike, monomeric gp120 and scaffolded V1/V2. a–**c**, Quaternary-structure-preferring antibodies show different affinities for oligomeric, monomeric and scaffolded V1/V2. Both structural and arginine-scanning mapping, however, suggest that the epitopes of PG9 and PG16 are mostly present in scaffolded V1/V2. **a**, Affinities of PG9 (filled symbols) and PG16 (open symbols) are shown for the functional viral spike (gp120/gp41)$_3$ (circles), monomeric gp120 (triangles), and scaffold-V1/V2 (squares), based on neutralization (black), ELISA (blue) and surface plasmon resonance (red). **b**, Negative stained class averages are shown for ternary complexes of wild-type gp120 (HIV-1 strain 16055) in complex with antibody PG9 and the CD4-binding-site antibody T13. Six different classifications were observed, and are superimposed in the left panel and labelled PG9-1 to PG9-6. Individual fitting for classes PG9-1, PG9-3 and PG9-5 are shown after rigid-body alignment of Fab PG9–scaffold-V1/V2, Fab T13 and core gp120 (in the conformation bound by the CD4-binding site antibody F105; ref. 20). **c**, Comparison of crystallographically defined PG9 paratope with neutralization-defined PG16 paratope. Scaffold-V1/V2 interactive surface of PG9 in ZM109 (left) and CAP45 (middle) contexts is shown along with the PG16 paratope (right) as defined by arginine-scanning mutagenesis (residues mutated to arginine are coloured according to the fold-increase in IC_{50} for the mutant relative to wild type: yellow for <50, orange for <100 and red for >100; orange-highlighted residue is Trp 64 in the CDR H2). Perpendicular views of the paratope, rotated by 90° about a horizontal axis, are shown in top and bottom rows.

regard that many V1/V2-directed antibodies are substantially more quaternary-structure preferring than PG9 (refs 10–12, 31). The quaternary-specific nature of the epitope may thus reflect a functional adaptation of HIV-1.

A conserved CDR H3 motif for V1/V2 recognition

Sequences of other V1/V2-directed broadly neutralizing antibodies indicate the presence of long CDR H3s, but little other sequence conservation (Fig. 5a). We have not yet been able to determine structures of other class members in complex with V1/V2, but nonetheless sought to provide insight into their conserved features of recognition by analysing unbound Fab structures.

The structure of unbound PG9 Fab (3.3-Å resolution, four molecules per asymmetric unit; Supplementary Fig. 16 and Supplementary Table 19) revealed considerable CDR H3 flexibility, similar to that observed previously with PG16 (ref. 30). For CH01–CH04 antibodies[11], crystallization was attempted for antigen-binding fragments and for six heavy/light-chain somatic chimaeras (Supplementary Table 20). Structures were determined for CH04 Fab and also for the CH04H/CH02L Fab, the latter in two different crystal forms (Supplementary Fig. 17 and Supplementary Table 19). These structures revealed an anionic CDR H3 for CH04, which extended above the rest of the combining site in a manner similar to the CDR H3s of PG9 and PG16 (Fig. 5b). With CH04, however, the extended hairpin was twisted ~90°, to an orientation that bisected heavy and light chains. The spacing between the protruding CDR H3 and the rest of the combining region was reduced by 8 Å relative to that of PG9, and no CDR H3 tyrosine sulphation was observed.

With PGT141–145 antibodies[12], Fab crystals of unbound PGT145 diffracted to 2.3 Å and revealed an extended, tyrosine-sulphated CDR H3 loop, which, like those of PG9, PG16 and CH04, reached substantially beyond the rest of the CDR loops. In contrast, the β-hairpin of CDR H3 extended vertically (parallel to the long axis of the Fab) (Fig. 5b, Supplementary Fig. 18 and Supplementary Table 19) and was rigidified by extensive tyrosine stacking (along with the standard strand–strand hydrogen bonding). Its negatively charged tip (including two sulphated tyrosines) was followed by a Gly-containing potential 'hinge' and resembled an extended version of the CDR H3 of antibody 2909 (refs 32, 33), a highly quaternary-structure-sensitive antibody[31,34] that recognizes an immunotype variant of the V1/V2 target site in which a Lys is substituted for the *N*-linked glycan at position 160 (ref. 35).

Thus, despite having been derived from three different individuals, antibodies from this class of V1/V2-directed broadly neutralizing antibodies all showed anionic protruding CDR H3s (Fig. 5b), most of which were tyrosine sulphated. All also displayed β-hairpins and, although these varied substantially in orientation relative to the rest of the combining site, all appeared capable of penetrating an *N*-linked glycan shield to reach a cationic protein surface.

A V1/V2 site of HIV-1 vulnerability

With both CAP45 and ZM109 strains of gp120, the V1/V2 site recognized by PG9 consists primarily of two glycans and a strand (Fig. 6a).

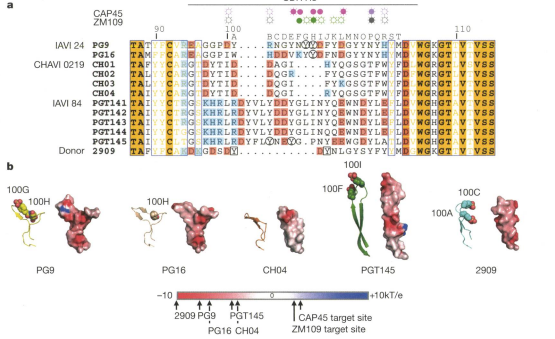

Figure 5 | CDR H3 features of V1/V2-directed broadly neutralizing antibodies. a, **b**, A protruding anionic CDR H3 is preserved in members of this broadly neutralizing class of antibodies. **a**, CDR H3 sequence alignment. Cohort, donor information and sequences in the CDR H3 are shown for V1/V2-directed antibodies (note that Kabat[29] numbering and formatting is shown for PG9, to which other antibodies are aligned). Positively charged residues are boxed in blue and negatively charged residues in red. Residues that make hydrogen bonds to CAP45 residues (magenta) or glycans (purple) are denoted with symbols above the alignment (side-chain hydrogen bonds are indicated by open circles with dashes, main-chain hydrogen bonds by closed circles, or main-chain and side-chain hydrogen bonds by closed circles with dashes). Similar contacts are shown for ZM109 residues (green) or glycans (grey). Sulphated tyrosines are circled or squared if the post-translational modification has been confirmed crystallographically or by mass spectrometry, respectively. The sequence for the V1/V2-directed strain-specific antibody, 2909, is also included. **b**, Protruding CDR H3, displayed as ribbon diagrams with sulphated tyrosines shown in spheres and paired with electrostatic surface potentials coloured blue to red, corresponding to positive and negative surface potentials, respectively. All CDR H3s are aligned so that the light chain would be on the left and the heavy chain on the right (as in Supplementary Fig. 17). Average electrostatic potentials are shown for specified CDR H3 and V1V2 surfaces.

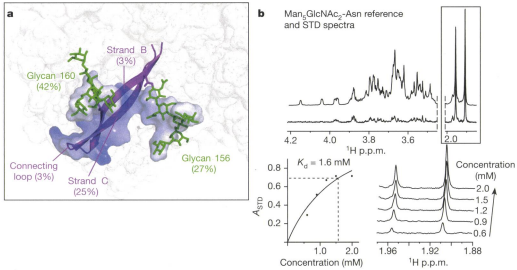

Figure 6 | Two glycans and a strand comprise a V1/V2 site of vulnerability. a, **b**, Glycan, electrostatic and sequence-independent interactions allow PG9 to recognize a glycopeptide site on V1/V2. **a**, Site characteristics in CAP45 strain of HIV-1. Glycans 160 and 156 (173 with ZM109) are highlighted in green, and strands B and C are highlighted in magenta, with the rest of V1/V2 in semi-transparent white. The interactive surface of V1/V2 with PG9 is shown, coloured according to the local electrostatic potential as in Fig. 5b. The contribution of each structural element to that surface is provided as a percentage of the total. Although the V1/V2 scaffolds used here do not allow a comprehensive analysis of the overall antibody response to this region of gp120, in addition to assisting with structural definition of effective V1/V2-directed neutralization, the V1/V2 scaffolds may have utility in attempts to direct the V1/V2-elicited response away from the hypervariable loops to the conserved strands—especially the site of vulnerability highlighted here. **b**, Saturation transfer difference (STD) NMR for $Man_5GlcNAc_2$-Asn binding to PG9. Top, STD spectrum of 1.5 mM $Man_5GlcNAc_2$-Asn in the presence of 15 μM Fab PG9 (lower spectrum) is paired with the corresponding reference spectrum (upper spectrum). Bottom left, Langmuir binding curve as a function of glycan concentration, used to obtain the K_d (A_{STD} signals correspond to *N*-acetyl protons, which are shown in the boxed area of the top panel). Bottom right, stacked STD NMR spectra as a function of $Man_5GlcNAc_2$-Asn concentration.

Minor interaction with strand B and with the B–C connecting loop (3% and 3–5% of the total interactive surface, respectively) complete the epitope, with the entire PG9-recognized surface of V1/V2 contained within the B–C hairpin (Supplementary Table 21). The minimal nature of this epitope suggests that it might be easier to engineer and to present to the immune system than other, more complex, epitopes. The epitopes for antibodies b12 and VRC01, for example, are comprised of seven and six independent protein segments[19,36], respectively. The presence in the PG9 epitope of *N*-linked glycosylation, which is added by host cell machinery, does provide a potentially complicating factor for humoral recognition.

To assess glycan affinities, we used saturation transfer difference NMR. In the crystal structure, recognition by PG9 occurs with protein-proximal *N*-acetylglucosamine and terminal mannose saccharides. With 1.5 mM (N-acetylglucosamine)$_2$, interaction with PG9 was not observed (Supplementary Fig. 19), whereas with 1.5 mM oligomannose-5, weak interactions were observed (Supplementary Fig. 20). We further carried out a titration series with Asn-(N-acetylglucosamine)$_2$(mannose)$_5$ and determined its affinity for PG9 to be 1.6 ± 0.9 mM (Fig. 6b). The weak affinity for glycan (surprising in the face of such a large contact surface and multiple hydrogen bonds) provides a potential explanation for the reported lack of PG9 autoreactivity despite its *N*-glycan dependence[10] (specificity for oligomannose-5 probably also reduces PG9 autoreactivity, as this glycan is infrequently displayed on the surface of mammalian cells).

Strand C is the most cationic of the V1/V2 strands. This conserved cationic character—present in the target-cell-facing V1/V2 cap of the viral spike—may relate to the observed anionic interactions of the viral spike, both with dextran sulphate[37,38] and other polyanions[39,40] or with heparan sulphate on the cell surface[41]. In terms of the ionic interactions of PG9 itself, we observed sulphation to increase affinity and neutralization potency by ~10-fold[27] (Supplementary Fig. 5). Ionic PG9 interactions may thus mimic the functional polyanion–V1/V2 interactions that HIV-1 uses for cell surface attachment during the initial stages of virus cell entry.

Strand C is also the most variable of the V1/V2 strands. Its location, at the edge of the sheet, however, provides an opportunity for sequence-independent recognition, through its exposed main-chain atoms. Whereas the four hydrogen bonds made by the main chain of PG9 probably contribute only a small portion of the overall binding energy, the surface of V1/V2 involved in main-chain interactions with PG9 totals 348 and 350 Å^2 in the CAP45 and ZM109 complexes, respectively, potentially providing a substantial contribution to the overall binding energy (Supplementary Table 21). This type of β-sheet interaction, for example, is the primary interaction between the CDR H3 of antibody 447-52D and the V3 of gp120 (ref. 42) in a 3-and-almost-4-stranded β-sheet.

Vaccine implications

The different types of PG9 interaction, involving glycan, electrostatic and sequence-independent interactions, all seem to be necessary for PG9 function. Such multicomponent recognition may also provide a mechanism that enables the immune system to overcome evasion associated with individual components of the interaction. Thus, for example, glycan-only affinity might lead to autoreactivity, and surface areas of electrostatic and sequence-independent interactions might be individually too small to generate sufficient affinity for tight interactions. Together, however, the glycan, electrostatic and sequence-independent interactions achieve the substantial level of affinity required for potent neutralization.

In longitudinal studies, antibody responses that require glycan, either at residue 160, as described here, or at residue 332, constitute the most commonly elicited initial broadly neutralizing responses[43], an observation also seen with elite neutralizers[13]. In such studies, transmitted/founder viruses in some cases did not show canonical glycosylation (for example, at positions 160 or 332), but acquired these under immune selection[44]. Thus it seems that *N*-linked glycosylation at particular residues is selected as a means of immune evasion, but that these same glycans—now part of a homogeneous glycan array—can be recognized by very broadly neutralizing antibodies. Recent structural results indicate that a number of 332-glycan-dependent antibodies also use protruding CDR H3s and, in at least one case, the antibody (PGT128) recognizes an epitope composed of two glycans and a strand[45]. Collectively these results suggest that an antibody with a penetrating CDR H3 that recognizes a conserved glycan and neighbouring polypeptide is a paradigm for humoral recognition of heavily glycosylated antigens.

Lastly, we note that recent immune analyses of the RV144 vaccine trial suggest that the presence of V1/V2-reactive antibodies associates inversely with HIV-1-infection risk[46,47]. What role these antibodies have in protection, however, is unknown. It is nonetheless fascinating that the V1/V2 domain—which functions in evading antibody-mediated neutralization—is itself a site of effective neutralization by a number of broadly neutralizing antibodies (for example, by PG9, CH04 and PGT145) and that antibodies against this domain seem to be an indicator of a successful vaccine outcome.

METHODS SUMMARY

Proteins that could accommodate backbone grafting of the V1/V2 stub from HIV-1 gp120 were identified using the Multigraft Match algorithm[48] implemented in Rosetta. Potential V1/V2 scaffolds were examined manually and, if necessary, optimizations were made to accommodate full-length V1/V2 loops (residues 126–196) or to alter scaffold properties (for example, mutating the intrinsic immunoglobulin affinity of 1FD6; ref. 49). For each V1/V2 scaffold, protein-A-purified PG9, altered to remove light-chain glycosylation and to introduce an HRV3C cleavage site in the hinge, was bound to Protein A Plus agarose, and the V1/V2 scaffold added. After washing away unbound scaffold, HRV3C protease was added to elute the PG9 Fab–V1/V2 scaffold complex. Complexes of PG9 Fab bound to 1FD6-CAP45 or 1FD6-ZM109 crystallized in similar conditions[50] (8–17% (w/v) PEG 3350, 5–10% (v/v) 2-methyl-2,4-pentanediol, 0.2 M lithium sulphate, 0.1 M imidazole pH 6.5). Crystals were cryoprotected with 15% (v/v) 2*R*,3*R*-butanediol, diffraction data were collected to 2.19 and 1.80 Å for PG9–1FD6-CAP45 and PG9–1FD6-ZM109, respectively, and structures solved by molecular replacement.

Full Methods and any associated references are available in the online version of the paper at www.nature.com/nature.

Received 1 September; accepted 4 November 2011.
Published online 23 November 2011.

1. Wyatt, R. & Sodroski, J. The HIV-1 envelope glycoproteins: fusogens, antigens, and immunogens. *Science* **280,** 1884–1888 (1998).
2. Liu, J., Bartesaghi, A., Borgnia, M. J., Sapiro, G. & Subramaniam, S. Molecular architecture of native HIV-1 gp120 trimers. *Nature* **455,** 109–113 (2008).
3. Wu, S. R. *et al.* Single-particle cryoelectron microscopy analysis reveals the HIV-1 spike as a tripod structure. *Proc. Natl Acad. Sci. USA* **107,** 18844–18849 (2010).
4. White, T. A. *et al.* Molecular architectures of trimeric SIV and HIV-1 envelope glycoproteins on intact viruses: strain-dependent variation in quaternary structure. *PLoS Pathog.* **6,** e1001249 (2010).
5. Hu, G., Liu, J., Taylor, K. A. & Roux, K. H. Structural comparison of HIV-1 envelope spikes with and without the V1/V2 loop. *J. Virol.* **85,** 2741–2750 (2011).
6. Cao, J. *et al.* Replication and neutralization of human immunodeficiency virus type 1 lacking the V1 and V2 variable loops of the gp120 envelope glycoprotein. *J. Virol.* **71,** 9808–9812 (1997).
7. Stamatatos, L. & Cheng-Mayer, C. An envelope modification that renders a primary, neutralization-resistant clade B human immunodeficiency virus type 1 isolate highly susceptible to neutralization by sera from other clades. *J. Virol.* **72,** 7840–7845 (1998).
8. Pinter, A. *et al.* The V1/V2 domain of gp120 is a global regulator of the sensitivity of primary human immunodeficiency virus type 1 isolates to neutralization by antibodies commonly induced upon infection. *J. Virol.* **78,** 5205–5215 (2004).
9. Rusert, P. *et al.* Interaction of the gp120 V1/V2 loop with a neighboring gp120 unit shields the HIV envelope trimer against cross-neutralizing antibodies. *J. Exp. Med.* **208,** 1419–1433 (2011).
10. Walker, L. M. *et al.* Broad and potent neutralizing antibodies from an African donor reveal a new HIV-1 vaccine target. *Science* **326,** 285–289 (2009).
11. Bonsignori, M. *et al.* Analysis of a clonal lineage of HIV-1 envelope V2/V3 conformational epitope-specific broadly neutralizing antibodies and their inferred unmutated common ancestors. *J. Virol.* **85,** 9998–10009 (2011).
12. Walker, L. M. *et al.* Broad neutralization coverage of HIV by multiple highly potent antibodies. *Nature* **477,** 466–470 (2011).

13. Walker, L. M. *et al.* A limited number of antibody specificities mediate broad and potent serum neutralization in selected HIV-1 infected individuals. *PLoS Pathog.* **6,** e1001028 (2010).
14. Moore, P. L., *et al.* Potent and broad neutralization of HIV-1 subtype C by plasma antibodies targeting a quaternary epitope including residues in the V2 loop. *J. Virol.* **85,** 3128–3141 (2011).
15. Kwong, P. D. *et al.* Probability analysis of variational crystallization and its application to gp120, the exterior envelope glycoprotein of type 1 human immunodeficiency virus (HIV-1). *J. Biol. Chem.* **274,** 4115–4123 (1999).
16. Huang, C. C. *et al.* Structure of a V3-containing HIV-1 gp120 core. *Science* **310,** 1025–1028 (2005).
17. Pancera, M. *et al.* Structure of HIV-1 gp120 with gp41-interactive region reveals layered envelope architecture and basis of conformational mobility. *Proc. Natl Acad. Sci. USA* **107,** 1166–1171 (2010).
18. Kwong, P. D. *et al.* Structure of an HIV gp120 envelope glycoprotein in complex with the CD4 receptor and a neutralizing human antibody. *Nature* **393,** 648–659 (1998).
19. Zhou, T. *et al.* Structural definition of a conserved neutralization epitope on HIV-1 gp120. *Nature* **445,** 732–737 (2007).
20. Chen, L. *et al.* Structural basis of immune evasion at the site of CD4 attachment on HIV-1 gp120. *Science* **326,** 1123–1127 (2009).
21. Kwong, P. D. *et al.* Structures of HIV-1 gp120 envelope glycoproteins from laboratory-adapted and primary isolates. *Structure* **8,** 1329–1339 (2000).
22. Chen, B. *et al.* Structure of an unliganded simian immunodeficiency virus gp120 core. *Nature* **433,** 834–841 (2005).
23. Ross, S. A., Sarisky, C. A., Su, A. & Mayo, S. L. Designed protein G core variants fold to native-like structures: sequence selection by ORBIT tolerates variation in backbone specification. *Protein Sci.* **10,** 450–454 (2001).
24. Fazi, B. *et al.* Unusual binding properties of the SH3 domain of the yeast actin-binding protein Abp1: structural and functional analysis. *J. Biol. Chem.* **277,** 5290–5298 (2002).
25. Arthos, J. *et al.* HIV-1 envelope protein binds to and signals through integrin $\alpha_4\beta_7$, the gut mucosal homing receptor for peripheral T cells. *Nature Immunol.* **9,** 301–309 (2008).
26. Reeves, P. J., Callewaert, N., Contreras, R. & Khorana, H. G. Structure and function in rhodopsin: high-level expression of rhodopsin with restricted and homogeneous *N*-glycosylation by a tetracycline-inducible *N*-acetylglucosaminyltransferase I-negative HEK293S stable mammalian cell line. *Proc. Natl Acad. Sci. USA* **99,** 13419–13424 (2002).
27. Pejchal, R. *et al.* Structure and function of broadly reactive antibody PG16 reveal an H3 subdomain that mediates potent neutralization of HIV-1. *Proc. Natl Acad. Sci. USA* **107,** 11483–11488 (2010).
28. Richardson, J. S. The anatomy and taxonomy of protein structure. *Adv. Protein Chem.* **34,** 167–339 (1981).
29. Kabat, E. A., Wu, T. T., Perry, H. M., Gottesman, K. S. & Foeller, C. *Sequences of Proteins of Immunological Interest* 5th edn (US Department of Health and Human Service, National Institutes of Health, 1991).
30. Pancera, M. *et al.* Crystal structure of PG16 and chimeric dissection with somatically related PG9: structure–function analysis of two quaternary-specific antibodies that effectively neutralize HIV-1. *J. Virol.* **84,** 8098–8110 (2010).
31. Gorny, M. K. *et al.* Identification of a new quaternary neutralizing epitope on human immunodeficiency virus type 1 virus particles. *J. Virol.* **79,** 5232–5237 (2005).
32. Changela, A. *et al.* Crystal structure of human antibody 2909 reveals conserved features of quaternary structure-specific antibodies that potently neutralize HIV-1. *J. Virol.* **85,** 2524–2535 (2011).
33. Spurrier, B. *et al.* Structural analysis of human and macaque mAbs 2909 and 2.5B: implications for the configuration of the quaternary neutralizing epitope of HIV-1 gp120. *Structure* **19,** 691–699 (2011).
34. Honnen, W. J. *et al.* Type-specific epitopes targeted by monoclonal antibodies with exceptionally potent neutralizing activities for selected strains of human immunodeficiency virus type 1 map to a common region of the V2 domain of gp120 and differ only at single positions from the clade B consensus sequence. *J. Virol.* **81,** 1424–1432 (2007).
35. Wu, X. *et al.* Immunotypes of a quaternary site of HIV-1 vulnerability and their recognition by antibodies. *J. Virol.* **85,** 4578–4585 (2011).
36. Zhou, T. *et al.* Structural basis for broad and potent neutralization of HIV-1 by antibody VRC01. *Science* **329,** 811–817 (2010).
37. Mitsuya, H. *et al.* Dextran sulfate suppression of viruses in the HIV family: inhibition of virion binding to CD4+ cells. *Science* **240,** 646–649 (1988).
38. Schols, D., Pauwels, R., Desmyter, J. & De Clercq, E. Dextran sulfate and other polyanionic anti-HIV compounds specifically interact with the viral gp120 glycoprotein expressed by T-cells persistently infected with HIV-1. *Virology* **175,** 556–561 (1990).
39. Moulard, M. *et al.* Selective interactions of polyanions with basic surfaces on human immunodeficiency virus type 1 gp120. *J. Virol.* **74,** 1948–1960 (2000).
40. Fletcher, P. S., Wallace, G. S., Mesquita, P. M. & Shattock, R. J. Candidate polyanion microbicides inhibit HIV-1 infection and dissemination pathways in human cervical explants. *Retrovirology* **3,** 46 (2006).
41. Mondor, I., Ugolini, S. & Sattentau, Q. J. Human immunodeficiency virus type 1 attachment to HeLa CD4 cells is CD4 independent and gp120 dependent and requires cell surface heparans. *J. Virol.* **72,** 3623–3634 (1998).
42. Stanfield, R. L., Gorny, M. K., Williams, C., Zolla-Pazner, S. & Wilson, I. A. Structural rationale for the broad neutralization of HIV-1 by human monoclonal antibody 447-52D. *Structure* **12,** 193–204 (2004).
43. Gray, E. S. *et al.* The neutralization breadth of HIV-1 develops incrementally over four years and is associated with CD4 T cell decline and high viral load during acute infection. *J. Virol.* **85,** 4828–4840 (2011).
44. Moore, P. L. *et al.* Evolution of HIV-1 transmitted/founder viruses results in the formation of epitopes for later broadly cross-neutralizing antibodies. *AIDS Res. Hum. Retroviruses* **27,** A-29 (2011).
45. Pejchal, R. *et al.* A potent and broad neutralizing antibody recognizes and penetrates the HIV glycan shield. *Science* doi:10.1126/science.1213256 (13 October 2011).
46. Karasavvas, N. *et al.* The Thai Phase III clinical trial (RV144) induces the generation of antibodies that target a conserved region within the V2 loop of gp120. *AIDS Res. Hum. Retroviruses* **27,** A-29 (2011).
47. Zolla-Pazner, S. *et al.* V2-reactive antibodies in RV144 vaccinees' plasma. *AIDS Res. Hum. Retroviruses* **27,** A-21 (2011).
48. Azoitei, M. L. *et al.* Computation-guided backbone grafting of a discontinuous motif onto a protein scaffold. *Science* **334,** 373–376 (2011).
49. Sloan, D. J. & Hellinga, H. W. Dissection of the protein G B1 domain binding site for human IgG Fc fragment. *Protein Sci.* **8,** 1643–1648 (1999).
50. Majeed, S. *et al.* Enhancing protein crystallization through precipitant synergy. *Structure* **11,** 1061–1070 (2003).

Supplementary Information is linked to the online version of the paper at www.nature.com/nature.

Acknowledgements We thank A. Changela and X. Wu for assistance with mapping the PG16 paratope, J. Sodroski for discussions, J. Stuckey for assistance with figures, and members of the Structural Biology Section and Structural Bioinformatics Core, Vaccine Research Center, for discussions and comments on the manuscript. Support for this work was provided by the Intramural Research Program of the National Institutes of Health (NIH), by the International AIDS Vaccine Initiative, by the Ragon Institute, by the Canadian Institute of Health Research and by grants from the NIH. The three-dimensional reconstructions were conducted at the National Resource for Automated Molecular Microscopy (NRAMM), which is supported by the NIH through the National Center for Research Resources' P41 program (RR017573). Use of sector 22 (Southeast Regional Collaborative Access Team) at the Advanced Photon Source was supported by the US Department of Energy, Basic Energy Sciences, Office of Science, under contract number W-31-109-Eng-38.

Author Contributions J.S.M., M.P., M.S., T.Z., J.Z., J.A., C.A.B., J.R.M., G.J.N., W.R.S., A.B.W., I.A.W. and P.D.K. designed research and analysed the data; J.S.M., M.P., C.C., J.G., J.-P.J., R.K., R.L., R.P., M.S., K.D., S.O'D., N.P., S.S.H., Y.Y., T.Z., J.C.B., G.-Y.C., D.D., I.G., Y.D.K., D.L., M.K.L., S.M., S.D.S., Z.-Y.Y. and B.Z. performed research and are listed in four alphabetical groups: J.S.M. and M.P. performed the majority of research and, with C.C., J.G., J.-P.J., R.K., R.L., R.P. and M.S., determined structures; K.D., S.O'D., N.P., S.S.H., Y.Y., B.Z., T.Z. and J.Z. contributed substantial experiments; J.C.B., G.-Y.C., D.D., I.G., Y.D.K., D.L., M.K.L., S.M., S.D.S. and Z.-Y.Y. contributed supporting research; M.B., J.A.C., S.H.K., N.E.S. and B.F.H. contributed donor 0219 materials; D.R.B., W.C.K. and L.M.W. contributed donor 24 and donor 84 materials and T13 antibody; S.P. and R.W. contributed 16055 gp120; J.O. and L.-X.W. contributed polysaccharides. J.S.M., M.P., G.J.N., I.A.W. and P.D.K. wrote the paper, with all principal investigators providing comments or revisions.

Author Information Coordinates and structure factors for PG9 Fab in complexes with V1/V2 from CAP45 and ZM109 strains of HIV-1 have been deposited with the Protein Data Bank under accession codes 3U4E and 3U2S, respectively. Coordinates and structure factors for unbound Fab structures of PG9, CH04, CH04H/CH02L (in two lattices) and PGT145 have been deposited with the Protein Data Bank under accession codes, 3U36, 3TCL, 3U46, 3U4B and 3U1S, respectively. Reprints and permissions information is available at www.nature.com/reprints. The authors declare no competing financial interests. Readers are welcome to comment on the online version of this article at www.nature.com/nature. Correspondence and requests for materials should be addressed to P.D.K. (pdkwong@nih.gov).

LETTER

doi:10.1038/nature10644

Supernova SN 2011fe from an exploding carbon–oxygen white dwarf star

Peter E. Nugent[1,2], Mark Sullivan[3], S. Bradley Cenko[2], Rollin C. Thomas[1], Daniel Kasen[1,4], D. Andrew Howell[5,6], David Bersier[7], Joshua S. Bloom[2], S. R. Kulkarni[8], Michael T. Kandrashoff[2], Alexei V. Filippenko[2], Jeffrey M. Silverman[2], Geoffrey W. Marcy[2], Andrew W. Howard[2], Howard T. Isaacson[2], Kate Maguire[3], Nao Suzuki[1], James E. Tarlton[3], Yen-Chen Pan[3], Lars Bildsten[6,9], Benjamin J. Fulton[5,6], Jerod T. Parrent[5,10], David Sand[5,6], Philipp Podsiadlowski[3], Federica B. Bianco[5,6], Benjamin Dilday[5,6], Melissa L. Graham[5,6], Joe Lyman[7], Phil James[7], Mansi M. Kasliwal[8], Nicholas M. Law[11], Robert M. Quimby[12], Isobel M. Hook[3,13], Emma S. Walker[14], Paolo Mazzali[15,16], Elena Pian[15,16], Eran O. Ofek[8,17], Avishay Gal-Yam[17] & Dovi Poznanski[1,2,18]

Type Ia supernovae have been used empirically as 'standard candles' to demonstrate the acceleration of the expansion of the Universe[1–3] even though fundamental details, such as the nature of their progenitor systems and how the stars explode, remain a mystery[4–6]. There is consensus that a white dwarf star explodes after accreting matter in a binary system, but the secondary body could be anything from a main-sequence star to a red giant, or even another white dwarf. This uncertainty stems from the fact that no recent type Ia supernova has been discovered close enough to Earth to detect the stars before explosion. Here we report early observations of supernova SN 2011fe in the galaxy M101 at a distance[7] from Earth of 6.4 megaparsecs. We find that the exploding star was probably a carbon–oxygen white dwarf, and from the lack of an early shock we conclude that the companion was probably a main-sequence star. Early spectroscopy shows high-velocity oxygen that slows rapidly, on a timescale of hours, and extensive mixing of newly synthesized intermediate-mass elements in the outermost layers of the supernova. A companion paper[8] uses pre-explosion images to rule out luminous red giants and most helium stars as companions to the progenitor.

Supernova 2011fe was detected in the Pinwheel galaxy (M101; Fig. 1) on 2011 August 24.167 (03:59 UT) with a g-band magnitude of 17.35 mag by the Palomar Transient Factory (PTF). Observations on the previous night revealed no source to a limiting magnitude of 21.5 mag. Given the distance to M101 of 6.4 Mpc (ref. 7), this first observation identified the supernova at an absolute magnitude of −11.7, roughly 1/1,000 of its peak brightness.

Following an alert sent to the PTF consortium (at 19:51 UT), observations were immediately undertaken by NASA's Swift satellite, and spectroscopic observations were carried out at 20:42 UT on the robotic Liverpool Telescope (La Palma, Canary Islands) equipped with the FRODOSpec spectrograph. After the calibration of this spectrum, at 23:47 UT an Astronomer's Telegram was issued[9] identifying SN 2011fe as a young supernova of type Ia. Eight hours later, a low-resolution spectrum was obtained with the Kast spectrograph at the Lick 3-m Shane telescope (Mt Hamilton, California) and a high-resolution spectrum was obtained with the HIRES spectrograph at the Keck I telescope (Mauna Kea, Hawaii). These spectra are presented in Fig. 2 (Supplementary Information).

The discovery and extensive follow-up photometry allow us to estimate the time of explosion to high precision (Fig. 3). At very early times, the luminosity should scale as the surface area of the expanding fireball and thus is expected to increase as t^2, where t is the time since the explosion. This assumes that neither the photospheric temperature nor the velocity changes significantly and that the input energy from the radioactive decay of ^{56}Ni to ^{56}Co is relatively constant over this period and occurs near the photosphere. Observations by Swift show only small changes in the relative flux between the optical and ultraviolet spectral ranges, and the velocity evolution over the first 24 h is small—consistent with these assumptions (Supplementary Information).

Using this 't^2 model', we find an explosion time at modified Julian date (MJD) 55796.696 ± 0.003 (Fig. 3). Letting the exponent of the power law differ from two, which captures some of the deviations from the fireball model, and fitting just the first three nights of data, results in a best-fit explosion date of MJD 55796.687 ± 0.014 (2011 August 23, 16:29 ± 20 min UT). The exponent of the power law is 2.01 ± 0.01,

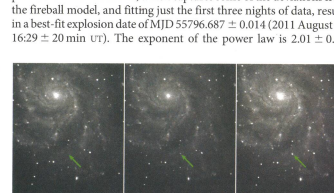

Figure 1 | PTF g-band image sequence of the field of M101 showing the appearance of SN 2011fe. From left to right, images are from August 23.22, 24.17 and 25.16 UT. The supernova was not detected on the first night to a 3σ limiting magnitude of 21.5 mag, was discovered at magnitude 17.35 mag and increased by a factor of ten in brightness to 14.86 mag the following night. The supernova peaked at magnitude ~9.9 mag, making it the fifth-brightest supernova in the past century. The PTF is a wide-field optical experiment designed to explore the variable sky systematically on a variety of timescales, with one particular focus being the very early detection of supernovae[22,23]. Discoveries such as this one have been made possible by coupling real-time computational tools to extensive astronomical follow-up observations[24,25].

[1]Lawrence Berkeley National Laboratory, Berkeley, California 94720, USA. [2]Department of Astronomy, University of California, Berkeley, California 94720-3411, USA. [3]Department of Physics (Astrophysics), University of Oxford, Keble Road, Oxford OX1 3RH, UK. [4]Department of Physics, University of California, Berkeley, California 94720, USA. [5]Las Cumbres Observatory Global Telescope Network, Goleta, California 93117, USA. [6]Department of Physics, University of California, Santa Barbara, California 93106, USA. [7]Astrophysics Research Institute, Liverpool John Moores University, Birkenhead CH41 1LD, UK. [8]Cahill Center for Astrophysics, California Institute of Technology, Pasadena, California 91125, USA. [9]Kavli Institute for Theoretical Physics, University of California, Santa Barbara, California 93106, USA. [10]Department of Physics and Astronomy, Dartmouth College, Hanover, New Hampshire 03755, USA. [11]Dunlap Institute for Astronomy and Astrophysics, University of Toronto, 50 St George Street, Toronto, Ontario M5S 3H4, Canada. [12]IPMU, University of Tokyo, Kashiwanoha 5-1-5, Kashiwa, 277-8583, Japan. [13]INAF, Osservatorio Astronomico di Roma, via Frascati 33, 00040 Monteporzio (RM), Italy. [14]Scuola Normale Superiore, Piazza dei Cavalieri 7, 56126 Pisa, Italy. [15]INAF, Osservatorio Astronomico di Padova, Vicolo dell'Osservatorio 5, 35122 Padova, Italy. [16]Max-Planck Institut für Astrophysik Karl-Schwarzschildstrasse 1, 85748 Garching, Germany. [17]Benozyo Center for Astrophysics, The Weizmann Institute of Science, Rehovot 76100, Israel. [18]School of Physics and Astronomy, Tel-Aviv University, Tel-Aviv 69978, Israel.

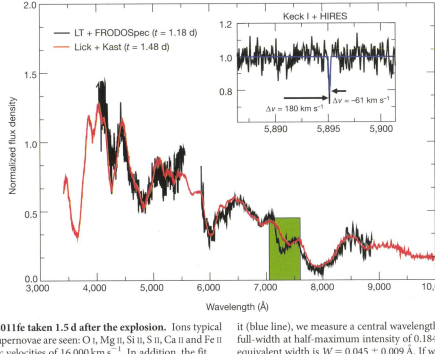

Figure 2 | Spectra of SN 2011fe taken 1.5 d after the explosion. Ions typical of pre-maximum type Ia supernovae are seen: O I, Mg II, Si II, S II, Ca II and Fe II are present at photospheric velocities of 16,000 km s^{-1}. In addition, the fit shows the presence of C II at wavelengths of $\lambda = 6{,}580$ and 7,234 Å. Both high-velocity Si II and Ca II are seen (with velocities exceeding 21,000 km s^{-1}), as is high-velocity O I (green highlighted region), the first evidence of such a feature in a type Ia supernova. This feature evolves in ~8 h, between the measurements of the first two low-resolution spectra. LT, Liverpool Telescope. Inset, Keck I + HIRES spectrum centred on the Na I D line. In this wavelength range, we identify only a single significant absorption feature. Fitting a Gaussian profile to it (blue line), we measure a central wavelength of $\lambda = 5{,}893.75 \pm 0.02$ Å and a full-width at half-maximum intensity of 0.184 ± 0.009 Å. The inferred line equivalent width is $W = 0.045 \pm 0.009$ Å. If we associate this feature with Na I at $\lambda = 5{,}889.95$ Å (the stronger of the two components in the Na I doublet), the observed wavelength is offset from the rest wavelength by $\Delta v = c(\lambda_{obs}/\lambda_{rest} - 1) = 180$ km s^{-1} (where c denotes the speed of light). Similarly, the line is blueshifted from the systemic velocity of M101 ($v = 241 \pm 2$ km s^{-1}; ref. 26) by $\Delta v_{M101} = -61$ km s^{-1}. Given the high galactic latitude ($b = 59.8°$), we consider it likely that the absorbing material originates in M101 and that the total extinction to the supernova is negligible.

consistent with the model discussed above. On the basis of these fits, our first data points were obtained just over 11 h after SN 2011fe exploded.

We analysed the Lick spectrum of SN 2011fe using the automated supernova spectrum interpretation code SYNAPPS[10] (Supplementary Information). At this time only a few hundredths of a solar mass of material are visible above the photosphere, yet ions typical[11] of pre-maximum type Ia supernovae are seen: O I, Mg II, Si II, S II, Ca II and Fe II are present with velocities of 16,000 km s^{-1}. The fit also shows the presence of C II at rest wavelengths of $\lambda = 6{,}580$ and 7,234 Å. Iron III was not needed in the fit. Both high-velocity Si II and Ca II are confirmed by SYNAPPS (with velocities surpassing 21,000 km s^{-1}). Notably, SYNAPPS finds high-velocity O I (velocity in excess of 20,000 km s^{-1}) for the absorption centred at 7,400 Å. This feature evolved significantly in only 8 h, between the times at which data was taken at the Liverpool Telescope and the Lick telescope, with the minimum of the O I absorption slowing from 18,000 to 14,000 km s^{-1}. The rapid evolution in these optically thin layers is best explained in terms of geometrical dilution during the early phases. To our knowledge, this is the first identification of rapidly evolving high-velocity oxygen in the ejecta of a type Ia supernova.

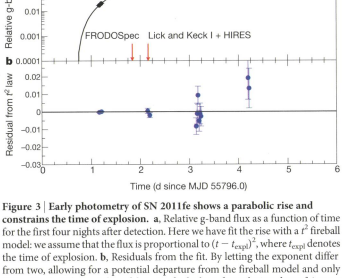

Figure 3 | Early photometry of SN 2011fe shows a parabolic rise and constrains the time of explosion. a, Relative g-band flux as a function of time for the first four nights after detection. Here we have fit the rise with a t^2 fireball model: we assume that the flux is proportional to $(t - t_{exp})^2$, where t_{exp} denotes the time of explosion. **b**, Residuals from the fit. By letting the exponent differ from two, allowing for a potential departure from the fireball model and only fitting the first three nights of data, we find a best-fit explosion date of August 23.687 ± 0.014 UT. On the basis of these fits, our first data points were obtained just over 11 h after SN 2011fe exploded. Error bars, 1σ.

The early-time spectra provide fundamental insight into the explosion physics of this supernova. As in previous[12] type Ia supernovae, intermediate-mass elements dominate the spectrum. In addition, we see strong features from unburnt material (carbon and high-velocity oxygen). The overlap in velocity space implies that the explosion processed the outer layers of the progenitor white dwarf but left behind (at least some) carbon and oxygen. The unburnt material could be confined to pockets, or the ejecta in the outer layers may be thoroughly mixed. The doubly ionized species (for example Si III and Fe III), which are often seen in the spectra of many early and maximum-light type Ia supernovae[13,14], are absent even though our observations were made ~1 d after the explosion, when the energy input from radioactive decay is near its peak. Supernova 2011fe is spectroscopically most similar to the slightly underluminous type Ia SN 1992A and SN 1994D[15,16], the second of which also has high-velocity features in the −12-d spectrum[17]. One potential explanation for this is that although some ^{56}Ni has been mixed out to the photosphere, the majority produced in

the explosion is confined to the innermost layers of the atmosphere and the bulk of the heating is thus well separated from the portion of the atmosphere we view in these spectra.

The early detection of SN 2011fe allows us to put considerable constraints on the progenitor system of this type Ia supernova. At early times (about 1 d or less after explosion), radiative diffusion from the shock-heated outer layers of the ejecta is a contributor to the supernova luminosity. The shock can originate either in the detonation of the white dwarf[18] or in a later collision with the companion star[19]. Dimensionally, the shock luminosity in this cooling, expanding envelope phase is $L \propto E(t)/t_{\rm d}$, where $E(t)$ is the ejecta internal energy at the elapsed time, t, and $t_{\rm d}$ is the effective diffusion time through the homologously expanding remnant. Because the ejecta in these phases are heavily radiation dominated, the internal energy decreases during adiabatic expansion as $E(t) \propto R_0/vt$, where R_0 is the initial radius of the star and v is the velocity of the ejecta. Thus, the early-time luminosity is proportional to R_0 and the effective temperature, $T_{\rm eff}$ is proportional to $L^{1/4} \propto R_0^{1/4}$ (Supplementary Information).

Although there must be radioactive heating in the outer layers of the supernova, we can make the very conservative upper-limit approximation that the earliest g-band photometric point ($L \approx 10^{40}\,{\rm erg\,s^{-1}}$ at $\sim$0.5 d) is entirely due to the explosion. We then infer an upper limit to the radius of the progenitor star, $R_0 < 0.1R_\odot$ (Fig. 4), where $R_\odot$ is the solar radius. This provides compelling, direct evidence that the progenitor of SN 2011fe was a compact star, namely a white dwarf. When we add the early carbon and oxygen observations, we conclude that the progenitor must have been a carbon–oxygen white dwarf.

The early-time light curve also constrains the properties of a binary star system[19], because the collision of the supernova with a companion star will shock and reheat a portion of the ejecta. The resulting luminosity is proportional to the separation distance, a, between the stars, and will be most prominent for observers aligned with the symmetry axis. If the companion were a red giant, the early luminosity would be several orders of magnitude greater than that observed, and this possibility

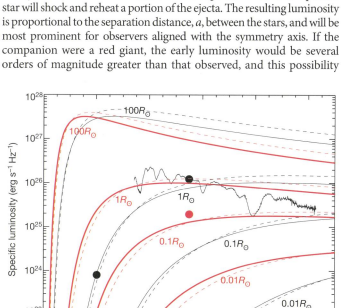

Figure 4 | Models and early data limit the radius of the exploding star of SN 2011fe. The thick red lines show black-body models for the spectrum at 0.5 d assuming different values of the progenitor star radius, R_0. The solid lines and the dashed lines are derived from two separate analyses[18,27]. The observed g-band photometry point at this time (red circle) constrains the radius of the progenitor star (or the surrounding opaque circumstellar medium) to be $\leq 10^{10}$ cm$\approx 0.1R_\odot$. The black spectrum and circles show corresponding model predictions (circles) and observations (spectrum) at 1.45 d. In all models, we have assumed an ejecta mass equal to the Chandrasekhar mass, an explosion energy of 10^{51} erg and an opacity of $0.2\,{\rm cm^2\,g^{-1}}$, appropriate for electron scattering in a singly ionized medium with a mass number/atomic number ratio of two. The early-time data indicate that the progenitor of SN 2011fe was a compact star, namely a white dwarf.

can be ruled out regardless of the viewing angle. A main-sequence companion is compatible with the data, unless SN 2011fe happened to be seen on-axis (within $\sim$40° of the symmetry axis), in which case the luminosity at 0.5 d rules out any binary with $a \leq 0.1R_\odot$. Despite this caveat, we conclude that the companion is most likely to be a main-sequence star.

Recent simulations of double-degenerate mergers have found that some material from the disrupted secondary white dwarf may get pushed out to large radius (10^{13}–10^{14} cm), either in the dynamics of the merger[20] or in the subsequent long-term thermal evolution of the system[21]. The interaction of the ejecta with this roughly spherical medium should produce (for all viewing angles) bright, early ultraviolet–optical emission, in conflict with what is observed. Our restriction that the dense circumstellar medium must reside at a radius of $\leq 10^{10}$ cm thus presents a tight constraint for merger models, and only a few of those proposed so far may be applicable to this supernova[6].

We caution that the conclusions we have come to regarding SN 2011fe rely on a theoretical interpretation. A companion paper[8] uses independent methodology to place direct observational limits on the companion star from historical imaging $\sim$100 times deeper in absolute luminosity than previous attempts using other type Ia supernovae.

These results come from only the first week or so of observation of SN 2011fe. Being the first close type Ia supernova to be detected in the era of modern instrumentation, SN 2011fe will undoubtedly become the best-recorded thermonuclear supernova in history, and will be studied daily across the spectral range from the ultraviolet to the infrared well into the faint nebular phase. As such, it will form the foundation on which our knowledge of more distant type Ia supernovae is built.

Received 8 September; accepted 14 October 2011.

1. Riess, A. G. *et al.* Observational evidence from supernovae for an accelerating universe and a cosmological constant. *Astron. J.* **116,** 1009–1038 (1998).
2. Perlmutter, S. *et al.* Measurements of Ω and Λ from 42 high-redshift supernovae. *Astrophys. J.* **517,** 565–586 (1999).
3. Sullivan, M. *et al.* SNLS3: constraints on dark energy combining the supernova legacy survey three-year data with other probes. *Astrophys. J.* **737,** 102–121 (2011).
4. Howell, D. A. Type Ia supernovae as stellar endpoints and cosmological tools. *Nature Commun.* **2,** 350 (2011).
5. Kasen, D., Röpke, F. K. & Woosley, S. E. The diversity of type Ia supernovae from broken symmetries. *Nature* **460,** 869–872 (2009).
6. Yoon, S.-C., Podsiadlowski, P. & Rosswog, S. Remnant evolution after a carbon-oxygen white dwarf merger. *Mon. Not. R. Astron. Soc.* **380,** 933–948 (2007).
7. Shappee, B. J. & Stanek, K. Z. A new Cepheid distance to the giant spiral M101 based on image subtraction of Hubble Space Telescope/Advanced Camera for Surveys observations. *Astrophys. J.* **733,** 124–149 (2011).
8. Li, W. *et al.* Exclusion of a luminous red giant as a companion star to the progenitor of supernova SN 2011fe. *Nature* http://dx.doi.org/10.1038/nature10646 (this issue).
9. Nugent, P. E. *et al.* Young type Ia supernova PTF11kly in M101. *Astron. Telegr.* **3581,** 1 (2011).
10. Thomas, R. C., Nugent, P. E. & Meza, J. C. SYNAPPS: data-driven analysis for supernova spectroscopy. *Publ. Astron. Soc. Pacif.* **123,** 237–248 (2011).
11. Filippenko, A. V. Optical spectra of supernovae. *Annu. Rev. Astron. Astrophys.* **35,** 309–355 (1997).
12. Branch, D. *et al.* The Type I supernova 1981b in NGC 4536 - the first 100 days. *Astrophys. J.* **270,** 123–125 (1983).
13. Leibundgut, B. *et al.* Premaximum observations of the type IA SN 1990N. *Astrophys. J.* **371,** L23–L26 (1991).
14. Nugent, P., Phillips, M., Baron, E., Branch, D. & Hauschildt, P. Evidence for a spectroscopic sequence among type 1a supernovae. *Astrophys. J.* **455,** L147–L151 (1995).
15. Kirshner, R. P. *et al.* SN 1992A: ultraviolet and optical studies based on HST, IUE, and CTIO observations. *Astrophys. J.* **415,** 589–615 (1993).
16. Patat, F. *et al.* The type IA supernova 1994D in NGC 4526: the early phases. *Mon. Not. R. Astron. Soc.* **278,** 111–124 (1996).
17. Hatano, K., Branch, D., Fisher, A., Baron, E. & Filippenko, A. V. On the high-velocity ejecta of the type Ia supernova SN 1994D. *Astrophys. J.* **525,** 881–885 (1999).
18. Piro, A. L., Chang, P. & Weinberg, N. N. Shock breakout from type Ia supernova. *Astrophys. J.* **708,** 598–604 (2010).
19. Kasen, D. Seeing the collision of a supernova with its companion star. *Astrophys. J.* **708,** 1025–1031 (2010).
20. Fryer, C. L. *et al.* Spectra of type Ia supernovae from double degenerate mergers. *Astrophys. J.* **725,** 296–308 (2010).

21. Shen, K. J., Bildsten, L., Kasen, D. & Quataert, E. The long-term evolution of double white dwarf mergers. Preprint at (http://arxiv.org/abs/1108.4036) (2011).
22. Rau, A. *et al.* Exploring the optical transient sky with the Palomar Transient Factory. *Publ. Astron. Soc. Pacif.* **121,** 1334–1351 (2009).
23. Law, N. M. *et al.* The Palomar Transient Factory: system overview, performance, and first results. *Publ. Astron. Soc. Pacif.* **121,** 1395–1408 (2009).
24. Gal-Yam, A. *et al.* Real-time detection and rapid multiwavelength follow-up observations of a highly subluminous type II-P supernova from the Palomar Transient Factory survey. *Astrophys. J.* **736,** 159–166 (2011).
25. Bloom, J. S. *et al.* Automating discovery and classification of transients and variable stars in the synoptic survey era. Preprint at (http://arxiv.org/abs/1106.5491) (2011).
26. de Vaucouleurs, G. *et al. Third Reference Catalogue of Bright Galaxies* (Springer, 1991).
27. Rabinak, I., Livne, E. & Waxman, E. Early emission from type Ia supernovae. Preprint at (http://arxiv.org/abs/1108.5548) (2011).

Supplementary Information is linked to the online version of the paper at www.nature.com/nature.

Acknowledgements The PTF project is a scientific collaboration between the California Institute of Technology, Columbia University, Las Cumbres Observatory, the Lawrence Berkeley National Laboratory, the National Energy Research Scientific Computing Center, the University of Oxford and the Weizmann Institute of Science. The National Energy Research Scientific Computing Center, supported by the Office of Science of the US Department of Energy (DOE), provided staff, computational resources and data storage for this project. P.E.N. acknowledges support from the US DOE Scientific Discovery through Advanced Computing programme. M.S. acknowledges support from the Royal Society. J.S.B. and L.B. were supported by the National Science Foundation (NSF). The work of A.V.F. is funded by the NSF, the TABASGO Foundation, Gary and Cynthia Bengier, and the Richard and Rhoda Goldman Fund. A.G. thanks the ISF and BSF. The Liverpool Telescope is operated by Liverpool John Moores University in the Spanish Observatorio del Roque de los Muchachos of the Instituto de Astrofisica de Canarias with financial support from the UK Science and Technology Facilities Council. Some of the data presented here were obtained at the W. M. Keck Observatory, which is operated as a scientific partnership among the California Institute of Technology, the University of California and NASA; the observatory was made possible by the generous financial support of the W. M. Keck Foundation. We thank the staffs of the many observatories at which data were obtained for their assistance.

Author Contributions P.E.N., M.S. and D.A.H. oversee the PTF programme on type Ia supernovae. P.E.N. oversaw the preparation of the manuscript. M.S., D.B., K.M., Y.-C.P., J.L. and P.J. performed and reduced the FRODOSpec observations. S.B.C., M.T.K., A.V.F. and J.M.S. obtained and reduced the Lick spectrum. G.W.M., A.W.H. and H.T.I. obtained the HIRES observations. S.B.C., J.S.B., S.R.K., M.M.K., N.M.L., E.O.O., R.M.Q. and D.P. assisted in the operation of the Palomar 48-inch telescope as part of the PTF collaboration. R.C.T. and J.E.T. performed the SYNAPPS analysis. D.K., L.B. and P.P. assisted with the theoretical interpretation of our observations. N.S., B.J.F., J.T.P., D.S., F.B.B., B.D., M.L.G., I.M.H., P.M., E.P., E.S.W. and A.G. assisted in follow-up observations of SN 2011fe.

Author Information Reprints and permissions information is available at www.nature.com/reprints. The authors declare no competing financial interests. Readers are welcome to comment on the online version of this article at www.nature.com/nature. Correspondence and requests for materials should be addressed to P.E.N. (penugent@lbl.gov).

LETTER

doi:10.1038/nature10646

Exclusion of a luminous red giant as a companion star to the progenitor of supernova SN 2011fe

Weidong Li[1], Joshua S. Bloom[1], Philipp Podsiadlowski[2], Adam A. Miller[1], S. Bradley Cenko[1], Saurabh W. Jha[3], Mark Sullivan[2], D. Andrew Howell[4,5], Peter E. Nugent[1,6], Nathaniel R. Butler[7], Eran O. Ofek[8,9], Mansi M. Kasliwal[10], Joseph W. Richards[1,11], Alan Stockton[12], Hsin-Yi Shih[12], Lars Bildsten[5,13], Michael M. Shara[14], Joanne Bibby[14], Alexei V. Filippenko[1], Mohan Ganeshalingam[1], Jeffrey M. Silverman[1], S. R. Kulkarni[8], Nicholas M. Law[15], Dovi Poznanski[16], Robert M. Quimby[17], Curtis McCully[3], Brandon Patel[3], Kate Maguire[2] & Ken J. Shen[1]

Type Ia supernovae are thought to result from a thermonuclear explosion of an accreting white dwarf in a binary system[1,2], but little is known of the precise nature of the companion star and the physical properties of the progenitor system. There are two classes of models[1,3]: double-degenerate (involving two white dwarfs in a close binary system[2,4]) and single-degenerate models[5,6]. In the latter, the primary white dwarf accretes material from a secondary companion until conditions are such that carbon ignites, at a mass of 1.38 times the mass of the Sun. The type Ia supernova SN 2011fe was recently detected in a nearby galaxy[7]. Here we report an analysis of archival images of the location of SN 2011fe. The luminosity of the progenitor system (especially the companion star) is 10–100 times fainter than previous limits on other type Ia supernova progenitor systems[8–10], allowing us to rule out luminous red giants and almost all helium stars as the mass-donating companion to the exploding white dwarf.

In a double-degenerate model, the orbit of the two white dwarfs shrinks owing to the release of gravitational radiation[2,4]. Ultimately, the lighter object (the secondary) is disrupted and accretion onto the primary ignites runaway thermonuclear fusion. Different single-degenerate models can be distinguished by the nature of the secondary: the white dwarf can accrete either from a wind (the "symbiotic channel"[11]), by Rochelobe overflow (the "RLOF channel"[12]), or by mass transfer from a helium star (the "helium-star channel"[11,13,14]). The secondary star in the symbiotic channel is often a red-giant star, and it is often a subgiant or main-sequence star in the RLOF channel.

We have analysed the available Hubble Space Telescope observations of the nearby galaxy Messier 101 (M101; see Supplementary Information). To pinpoint the precise supernova location in the Hubble Space Telescope images, we obtained a mosaic image of the field of SN 2011fe with the Near-Infrared Camera 2 (NIRC2) mounted behind the adaptive optics system on the Keck II telescope[15]. The Keck adaptive optics image was astrometrically registered to the Hubble Space Telescope/Advanced Camera for Surveys images, yielding a 1σ precision of 0.021″ (or 21 mas) for the supernova position (see Supplementary Information). Figure 1 shows the site of SN 2011fe at different scales. No object is detected at the nominal supernova location in four different Hubble Space Telescope filters, or within the approximately 8σ error radius.

This nondetection can be directly translated into limits on the progenitor system brightness and temperature. Indeed, each of the four Hubble Space Telescope bands places different limits on the progenitor brightness depending on the (unknown) effective temperature and luminosity class. Figure 2 shows the region in effective temperature versus absolute V-band magnitude excluded by the Hubble Space Telescope imaging analysis (see Supplementary Information). At 3,000 K, progenitor systems of SN 2011fe are excluded for V-band absolute magnitude $M_V \leq 1$ mag, and for effective temperatures larger than 5,000 K, the exclusion is $M_V \leq -0.5$ mag. These limits rule out a symbiotic binary progenitor with brightness and colour similar to the well-observed Galactic systems RS Ophiuchi (RS Oph) and probably T Coronae Borealis (T CrB). Both of these binary systems have been advanced as possible prototypes of type Ia supernova progenitor systems[16]. Similarly, the helium-star binary V445 Puppis (V445 Pup)[17] is excluded, although the entire He-star channel cannot be completely ruled out (see the blue-shaded area in Fig. 2). In contrast, RLOF from a main-sequence or subgiant star such as U Scorpii (U Sco)[18] can easily be reconciled with the Hubble Space Telescope constraints. Finally, all variations of the double-degenerate model are consistent with the nondetection of a source at the position of SN 2011fe, because the model does not predict a bright source in the visible range. The brightness limits we have deduced also rule out a globular cluster, or any open star cluster with more than about 300 members, as the site of SN 2011fe. In addition, Fig. 2 shows that a mass donor with an effective temperature less than 4,800 K (spectral type redder than about G5) needs to have a zero-age main-sequence mass less than $2.2M_{\odot}$, where $M_{\odot}$ is the mass of the Sun. For stars with spectral type redder than an A0 star (effective temperature about 10,000 K), the companion star would need to be less massive than $3.5M_{\odot}$.

The single-degenerate models predict episodes of nondestructive eruptions (novae) in the decades leading up to the supernova explosion. Indeed, RS Oph, T CrB and U Sco are all recurrent novae in the Milky Way. The recurrence time of white-dwarf binaries where the white dwarfs are close to the Chandrasekhar mass is expected[19] to be 10–20 years. Although our historical images had sufficient sensitivity to detect classical novae, we find no evidence for any such outburst in the past 12 years at the site of SN 2011fe. However, we estimate an approximately 37% chance that a typical nova could have occurred in the past 5 years and have been missed given the particular cadence of the imaging (see Supplementary Information).

Historical imaging at other wavebands complements these visible-light progenitor system constraints. We have analysed 11 epochs of

[1]Department of Astronomy, University of California, Berkeley, California 94720-3411, USA. [2]Department of Physics (Astrophysics), University of Oxford, Keble Road, Oxford OX1 3RH, UK. [3]Department of Physics and Astronomy, Rutgers, The State University of New Jersey, Piscataway, New Jersey 08854, USA. [4]Las Cumbres Observatory Global Telescope Network, Goleta, California 93117, USA. [5]Department of Physics, University of California, Santa Barbara, California 93106, USA. [6]Computational Cosmology Center, Lawrence Berkeley National Laboratory, 1 Cyclotron Road, Berkeley, California 94720, USA. [7]Department of Physics, Arizona State University, Tempe, Arizona 85287-1504, USA. [8]Cahill Center for Astrophysics 249-17, California Institute of Technology, Pasadena, California 91125, USA. [9]Benoziyo Center for Astrophysics, Faculty of Physics, Weizmann Institute of Science, 76100 Rehovot, Israel. [10]Carnegie Institution for Science, 813 Santa Barbara Street, Pasadena, California 91101, USA. [11]Department of Statistics, University of California, Berkeley, California 94720-7450, USA. [12]Institute for Astronomy, University of Hawaii, Honolulu, Hawaii 96822, USA. [13]Kavli Institute for Theoretical Physics, University of California, Santa Barbara, California 93106, USA. [14]Department of Astrophysics, American Museum of Natural History, Central Park West and 79th Street, New York, New York 10024-5192, USA. [15]Dunlap Institute for Astronomy and Astrophysics, University of Toronto, 50 St George Street, Toronto M5S 3H4, Ontario, Canada. [16]School of Physics and Astronomy, Tel-Aviv University, Tel-Aviv 69978, Israel. [17]IPMU, University of Tokyo, Kashiwanoha 5-1-5, Kashiwa-shi, Chiba, Japan.

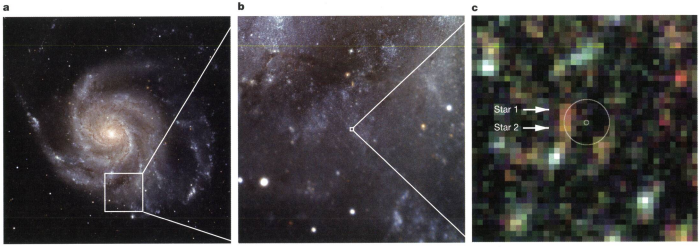

Figure 1 | The site of SN 2011fe in galaxy M101 as imaged by the Hubble Space Telescope/Advanced Camera for Surveys. a, A full-view colour picture of the face-on spiral galaxy M101 ($18' \times 18'$ field of view) constructed from the three-colour Hubble Space Telescope/Advanced Camera for Surveys images taken at multiple mosaic pointings. North is up and east to the left. M101 displays several well-defined spiral arms. With a diameter of 170,000 light years, M101 is nearly twice the size of our Milky Way Galaxy, and is estimated to contain at least one trillion stars. **b**, A cutout section ($3' \times 3'$) of **a**, centred on the supernova location. SN 2011fe is spatially projected on a prominent spiral arm. **c**, A cutout section ($2'' \times 2''$) of **b** centred on the supernova location, which is marked by two circles. The smaller circle has a radius of our 1σ astrometric uncertainty (21 mas), and the bigger circle has a radius of nine times that. No object is detected at the nominal supernova location, or within the 8σ error radius. Two nearby red sources are labelled 'Star 1' and 'Star 2'; they are displaced from our nominal supernova location by about 9σ, and hence are formally excluded as viable candidate objects involved in the progenitor system of SN 2011fe. Credit for the colour picture in **a** (from http://hubblesite.org): NASA, ESA, K. Kuntz (JHU), F. Bresolin (University of Hawaii), J. Trauger (Jet Propulsion Lab), J. Mould (NOAO), Y.-H. Chu (University of Illinois, Urbana) and STScI.

archival Chandra X-ray observations of M101 taken in 2004 (see Supplementary Information), and derived upper limits for the X-ray luminosity at the location of SN 2011fe in the range $(4–25) \times 10^{38}$ erg s^{-1} (depending on the details of the assumed spectrum). Single-degenerate progenitor systems are thought to undergo a prolonged period ($\Delta t \approx 10^6$ years) of steady nuclear burning during the mass-transfer process. Such systems should appear as luminous X-ray sources: 10^{36}–10^{38} erg s^{-1} ($kT \approx 100$ eV). Indeed, nearly a hundred of these 'supersoft' sources have been identified so far in the Milky Way and other nearby galaxies, including M101 itself[20,21]. Double-degenerate

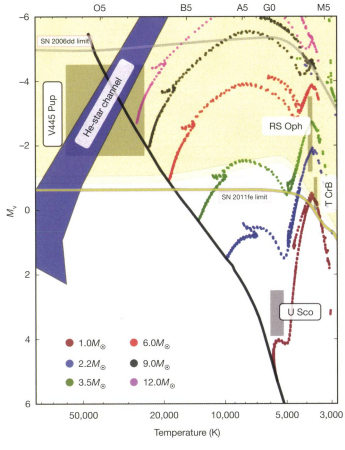

Figure 2 | Progenitor system constraints in a Hertzsprung–Russell diagram. The thick yellow line is the 2σ limit in M_V against effective temperature at the supernova location (see text) from a combination of the four Hubble Space Telescope filters, weighted using synthetic colours of redshifted stellar spectra at solar metallicity for that temperature and luminosity class. A more conservative limit comes from taking the single filter that most constrains the stellar type and luminosity class; shown is the 2σ limit assuming the adopted distance modulus[27,28] of 29.05 mag (middle grey curve at the bottom of the yellow shading) with a total uncertainty of 0.23 mag (top/bottom grey curve at the bottom of the yellow shading). We also show the theoretical estimates (He-star channel[13,14] and observed candidate systems (V445 Pup[17], RS Oph[16], U Sco[18,29] and T CrB[16]). The grey-shaded rectangle shows the location of V445 Pup. Also plotted are the theoretical evolutionary tracks (from 1 Myr to 13 Gyr) of isolated stars for a range of masses for solar metallicity; note that the limits on the progenitor mass of SN 2011fe under the supersolar metallicity assumption are similar to those represented here. The grey curve at top is the limit inferred from Hubble Space Telescope analysis of SN 2006dd, representative of the other nearby type Ia supernova progenitor limits (see Supplementary Information). For the helium-star channel, bolometric luminosity corrections to the V band are adopted on the basis of effective temperature[30]. For an effective temperature of 3,000–4,000 K, as expected for the red-giant-branch stars, the M_V limit excludes progenitors brighter than an absolute I-band magnitude of $M_I \approx -2$. This limit is 2 mag fainter than the observed[29] tip of the red-giant branch in M101 and places an upper bound to the radius of $R \lesssim 60R_\odot$ for an effective temperature of 3,500 K on any red-giant branch progenitor. In a progenitor model that requires RLOF, this limit then demands an orbital period smaller than 260 to 130 days in a binary system with a $1.3M_\odot$ white dwarf (where the range of orbital period accommodates the $0.5M_\odot - 2.5M_\odot$ range allowed for a red-giant-branch star). The foreground Galactic and M101 extinction due to dust is negligible[7] and is taken to be $A_V = 0$ mag here. Had a source at the 2.0σ photometric level been detected in the Hubble Space Telescope images at the precise location of the supernova, we would have been able to rule out the null hypothesis of no significant progenitor with 95% confidence. We therefore use the 2σ photometric uncertainties in quoting the brightness limits on the progenitor system.

progenitor systems have also been predicted to emit X-rays[22,23], with X-ray luminosity of 10^{36}–10^{37} erg s^{-1}. Our historical X-ray limits are, unfortunately, not deep enough to rule out either channel.

We have also analysed pre-explosion mid-infrared data on M101 taken in 2004 with the Spitzer space telescope (see Supplementary Information). No point source was detected at the supernova location, to a mid-infrared luminosity of less than $(1–13) \times 10^{36}$ erg s^{-1}. These limits rule out bright red-giant mass donors for SN 2011fe in the symbiotic channel, but are consistent with a relatively faint secondary star in the RLOF channel. For a double-degenerate merger to produce a type Ia supernova, the merger product may need to evolve and cool slowly[24] for over a million years. This requires the radiated luminosity (mostly in the infrared) to be less than 4×10^{36} erg s^{-1}. The Spitzer nondetection limits are certainly consistent with the requirement of low-infrared luminosity for the double-degenerate models.

One test to determine whether SN 2011fe comes from the RLOF channel of the single-degenerate model, or from a double-degenerate merger, is to detect the surviving companion in the RLOF channel. But with our current resources, it would be very challenging to observe a subgiant mass donor, and nearly impossible to observe a main-sequence companion, unless there is excessive heating caused by the interaction between the companion star and the supernova ejecta.

Using historical imaging we have placed a limit on the progenitor of a type Ia supernova that is about a hundred times fainter than those previously achieved, showing that any evolved secondary star in the progenitor system of SN 2011fe must be less massive than $3.5 M_{\odot}$. This rules out symbiotic progenitors like RS Oph and probably T CrB. These are fairly straightforward observational constraints, but in a companion paper[7] we use more indirect theoretical arguments to place additional limits. Expanding supernova ejecta should be shocked by contact with a large secondary[25], and the absence of this signature suggests that that secondary was not an evolved star. Furthermore, the ejecta could be shocked by debris that some studies[26] suggest should be present in a double-degenerate merger, although such shocked ejecta have not been seen. Taking all observational and theoretical limits together, the scenario of a white dwarf accreting from a main-sequence or subgiant companion is consistent with all constraints. Given the observed diversity of type Ia supernovae, however, the possibility of more than one progenitor channel for the class remains. As the trove of high-resolution wide-field imaging grows, covering more and more future supernova explosion sites, similar analyses may eventually resolve this possibility.

Received 7 September; accepted 14 October 2011.

1. Nomoto, K. Accreting white dwarf models for type I supernovae. I—Presupernova evolution and triggering mechanisms. *Astrophys. J.* **253,** 798–810 (1982).
2. Iben, I. Jr & Tutukov, A. V. Supernovae of type I as end products of the evolution of binaries with components of moderate initial mass (*M* not greater than about 9 solar masses). *Astrophys. J. Suppl. Ser.* **54,** 335–372 (1984).
3. Whelan, J. & Iben, I. Jr. Binaries and supernovae of type I. *Astrophys. J.* **186,** 1007–1014 (1973).
4. Webbink, R. F. Double white dwarfs as progenitors of R Coronae Borealis stars and type I supernovae. *Astrophys. J.* **277,** 355–360 (1984).
5. Nomoto, K., Iwamoto, K. & Kishimoto, N. Type Ia supernovae: their origin and possible applications in cosmology. *Science* **276,** 1378–1382 (1997).
6. Podsiadlowski, P., Mazzali, P., Lesaffre, P., Han, Z. & Förster, F. The nuclear diversity of type Ia supernova explosions. *N. Astron. Rev.* **52,** 381–385 (2008).
7. Nugent, P. *et al.* Supernova SN 2011fe from an exploding carbon–oxygen white dwarf star. *Nature* http://dx.doi.org/10.1038/nature10644 (this issue).
8. Maoz, D. & Mannucci, F. A search for the progenitors of two type Ia supernovae in NGC 1316. *Mon. Not. R. Astron. Soc.* **388,** 421–428 (2008).
9. Nelemans, G., Voss, R., Roelofs, G. & Bassa, C. Limits on the X-ray and optical luminosity of the progenitor of the type Ia supernova 2007sr. *Mon. Not. R. Astron. Soc.* **388,** 487–494 (2008).
10. Voss, R. & Nelemans, G. Discovery of the progenitor of the type Ia supernova 2007on. *Nature* **451,** 802–804 (2008).
11. Munari, U. & Renzini, A. Are symbiotic stars the precursors of type Ia supernovae? *Astrophys. J.* **397,** L87–L90 (1992).
12. van den Heuvel, E. P. J., Bhattacharya, D., Nomoto, K. & Rappaport, S. A. Accreting white dwarf models for CAL 83, CAL 87, and other ultrasoft X-ray sources in the LMC. *Astron. Astrophys.* **262,** 97–105 (1992).
13. Liu, W.-M., Chen, W.-C., Wang, B. & Han, Z. W. Helium-star evolutionary channel to super-Chandrasekhar mass type Ia supernovae. *Astron. Astrophys.* **523,** A3 (2010).
14. Yoon, S.-C. & Langer, N. The first binary star evolution model producing a Chandrasekhar mass white dwarf. *Astron. Astrophys.* **412,** L53–L56 (2003).
15. Wizinowich, P. L. *et al.* The W. M. Keck Observatory laser guide star adaptive optics system: overview. *Publ. Astron. Soc. Pacif.* **118,** 297–309 (2006).
16. Hachisu, I. & Kato, M. Recurrent novae as a progenitor system of type Ia supernovae. I. RS Ophiuchi subclass: systems with a red giant companion. *Astrophys. J.* **558,** 323–350 (2001).
17. Woudt, P. A. *et al.* The expanding bipolar shell of the helium nova V445 Puppis. *Astrophys. J.* **706,** 738–746 (2009).
18. Thoroughgood, T. D., Dhillon, V. S., Littlefair, S. P., Marsh, T. R. & Smith, D. A. The mass of the white dwarf in the recurrent nova U Scorpii. *Mon. Not. R. Astron. Soc.* **327,** 1323–1333 (2001).
19. Schaefer, B. E. Comprehensive photometric histories of all known Galactic recurrent novae. *Astrophys. J. Suppl. Ser.* **187,** 275–373 (2010).
20. Greiner, J. Catalog of supersoft X-ray sources. *N. Astron.* **5,** 137–141 (2000).
21. Di Stefano, R. The progenitors of type Ia supernovae. I. Are they supersoft sources? *Astrophys. J.* **712,** 728–733 (2010).
22. Di Stefano, R. The progenitors of type Ia supernovae. II. Are they double-degenerate binaries? The symbiotic channel. *Astrophys. J.* **719,** 474–482 (2010).
23. Yoon, S.-C., Podsiadlowski, P. & Rosswog, S. Remnant evolution after a carbon-oxygen white dwarf merger. *Mon. Not. R. Astron. Soc.* **380,** 933–948 (2007).
24. Shen, K. J., Bildsten, L., Kasen, D. & Quataert, E. The long-term evolution of double white dwarf mergers. Preprint at http://arxiv.org/abs/1108.4036 (2011).
25. Kasen, D. Seeing the collision of a supernova with its companion star. *Astrophys. J.* **708,** 1025–1031 (2010).
26. Fryer, C. L. *et al.* Spectra of type Ia supernovae from double degenerate mergers. *Astrophys. J.* **725,** 296–308 (2010).
27. Stetson, P. B. *et al.* The extragalactic distance scale key project. XVI. Cepheid variables in an inner field of M101. *Astrophys. J.* **508,** 491–517 (1998).
28. Shappee, B. J. & Stanek, K. Z. A new Cepheid distance to the giant spiral M101 based on image subtraction of Hubble Space Telescope/Advanced Camera for Surveys observations. *Astrophys. J.* **733,** 124–148 (2011).
29. Hachisu, I., Kato, M., Nomoto, K. & Umeda, H. A new evolutionary path to type Ia supernovae: a helium-rich supersoft x-ray source channel. *Astrophys. J.* **519,** 314–323 (1999).
30. Torres, G. On the use of empirical bolometric corrections for stars. *Astron. J.* **140,** 1158–1162 (2010).

Supplementary Information is linked to the online version of the paper at www.nature.com/nature.

Acknowledgements We thank D. Maoz and S. Starrfield for comments, and the staff of the W. M. Keck Observatory, especially J. Lyke and R. Campbell, for their assistance in obtaining the NIRC adaptive optics imaging. P.P. acknowledges discussions on symbiotic binaries with J. Mikolajewska. M.M.K. acknowledges support by NASA's Hubble Fellowship and the Carnegie-Princeton Fellowship. J.S.B.'s group was partially supported by NASA. J.S.B., A.V.F., L.B. and S.W.J. acknowledge support from the US National Science Foundation. A.V.F.'s group at UC Berkeley, and the Katzman Automatic Imaging Telescope (KAIT) and its ongoing operation, have received financial assistance from NASA, Gary and Cynthia Bengier, the Richard & Rhoda Goldman Fund, the Sylvia and Jim Katzman Foundation, and the TABASGO Foundation. E.O.O. is supported by an Einstein Fellowship from NASA. M.M.S. and J.B. acknowledge the support of Hilary Lipsitz and the American Museum of Natural History for essential funding. M.S. acknowledges support from the Royal Society. Some of the data presented here were obtained at the W. M. Keck Observatory, which is operated as a scientific partnership among the California Institute of Technology, the University of California, and NASA; the observatory was made possible by the generous financial support of the W. M. Keck Foundation. Observations were obtained with the Samuel Oschin Telescope at the Palomar Observatory as part of the Palomar Transient Factory project, a scientific collaboration between the California Institute of Technology, Columbia University, La Cumbres Observatory, the Lawrence Berkeley National Laboratory, the National Energy Research Scientific Computing Center, the University of Oxford, and the Weizmann Institute of Science. The National Energy Research Scientific Computing Center, provided staff, computational resources, and data storage for this project.

Author Contributions W.L., J.S.B., S.W.J., C.M. and B.P. analysed the Hubble Space Telescope photometry in the context of progenitor limits. P.P. contributed the analysis of progenitor models. A.A.M., J.W.R. and S.B.C. analysed historical imaging from the Palomar Transient Factory (PTF) and KAIT in the context of *nova* limits. M.M.K. and K.J.S. provided the analysis of Spitzer observations. M.M.S. and J.B. provided analysis of the Hubble Space Telescope imaging. M.M.S. also contributed interpretation of the progenitor limits. N.R.B., E.O.O. and L.B. contributed analysis and interpretation of the historical X-ray imaging. D.P., R.M.Q., S.R.K., N.M.L., E.O.O., S.B.C., M.S., D.A.H., J.S.B., P.E.N., M.M.K., L.B. and K.M. were responsible for obtaining, reducing, and analysing the PTF observations. A.S. and H.-Y.S. obtained the Keck adaptive optics imaging and S.B.C. reduced and analysed those images. A.V.F., M.G., W.L. and J.M.S. were responsible for the KAIT imaging and analysis.

Author Information Reprints and permissions information is available at www.nature.com/reprints. The authors declare no competing financial interests. Readers are welcome to comment on the online version of this article at www.nature.com/nature. Correspondence and requests for materials should be addressed to W.L. (weidong@berkeley.edu).

LETTER

doi:10.1038/nature10628

Microwave amplification with nanomechanical resonators

F. Massel[1], T. T. Heikkilä[1], J.-M. Pirkkalainen[1], S. U. Cho[1], H. Saloniemi[2], P. J. Hakonen[1] & M. A. Sillanpää[1]

The sensitive measurement of electrical signals is at the heart of modern technology. According to the principles of quantum mechanics, any detector or amplifier necessarily adds a certain amount of noise to the signal, equal to at least the noise added by quantum fluctuations[1,2]. This quantum limit of added noise has nearly been reached in superconducting devices that take advantage of nonlinearities in Josephson junctions[3,4]. Here we introduce the concept of the amplification of microwave signals using mechanical oscillation, which seems likely to enable quantum-limited operation. We drive a nanomechanical resonator with a radiation pressure force[5–7], and provide an experimental demonstration and an analytical description of how a signal input to a microwave cavity induces coherent stimulated emission and, consequently, signal amplification. This generic scheme, which is based on two linear oscillators, has the advantage of being conceptually and practically simpler than the Josephson junction devices. In our device, we achieve signal amplification of 25 decibels with the addition of 20 quanta of noise, which is consistent with the expected amount of added noise. The generality of the model allows for realization in other physical systems as well, and we anticipate that near-quantum-limited mechanical microwave amplification will soon be feasible in various applications involving integrated electrical circuits.

Since the early days of quantum mechanics, the effect of quantum zero-point fluctuations on measurement accuracy has been actively investigated. The measurement of the position, x, of an object, necessarily disturbs its subsequent motion by introducing a change in its momentum, p. The Heisenberg uncertainty principle states that the uncertainties in the two quantities are related by the fundamental limit $\Delta x \Delta p \geq \hbar/2$, where $\hbar$ is Planck's constant divided by 2π. The optimal compromise between the two uncertainties results in the lowest added noise power per unit bandwidth, $\hbar\omega/2$, which equals the quantum fluctuations of the system at the signal frequency, ω. However, if only one observable, for example position, or a single quadrature of oscillation is measured, noise in this measurement can be reduced below the quantum limit at the expense of increased noise in the complementary observable or quadrature. In this case, the amplifier is said to be phase sensitive.

State-of-the-art cryogenic amplifiers using high-electron-mobility transistors operate at best at a few decades above the fundamental noise limit. Substantial improvements are difficult, owing to the strong current dissipation within such devices. Superconducting Josephson junction parametric amplifiers[3,4,8,9], working near the absolute zero of temperature, rely instead on reactive electrical elements. They operate at the level of only a few added noise quanta (above the quantum limit) at microwave frequencies. The quantum limit has not yet been approached using a mechanical amplifier; moreover, little work of any kind has been done on amplifying electrical signals by mechanical means[10], primarily as a result of the electromechanical interaction, which is typically small. In this Letter, we describe a way to approach quantum-limited microwave amplification using a mechanical device. Our system, which is mostly reactive, consists of a mechanical resonator affected by radiation pressure forces produced by an electromagnetic field confined in a lithographically patterned thin-film microwave cavity. Depending on the configuration, it is capable of either phase-sensitive or phase-insensitive amplification.

In our system, two coupled linear oscillators are arranged to form possibly the simplest means of quantum amplification of external signals realizable in principle at any frequency of the electromagnetic spectrum or in any other medium. Analysis of this system could give direct insight into the potential quantum behaviour of macroscopic mechanical objects[11–13], used here as the active modes of the amplifier, and the emergence of macroscopic phenomena from the quantum mechanical laws governing nature on the microscopic scale. Apart from this fundamental significance, the use of mechanical objects as building blocks of low-noise amplification might be advantageous over amplification by purely electrical means because of the possibility of developing a device based on an elementary physical structure: ultimately, these amplifiers could be made using single-crystalline resonant beams or membranes.

More specifically, our system involves an on-chip microwave cavity parametrically interacting with a micromechanical resonator[14–16], such that the mechanical motion, with resonance frequency ω_m, couples with the cavity (Fig. 1). We first review the archetypal case, namely a cavity driven by a single, strong tone with amplitude α_p (hereafter denoted as the pump), having a frequency, ω_p, near the resonant frequency, ω_c, of the cavity (Fig. 2a). The interaction is described by the Hamiltonian $H_{\rm int} = -\hbar g(n_c + 1/2)x$, where n_c is the number of coherently driven photons in the cavity, $g = (\omega_c/2C)\partial C_g/\partial x$ is the electromechanical interaction and x is the displacement of the mechanical resonator. In the expression for g, C denotes the capacitance of the cavity and C_g is the coupling capacitance to the mechanical resonator.

The sign of the detuning $\Delta = \omega_p - \omega_c$ determines the direction of the energy transfer between the two systems due to the interaction. Under the red-detuning condition, where $\Delta \approx -\omega_m$, the microwave–mechanics coupling generates a net energy transfer from the mechanical degrees of freedom into the cavity, hence effectively leading to the cooling of the mechanics. This sideband cooling regime has been reached both in electromechanical and in optomechanical systems[6,16–18].

By contrast, for blue detuning, where $\Delta > 0$, the pump gives rise to an energy transfer into the mechanical degrees of freedom. Adding a weak probe tone with a frequency near ω_c induces stimulated emission of microwave photons, effectively leading to an amplification of the probe signal. The energy levels corresponding to this process are shown in Fig. 2b. This type of pump–probe scheme underlies our device and is the topic of the remainder of the paper.

An image of our device, with relevant details indicated, is shown in Fig. 1b. The mechanical device consists of an aluminium micromechanical beam resonator of length 8.5 μm and width 320 nm. For this, the lowest flexural mode has frequency $\omega_m/2\pi = 32.5$ MHz and the linewidth is $\gamma_m/2\pi \approx 500$–$1{,}200$ Hz (depending on temperature). By varying an ultranarrow vacuum gap[19], the displacement affects the end-to-end capacitance of the cavity, which is a superconducting microstrip resonator having the natural frequency $\omega_c \gg \omega_m$ and linewidth γ_c. To obtain the largest possible electromechanical coupling, in

[1]Low Temperature Laboratory, Aalto University, PO Box 15100, FI-00076 Aalto, Finland. [2]Microsystems and Nanoelectronics, VTT Technical Research Centre of Finland, PO Box 1000, FI-02044 VTT, Finland.

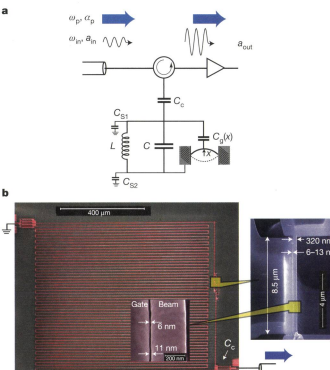

Figure 1 | Electromechanical microwave amplification. a, The variable capacitor of the micromechanical resonator is in parallel with the cavity, as shown in the lumped-element model. The input microwave field is decomposed into a blue-detuned pump coherent field, α_p (frequency, ω_p) and a signal (frequency, ω_s) plus noise, $a_{in} = \alpha_{in} + \delta a_{in}$. The output signal, a_{out}, is the amplified input signal. **b**, The device is dominated by the meandering high-impedance cavity (false colour in red), which resonates at $\omega_c/2\pi = 6.982$ GHz. During operation, this cavity is connected to coaxial cables via a coupling capacitor. The micromechanical beam resonator (frequency, $\omega_m/2\pi = 32.5$ MHz) couples the ends of the meander via the protrusions from either end and through a 6–13-nm vacuum gap[19] (right and inset).

designing the cavity we decided to fabricate the device on a fused silica substrate. This material has a low dielectric constant ($\varepsilon_r \approx 4$) relative to, for instance, silicon ($\varepsilon_r \approx 12$), which is frequently used. This low value contributes to minimizing the stray capacitance and allows us to obtain the lowest value so far, $C \approx 18$ fF, for the effective parallel capacitance of the nearly millimetre-sized cavity. These measures, and the remaining parameters ($L = 21$ nH, $C_{S1} = 6$ fF, $C_{S2} = 12$ fF and $C_g = 0.6$ fF; Fig. 1a), create a strong electromechanical coupling of $g/2\pi = 1.8$ MHz nm^{-1} (equivalently, $g/2\pi$ multiplied by the zero-point amplitude, x_0, equals 40 Hz per phonon). An interdigital coupling capacitor, $C_c \approx 6$ fF, results in the external damping rate, $\gamma_E/2\pi = 4.8$ MHz. The total cavity linewidth is $\gamma_c = \gamma_E + \gamma_i \approx 2\pi \times 6.2$ MHz, where $\gamma_i/2\pi = 1.4$ MHz is the damping rate due to internal losses.

The theoretical framework suitable to describe the amplification is closely related to the methodology used to describe the sideband cooling in optomechanical systems[17,18,20–22]. We describe the system in terms of quantum Langevin equations with the aim of analysing the effect of the pumping on the signal, and especially to detail the effects of different types of fluctuation coupling to the system. The latter comprise the quantum and thermal fluctuations related to the input signal, the cavity and the mechanical resonator. In general, the parametric coupling between the cavity and the mechanical resonator gives rise to the possibility of squeezed states[23,24] and, hence, to back-action-evading measurements.

Our detailed theoretical analysis (Supplementary Information) gives the explicit value of the gain in each preferred quadrature, G_x

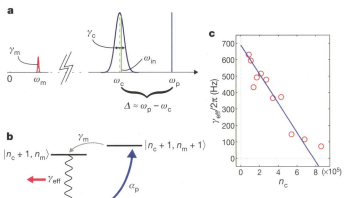

Figure 2 | Amplification mechanism. a, Explanation of the various frequencies involved. The cavity is driven by a coherent field (the pump, α_p) oscillating at $\omega_p = \omega_c + \Delta$, where ω_c is the cavity resonant frequency and $\Delta = \omega_m \ll \omega_c$. The weak input signal to be amplified, a_{in}, is applied with a frequency near the cavity resonance, such that $\omega_s = \omega_p - \omega_m$. **b**, The physics of the electromechanical amplifier can be intuitively understood by considering a block of three energy levels in the system. The (blue-detuned) pump, α_p, induces a transition between a state characterized by n_c cavity photons and n_m mechanical quanta, $|n_c, n_m\rangle$, and a state characterized by $n_c + 1$ photons and $n_m + 1$ mechanical quanta, $|n_c + 1, n_m + 1\rangle$. A key part of the amplification process is the effective damping, γ_{eff}, which in the simplified scheme presented here represents the effective lifetime for the cavity photons and thus models the parametric down-conversion of the pump photons to the cavity resonant frequency. **c**, The damping decreases as the pump field increases in power, and as $\gamma_{eff} \to 0$ instability and parametric oscillations set in. The circles are fitted from the measured mechanical peak in the output spectrum, and the solid line is the theoretical result.

and G_y, and the average gain, $G_{av} = (G_x + G_y)/2$. The expressions for the gains are well approximated by

$$G_{x,y} = 4|\Gamma_M(\omega)|^2 \left(\frac{\gamma_E}{\gamma_c}\right)^2 \left(\sqrt{1 + \frac{\gamma_c}{4\Delta}} \pm \frac{\gamma_c}{4\Delta}\right)^2 \qquad (1)$$

where the upper sign gives the expression for G_x and the lower sign gives the expression for G_y. The main contribution to the amplification is described by the ratio between the mechanical response functions in the presence and the absence of the pump, $\Gamma_M(\omega) = \left(\omega_m^2 - \omega^2 - i\gamma_m\omega\right)/\left(\omega_{eff}^2 - \omega^2 - i\gamma_{eff}\omega\right)$, where $\omega_{eff} \approx \omega_m$.

The key role in the microwave amplification is that of the effective mechanical damping, $\gamma_{eff} = \gamma_m - \delta\gamma_{eff}(\omega, n_c)$ (Fig. 2c and Supplementary Information). The value of $\delta\gamma_{eff}$ can be tuned by the pump. In particular, blue-detuned driving results in a sizable reduction in the mechanical damping. This reduction causes the amplification of the signal, described by the factor $\Gamma_M(\omega \approx \omega_m) \approx \gamma_m/\gamma_{eff}$. From equation (1) and the definition of γ_{eff}, we establish the optimal value for the pumped occupancy to be $n_{c,opt} = \gamma_c\gamma_m/4g^2x_0^2$. The corresponding maximum average gain is $G_{av}(\omega = \omega_m) \approx 4(4\Delta/\gamma_c)^2$. Above this threshold, $\gamma_{eff} \to 0$ and the coupled system becomes unstable[5,7,25,26].

As indicated by the unequal values of G_x and G_y, the amplifier shows a variable amount of squeezing. In particular, in the 'good-cavity' limit ($\gamma_c/\Delta \ll 1$) used in our experiment, the squeezing is expected to be negligible and the amplifier hence behaves as a typical phase-insensitive amplifier characterized by the average gain, G_{av}. However, it is noteworthy that by varying the parameters towards the 'bad-cavity' limit ($\gamma_c/\Delta > 1$), it is possible to achieve strong squeezing and, consequently, noise-free amplification in one quadrature. This situation is opposite to the findings in studies on two-tone back-action-evading measurements, where the strongest squeezing is found in the good-cavity limit.

We use a cryostat with the temperature stabilized between 350 and 25 mK to carry out the measurements. The pump and signal tones are combined at room temperature using a power splitter. Inside the cryostat, the incoming irradiation is attenuated by 43 ± 1.5 dB. The

uncertainty in the cryogenic attenuation sets relatively large error bars for n_c. The signals reflected from the device chip are directed towards a conventional cryogenic amplifier. Following amplification, we used a sharp low-pass filter to remove the strong pump microwave, because we consider only the signal frequency in the processing. The signal is recorded using a vector network analyser or, for noise measurements, is fed into a spectrum analyser. Although it is possible to distinguish the different quadrature gains (G_x and G_y), to begin with we consider only the phase-insensitive gain (G_{av}). More details of the practical set-up are given in Supplementary Information.

At the lowest pump power, $n_c \ll n_{c,crit}$, we observe attenuation of the reflected signal resulting from cavity absorption at the applied signal frequency, $\omega_{in}/2\pi \approx 6.98$ GHz, of about −5.5 dB for $\omega_{in} \approx \omega_c$ (Fig. 3a). At higher values of n_c, a mechanical peak at $\omega_p - \omega_{in} \approx \omega_m$ indicates a decrease in absorption. The absorption vanishes when $2\gamma_m/\gamma_{eff} \approx \gamma_c/\gamma_E$, that is, when reduced damping balances external losses. This behaviour, observed recently in optomechanical crystals[27], has a similar effect on the direct transmission of radiation as the electromagnetically induced transparency. The latter phenomenon, which is associated with increased damping and slowing down and storage of light, is obtained using red-detuned pumping. In the present context, it is called electromechanically induced transparency[28,29]. Blue-detuned pumping, however, transfers energy to the cavity frequency, and we therefore also observe amplification of the signal tone (Fig. 3b).

The theoretical prediction, overlaid on the experimental data in Fig. 3b, shows a remarkable agreement with the measurement, with the only adjustable parameter being n_c, whose values, nevertheless, are independently known to within a factor of two. A maximum gain of 25 dB is observed close to the instability associated with the $\gamma_{eff} \to 0$ limit, but it comes with a markedly increased amount of fluctuation, typical of parametric systems. The range of useful gain, where noise is not increased, is up to about 15 dB in this measurement. The operational frequency of the amplifier may be tuned by roughly the amount of the cavity linewidth by detuning the pump slightly from the exact blue-sideband condition. Although the data was measured with a small input signal exciting about 0.3 signal photons (before amplification) in the cavity, a favourable property of the mechanical amplification is its high dynamic range: amplification is observed at input powers corresponding to at least 10^4 such photons. This high power-handling capability contrasts with the Josephson parametric amplifiers, which usually work near the single-quantum regime.

We can also confirm the theory predictions by inverting the pump frequency to the red sideband, where $\Delta = -\omega_m$ (Fig. 3c). By analogy with the enhanced damping leading to sideband cooling under these conditions, we observe de-amplification of the input signal. Even at a stronger pump power, $n_c > n_{c,crit}$, decreased absorption indicates that the eigenmode splitting[29] starts to set in. The observed gains (Fig. 3d) as a function of the pumped occupancy are in a good agreement with theory.

Finally, an amplifier should be characterized by its added noise, which is commonly referred to the input signal. Because of its simple structure, we expect the mechanical amplifier to be less influenced by the strong electrical flicker noise typical of nonlinear transistor or Josephson junction devices. What remain as noise sources are thermal fluctuations and, ultimately, quantum fluctuations in the numbers of quanta of both the cavity and the mechanics. In the case of optimal gain, the quadrature-averaged added noise at the cavity frequency is

$$n_{add} = \frac{\gamma_I}{\gamma_c}\left(n_c^T + \frac{1}{2}\right) + \frac{\gamma_c}{\gamma_E}\left(n_m + \frac{1}{2}\right)$$
$$\geq \frac{1}{2}\left[1 - (G_x G_y)^{-1/2}\right]$$
$$\approx \frac{1}{2}$$

Here n_c^T and n_m represent the finite number of cavity photons associated with the internal losses and, respectively, the number of mechanical quanta due to the thermal fluctuations in the mechanical bath. The large-gain quantum limit of $n_{add} = 1/2$ may thus be reached for $n_c^T \approx 0$ and $n_m \approx 0$ if information is not lost inside the system, that is, if external dissipation of the cavity related to the measurement dominates over internal losses. Whereas in cryogenic experiments n_c^T is typically approximately zero owing to gigahertz-range cavity frequencies, standard mechanical frequencies of $\omega_m/2\pi \leq 50$ MHz tend to pose a practical noise limit of $n_{add} > n_m \gtrsim 10$. We note that Josephson parametric amplifiers are more favourable in this sense because they are in the ground state at standard cryogenic temperatures. Nevertheless, in what follows and in Supplementary Information we discuss ways closely to approach the quantum limit with mechanical amplifiers as well.

We measured the added noise by comparing it with a known noise source. Here the noise floor is set by the effective noise temperature of

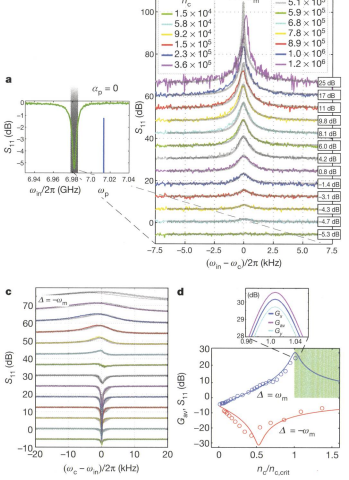

Figure 3 | Amplifier gain. a, Reflection magnitude, S_{11}, of the signal microwave over a wide frequency range about the cavity resonance, measured without applying the pump. **b**, Measured gain (coloured lines) in a narrow frequency range (shaded grey in **a**) for values of the pump occupation number, n_c, that increase by 2 dB per curve (bottom to top). For clarity, the curves are displaced vertically by 3 dB. The baseline of each curve roughly corresponds to the cavity absorption of −5.5 dB. The maximum gain is quoted for each curve. The grey curves are theoretical predictions for the average gain over quadratures, G_{av}. **c**, As in **b**, but with red-detuned pumping and n_c increasing by 2 dB per curve (bottom to top) from a minimum value of $n_c = 4.6 \times 10^4$. Here de-amplification of the signal field (sharp dip) is observed. **d**, Calculated average gain (at $\omega_p - \omega_m$) and, inset, the quadrature gains G_x and G_y as functions of the scaled cavity occupancy. The blue and red traces correspond to amplification ($\Delta > 0$) and de-amplification ($\Delta < 0$), respectively. The shaded region is the unstable regime (see text). The experimental points are extracted from **b** and **c**.

the system, ~6–7 K. We worked at a temperature of 30 mK and used a weak input signal as a marker (Supplementary Information). We obtained a slight improvement, by 0.6 dB, in the signal-to-noise ratio, which corresponds to $n_{\mathrm{add}} \approx 20$ added noise quanta at the signal frequency of 7 GHz. This finding agrees remarkably well with the ideal prediction, which equals the thermal phonon number, and shows that no extra noise other than thermal noise was generated in the process. Hence, even further improvement, bringing the device's performance closer to the quantum limit, $n_{\mathrm{add}} = 1/2$, seems possible.

We have shown that interaction of a micromechanical device and radiation pressure can be used to amplify weak electrical signals. This positions such amplifiers as alternatives to conventional electrical microwave amplifiers, and may facilitate radiation detection in the terahertz band, where such detection is difficult. From a theoretical point of view, the set-up represents one of the simplest realizations of a quantum amplifier that could potentially operate at the noise limit set by the Heisenberg uncertainty principle. In the first proof-of-principle device, the mechanical amplifier showed no added noise beyond that predicted by the ideal theoretical model. In practice, the frequency band can be made variable over a larger span by using tunable cavities[3]. A higher electromechanical coupling, achieved, for instance, through the use of piezoelectric materials[13], could allow for an increase in the bandwidth through an engineerd increase in damping. At a higher mechanical frequency, in the gigahertz range, or potentially with the help of pre-cooling to the ground state[30] by red-detuned pumping at even higher operating temperatures than here, devices based on the amplification principle set out here could, we believe, offer near-quantum-limited operation.

METHODS SUMMARY

Both the cavity and the structures for the beam were patterned in a single electron beam lithography step, followed by evaporation of a 150-nm layer of aluminium. To minimize the stray capacitance, C, of the cavity, the device was fabricated on a fused silica (SiO_2) substrate, which has a low dielectric constant ($\varepsilon_r \approx 4$). The beam was partly released by etching the substrate by the use of hydrofluoric acid vapour etcher, for 500 s at a pressure of 150 torr. The mechanical beams were defined by focused ion beam etching, as in ref. 19.

The measurements were carried out in a cryostat at temperatures as low as 25 mK. The pump and probe signals were combined at room temperature (~300 K) using a power splitter. Before the signals entered the cryostat, a sharp high-pass filter at room temperature was used to attenuate the phase noise of the generators near the cavity frequency. This filter provides 50 dB more attenuation at the cavity frequency than at the blue sideband. Inside the cryostat, the incoming signals are heavily attenuated.

We use the notion of preferred quadratures[1] for a phase-sensitive amplifier, for which the output quadrature fields, X_{out} and Y_{out}, are independent of the respective input fields, Y_{in} and X_{in}. The solution of the quantum Langevin equations gives the relation between the input and output fields. In particular, the output signal from the microwave cavity is determined from the gains for the input signal, M and L, and those for the input noise, M_1 and L_1:

$$a_{\mathrm{out}} = Ma_{\mathrm{in}} + La_{\mathrm{in}}^{\dagger} + M_1 a_{\mathrm{in}}^{\prime} + L_1 a_{\mathrm{in}}^{\prime\dagger} + Q\xi$$

Here $a_{\mathrm{in}}^{\prime}(\omega)$ and $\xi(\omega)$ represent the noise introduced by the internal losses of the cavity and the mechanical bath, respectively, and $a_{\mathrm{in}}(\omega) = \alpha_{\mathrm{in}} + \delta a_{\mathrm{in}}$ is the sum of the input (coherent) signal and the input noise. The output field is then expressed in terms of the preferred quadratures as $X_{\mathrm{out}} = \sqrt{G_c}X_{\mathrm{in}} + (\text{noise terms})_x$ and $Y_{\mathrm{out}} = \sqrt{G_c}Y_{\mathrm{in}} + (\text{noise terms})_y$.

Received 12 July; accepted 10 October 2011.

1. Caves, C. M. Quantum limits on noise in linear-amplifiers. *Phys. Rev. D* **26,** 1817–1839 (1982).
2. Haus, H. A. *Electromagnetic Noise and Quantum Optical Measurements* 267–277 (Advanced Texts in Physics, Springer, 2000).
3. Castellanos-Beltran, M. A., Irwin, K. D., Hilton, G. C., Vale, L. R. & Lehnert, K. W. Amplification and squeezing of quantum noise with a tunable Josephson metamaterial. *Nature Phys.* **4,** 929–931 (2008).
4. Bergeal, N. *et al.* Phase-preserving amplification near the quantum limit with a Josephson ring modulator. *Nature* **465,** 64–68 (2010).
5. Braginsky, V. B., Strigin, S. E. & Vyatchanin, S. P. Parametric oscillatory instability in Fabry-Perot interferometer. *Phys. Lett. A* **287,** 331–338 (2001).
6. Metzger, C. H. & Karrai, K. Cavity cooling of a microlever. *Nature* **432,** 1002–1005 (2004).
7. Kippenberg, T. J., Rokhsari, H., Carmon, T., Scherer, A. & Vahala, K. J. Analysis of radiation-pressure induced mechanical oscillation of an optical microcavity. *Phys. Rev. Lett.* **95,** 033901 (2005).
8. Yurke, B. *et al.* Observation of 4.2-K equilibrium-noise squeezing via a Josephson-parametric amplifier. *Phys. Rev. Lett.* **60,** 764–767 (1988).
9. André, M. O., Mück, M., Clarke, J., Gail, J. & Heiden, C. Radio-frequency amplifier with tenth-kelvin noise temperature based on a microstrip direct current superconducting quantum interference device. *Appl. Phys. Lett.* **75,** 698–700 (1999).
10. Raskin, J. P., Brown, A. R., Khuri-Yakub, B. T. & Rebeiz, G. M. A novel parametric-effect MEMS amplifier. *J. Microelectromech. Syst.* **9,** 528–537 (2000).
11. Leggett, A. J. Testing the limits of quantum mechanics: motivation, state of play, prospects. *J. Phys. Condens. Matter* **14,** R415–R451 (2002).
12. Marshall, W., Simon, C., Penrose, R. & Bouwmeester, D. Towards quantum superpositions of a mirror. *Phys. Rev. Lett.* **91,** 130401 (2003).
13. O'Connell, A. D. *et al.* Quantum ground state and single-phonon control of a mechanical resonator. *Nature* **464,** 697–703 (2010).
14. Regal, C. A., Teufel, J. D. & Lehnert, K. W. Measuring nanomechanical motion with a microwave cavity interferometer. *Nature Phys.* **4,** 555–560 (2008).
15. Sillanpää, M. A., Sarkar, J., Sulkko, J., Muhonen, J. & Hakonen, P. J. Accessing nanomechanical resonators via a fast microwave circuit. *Appl. Phys. Lett.* **95,** 011909 (2009).
16. Rocheleau, T. *et al.* Preparation and detection of a mechanical resonator near the ground state of motion. *Nature* **463,** 72–75 (2010).
17. Marquardt, F., Chen, J. P., Clerk, A. A. & Girvin, S. M. Quantum theory of cavity-assisted sideband cooling of mechanical motion. *Phys. Rev. Lett.* **99,** 093902 (2007).
18. Wilson-Rae, I., Nooshi, N., Zwerger, W. & Kippenberg, T. J. Theory of ground state cooling of a mechanical oscillator using dynamical backaction. *Phys. Rev. Lett.* **99,** 093901 (2007).
19. Sulkko, J. *et al.* Strong gate coupling of high-*Q* nanomechanical resonators. *Nano Lett.* **10,** 4884–4889 (2010).
20. Mancini, S. & Tombesi, P. Quantum-noise reduction by radiation pressure. *Phys. Rev. A* **49,** 4055–4065 (1994).
21. Genes, C., Vitali, D., Tombesi, P., Gigan, S. & Aspelmeyer, M. Ground-state cooling of a micromechanical oscillator: comparing cold damping and cavity-assisted cooling schemes. *Phys. Rev. A* **77,** 033804 (2008).
22. Clerk, A. A., Devoret, M. H., Girvin, S. M., Marquardt, F. & Schoelkopf, R. J. Introduction to quantum noise, measurement, and amplification. *Rev. Mod. Phys.* **82,** 1155–1208 (2010).
23. Rugar, D. & Grütter, P. Mechanical parametric amplification and thermomechanical noise squeezing. *Phys. Rev. Lett.* **67,** 699–702 (1991).
24. Woolley, M. J., Doherty, A. C., Milburn, G. J. & Schwab, K. C. Nanomechanical squeezing with detection via a microwave cavity. *Phys. Rev. A* **78,** 062303 (2008).
25. Carr, D. W., Evoy, S., Sekaric, L., Craighead, H. G. & Parpia, J. M. Parametric amplification in a torsional microresonator. *Appl. Phys. Lett.* **77,** 1545–1547 (2000).
26. Arcizet, O., Cohadon, P. F., Briant, T., Pinard, M. & Heidmann, A. Radiation-pressure cooling and optomechanical instability of a micromirror. *Nature* **444,** 71–74 (2006).
27. Safavi-Naeini, A. H. *et al.* Electromagnetically induced transparency and slow light with optomechanics. *Nature* **472,** 69–73 (2011).
28. Weis, S. *et al.* Optomechanically induced transparency. *Science* **330,** 1520–1523 (2010).
29. Teufel, J. D. *et al.* Circuit cavity electromechanics in the strong-coupling regime. *Nature* **471,** 204–208 (2011).
30. Teufel, J. D. *et al.* Sideband cooling of micromechanical motion to the quantum ground state. *Nature* **475,** 359–363 (2011).

Supplementary Information is linked to the online version of the paper at www.nature.com/nature.

Acknowledgements We would like to thank S. Paraoanu and H. Seppä for discussions. This work was supported by the Academy of Finland and by the European Research Council (grant numbers 240362-Heattronics and 240387-NEMSQED) and EU-FP7-NMP-246026.

Author Contributions F.M. and T.T.H. developed the theory. J.-M.P. and S.U.C. contributed to the design and fabrication of the samples and to the cryogenic set-up. H.S. made the samples. P.J.H. and M.A.S. designed the experimental set-up. M.A.S. initiated the work and carried out the measurements.

Author Information Reprints and permissions information is available at www.nature.com/reprints. The authors declare no competing financial interests. Readers are welcome to comment on the online version of this article at www.nature.com/nature. Correspondence and requests for materials should be addressed to F.M. (francesco.massel@aalto.fi).

LETTER

doi:10.1038/nature10667

Jamming by shear

Dapeng Bi[1], Jie Zhang[2,3,4], Bulbul Chakraborty[1] & R. P. Behringer[4]

A broad class of disordered materials including foams, glassy molecular systems, colloids and granular materials can form jammed states. A jammed system can resist small stresses without deforming irreversibly, whereas unjammed systems flow under any applied stresses. The broad applicability of the Liu–Nagel jamming concept[1,2] has attracted intensive theoretical and modelling interest but has prompted less experimental effort[1–6]. In the Liu–Nagel framework, jammed states of athermal systems exist only above a certain critical density. Although numerical simulations for particles that do not experience friction broadly support this idea[7–13], the nature of the jamming transition for frictional grains is less clear[14–17]. Here we show that jamming of frictional, disk-shaped grains can be induced by the application of shear stress at densities lower than the critical value, at which isotropic (shear-free) jamming occurs. These jammed states have a much richer phenomenology than the isotropic jammed states: for small applied shear stresses, the states are fragile, with a strong force network that percolates only in one direction. A minimum shear stress is needed to create robust, shear-jammed states with a strong force network percolating in all directions. The transitions from unjammed to fragile states and from fragile to shear-jammed states are controlled by the fraction of force-bearing grains. The fractions at which these transitions occur are statistically independent of the density. Jammed states with densities lower than the critical value have an anisotropic fabric (contact network). The minimum anisotropy of shear-jammed states vanishes as the density approaches the critical value from below, in a manner reminiscent of an order–disorder transition.

Cohesionless granular materials form jammed states only under external stress, as explored extensively in the soil mechanics literature[18]. In the zero-temperature ($T = 0$) plane of the Liu–Nagel jamming diagram[1–5] (Fig. 1a), increased packing fraction (ϕ) induces jamming and positive pressure, and shear stress (τ) induces irreversible flow at the yield stress line (Fig. 1a, black line). Simulations of frictionless grains typically probe jamming near the critical point at $T = 0$, $\tau = 0$ and $\phi = \phi_J$, through isotropic compression or decompression[7–9], or along the yield stress line[11–13,19,20]. The numerical value of ϕ_J depends on the protocol for preparing the jammed states. However, the characteristics of the transition are robust[21]. Only a few experiments[4–6,22] have investigated the Liu–Nagel jamming model[1,2] for physical systems consisting of particles with friction. For example, by using isotropically confined frictional disks it was found[4] that friction only weakly affects certain aspects of jamming, such as the packing fraction ($\phi \approx 0.842$), but that other aspects, such as average number of contacts at jamming, are more strongly dependent on friction, as expected[15].

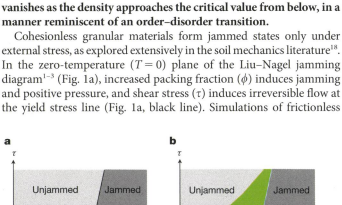

Figure 1 | Jamming phase diagrams in the $T = 0$ plane. a, Original Liu–Nagel jamming phase diagram[1]. The boundary between unjammed and jammed regions is the yield stress line. Unjamming can be induced by decreasing the packing fraction or increasing the shear stress. **b**, Generalized jamming diagram including the shear-jammed (SJ) and fragile (F) states. Along the ϕ axis, there are two special densities: ϕ_S, below which there is no shear jamming, and ϕ_J, above which isotropically jammed states exist. For $\phi_S \leq \phi \leq \phi_J$, jamming can occur with application of shear stress.

We report stable static states that jam only under a minimum shear stress. These states are outside the jammed region of Fig. 1a and alter the jamming diagram as illustrated in Fig. 1b. Of special note is the line separating two qualitatively different classes of states: the fragile states and the shear-jammed states. As we show below, this line is the locus of shear stresses marking a percolation transition. Shear-jammed states have not been reported in typical (that is, frictionless) models of jamming, which involve isotropically compressed particles and where additional relaxation may be induced to find a lower-energy state[7,15]. Our systems differ from these models in several key aspects: they consist of frictional (photoelastic) disks (Supplementary Fig. 1) prepared at densities below (and above) ϕ_J; they are subjected to pure (volume-preserving) shear applied in small strain steps, allowing the system spontaneously to relax between steps; and they rest on a weakly frictional substrate, with forces that are an order of magnitude smaller than typical interparticle forces at jamming. We obtained stress data, that is, values of τ, pressure (P) and the fabric tensor ($\bar{R}$). The eigenvalues, R_1 and R_2, of $\bar{R}$ yield the mean contact number, $Z = R_1 + R_2$, and a measure of contact anisotropy, $\rho = R_2 - R_1$. In addition, we analysed the spatial organization of contact forces. Experimental details can be found in Methods.

Ascertaining that states are macroscopically jammed is non-trivial. Necessary requirements are non-zero P and τ and the ability to resist any small incremental stress. For frictionless grains, these conditions are met if Z exceeds Z_{iso} (refs 7, 11), where the number of mechanical equilibrium constraints equals the number of degrees of freedom. For large N, isotropic jammed states exist for $\phi \geq \phi_J$, where ϕ_J depends only on the spatial dimension for a given protocol[7].

For frictional grains, a minimal parameter set for jamming has not been clearly determined. Although Z is a key parameter for mechanical stability, the minimum number of contacts needed for jamming can span a range of values, depending on friction and preparation[14,15,23]. For the disks used here, a reasonable criterion for isotropic jamming was found to be $Z \geq 3.0$ to ~ 3.1 (ref. 4), for which $\phi_J \approx 0.842$ (Supplementary Fig. 3).

A distinguishing property of granular jammed states is the existence of force networks. To characterize the states obtained by shearing at $\phi < \phi_J$, we consider the contact force and fabric networks, and their correlation with the properties of the stress tensor[24] and the fraction of non-rattler grains, f_{NR} (Supplementary Figs 2 and 4). It is known from earlier studies that force networks in jammed packings of dry grains

[1]Martin Fisher School of Physics, Brandeis University, Waltham, Massachusetts 02454, USA. [2]Institute of Natural Sciences and Department of Physics, Shanghai Jiao Tong University, Shanghai 200240, China. [3]Department of Physics, Indiana University Purdue University Fort Wayne, Fort Wayne, Indiana 46805, USA. [4]Department of Physics, Duke University, Durham, North Carolina 27708, USA.

can be separated into a strong network (in which each contact force magnitude satisfies $f > f_{avg}$ where f_{avg} is the average of all contact force magnitudes over all force-bearing contacts in the system) and a complementary weak network[24,25]. We identify a strong force network with the largest cluster of grains that is connected via contact forces with magnitudes $f > f_{avg}$.

Starting from an unjammed state (Fig. 2), the strong force network undergoes two sequential percolation transitions controlled by the non-rattler fraction, f_{NR} (ref. 26; here we define grains with at least two force-bearing contacts as non-rattler grains). Experimentally, the shear strain controls f_{NR}. Monotonic increases in shear strain generally increase f_{NR} (Supplementary Fig. 5) and tune the system through the percolation transitions. For $f_{NR} < 0.4$, the network of force-bearing grains does not percolate in any direction of the sheared packing. There are small residual values of P and τ for these states due only to experimental noise and the small frictional forces exerted on the grains by the base (Methods). We refer to these states as 'unjammed'. As f_{NR} increases above ~0.7, the strong force network percolates in the compressive direction but not transverse to it. We refer to these states as 'fragile'; they have a strong force network that carries the majority of the shear stress (deviatoric stress) but which spans the system only in the compressive direction. The weak force network, by contrast, acts like a fluid, supporting a less anisotropic stress tensor[24]. We expect that in the limit of infinitely rigid grains, these fragile states would be able to support only loads along the compressive direction without undergoing plastic rearrangement[27]. Because the experimental system is composed of deformable grains, there is a small regime of elastic response in the dilational direction even for the fragile states. At $f_{NR} = 0.83 \pm 0.02$, the strong force network percolates in both directions. These states, which we refer to as 'shear jammed', are characterized by two non-parallel populations of force chains. The classification of shear-jammed, fragile and unjammed states has relied on identifying the $f > kf_{avg}$ (with $k = 1$) cluster as the strong force network (where f refers to the individual contact force magnitude). We show in Supplementary Fig. 6 that this definition is robust with respect to the choice of the threshold (k), and that at $f_{NR} = 0.83$ all k-clusters with $0 \leq k \leq 1.2$ have percolated in the dilational direction. The experiment shown in Supplementary Movie 1 illustrates the evolution of force networks and the percolation events.

The Liu–Nagel jamming diagram needs to be modified to include the fragile and shear-jammed states. Figure 2c shows a τ–ϕ plot of shear-jammed (green), fragile (red) and unjammed (black) states, as distinguished by the natures of their force networks. For each $\phi < \phi_J$, there is a minimum shear stress, $\tau_0(\phi)$, needed to create a shear-jammed state, and $\tau_0 \to 0$ as $\phi \to \phi_J$ from below. As shown in Fig. 2b (see also Supplementary Figs 5 and 6), the pure shear strain imposed in the experiment induces shear jamming by increasing the non-rattler fraction, f_{NR}, which leads to the two percolation transitions. Continued shear pushes the system to the yield stress line (Fig. 2c, purple symbols). For $\phi > \phi_J$, jammed states with a strong force network percolating in all directions occur along the ϕ axis at $\tau = 0$.

The formation of fragile and shear-jammed states depends on the possibility of creating anisotropic contact networks (fabric[24,28,29]; discussed in detail in Supplementary Figs 5, 7 and 8), which form a backbone for the stresses[27]. The anisotropies of the stress tensor and the fabric tensor are intimately related in these states[24,29]. Models, physical particle properties or protocols that preclude the formation of this backbone would not lead to these states.

Theoretical support for shear-jammed states comes from recent simulations[16] that probed systems of frictional grains subject to quasi-static steady shear along the yield stress line and showed a discontinuous transition in the τ–ϕ phase curve from jammed to unjammed states at a value of ϕ that is consistent with our observations for ϕ_S, the lowest value of ϕ for which shear jamming occurs. These simulations correspond to moving along the yield stress line in Fig. 2c (purple) towards lower values of ϕ and arriving at the 'nose' of the jamming curve at ϕ_S.

The relationship between the fabric and stress anisotropies, expressed in Fig. 3a as a plot of ρ versus τ for all sheared states, is analogous to that between magnetization and magnetic field in a magnetic system. As

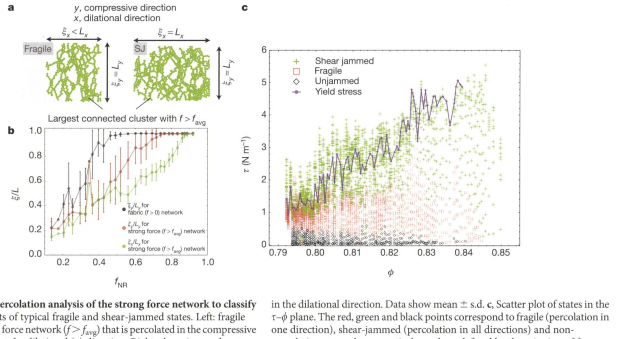

Figure 2 | Using percolation analysis of the strong force network to classify states. a, Snapshots of typical fragile and shear-jammed states. Left: fragile states have a strong force network ($f > f_{avg}$) that is percolated in the compressive (y) direction but not the dilational (x) direction. Right: shear-jammed states have a strong force network that is percolated in all directions. ξ_x and ξ_y are the linear sizes associated with the largest connected cluster in the strong force network. L_x and L_y are box dimensions. **b**, Plots of cluster size/box dimension ratio (ξ/L) versus f_{NR} for the fabric and the strong force networks (Supplementary Fig. 6): black, fabric network in the compressive direction; red, strong force network in the compressive direction; green, strong force network in the dilational direction. Data show mean ± s.d. **c**, Scatter plot of states in the τ–ϕ plane. The red, green and black points correspond to fragile (percolation in one direction), shear-jammed (percolation in all directions) and non-percolating networks, respectively, and are defined by the criterion of force network percolation as shown in **b**. The purple line is the yield stress line. For each $\phi < \phi_J$, the yield stress is obtained by averaging over the stress values just before plastic rearrangements occur in the forward shear time trace[11]. For $\phi > \phi_J$, owing to experimental limitations, we do not have enough statistics to calculate the yield stress.

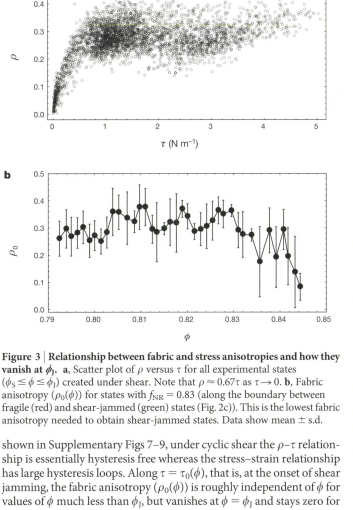

Figure 3 | Relationship between fabric and stress anisotropies and how they vanish at ϕ_1. **a**, Scatter plot of ρ versus τ for all experimental states ($\phi_S \leq \phi \leq \phi_1$) created under shear. Note that $\rho \approx 0.67\tau$ as $\tau \to 0$. **b**, Fabric anisotropy ($\rho_0(\phi)$) for states with $f_{NR} = 0.83$ (along the boundary between fragile (red) and shear-jammed (green) states (Fig. 2c)). This is the lowest fabric anisotropy needed to obtain shear-jammed states. Data show mean ± s.d.

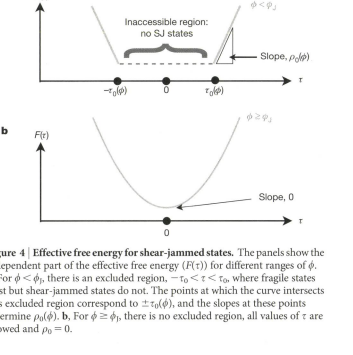

Figure 4 | Effective free energy for shear-jammed states. The panels show the τ-dependent part of the effective free energy ($F(\tau)$) for different ranges of ϕ. **a**, For $\phi < \phi_1$, there is an excluded region, $-\tau_0 < \tau < \tau_0$, where fragile states exist but shear-jammed states do not. The points at which the curve intersects this excluded region correspond to $\pm\tau_0(\phi)$, and the slopes at these points determine $\rho_0(\phi)$. **b**, For $\phi \geq \phi_1$, there is no excluded region, all values of τ are allowed and $\rho_0 = 0$.

shown in Supplementary Figs 7–9, under cyclic shear the ρ–τ relationship is essentially hysteresis free whereas the stress–strain relationship has large hysteresis loops. Along $\tau = \tau_0(\phi)$, that is, at the onset of shear jamming, the fabric anisotropy ($\rho_0(\phi)$) is roughly independent of ϕ for values of ϕ much less than ϕ_1, but vanishes at $\phi = \phi_1$ and stays zero for $\phi > \phi_1$ (Fig. 3b). This suggests that ρ_0 acts as an order parameter for the shear-jammed states (it is non-zero for such states and zero for isotropic jammed states) and that ϕ_1 marks an order–disorder transition at which jammed states become isotropic. For a magnet, the order parameter is the zero-field magnetization, whereas the order parameter for the shear-jammed states, ρ_0, is measured along the $\tau_0(\phi)$ line, the lower limit for jammed states to exist. For systems in thermal equilibrium, derivatives of the free energy define relationships between an order parameter and the conjugate external field. In analogy, we define an 'effective free energy' (F) through the relationship $\rho = \partial F/\partial\tau$. The results for $\rho_0(\phi)$ and $\tau_0(\phi)$ suggest an empirical form for F that is illustrated in Fig. 4. This form is consistent with the ρ–τ relationship for cyclically sheared states (Supplementary Figs 7–9). For $\phi_S < \phi < \phi_1$, there is an excluded region, $-\tau_0 < \tau < \tau_0$, with fragile but not shear-jammed states, and the slope of F (as a function of τ) at the boundary of this regime is ρ_0. As $\phi \to \phi_1$ from below, the excluded region vanishes and $\rho_0 \to 0$. Ideally, such an effective free energy would be related to the probability density of shear-jammed states at given values of ϕ and τ, which could be obtained from simulations of sheared frictional grains.

The present jamming diagram, deduced from physical experiments with frictional particles, differs substantially from the jamming diagram based on simulations of frictionless particles. We observe new classes of states that exist only under shear, have anisotropic force and fabric networks, and have an order parameter that vanishes as ϕ increases beyond a threshold comparable to ϕ_1 for isotropic jammed states. The fraction of non-rattler grains (f_{NR}) controls the percolation of the force networks and emerges as the single parameter distinguishing between unjammed, fragile and shear-jammed states. The shear-jammed states occupy a large region of parameter space and are important in determining the response of frictional granular materials to external stresses. The yield stress of shear-jammed states vanishes discontinuously at $\phi_S < \phi_1$ (ref. 16). The origin of these states is probably related to dilatancy, that is, the tendency of dense granular matter, under constant pressure, to expand under shear. Under constant-area conditions such as in the experiments studied here, shearing leads to jamming[17,27]. Our systems are quasi-two-dimensional and an important question for further study is what happens in fully three-dimensional systems.

METHODS SUMMARY

We applied pure shear strain to a system of 1,568 frictional, bidisperse, photoelastic disks contained in a biaxial device[4,22,30]. This device can deform the system, keeping the area (A) and ϕ fixed, to perform isotropic compression or pure shear. In many soil mechanics approaches, biaxial deformations are achieved by compressing in one direction while keeping the normal stress constant in the remaining direction[28,29]. Using photoelastic particles, we determine the location of, and forces ($\mathbf{f}$) at, interparticle contacts[30], and from these construct the stress tensor ($\tilde{\sigma}$) and a contact fabric tensor[24,29] ($\tilde{R}$):

$$\tilde{\sigma} = \frac{1}{V}\sum_{i \neq j} \mathbf{r}_{ij} \otimes \mathbf{f}_{ij}$$

$$\tilde{R} = \frac{1}{N}\sum_{i \neq j} \frac{\mathbf{r}_{ij}}{\|\mathbf{r}_{ij}\|} \otimes \frac{\mathbf{r}_{ij}}{\|\mathbf{r}_{ij}\|}$$

Here $\mathbf{r}_{ij}$ is the contact vector from the centre of grain i to the interparticle contact between grains i and j, $\mathbf{f}_{ij}$ is the force vector associated with this contact and '$\otimes$' denotes a vector outer product. Also, V is the volume of the system (or area in two dimensions) and N is the number of non-rattler particles (particles with at least two contacts[4,22]). Denoting the principal stresses by σ_1 and σ_2, the pressure is given by $P = (\sigma_1 + \sigma_2)/2$ and the shear stress is given by $\tau = (\sigma_2 - \sigma_1)/2$. Denoting the eigenvalues of $\tilde{R}$ by R_1 and R_2, the mean contact number per particle is $Z = R_1 + R_2$ and $\rho = R_2 - R_1$ or ρ/Z characterizes the contact network anisotropy.

The experiments span $\phi_S \leq \phi \leq \phi_1$, where $\phi_S = 0.792$ and $\phi_1 = 0.850$. For each value of ϕ, the walls of the biaxial device were initially configured in a square, with the particles in nominally random positions. For $\phi < \phi_1 = 0.842$, the initial isotropic state was unjammed. For $\phi > \phi_1$, we initialized the system by tapping gently to relax the stresses to their lowest value. For all ϕ, after initializing the system we subsequently made small quasi-static pure shear steps, allowing the system spontaneously to relax for at least several minutes between steps. The typical strain step was of size $\delta\varepsilon \approx 0.003$. For sufficient shear, the system achieved a manifestly

jammed state, with a network of force chains (Supplementary Fig. 1) provided that $\phi > \phi_S$. We also carried out some cyclic shear experiments[22] (Supplementary Figs 7–9). These experiments involved six cycles, each consisting of a forward and a reverse shear strain, and the data from these cycles provide valuable information about the evolution of the relevant networks.

Received 14 March; accepted 25 October 2011.

1. Liu, A. & Nagel, S. Jamming is not just cool any more. *Nature* **396,** 21–22 (1998).
2. Liu, A. J. & Nagel, S. R. Granular and jammed materials. *Soft Matter* **6,** 2869–2870 (2010).
3. Trappe, V., Prasad, V., Cipelletti, L., Segre, P. N. & Weitz, D. A. Jamming phase diagram for attractive particles. *Nature* **411,** 772–775 (2001).
4. Majmudar, T. S., Sperl, M., Luding, S. & Behringer, R. P. Jamming transition in granular systems. *Phys. Rev. Lett.* **98,** 058001 (2007).
5. Lechenault, F. *et al.* Critical scaling and heterogeneous superdiffusion across the jamming/rigidity transition of a granular glass. *Europhys. Lett.* **83,** 46003 (2008).
6. Candelier, R. & Dauchot, O. Creep motion of an intruder within a granular glass close to jamming. *Phys. Rev. Lett.* **103,** 128001 (2009).
7. O'Hern, C. S., Silbert, L. E., Liu, A. J. & Nagel, S. R. Jamming at zero temperature and zero applied stress: the epitome of disorder. *Phys. Rev. E* **68,** 011306 (2003).
8. Silbert, L. E., Liu, A. J. & Nagel, S. R. Structural signatures of the unjamming transition at zero temperature. *Phys. Rev. E* **73,** 041304 (2006).
9. Silbert, L. E., Liu, A. J. & Nagel, S. R. Vibrations and diverging length scales near the unjamming transition. *Phys. Rev. Lett.* **95,** 098301 (2005).
10. Wyart, M. On the rigidity of amorphous solids. *Ann. Phys. Fr.* **30,** 1–96 (2005).
11. Heussinger, C. & Barrat, J.-L. Jamming transition as probed by quasistatic shear flow. *Phys. Rev. Lett.* **102,** 218303 (2009).
12. Olsson, P. & Teitel, S. Critical scaling of shear viscosity at the jamming transition. *Phys. Rev. Lett.* **99,** 178001 (2007).
13. Olsson, P. & Teitel, S. Glassiness, rigidity and jamming of frictionless soft core disks. *Phys. Rev. E* **83,** 031307 (2011).
14. Makse, H., Johnson, D. L. & Schwartz, L. M. Packing of compressible granular materials. *Phys. Rev. Lett.* **84,** 4160–4163 (2000).
15. Silbert, L. E. Jamming of frictional spheres and random loose packing. *Soft Matter* **6,** 2918–2924 (2010).
16. Otsuki, M. & Hayakawa, H. Critical scaling near jamming transition for frictional granular particles. *Phys. Rev. E* **83,** 051301 (2011).
17. Pastore, M., Ciamarra, M. P. & Coniglio, A. Flow and jam of frictional athermal systems under shear stress. *Phil. Mag.* **91,** 2006–2013 (2011).
18. Nedderman, R. M. *Statics and Kinematics of Granular Materials* (Cambridge Univ. Press, 1992).
19. Hatano, T. Scaling properties of granular rheology near the jamming transition. *J. Phys. Soc. Jpn* **77,** 123002 (2008).
20. Peyneau, P.-E. & Roux, J.-N. Frictionless bead packs have macroscopic friction, but no dilatancy. *Phys. Rev. E* **78,** 011307 (2008).
21. Ciamarra, M. P. Nicodemi, M. & Coniglio, A. Recent results on the jamming phase diagram. *Soft Matter* **6,** 2871–2874 (2010).
22. Zhang, J., Majmudar, T. S., Tordesillas, A. & Behringer, R. P. Statistical properties of a 2D granular material subjected to cyclic shear. *Granul. Matter* **12,** 159–172 (2010).
23. Henkes, S., van Hecke, M. & van Saarloos, W. Critical jamming of frictional grains in the generalized isostaticity picture. *Europhys. Lett.* **90,** 14003 (2010).
24. Radjai, F., Wolf, D. E., Jean, M. & Moreau, J.-J. Bimodal character of stress transmission in granular packings. *Phys. Rev. Lett.* **80,** 61–64 (1998).
25. Walker, D. M. *et al.* Percolating contact subnetworks on the edge of isostaticity. *Granul. Matter* **13,** 233–240 (2011).
26. Göncü, F., Duran, O. & Luding, S. Constitutive relations for the isotropic deformation of frictionless packings of polydisperse spheres. *C.R. Méc.* **338,** 570–586 (2010).
27. Cates, M. E., Wittmer, J. P., Bouchaud, J.-P. & Claudin, P. Jamming, force chains, and fragile matter. *Phys. Rev. Lett.* **81,** 1841–1844 (1998).
28. Goddard, J. D. *Continuum Modeling of Granular Assemblies* 1–24 (Kluwer, 1998).
29. Alonso-Marroquín, F., Luding, S., Herrmann, H. J. & Vardoulakis, I. Role of anisotropy in the elastoplastic response of a polygonal packing. *Phys. Rev. E* **71,** 051304 (2005).
30. Majmudar, T. S. & Behringer, R. P. Contact force measurements and stress-induced anisotropy in granular materials. *Nature* **435,** 1079–1082 (2005).

Supplementary Information is linked to the online version of the paper at www.nature.com/nature.

Acknowledgements D.B. and B.C. acknowledge support from US NSF grant DMR-0905880. R.P.B. and J.Z. acknowledge support from US NSF grants DMR-0906908 and NSF-0835571, and from US ARO grant W911NF-07-1-1031. B.C. and R.P.B. acknowledge the hospitality of the Aspen Center for Physics and discussions with S. Teitel, H. Hayakawa and M. Otsuki. D.B. and B.C. acknowledge discussions with M. Mailman.

Author Contributions All authors contributed in comparably equal ways. Specifically, R.P.B. and J.Z. designed the experimental project, including the force-inverse algorithm, and performed the experiments. B.C. and D.B. performed the theoretical analysis. D.B. and J.Z. carried out the data analysis. All authors contributed equally to writing the manuscript.

Author Information Reprints and permissions information is available at www.nature.com/reprints. The authors declare no competing financial interests. Readers are welcome to comment on the online version of this article at www.nature.com/nature. Correspondence and requests for materials should be addressed to R.P.B. (bob@phy.duke.edu).

LETTER

doi:10.1038/nature10651

Messinian salinity crisis regulated by competing tectonics and erosion at the Gibraltar arc

D. Garcia-Castellanos[1] & A. Villaseñor[1]

The Messinian salinity crisis[1,2] (5.96 to 5.33 million years ago) was caused by reduced water inflow from the Atlantic Ocean to the Mediterranean Sea resulting in widespread salt precipitation and a decrease in Mediterranean sea level of about 1.5 kilometres due to evaporation[3]. The reduced connectivity between the Atlantic and the Mediterranean at the time of the salinity crisis is thought to have resulted from tectonic uplift of the Gibraltar arc seaway and global sea-level changes, both of which control the inflow of water required to compensate for the hydrological deficit of the Mediterranean[1,4]. However, the different timescales on which tectonic uplift and changes in sea level occur are difficult to reconcile with the long duration of the shallow connection between the Mediterranean and the Atlantic[5] needed to explain the large amount of salt precipitated. Here we use numerical modelling to show that seaway erosion caused by the Atlantic inflow could sustain such a shallow connection between the Atlantic and the Mediterranean by counteracting tectonic uplift. The erosion and uplift rates required are consistent with previous mountain erosion studies, with the present altitude of marine sediments in the Gibraltar arc[6,7] and with geodynamic models suggesting a lithospheric slab tear underneath the region[8–10]. The moderate Mediterranean sea-level drawdown during the early stages of the Messinian salinity crisis[3,5] can be explained by an uplift of a few millimetres per year counteracted by similar rates of erosion due to Atlantic inflow. Our findings suggest that the competition between uplift and erosion can result in harmonic coupling between erosion and the Mediterranean sea level, providing an alternative mechanism for the cyclicity observed in early salt precipitation deposits and calling into question previous ideas regarding the timing of the events that occurred during the Messinian salinity crisis[1].

It is broadly accepted that the period of widespread salt precipitation in the Mediterranean known as the Messinian salinity crisis (MSC) spanned from 5.96 to 5.33 Myr ago[1,2]. Although there is debate on how the events recorded in strata correlate between the marginal shallow basins and the deeper parts of the Mediterranean, biostratigraphic analyses[2,11] agree on the occurrence of two stages in both environments: stage 1 encompasses the early salt precipitation (forming the lower evaporites), producing massive gypsum deposits at the basin margins and involving minor sea-level drawdown; stage 2 includes the formation of the upper evaporites and Lago Mare deposits, and a kilometre-scale Mediterranean sea-level drop evidenced by the widespread presence of Messinian erosion surfaces[11]. During stage 2, the largest rivers flowing to the nearly desiccated Mediterranean excavated canyons about 2,500 m deep in the Nile delta[12] and 1,000 m deep at the mouth of the Rhone[13]. Strontium isotope data[14] indicate that stage 1 took place in a restricted Mediterranean, that is, one with reduced connectivity with the Atlantic, whereas stage 2 occurred in predominantly continental waters with little or no connection to the ocean. The durations of these two phases have been estimated at 360 and 270 kyr, respectively, on the basis of the assumption that the 14 to 17 cycles observed in the gypsum of stage 1 are due to Milankovitch precessional cycles of insolation.

Three mechanisms have been proposed as responsible for the closure of the seaways. A global sea-level drop can be discarded because the open-ocean benthic $^{18}O/^{16}O$ ratio, a proxy for glacio-eustasy, does not match the onset of evaporite deposition[1,15]. Similarly, no evidence has yet linked local tectonic fault deformation[16] along the corridors to the onset of the MSC, a period when tectonic activity was relatively low both in the Betic[17] and the Rifean corridors[18]. Accordingly, a long-wavelength, mantle-sourced tectonic uplift of the Betic and/or Rif mountains[6,18–21] is seen as the most plausible cause for the isolation of the Mediterranean[8], and is supported by the presence of uplifted, pre-Messinian marine sediments near the seaways in the Rif[6,18] and the Betics[7,19]. However, the physical feasibility of this mechanism has not yet been quantitatively tested, because former models of the MSC[4,21,22] predefined the connectivity conditions at the seaway. Because sea level varies on much shorter timescales than tectonic uplift, previous attempts at linking both processes[8] predict a succession of short desiccations and floods during both stages of the MSC. This may explain the large amount of salt precipitated during the MSC[3,22–24], which requires the evaporation of about 50 times the volume of the Mediterranean, but is in conflict with the notion of a two-stage MSC. Furthermore, the erosion produced by each flood would deepen and widen the inflow channel[25,26], implying a succession of multiple tectonic uplift and subsidence episodes[20,26] for which no geodynamic mechanism is known.

The alternative to multiple flooding is a long period of continuous inflow and limited outflow caused by a shallow connection between the Mediterranean and the Atlantic. This does not imply a large sea-level drawdown in the Mediterranean during stage 1, and allows for the required amount of salt to be precipitated in a few hundred thousand years. However, to avoid both interoceanic mixing and complete disconnection[5] this mechanism would require a fortuitous, *ad hoc* evolution of both sea level and uplift closely following each other with a deviation of only a few tens of metres[4]. Here we postulate that such a long-lasting, shallow connection can be naturally sustained by a competition between the tectonic obstruction of the seaway and its erosional deepening by water inflow, and that this competition was responsible for the salt precipitation during the first stage of the MSC.

To test this hypothesis, we combine a model of rock erosion with classical hydrodynamic equations and a climate-based water budget (Fig. 1 and Supplementary Methods) to calculate the timing of water and salt flow between the Atlantic and the Mediterranean and the erosion produced along the connecting corridor. The evolution of the reference model in Fig. 2 starts with a 60-m-deep seaway that is uplifted at a constant rate. As the seaway becomes shallower, less water is able to cross the strait, and the Mediterranean sea level decreases evaporatively. When the seaway becomes shallower than a few tens of metres, the Mediterranean sea level decreases at rates of centimetres per year. As this sea-level difference across the Gibraltar arc increases, so does the shear stress of the inflow and the associated seaway erosion rate, which eventually compensates the imposed uplift rate. This keeps the inlet neither open enough to allow double circulation nor completely closed. If the uplift rate exceeds a critical value, U_c, then it overcomes erosion and the threshold rises above global sea level, cancelling the

[1]Instituto de Ciencias de la Tierra Jaume Almera, CSIC, Solé i Sabarís s/n, 08028 Barcelona, Spain.

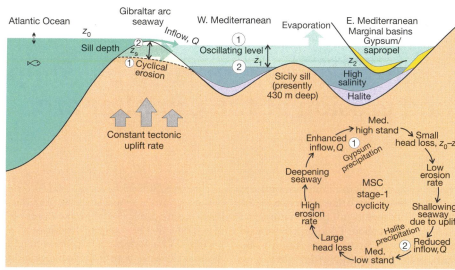

Figure 1 | Competition between uplift and erosion along the last corridor connecting the Atlantic and the Mediterranean during stage 1 of the MSC. Erosion at the sill is controlled by rock erodibility and water inflow, which is calculated as a function of sill depth, $z_0 - z_s$, and head loss, $z_0 - z_1$. Oscillations in water level and salinity can result from feedback (harmonic coupling) between tectonic uplift, water flow, evaporation and sill erosion. Sketch not drawn to scale.

connection permanently. The reference model in Fig. 2 corresponds to the critical uplift rate (4.9 mm yr^{-1}) for the reference erodibility and climatic parameters. We searched systematically for the critical uplift rates for a range of erodibility values consistent with previous river incision studies (Fig. 3) and found that values greater than 1 mm yr^{-1} are needed. These values are close to uplift rates expected from mantle geodynamic models simulating slab detachment[9,10]. Critical uplift rates are also dependent on the hydrological deficit. Changing the climatic

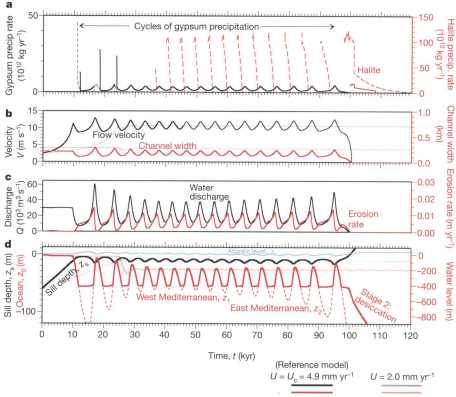

Figure 2 | Calculated evolution of the reference model resulting from competition between seaway uplift and erosion. The uplift rate is set to $U = 4.9$ mm yr^{-1}, close to the critical value causing complete disconnection, and undergoes a minor acceleration to force the formation of exactly 17 precipitation cycles before closure at $t = 100$ kyr. The model starts with a 60-m-deep seaway at $t = 0$. At $t = 11$ and $t = 12$ kyr, the saturation of gypsum is reached in the eastern and western Mediterranean, respectively. **a**, Halite and gypsum precipitation rates; **b**, flow velocity and width of the seaway; **c**, inflow water discharge and erosion at the seaway; **d**, seaway depth (black), level of the Atlantic (blue), and level of the Mediterranean (red). At $t = 10$ kyr, the seaway becomes shallow enough to reduce water discharge and velocity, allowing a Mediterranean evaporative drawdown that leads to higher slope and erosion along the seaway. The subsequent oscillations in sea level and salt precipitation are the result of dynamic harmonic coupling between the drawdown and the refill triggered when erosion deepens the seaway. The amplitude of sea-level oscillations in this example is an upper limit. For comparison, the results obtained for an uplift rate of 2.0 mm yr^{-1} are also displayed, by lighter lines, in **b** and **d**. Dashed lines in **a** and **d** indicate values for the eastern Mediterranean.

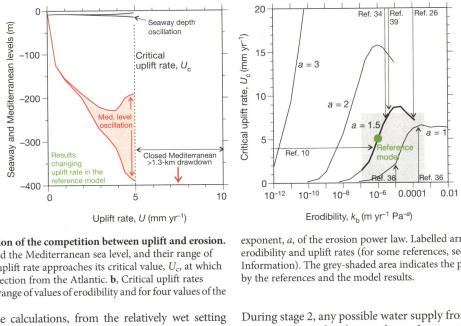

Figure 3 | Parameterization of the competition between uplift and erosion. **a**, Depth of the seaway and the Mediterranean sea level, and their range of oscillation as the seaway uplift rate approaches its critical value, U_c, at which there is complete disconnection from the Atlantic. **b**, Critical uplift rates required for closure, for a range of values of erodibility and for four values of the exponent, a, of the erosion power law. Labelled arrows indicate references for erodibility and uplift rates (for some references, see Supplementary Information). The grey-shaded area indicates the parameter ranges supported by the references and the model results.

conditions used for the calculations, from the relatively wet setting deduced for the MSC[27] to the present dryer conditions, implies an increase of the critical uplift rate by a factor of almost three. Thus, a relatively humid climate during the early Messinian may have facilitated the isolation and eventual evaporation of the Mediterranean by decreasing the amount of water crossing and eroding the seaway.

We found that uplift rates only slightly lower than the critical value produce a cyclic change in the sea level of the Mediterranean, even if uplift occurs at a constant rate. The dynamic equilibrium between uplift and erosion attained at low uplift rates develops into an apparent sea-level harmonic oscillation for values comparable to U_c. This happens as follows (Fig. 1). Inflow reduction by tectonic uplift leads to a delayed evaporative drawdown in the Mediterranean, with the time lag depending on the sea's hydrological deficit. The drawdown induces greater flow energy in the corridor and larger incision rates that deepen the seaway, allowing more water inflow and the recovery of the normal Mediterranean sea level. This reduction in sea-level difference leads to slower inflow and erosion that can be again overcome by tectonic uplift. This cyclic process produces salt precipitation and sea-level cycles of higher intensity as the uplift rate gets closer to the critical value (Fig. 3a). The period of these cycles is dependent on uplift rate and on the hydrological deficit, and using climatic parameters closer to the present drier climate scenario produces a reduction in the oscillation period by a factor of two relative to the reference model. This suggests that the cyclicity of the lower evaporites (stage 1) might be a result of the competition between tectonic uplift and water flow erosion, rather than of Milankovitch insolation changes as previously proposed[1]. In that case, the duration of stage 1 may have been half of previous estimates[1] or less, because the cycle periods that we obtain (<10 kyr) are less than half of the precession cycle (21 kyr). The uncertainty in erodibility and uplift data does not allow us definitively to state this as an origin for the cycles on the basis of only modelling techniques, and global sea-level changes might also have modulated shorter-term sediment sequences[4]. However, within the approaches taken here the coupling between uplift and erosion is dominant as long as global oscillations are smaller than about 10 m (Supplementary Fig. 3).

Regardless of the origin of the cycles, the results imply that stage 1 was sustained by a competition between uplift and erosion at the seaway, allowing for limited but uninterrupted Atlantic inflow. This is consistent with the observation that the Mediterranean underwent relatively small sea-level drawdown, of a few hundred meters or less[3], during stage 1, allowing the formation of coastal erosional surfaces[28]. During stage 2, any possible water supply from the Atlantic could not last more than a few thousand years because the large head loss across the Betic–Rifean orogen would imply high incision rates and lead irreversibly to a complete refill[29], leading back to the initial pre-MSC situation. Therefore, the simplest picture consistent with the physics of our model includes, first, a single stage of sustained inflow of Atlantic waters and limited or no outflow (stage 1), then a single stage of complete disconnection and kilometric drawdown with sea level controlled mainly by changes in the Mediterranean hydrological budget (stage 2), and then a single, final flood (Supplementary Fig. 1).

Evidence for the tectonic uplift required by the model is found near the last corridors connecting both oceanic domains. In the Betic internal basins, the pre-Messinian marine–continental transition is at present at altitudes close to 1,000 m (Fig. 4), with most intramountain basins emerging between 7.6 and 5.3 Myr ago[7]. In the Rifean corridor, palaeodepth reconstructions indicate a rapid shallowing starting 7.2 Myr ago at rates as high as 3.6 mm yr^{-1}, with the transition from marine to continental deposits occurring by 6.0 Myr ago[18] and lying at present at an altitude higher than 600 m. This is consistent with a long-wavelength uplift of at least that amount across the Rif–Atlas corridor[6,18]. Either of these uplifts can explain the closure of the Mediterranean according to the model presented here, which requires uplift of more than 1 mm yr^{-1} (Fig. 3b) over a period of at least 80 kyr.

Lithospheric slab detachment and roll back has previously been suggested as the possible cause for uplift that initiated the MSC[9]. Our model allows to bridge the gap quantitatively between such geodynamic processes and the MSC events. Slab detachment models predict uplifts of kilometre scale, with uplift rates ranging from 0.07 mm yr^{-1} (ref. 29) to 4 mm yr^{-1} (ref. 10). The higher values within this range are consistent with the rates needed to close the seaway in our model. Moreover, tear propagation of a hanging lithospheric slab underneath the Gibraltar arc[8] provides a mechanism of westwards propagation of both uplift and subsidence (Fig. 4). Recent seismic tomography obtained from the inversion of P-wave arrival times[30] supports the presence of such lithospheric tearing (Fig. 4 and Supplementary Information). The location of this tear point between the last pre-Messinian corridor and the strait of Gibraltar (Fig. 4) could explain the uplift and closure of the Betic seaways[9], and a later subsidence in Gibraltar, leading to the Zanclean flood[26]. But other modes of tectonic uplift cannot be completely ruled out as responsible for the tectonic uplift cannot be completely ruled out as responsible for the closure of the Mediterranean: the ongoing tectonic convergence between Europe and Africa (about 4 mm yr^{-1} since the Tertiary

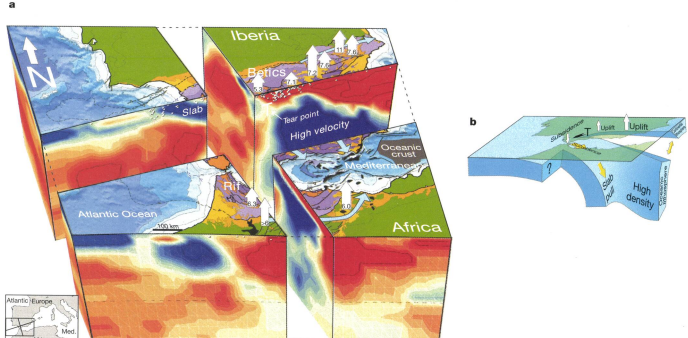

Figure 4 | Geodynamic interpretation of the results invokes the lateral migration of a tearing[6] of the lithospheric slab originally attached to the south Iberian margin. a, Geological map of the Gibraltar arc and subjacent mantle structure derived from seismic tomography. White arrows indicate uplift of intramountain basins within the Betics[7,8] and the Rif[9,10], and ages of their transition from marine to continental conditions[7]. White dots locate earthquake hypocentres used for the tomographic inversion and blue arrows locate proposed connecting corridors. **b**, Interpretative sketch: T marks the proposed lithosphere tearing point, separating areas where the sinking lithospheric slab (blue) is detached from Iberia, inducing surface uplift (to the east), from areas where it remains attached to the crust (to the west).

period) could also have contributed to uplift rates through faulting or doming[7].

The MSC has implications beyond its effects on the Mediterranean landscape. During stage 1, the Mediterranean basin sequestered about 10% of the salt of Earth's oceans, raising its freezing point by about 0.2 °C. During desiccation (stage 2), the evaporated Mediterranean waters were redistributed through the atmosphere to the world oceans, raising global sea level by about 10 m, as recorded in reef stratigraphy in the Pacific Ocean[31]. However, the climatic impact of the MSC remains elusive, as model results are ambiguous[27,32] and not well reflected in palynological data[33]. Final evidence on the timing and magnitude of these events may come in future from improved global climate models that could in turn benefit from the uniquely extreme conditions imposed by the Messinian natural laboratory.

METHODS SUMMARY

We calculate sea-level changes in the Mediterranean by developing a one-dimensional model of the depth of the seaway that limits the water inflow from the Atlantic. The feedback between water-flow-controlled incision and seaway-depth-controlled water flow is implemented by developing a formulation based on previous river incision studies and on standard hydrodynamic formulae. The model is based on the assumption that the depth of the seaway, z_s, depends on uplift and erosion, the last being a power-law function of basal shear stress. The level of the Mediterranean is a function of precipitation, evaporation, river supply and Atlantic inflow along the seaway. The evaporation surface of the Mediterranean is calculated as a function of its level, using a reconstructed hypsometry[21]. The interplay between tectonic uplift, incision and the driving role of hydraulic gradient across the seaway (resulting from the competition between inflow through Gibraltar and the water deficit in the Mediterranean) is calculated using an explicit finite-difference, time-iterative technique. At each time step, the water discharge, Q, is calculated on the basis of the depth of the sill and the head loss, and then seaway erosion is calculated from the basal shear stress of the flow. See Methods for further details.

Full Methods and any associated references are available in the online version of the paper at www.nature.com/nature.

Received 22 February; accepted 6 October 2011.

1. Krijgsman, W., Hilgen, F. J., Raffi, I., Sierro, F. J. & Wilson, D. S. Chronology, causes and progression of the Messinian salinity crisis. *Nature* **400,** 652–655 (1999).
2. Briand, F. (ed.) *The Messinian Salinity Crisis from Mega-Deposits to Microbiology – A Consensus Report* (CIESM Workshop Monographs 30, CIESM, 2008).
3. Hsü, K. J., Ryan, W. B. F. & Cita, M. B. Late Miocene desiccation of the Mediterranean. *Nature* **242,** 240–244 (1973).
4. Rohling, E. J., Schiebel, R. & Siddall, M. Controls on Messinian Lower Evaporite cycles in the Mediterranean. *Earth Planet. Sci. Lett.* **275,** 165–171 (2008).
5. Gargani, J. & Rigollet, C. Mediterranean sea level variations during the Messinian salinity crisis. *Geophys. Res. Lett.* **34,** L10405 (2007).
6. Babault, J., Teixell, A., Arboleya, M. L. & Charroud, M. A late Cenozoic age for long-wavelength surface uplift of the Atlas Mountains of Morocco. *Terra Nova* **20,** 102–107 (2008).
7. Iribarren, L., Vergés, J. & Fernández, M. Sediment supply from the Betic-Rif orogen to basins through Neogene. *Tectonophysics* **475,** 68–84 (2009).
8. Spakman, W. & Wortel, M. J. R. in *The TRANSMED Atlas: The Mediterranean Region from Crust to Mantle* (eds Cavazza, W. *et al.*) 31–52 (Springer, 2004).
9. Duggen, S., Hoernle, K., Van den Bogaard, P., Rüpke, L. & Morgan, J. P. Deep roots of the Messinian salinity crisis. *Nature* **422,** 602–606 (2003).
10. Andrews, E. R. & Billen, M. I. Rheologic controls on the dynamics of slab detachment. *Tectonophysics* **464,** 60–69 (2009).
11. Clauzon, G., Suc, J.-P., Gautier, F., Berger, A. & Loutre, M.-F. Alternate interpretation of the Messinian salinity crisis: controversy resolved? *Geology* **24,** 363–366 (1996).
12. Barber, P. M. Messinian subaerial erosion of the proto-Nile Delta. *Mar. Geol.* **44,** 253–272 (1981).
13. Clauzon, G. The Messinian Var canyon (Provence, southern France): paleogeographic implications. *Mar. Geol.* **27,** 231–246 (1978).

14. Flecker, R. & Ellam, R. M. Identifying late Miocene episodes of connection and isolation in the Mediterranean-Paratethyan realm using Sr isotopes. *Sedim. Geol.* **188–189,** 189–203 (2006).
15. Hilgen, F., Kuiper, K., Krijgsman, W., Snel, E. & van der Laan, E. Astronomical tuning as the basis for high resolution chronostratigraphy: the intricate history of the Messinian Salinity Crisis. *Stratigraphy* **4,** 231–238 (2007).
16. Weijermars, R. Neogene tectonics in the Western Mediterranean may have caused the Messinian salinity crisis and an associated glacial event. *Tectonophysics* **148,** 211–219 (1988).
17. Comas, M. C., Platt, J. P., Soto, J. I. & Watts, A. B. The origin and tectonic history of the Alboran Basin. *Proc. ODP Sci. Res.* **161,** 555–580 (1999).
18. Krijgsman, W. Late Neogene evolution of the Taza-Guercif Basin (Rifean Corridor; Morocco) and implications for the Messinian salinity crisis. *Mar. Geol.* **153,** 147–160 (1999).
19. Garcés, M., Krijgsman, W. & Agustí, J. Chronology of the late Turolian deposits of the Fortuna basin (SE Spain): implications for the Messinian evolution of the eastern Betics. *Earth Planet. Sci. Lett.* **163,** 69–81 (1998).
20. Govers, R. Choking the Mediterranean to dehydration: the Messinian salinity crisis. *Geology* **37,** 167–170 (2009).
21. Meijer, P., Th. & Krijgsman, W. A quantitative analysis of the desiccation and re-filling of the Mediterranean during the Messinian Salinity Crisis. *Earth Planet. Sci. Lett.* **240,** 510–520 (2005).
22. Blanc, P.-L. Improved modelling of the Messinian Salinity Crisis and conceptual implications. *Palaeogeogr. Palaeoclimatol. Palaeoecol.* **238,** 349–372 (2006).
23. Rouchy, J.-M. & Saint Martin, J. P. Late Miocene events in the Mediterranean as recorded by carbonate-evaporite relations. *Geology* **20,** 629–632 (1992).
24. Ryan, W. B. F. Decoding the Mediterranean salinity crisis. *Sedimentology* **56,** 95–136 (2009).
25. Blanc, P.-L. The opening of the Plio-Quaternary Gibraltar Strait: assessing the size of a cataclysm. *Geodin. Acta* **15,** 303–317 (2002).
26. Garcia-Castellanos, D. *et al.* Catastrophic flood of the Mediterranean after the Messinian Crisis. *Nature* **462,** 778–781 (2009).
27. Gladstone, R., Flecker, R., Valdes, P., Lunt, D. & Markwick, P. The Mediterranean hydrologic budget from a Late Miocene global climate simulation. *Palaeogeogr. Palaeoclimatol. Palaeoecol.* **251,** 254–267 (2007).
28. Just, J., Hübscher, C., Betzler, C., Lüdmann, T. & Reicherter, K. Erosion of continental margins in the Western Mediterranean due to sea-level stagnancy during the Messinian Salinity Crisis. *Geo-Mar. Lett.* **31,** 51–64 (2011).
29. Gerya, T. V., Yuen, D. A. & Maresch, W. V. Thermomechanical modelling of slab detachment. *Earth Planet. Sci. Lett.* **226,** 101–116 (2004).
30. Villaseñor, A., Spakman, W. & Engdahl, E. R. Influence of regional travel times in global tomographic models. *Geophys. Res. Abstr.* **5,** abstr. EAE03-A-08614 (2003).
31. Aharon, P., Goldstein, S. L., Wheeler, C. W. & Jacobson, G. Sea-level events in the South Pacific linked with the Messinian salinity crisis. *Geology* **21,** 771–775 (1993).
32. Schneck, R., Micheels, A. & Mosbrugger, V. Climate modelling sensitivity experiments for the Messinian Salinity Crisis. *Palaeogeogr. Palaeoclimatol. Palaeoecol.* **286,** 149–163 (2010).
33. Fauquette, S. *et al.* How much did climate force the Messinian salinity crisis? Quantified climatic conditions from pollen records in the Mediterranean region. *Palaeogeogr. Palaeoclimatol. Palaeoecol.* **238,** 281–301 (2006).

Supplementary Information is linked to the online version of the paper at www.nature.com/nature.

Acknowledgements We thank P. Meijer, S. Giralt, L. Matenco and C. Ayora for comments and criticisms on earlier versions of the manuscript. This work was funded by the Spanish government through the projects ATLA (CGL2009-09662), TopoAtlas (CGL2006-05493), TopoMed (CGL2008-03474-E/BTE) and Topolberia (CSD2006-00041).

Author Contributions D.G.-C. planned the study, performed the modelling and wrote the paper; A.V. processed and interpreted the seismic data and tomography; and both authors interpreted and discussed the results.

Author Information The source code developed for the calculations can be downloaded from https://sites.google.com/site/danigcc/research-interests/messinian. Reprints and permissions information is available at www.nature.com/reprints. The authors declare no competing financial interests. Readers are welcome to comment on the online version of this article at www.nature.com/nature. Correspondence and requests for materials should be addressed to D.G.-C. (danielgc@ictja.csic.es).

LETTER

doi:10.1038/nature10526

Resolving the evolutionary relationships of molluscs with phylogenomic tools

Stephen A. Smith[1,2], Nerida G. Wilson[3,4], Freya E. Goetz[1], Caitlin Feehery[1,4], Sónia C. S. Andrade[5], Greg W. Rouse[4], Gonzalo Giribet[5] & Casey W. Dunn[1]

Molluscs (snails, octopuses, clams and their relatives) have a great disparity of body plans and, among the animals, only arthropods surpass them in species number. This diversity has made Mollusca one of the best-studied groups of animals, yet their evolutionary relationships remain poorly resolved[1]. Open questions have important implications for the origin of Mollusca and for morphological evolution within the group. These questions include whether the shell-less, vermiform aplacophoran molluscs diverged before the origin of the shelled molluscs (Conchifera)[2–4] or lost their shells secondarily. Monoplacophorans were not included in molecular studies until recently[5,6], when it was proposed that they constitute a clade named Serialia together with Polyplacophora (chitons), reflecting the serial repetition of body organs in both groups[5]. Attempts to understand the early evolution of molluscs become even more complex when considering the large diversity of Cambrian fossils. These can have multiple dorsal shell plates and sclerites[7–10] or can be shell-less but with a typical molluscan radula and serially repeated gills[11]. To better resolve the relationships among molluscs, we generated transcriptome data for 15 species that, in combination with existing data, represent for the first time all major molluscan groups. We analysed multiple data sets containing up to 216,402 sites and 1,185 gene regions using multiple models and methods. Our results support the clade Aculifera, containing the three molluscan groups with spicules but without true shells, and they support the monophyly of Conchifera. Monoplacophora is not the sister group to other Conchifera but to Cephalopoda. Strong support is found for a clade that comprises Scaphopoda (tusk shells), Gastropoda and Bivalvia, with most analyses placing Scaphopoda and Gastropoda as sister groups. This well-resolved tree will constitute a framework for further studies of molluscs evolution, development and anatomy.

Since the first animal phylogenies based on molecular data, many researchers have struggled to resolve mollusc phylogenies even as taxon sampling improved[5,6,12] (see Fig. 1 for some hypotheses that have been proposed). Little support, if any, was found for the monophyly of Mollusca or most of its larger subclades. Better results were achieved for some internal relationships of these groups, including Polyplacophora, Bivalvia, Cephalopoda, Scaphopoda and Gastropoda, although often with difficulties recovering monophyly of the two largest clades, the gastropods and bivalves[5,13,14]. Unfortunately, fundamental questions in mollusc evolution remain largely unanswered by the molecular and morphological data. These questions include whether the aplacophoran molluscs are monophyletic[2] or paraphyletic[3,4]. There has also been conflicting evidence for the placement of Polyplacophora, which has been placed with the aplacophorans (forming the clade Aculifera), as the sister group to the shelled molluscs (forming the clade Testaria) or as the sister group to Monoplacophora (forming the clade Serialia). In addition, many hypotheses have been proposed for the interrelationships of the conchiferan groups. The extensive fossil record of Mollusca (which dates back to the Cambrian), combined with the numerous Palaeozoic forms that are considered stem-group molluscs and the lack of resolution in targeted-gene approaches to molluscan phylogenetics, pointed towards a possible rapid radiation with little phylogenetic signal left in the genomes of molluscs. However, the same has been argued for the radiation of Metazoa in the Cambrian or earlier[15], but large increases in gene representation using phylogenomic analyses have clearly ameliorated this problem and identified relationships that seemed impossible to resolve with target-gene

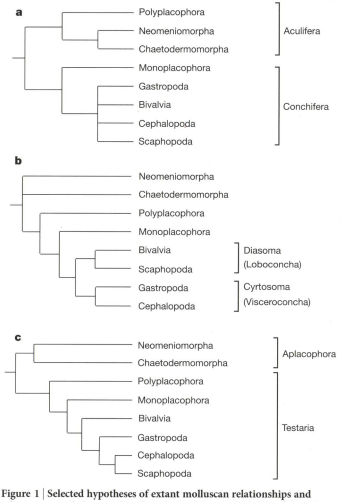

Figure 1 | Selected hypotheses of extant molluscan relationships and relevant taxa. Phylograms based on the hypotheses of Scheltema[1] (**a**), Salvini-Plawen and Steiner[2] (**b**) and Waller[28] (**c**). Most controversy centres on the monophyly of Aplacophora, the relationships within Conchifera and the placement of Polyplacophora (for example, in Aculifera versus in Testaria).

[1]Department of Ecology and Evolutionary Biology, Brown University, Providence, Rhode Island 02912, USA. [2]Heidelberg Institute for Theoretical Studies, Heidelberg D-69118, Germany. [3]The Australian Museum, Sydney, New South Wales 2010, Australia. [4]Scripps Institution of Oceanography, University of California San Diego, La Jolla, California 92093, USA. [5]Museum of Comparative Zoology, Department of Organismic and Evolutionary Biology, Harvard University, Cambridge, Massachusetts 02138, USA.

approaches[16,17]. We applied the same principles to Mollusca, one of the most challenging problems to solve in animal phylogenetics.

Only phylogenomic analyses have been able to recover molluscan monophyly with high support[17]; however, few molluscs were included in earlier analyses, and not all of the major subclades were represented. Therefore, little could be concluded about the interrelationships of the major molluscan groups. Morphology-based cladistic analyses have often relied on 'idealized' composite ground patterns to represent entire clades[2-4], a practice that has now been largely replaced with the use of exemplar species[18] and more detailed character descriptions. But an analysis of molluscan morphological features coding real exemplars has yet to be published, and the exemplar approach is much more amenable to molecular data.

Analyses of our broadly sampled, new phylogenomic data (see Methods, Supplementary Table 1 and Supplementary Fig. 1) result in a well-resolved and highly supported phylogeny of Mollusca (Fig. 2), in contrast to all previous molecular attempts[5,6,12]. These results are consistent across analytical methods, phylogenetic inference programs, matrices that vary in occupancy and the number of genes considered (Fig. 2 and Supplementary Figs 2–6 and 9), and the inclusion of different outgroup taxa (Supplementary Fig. 7).

Our results (Fig. 2) show a sister group relationship between the aculiferan molluscs and the conchiferan groups. Aculifera[3,19] includes Polyplacophora as the sister group to the two aplacophoran groups (Neomeniomorpha and Chaetodermomorpha). This topology lends support to the idea that the vermiform Aplacophora are not plesiomorphic but are derived from plated Palaeozoic molluscs such as *Acaenoplax*[10]. The aculiferans are characterized by spicules and dorsal shell plates. Chitons have eight dorsal shell plates, but their larva has an anlagen with seven rows of dorsal papillae, as observed in the serially arranged spiculoblasts of a chaetodermomorph larva[20], a character that may constitute a synapomorphy of the clade.

Conchifera is supported as a clade, suggesting that true shells may have originated only once, perhaps by the concentration of a diffuse shell gland into a single zone of the mantle (two zones in bivalves), at least as defined by the role of *engrailed* during organogenesis[21]. The support here for Conchifera rejects the recent Serialia hypothesis[5,6]. Comparing the site likelihoods in analyses in which Serialia is constrained with those in which it is not constrained reveals that there are many more characters that are incongruent with Serialia than support Serialia (Supplementary Fig. 8). Monoplacophora is not, however, the sister group of all other Conchifera, as has been suggested by most authors, and is instead the sister group to Cephalopoda, as has been proposed based on some palaeontological data[22]. Many palaeontologists have accepted the monoplacophoran 'ancestry' of Cephalopoda[23,24], although this relationship has been rejected by neontologists, who

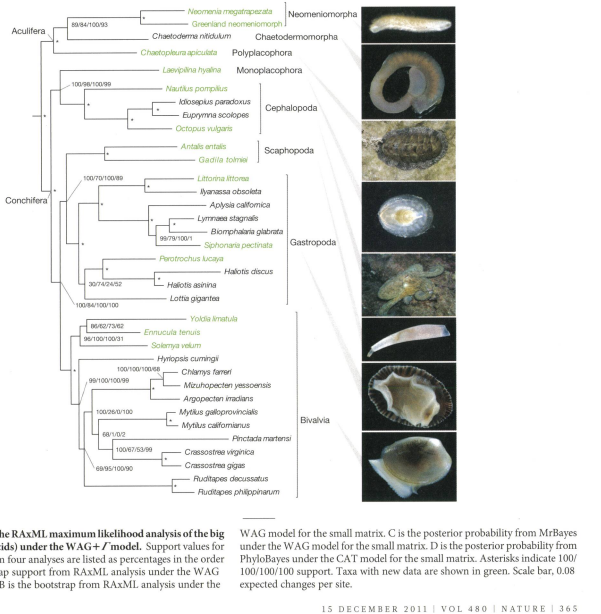

Figure 2 | Phylogram of the RAxML maximum likelihood analysis of the big matrix (216,402 amino acids) under the WAG+*Γ* model. Support values for the topology obtained from four analyses are listed as percentages in the order A/B/C/D. A is the bootstrap support from RAxML analysis under the WAG model for the big matrix. B is the bootstrap from RAxML analysis under the WAG model for the small matrix. C is the posterior probability from MrBayes under the WAG model for the small matrix. D is the posterior probability from PhyloBayes under the CAT model for the small matrix. Asterisks indicate 100/100/100/100 support. Taxa with new data are shown in green. Scale bar, 0.08 expected changes per site.

consider that cephalopods and gastropods share important morphological features such as the presence of cephalic eyes, the isolation of the head from the visceral mass, the terminal position of the mantle cavity and the occurrence of muscle antagonistic systems[2,23]. The presence of multiseptate shells in fossil Hypseloconidae monoplacophorans, a character that is found in *Nautilus* and fossil cephalopods, has been interpreted as supporting this relationship between Cephalopoda and Monoplacophora[24]. The presence of two pairs of gills, kidneys and atria in the chambered *Nautilus* has been interpreted as an indication that secondary simplification took place during the early evolution of cephalopods from an ancestor with serially repeated structures[23]. This interpretation and the present trees suggest that the most recent common ancestor of Cephalopoda and Monoplacophora had some serially repeated structures.

The internal resolution of Cephalopoda is in agreement with all of the current hypotheses, with the chambered *Nautilus* forming the sister group of Coleoidea, and also identifies the monophyly of Decapoda[25,26]. Scaphopoda, Gastropoda and Bivalvia form a clade with thick multilayered shells, but this clade has received little attention in the literature[25]. Most morphological hypotheses place scaphopods as the sister group to bivalves in a clade named Diasoma[2,27] and, recently, molecular and developmental data have favoured a cephalopod–scaphopod relationship. Although there is strong support for the placement of Scaphopoda as the sister group to Gastropoda in maximum likelihood analyses of the big matrix (Fig. 2 and Supplementary Figs 2 and 4), maximum likelihood analyses of the small matrix recover this same relationship but with less support (Fig. 2 and Supplementary Figs 3 and 5). Bayesian analyses using the site-heterogeneous CAT model of protein evolution also place Scaphopoda as the sister group to Gastropoda, with a posterior probability of 89% (Supplementary Fig. 9).

Within Bivalvia, maximum likelihood analyses and Bayesian analyses under the Whelan and Goldman (WAG) model support the monophyly of Protobranchia, which includes bivalves with plesiomorphic ctenidia—gills comparable to those of many other molluscs. This contradicts some earlier bivalve phylogenies, based on fewer data, that proposed paraphyly of protobranchs[14] but supports the traditional morphological views[2,28]. Bayesian analyses with the CAT model are consistent with Protobranchia but do not provide strong support for it. The hypertrophied bivalve gill, which is responsible for filter feeding, had a single origin, and organisms with this type of gill constitute the well-recognized clade Autolamellibranchiata. Palaeoheterodonta (the group that includes freshwater pearl mussels) is the sister group to all other autolamellibranchiates, which can be divided into heterodonts and pteriomorphians. This hypothesis is similar to that proposed by some palaeontologists, although additional taxa, especially *Neotrigonia*, Anomalodesmata and Archiheterodonta, must be included before concluding more about the internal autolamellibranchiate relationships.

Likewise, the internal relationships of Gastropoda, although still limited in their taxonomic representation (the group includes nearly 100,000 living species), support some of the major divisions that are currently accepted[29]. The patellogastropod *Lottia* is either the sister group to Vetigastropoda (as in Thiele's Archaeogastropoda hypothesis) or the sister group to all other gastropods[29], depending on the data set that is analysed. The former alternative has been recovered in recent molecular analyses of gastropods[30]. The two representatives of Caenogastropoda form a sister clade to the representatives of Heterobranchia, including opisthobranchs and pulmonates, as suggested in all of the modern analyses of gastropod relationships[13,29].

For the first time, our data and analyses resolve the broad-scale relationships within Mollusca with strong support. This allows us to gain an understanding not only of the relationships of modern molluscs but also of the numerous Palaeozoic forms of molluscs. It also allows us to investigate several key characters that define the group. Molluscs are related to other animals with spiral development and a trochophore larva and have now been shown to share a close ancestor with annelids and brachiopods[16], both of which use chaetoblasts to produce chaetae. Spicules and chaetae may share a similar developmental mechanism[17]. Likewise, the appearance of dorsal plates or shells in addition to sclerites is now well documented in halwaxiids, *Acaenoplax* and Polyplacophora. These features are generated by multiple rows of secretory papillae in chiton and aplacophoran larvae. They may be plesiomorphic among molluscs, especially if halwaxiids are interpreted as stem-group molluscs, but they could also be apomorphic for Aculifera. The condensation of such papillae into a single shell gland[21] could be responsible for the origin of the conchiferan shell, arguably the single event that led to the extraordinary success of molluscs, first in the Cambrian oceans and later in many limnic and terrestrial environments. In addition to the presence of shell glands that can deposit calcium carbonate, the primitive mollusc may have had a rasping radula and serially repeated ctenidia along the mantle cavity, because both characters appear in the two lineages of extant molluscs, Aculifera and Conchifera, as well as in several extinct Palaeozoic stem molluscs. Like the arthropods, with their hardened exoskeletons, molluscs are true conquerors of our land and waters.

METHODS SUMMARY

New transcriptome data were collected for 14 mollusc species that had been selected to optimize taxonomic representation (Supplementary Table 1). Collecting efforts included an oceanographic campaign to collect members of the key taxon Monoplacophora. Using several protocols, messenger RNA was extracted, and cDNA samples were sequenced on a 454 Genome Sequencer FLX Titanium (Roche) or a Genome Analyzer IIx (Illumina). After assembly and translation, the sequences from all taxa were compared to each other with BLASTP. These pairwise comparisons were used to cluster genes into homologues using the algorithm MCL. The phylogenetic analyses divided sets of homologues into orthologues, which were aligned, trimmed and concatenated into two supermatrices that differed in the number of genes and the average fraction of genes available for each species. The 'small' matrix consists of 301 genes that are present in at least 20 taxa. This matrix has 50% gene occupancy (that is, sequence data were available for an average of 50% of the genes across the taxa), 27% character occupancy (that is, 27% of the matrix consists of unambiguous amino acid data, with the remainder being missing data or alignment gaps) and is 50,930 sites in length. The 'big' matrix consists of 1,185 genes that are present in at least 15 taxa. This matrix has 40% gene occupancy, 21% character occupancy and is 216,402 sites long. Both matrices contain data for all of the 46 species that were included in the study. The matrices were analysed with the programs RAxML, MrBayes and PhyloBayes to infer relationships.

Full Methods and any associated references are available in the online version of the paper at www.nature.com/nature.

Received 7 April; accepted 31 August 2011.
Published online 26 October 2011.

1. Ponder, W. F. & Lindberg, D. R. (eds) *Phylogeny and Evolution of the Mollusca* (Univ. California Press, 2008).
2. Salvini-Plawen, L. V. & Steiner, G. in *Origin and Evolutionary Radiation of the Mollusca* (ed. Taylor, J. D.) 29–51 (Oxford Univ. Press, 1996).
3. Scheltema, A. H. in *Origin and Evolutionary Radiation of the Mollusca* (ed. Taylor, J. D.) 53–58 (Oxford Univ. Press, 1996).
4. Haszprunar, G. Is the Aplacophora monophyletic? A cladistic point of view. *Am. Malacol. Bull.* **15,** 115–130 (2000).
5. Giribet, G. *et al.* Evidence for a clade composed of molluscs with serially repeated structures: monoplacophorans are related to chitons. *Proc. Natl Acad. Sci. USA* **103,** 7723–7728 (2006).
6. Wilson, N. G., Rouse, G. W. & Giribet, G. Assessing the molluscan hypothesis Serialia (Monoplacophora + Polyplacophora) using novel molecular data. *Mol. Phylogenet. Evol.* **54,** 187–193 (2010).
7. Vinther, J. & Nielsen, C. The Early Cambrian *Halkieria* is a mollusc. *Zool. Scr.* **34,** 81–89 (2005).
8. Scheltema, A. H., Kerth, K. & Kuzirian, A. M. Original molluscan radula: comparisons among Polyplacophora, Polyplacophora, Gastropoda, and the Cambrian fossil *Wiwaxia corrugata*. *J. Morphol.* **257,** 219–245 (2003).
9. Morris, S. C. & Caron, J. B. Halwaxiids and the early evolution of the lophotrochozoans. *Science* **315,** 1255–1258 (2007).
10. Sutton, M. D., Briggs, D. E. G., Siveter, D. J. & Siveter, D. J. Computer reconstruction and analysis of the vermiform mollusc *Acaenoplax hayae* from the Herefordshire Lagerstätte (Silurian, England), and implications for molluscan phylogeny. *Palaeontology* **47,** 293–318 (2004).
11. Caron, J.-B., Scheltema, A., Schander, C. & Rudkin, D. A soft-bodied mollusc with radula from the Middle Cambrian Burgess Shale. *Nature* **442,** 159–163 (2006).

12. Passamaneck, Y. J., Schander, C. & Halanych, K. M. Investigation of molluscan phylogeny using large-subunit and small-subunit nuclear rRNA sequences. *Mol. Phylogenet. Evol.* **32,** 25–38 (2004).
13. Aktipis, S. W., Giribet, G., Lindberg, D. R. & Ponder, W. F. in *Phylogeny and Evolution of the Mollusca* (eds Ponder, W. F. & Lindberg, D. R.) 201–237 (Univ. California Press, 2008).
14. Giribet, G. & Distel, D. L. in *Molecular Systematics and Phylogeography of Mollusks* (eds Lydeard, C. & Lindberg, D. R.) 45–90 (Smithsonian Books, 2003).
15. Rokas, A., Krüger, D. & Carroll, S. B. Animal evolution and the molecular signature of radiations compressed in time. *Science* **310,** 1933–1938 (2005).
16. Hejnol, A. *et al.* Assessing the root of bilaterian animals with scalable phylogenomic methods. *Proc. R. Soc. B* **276,** 4261–4270 (2009).
17. Dunn, C. W. *et al.* Broad taxon sampling improves resolution of the animal tree of life. *Nature* **452,** 745–749 (2008).
18. Prendini, L. Species or supraspecific taxa as terminals in cladistic analysis? Groundplans versus exemplars revisited. *Syst. Biol.* **50,** 290–300 (2001).
19. Vendrasco, M. J., Wood, T. E. & Runnegar, B. N. Articulated Palaeozoic fossil with 17 plates greatly expands disparity of early chitons. *Nature* **429,** 288–291 (2004).
20. Nielsen, C., Haszprunar, G., Ruthensteiner, B. & Wanninger, A. Early development of the aplacophoran mollusc *Chaetoderma*. *Acta Zool.* **88,** 231–247 (2007).
21. Wanninger, A., Koop, D., Moshel-Lynch, S. & Degnan, B. M. in *Phylogeny and Evolution of the Mollusca* (eds Ponder, W. F. & Lindberg, D. R.) 427–445 (Univ. California Press, 2008).
22. Yochelson, E. L. An alternative approach to the interpretation of the phylogeny of ancient mollusks. *Malacologia* **17,** 165–191 (1978).
23. Runnegar, B. in *Origin and Evolutionary Radiation of the Mollusca* (ed. Taylor, J. D.) 77–87 (Oxford Univ. Press, 1996).
24. Yochelson, E. L., Flower, R. H. & Webers, G. F. The bearing of the new Late Cambrian monoplacophoran genus *Knightoconus* upon the origin of Cephalopoda. *Lethaia* **6,** 275–309 (1973).
25. Lindgren, A. R., Giribet, G. & Nishiguchi, M. K. A combined approach to the phylogeny of Cephalopoda (Mollusca). *Cladistics* **20,** 454–486 (2004).
26. Strugnell, J. & Nishiguchi, M. K. Molecular phylogeny of coleoid cephalopods (Mollusca: Cephalopoda) inferred from three mitochondrial and six nuclear loci: a comparison of alignment, implied alignment and analysis methods. *J. Molluscan Stud.* **73,** 399–410 (2007).
27. Runnegar, B. & Pojeta, J. Jr. Molluscan phylogeny: the paleontological viewpoint. *Science* **186,** 311–317 (1974).
28. Waller, T. R. in *Bivalves: An Eon of Evolution* (eds Johnston, P. A. & Haggart, J. W.) 1–45 (Univ. Calgary Press, 1998).
29. Ponder, W. F. & Lindberg, D. R. Towards a phylogeny of gastropod molluscs: an analysis using morphological characters. *Zool. J. Linn. Soc.* **119,** 83–265 (1997).
30. Aktipis, S. W. & Giribet, G. A phylogeny of Vetigastropoda and other 'archaeogastropods': re-organizing old gastropod clades. *Invertebr. Biol.* **129,** 220–240 (2010).

Supplementary Information is linked to the online version of the paper at www.nature.com/nature.

Acknowledgements This research was supported by the US National Science Foundation through the Systematics Program (awards 0844596, 0844881 and 0844652), the ATOL Program (EF-0531757), EPSCoR (Infrastructure to Advance Life Sciences in the Ocean State, 1004057) and the iPlant Collaborative (0735191). Support was also provided by the Scripps Institution of Oceanography, the University of California Ship Funds and the Museum of Comparative Zoology. Collecting in Greenland was supported by the Carlsberg Foundation. A. Riesgo and J. Harasewych provided tissue samples of *Octopus* and *Perotrochus*, respectively. E. Röttinger assisted with *Nautilus*. C. Palacín allowed us to use an *Octopus vulgaris* photograph. At Brown University, Illumina sequencing was enabled by the Genomics Core Facility, and computational analyses were facilitated by L. Dong and the Center for Computing and Visualization. At Harvard University, Illumina sequencing was enabled by the Bauer Core in the Faculty of Arts and Sciences (FAS) Center for Systems Biology, and analyses were supported by the staff of the Research Computing cluster Odyssey facility in the FAS.

Author Contributions C.W.D., G.G. and N.G.W. conceived of and oversaw the study. S.A.S. and C.W.D. designed and implemented the data analyses. N.G.W., G.G. and G.W.R. collected the specimens. F.E.G., S.C.S.A. and C.F. prepared the specimens for sequencing. S.A.S., C.W.D., G.G., G.W.R. and N.G.W. wrote the manuscript. All authors read and provided input into the manuscript and approved the final version.

Author Information Illumina and 454 reads have been deposited in the National Center for Biotechnology Information (NCBI) Sequence Read Archive under accession number SRA044948. Sanger reads for *Laevipilina hyalina* have been deposited in the NCBI Trace Archive under the sequencing centre name BUDL with TI range 2317135955-2317139410. The assembled data, matrices and trees have been deposited in Dryad (http://dx.doi.org/10.5061/dryad.24cb8). Reprints and permissions information is available at www.nature.com/reprints. The authors declare no competing financial interests. Readers are welcome to comment on the online version of this article at www.nature.com/nature. Correspondence and requests for materials should be addressed to N.G.W. (nerida.wilson@austmus.gov.au), G.G. (ggiribet@oeb.harvard.edu) or C.W.D. (casey_dunn@brown.edu).

LETTER

doi:10.1038/nature10576

Metagenomic analysis of a permafrost microbial community reveals a rapid response to thaw

Rachel Mackelprang[1,2], Mark P. Waldrop[3], Kristen M. DeAngelis[4], Maude M. David[4], Krystle L. Chavarria[4], Steven J. Blazewicz[5], Edward M. Rubin[2,6] & Janet K. Jansson[2,4]

Permafrost contains an estimated 1672 Pg carbon (C), an amount roughly equivalent to the total currently contained within land plants and the atmosphere[1–3]. This reservoir of C is vulnerable to decomposition as rising global temperatures cause the permafrost to thaw[2]. During thaw, trapped organic matter may become more accessible for microbial degradation and result in greenhouse gas emissions[4,5]. Despite recent advances in the use of molecular tools to study permafrost microbial communities[6–9], their response to thaw remains unclear. Here we use deep metagenomic sequencing to determine the impact of thaw on microbial phylogenetic and functional genes, and relate these data to measurements of methane emissions. Metagenomics, the direct sequencing of DNA from the environment, allows the examination of whole biochemical pathways and associated processes, as opposed to individual pieces of the metabolic puzzle. Our metagenome analyses reveal that during transition from a frozen to a thawed state there are rapid shifts in many microbial, phylogenetic and functional gene abundances and pathways. After one week of incubation at 5 °C, permafrost metagenomes converge to be more similar to each other than while they are frozen. We find that multiple genes involved in cycling of C and nitrogen shift rapidly during thaw. We also construct the first draft genome from a complex soil metagenome, which corresponds to a novel methanogen. Methane previously accumulated in permafrost is released during thaw and subsequently consumed by methanotrophic bacteria. Together these data point towards the importance of rapid cycling of methane and nitrogen in thawing permafrost.

We collected three intact frozen permafrost soil cores with their overlying seasonally thawed active layers from Hess Creek, Alaska. This is a black-spruce forest site containing many metres of frozen peat and the C was dated to 1200 yr BP[10]. Other soil properties and microbial respiration rates were previously characterized[10]. Frozen active layer and permafrost layer samples from each core were thawed and incubated for 7 days at 5 °C under a helium headspace. During the incubations, CH_4 (Fig. 1a) and CO_2 (Supplementary Fig. 1) concentrations were monitored in the headspace and DNA was extracted for 16S ribosomal RNA (rRNA) and metagenome sequencing.

There was a burst of CH_4 from the permafrost within 48 h of thaw, followed by a significant ($P = 0.05$) decrease in concentration from day 2 to day 7 (Fig. 1a). To determine (1) if methane release was due to post-thaw production or from trapped gas, (2) whether the methane was consumed by methanotrophs or anaerobic methane oxidizers, and (3) the CH_4 oxidation potential over time, we treated additional samples with 1500 p.p.m. CH_4 and 2-bromoethane sulphonic acid (BES) and measured CH_4 levels daily. BES is an inhibitor of archaeal methanogenesis and methyl-coenzyme M reductase-dependent anaerobic methane oxidation. Rapid release of CH_4 from samples treated with BES suggested that the CH_4 primarily originated from gas present in the permafrost before thaw (Supplementary Fig. 2), as previously reported[11]. Subsequent CH_4 consumption in both BES- and non-BES-treated samples was indicative of CH_4 oxidation by methanotrophic bacteria (Fig. 1b). The oxygen used for methane oxidation presumably originated from permafrost water or aerobic microsites in the samples[12]. Together these data indicate CH_4 levels are dynamic in thawing permafrost.

To determine the phylogenetic and functional gene repertoire before and after thaw, we performed deep metagenome sequencing of samples from two of the three replicate cores (cores 1 and 2). DNA was extracted from frozen active layer and permafrost samples and from samples thawed at 5 °C for 2 and 7 days. This resulted in 12 samples for metagenome sequencing.

Owing to low DNA yield we used emulsion PCR (emPCR) to generate random shotgun short insert libraries with minimum amplification bias[13]. Sequencing yielded a total of 176 million reads and 39.8 Gb of raw sequence. The individual metagenome reads were annotated by comparison with protein-coding and small subunit (SSU) rRNA genes (Supplementary Table 1). We achieved relatively good assembly of the metagenome data, despite the high microbial diversity of soil. In total we obtained 9.7 Mb of sequence in 3,758 contigs greater than 1 kb in length. The longest contig was 67.4 kb in length and 98 contigs were greater than 10 kb.

A draft genome of a novel methanogen was constructed from the metagenome data (Fig. 2), owing to the relatively high abundance of methanogens in the samples (0.2–4% of total 16S rRNA gene sequences) and its low population heterogeneity. To generate the draft genome, contigs were binned by tetranucleotide frequency and read coverage[14]. The draft genome comprised 1.9 Mb of sequence in 174 contigs. To confirm that the clustered contigs represented a draft genome, we validated the assembly through single-copy gene analysis (Supplementary Table 2) and by alignment of the draft genome to a related reference genome (Supplementary Fig. 3). This is the first example of successful assembly of a draft genome from a highly complex soil metagenome. The nearest sequenced relative was the recently

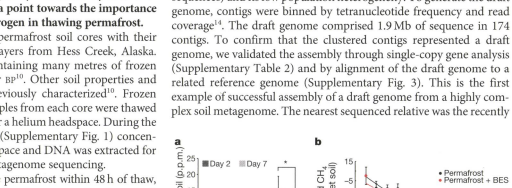

Figure 1 | Bacterial oxidation of trapped CH_4 released from Hess Creek permafrost after thaw. a, CH_4 headspace concentration during incubation of permafrost and active layer samples at 5 °C for 2 and 7 days. Values are means ± s.e.m. **b**, CH_4 headspace concentrations during 7 days incubation at 5 °C from permafrost samples without BES and with BES. Values are normalized to CH_4 concentrations after the initial release of CH_4 during thaw (day 1). *$P = 0.05$ ($n = 3$).

[1]Department of Biology, California State University at Northridge, Northridge, California 91330, USA. [2]United States Department of Energy Joint Genome Institute, Walnut Creek, California 94598, USA. [3]United States Geological Survey, Menlo Park, California 94025, USA. [4]Lawrence Berkeley National Laboratory, Earth Sciences Division, Berkeley, California 94720, USA. [5]Department of Environmental Science, Policy and Management, University of California at Berkeley, Berkeley, California 94720, USA. [6]Lawrence Berkeley National Laboratory, Genomics Division, Berkeley, California 94720, USA.

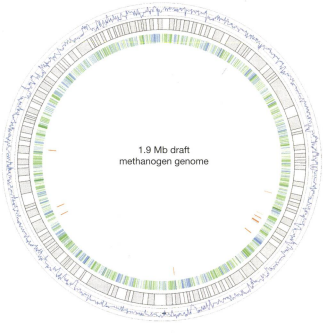

Figure 2 | Draft methanogen genome assembly. Draft methanogen genome. Features correspond to concentric circles, starting with the outermost circle. (1) Illumina sequence coverage averaging 73×. (2) One hundred and seventy-four contigs making up the draft genome; contigs shown are scaled according to size and are roughly ordered by mapping to the reference genome (65% identity at the nucleotide level). (3) GC content heat map (dark blue to light green represent low to high values). (4) Methanogenesis genes (orange) and nitrogen fixation genes (blue). The true size of the genome is not known owing to gaps between the contigs.

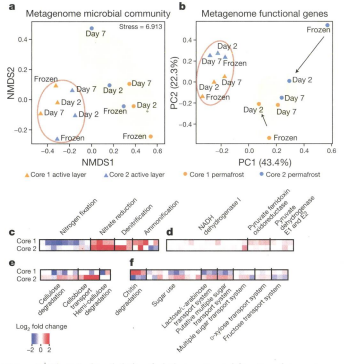

Figure 3 | Thaw-induced shifts of phylogenetic and functional genes in metagenomes. a, nMDS analysis of the relative abundance of 16S rRNA genes from the metagenomes. **b**, Principal component analysis of relative abundance of KEGG genes in metagenomes. The percentage variation explained by the principal components is indicated on the axes. Arrows illustrate rapid shift in functional gene composition upon thaw in two disparate permafrost samples. **c**–**f**, Heat maps indicating differences in relative abundances of specific genes between frozen (day 0) and thawed (day 7) permafrost metagenomes (Hess Creek cores 1 and 2). **c**, Nitrogen cycle; **d**, central metabolism; **e**, cellulose degradation; **f**, chitin degradation, sugar metabolism and transport.

described Methanocellales[15] order at a nucleotide identity level of approximately 65% (Fig. 2). Single-copy gene analysis demonstrated it was related to members of *Methanomicrobia* (Supplementary Fig. 4). The abundance of this novel methanogen correlates with the observed CH_4 in the samples and suggests that it may be an important player in CH_4 production under frozen conditions. It has previously been reported that trapped CH_4 in permafrost is biological in origin and that methanogenesis can occur at sub-zero temperatures[11]. The draft genome also included genes for nitrogen fixation. Although nitrogen-fixing methanogens have been previously described[16], this draft genome is the first indication that they are present in permafrost.

The metagenome data revealed core-specific shifts in some community members (Fig. 3a), including the orders Proteobacteria, Bacteriodetes and Firmicutes. We found that Actinobacteria increased in both cores during thaw (Supplementary Fig. 5). Actinobacteria have previously been found at high abundance in permafrost[8], which is thought to be caused by their maintenance of metabolic activity and DNA repair mechanisms at low temperatures[17]. Most archaeal sequences identified in the metagenomic data were methanogens in the phylum Euryarchaeota (62–95%), including the Methanomicrobia that was represented in our draft genome. In total, four orders of methanogens (Methanosarcinales, Methanomicrobiales, Methanomicrobia and Methanobacterales) were detected. As the permafrost thawed, the methanogens (including Methanomicrobia) increased in relative abundance (Supplementary Fig. 6). These orders are known to be metabolically versatile and can use a variety of substrates[18].

18S rRNA gene sequences from land plants (Streptophyta) were the most abundant eukaryotic reads in the metagenome data, probably originating from undecomposed detritus. 18S rRNA gene sequences also originated from fungi, protists, ameobae, algae and other eukaryotic phyla (Supplementary Fig. 7.) Few consistent changes in the Eukarya were observed after thaw, although the Streptophyta decreased in core 2, presumably owing to microbial degradation of plant material (Supplementary Fig. 7).

A greater phylogenetic distance was observed between frozen and day 2 samples than between day 2 and day 7 samples (Supplementary Fig. 8), based on 454 pyrotag sequencing of 16S rRNA genes, suggesting that the community composition shifted rapidly upon thaw. The difference was more pronounced in the permafrost than in the active layer. Operational taxonomic units changing significantly ($P < 0.05$) in abundance during thaw were largely from uncultivated taxa (Supplementary Fig. 9 and Supplementary Table 3).

We used quantitative PCR (qPCR) to measure the absolute abundances of specific phyla before and after thaw. The qPCR results confirmed that there was a significant increase in Actinobacteria in both cores after thaw, Bacteriodetes changed in a core-dependent manner, and no significant changes were observed in Chloroflexi (Supplementary Fig. 10).

Our observation that methane was consumed after thaw (Fig. 1) was correlated to detection of sequences representative of bacterial methanotrophs in relatively high amounts (approximately 0.25–0.65% relative abundance). Two forms of methane monooxygenases were detected: particulate methane monooxygenase (*pmoA*) represented most (~80%) and the rest were soluble methane monooxygenase (*mmoX*). The metagenomic results were confirmed by qPCR of *pmoA*, *mcrA* (encoding the methyl coenzyme-M reductase alpha subunit) and 16S rRNA genes from type I and type II methanotrophs. Both the *pmoA* gene and type II methanotrophs significantly increased in abundance after thaw ($P < 0.01$). Although type I methanotrophs were detectable at low levels (fewer than 100 copies per nanogram), they did not differ in abundance between the frozen and thawed samples. *McrA* sequences from methanogenic archaea were detected but did not change significantly during thaw (Supplementary Fig. 11). *McrA* and 16S sequences

originating from anaerobic methane oxidizers were not detected. Collectively, these data and our BES incubation experiments (Fig. 1b) suggest that bacterial type II methanotrophs and the particulate methane monooxygenase enzyme were involved in consumption of methane released during permafrost thaw.

We tracked simultaneous shifts in the total gene complement from the metagenome data to obtain a global view of functional response to thaw. The active layer samples were relatively similar before and after thaw. By contrast, the two frozen permafrost metagenomes differed dramatically before thaw (Fig. 3b). In addition, functional genes in frozen active layer and permafrost samples were distinct from each other, including differences in several key metabolic pathways such as energy metabolism, nitrogen fixation, amino-acid transport, oxidative phosphorylation and anaerobic respiration (Supplementary Fig. 12). During thaw, the permafrost metagenomes rapidly converged and neared those in the active layer samples (Fig. 3b). The convergence of function was not matched by a convergence of phylogenetic composition during this short-term incubation (Fig. 3a), suggesting that disparate community responses to thaw can have similar functional consequences.

The high sequencing depth used provided the sensitivity necessary to characterize subtle changes in the abundance of thousands of genes that had a cumulative significant affect, as confirmed by multiple statistical analyses (Supplementary Figs 13–15 and Supplementary Table 4). We specifically targeted genes involved in C and N cycling by grouping Kyoto Encyclopedia of Gene and Genomes (KEGG) genes into subsets (Fig. 3c–f). Several genes involved in the N cycle shifted in abundance during thaw (Fig. 3c). For example, nitrate reductase I genes significantly increased, suggesting nitrate was available as a terminal electron acceptor, which was confirmed by its presence in the chemical data[10]. Ammonification and denitrification genes increased during thaw in both cores. However, core 1 did not show an increase in the *nosZ* gene, responsible for converting N_2O to N_2, suggesting that it had potential for N_2O greenhouse gas emission during thaw. By contrast, several genes in the nitrogen fixation pathway decreased during thaw in both cores. Changes in the N cycle observed in the metagenomic data were confirmed by qPCR of specific genes for nitrate reduction (*narG*, encoding nitrate reductase I, alpha subunit) and nitrogen fixation (*nifH*, encoding the nitrogenase iron protein), which increased and decreased in abundance after thaw, respectively (Supplementary Fig. 16).

The metagenomic strategy also allowed us to identify changes in a diverse set of C cycle genes not easily accessed by other approaches such as qPCR or analysis of enzymatic activities. These included genes involved in central metabolism that increased during thaw (Fig. 3d). Genes involved in the transport and metabolism of specific carbohydrates were also enriched after thaw, but these changes were mainly core specific. For example, in core 2, we observed significant increases ($P < 0.01$) in the cellobiose transport system and a corresponding increase in cellulose degradation and hemicellulose degradation (Fig. 3f). Chitin degradation genes and some sugar transport systems were specifically enriched in core 1 (Fig. 3g) (see Supplementary Table 5 for a complete list). It is important to keep in mind that decreases in relative abundance may also be due to growth of other community members lacking those particular genes. These data reflect a rapid response of specific members of the microbial community in permafrost to thaw, probably owing to the availability of particular substrates that become accessible. Although the cores were taken from the same site within metres of each other and would presumably have similar chemical and physical properties, there were subtle differences between the genetic responses to thaw in the replicate cores. For example, we observed a higher level of dissolved organic carbon and higher C density in core 2 (Supplementary Table 6) that is correlated with the core-2-specific enrichment of C processing genes during thaw. These findings emphasize the importance of replication, even for complex soil metagenomes.

In summary, these detailed analyses reveal for the first time the rapid and dynamic response of permafrost microbial communities to thaw. The thaw-induced shifts that we detected directly support conceptual models of C and N cycling in Arctic soils (Fig. 4), in which microbes play a central role in greenhouse gas emissions and destabilization of stored permafrost C.

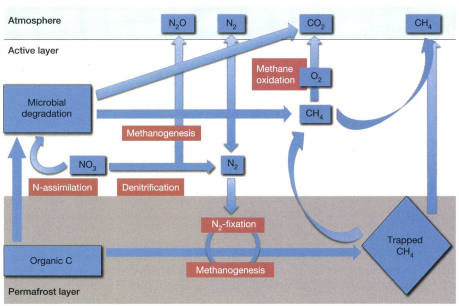

Figure 4 | Conceptual model of C and N cycling in Arctic soils based on metagenome data. Slow rates of methanogenesis by cold-adapted methanogens occur in permafrost and active layer soils. Over time, methane accumulates in the permafrost and is initially consumed by bacterial methanotrophs upon thaw. In the permafrost, N_2 fixation genes are abundant. As the permafrost thaws, microbial degradation of organic C occurs rapidly and other nitrogen sources become available with an increase in dissimilatory and assimilatory nitrate reduction processes.

METHODS SUMMARY

Triplicate frozen permafrost cores were collected from Hess Creek, Alaska, to a depth of 1 m. Active layer (approximately 35cm depth) and permafrost (approximately 85 cm depth) samples were cut from the frozen cores using a band saw in a −20 °C cold room. Approximately 10 g of frozen soil were incubated at 5 °C for one week under a helium headspace. CH_4 and CO_2 concentrations were measured on days 2 and 7 of incubation. In separate experiments, CH_4 oxidation was measured in permafrost samples incubated with 2-bromoethane sulphonic acid and CH_4 (1500 p.p.m.). CH_4 was subsequently measured in the headspace every 24 h for 7 days.

Shotgun metagenomic sequencing was conducted on DNA extracted from two replicate cores (active layer and permafrost) while frozen and after 2 and 7 days of incubation. Because the DNA yield was too low to prepare standard sequencing libraries, we used emPCR[13,19], for amplification before sequencing. This method escapes biases common in other amplification methods. The DNA was sequenced using the Illumina GAII platform with 2×113-base-pair (bp) cycles. Metagenomic reads were annotated by comparison with the KEGG genes database[20] using BLASTX[21] ($E \leq 1 \times 10^{-5}$) and with the Greengenes[22] and SILVA[23] databases using BLASTN[21] ($E \leq 1 \times 10^{-20}$). For assembly, raw reads from all samples were combined. After quality filtering and de-replication, *k*-mers (32-mers) with a depth less than two were removed from the data set[14]. The filtered reads were then assembled using Velvet[14]. Approximately ten assemblies were generated, and the one generating the longest contigs was chosen for further analysis. Contigs were annotated through the Integrated Microbial Genomes & Metagenomics (IMG/M) system[25]. To group contigs into a draft genome, large contigs (greater than 15 kb in length) were clustered based on tetranucleotide frequency and coverage. The largest bin was grown by the recruitment of smaller contigs to the large cluster[24].

Full Methods and any associated references are available in the online version of the paper at www.nature.com/nature.

Received 28 April; accepted 20 September 2011.
Published online 6 November 2011.

1. Schuur, E. A. G. *et al.* Vulnerability of permafrost carbon to climate change: Implications for the global carbon cycle. *Bioscience* **58,** 701–714 (2008).
2. Tarnocai, C. *et al.* Soil organic carbon pools in the northern circumpolar permafrost region. *Glob. Biogeochem. Cycles* **23,** GB2023 (2009).
3. Zimov, S. A., Schuur, E. A. & Chapin, F. S. Climate change. Permafrost and the global carbon budget. *Science* **312,** 1612–1613 (2006).
4. Osterkamp, T. Characteristics of the recent warming of permafrost in Alaska. *J. Geophys. Res.* **112,** F02S02 (2007).
5. Prater, J. L., Chanton, J. P. & Whiting, G. J. Variation in methane production pathways associated with permafrost decomposition in collapse scar bogs of Alberta, Canada. *Glob. Biogeochem. Cycles* **21,** GB4004 (2007).
6. Chu, H. *et al.* Soil bacterial diversity in the Arctic is not fundamentally different from that found in other biomes. *Environ. Microbiol.* **12,** 2998–3006 (2010).
7. Hansen, A. A. *et al.* Viability, diversity and composition of the bacterial community in a high Arctic permafrost soil from Spitsbergen, Northern Norway. *Environ. Microbiol.* **9,** 2870–2884 (2007).
8. Steven, B., Pollard, W. H., Greer, C. W. & Whyte, L. G. Microbial diversity and activity through a permafrost/ground ice core profile from the Canadian high Arctic. *Environ. Microbiol.* **10,** 3388–3403 (2008).
9. Yergeau, E., Hogues, H., Whyte, L. G. & Greer, C. W. The functional potential of high Arctic permafrost revealed by metagenomic sequencing, qPCR and microarray analyses. *ISME J.* **4,** 1206–1214 (2010).
10. Waldrop, M. P. *et al.* Molecular investigations into a globally important carbon pool: permafrost-protected carbon in Alaskan soils. *Glob. Change Biol.* **16,** 2543–2544 (2010).
11. Rivkina, R. *et al.* Biogeochemistry of methane and methanogenic archaea in permafrost. *FEMS Microbiol. Ecol.* **61,** 1–15 (2007).
12. Trotsenko, Y. A. & Khmelenian, V. N. Aerobic methanotrophic bacteria of cold ecosystems. *FEMS Microbiol. Ecol.* **53,** 15–26 (2005).
13. Blow, M. *et al.* Identification of ancient remains through genomic sequencing. *Genome Res.* **18,** 1347–1353 (2008).
14. Hess, M. *et al.* Metagenomic discovery of biomass-degrading genes and genomes from cow rumen. *Science* **331,** 463–467 (2011).
15. Sakai, S. *et al. Methanocella paludicola* gen. nov., sp. nov., a methane-producing archaeon, the first isolate of the lineage 'Rice Cluster I', and proposal of the new archaeal order Methanocellales ord. nov. *Int. J. Syst. Evol. Microbiol.* **58,** 929–936 (2008).
16. Murray, P. A. & Zinder, S. H. Nitrogen-fixation by a methanogenic archaebacterium. *Nature* **312,** 284–286 (1984).
17. Johnson, S. S. *et al.* Ancient bacteria show evidence of DNA repair. *Proc. Natl Acad. Sci. USA* **104,** 14401–14405 (2007).
18. Ferry, J. G. How to make a living by exhaling methane. *Annu. Rev. Microbiol.* **64,** 453–473 (2010).
19. Williams, R. *et al.* Amplification of complex gene libraries by emulsion PCR. *Nature Methods* **3,** 545–550 (2006).
20. Kanehisa, M. & Goto, S. KEGG: Kyoto Encyclopedia of Genes and Genomes. *Nucleic Acids Res.* **28,** 27–30 (2000).
21. Altschul, S. F., Gish, W., Miller, W., Myers, E. W. & Lipman, D. J. Basic local alignment search tool. *J. Mol. Biol.* **215,** 403–410 (1990).
22. DeSantis, T. Z. *et al.* Greengenes, a chimera-checked 16S rRNA gene database and workbench compatible with ARB. *Appl. Environ. Microbiol.* **72,** 5069–5072 (2006).
23. Pruesse, E. C. *et al.* SILVA: a comprehensive online resource for quality checked and aligned ribosomal RNA sequence data compatible with ARB. *Nucleic Acids Res.* **35,** 7188–7196 (2007).
24. Zerbino, D. R. & Birney, E. Velvet: algorithms for de novo short read assembly using de Bruijn graphs. *Genome Res.* **18,** 821–829 (2008).
25. Markowitz, V. M. *et al.* IMG/M: a data management and analysis system for metagenomes. *Nucleic Acids Res.* **36,** D534–D538 (2008).

Supplementary Information is linked to the online version of the paper at www.nature.com/nature.

Acknowledgements The work conducted by the Lawrence Berkeley National Laboratory Earth Sciences Division (Laboratory Directed Research Development) and the Joint Genome Institute was supported in part by the Office of Science of the US Department of Energy under Contract no. DE-AC02-05CH11231. This study was also supported by the Venture Capital and Yukon River Basin project of the United States Geological Survey. We acknowledge the technical support by the Joint Genome Institute production team. We thank A. Sczyrba, R. Egan and S. Canon for discussions and advice.

Author Contributions J.K.J., M.P.W. and K.M.D. conceived the incubation experiments. M.P.W. collected the samples. M.P.W. and S.J.B. conducted the incubation experiments. R.M., K.L.C. and K.M.D. performed the DNA extractions. R.M. created the shotgun sequencing libraries and conducted bioinformatics analyses. R.M. and K.M.D. performed statistical analyses. R.M. and M.M.D. performed qPCR experiments. R.M. and J.K.J. wrote the paper. All authors discussed the results and commented on the manuscript. E.M.R. M.P.W. and J.K.J. obtained funding for the study.

Author Information All annotated assembled sequences were incorporated into the IMG/M system with the Taxon Object ID 2067725009. Raw Illumina and 454 pyrotag sequence reads and a list containing the subset of contigs belonging to the draft methanogen genome are available at https://www.jgi.doe.gov/downloads/Permafrost_metagenome. Reprints and permissions information is available at www.nature.com/reprints. The authors declare no competing financial interests. Readers are welcome to comment on the online version of this article at www.nature.com/nature. Correspondence and requests for materials should be addressed to J.K.J. (jrjansson@lbl.gov).

LETTER

doi:10.1038/nature10594

Sustained axon regeneration induced by co-deletion of PTEN and SOCS3

Fang Sun[1], Kevin K. Park[2], Stephane Belin[1], Dongqing Wang[3], Tao Lu[4], Gang Chen[1], Kang Zhang[5], Cecil Yeung[1], Guoping Feng[3], Bruce A. Yankner[4] & Zhigang He[1]

A formidable challenge in neural repair in the adult central nervous system (CNS) is the long distances that regenerating axons often need to travel in order to reconnect with their targets. Thus, a sustained capacity for axon regeneration is critical for achieving functional restoration. Although deletion of either phosphatase and tensin homologue (PTEN), a negative regulator of mammalian target of rapamycin (mTOR), or suppressor of cytokine signalling 3 (SOCS3), a negative regulator of Janus kinase/signal transducers and activators of transcription (JAK/STAT) pathway, in adult retinal ganglion cells (RGCs) individually promoted significant optic nerve regeneration, such regrowth tapered off around 2 weeks after the crush injury[1,2]. Here we show that, remarkably, simultaneous deletion of both *PTEN* and *SOCS3* enables robust and sustained axon regeneration. We further show that PTEN and SOCS3 regulate two independent pathways that act synergistically to promote enhanced axon regeneration. Gene expression analyses suggest that double deletion not only results in the induction of many growth-related genes, but also allows RGCs to maintain the expression of a repertoire of genes at the physiological level after injury. Our results reveal concurrent activation of mTOR and STAT3 pathways as key for sustaining long-distance axon regeneration in adult CNS, a crucial step towards functional recovery.

During development axons reach their targets first through *de novo* outgrowth in embryos, followed by 'networked growth' in which axons elongate with termini tethered to their targets. As animals increase in body size during postnatal and adolescent stages, the distance resulted from the 'networked growth' could be much longer than that travelled by the initial *de novo* growth. After injury in the adult CNS, regenerating axons need to carry out *de novo* growth over relatively vast distances to reach their targets. Thus, the robustness of axon regeneration, in terms of both speed and duration of axon regrowth, is critical for making functional reconnections in adulthood. Approaches that have been shown to promote axon regeneration in the adult CNS include reducing extracellular inhibitory activity and increasing intrinsic growth ability[1–9]. However, the extents of axon regeneration observed in these studies are still limited. For example, our previous studies demonstrated that the injured optic nerve could undergo significant axon regeneration after conditional deletion of *PTEN* or *SOCS3* in adult RGCs, but the regrowth only occurred during the first 2 weeks after injury, and then subsided afterwards[1,2].

To identify a strategy for promoting sustained robust axon regeneration, we assessed the effects of deleting both *PTEN* and *SOCS3* in adult RGCs on optic nerve regeneration. Adeno-associated viruses (AAV)-Cre (AAV–GFP (green fluorescent protein) as a control) were injected into the vitreous body of $PTEN^{f/f/+}$, or $SOCS3^{f/f/+}$, or $PTEN^{f/f}/SOCS3^{f/f}$ mice to delete the floxed genes 2 weeks before optic nerve injury. In addition, ciliary neurotrophic factor (CNTF) was applied intravitreously to the $SOCS3^{f/f}$ or $PTEN^{f/f}/SOCS3^{f/f}$ mice, as this enhances axon regeneration induced by *SOCS3* deletion[2].

At 2 weeks after injury, we observed a significant increase in axon regeneration in the double knockout group (Supplementary Fig. 1a, b). The synergistic effects of the double deletion became even more dramatic at 4 weeks after injury (Fig. 1). At 2 mm distal to the lesion site, deletion of both genes resulted in more than tenfold increase in the number of regenerating axons compared with deletion of either gene alone (Fig. 1a, b, d). In the double mutants, more than 20% of the regenerating axons reached the region proximal to the optic chiasm (Fig. 1c, d). Among the regenerating axons passing the chiasm, some crossed the midline and projected to the contralateral side, while others remained ipsilateral. Occasionally, a few axons could be seen projecting into the opposite uninjured optic nerve (Fig. 1c). Interestingly, several regenerating axons could grow even further, reaching the optic-tract brain entry zone and in the hypothalamus, the suprachiasmatic nuclei area (Supplementary Fig. 2).

Compared with wild-type animals, all three mutant groups showed significantly increased RGC survival after injury. At 2 weeks after injury, the survival was comparable among the three mutant groups (Supplementary Fig. 1c). At 4 weeks after injury, however, the number of surviving RGCs declined in the PTEN or SOCS3 single mutants, whereas the survival rate was maintained in the double mutants (Fig. 1e).

To mimic a clinically relevant situation, we examined whether a delayed deletion of *PTEN* and/or *SOCS3* still promoted sustained optic nerve regeneration. Thus, we performed intravitreal AAV-Cre injection immediately after optic nerve injury (Fig. 2). It takes at least 3–6 days for Cre-dependent reporter expression to be observed (Supplementary Fig. 3a). We thus examined RGC survival and axon regeneration 3 weeks after injury in these animals. Despite similar survivals in all groups (Supplementary Fig. 3b, c), double and single mutants showed significant differences in the extents of axon regeneration (Fig. 2). At 2 mm distal to the lesion site, up to 20-fold more regenerating axons were seen in double mutants, compared with individual single mutants. Thus, adult RGCs with concomitant deletion of *PTEN* and *SOCS3* can activate a program for sustained *de novo* axon growth after injury.

We next examined what mechanism(s) contribute to the synergy produced by concurrent deletion of *PTEN* and *SOCS3*. Although mTOR activation is likely to be a major mediator of *PTEN* deletion[1], the regeneration phenotype of *SOCS3* deletion is dependent on gp130, a shared receptor component for cytokines[12,13]. However, multiple downstream effectors have been implicated in cytokines–gp130 signalling[12–15]. Because of a suggested relevance to axon regeneration[16–18], we tested the specific involvement of the transcription factor STAT3, a major target of the JAK/STAT pathway[19]. Upon phosphorylation-mediated activation, STAT3 accumulates in the nucleus to initiate

[1]F.M. Kirby Neurobiology Center, Children's Hospital, and Department of Neurology, Harvard Medical School, 300 Longwood Avenue, Boston, Massachusetts 02115, USA. [2]Miami Project to Cure Paralysis, Department of Neurological Surgery, Miller School of Medicine, University of Miami, Miami, Florida 33136, USA. [3]McGovern Institute for Brain Research, Department of Brain and Cognitive Sciences, Massachusetts Institute of Technology, Cambridge, Massachusetts 02139, USA. [4]Department of Genetics, Harvard Medical School, Boston, Massachusetts 02115, USA. [5]Shiley Eye Center, University of California at San Diego, La Jolla, California 92093, USA.

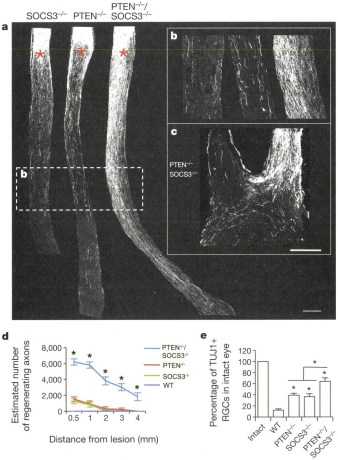

Figure 1 | Synergistic effects of double deletion of *PTEN* and *SOCS3* on axon regeneration observed at 4 weeks after injury. **a**, Images of the optic nerve sections showing CTB-labelled axons in AAV-Cre-injected $SOCS3^{f/f}$ with CNTF ($SOCS3^{-/-}$), $PTEN^{f/f}$ ($PTEN^{-/-}$) or $PTEN^{f/f}/SOCS3^{f/f}$ with CNTF ($PTEN^{-/-}/SOCS3^{-/-}$) mice. Asterisks, lesion sites. **b**, High-magnification images of the boxed area in **a**, which is about 1.5–2.0 mm from the lesion sites. **c**, Regenerating axons at the optic chiasm. **d**, Estimated numbers of regenerating axons. There was a significant difference between the $PTEN^{-/-}/SOCS3^{-/-}$ group and others. $^{*}P < 0.001$, ANOVA, Bonferroni's post-hoc test. **e**, Percentages of TUJ1-positive RGCs in each group compared with that in the intact retinas. $^{*}P < 0.001$, ANOVA, Tukey's post-hoc test. $N = 7$–8 per group. Error bars, s.d. Scale bars, 200 μm.

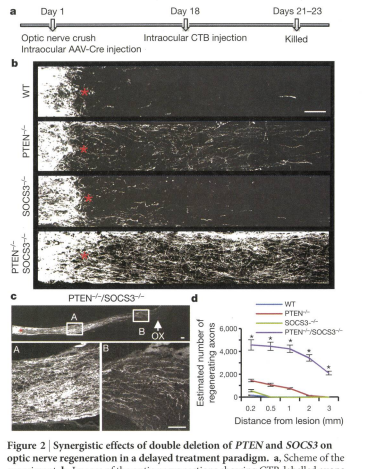

Figure 2 | Synergistic effects of double deletion of *PTEN* and *SOCS3* on optic nerve regeneration in a delayed treatment paradigm. **a**, Scheme of the experiment. **b**, Images of the optic nerve sections showing CTB-labelled axons in AAV-Cre-injected $SOCS3^{f/f}$ with CNTF ($SOCS3^{-/-}$), $PTEN^{f/f}$ ($PTEN^{-/-}$) or $PTEN^{f/f}/SOCS3^{f/f}$ with CNTF ($PTEN^{-/-}/SOCS3^{-/-}$) mice. Asterisks, lesion sites. **c**, Extensive axon regeneration is only evident in double mutants. Top panel shows the entire optic nerve up to the chiasm. Bottom panels show high-magnified areas (**a** and **b**) as indicated in the top panel. OX, optic chiasm. **d**, Estimated numbers of regenerating axons. At all distances quantified, there was a significant difference between the $PTEN^{-/-}/SOCS3^{-/-}$ group and the remaining groups. $^{*}P < 0.001$, ANOVA, Bonferroni's post-hoc test. $N = 5$–6 per group. Error bars, s.d. Scale bars, 100 μm.

transcription[19]. By immunostaining with anti-phospho-STAT3, we found that phospho-STAT3 expression was rarely detectable in intact RGCs. In wild-type mice, optic nerve injury increased phospho-STAT3 levels in RGCs, but such signals were mainly localized in the cytosol (Fig. 3a, b). In contrast, phospho-STAT3 was evident in the nuclei of axotomized RGCs with both *SOCS3* single and *SOCS3*/*PTEN* double mutants (Fig. 3a, b), suggesting the activation of STAT3 under these conditions.

We then evaluated the contribution of STAT3 to the axon regeneration induced by *SOCS3* deletion and CNTF administration. Deletion of *STAT3* had no significant effects on RGC survival (Supplementary Fig. 4) and axon regeneration (Fig. 3c). However, double deletion of *STAT3* and *SOCS3* abolished injury-induced phospho-STAT3 signal (Fig. 3a, b), RGC survival (Supplementary Fig. 4) and axon regeneration (Fig. 3c, d) seen in *SOCS3* single mutants, suggesting that STAT3 is a critical mediator of SOCS3 regulated axon regeneration and RGC survival.

We next examined possible interactions of the PTEN- and SOCS3-regulated pathways on optic nerve regeneration. Similar to wild type, phospho-STAT3 expression in *PTEN*-deleted RGCs after injury was rarely detectable (Supplementary Fig. 5), arguing against STAT3 activation after *PTEN* deletion. Importantly, the extents of axon regeneration and RGC survival were similar in the animals with *PTEN* single deletion and *PTEN*/*STAT3* or *PTEN*/*gp130* double deletion (Fig. 4a, c and Supplementary Fig. 6a, b), suggesting that STAT3 is unlikely to be an important mediator of *PTEN* deletion.

We also evaluated the potential role of mTOR activation in axon regeneration induced by *SOCS3* deletion. Although systematic administration of rapamycin, a specific mTOR inhibitor, abolished most of the axon regeneration after *PTEN* deletion (Fig. 4a, c), the same treatment did not affect axon regeneration from *SOCS3*-deleted RGCs (Fig. 4b, d). These results suggest that these two pathways act independently in regulating axon regeneration.

To assess possible gene expression alteration triggered by *PTEN*/*SOCS3* double-deletion, we performed gene-expression profiling studies. Transgenic YFP17 mice expressing yellow fluorescent protein (YFP) in most RGCs (with only few amacrine cells, Supplementary Fig. 7a), either in a control background or crossed to three different mutants, were subjected to AAV-Cre injection and optic nerve injury. Three days after injury, RNA was extracted from fluorescence-activated cell sorted (FACS) RGCs for microarray analysis (Supplementary Fig. 7b–e).

The first potential mechanism is that certain key regeneration-promoting genes are significantly altered by *PTEN*/*SOCS3* double deletion, when compared with both single deletions and the wild-type

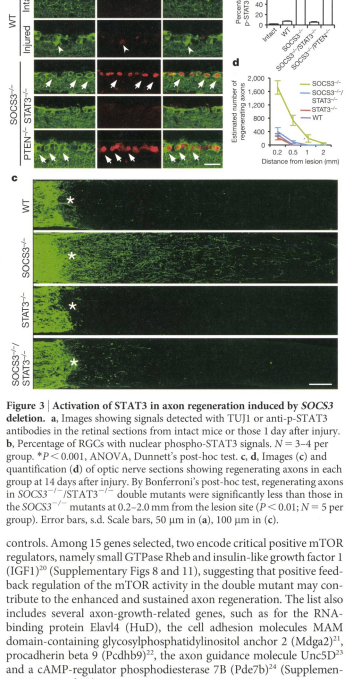

Figure 3 | Activation of STAT3 in axon regeneration induced by *SOCS3* deletion. **a**, Images showing signals detected with TUJ1 or anti-p-STAT3 antibodies in the retinal sections from intact mice or those 1 day after injury. **b**, Percentage of RGCs with nuclear phospho-STAT3 signals. $N = 3$–4 per group. $^*P < 0.001$, ANOVA, Dunnett's post-hoc test. **c**, **d**, Images (**c**) and quantification (**d**) of optic nerve sections showing regenerating axons in each group at 14 days after injury. By Bonferroni's post-hoc test, regenerating axons in *SOCS3*$^{-/-}$/*STAT3*$^{-/-}$ double mutants were significantly less than those in the *SOCS3*$^{-/-}$ mutants at 0.2–2.0 mm from the lesion site ($P < 0.01$; $N = 5$ per group). Error bars, s.d. Scale bars, 50 μm in (**a**), 100 μm in (**c**).

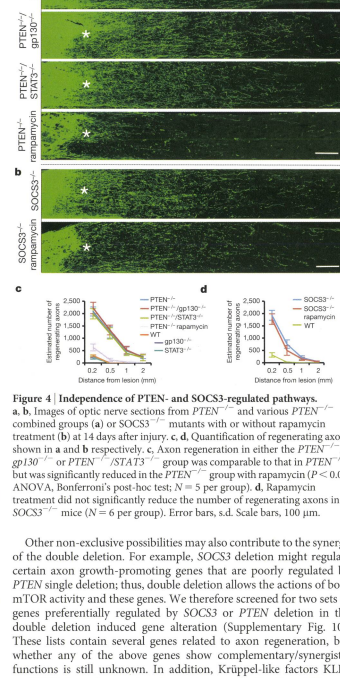

Figure 4 | Independence of PTEN- and SOCS3-regulated pathways. **a**, **b**, Images of optic nerve sections from *PTEN*$^{-/-}$ and various *PTEN*$^{-/-}$ combined groups (**a**) or SOCS3$^{-/-}$ mutants with or without rapamycin treatment (**b**) at 14 days after injury. **c**, **d**, Quantification of regenerating axons shown in **a** and **b** respectively. **c**, Axon regeneration in either the *PTEN*$^{-/-}$/*gp130*$^{-/-}$ or *PTEN*$^{-/-}$/*STAT3*$^{-/-}$ group was comparable to that in *PTEN*$^{-/-}$, but was significantly reduced in the *PTEN*$^{-/-}$ group with rapamycin ($P < 0.01$, ANOVA, Bonferroni's post-hoc test; $N = 5$ per group). **d**, Rapamycin treatment did not significantly reduce the number of regenerating axons in *SOCS3*$^{-/-}$ mice ($N = 6$ per group). Error bars, s.d. Scale bars, 100 μm.

controls. Among 15 genes selected, two encode critical positive mTOR regulators, namely small GTPase Rheb and insulin-like growth factor 1 (IGF1)[20] (Supplementary Figs 8 and 11), suggesting that positive feedback regulation of the mTOR activity in the double mutant may contribute to the enhanced and sustained axon regeneration. The list also includes several axon-growth-related genes, such as for the RNA-binding protein Elavl4 (HuD), the cell adhesion molecules MAM domain-containing glycosylphosphatidylinositol anchor 2 (Mdga2)[21], procadherin beta 9 (Pcdhb9)[22], the axon guidance molecule Unc5D[23] and a cAMP-regulator phosphodiesterase 7B (Pde7b)[24] (Supplementary Figs 8 and 11).

In addition, double deletion may 'enhance' the regeneration-related gene-expression changes that occur poorly or moderately in the single mutants. By the criteria of significant changes ($q > 0.05$, fold change <1.6) for comparisons between the double mutants and wild-type controls, but not between the single mutants and wild-type controls, we revealed the gene set shown in Supplementary Fig. 9a. This includes most of genes shown in Supplementary Fig. 8. Further, it shows the upregulation of several axon-growth-related genes, such as those for the signalling molecule mitogen-activated protein kinase kinase (Map2k4)[25] and the axon transport components dynein component Dync1li2, kinesin family member Kif21a and kinesin-associated protein 3 (Kifap3)[26,27] (Supplementary Fig. 9a, 11). Consistently, pathway analysis indicates that this list is enriched in genes serving cellular functions related to axon growth (Supplementary Fig. 9b).

Other non-exclusive possibilities may also contribute to the synergy of the double deletion. For example, *SOCS3* deletion might regulate certain axon growth-promoting genes that are poorly regulated by *PTEN* single deletion; thus, double deletion allows the actions of both mTOR activity and these genes. We therefore screened for two sets of genes preferentially regulated by *SOCS3* or *PTEN* deletion in the double deletion induced gene alteration (Supplementary Fig. 10). These lists contain several genes related to axon regeneration, but whether any of the above genes show complementary/synergistic functions is still unknown. In addition, Krüppel-like factors KLF4 and KLF6 showed expression changes in opposite directions (although the changes of KLF4 did not reach statistical significance (Supplementary Fig. 11)), consistent with proposed opposite functions of these regeneration regulators[8].

Complementarily, we assessed the expression of a subset of genes in both intact and injured RGCs by *in situ* hybridization. When compared with the expression in intact RGCs, some genes, such as *Elavl4* and *KLF6*, were induced in the mutant(s) after injury (Supplementary Fig. 12a, b), consistent with the model of the activation of axon-growth-related genes in these mutants. However, some other genes, such as axon transport genes *Dync1li2*, *Kif21a* and *Kifap3*, and a transcription factor ZFP40, were maintained in the double-mutant RGCs but downregulated in both wild-type and single mutant RGCs after injury (Supplementary Fig. 12c–f). These results suggested that, in addition to inducing growth-related gene expression, the double

deletion enables injured neurons to maintain their pre-injury physiological states, which might be an important contributing mechanism for the enhanced and sustained axon regeneration.

Together, our experiments reveal an important strategy for achieving sustainable *de novo* axon regrowth in the adult CNS neurons: co-activation of specific protein translations and gene transcriptions by concomitant inactivation of PTEN and SOCS3. Notably, the mTOR increased activity is maintained and phospho-STAT3 levels are increased in adult peripheral sensory neurons after injury[17,28]. Thus, the activation states of these two pathways may underlie the differential regenerative abilities of CNS and PNS neurons. However, deletion of *PTEN* and *SOCS3* is not converting the CNS neurons to a PNS-like state, because *PTEN* is similarly expressed in adult PNS neurons and *SOCS3* is increased during PNS regeneration[17,29]. Nonetheless, enhancing mTOR activity through deletion of *PTEN* or *TSC2* also drastically increases axon re-growth in PNS neurons[29,30], indicating deletion of *PTEN* and *SOCS3* may make an end-run around different growth-suppressive mechanisms. Considering the formidable long distances that regenerating axons must travel in the adult after injury, the synergistic effects of two different pathways suggest a potential solution to this challenge, making the goal of functional recovery more realistic.

METHODS SUMMARY

AAV-Cre injection and optic nerve injury. Adult mice were intravitreally injected with AAV-Cre and/or CNTF to the left eyes. Optic nerve injury and quantifications were done with the methods described previously[1,2].

Purification of RGCs. Seventy-two hours after injury, isolated retinas were incubated in digestion solution, dissociated by gentle trituration and then filtered before FACS sorting.

RNA extraction and microarray. Isolated RNA was subjected to microarray analysis. Data were $\log_2$ transformed at probe level, and the perfect match) model-based expression values were annotated and normalized using dChip. Statistical significance of gene expression differences between groups was determined by Significance Analysis of Microarrays software. After an initial filter of very low expressed genes (average $\log_2$ transformed value <5), a false discovery rate, or q value, less than 0.05 was used to generate the significant gene lists. Functional analyses were performed using the Database for Annotation, Visualization and Integrated Discovery.

Full Methods and any associated references are available in the online version of the paper at www.nature.com/nature.

Received 1 June; accepted 28 September 2011.
Published online 6 November 2011.

1. Park, K. K. *et al.* Promoting axon regeneration in the adult CNS by modulation of the PTEN/mTOR pathway. *Science* **322,** 963–966 (2008).
2. Smith, P. D. *et al.* SOCS3 deletion promotes optic nerve regeneration *in vivo*. *Neuron* **64,** 617–623 (2009).
3. Fawcett, J. Molecular control of brain plasticity and repair. *Prog. Brain Res.* **175,** 501–509 (2009).
4. Filbin, M. T. Recapitulate development to promote axonal regeneration: good or bad approach? *Phil. Trans. R. Soc. B* **361,** 1565–1574 (2006).
5. Fitch, M. T. & Silver, J. CNS injury, glial scars, and inflammation: inhibitory extracellular matrices and regeneration failure. *Exp. Neurol.* **209,** 294–301 (2008).
6. Hellal, F. *et al.* Microtubule stabilization reduces scarring and causes axon regeneration after spinal cord injury. *Science* **331,** 928–931 (2011).
7. Leibinger, M. *et al.* Neuroprotective and axon growth-promoting effects following inflammatory stimulation on mature retinal ganglion cells in mice depend on ciliary neurotrophic factor and leukemia inhibitory factor. *J. Neurosci.* **29,** 14334–14341 (2009).
8. Moore, D. L. *et al.* KLF family members regulate intrinsic axon regeneration ability. *Science* **326,** 298–301 (2009).
9. Winzeler, A. M. *et al.* The lipid sulfatide is a novel myelin-associated inhibitor of CNS axon outgrowth. *J. Neurosci.* **31,** 6481–6492 (2011).
10. Groszer, M. *et al.* Negative regulation of neural stem/progenitor cell proliferation by the Pten tumor suppressor gene *in vivo*. *Science* **294,** 2186–2189 (2001).
11. Mori, H. *et al.* Socs3 deficiency in the brain elevates leptin sensitivity and confers resistance to diet-induced obesity. *Nature Med.* **10,** 739–743 (2004).
12. Fasnacht, N. & Muller, W. Conditional gp130 deficient mouse mutants. *Semin. Cell Dev. Biol.* **19,** 379–384 (2008).
13. Ernst, M. & Jenkins, B. J. Acquiring signalling specificity from the cytokine receptor gp130. *Trends Genet.* **20,** 23–32 (2004).
14. Park, K. K. *et al.* Cytokine-induced SOCS expression is inhibited by cAMP analogue: impact on regeneration in injured retina. *Mol. Cell. Neurosci.* **41,** 313–324 (2009).
15. Park, K., Luo, J. M., Hisheh, S., Harvey, A. R. & Cui, Q. Cellular mechanisms associated with spontaneous and ciliary neurotrophic factor-cAMP-induced survival and axonal regeneration of adult retinal ganglion cells. *J. Neurosci.* **24,** 10806–10815 (2004).
16. Bareyre, F. M. *et al. In vivo* imaging reveals a phase-specific role of STAT3 during central and peripheral nervous system axon regeneration. *Proc. Natl Acad. Sci. USA* **108,** 6282–6287 (2011).
17. Miao, T. *et al.* Suppressor of cytokine signaling-3 suppresses the ability of activated signal transducer and activator of transcription-3 to stimulate neurite growth in rat primary sensory neurons. *J. Neurosci.* **26,** 9512–9519 (2006).
18. Qiu, J., Cafferty, W. B., McMahon, S. B. & Thompson, S. W. Conditioning injury-induced spinal axon regeneration requires signal transducer and activator of transcription 3 activation. *J. Neurosci.* **25,** 1645–1653 (2005).
19. Aaronson, D. S. & Horvath, C. M. A road map for those who don't know JAK-STAT. *Science* **296,** 1653–1655 (2002).
20. Sengupta, S., Peterson, T. R. & Sabatini, D. M. Regulation of the mTOR complex 1 pathway by nutrients, growth factors, and stress. *Mol. Cell* **40,** 310–322 (2010).
21. Joset, P. *et al.* Rostral growth of commissural axons requires the cell adhesion molecule MDGA2. *Neural Develop.* **6,** 22 (2011).
22. Junghans, D., Haas, I. G. & Kemler, R. Mammalian cadherins and protocadherins: about cell death, synapses and processing. *Curr. Opin. Cell Biol.* **17,** 446–452 (2005).
23. Low, K., Culbertson, M., Bradke, F., Tessier-Lavigne, M. & Tuszynski, M. H. Netrin-1 is a novel myelin-associated inhibitor to axon growth. *J. Neurosci.* **28,** 1099–1108 (2008).
24. Hannila, S. S. & Filbin, M. T. The role of cyclic AMP signaling in promoting axonal regeneration after spinal cord injury. *Exp. Neurol.* **209,** 321–332 (2008).
25. Nix, P., Hisamoto, N., Matsumoto, K. & Bastiani, M. Axon regeneration requires coordinate activation of p38 and JNK MAPK pathways. *Proc. Natl Acad. Sci. USA* **108,** 10738–10743 (2011).
26. Hanz, S. & Fainzilber, M. Retrograde signaling in injured nerve–the axon reaction revisited. *J. Neurochem.* **99,** 13–19 (2006).
27. Hoffman, P. N. A conditioning lesion induces changes in gene expression and axonal transport that enhance regeneration by increasing the intrinsic growth state of axons. *Exp. Neurol.* **223,** 11–18 (2010).
28. Park, K. K., Liu, K., Hu, Y., Kanter, J. L. & He, Z. PTEN/mTOR and axon regeneration. *Exp. Neurol.* **223,** 45–50 (2010).
29. Abe, N., Borson, S. H., Gambello, M. J., Wang, F. & Cavalli, V. Mammalian target of rapamycin (mTOR) activation increases axonal growth capacity of injured peripheral nerves. *J. Biol. Chem.* **285,** 28034–28043 (2010).
30. Christie, K. J., Webber, C. A., Martinez, J. A., Singh, B. & Zochodne, D. W. PTEN inhibition to facilitate intrinsic regenerative outgrowth of adult peripheral axons. *J. Neurosci.* **30,** 9306–9315 (2010).

Supplementary Information is linked to the online version of the paper at www.nature.com/nature.

Acknowledgements We thank M. Curry and C. Wang for technical support, H. Sasaki and F. Wang for providing Stat3$^{f/f}$ and Rosa-lox-STOP-lox-Tomato mice. J. Gray, M. Hemberg, J. Choi, J. Ngai and W. Wang for advice on microarray and data analysis, and J. Gray, X. He, T. Schwarz, F. Wang, W. Wang and C. Woolf for reading the manuscript. This study was supported by grants from Wings for Life (to F.S.), Miami Project to Cure Paralysis (to K.K.P.) and NEI (to Z.H.).

Author Contributions F.S, K.K.P., K.Z. and Z.H. conceived and F.S., K.K.P., S.B., G.C. and C.Y. performed the experiments. D.W. and G.F. provided YFP-17 mice. F.S., T.L., B.A.Y. and Z.H. analysed gene array data. F.S., K.K.P. and Z.H. prepared the manuscript.

Author Information Microarray data are deposited in Gene Expression Omnibus under accession number GSE32309. Reprints and permissions information is available at www.nature.com/reprints. The authors declare competing financial interests: details accompany the full-text HTML version of the paper at www.nature.com/nature. Readers are welcome to comment on the online version of this article at www.nature.com/nature. Correspondence and requests for materials should be addressed to Z.H. (Zhigang.he@childrens.harvard.edu).

LETTER

doi:10.1038/nature10590

Experimental infection of bats with *Geomyces destructans* causes white-nose syndrome

Jeffrey M. Lorch[1,2], Carol U. Meteyer[2], Melissa J. Behr[3], Justin G. Boyles[4], Paul M. Cryan[5], Alan C. Hicks[6], Anne E. Ballmann[2], Jeremy T. H. Coleman[7], David N. Redell[8], DeeAnn M. Reeder[9] & David S. Blehert[2]

White-nose syndrome (WNS) has caused recent catastrophic declines among multiple species of bats in eastern North America[1,2]. The disease's name derives from a visually apparent white growth of the newly discovered fungus *Geomyces destructans* on the skin (including the muzzle) of hibernating bats[1,3]. Colonization of skin by this fungus is associated with characteristic cutaneous lesions that are the only consistent pathological finding related to WNS[4]. However, the role of *G. destructans* in WNS remains controversial because evidence to implicate the fungus as the primary cause of this disease is lacking. The debate is fuelled, in part, by the assumption that fungal infections in mammals are most commonly associated with immune system dysfunction[5–7]. Additionally, the recent discovery that *G. destructans* commonly colonizes the skin of bats of Europe, where no unusual bat mortality events have been reported[8–10], has generated further speculation that the fungus is an opportunistic pathogen and that other unidentified factors are the primary cause of WNS[11,12]. Here we demonstrate that exposure of healthy little brown bats (*Myotis lucifugus*) to pure cultures of *G. destructans* causes WNS. Live *G. destructans* was subsequently cultured from diseased bats, successfully fulfilling established criteria for the determination of *G. destructans* as a primary pathogen[13]. We also confirmed that WNS can be transmitted from infected bats to healthy bats through direct contact. Our results provide the first direct evidence that *G. destructans* is the causal agent of WNS and that the recent emergence of WNS in North America may represent translocation of the fungus to a region with a naive population of animals[8]. Demonstration of causality is an instrumental step in elucidating the pathogenesis[14] and epidemiology[15] of WNS and in guiding management actions to preserve bat populations against the novel threat posed by this devastating infectious disease.

To test the ability of *G. destructans* to act as a primary pathogen, we housed healthy little brown bats (*Myotis lucifugus*; $n = 29$) in the laboratory under hibernation conditions and treated them with conidia of *G. destructans* harvested from pure culture. Histological examination of treated bats that died during the course of the experiment showed that lesions diagnostic for WNS were apparent by 83 days after treatment. All treated bats were positive for WNS by histology when the trial was terminated at 102 days after treatment. In contrast, at the end of the experiment, all bats from the negative control group (bats treated identically but not exposed to conidia of *G. destructans*; $n = 34$) were negative for WNS by histology.

We also investigated the potential for WNS to be transmitted from infected to healthy animals by co-housing hibernating bats naturally infected with WNS (collected from an affected hibernaculum and showing clinical signs of the disease; $n = 25$) with healthy bats (contact exposure group; $n = 18$). Eighty-nine per cent of bats in the contact exposure group developed WNS lesions by day 102, demonstrating for the first time that WNS is transmissible. This has important epidemiological and disease management implications, because many of the bat species most commonly impacted by WNS often form tight, occasionally mixed-species clusters during hibernation, facilitating the transfer of fungus among individuals and species. In addition, bat species affected by WNS engage in 'swarming' behaviour at hibernacula just before hibernation. During this time, there is much direct contact between individuals as they participate in a promiscuous mating system[16]. Furthermore, individual bats have been documented to move long distances between hibernacula during this period[17], which may, in part, facilitate the spread of WNS across the landscape.

To determine if WNS could be spread between bats through the air, healthy bats ($n = 36$) were placed in mesh cages in close proximity to (separated by 1.3 cm), but not in direct contact with, the positive control and treated groups. After a period of 102 days, none of the animals exposed to possible airborne conidia from bats with WNS showed histopathological evidence of infection. This may be due to an inability of *G. destructans* conidia to travel through air at levels sufficient to establish infections in neighbouring individuals over the experimental interval or could reflect that conditions within the incubators (for example, airflow patterns and/or static charges) were not conducive to airborne transfer of conidia.

The fungal skin lesions that developed in treated and contact-exposed animals were indistinguishable from those that occurred in the positive control bats (Fig. 1). Additionally, the prevalence of infection was similar between the two groups (Table 1), indicating that the treated group did not develop disease from exposure to an excessively high dose of conidia. Similar disease pathology between groups also indicates that the contact-exposed bats did not develop WNS through exposure to an agent other than *G. destructans*. Histological examination of hearts, intestines, livers, lungs and kidneys from a subset of animals (positive control group $n = 5$, negative control group $n = 3$, treated group $n = 10$, contact exposure group $n = 5$) did not reveal any tissue damage or other signs of infectious processes that might have predisposed the animals to skin infection by *G. destructans*. Furthermore, live *G. destructans* was cultured from the skin of bats confirmed to have WNS lesions. Development of lesions diagnostic for WNS in the absence of other signs of disease provides the first experimental evidence that *G. destructans* is a primary pathogen and causes WNS in healthy bats.

The large-scale mortality seen in wild bat populations with WNS was not observed in the treated or contact exposure groups. Although all of the positive control animals died before the termination of the trial, survivorship ($P = 0.72$) and body mass index (BMI; $P = 0.96$) of the remaining groups did not significantly differ from the negative control group (Fig. 2a). The lack of WNS-related mortality in the treated and contact exposure groups is best explained by the short period of time these groups were exposed to *G. destructans*. On the basis of an analysis of wild bats submitted to the US Geological

[1]Molecular and Environmental Toxicology Center, University of Wisconsin-Madison, Madison, Wisconsin 53706, USA. [2]National Wildlife Health Center, US Geological Survey, Madison, Wisconsin 53711, USA. [3]Wisconsin Veterinary Diagnostic Laboratory, Madison, Wisconsin 53706, USA. [4]Department of Ecology and Evolutionary Biology, University of Tennessee, Knoxville, Tennessee 37996, USA. [5]Fort Collins Science Center, US Geological Survey, Fort Collins, Colorado 80526, USA. [6]New York Department of Environmental Conservation, Albany, New York 12233, USA. [7]US Fish and Wildlife Service, Hadley, Massachusetts 01035, USA. [8]Wisconsin Department of Natural Resources, Madison, Wisconsin 53707, USA. [9]Department of Biology, Bucknell University, Lewisburg, Pennsylvania 17837, USA.

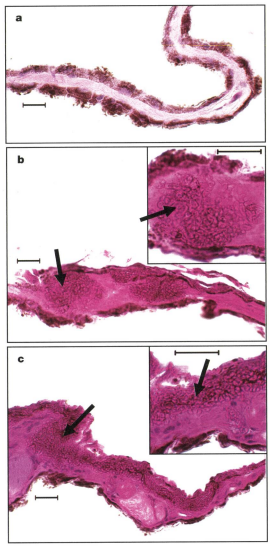

Figure 1 | Histological sections of representative wing membranes (periodic acid-Schiff stain). **a**, Normal wing membrane of a healthy bat from the negative control group showing no signs of fungal growth. **b**, **c**, WNS lesions, including invasion of the underlying connective tissue by fungal hyphae (arrows), are visible in sections from a bat with WNS from the positive control group (**b**) and a bat from the treated group that developed WNS after experimental exposure to *G. destructans* (**c**). Insets are higher magnification images and scale bars indicate 20 μm.

Survey (USGS)–National Wildlife Health Center (NWHC) for diagnostic testing (January 2008 to June 2011), WNS lesions have seasonally first been detected during autumn (late September), just before the start of long-term hibernation; major mortality events caused by WNS have seasonally not been observed among wild bats until the end of January (Fig. 2b). These data indicate that mortality

Table 1 | Development of WNS in experimentally infected bats

Treatment group	Number with WNS lesions present	Number with no WNS lesions	Total	Per cent infected
Negative control	0	34	34	0
Treated	29	0	29	100
Contact exposure	16	2	18	89
Airborne exposure	0	36	36	0
Positive control	25	0	25	100

The data show prevalence of WNS-associated fungal infections established in groups of healthy little brown bats inoculated with conidia of *G. destructans* from pure culture or exposed to bats known to have WNS (positive control group). Infection status was determined by histological examination of the wing.

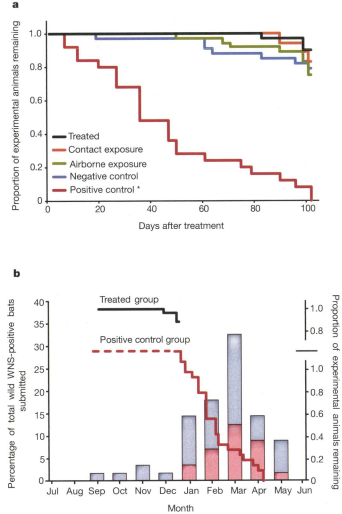

Figure 2 | Survival curves. **a**, Survival curves for the treated ($n = 29$), contact exposure ($n = 18$), airborne exposure ($n = 36$), negative control ($n = 34$) and positive control ($n = 25$) groups. Bats in the positive control group, which consisted of animals naturally infected with WNS at the time they were collected, exhibited significantly decreased survival (asterisk) relative to the other groups ($P < 0.001$). Survival among bats of the remaining groups did not differ significantly from one another ($P = 0.72$). **b**, Percentage of bats submitted by month (January 2008 to June 2011) to the USGS–National Wildlife Health Center that tested positive for WNS ($n = 54$ submission events). The blue bars represent submissions that were not associated with major mortality events; the red bars depict submissions associated with high mortality. Annually, WNS-associated mortality events are first observed in January; the number of submissions involving mortality events for a given month peaks in March. Assuming the positive control bats were first exposed to *G. destructans* in late September, mortality due to WNS did not occur in the laboratory until approximately 120 days after exposure, consistent with what is observed in free-ranging wild bats (the dotted line represents the exposure period in the wild before the animals were collected for this study). The duration of this infection trial (102 days) was insufficient to observe WNS-associated mortality in the treated and contact exposure groups (the treated group mortality curve is shifted such that duration of exposure corresponds to that of the positive control group; contact and airborne exposure group mortality curves are not shown).

from WNS does not manifest until approximately 120 days after bats enter hibernation and assume a cold physiological state conducive to proliferation of *G. destructans*; mortality subsequently peaks about 180 days after bats first enter hibernacula (in the month of March). Assuming that initial exposure of positive-control bats to the fungus occurred in late September, these animals survived about 110 to 205 days after exposure, with approximately 50% having died by the

150-day mark. The treated and contact-exposure bats were only exposed to *G. destructans* for 102 days. Thus, the experiment was terminated before the disease had progressed to the degree that mortality would be expected among treated and contact-exposed animals.

Our work demonstrates experimental infection of little brown bats by *G. destructans* with subsequent development of WNS in the absence of underlying health conditions. It follows that the recent widespread detection of *G. destructans* in Europe without apparent detriment to bat populations indicates that the fungus may be endemic to that region where it co-evolved with continental bat species[8,10]. In North America, the data indicate that WNS originated at a single site[1,18] with high tourist traffic, consistent with the introduction of an exotic species[19]. Thus, the pathological effects caused by *G. destructans* in North American bats may reflect exposure of a naive host population to a novel pathogen. Future studies are needed to investigate the origin of *G. destructans* in North America and to elucidate differences in physiology and behaviour between North American and European bats that might account for disparate disease outcomes observed among the two continents.

Fungal pathogens have the unique capacity to drive host populations to extinction because of their ability to survive in host-free environments[2]. Given the high mortality rate and speed at which WNS has spread, the disease has the potential to decimate North American bat populations and cause species extinctions[20] similar to those documented for amphibians affected by chytridiomycosis[21]. Advancement of WNS research and management has been limited by uncertainty over the causative agent of this disease. With the causative agent now conclusively identified through fulfilment of Koch's postulates, future research efforts can focus on mitigating the effects of WNS before hibernating bat populations suffer losses beyond the point of recovery.

METHODS SUMMARY

Little brown bats (*Myotis lucifugus*) naturally infected with WNS (positive control group; $n = 25$) were collected from a hibernaculum in New York. Healthy (based upon body condition and histopathology findings) little brown bats were collected from a hibernaculum in Wisconsin outside of the known range of WNS. Healthy bats were divided into four groups: negative control ($n = 34$), treated ($n = 29$), contact exposure ($n = 18$) and airborne exposure ($n = 36$). Conidia of *G. destructans* (5×10^5 conidia suspended in 20 µl of phosphate buffered saline solution containing 0.5% Tween 20 (PBST)) were applied to one of the wings of bats in the treated group, and an additional 5×10^5 conidia were applied to the fur between the eye and ear. Negative control bats were treated identically with PBST lacking conidia. Animals were maintained in mesh enclosures (Supplementary Fig. 1) under conditions approximating bat hibernacula for 102 days. The experimental end point was set to correspond with the timing by which wild bats naturally emerge from hibernation. Infection status was determined by histological examination of the muzzle and skin from each wing[4], and *G. destructans* was re-isolated from wing skin as previously described[22]. The identity of fungal isolates resembling *G. destructans* was confirmed by PCR amplification/double-stranded sequence analysis of the rRNA gene internal transcribed spacer[23].

Full Methods and any associated references are available in the online version of the paper at www.nature.com/nature.

Received 17 August; accepted 22 September 2011.
Published online 26 October 2011.

1. Blehert, D. S. *et al.* Bat white-nose syndrome: an emerging fungal pathogen? *Science* **323,** 227 (2009).
2. Turner, G. G., Reeder, D. M. & Coleman, J. T. H. A five-year assessment of mortality and geographic spread of white-nose syndrome in North American bats and a look to the future. *Bat Res. News* **52,** 13–27 (2011).
3. Gargas, A., Trest, M. T., Christensen, M., Volk, T. J. & Blehert, D. S. *Geomyces destructans* sp. nov. associated with bat white-nose syndrome. *Mycotaxon* **108,** 147–154 (2009).
4. Meteyer, C. U. *et al.* Histopathologic criteria to confirm white-nose syndrome in bats. *J. Vet. Diagn. Invest.* **21,** 411–414 (2009).
5. Casadevall, A. Fungal virulence, vertebrate endothermy, and dinosaur extinction: is there a connection? *Fungal Genet. Biol.* **42,** 98–106 (2005).
6. Blanco, J. L. & Garcia, M. E. Immune response to fungal infections. *Vet. Immunol. Immunopathol.* **125,** 47–70 (2008).
7. Maschmeyer, G., Calandra, T., Singh, N., Wiley, J. & Perfect, J. Invasive mould infections: a multi-disciplinary update. *Med. Mycol.* **47,** 571–583 (2009).
8. Wibbelt, G. *et al.* White-nose syndrome fungus (*Geomyces destructans*) in bats, Europe. *Emerg. Infect. Dis.* **16,** 1237–1242 (2010).
9. Martínková, N. *et al.* Increasing incidence of *Geomyces destructans* fungus in bats from the Czech Republic and Slovakia. *PLoS ONE* **5,** e13853 (2010).
10. Puechmaille, S. J. *et al.* Pan-European distribution of white-nose syndrome fungus (*Geomyces destructans*) not associated with mass mortality. *PLoS ONE* **6,** e19167 (2011).
11. Turner, G. G. & Reeder, D. M. Update of white-nose syndrome in bats, September 2009. *Bat Res. News* **50,** 47–53 (2009).
12. Puechmaille, S. J. *et al.* White-nose syndrome fungus (*Geomyces destructans*) in bat, France. *Emerg. Infect. Dis.* **16,** 290–293 (2010).
13. Koch, R. Die aetiologie der tuberkulose. *Mitt. Kaiser. Gesundh.* **2,** 1–88 (1884).
14. Cryan, P. M., Meteyer, C. U., Boyles, J. G. & Blehert, D. S. Wing pathology of white-nose syndrome in bats suggests life-threatening disruption of physiology. *BMC Biol.* **8,** 135 (2010).
15. Foley, J., Clifford, D., Castle, K., Cryan, P. M. & Ostfeld, R. S. Investigating and managing the rapid emergence of white-nose syndrome, a novel, fatal, infectious disease of hibernating bats. *Conserv. Biol.* **25,** 223–231 (2011).
16. Thomas, D. W., Fenton, M. B. & Barclay, M. R. Social behavior of the little brown bat, *Myotis lucifugus*. *Behav. Ecol. Sociobiol.* **6,** 129–136 (1979).
17. Fenton, M. B. Summer activity of *Myotis lucifugus* (Chiroptera:Vespertilionidae) at hibernacula in Ontario and Quebec. *Can. J. Zool.* **47,** 597–602 (1969).
18. Rajkumar, S. S. *et al.* Clonal genotype of *Geomyces destructans* among bats with white-nose syndrome, New York, USA. *Emerg. Infect. Dis.* **17,** 1273–1276 (2011).
19. Desprez-Loustau, M. L. *et al.* The fungal dimension of biological invasions. *Trends Ecol. Evol.* **22,** 472–480 (2007).
20. Frick, W. F. *et al.* An emerging disease causes regional population collapse of a common North American bat species. *Science* **329,** 679–682 (2010).
21. Skerratt, L. F. *et al.* Spread of chytridiomycosis has caused the rapid global decline and extinction of frogs. *EcoHealth* **4,** 125–134 (2007).
22. Lorch, J. M. *et al.* Rapid polymerase chain reaction diagnosis of white-nose syndrome in bats. *J. Vet. Diagn. Invest.* **22,** 224–230 (2010).
23. White, T. J., Bruns, T., Lee, S. & Taylor, J. Amplification and direct sequencing of fungal ribosomal RNA genes for phylogenetics. In *PCR Protocols: A Guide to Methods and Applications* 315–322 (Academic Press, 1990).

Supplementary Information is linked to the online version of the paper at www.nature.com/nature.

Acknowledgements Financial support for this project was provided by the US Geological Survey, the US Fish and Wildlife Service, Bat Conservation International, and the Indiana State University Center for North American Bat Research and Conservation. Use of trade, product, or firm names is for descriptive purposes only and does not imply endorsement by the US Government. We acknowledge E. Buckles, S. Darling and T. Tomasi for discussions during the development of this project. We thank N. Keller for comments during the preparation of this manuscript. We also thank J. P. White, R. Dusek, A. Klein, L. Leppert, K. Schuler, C. L. White and NWHC Animal Care Staff for their help with set-up and maintenance of animals, and D. Berndt, L. Muller, A. Pike and M. Verant for their assistance during necropsies. We thank X. Yu for help with statistical analyses.

Author Contributions D.S.B., A.C.H., P.M.C. and D.M.R. designed the study. A.C.H., J.T.H.C. and D.N.R. collected wild animals for the study. J.M.L., D.S.B., C.U.M., M.J.B., J.G.B., A.C.H., A.E.B., J.T.H.C., D.N.R. and D.M.R. performed the experiment and/or assisted to collect samples upon completion. C.U.M. and M.J.B. read and interpreted histopathology. J.M.L. and J.G.B. analysed the experimental data. A.E.B. compiled data on wild bats submitted to the NWHC for diagnostic testing. J.M.L. wrote the manuscript and all co-authors provided input. D.S.B. supervised data analyses and edited the manuscript.

Author Information Reprints and permissions information is available at www.nature.com/reprints. The authors declare no competing financial interests. Readers are welcome to comment on the online version of this article at www.nature.com/nature. Correspondence and requests for materials should be addressed to D.S.B. (dblehert@usgs.gov).

LETTER

doi:10.1038/nature10623

HIV-1 restriction factor SAMHD1 is a deoxynucleoside triphosphate triphosphohydrolase

David C. Goldstone[1]*, Valerie Ennis-Adeniran[1]*, Joseph J. Hedden[1], Harriet C. T. Groom[2], Gillian I. Rice[3], Evangelos Christodoulou[1], Philip A. Walker[1], Geoff Kelly[4], Lesley F. Haire[1], Melvyn W. Yap[2], Luiz Pedro S. de Carvalho[5], Jonathan P. Stoye[2], Yanick J. Crow[3], Ian A. Taylor[1] & Michelle Webb[3]

SAMHD1, an analogue of the murine interferon (IFN)-γ-induced gene *Mg11* (ref. 1), has recently been identified as a human immunodeficiency virus-1 (HIV-1) restriction factor that blocks early-stage virus replication in dendritic and other myeloid cells[2,3] and is the target of the lentiviral protein Vpx, which can relieve HIV-1 restriction[4–7]. SAMHD1 is also associated with Aicardi–Goutières syndrome (AGS), an inflammatory encephalopathy characterized by chronic cerebrospinal fluid lymphocytosis and elevated levels of the antiviral cytokine IFN-α[8]. The pathology associated with AGS resembles congenital viral infection, such as transplacentally acquired HIV. Here we show that human SAMHD1 is a potent dGTP-stimulated triphosphohydrolase that converts deoxynucleoside triphosphates to the constituent deoxynucleoside and inorganic triphosphate. The crystal structure of the catalytic core of SAMHD1 reveals that the protein is dimeric and indicates a molecular basis for dGTP stimulation of catalytic activity against dNTPs. We propose that SAMHD1, which is highly expressed in dendritic cells, restricts HIV-1 replication by hydrolysing the majority of cellular dNTPs, thus inhibiting reverse transcription and viral complementary DNA (cDNA) synthesis.

SAMHD1 was originally identified in a human dendritic cell cDNA library as an orthologue of the mouse IFN-γ-induced gene *Mg11* (ref. 1). SAMHD1 is expressed at basal levels in a large number of tissues[1] but is highly expressed in dendritic cells and other cells of the myeloid lineage[2,9] (http://biogps.gnf.org/#goto=genereport&id=25939). However, although it is mutated in patients with AGS and upregulated in response to viral infection[10,11], the cellular functions of SAMHD1 are unclear; although a role as a negative regulator of the innate immune response to interferon stimulatory DNA (ISD) has been proposed[8]. More recently, it has been demonstrated that SAMHD1 is a restriction factor that blocks the early stages of HIV-1 replication in dendritic cells[2]. To understand the mechanism of HIV-1 restriction we have characterized its enzymatic activity and determined the crystal structure of the catalytic core of SAMHD1 (residues 120–626).

Given the known nucleic acid metabolising functions of proteins associated with AGS[12–14] and given that SAMHD1 contains an HD motif, which have been proposed to have phosphohydrolase activities[15], we investigated the potential hydrolytic activity of the protein. SAMHD1(120–626) (hereafter SAMHD1c) was incubated with nucleotides and/or nucleic acid substrates. The products of nucleotide hydrolysis were analysed by anion-exchange high-performance liquid chromatography (HPLC) and nuclease activity directed against nucleic acid polymers was assessed using gel electrophoresis. The chromatograms produced from activity assays testing potential substrates are shown for individual deoxynucleoside triphosphates (Fig. 1a–d) and for nucleoside triphosphates and single-stranded (ss)DNA, double-stranded (ds)DNA and RNA (Supplementary Figs 1

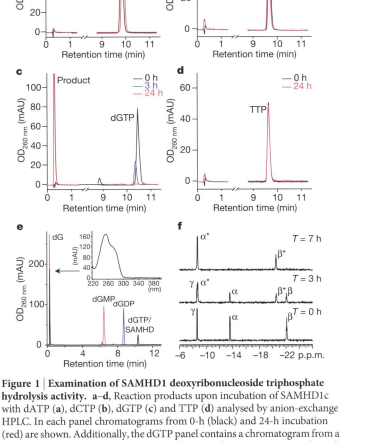

Figure 1 | Examination of SAMHD1 deoxyribonucleoside triphosphate hydrolysis activity. a–d, Reaction products upon incubation of SAMHD1c with dATP (**a**), dCTP (**b**), dGTP (**c**) and TTP (**d**) analysed by anion-exchange HPLC. In each panel chromatograms from 0-h (black) and 24-h incubation (red) are shown. Additionally, the dGTP panel contains a chromatogram from a 3-h incubation (blue). The hydrolysis product that elutes at 0.5 min is indicated. **e**, Identification of the hydrolysis product from the dGTP reaction. Chromatograms of individual standards of deoxyguanosine (red), dGMP (magenta) and dGDP (blue) are shown together with that of a 3-h incubation of SAMHD1c with dGTP (black). Inset, ultraviolet/visible-light spectrum recorded during elution of the SAMHD1/dGTP product peak co-eluting with deoxyguanosine. **f**, Analysis of SAMHD1c/dGTP hydrolysis by ^{31}P NMR spectroscopy after 0, 3 and 7 h of incubation. Assigned ^{31}P resonances from of the α-, β- and γ-phosphate of dGTP and α- and β-phosphate of the triphosphate product species are labelled. Product resonances are marked with asterisks.

[1]Division of Molecular Structure, MRC National Institute for Medical Research, the Ridgeway, Mill Hill, London NW7 1AA, UK. [2]Division of Virology, MRC National Institute for Medical Research, the Ridgeway, Mill Hill, London NW7 1AA, UK. [3]Genetic Medicine, University of Manchester, Manchester Academic Health Science Centre, Central Manchester Foundation Trust University Hospitals, Manchester M13 9PT, UK. [4]MRC Biomedical NMR Centre, National Institute for Medical Research, the Ridgeway, Mill Hill, London NW7 1AA, UK. [5]Division of Mycobacterial Research, MRC National Institute for Medical Research, the Ridgeway, Mill Hill, London NW7 1AA, UK.
*These authors contributed equally to this work.

and 2, respectively). These data reveal that SAMHD1 rapidly hydrolyses dGTP but not dATP, dCTP and TTP (5-methyl deoxyuridine triphosphate) (Fig. 1c), has no nuclease activity against the three nucleic acid substrates and does not hydrolyse nucleoside triphosphates. Thus SAMHD1 is a deoxyguanosine triphosphate triphosphohydrolase.

To determine the products of dGTP hydrolysis by SAMHD1c, two approaches were taken. First, the reaction products after a 3-h incubation of SAMHD1c with dGTP were again characterized by anion-exchange HPLC (Fig. 1e). The reaction product co-elutes with the deoxyguanosine standard, and analysis of the ultraviolet/visible-light absorption spectrum confirms the product as deoxyguanosine. Second, the ^{31}P NMR spectrum of 0, 3 and 7-h dGTP incubation with SAMHD1 (Fig. 1f) shows that the SAMHD1c hydrolysis reaction produces triphosphate with no indication of sequential release of monophosphate. Taken together, these data demonstrate that SAMHD1c possesses an unusual triphosphohydrolase activity that rapidly converts dGTP to guanosine and inorganic triphosphate, which, to our knowledge, has not been reported in eukaryotes and has only been partially characterized in some bacteria[16–18]. Release of triphosphate combined with subsequent turnover to inorganic phosphate by cellular exopolyphosphatases and pyrophosphatases would strongly drive the triphosphohydrolase reaction, leading to substantial reductions in the cellular dNTP pool.

Intriguingly, although assays carried out using individual deoxynucleoside and nucleoside triphosphates suggested that SAMHD1 only shows dGTP triphosphohydrolase activity, when all four deoxynucleoside triphosphates are incubated together it is apparent that all of the deoxynucleoside triphosphates are rapidly hydrolysed (Fig. 2a). To understand the basis of this more promiscuous activity, pairs of deoxynucleoside triphosphates were incubated with SAMHD1c. In this case hydrolysis of dATP, dCTP and TTP occurs only when dGTP is also present (Fig. 2b–f), suggesting that in addition to being a preferred substrate, dGTP also activates the enzyme to hydrolyse the other dNTPs. To examine if dGTP could also activate the enzyme to hydrolyse NTPs, additional reactions were carried out (Supplementary Fig. 3), which showed that only hydrolysis of the dGTP occurs, indicating that the enzyme is not able to utilize NTPs as substrates. Thus SAMHD1 has strict specificity for deoxynucleotides, and dGTP is both a substrate and an activator of the enzyme against the other dNTPs.

The crystal structure of SAMHD1c was solved by single-wavelength anomalous dispersion (SAD) (Supplementary Table 1), and is represented in Fig. 3. The molecule comprises 19 α-helices (α1–α19) and 9 β-strands (β1–β9) arranged in a mixed α/β fold (Supplementary Fig. 4) and comprises a large domain (residues 120–451) containing a major and minor lobe, together with a smaller carboxy-terminal region (residues 455–583). The dimer interface buries approximately 2,000 Å^2 of surface (Supplementary Fig. 5) and, consistent with the crystal structure, our solution hydrodynamic data (Supplementary Fig. 6) demonstrate that SAMHD1 is largely dimeric in solution.

Although we have been unable to co-crystallize SAMHD1c with substrates, a phosphate ion from the crystallization buffer is found close to the sequence-conserved HD motif and co-ordinated to a zinc ion. This locates the active site to a cavity between the major and minor lobes that extends beneath the C-terminal region (Fig. 3 and Supplementary Fig. 7). The catalytic centre lies at the bottom of the cavity and contains the zinc ion together with the coordinated phosphate group and surrounding aspartate, histidine and arginine side chains (Fig. 3). The zinc ion is coordinated by the side chains of His 206 and Asp 207, a phosphate oxygen and the side chains of His 167 and Asp 311. The side chains of the two zinc coordinating aspartic acid residues, 207 and 311, also form hydrogen bonds with other phosphate oxygens, thus extending the linkage between the zinc ion and phosphate ion. The phosphate also forms salt bridges with the side chains of four basic residues adjacent to the active site, Arg 164 and histidine residues at positions 210, 215 and 233 as well as hydrogen bonding to a water molecule. We believe the position of the bound phosphate is

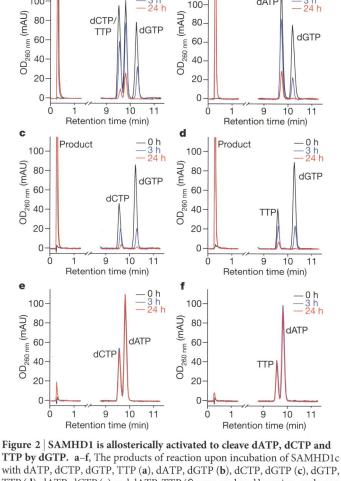

Figure 2 | SAMHD1 is allosterically activated to cleave dATP, dCTP and TTP by dGTP. a–f, The products of reaction upon incubation of SAMHD1c with dATP, dCTP, dGTP, TTP (**a**), dATP, dGTP (**b**), dCTP, dGTP (**c**), dGTP, TTP (**d**), dATP, dCTP (**e**) and dATP, TTP (**f**) were analysed by anion-exchange HPLC. In each panel chromatograms produced from 0 h (black), 3 h (blue) and 24 h (red) of incubation are shown. Peaks corresponding to nucleoside triphosphates elute in the order C/T, A, G between 9 and 11 min.

significant, as its close association with the zinc ion and its proximity to the HD catalytic motif helps to define the active site and serves as a marker for the position of the α-nucleotidyl phosphate.

Comparison of the SAMHD1c structure with a related HD protein from *Aquifex aeolicus* (PDB code 2HEK) suggests a mechanism for the allosteric activation of the enzyme by dGTP (Supplementary Fig. 8). The 2HEK dimer interface incorporates two nucleotide-binding sites, each containing GDP. Examination of the residues that interact with the guanine base in 2HEK reveals that they equate to the conserved residues Asp 137, Gln 142, Arg 145 and Arg 451 in SAMHD1. This analysis strongly suggests the location of the allosteric nucleotide-binding sites in SAMHD1 and enables us to model guanine nucleotides into the SAMHD1 structure (Fig. 3). The resulting model shows that Asp 137, Gln 142 and Arg 145 are likely to be the residues that recognize the base edge, accounting for guanine selectivity at the allosteric sites of SAMHD1. Gln 142 and Arg 145 are located on the same face of α2 whereas Asp 137 is in the preceding loop (Fig. 3). Arg 143 neighbours both Gln 142 and Arg 145 but is located on the opposing face of the α2 helix where its side chain projects into the active site and is hydrogen bonded to the main-chain carbonyls of Leu 208 and His 210. In this way the presence of bound dGTP in the allosteric site is likely to alter the environment and thus catalytic properties of the enzyme's active site. Importantly, several AGS mutations also cluster around this proposed allosteric site (Arg145Gln, Arg143Cys, Arg143His and Gly209Ser) and we propose that they cause loss of SAMHD1 function by interfering with the allosteric activation mechanism. To test this model, alanine

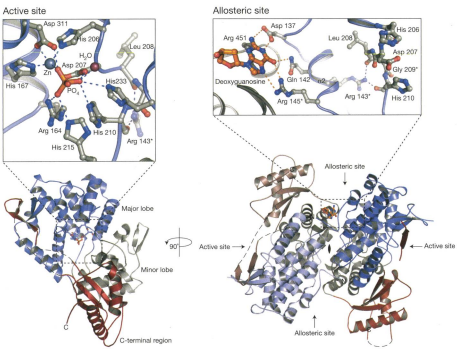

Figure 3 | Crystal structure of the extended HD domain of human SAMHD1. Ribbon representation of the SAMHD1 dimer with the major lobe (blue), minor lobe (grey) and C-terminal region (red). The SAMHD1 active site is located at the intersection of helices α4, α5, α7 and α11 in a cavity on the face of the monomer. Residues coordinating the active-site zinc and phosphate are shown as a stick representation. An expanded view of the allosteric site at the dimer interface is shown. Deoxyguanosine has been modelled into the site by comparison with 2HEK. Potential hydrogen bonds are represented as dashed orange lines. Residues on opposing sides of helix α2 link bound deoxyguanosine to residues in the active site of SAMHD1. Asterisks indicate the residues where mutations are found in AGS patients.

substitution mutants were made at residues in the allosteric and catalytic sites of SAMHD1 as well as the AGS mutation Arg145Gln. Analysis of the catalytic activity of these substitution mutants (Supplementary Table 2) revealed that mutations at 137 and 145 in the allosteric site abolished SAMHD1 hydrolysis activity entirely whereas alanine substitution at Gln 142 resulted in a fivefold reduction in activity. Similarly, mutations in the active site at residues 206–207, 311 and 164 abolished activity, and substitution of His 233 by alanine resulted in a sixfold reduction in the rate of dGTP-activated TTP hydrolysis. Further support for the role of dGTP at the allosteric binding sites comes from sedimentation velocity analysis, which reveals that the presence of dGTP promotes the formation of the dimer (Supplementary Fig. 9).

The other proteins that have been identified in which mutations are associated with AGS are TREX1 and the three constituent subunits of RNase H2 (refs 8, 19, 20). Both TREX1 and RNase H2 have nucleic acid metabolising functions[12–14] and it has been proposed that TREX1 functions in the clearing of reverse transcripts produced from endogenous retroviral elements[21]. We show that SAMHD1 activity is probably associated with degradation of DNA precursors rather than polymeric nucleic acids. However, considering the same human disease phenotype is associated with mutations in either, SAMHD1 and TREX1 activities might act to control synthesis as well as degradation of cytosolic nucleic acids derived from endogenous retroelements. Moreover, it is proposed that the accumulation of cytosolic ssDNA resulting from loss of TREX1 function is the cause of the autoimmunity observed in AGS[21]. Similarly, loss of a SAMHD1 function, which would otherwise inhibit endogenous reverse transcription by limiting the dNTP pools, would also result in a build-up of cytosolic DNA and trigger the inappropriate interferon response reported in AGS (Fig. 4a, b).

The pattern of SAMHD1 expression in cells is also likely to be important in exogenous virus infection. Although basal levels of SAMHD1 expression are observed in a variety of organs and tissues, it is highly expressed in the myeloid-derived cells in which HIV-1 is restricted, including dendritic cells, monocytes and, to a lesser extent, macrophages[9] (http://biogps.gnf.org/#goto=genereport&id=25939). In contrast, SAMHD1 is not expressed in HIV-1-permissive T-cell lines[2]. Importantly, the concentration of the dNTP pool in non-permissive cells is low, 40–70 nM in macrophages compared to 1.5–16 μM in peripheral blood mononuclear cells (PBMCs)[22,23]. Further, upon phorbal 12-myristate 13-acetate (PMA)-induced differentiation of THP-1 cells, the TTP concentration is reduced, and when the SAMHD1 expression level is increased, the TTP level is reduced further (Supplementary Fig. 10). In addition, HIV-1 variants with reverse transcriptase that has reduced dNTP binding affinity are incapable of replication in macrophages[24]. The combination of high SAMHD1

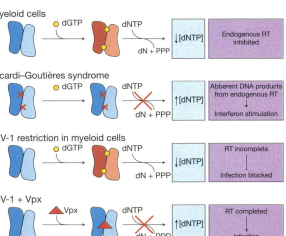

Figure 4 | Model for SAMHD1 function. a, Dimeric inactive SAMHD1 (blue) binds dGTP at the dimer interface. Activated SAMHD1 (red) catalyses the cleavage of dNTPs into the composite deoxynucleoside and inorganic triphosphate. The deoxynucleotide pool is suppressed and endogenous reverse transcriptase (RT) activity is inhibited. **b**, AGS mutations in the allosteric binding site of SAMHD1 prevent dGTP binding or allosteric activation rendering the protein inactive. As a result, deoxynucleotide levels rise and aberrant DNA products arising from reverse transcription of endogenous retroviruses accumulate within the cytoplasm, triggering the inappropriate production of interferon observed in AGS. **c**, In HIV-1-infected dendritic cells SAMHD1 activity suppresses the deoxynucleotide pool, inhibiting reverse transcriptase and blocking infection. **d**, In the presence of Vpx, SAMHD1 is recruited by the DDB–CUL4–DCAF1 E3 ubiquitin ligase complex and targeted to the proteasome for degradation. Control on the dNTP pool is released and sufficient dNTPs are available for reverse transcription to be completed, releasing the HIV-1 block.

expression with low dNTP pool concentration in cells that restrict HIV-1 links powerfully to our finding that SAMHD1 is a potent deoxynucleoside triphosphate triphosphohydrolase. The observation that the lentiviral accessory protein Vpx can restore HIV-1 replication in dendritic and other myeloid cells by targeting SAMHD1 for proteasomal degradation[2,4–7] also lends further weight to this argument (Fig. 4c, d). However, paradoxically, SAMHD1-mediated restriction may not be beneficial for the host, as *in vitro* studies indicate that Vpx rescue of HIV-1 infection actually results in increased maturation of dendritic cells[25]. This raises the possibility of an enhanced immune response *in vivo* in individuals with low SAMHD1 activity.

METHODS SUMMARY

SAMHD1c was expressed in *E. coli* strain BL21 (DE3) and purified using streptactin affinity and size-exclusion chromatography. For structure determination selenium was incorporated into the protein by supplementing defined culture media with seleno-methionine. Products of nucleic acid hydrolysis by SAMHD1c were analysed by gel electrophoresis using 15% polyacrylamide gels for DNA substrates and 1.5% agarose gel for RNA substrates. Nucleotide hydrolysis reactions were analysed by anion-exchange HPLC using a DNA-PAC100 (4×50 mm) column (Dionex) and ^{31}P NMR. Spectra were recorded at 25 °C on a 600 MHz Varian Inova spectrometer using a broadband X-nucleus detection probe. Solution oligomerization state was analysed using on-line size-exclusion chromatography coupled to multi-angle laser light scattering (SEC-MALLS) and sedimentation velocity/equilibrium. For SEC-MALLS scattered light intensities were recorded using a DAWN-HELEOS laser photometer and protein concentration was measured using an OPTILAB-rEX differential refractometer. Weight-averaged molecular masses were determined from the combined data using ASTRA software (Wyatt Technology). Sedimentation velocity/equilibrium experiments were performed in a Beckman XL-I analytical ultracentrifuge. Velocity data were analysed using the program SEDFIT[26] and equilibrium data were analysed using the program SEDPHAT[27]. Protein crystals were grown in 20% PEG3350, 0.1 M Na_2HPO_4 by micro-seeding and snap frozen with the addition of 20% glycerol as cryoprotectant. X-ray diffraction data were collected at the Diamond Light Source and processed using the HKL suite[28]. The structure was determined by SAD and refined using methods implemented in Phenix[29]. Structure figures were generated using PyMOL (http://pymol.sourceforge.net/). For cellular TTP quantification, THP-1 cells were transduced with codon-optimized SAMHD1 and parental and transduced cell lines differentiated by PMA treatment. TTP were isolated from both undifferentiated and differentiated cells by methanol extraction and quantified using a fluorescence-based primer extension assay[30].

Full Methods and any associated references are available in the online version of the paper at www.nature.com/nature.

Received 7 June; accepted 11 October 2011.
Published online 6 November 2011.

1. Li, N., Zhang, W. & Cao, X. Identification of human homologue of mouse IFN-γ induced protein from human dendritic cells. *Immunol. Lett.* **74,** 221–224 (2000).
2. Laguette, N. *et al.* SAMHD1 is the dendritic- and myeloid-cell-specific HIV-1 restriction factor counteracted by Vpx. *Nature* **474,** 654–657 (2011).
3. Hrecka, K. *et al.* Vpx relieves inhibition of HIV-1 infection of macrophages mediated by the SAMHD1 protein. *Nature* **474,** 658–661 (2011).
4. Goujon, C. *et al.* SIVSM/HIV-2 Vpx proteins promote retroviral escape from a proteasome-dependent restriction pathway present in human dendritic cells. *Retrovirology* **4,** 2 (2007).
5. Kaushik, R., Zhu, X., Stranska, R., Wu, Y. & Stevenson, M. A cellular restriction dictates the permissivity of nondividing monocytes/macrophages to lentivirus and gammaretrovirus infection. *Cell Host Microbe* **6,** 68–80 (2009).
6. Srivastava, S. *et al.* Lentiviral Vpx accessory factor targets VprBP/DCAF1 substrate adaptor for cullin 4 E3 ubiquitin ligase to enable macrophage infection. *PLoS Pathog.* **4,** e1000059 (2008).
7. Bergamaschi, A. *et al.* The human immunodeficiency virus type 2 Vpx protein usurps the CUL4A-DDB1^{DCAF1} ubiquitin ligase to overcome a postentry block in macrophage infection. *J. Virol.* **83,** 4854–4860 (2009).
8. Rice, G. I. *et al.* Mutations involved in Aicardi–Goutières syndrome implicate SAMHD1 as regulator of the innate immune response. *Nature Genet.* **41,** 829–832 (2009).
9. Wu, C. *et al. BioGPS*: an extensible and customizable portal for querying and organizing gene annotation resources. *Genome Biol.* **10,** R130 (2009).
10. Prehaud, C., Megret, F., Lafage, M. & Lafon, M. Virus infection switches TLR-3-positive human neurons to become strong producers of beta interferon. *J. Virol.* **79,** 12893–12904 (2005).
11. Hartman, Z. C. *et al.* Adenovirus infection triggers a rapid, MyD88-regulated transcriptome response critical to acute-phase and adaptive immune responses *in vivo*. *J. Virol.* **81,** 1796–1812 (2007).
12. Lindahl, T., Barnes, D. E., Yang, Y. G. & Robins, P. Biochemical properties of mammalian TREX1 and its association with DNA replication and inherited inflammatory disease. *Biochem. Soc. Trans.* **37,** 535–538 (2009).
13. Rydberg, B. & Game, J. Excision of misincorporated ribonucleotides in DNA by RNase H (type 2) and FEN-1 in cell-free extracts. *Proc. Natl Acad. Sci. USA* **99,** 16654–16659 (2002).
14. Qiu, J., Qian, Y., Frank, P., Wintersberger, U. & Shen, B. *Saccharomyces cerevisiae* RNase H(35) functions in RNA primer removal during lagging-strand DNA synthesis, most efficiently in cooperation with Rad27 nuclease. *Mol. Cell. Biol.* **19,** 8361–8371 (1999).
15. Aravind, L. & Koonin, E. V. The HD domain defines a new superfamily of metal-dependent phosphohydrolases. *Trends Biochem. Sci.* **23,** 469–472 (1998).
16. Kondo, N. *et al.* Structure of dNTP-inducible dNTP triphosphohydrolase: insight into broad specificity for dNTPs and triphosphohydrolase-type hydrolysis. *Acta Crystallogr. D Biol. Crystallogr.* **63,** 230–239 (2007).
17. Kondo, N., Kuramitsu, S. & Masui, R. Biochemical characterization of TT1383 from *Thermus thermophilus* identifies a novel dTTP triphosphohydrolase activity stimulated by dATP and dTTP. *J. Biochem.* **136,** 221–231 (2004).
18. Seto, D., Bhatnagar, S. K. & Bessman, M. J. The purification and properties of deoxyguanosine triphosphate triphosphohydrolase from *Escherichia coli*. *J. Biol. Chem.* **263,** 1494–1499 (1988).
19. Crow, Y. J. *et al.* Mutations in the gene encoding the 3′–5′ DNA exonuclease TREX1 cause Aicardi–Goutières syndrome at the *AGS1* locus. *Nature Genet.* **38,** 917–920 (2006).
20. Crow, Y. J. *et al.* Mutations in genes encoding ribonuclease H2 subunits cause Aicardi–Goutières syndrome and mimic congenital viral brain infection. *Nature Genet.* **38,** 910–916 (2006).
21. Stetson, D. B., Ko, J. S., Heidmann, T. & Medzhitov, R. Trex1 prevents cell-intrinsic initiation of autoimmunity. *Cell* **134,** 587–598 (2008).
22. Kennedy, E. M. *et al.* Ribonucleoside triphosphates as substrate of human immunodeficiency virus type 1 reverse transcriptase in human macrophages. *J. Biol. Chem.* **285,** 39380–39391 (2010).
23. Diamond, T. L. *et al.* Macrophage tropism of HIV-1 depends on efficient cellular dNTP utilization by reverse transcriptase. *J. Biol. Chem.* **279,** 51545–51553 (2004).
24. Jamburuthugoda, V. K. *et al.* Reduced dNTP binding affinity of 3TC-resistant M184I/V HIV-1 reverse transcriptase variants responsible for viral infection failure in macrophage. *J. Biol. Chem.* **283,** 9206–9216 (2008).
25. Manel, N. *et al.* A cryptic sensor for HIV-1 activates antiviral innate immunity in dendritic cells. *Nature* **467,** 214–217 (2010).
26. Brown, P. H. & Schuck, P. Macromolecular size-and-shape distributions by sedimentation velocity analytical ultracentrifugation. *Biophys. J.* **90,** 4651–4661 (2006).
27. Vistica, J. *et al.* Sedimentation equilibrium analysis of protein interactions with global implicit mass conservation constraints and systematic noise decomposition. *Anal. Biochem.* **326,** 234–256 (2004).
28. Otwinowski, Z. & Minor, W. Processing of X-ray diffraction data collected in oscillation mode. *Methods Enzymol.* **276,** 307–326 (1997).
29. Zwart, P. H. *et al.* Automated structure solution with the PHENIX suite. *Methods Mol. Biol.* **426,** 419–435 (2008).
30. Wilson, P. M. *et al.* A novel fluorescence-based assay for the rapid detection and quantification of cellular deoxyribonucleoside triphosphates. *Nucleic Acids Res.* doi:10.1093/nar/gkr350 (16 May 2011).

Supplementary Information is linked to the online version of the paper at www.nature.com/nature.

Acknowledgements We thank S. Gamblin for comments on the manuscript and we acknowledge the Diamond Light Source for synchrotron access. This work was supported by the UK Medical Research Council, file references U117565647 (I.A.T.) and U117512710 (J.P.S.). Y.J.C. acknowledges the European Union Seventh Framework Programme (FP7/2007-2013) grant agreement number 241779 (NIMBL: http://www.NIMBLeu/), and the European Leukodystrophy Association. Y.J.C. and M.W. acknowledge the Manchester National Institute for Health Research Biomedical Research Centre.

Author Contributions D.C.G., V.E.-A., J.J.H., H.C. T. G., E.C., P.A.W., G.K., L.F.H., M.W.Y., I.A.T. and M.W. performed experiments. All authors contributed to data analysis, experimental design and manuscript writing.

Author Information The coordinates and structure factors of SAMHD1c have been deposited in the Protein Data Bank under accession number 3U1N. Reprints and permissions information is available at www.nature.com/reprints. The authors declare no competing financial interests. Readers are welcome to comment on the online version of this article at www.nature.com/nature. Correspondence and requests for materials should be addressed to I.A.T. (itaylor@nimr.mrc.ac.uk) or M.W. (Michelle.Webb@manchester.ac.uk).

LETTER

doi:10.1038/nature10595

Regulatory evolution through divergence of a phosphoswitch in the transcription factor CEBPB

Vincent J. Lynch[1], Gemma May[1] & Günter P. Wagner[1]

There is an emerging consensus that gene regulation evolves through changes in *cis*-regulatory elements[1,2] and transcription factors[3–6]. Although it is clear how nucleotide substitutions in *cis*-regulatory elements affect gene expression, it is not clear how amino-acid substitutions in transcription factors influence gene regulation[4–10]. Here we show that amino-acid changes in the transcription factor CCAAT/enhancer binding protein-β (CEBPB, also known as C/EBP-β) in the stem-lineage of placental mammals changed the way it responds to cyclic AMP/protein kinase A (cAMP/PKA) signalling. By functionally analysing resurrected ancestral proteins, we identify three amino-acid substitutions in an internal regulatory domain of CEBPB that are responsible for the novel function. These amino-acid substitutions reorganize the location of key phosphorylation sites, introducing a new site and removing two ancestral sites, reversing the response of CEBPB to GSK-3β-mediated phosphorylation from repression to activation. We conclude that changing the response of transcription factors to signalling pathways can be an important mechanism of gene regulatory evolution.

A major challenge in evolutionary and developmental biology is discovering the molecular mechanisms of gene regulatory evolution. Although it is clear that changes in transcription factors have contributed to the evolution of gene regulation[7–11], most studies of gene regulatory evolution have focused on *cis*-regulatory elements[1,2,12–15]. Thus, how mutations in transcription factors generate new regulatory functions is not well understood.

The mammalian transcription factor CEBPB plays an essential role during pregnancy[16–18], including physically and functionally interacting with FOXO1A to activate prolactin (PRL) expression in endometrial stromal cells (ESCs)[19–21] (Supplementary Fig. 1a). To test if this function evolved coincident with the origin of pregnancy in placental mammals, we assayed chicken, opossum and human CEBPB (LAP) and FOXO1A for their ability to transactivate luciferase expression from the ESC *PRL* enhancer. We found that each species' CEBPB moderately transactivated luciferase expression in HeLa and ESC (Fig. 1a, b). Co-expressed human FOXO1A and CEBPB cooperatively transactivated luciferase expression approximately 3.6-fold (Fig. 1a, b). In stark contrast, co-expression of CEBPB and FOXO1A from opossum and chicken were unable to transactivate luciferase expression cooperatively (Fig. 1a, b).

These results suggest that the cooperative CEBPB/FOXO1A interaction evolved in placental mammals. To test this hypothesis we used maximum likelihood to reconstruct the sequence of the ancestral therian (AncTherian) and eutherian (AncEutherian) CEBPB and FOXO1A genes, synthesized them using human codon-usage and tested their function in the assay described above. We found that the AncEutherian CEBPB/FOXO1A complex strongly transactivated luciferase expression whereas the AncTherian complex was unable to do so (Fig. 1a, b). This derived cooperativity in placental mammals, however, does not result from a newly evolved physical interaction between CEBPB and FOXO1A because both the AncEutherian and AncTherian CEBPB proteins are able to interact physically with ancestral FOXO1A proteins (Fig. 1c).

Previous studies have characterized several functionally distinct regions in CEBPB including three activation domains (ADM1–3), two internal regulatory domains (RD1–2) and a DNA-binding domain (DBD)[22–24]. To determine which domains and amino-acid substitutions are responsible for the derived function of CEBPB, we made

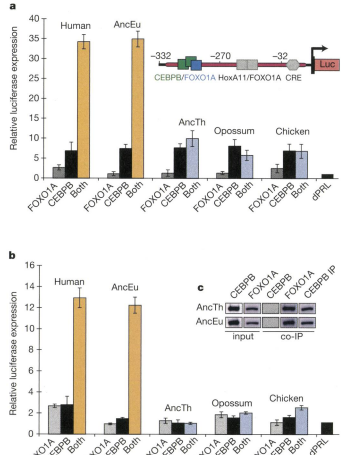

Figure 1 | CEBPB cooperatively regulates gene expression with FOXO1A in placental mammals. CEBPB and FOXO1A from human and the reconstructed ancestor of eutherian mammals (AncEu) cooperatively transactivate luciferase expression from the decidual prolactin promoter (dPRL) when co-transfected into HeLa (**a**) or human ESCs (**b**). Inset, the structure of the luciferase reporter vector and experimentally characterized transcription-factor binding sites. CEBPB and FOXO1A from non-mammals, including the reconstructed ancestor of therian mammals (AncTh), do not show cooperative upregulation. Luciferase values are shown as fold changes (mean ± s.e.m., $n = 6$) relative to the reporter control (dPRL). **c**, Both the ancestral therian and eutherian CEBPB proteins directly interact. CEBPB-V5/His and FOXO1A–Flag were expressed in HeLa cells and immunoprecipitated with anti-Flag agarose beads followed by DNase treatment.

[1]Yale Systems Biology Institute and Department of Ecology and Evolutionary Biology, Yale University, New Haven, Connecticut 06511, USA.

amino (N)-terminal truncation mutants of the AncTherian and AncEutherian CEPBPB genes and tested their ability to transactivate luciferase expression when co-expressed with FOXO1A. Deletion of ADM1 (Δ39) or ADM1–2 (Δ109) abrogated the transactivation ability of the AncEutherian protein whereas the ADM1–3 (Δ131) deletion restored transactivation. Deletion of RD1 (Δ175) and the region between RD1 and RD2 (Δ200) had little effect on the enhanced activation of Δ131. Deletion of RD2 (Δ236), however, reduced the transactivation ability of the AncEutherian protein to that observed for the AncTherian protein (Fig. 2a), indicating that RD2 plays a critical role in PRL regulation.

To test if the five eutherian-specific amino-acid changes within this region are responsible for the derived function in placental mammals, we reverted the derived amino acids in AncEutherian RD2 back to their ancestral state in the AncTherian protein and tested their ability to transactivate luciferase expression. We found that back mutation of derived sites one and two had no effect on transactivation, whereas back mutation of sites three, four and five resulted in a pronounced loss of transactivation ability (Fig. 2b). Next, we tested whether forward mutation of sites three, four and five was sufficient to impart a transactivation function to the AncTherian CEBPB. Unlike the progressive loss of function observed for reverse mutations, forward mutation of sites three and four, alone or in combination, had no effect on the ability of AncTherian CEBPB to transactivate luciferase expression (Fig. 2b). Forward mutation of site five only modestly enhanced transactivation; however, forward mutation of sites three and four in combination with site five dramatically enhanced transactivation by the AncTherian CEBPB (Fig. 2b). Thus, although the amino-acid substitutions at sites three and four contribute to the derived regulatory ability of CEBPB in placental mammals, they are dependent on the amino-acid substitution at site five.

Previous studies have shown that CEBPB is phosphorylated in response to cell-signalling, differentiation[25] and cAMP/PKA stimulation[26]. We mapped known and predicted phosphorylation sites in CEBPB and identified several differences between non-placental and placental mammals, including the loss of two ancestral serine phosphosites at sites three (S3A) and four (S4A) and the gain of a serine phosphosite at site five (N5S) in placental mammals. These sites are generally conserved at state S-(S/T)-N outside placental mammals and at state A-A-S within placental mammals, suggesting they are functionally constrained (Fig. 2c). Remarkably, the eutherian-specific serine at site five has previously been shown to be phosphorylated by GSK-3β kinase in rat CEBPB[27]. We confirmed that this site was phosphorylated in the AncEutherian CEBPB using nano-LC-ESI-MS/MS on purified protein *in vitro* phosphorylated with MAPK and GSK-3β kinases. Automated analysis of the tandem mass spectrometry (MS/MS) spectra indicated that the derived serine at site five is phosphorylated by GSK-3β kinases.

To test if phosphorylation by GSK-3β plays a role in potentiating transactivation by CEBPB, we repeated our luciferase reporter assays with the ancestral CEBPB and FOXO1A proteins but blocked GSK-3β phosphorylation with the kinase inhibitor 6-bromoindirubin 3′-oxime (BIO); if phosphorylation by GSK-3β is functionally important for transactivation of reporter gene expression by CEBPB, then inhibiting this kinase should block transactivation. Indeed, we found that inhibiting GSK-3β blocked the ability of the AncEutherian CEBPB to transactivate luciferase expression from the dPRL enhancer (Fig. 2b). Unexpectedly, however, inhibiting GSK-3β dramatically potentiated transactivation by AncTherian CEBPB. These results indicate that the AncEutherian CEBPB is activated by GSK-3β, whereas the AncTherian CEBPB is repressed by GSK-3β (Fig. 2b).

To determine which amino acids are responsible for interpreting GSK-3β-mediated phosphorylation as an inhibiting signal in AncTherian CEBPB and an activating signal in AncEutherian CEBPB, we compared the ability of back and forward mutated proteins to cooperatively transactivate luciferase expression with FOXO1A in the presence of BIO. We found that back mutation of site three, four and three/four in the AncEutherian CEBPB protein, which restores ancestral putative

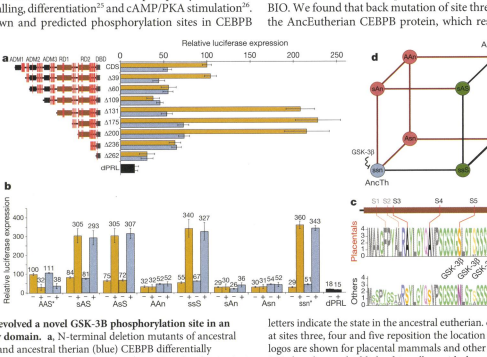

Figure 2 | CEBPB evolved a novel GSK-3B phosphorylation site in an internal regulatory domain. **a**, N-terminal deletion mutants of ancestral eutherian (yellow) and ancestral therian (blue) CEBPB differentially transactivate the dPRL-luciferase reporter when co-transfected with FOXO1A. Deletion of regulatory domain 2 (RD2; Δ236) in the ancestral eutherian CEBPB protein reduces its transactivating ability to that of the ancestral therian protein. Luciferase values are shown as fold changes relative to the full-length (CDS) ancestral eutherian CEBPB protein (mean ± s.e.m., $n = 6$). Red lines indicate the position of eutherian-specific amino-acid changes. **b**, Effect of forward and back mutation of sites three, four, and five in the ancestral therian (blue) and eutherian (yellow) CEBPB on transactivation in the presence of BIO (+) or BIO control (−) media. Luciferase values are shown relative to wild-type ancestral eutherian CEBPB (mean ± s.e.m., $n = 6$); *wild-type proteins; lower-case letters indicate amino-acid state in the ancestral therian whereas upper-case letters indicate the state in the ancestral eutherian. **c**, Amino-acid substitutions at sites three, four and five reposition the location of key phosphosites. RD2 logos are shown for placental mammals and other species with the location of S/T phosphosites highlighted in yellow with the name of the phosphorylating kinases; nano-liquid chromatography–electrospray ionization/tandem mass spectrometry of *in vitro* phosphorylated ancestral eutherian CEBPB confirmed site five (S5) is phosphorylated by GSK-3β. **d**, Mutational pathway between the ancestral therian (AncTh, blue) and eutherian (AncEu, yellow) functions. Each corner of the cube represents a possible intermediate state for amino acids at sites three, four and five; amino-acid identity at each state is shown as single letter amino code. Red edges show unlikely evolutionary paths through intermediate states that cannot transactivate reporter gene expression (red nodes), black edges show paths through functional intermediate states (green nodes).

phosphorylation sites that were lost in the stem lineage of placental mammals, recapitulated the dramatic enhancement of transactivation observed for AncTherian CEBPB in the presence of BIO (Fig. 2b). Conversely, forward mutations of sites three, four and three/four in the AncTherian CEBPB protein, which abolish the ancestral phosphorylation sites but do not introduce the derived phosphosite at site five, blocked its ability to transactivate reporter gene expression regardless of BIO treatment, leading to an essentially functionless protein in this assay (Fig. 2b). Incorporating a forward mutation at site five increased the transactivation ability of AncTherian CEBPB in the absence of BIO while maintaining a strong enhancement of transactivation with BIO treatment; however, transactivation with BIO was lost upon forward mutations of sites three and four (Fig. 2b). We conclude that the N5S substitution probably came before S3A and S4A because these substitutions lead to non-functional proteins when not paired with N5S and evolution is unlikely to pass through such non-functional intermediates (Fig. 2d).

Previous studies suggest that phosphorylation of RD2 induces a conformation change in CEBPB that disrupts intramolecular contacts between RD1–2, ADM1-3 and the bZIP/DNA-binding domain, leading to activation of the intrinsically repressed protein[17,22–24,28]. To infer the structural consequences of repositioning phosphorylation sites, we generated structural models of unphosphorylated and phosphorylated proteins using Rosetta/Robetta[29]. The model of the unphosphorylated AncEutherian protein suggests that ADM1–3 and RD1–2 are intrinsically unstructured and collapsed into a tight knot-like bundle in close contact with the helical bZIP/DNA-binding domain (Fig. 3a) similar to previous molecular and biochemical models[22–24]. In contrast, ADM1–3 and RD1–2 associate with neither each other nor the bZIP/DNA-binding domain in the model of the phosphorylated AncEutherian CEBPB (Fig. 3a), freeing residues critical for nuclear localization and DNA binding from an intramolecular masking. Unlike the phosphorylated AncEutherian CEBPB, the model of the AncTherian CEBPB phosphorylated at ancestral sites three and four assumes the repressed, transcriptionally inactive, conformation (Fig. 3a). These structural models suggest the differential response of AncEutherian and AncTherian proteins to GSK-3β stimulation results from the acquisition of different conformational states upon phosphorylation.

To test if GSK-3β-mediated phosphorylation induces a conformation change in CEBPB, we immunoprecipitated AncEutherian and AncTherian proteins from BIO-treated or control HeLa cells and incubated the purified protein with 20S proteasome, which degrades proteins with extended unstructured regions[30]. We found that the AncEutherian CEBPB isolated from BIO-treated cells was less efficiently degraded than protein from untreated cells, suggesting that inhibiting GSK-3β shifts the conformation of the AncEutherian CEBPB to the inactive state, which prevents digestion by the 20S proteasome (Fig. 3b). In contrast, AncTherian CEBPB isolated from BIO-treated cells was more efficiently degraded than protein isolated from untreated cells, suggesting that inhibiting GSK-3β shifted the conformation of the AncTherian CEBPB to the active state (Fig. 3b).

To test if GSK-3β-mediated phosphorylation of site five is important for inducing a conformation change in AncEutherian CEBPB, we immunopurified transiently expressed wild-type and site five back-mutated AncEutherian CEBPB in HeLa cells, and either *in vitro* phosphorylated the protein with MAPK/GSK-3β kinases or dephosphorylated it with calf intestinal alkaline phosphatase. We found that *in vitro* phosphorylated wild-type AncEutherian CEBPB was nearly completely degraded by the 20S proteasome, but that back mutation at site five and dephosphorylation protected the protein from degradation (Fig. 3c). These results suggest that in the ancestral state (likely) phosphorylation of sites three and/or four flips the conformation of CEBPB to the closed, transcriptionally repressed state. In contrast, in the derived-state phosphorylation at site five flips the switch to the open, transcriptionally active conformation (Fig. 3d).

These results uncover a potentially important mechanism of gene regulatory evolution and suggest that evolution can affect transcription factor functions in a cell-type-dependent way, probably avoiding deleterious pleiotropic effects on functions in different cellular and developmental contexts. Thus, modification of phosphorylation sites

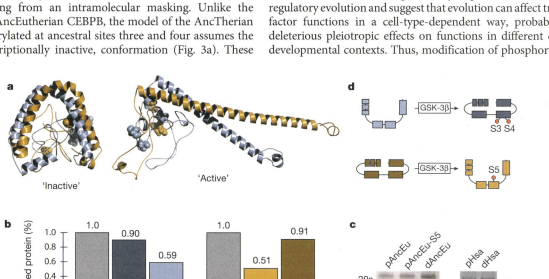

Figure 3 | Phosphorylation induces a conformation change in CEBPB. **a**, Structural models of unphosphorylated and phosphorylated ancestral therian (blue) and eutherian (yellow) CEBPB proteins. The model of the phosphorylated ancestral eutherian CEBPB is in the 'active' conformation whereas the model of the unphosphorylated ancestral therian CEBPB is in the 'active' conformation. Sites three, four and five are shown as spheres. **b**, Ancestral therian (AncTh) and ancestral eutherian (AncEu) CEBPB protein grown in cells treated with the GSK-3β inhibitor BIO (+) or control (−) media are differentially digested by the 20S proteasome. The percentage of undigested protein after a 30-min digestion with the 20S proteasome is shown relative to input. **c**, Phosphorylation of site five induces a conformation change in the ancestral eutherian CEBPB. Incubation of *in vitro* phosphorylated human (pHsa) and ancestral eutherian (pAncEu) CEBPB with purified 20S proteasome leads to protein degradation whereas dephosphorylated proteins (dHsa, dAncEu) are protected from degradation. Back mutation of site 5 (pAncEu-S5) decreases susceptibility of the *in vitro* phosphorylated protein to degradation. Arrows indicate CEBPB bands in Coomassie-blue-stained gel. **d**, Models of the conformational phospho-switch in CEBPB. Phosphorylation of the ancestral therian CEBPB (top) at sites three (S3) and four (S4) by GSK-3β flips the switch from the 'active' conformation (light blue) to the 'inactive' conformation (dark blue). In contrast, phosphorylation of the ancestral eutherian CEBPB (bottom) at site five (S5) by GSK-3β flips the switch from the 'inactive' conformation (dark yellow) to the 'active' conformation (yellow).

in transcription factors can facilitate gene regulatory innovation by altering kinase-signalling-dependent transcriptional networks.

METHODS SUMMARY

We used maximum-likelihood models implemented in CODEML in the PAML4 package of programs to reconstruct ancestral sequences under a $JTT+F_4$ model and the phylogeny shown in Supplementary Fig. 1. HeLa and human ESCs were transiently transfected with 2 ng of *Renilla* control (pGL4.71), 50 ng of dPRL luciferase reporter (dPRL-332/Luc3) and 200 ng of expression vector. Protein samples for co-immunoprecipitation, 20S assay and proteomics were isolated from the nuclear fraction of cell protein, treated with 50 U DNase (Roche) and 2.5 μg RNase (Roche) for 60 min at room temperature and washed three times with 1 ml of lysis buffer. For *in vitro* phosphorylation assays, immunoprecipitated proteins were either incubated with MAPK/GSK-3β and ATP or calf intestinal phosphatase. For 20S assays, *in vitro* phosphorylated and dephosphorylated protein was incubated for 1 h at 37 °C with 1 μg purified human 20S proteosome (Enzo Life Sciences). Immunoprecipitated proteins were either excised from SDS–polyacrylamide gel electrophoresis gels and processed for nano-LC-ESI-MS/MS or transferred to a PVDF membrane for western blotting.

Full Methods and any associated references are available in the online version of the paper at www.nature.com/nature.

Received 14 October 2010; accepted 28 September 2011.
Published online 13 November 2011.

1. Stern, D. L. Evolutionary developmental biology and the problem of variation. *Evolution* **54,** 1079–1091 (2000).
2. Carroll, S. B. Evolution at two levels: on genes and form. *PLoS Biol.* **3,** e245 (2005).
3. Hsia, C. C. & McGinnis, W. Evolution of transcription factor function. *Curr. Opin. Genet. Dev.* **13,** 199–206 (2003).
4. Lynch, V. J. & Wagner, G. P. Resurrecting the role of transcription factor change in developmental evolution. *Evolution* **62,** 2131–2154 (2008).
5. Wagner, G. P. & Lynch, V. J. Molecular evolution of evolutionary novelties: the vagina and uterus of therian mammals. *J. Exp. Zool. B* **304,** 580–592 (2005).
6. Wagner, G. P. & Lynch, V. J. Evolutionary novelties. *Curr. Biol.* **20,** R48–R52 (2010).
7. Lynch, V. J. *et al.* Adaptive changes in the transcription factor HoxA-11 are essential for the evolution of pregnancy in mammals. *Proc. Natl Acad. Sci. USA* **105,** 14928–14933 (2008).
8. Galant, R. & Carroll, S. B. Evolution of a transcriptional repression domain in an insect Hox protein. *Nature* **415,** 910–913 (2002).
9. Ronshaugen, M., McGinnis, N. & McGinnis, W. Hox protein mutation and macroevolution of the insect body plan. *Nature* **415,** 914–917 (2002).
10. Löhr, U., Yussa, M. & Pick, L. *Drosophila fushi tarazu*: a gene on the border of homeotic function. *Curr. Biol.* **11,** 1403–1412 (2001).
11. Chen, L. *et al.* Mouse and zebrafish Hoxa3 orthologues have nonequivalent *in vivo* protein function. *Proc. Natl Acad. Sci. USA* **107,** 10555–10560 (2010).
12. Carroll, S. B. Evo-devo and an expanding evolutionary synthesis: a genetic theory of morphological evolution. *Cell* **134,** 25–36 (2008).
13. Prud'homme, B., Gompel, N. & Carroll, S. B. Emerging principles of regulatory evolution. *Proc. Natl Acad. Sci. USA* **104,** 8605–8612 (2007).
14. Wray, G. A. The evolutionary significance of cis-regulatory mutations. *Nature Rev. Genet.* **8,** 206–216 (2007).
15. Stern, D. L. & Orgogozo, V. The loci of evolution: how predictable is genetic evolution? *Evolution* **62,** 2155–2177 (2008).
16. Shen, F. *et al.* IL-17 receptor signaling inhibits C/EBPβ by sequential phosphorylation of the regulatory 2 domain. *Sci. Signal.* **2,** ra8 (2009).
17. Spooner, C. J., Guo, X., Johnson, P. F. & Schwartz, R. C. Differential roles of C/EBPβ regulatory domains in specifying MCP-1 and IL-6 transcription. *Mol. Immunol.* **44,** 1384–1392 (2007).
18. Friedman, J. R. *et al.* Orthogonal analysis of C/EBPβ targets *in vivo* during liver proliferation. *Proc. Natl Acad. Sci. USA* **101,** 12986–12991 (2004).
19. Christian, M., Pohnke, Y., Kempf, R., Gellersen, B. & Brosens, J. J. Functional association of PR and CCAAT/enhancer-binding proteinβ isoforms: promoter-dependent cooperation between PR-B and liver-enriched inhibitory protein, or liver-enriched activatory protein and PR-A in human endometrial stromal cells. *Mol. Endocrinol.* **16,** 141–154 (2002).
20. Christian, M. *et al.* Cyclic AMP-induced forkhead transcription factor, FKHR, cooperates with CCAAT/enhancer-binding protein β in differentiating human endometrial stromal cells. *J. Biol. Chem.* **277,** 20825–20832 (2002).
21. Pohnke, Y., Kempf, R. & Gellersen, B. CCAAT/enhancer-binding proteins are mediators in the protein kinase A-dependent activation of the decidual prolactin promoter. *J. Biol. Chem.* **274,** 24808–24818 (1999).
22. Williams, S. C., Baer, M., Dillner, A. J. & Johnson, P. F. CRP2 (C/EBPβ) contains a bipartite regulatory domain that controls transcriptional activation, DNA binding and cell specificity. *EMBO J.* **14,** 3170–3183 (1995).
23. Kowenz-Leutz, E., Twamley, G., Ansieau, S. & Leutz, A. Novel mechanism of C/EBPβ (NF-M) transcriptional control: activation through derepression. *Genes Dev.* **8,** 2781–2791 (1994).
24. Lee, S., Miller, M., Shuman, J. D. & Johnson, P. F. CCAAT/enhancer-binding protein β DNA binding is auto-inhibited by multiple elements that also mediate association with p300/CREB-binding protein (CBP). *J. Biol. Chem.* **285,** 21399–21410 (2010).
25. Kowenz-Leutz, E., Pless, O., Dittmar, G., Knoblich, M. & Leutz, A. Crosstalk between C/EBPβ phosphorylation, arginine methylation, and SWI/SNF/mediator implies an indexing transcription factor code. *EMBO J.* **29,** 1105–1115 (2010).
26. Metz, R. & Ziff, E. cAMP stimulates the C/EBP-related transcription factor rNFIL-6 to trans-locate to the nucleus and induce c-fos transcription. *Genes Dev.* **5,** 1754–1766 (1991).
27. Zhao, X., Zhuang, S., Chen, Y., Boss, G. R. & Pilz, R. B. Cyclic GMP-dependent protein kinase regulates CCAAT enhancer-binding protein β functions through inhibition of glycogen synthase kinase-3. *J. Biol. Chem.* **280,** 32683–32692 (2005).
28. Trautwein, C., Walker, D. L., Plümpe, J. & Manns, M. P. Transactivation of LAP/NF-IL6 is mediated by an acidic domain in the N-terminal part of the protein. *J. Biol. Chem.* **270,** 15130–15136 (1995).
29. Kim, D. E., Chivian, D. & Baker, D. Protein structure prediction and analysis using the Robetta server. *Nucleic Acids Res.* **32,** W526–W531 (2004).
30. Tsvetkov, P. *et al.* Operational definition of intrinsically unstructured protein sequences based on susceptibility to the 20S proteasome. *Proteins Struct. Funct. Bioinf.* **70,** 1357–1366 (2008).

Supplementary Information is linked to the online version of the paper at www.nature.com/nature.

Acknowledgements This work was funded by a grant from the John Templeton Foundation, number 12793 Genetics and the Origin of Organismal Complexity; results presented here do not necessarily reflect the views of the John Templeton Foundation. The funders had no role in study design, data collection and analysis, decision to publish or preparation of the manuscript.

Author Contributions V.J.L. and G.P.W. designed experiments and wrote the manuscript. V.J.L. performed experiments and analysed data. G.M. cloned and sequenced CEBPB genes from non-mammalian species.

Author Information Reprints and permissions information is available at www.nature.com/reprints. The authors declare no competing financial interests. Readers are welcome to comment on the online version of this article at www.nature.com/nature. Correspondence and requests for materials should be addressed to V.J.L. (vincent.j.lynch@yale.edu).

LETTER

doi:10.1038/nature10662

RAF inhibitor resistance is mediated by dimerization of aberrantly spliced BRAF(V600E)

Poulikos I. Poulikakos[1], Yogindra Persaud[2], Manickam Janakiraman[2], Xiangju Kong[3], Charles Ng[4], Gatien Moriceau[3], Hubing Shi[3], Mohammad Atefi[4], Bjoern Titz[5], May Tal Gabay[1], Maayan Salton[6], Kimberly B. Dahlman[7], Madhavi Tadi[1], Jennifer A. Wargo[8], Keith T. Flaherty[9], Mark C. Kelley[10], Tom Misteli[6], Paul B. Chapman[11], Jeffrey A. Sosman[7], Thomas G. Graeber[5], Antoni Ribas[4,5], Roger S. Lo[3,5], Neal Rosen[1,11] & David B. Solit[4,11]

Activated RAS promotes dimerization of members of the RAF kinase family[1–3]. ATP-competitive RAF inhibitors activate ERK signalling[4–7] by transactivating RAF dimers[4]. In melanomas with mutant BRAF(V600E), levels of RAS activation are low and these drugs bind to BRAF(V600E) monomers and inhibit their activity. This tumour-specific inhibition of ERK signalling results in a broad therapeutic index and RAF inhibitors have remarkable clinical activity in patients with melanomas that harbour mutant BRAF(V600E)[8]. However, resistance invariably develops. Here, we identify a new resistance mechanism. We find that a subset of cells resistant to vemurafenib (PLX4032, RG7204) express a 61-kDa variant form of BRAF(V600E), p61BRAF(V600E), which lacks exons 4–8, a region that encompasses the RAS-binding domain. p61BRAF(V600E) shows enhanced dimerization in cells with low levels of RAS activation, as compared to full-length BRAF(V600E). In cells in which p61BRAF(V600E) is expressed endogenously or ectopically, ERK signalling is resistant to the RAF inhibitor. Moreover, a mutation that abolishes the dimerization of p61BRAF(V600E) restores its sensitivity to vemurafenib. Finally, we identified BRAF(V600E) splicing variants lacking the RAS-binding domain in the tumours of six of nineteen patients with acquired resistance to vemurafenib. These data support the model that inhibition of ERK signalling by RAF inhibitors is dependent on levels of RAS–GTP too low to support RAF dimerization and identify a novel mechanism of acquired resistance in patients: expression of splicing isoforms of BRAF(V600E) that dimerize in a RAS-independent manner.

RAF inhibitors have remarkable clinical activity in mutant BRAF melanomas that is limited by acquisition of drug resistance[8]. To identify new mechanisms of resistance, we generated cell lines resistant to vemurafenib by exposing the BRAF-mutant (V600E) melanoma cell line SKMEL-239 to a high dose of drug (2 μM). At this concentration, vemurafenib effectively inhibited ERK signalling and induced cell cycle arrest and cell death (Fig. 1a–c, Supplementary Fig. 2a and data not shown). Five independent vemurafenib-resistant cell populations were generated after approximately 2 months of continuous drug exposure (Fig. 1a). We chose this approach rather than one of gradual adaptation to increasing concentrations of drug because it more closely represents the clinical situation[8].

Resistance of SKMEL-239 cells to vemurafenib was associated with decreased sensitivity of ERK signalling to the drug (Fig. 1b, c and Supplementary Fig. 2b). Analysis revealed the presence of two distinct classes of resistant clones. In the first, exemplified by the C3 clone, the half-maximum inhibitory concentration (IC_{50}) for phosphorylated MEK (pMEK) inhibition was more than 100-fold higher than that of the parental cell line (Fig. 1d, e). Despite a similar degree of resistance to the anti-proliferative and pro-apoptotic effects of the drug, the second class of clones, exemplified by clone C5, demonstrated only a modest increase in pMEK IC_{50} (4.5-fold higher than the parental cell line). All five resistant clones retained sensitivity to the MEK inhibitor PD0325901 (ref. 9), albeit at slightly higher doses (Supplementary Fig. 3a, b).

Analysis of DNA and complementary DNA derived from the five resistant clones showed that all retained expression of BRAF(V600E) (Supplementary Fig. 4a, b). We did not detect mutation in BRAF at the gatekeeper site[10], RAS mutation, upregulation of receptor tyrosine kinase activity or COT overexpression (Supplementary Fig. 5a, b and data not shown). Analysis of BRAF protein expression showed that each of the resistant clones expressed a 90 kDa band that comigrated with the band observed in parental cells. In the C1, C3 and C4 clones, a new band was also identified, at an approximate molecular weight of 61 kDa (p61BRAF(V600E), Fig. 1c and Supplementary Fig. 2b). No band of this size was detected in parental SKMEL-239 cells or in a panel of 22 other melanoma cell lines (Supplementary Fig. 6).

PCR analysis of cDNA showed the expected single transcript of 2.3 kilobases, representing full-length BRAF, in parental cells and two transcripts of 2.3 kb and 1.7 kb in C3 cells. The 1.7-kb product was a BRAF transcript that contained the V600E mutation and an in-frame deletion of exons 4–8 (Fig. 2a and Supplementary Fig. 7). This 1.7-kb transcript is predicted to encode a protein of 554 amino acids (molecular mass 61 kDa), consistent with the lower BRAF band detected by immunoblotting. Exons 4–8 include domains critical for RAF activation, most notably, the RAS-binding domain (RBD) and the cysteine-rich domain (CRD)[3]. Analogous deletions in wild-type BRAF and CRAF promote RAF dimerization and render RAS activity dispensable for this process[1,4]. The 61-kDa BRAF variant identified in C3 was also detected in clones C1 and C4 by quantitative PCR, with a primer that anneals specifically to the exons 3/9 junction (Supplementary Fig. 8). Inspection of the *BRAF* locus on chromosome 7q34 by array CGH data suggested no evidence of an intragenic somatic deletion within the *BRAF* gene.

The 1.7-kb transcript was cloned into an expression vector and expressed in 293H cells, alone or together with full-length wild-type BRAF. ERK signalling was resistant to vemurafenib when p61BRAF(V600E) was ectopically expressed (Fig. 2b). Expression of p61BRAF(V600E) in parental SKMEL-239 cells or in HT-29 (BRAF(V600E)) cells also resulted in failure of vemurafenib to inhibit ERK signalling effectively (Supplementary Fig. 9a, b). To test whether ERK signalling in C3 cells was dependent on p61BRAF(V600E), we

[1]Department of Molecular Pharmacology and Chemistry, Memorial Sloan-Kettering Cancer Center, New York, New York 10065, USA. [2]Human Oncology and Pathogenesis Program, Memorial Sloan-Kettering Cancer Center, New York, New York 10065, USA. [3]Division of Dermatology, Department of Medicine, Jonsson Comprehensive Cancer Center, University of California at Los Angeles, Los Angeles, California 90095, USA. [4]Division of Hematology and Oncology, Department of Medicine, Jonsson Comprehensive Cancer Center, University of California at Los Angeles, Los Angeles, California 90095, USA. [5]Department of Molecular and Medical Pharmacology, Jonsson Comprehensive Cancer Center, University of California at Los Angeles, Los Angeles, California 90095, USA. [6]National Cancer Institute, NIH, Bethesda, Maryland 20892, USA. [7]Department of Medicine, Vanderbilt-Ingram Cancer Center, Nashville, Tennessee 37232, USA. [8]Department of Surgery, Massachusetts General Hospital Cancer Center, Boston, Massachusetts 02114, USA. [9]Department of Medicine, Massachusetts General Hospital Cancer Center, Boston, Massachusetts 02114, USA. [10]Department of Surgery, Vanderbilt-Ingram Cancer Center, Nashville, Tennessee 37232, USA. [11]Department of Medicine, Memorial Sloan-Kettering Cancer Center, New York, New York 10065, USA.

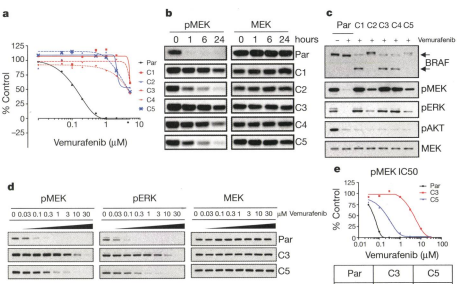

Par	C3	C5
0.04	4.30	0.191
1	107 fold	4.6 fold

Figure 1 | Resistance to the RAF inhibitor vemurafenib (PLX4032) is associated with failure of the drug to inhibit ERK signalling. a, Vemurafenib IC_{50} curves (at 5 days) for the SKMEL-239 parental cell line and five vemurafenib-resistant clones. **b**, Effects of 2 μM vemurafenib on ERK signalling in parental (Par) and resistant clones (C1–C5). **c**, Western blot for components of the ERK and AKT signalling pathways in parental and resistant clones (2 μM vemurafenib, 24 h). **d**, Dose–response of pMEK and pERK downregulation at 1 h to increasing concentrations of vemurafenib in parental and two representative resistant clones (C3 and C5). **e**, Graphic representation of the chemiluminescent signal intensities from **d** and IC_{50} values for inhibition of MEK phosphorylation by vemurafenib in the parental and C3 and C5 clones.

designed short interfering RNAs (siRNAs) directed against either the 3/9 splice junction or a region within the exon 4–8 deletion to suppress selectively the expression of p61BRAF(V600E) or full-length BRAF, respectively. In parental cells, ERK signalling was inhibited by knockdown of full-length BRAF(V600E) (Supplementary Fig. 10a). In C3 cells, phosphorylation of MEK, cyclin D1 expression and cell growth were inhibited upon knockdown of p61BRAF(V600E) but not of full-length wild-type BRAF, ARAF or CRAF (Supplementary Fig. 10b, c). Moreover, in C3 cells in which the expression of full-length BRAF or CRAF was knocked down, ERK signalling remained resistant to vemurafenib (Supplementary Fig. 10d).

Vemurafenib inhibits the kinase activity of RAF immunoprecipitated from cells, but activates intracellular RAF in BRAF wild-type cells[6]. This indicates that the conditions required for transactivation *in vivo* are not recapitulated in the *in vitro* assay. We tested whether p61BRAF(V600E) is also sensitive to this inhibitor *in vitro*. Although the *in vitro* activity of p61BRAF(V600E) was slightly higher than full-length BRAF(V600E), similar concentrations of vemurafenib caused their inhibition *in vitro* (Supplementary Fig. 11). These data indicate that resistance of p61BRAF(V600E) to vemurafenib is not due to its inability to bind the inhibitor.

It has been shown that the amino terminus of RAF negatively regulates the carboxy-terminal catalytic domain[11] and that truncation of the N terminus results in constitutive dimerization of the protein in the absence of activated RAS[1]. To ask whether deletion of exons 4–8 promotes dimerization of p61BRAF(V600E), we co-expressed two constructs encoding the same protein (either p61BRAF(V600E) or full-length BRAF(V600E)) but with different tags (Flag or V5) and then immunoblotted for V5 after immunoprecipitating Flag. As shown in Fig. 2c, dimerization of p61BRAF(V600E) was significantly elevated compared to that of full-length BRAF(V600E). The R509 residue is within the BRAF dimerization interface. Mutation of this residue to a histidine significantly diminishes dimerization of wild-type BRAF and results in loss of its catalytic activity in cells[4,12]. However, full-length BRAF(V600E/R509H) expressed in 293H cells retained its ability to fully activate ERK signalling and remained sensitive to vemurafenib (Fig. 2d). Moreover, BRAF(V600E/R509H) fully activated ERK signalling when expressed in either BRAF-null or ARAF/CRAF-null mouse embryonic fibroblasts (Supplementary Fig. 12a, b). These results show that, in contrast to wild-type BRAF, BRAF(V600E) can signal as a monomer and that active RAS and dimerization are not necessary for its activation.

Our model implies that, in tumours with BRAF(V600E), elevation of RAS–GTP or alterations that cause increased RAF dimerization in the absence of RAS activation will confer resistance to RAF inhibitors[4,13]. To test whether resistance mediated by p61BRAF(V600E) was the result of elevated dimer formation, we introduced the R509H dimerization-deficient mutation into p61BRAF(V600E). In 293H cells expressing p61BRAF(V600E), phosphorylation of ERK was elevated and was insensitive to vemurafenib (Fig. 2e). ERK activity was also elevated in cells expressing p61BRAF(V600E/R509H), but to a slightly lesser degree. p61BRAF(V600E/R509H) showed impaired dimerization, confirming that the R509H mutation located within the dimerization interface disrupts the formation of p61RAF(V600E) dimers (Fig. 2c and Supplementary Fig. 13). Finally, this monomeric p61BRAF(V600E/R509H) was sensitive to RAF inhibitors; in cells ectopically expressing this mutant, ERK signalling was inhibited by vemurafenib (Fig. 2e). Thus, the R509H mutation restores sensitivity to the RAF inhibitor by impairing dimerization of p61BRAF(V600E).

To determine whether BRAF variants can account for clinical resistance to RAF inhibitors, we analysed tumours from nineteen melanoma patients with acquired resistance to vemurafenib. PCR analysis of cDNA from pre-treatment samples showed a single band of the expected size (2.3 kb), which was sequenced and confirmed to include both BRAF(V600E) and wild-type BRAF transcripts (Fig. 3a, b and data not shown). We identified two PCR products in six of the post-treatment progression samples, including three with matching pre-treatment samples. The shorter PCR products encoded BRAF(V600E) transcripts lacking exons 4–10 (patient 1), exons 4–8, (patient 11, identical to the variant identified in the resistant cell lines), exons 2–8 (patient 12), or exons 2–10 (patients 5, 6 and 19) (Fig. 3a–c, Supplementary Table 1). Mutations in NRAS were identified in 4 of 19

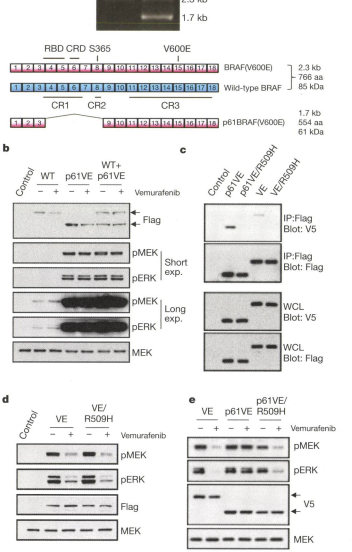

Figure 2 | A BRAF(V600E) variant that lacks exons 4–8 is resistant to the RAF inhibitor vemurafenib. a, PCR analysis of BRAF in cDNA from parental (Par) and C3 cells. Sequencing of the 1.7-kb product expressed in the C3 clones, but not in parental cells, revealed an in-frame deletion of five exons (4–8) in *cis* with the V600E mutation. aa, amino acids; CR1, conserved region 1; CR2, conserved region 2; CR3, conserved region 3; CRD, cystine-rich domain; RBD, RAS-binding domain. **b**, Full-length wild-type BRAF and the 1.7 kb/61 kDa splice variant of BRAF(V600E) (p61VE) were expressed in 293H cells. The effect of vemurafenib (2 μM for 1 h) on ERK signalling in the presence of p61BRAF(V600E) was analysed by western blot for pMEK and pERK. exp., exposure. **c**, To compare levels of dimerization, 293H cells co-expressing Flag-tagged and V5-tagged p61BRAF(V600E), full-length BRAF(V600E) and the corresponding dimerization-deficient mutants p61BRAF(V600E/R509H) and BRAF(V600E/R509H) were lysed followed by immunoprecipitation (IP) with Flag antibody. Western blotting (Blot) with anti-V5 or anti-Flag antibodies was performed as indicated. WCL, whole-cell lysate. **d**, Comparison of MEK/ERK activation and sensitivity of ERK signalling to vemurafenib (2 μM for 1 h) in 293H cells expressing either Flag-tagged BRAF(V600E) or the dimerization mutant Flag-tagged BRAF(V600E/R509H). **e**, Constructs expressing V5-tagged BRAF(V600E), p61BRAF(V600E) or the dimerization mutant p61BRAF(V600E/R509H) were transfected into 293H cells and treated with DMSO or 2 μM vemurafenib for 1 h.

progression samples and were found to be mutually exclusive with BRAF splicing variants. BRAF splicing variants were not detected in two samples derived from patients with intrinsic resistance (patient 20 shown) or in 27 additional melanomas resected from vemurafenib-naive

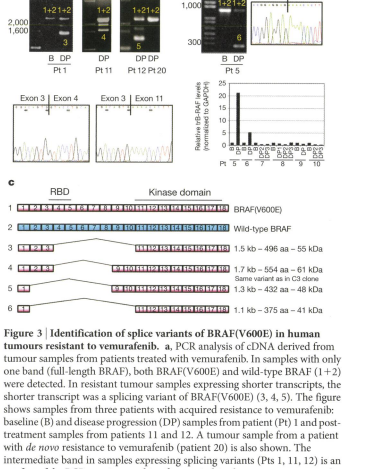

Figure 3 | Identification of splice variants of BRAF(V600E) in human tumours resistant to vemurafenib. a, PCR analysis of cDNA derived from tumour samples from patients treated with vemurafenib. In samples with only one band (full-length BRAF), both BRAF(V600E) and wild-type BRAF (1+2) were detected. In resistant tumour samples expressing shorter transcripts, the shorter transcript was a splicing variant of BRAF(V600E) (3, 4, 5). The figure shows samples from three patients with acquired resistance to vemurafenib: baseline (B) and disease progression (DP) samples from patient (Pt) 1 and post-treatment samples from patients 11 and 12. A tumour sample from a patient with *de novo* resistance to vemurafenib (patient 20) is also shown. The intermediate band in samples expressing splicing variants (Pts 1, 11, 12) is an artefact of the PCR reaction resulting from switching between two very similar templates. Representative Sanger sequencing traces showing the junction between exons 3 and 11 in the DP sample from patient 1 compared to the full-length transcript derived from the baseline pre-treatment sample. **b**, As in **a**, baseline (B) and disease progression (DP) samples from a patient with an exon 2–10 deletion. RNA/cDNA levels of the exon 2–10 deletion were determined by qPCR using an exon 1/11 junction primer. The data are shown as the average of duplicates and expressed as relative levels between patient-matched samples. **c**, Exon organization of the splicing variants found in tumours from six patients that initially responded and then progressed on vemurafenib.

patients (Fig. 3a, Supplementary Table 1 and data not shown). Thus, we did not detect significant levels of BRAF splicing variants in melanoma cell lines and tumours that have not been exposed to RAF inhibitors. However, the assay used cannot exclude the possibility that such variants may be expressed in small amounts before drug selection and subsequently selected under conditions of continuous treatment with the drug.

In tumours from patients that have been analysed, resistance to vemurafenib is frequently associated with inability of the drug to inhibit ERK signalling[14]. Our model indicates that this can be due to increased RAF dimer formation in the cell[4]. This can happen in at least two ways: increasing RAS–GTP levels and induction of RAS-independent dimerization (Supplementary Fig. 1a, b). NRAS mutation has recently been reported in resistant tumours[15]. Other mechanisms of resistance to RAF inhibitors in model systems and in patients have also been reported, including activation of receptor tyrosine kinases, COT over-expression and MEK1 mutation[15–18]. We now report a lesion in patient tumours that results in RAF inhibitor resistance by inducing increased, RAS-independent dimerization.

Expression of BRAF(V600E) splicing variants is the first resistance mechanism identified that involves a structural change in BRAF. In each case, the alternative splicing forms identified in the cell lines and patients were in-frame and confined to the mutant *BRAF* allele. This suggests that generation of the splicing variants is probably due to a mutation or epigenetic change that affects *BRAF* splicing and not to a loss of global splicing fidelity[19]. The identification of BRAF variants lacking the RAS-binding domain in six of nineteen patients with acquired resistance indicates that this mechanism is clinically important. Acquired resistance mediated by BRAF(V600E) splicing variants is due to insensitivity of the enzyme to RAF inhibitors. These tumours should retain sensitivity to inhibitors of downstream components of the pathway such as MEK, which was indeed the case (Supplementary Fig. 3). Therefore, MEK inhibitors used in combination with vemurafenib could delay or prevent resistance by this mechanism.

METHODS SUMMARY

Vemurafenib[20] (PLX4032) was obtained from Plexxikon. PD0325901 was synthesized in the MSKCC Organic Synthesis Core Facility by O. Ouerfelli. Flag-tagged BRAF constructs have been described previously[4]. All other plasmids were created using standard cloning methods, with pcDNA3.1 (Invitrogen) as a vector. Mutations were introduced using a site-directed mutagenesis kit (Stratagene). The C1-5 vemurafenib-resistant cells were generated by continuous exposure of parental SKMEL-239 cells to 2 μM of drug until the emergence of resistant colonies. Single-cell cloning was then performed before biological characterization.

For cDNA preparation, a Superscript III First-Strand Synthesis kit (Invitrogen) was used. Sanger sequencing of the products was performed by Genewiz. For qPCR analysis, cDNA synthesis was carried out with the High Capacity cDNA Reverse Transcription kit (Applied Biosystems). qPCR was performed with a iQ SYBR Green RT–PCR Super Mix (Bio-Rad) and a C1000 Thermal Cycler (Bio-Rad). The comparative C_t method was used to quantify transcripts and delta C_t was measured in triplicate. Sequences of all primers used are available upon request.

Melanoma tumour specimens from patients treated with vemurafenib were collected following IRB-approved protocols and were flash-frozen immediately after resection or biopsy. To determine tumour content, 5-μm sections were cut, stained with haematoxylin and eosin, and scored by a pathologist. If the specimen had >70% tumour content (excluding necrosis), the remainder of the frozen tumour was homogenized using a Bullet Blender (Next Advance) with 0.9–2 mm stainless steel beads for 5 min at a speed setting of 10. RNA was then extracted from the tumour homogenate using an RNeasy Mini kit (Qiagen) and quantified.

Full Methods and any associated references are available in the online version of the paper at www.nature.com/nature.

Received 4 May; accepted 20 October 2011.

Published online 23 November; corrected 14 December 2011 (see full-text HTML version for details).

1. Weber, C. K., Slupsky, J. R., Kalmes, H. A. & Rapp, U. R. Active Ras induces heterodimerization of cRaf and BRaf. *Cancer Res.* **61,** 3595–3598 (2001).
2. Rushworth, L. K., Hindley, A. D., O'Neill, E. & Kolch, W. Regulation and role of Raf-1/B-Raf heterodimerization. *Mol. Cell Biol.* **26,** 2262–2272 (2006).
3. Wellbrock, C., Karasarides, M. & Marais, R. The RAF proteins take centre stage. *Nature Rev. Mol. Cell Biol.* **5,** 875–885 (2004).
4. Poulikakos, P. I., Zhang, C., Bollag, G., Shokat, K. M. & Rosen, N. RAF inhibitors transactivate RAF dimers and ERK signalling in cells with wild-type BRAF. *Nature* **464,** 427–430 (2010).
5. Heidorn, S. J. *et al.* Kinase-dead BRAF and oncogenic RAS cooperate to drive tumor progression through CRAF. *Cell* **140,** 209–221 (2010).
6. Hatzivassiliou, G. *et al.* RAF inhibitors prime wild-type RAF to activate the MAPK pathway and enhance growth. *Nature* **464,** 431–435 (2010).
7. Joseph, E. W. *et al.* The RAF inhibitor PLX4032 inhibits ERK signaling and tumor cell proliferation in a V600E BRAF-selective manner. *Proc. Natl Acad. Sci. USA* **107,** 14903–14908 (2010).
8. Flaherty, K. T. *et al.* Inhibition of mutated, activated BRAF in metastatic melanoma. *N. Engl. J. Med.* **363,** 809–819 (2010).
9. Solit, D. B. *et al.* BRAF mutation predicts sensitivity to MEK inhibition. *Nature* **439,** 358–362 (2006).
10. Whittaker, S. *et al.* Gatekeeper mutations mediate resistance to BRAF-targeted therapies. *Sci. Transl. Med.* **2,** 35ra41 (2010).
11. Cutler, R. E. Jr, Stephens, R. M., Saracino, M. R. & Morrison, D. K. Autoregulation of the Raf-1 serine/threonine kinase. *Proc. Natl Acad. Sci. USA* **95,** 9214–9219 (1998).
12. Rajakulendran, T., Sahmi, M., Lefrancois, M., Sicheri, F. & Therrien, M. A dimerization-dependent mechanism drives RAF catalytic activation. *Nature* **461,** 542–545 (2009).
13. Poulikakos, P. I. & Rosen, N. Mutant BRAF melanomas–dependence and resistance. *Cancer Cell* **19,** 11–15 (2011).
14. McArthur, G. *et al.* Molecular analyses from a phase I trial of vemurafenib to study mechanism of action (MOA) and resistance in repeated biopsies from BRAF mutation–positive metastatic melanoma patients (pts). *J Clin Oncol* **29,** suppl; abstr 8502 (2011).
15. Nazarian, R. *et al.* Melanomas acquire resistance to B-RAF(V600E) inhibition by RTK or N-RAS upregulation. *Nature* **468,** 973–977 (2010).
16. Johannessen, C. M. *et al.* COT drives resistance to RAF inhibition through MAP kinase pathway reactivation. *Nature* **468,** 968–972 (2010).
17. Villanueva, J. *et al.* Acquired resistance to BRAF inhibitors mediated by a RAF kinase switch in melanoma can be overcome by cotargeting MEK and IGF-1R/PI3K. *Cancer Cell* **18,** 683–695, doi:S1535–6108(10)00484–8 (2010).
18. Wagle, N. *et al.* Dissecting therapeutic resistance to RAF inhibition in melanoma by tumor genomic profiling. *J. Clin. Oncol.* **29,** 3085–3096 (2011).
19. Luco, R. F., Allo, M., Schor, I. E., Kornblihtt, A. R. & Misteli, T. Epigenetics in alternative pre-mRNA splicing. *Cell* **144,** 16–26 (2011).
20. Bollag, G. *et al.* Clinical efficacy of a RAF inhibitor needs broad target blockade in BRAF-mutant melanoma. *Nature* **467,** 596–599 (2010).

Supplementary Information is linked to the online version of the paper at www.nature.com/nature.

Acknowledgements We are grateful to M. Baccarini and C. Pritchard for the RAF knockout mouse embryonic fibroblasts. We would like to thank K. Shokat, C. Zhang, S. Chandarlapaty, C. Pratilas and K. Robzyk for useful discussions, C. Liu for her technical expertise and T. J. Riley. We also thank D. Hucks for technical assistance, P. L. Lyle for scoring the tumour sections, and T. Chodon for assistance with tumour procurement. The ITR is supported by the Vanderbilt-Ingram Cancer Center and the T. J. Martell Foundation. This work has been funded by the National Institutes of Health (NIH; R.S.L., N.R., D.B.S.), the Beene Foundation (D.B.S.), the Melanoma Research Alliance (K.T.F., J.A.S. P.B.C., R.S.L., N.R., D.B.S.) and the STARR Foundation (N.R., D.B.S.). R.S.L. was supported by the Burroughs Wellcome Fund, American Skin Association, Joint Center for Translational Medicine, Sidney Kimmel Foundation, and Stand Up to Cancer. T.M. was supported in part by the Intramural Research Program of the NIH, NCI, Center for Cancer Research and P.B.C. was supported in part by the Danny Federici Melanoma Fund. P.I.P. was supported by T32 CACA062948-15.

Author Contributions P.I.P., M.J., T.G.G., A.R., R.S.L., N.R. and D.B.S. designed experiments and analysed data. P.I.P., Y.P., M.J., X.K., C.N., G.M., H.S., M.A., B.T., M.T.G., M.S., K.B.D. and M.T. performed experiments and analysed data. J.A.W., K.T.F., M.C.K., J.A.S., P.B.C. and R.S.L. provided tumours for analysis. All authors contributed to the writing of the paper.

Author Information Reprints and permissions information is available at www.nature.com/reprints. The authors declare competing financial interests: details accompany the full-text HTML version of the paper at www.nature.com/nature. Readers are welcome to comment on the online version of this article at www.nature.com/nature. Correspondence and requests for materials should be addressed to D.B.S. (solitd@mskcc.org).

LETTER

doi:10.1038/nature10492

Chromatin-associated RNA interference components contribute to transcriptional regulation in *Drosophila*

Filippo M. Cernilogar[1,2]†*, Maria Cristina Onorati[3]*, Greg O. Kothe[4], A. Maxwell Burroughs[5], Krishna Mohan Parsi[1,2], Achim Breiling[6], Federica Lo Sardo[1], Alka Saxena[5], Keita Miyoshi[7], Haruhiko Siomi[7], Mikiko C. Siomi[7,8], Piero Carninci[5], David S. Gilmour[4], Davide F. V. Corona[3] & Valerio Orlando[1]

RNA interference (RNAi) pathways have evolved as important modulators of gene expression that operate in the cytoplasm by degrading RNA target molecules through the activity of short (21–30 nucleotide) RNAs[1–4]. RNAi components have been reported to have a role in the nucleus, as they are involved in epigenetic regulation and heterochromatin formation[5–10]. However, although RNAi-mediated post-transcriptional gene silencing is well documented, the mechanisms of RNAi-mediated transcriptional gene silencing and, in particular, the role of RNAi components in chromatin dynamics, especially in animal multicellular organisms, are elusive. Here we show that the key RNAi components Dicer 2 (DCR2) and Argonaute 2 (AGO2) associate with chromatin (with a strong preference for euchromatic, transcriptionally active, loci) and interact with the core transcription machinery. Notably, loss of function of DCR2 or AGO2 showed that transcriptional defects are accompanied by the perturbation of RNA polymerase II positioning on promoters. Furthermore, after heat shock, both *Dcr2* and *Ago2* null mutations, as well as missense mutations that compromise the RNAi activity, impaired the global dynamics of RNA polymerase II. Finally, the deep sequencing of the AGO2-associated small RNAs (AGO2 RIP-seq) revealed that AGO2 is strongly enriched in small RNAs that encompass the promoter regions and other regions of heat-shock and other genetic loci on both the sense and antisense DNA strands, but with a strong bias for the antisense strand, particularly after heat shock. Taken together, our results show that DCR2 and AGO2 are globally associated with transcriptionally active loci and may have a pivotal role in shaping the transcriptome by controlling the processivity of RNA polymerase II.

Accumulating evidence indicates that RNAi components and small RNAs function in the nucleus to control heterochromatin formation, as well as repeat-induced gene silencing and transposable element mobilization[7–10]. However, the global association of RNAi components with chromatin and their role in transcriptional regulation remains to be elucidated. To investigate a role for RNAi in the chromatin dynamics of a multicellular organism and, possibly, in transcriptional gene silencing, we first determined whether any of the key RNAi components are present in the nucleus of *Drosophila* cells. Cellular fractionation of embryonic tissue culture cells (S2 cells) showed that the microRNA-processing factors DCR1 and AGO1, as well the RNAi component AGO2, are equally distributed between the cytoplasm and the nucleus (Supplementary Fig. 1a). By contrast, the RNAi protein DCR2 is greatly enriched in the nuclear fraction (Supplementary Fig. 1a). To evaluate the association of RNAi components with the different nuclear compartments, we carried out chromatin fractionation experiments[11] (Supplementary Fig. 1b, c). A substantial amount of DCR2 and AGO2 was detected in chromatin fractions, together with RNA polymerase II (RNA Pol II), Negative elongation factor E (NELF-E), Polycomb (Pc) and histone H3 (Supplementary Fig. 1c). By contrast, most of the cellular DCR1 and AGO1 was found in the Triton X-100 soluble fraction (S1 fraction), together with tubulin, a marker for proteins that are not associated with chromatin (Supplementary Fig. 1c). Taken together, our data indicate that the DCR2–AGO2 complex is mainly associated with chromatin, whereas the DCR1–AGO1 complex is mostly cytoplasmic, in accordance with its cytoplasmic function (that is, post-transcriptional gene silencing).

To determine whether RNAi components associate with chromatin *in vivo*, *Drosophila* polytene chromosomes were stained with AGO2- and DCR2-specific monoclonal antibodies[3,12,13]. Both AGO2 and DCR2 were detected at several hundred sites on polytene chromosomes from wild-type larvae (Supplementary Figs 1d, g and 2a, b). By contrast, little or no staining was detected in *Ago2*- or *Dcr2*-null chromosomes[1,2] (Supplementary Fig. 1f, i and Supplementary Table 1a). Strikingly, the majority of AGO2- and DCR2-associated loci correspond to interbands, suggesting that AGO2 and DCR2 preferentially associate with euchromatic, transcriptionally active, loci[14] (Supplementary Fig. 2a, b). In particular, the chromatin binding of DCR2 requires AGO2, but the converse is not true (Supplementary Fig. 3), suggesting that AGO2 also acts as the RNAi effector complex on chromatin.

Interestingly, AGO2 and DCR2 are present at the 87A and 87C cytogenetic loci (Supplementary Fig. 1e, h). These cytogenetic loci contain copies of the heat-shock gene *Hsp70*, thus providing well-characterized inducible candidate genes with which to investigate the role of DCR2 and AGO2 in transcription and, in particular, in RNA Pol II pausing regulation[15,16]. To determine whether DCR2 and AGO2 affect *Hsp70* transcription, *Hsp70* transcript levels were measured in control cells and in cells depleted of DCR2 or AGO2 (Supplementary Fig. 4). The knockdown of either RNAi component resulted in a significant increase in *Hsp70* transcripts in non-heat-shocked cells (Fig. 1a, b). Similar results were obtained for a second heat-shock gene, *Hsp68* (Fig. 1a, b). The increased expression of *Hsp70* and *Hsp68* in cells depleted of DCR2 could be reversed by the expression of a Flag-tagged wild-type copy of DCR2 (DCR2–Flag) (Fig. 1c), indicating that the change in expression was not the result of an off-target effect of the *Dcr2* RNAi. Interestingly, the levels of the endogenous AGO2 protein increased together with the expression of wild-type DCR2–Flag (Supplementary Fig. 4a), suggesting that the DCR2–Flag protein is integrated into the RNAi pathway and that re-establishment of functional levels of DCR2 and AGO2 rescues the observed transcriptional defects in heat-shock genes. However, the depletion of DCR2 and AGO2 did not affect the expression of *Hsp70* and *Hsp68*

[1]Dulbecco Telethon Institute, Epigenetics and Genome Reprogramming, IRCCS Fondazione Santa Lucia, Via del Fosso di Fiorano 64, 00143 Rome, Italy. [2]Dulbecco Telethon Institute, IGB ABT-CNR, Via Pietro Castellino 111, 80131 Naples, Italy. [3]Dulbecco Telethon Institute at Università degli Studi di Palermo, Dipartimento STEMBIO, Sezione Biologia Cellulare, Viale delle Scienze, Edificio 16, 90128 Palermo, Italy. [4]Department of Biochemistry and Molecular Biology, Center for Eukaryotic Gene Regulation, The Pennsylvania State University, University Park, Pennsylvania 16802, USA. [5]RIKEN Omics Science Center, RIKEN Yokohama Institute, 1-7-22 Suehiro-cho, Tsurumi-ku, Yokohama, Kanagawa 230-0045, Japan. [6]Division of Epigenetics, DKFZ-ZMBH Alliance, German Cancer Research Center, Im Neuenheimer Feld 580, 69120 Heidelberg, Germany. [7]Keio University School of Medicine, Tokyo 160-8582, Japan. [8]JST, CREST, Saitama 332-0012, Japan. †Present address: Helmholtz Center Munich, Institute of Developmental Genetics, Ingolstaedter Landstrasse 1, 85764 Munich-Neuherberg, Germany.

*These authors contributed equally to this work.

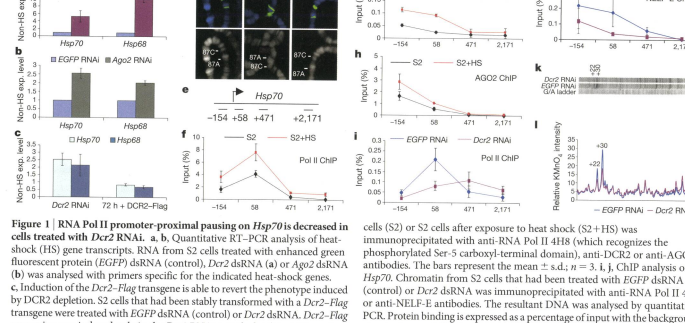

Figure 1 | RNA Pol II promoter-proximal pausing on *Hsp70* is decreased in cells treated with *Dcr2* RNAi. **a**, **b**, Quantitative RT–PCR analysis of heat-shock (HS) gene transcripts. RNA from S2 cells treated with enhanced green fluorescent protein (*EGFP*) dsRNA (control), *Dcr2* dsRNA (**a**) or *Ago2* dsRNA (**b**) was analysed with primers specific for the indicated heat-shock genes. **c**, Induction of the *Dcr2–Flag* transgene is able to revert the phenotype induced by DCR2 depletion. S2 cells that had been stably transformed with a *Dcr2–Flag* transgene were treated with *EGFP* dsRNA (control) or *Dcr2* dsRNA. *Dcr2–Flag* expression was induced only in the *Dcr2* RNAi sample, by the addition of copper. The samples were analysed before and after a 72-h induction of the transgene. The transcript levels are shown with respect to the *EGFP* control (experiment:control ratio); $n = 3$. The bars represent the mean ± s.d. **d**, *Hsp70* DNA-FISH on polytene chromosomes from wild type (WT), homozygous $Dcr2^{L811fsX}$ ($Dcr2^{-/-}$) or homozygous $Ago2^{414}$ ($Ago2^{-/-}$) mutant larvae, showing the merge of DNA (blue) and FISH (green) signals (top) and DNA staining (bottom). **e**, Schematic representation of the *Hsp70* transcription unit with the position of the PCR amplicons used in this study. The numbers indicate the middle of each amplicon with respect to the transcription start site (arrow). **f**–**h**, ChIP analysis of the heat-shock gene *Hsp70*. Chromatin from S2 cells (S2) or S2 cells after exposure to heat shock (S2+HS) was immunoprecipitated with anti-RNA Pol II 4H8 (which recognizes the phosphorylated Ser-5 carboxyl-terminal domain), anti-DCR2 or anti-AGO2 antibodies. The bars represent the mean ± s.d.; $n = 3$. **i**, **j**, ChIP analysis of *Hsp70*. Chromatin from S2 cells that had been treated with *EGFP* dsRNA (control) or *Dcr2* dsRNA was immunoprecipitated with anti-RNA Pol II 4H8 or anti-NELF-E antibodies. The resultant DNA was analysed by quantitative PCR. Protein binding is expressed as a percentage of input with the background signal subtracted. The bars represent the mean ± s.d.; $n = 3$. The differences in RNA Pol II ChIP values in Fig. 2f, i are due to different batches of antibody used in these assays. **k**, Permanganate (MnO_4) mapping of open transcription bubbles on *Hsp70*. Permanganate reacts with single-stranded thymine bases, such as those in an open transcription bubble, uncovering a transcriptionally engaged RNA Pol II. The autoradiograph includes a G/A ladder, which was used to determine the position of the bands, and shows the permanganate reactivity of thymines observed in S2 cells treated with *EGFP* dsRNA (control) or *Dcr2* dsRNA. The hyper-reactive thymines +22 and +30 are labelled. Two independent biological samples were analysed. **l**, The quantification of the autoradiograph is shown. exp., expression.

during heat shock, suggesting that RNAi activity is not involved in heat-shock-gene-mediated activation (Supplementary Fig. 5a, b).

Typically, the activation of heat-shock genes results in the chromosome decondensation of heat-shock loci, forming large puffs on polytene chromosomes[17]. Therefore, we used DNA fluorescence *in situ* hybridization (DNA-FISH) to look at the chromatin structure of heat-shock loci in polytene chromosomes with specific null mutations of *Dcr2* and *Ago2*: $Dcr2^{L811fsX}$ and $Ago2^{414}$. Interestingly, we observed that the 87C locus is partially decondensed in $Dcr2^{L811fsX}$ and $Ago2^{414}$ mutant chromosomes relative to the wild-type controls (Fig. 1d). The 87C locus contains four copies of *Hsp70* distributed over 30 kilobases. Decondensation was not evident at 87A, probably because this locus has only two copies of *Hsp70* within a region of less than 10 kilobases.

Because the data from PCR following reverse transcription (RT–PCR) and from cytogenetic analyses suggested that the maintenance of RNA Pol II pausing was defective, we used chromatin immunoprecipitation (ChIP) to measure the level of RNA Pol II with a phosphorylated Ser-5 residue that was present on the *Hsp70* gene before and after heat shock (Fig. 1e, f). The primers used for quantitative PCR analysis of the immunoprecipitated DNA spanned several regions of the *Hsp70* gene. An upstream primer set centred at −154 bases from the transcription start site was used to detect the heat-shock element; the +58 primer set encompassed the region of the paused polymerase[18]; and two other primer sets were downstream within the transcription unit, extending towards the end of the gene (Fig. 1e). Consistent with previous observations[18], the RNA Pol II profile observed in S2 cells showed a peak in the region of paused RNA Pol II (+58 primer set) (Fig. 1f), which increased after heat shock. Furthermore, ChIP analysis showed that DCR2 and AGO2 were present at the *Hsp70* promoter region (−154/+58) (Fig. 1g, h and Supplementary Fig. 6). Interestingly, after heat shock, the levels of both DCR2 and AGO2 proteins increased in the *Hsp70* promoter region (Fig. 1g, h, Supplementary Figs 1i, 6 and Methods). Consistent with RT–PCR and cytogenetic data, DCR2 depletion consistently decreased the level of RNA Pol II on *Hsp70* in the region of the paused polymerase (primer set +58) (Fig. 1i).

We extended our ChIP analysis to the NELF-E protein, which is part of the transcriptional regulatory complex that causes RNA Pol II pausing[16,19]. Depletion of DCR2 caused the level of NELF-E on *Hsp70* to decrease in the +58 region, where RNA Pol II pauses (Fig. 1j). The total cellular levels of RNA Pol II and NELF-E protein were not altered by DCR2 depletion (Supplementary Fig. 4b), indicating that the diminished level of RNA Pol II and NELF-E detected on *Hsp70* is not a consequence of a decrease in the amount of available protein. Conversely, in DCR2-depleted cells, we observed a reduction in the level of the AGO2 protein (Supplementary Fig. 4b). This was not simply a result of cross-targeting of the double-stranded RNA (dsRNA) because the level of the *Ago2* transcript was unaffected (Supplementary Fig. 4c). Likewise, *Ago2* dsRNA resulted in reduced DCR2 protein levels (Supplementary Fig. 4d) without affecting *Dcr2* messenger RNA levels (Supplementary Fig. 4e). These results suggest that DCR2 and AGO2 stabilize each other in a protein complex that is important for repressing heat-shock genes in uninduced cells.

To confirm that DCR2 depletion affected RNA Pol II pausing on *Hsp70*, we carried out permanganate footprinting analysis. Permanganate reacts with thymine bases in regions of single-stranded DNA, revealing the presence and location of transcriptionally engaged RNA Pol II. We observed a significant reduction in permanganate reactivity of thymine residues at +22 and +30 of *Hsp70* in DCR2-depleted cells (Fig. 1k, l), which is in agreement with the reduced occupancy of the DNA by RNA Pol II in this region (primer set +58) that was shown by ChIP (Fig. 1i).

Hence, DCR2 is involved in maintaining paused RNA Pol II at the observed *Hsp70* loci.

Heat-shock gene expression and loss of paused RNA Pol II on depletion of DCR2 could be a consequence of stress induced by depletion of the RNAi machinery in the cell. Therefore, we evaluated the impact of perturbing the RNAi pathway on the transcription of non-heat-shock genes. Four non-heat-shock genes (*CG9008*, *fz*, *rho* and *mfas*) that have paused RNA Pol II were analysed by permanganate footprinting[19,20]. Depletion of DCR2 was found also to alter the distribution of RNA Pol II in the promoter-proximal region of these genes (Supplementary Fig. 7). These changes were also accompanied by differences in transcript levels (Supplementary Fig. 8). Notably, the observed changes in RNA Pol II resulted both in upregulation (for *CG9008*, *fz* and *rho*) and downregulation (*mfas*) of the corresponding transcripts (Supplementary Fig. 8). Thus, the RNAi machinery can influence RNA Pol II pausing at non-heat-shock genes, arguing against a nonspecific DCR2-induced heat-shock response.

During heat shock, most of the *Drosophila* genome is transcriptionally quiescent. The elongating RNA Pol II dissociates from euchromatic interbands and accumulates at heat-shock loci[21]. We used this dynamic RNA Pol II relocalization behaviour to follow the chromatin binding and distribution of elongating RNA Pol II (which is Ser-2-phosphorylated), as well as AGO2 and DCR2, *in vivo*. In agreement with the ChIP results (Fig. 1h), we found that, after heat shock, AGO2 accumulated at heat-shock loci (Fig. 2a). However, in contrast to RNA Pol II, the association of AGO2 with other loci appears unchanged (Fig. 2a). When we analysed the dynamic chromatin repositioning of RNA Pol II after heat shock in *Ago2*-null mutant chromosomes, we found that RNA Pol II was still accumulated at the heat-shock loci (Fig. 2b). Strikingly, a substantial fraction of elongating RNA Pol II in $Ago2^{414}$ mutants was retained at many euchromatic sites after heat shock (Fig. 2b). The same behaviour was observed for the $Dcr2^{L811fsX}$ mutant (Supplementary Table 2). Taken together, these results show that AGO2 and DCR2 associate with many euchromatic sites and that their activity is probably required for the correct execution of global transcriptional repression after heat shock.

To dissect the role of RNAi in RNA Pol II regulation, we used three mutants that each carried a single amino acid substitution affecting the following RNAi activities: the helicase ($Dcr2^{L188F}$), the dicing ($Dcr2^{P1496L}$) and the AGO2 slicing ($Ago2^{V966M}$) activities[22,23] (Supplementary Table 1a). To check for DCR2- and AGO2-specific requirements, we first used DNA-FISH to analyse chromosome decondensation at *Hsp70* loci. Puffing frequencies were increased in all three mutants, particularly in the AGO2 slicing mutant ($Ago2^{V966M}$) (Supplementary Table 1b). In addition, in all of these mutants, the *Hsp70A*, *Hsp70B* and *Hsp68* transcripts were present at increased levels before heat shock, compared with wild type (Supplementary Fig. 9). Interestingly, the transcript increase was also evident at 87A (*Hsp70A*), where the chromatin decondensation was not appreciable at a cytogenetic level (Supplementary Fig. 9 and Supplementary Table 1b). Thus, all tested mutants induced transcript upregulation of the *Hsp70* genomic region, although this was not always accompanied by chromatin decondensation. The uncoupling of chromatin decondensation and transcriptional activation has been reported previously[24], although in this case we cannot exclude an RNAi-dependent post-transcriptional mechanism influencing the *Hsp70A* transcript levels.

Next, we analysed RNA Pol II distribution and dynamics on polytene chromosomes in the same *Dcr2* and *Ago2* mutants. Remarkably, although with a different degree of penetrance, all three mutants failed to relocalize elongating RNA Pol II after heat shock (Fig. 2c–f and Supplementary Table 2), suggesting that RNAi enzymatic activity is involved in the global RNA Pol II dynamics following the heat-shock stress response.

The association of RNAi components with RNA Pol II complexes has been reported in other systems[25–27]. To investigate the possibility that these proteins are part of a complex that regulates RNA Pol II

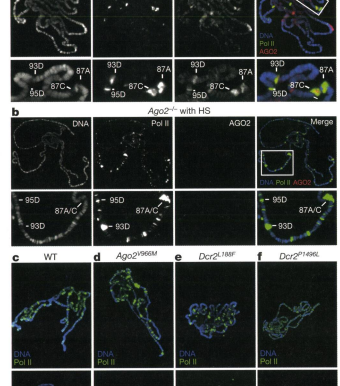

Figure 2 | Chromatin localization of RNA Pol II and AGO2 after heat shock. **a**, **b**, Co-immunolocalization of AGO2 (red) and elongating RNA Pol II (green) in WT (**a**) and homozygous $Ago2^{414}$ ($Ago2^{-/-}$) mutant chromosomes (**b**) after heat shock (HS). DNA is stained in blue. Single signals are shown in black and white. The bottom row shows a higher magnification of the boxed area (top right). **c**–**f**, Immunolocalization of elongating RNA Pol II (green) in WT (**c**) and homozygous $Ago2^{V966M}$ (**d**), homozygous $Dcr2^{L188F}$ (**e**) and homozygous $Dcr2^{P1496L}$ (**f**) chromosomes shows that missense mutations in DCR2 or AGO2 influence the behaviour of elongating RNA Pol II. DNA is stained in blue. Chromosomes in the bottom panel have been exposed to heat shock.

elongation, thus establishing a link with the observed 'pausing' defects, we tested for interactions between DCR2, NELF-E and RNA Pol II in nuclear extracts derived from *Drosophila* S2 cells. Immunoprecipitated fractions were evaluated by western blotting for the presence of RNA Pol II, DCR2, AGO2 and NELF-E (Fig. 3a). As expected, DCR2 interacted with AGO2 (ref. 28) (Fig. 3a). In addition, we found that DCR2 and AGO2 interacted with RNA Pol II and NELF-E (Fig. 3a). All of these interactions were resistant to RNase treatment, indicating that they are not an indirect consequence of protein trapping associated with emerging RNA molecules (Supplementary Fig. 10a). Compared with general transcription factors, the amount of RNA Pol II interacting with DCR2 seems to be in the same range as for the TATA-binding protein (TBP), confirming the association of DCR2 with many active loci on polytene chromosomes (Fig. 3b). When we tested the same interaction in DCR2-depleted cells, we observed a decrease in the levels of NELF-E and AGO2 associated with RNA Pol II (Supplementary Fig. 10b). These observations indicate that the DCR2–AGO2 complex influences the association of NELF-E with RNA Pol II, thereby providing a possible explanation for the observation that the

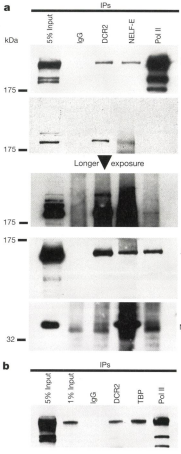

Figure 3 | DCR2 and the RNAi effector protein AGO2 associate with RNA Pol II and NELF-E. a, Nuclear extracts from *Drosophila* S2 cells were immunoprecipitated with antibodies specific for the indicated proteins (with IgG as a negative control, top), and the immunoprecipitates (IPs) were analysed by western blotting for the presence of RNA Pol II, DCR2, AGO2 and NELF-E proteins. **b**, Nuclear extracts from S2 cells were immunoprecipitated with antibodies specific for the indicated proteins (with IgG as a negative control, top) and analysed by western blotting for the presence of RNA Pol II.

depletion of DCR2 alters the behaviour of RNA Pol II in the promoter-proximal region of several genes.

Our data indicate an involvement of the RNAi machinery in the heat-shock stress response. To evaluate possible heat-shock-induced changes in the expression signature of AGO2-dependent small RNAs, we sequenced small RNAs bound to AGO2 before and after heat shock. Small RNA libraries from S2 cells were generated from RNA fractions obtained by immunoprecipitation with antibodies against AGO2 or with control IgG, with or without heat shock (Supplementary Fig. 11). Basic statistical parameters for the four libraries are listed in Supplementary Table 3. Many sequenced tags mapped to repeat regions in more than one location (Supplementary Fig. 12), which is consistent with previous *Drosophila* deep-sequenced AGO2-immunoprecipitation libraries[3,5]. First, we focused our attention on the heat-shock promoter regions (500 base pairs (bp) upstream and 50 bp downstream of the transcription start site). We found that heat-shock loci promoter regions were enriched in small RNAs and showed a marked increase in small RNA enrichment on heat shock. This was most noticeable for *Hsp23* and for all *Hsp70* loci (Supplementary Tables 4 and 5). This observation prompted us to consider whether the level of small RNAs increased across all promoters[29]. Strikingly, the most enriched promoters were the *Hsp70B* loci, and *Hsp23* was also one of the 20 most enriched loci, suggesting a direct role for AGO2 at these promoters (Fig. 4a). The possible function or role in the heat-shock response of other loci present in the top 20 list is not known.

Next, we tried to gauge shifts in small RNA tags derived from discrete transcribed regions at all gene loci in response to heat shock (Supplementary Fig. 14a). We observed little or no relative enrichment along different length intervals, suggesting that these tags are not derived exclusively from promoter regions but are equally distributed along the transcription unit (Supplementary Fig. 13). Although there was a sharp increase in AGO2-associated small RNAs in the heat-shock condition relative to the heat-shock condition negative control immunoprecipitation (confirming the specific association of these tags with AGO2), only a small increase was observed in the heat-shock condition AGO2 immunoprecipitation relative to the normal condition AGO2 immunoprecipitation, suggesting that these transcript-associating tags are present even under normal conditions (Supplementary Fig. 14a). These data suggest a role for AGO2 in regulating RNA Pol II processivity, in addition to promoter regulation.

We then analysed the strand bias of AGO2-associated small RNAs. Sense and antisense tags had a specular distribution within individual libraries, with the ratio of the sums of the sense and antisense small RNA tag counts mapping to heat-shock loci and the set of all *Drosophila* genes being equal to approximately 1 (Supplementary Fig. 14b). However, a comparison of normalized sense and antisense tag counts across AGO2-immunoprecipitation and negative-control-immunoprecipitation libraries showed a pronounced enrichment in antisense tags and little or no enrichment in sense tags, suggesting that antisense tags are highly specific in their association with AGO2 but that

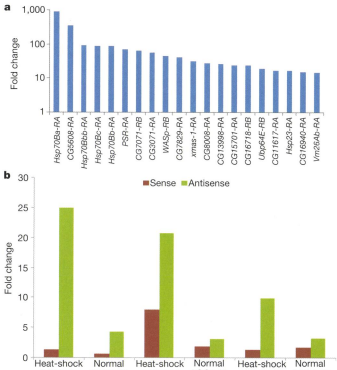

Figure 4 | Features of AGO2-associated small RNAs. a, The 20 promoters that are the most enriched in small RNAs under heat-shock versus non-heat-shock (normal) conditions. A comparison of the small RNA fold enrichment in the AGO2-immunoprecipitation (AGO2-IP) libraries between normal and heat-shock conditions is shown for all promoters. **b**, Relative enrichment calculated as fold change (*y*-axis) for the sum of all sense or antisense tags across different conditions. The analysed gene/promoter definitions and conditions are labelled below the graph. Little to no sense tag enrichment is observed across gene/promoter definitions, whereas antisense tags show enrichment across the groups, particularly under heat-shock conditions. Neg-IP, negative control immunoprecipitation.

sense tags are not. Additionally, the observed enrichment implies that antisense tag association is strongest in the heat-shock condition (Fig. 4b).

Next, we examined cap analysis of gene expression (CAGE) data that had been generated in *Drosophila* embryos for the modENCODE project[28], to survey the extent of antisense transcriptional activity at heat-shock loci (Supplementary Table 6). Antisense transcriptional activity was observed at almost all heat-shock loci and, surprisingly, many *Hsp70* loci had roughly equivalent levels of sense and antisense transcription (Supplementary Table 6), suggesting a possible source for the observed small RNA tags. Taken together, these data indicate that the observed small RNAs are probably derived from dsRNA precursors and that sequences that are antisense to the loci preferentially associate with AGO2, implying that sense targeting occurs.

In this study, we show that, in *Drosophila*, RNAi components operate in the nucleus, associate with transcriptionally active (rather then inactive) gene loci, interact with RNA Pol II and contribute to transcriptional control in a multicellular organism, particularly during the heat-shock stress response. Our results reveal that RNAi function has also evolved as a key nuclear pathway that operates in the context of pervasive sense and antisense transcription to regulate RNA-level homeostasis in the cell (see also Supplementary Discussion).

METHODS SUMMARY

Wild-type *Drosophila melanogaster* (Canton-S or w^{1118}) and the mutant stocks $Dcr\text{-}2^{L811fsX}$, $Ago2^{51B}$ ^{796fsX}, $Ago2^{414}$, $Dcr\text{-}2^{1898}$ and $Dcr\text{-}2^{214962}$ (refs 1, 2, 22, 23) were maintained under standard conditions. S2 cells were grown in serum-free insect culture medium. Protein–protein interactions were analysed by immunoprecipitations from nuclear extracts with specific antibodies. The production of dsRNAs was performed *in vitro* by T7 transcription, and the dsRNAs were transfected into S2 cells using FuGENE reagent (Roche). ChIP experiments were performed using formaldehyde-crosslinked chromatin from S2 cells. ChIP-purified DNA was analysed by using quantitative PCR with primer pairs specific for the *Hsp70* locus. Total RNA from S2 cells or larvae was reverse transcribed and analysed by quantitative PCR. Polytene chromosomes were prepared from third-instar larvae grown at 18 °C and were used for FISH. FISH signals were quantified by densitometric analysis using QFluoro software (Leica). To analyse RNA Pol II pausing on the promoters of *Hsp70* and non-heat-shock genes in S2 cells, permanganate footprinting was used. AGO2-associated RNAs were isolated from S2 cells as previously described[6]. Small RNA libraries were prepared and sequenced using a Genome Analyzer IIx (Illumina) in two lanes. For additional details see the Methods.

Full Methods and any associated references are available in the online version of the paper at www.nature.com/nature.

Received 13 July 2009; accepted 17 August 2011.
Published online 6 November 2011.

1. Okamura, K., Ishizuka, A., Siomi, H. & Siomi, M. C. Distinct roles for Argonaute proteins in small RNA-directed RNA cleavage pathways. *Genes Dev.* **18,** 1655–1666 (2004).
2. Lee, Y. S. *et al.* Distinct roles for *Drosophila* Dicer-1 and Dicer-2 in the siRNA/miRNA silencing pathways. *Cell* **117,** 69–81 (2004).
3. Kawamura, Y. *et al. Drosophila* endogenous small RNAs bind to Argonaute 2 in somatic cells. *Nature* **453,** 793–797 (2008).
4. Ghildiyal, M. *et al.* Endogenous siRNAs derived from transposons and mRNAs in *Drosophila* somatic cells. *Science* **320,** 1077–1081 (2008).
5. Czech, B. *et al.* An endogenous small interfering RNA pathway in *Drosophila*. *Nature* **453,** 798–802 (2008).
6. Okamura, K. *et al.* The *Drosophila* hairpin RNA pathway generates endogenous short interfering RNAs. *Nature* **453,** 803–806 (2008).
7. Allshire, R. C. & Karpen, G. H. Epigenetic regulation of centromeric chromatin: old dogs, new tricks? *Nature Rev. Genet.* **9,** 923–937 (2008).
8. Malone, C. D. & Hannon, G. J. Small RNAs as guardians of the genome. *Cell* **136,** 656–668 (2009).
9. Moazed, D. Small RNAs in transcriptional gene silencing and genome defence. *Nature* **457,** 413–420 (2009).
10. Teixeira, F. K. *et al.* A role for RNAi in the selective correction of DNA methylation defects. *Science* **323,** 1600–1604 (2009).
11. Llano, M. *et al.* Identification and characterization of the chromatin-binding domains of the HIV-1 integrase interactor LEDGF/p75. *J. Mol. Biol.* **360,** 760–773 (2006).
12. Miyoshi, K., Tsukumo, H., Nagami, T., Siomi, H. & Siomi, M. C. Slicer function of *Drosophila* Argonautes and its involvement in RISC formation. *Genes Dev.* **19,** 2837–2848 (2005).
13. Miyoshi, K., Okada, T. N., Siomi, H. & Siomi, M. C. Characterization of the miRNA-RISC loading complex and miRNA-RISC formed in the *Drosophila* miRNA pathway. *RNA* **15,** 1282–1291 (2009).
14. Weeks, J. R., Hardin, S. E., Shen, J., Lee, J. M. & Greenleaf, A. L. Locus-specific variation in phosphorylation state of RNA polymerase II *in vivo*: correlations with gene activity and transcript processing. *Genes Dev.* **7,** 2329–2344 (1993).
15. Lis, J. T. Imaging *Drosophila* gene activation and polymerase pausing *in vivo*. *Nature* **450,** 198–202 (2007).
16. Wu, C. H. *et al.* NELF and DSIF cause promoter proximal pausing on the *hsp70* promoter in *Drosophila*. *Genes Dev.* **17,** 1402–1414 (2003).
17. Simon, J. A., Sutton, C. A., Lobell, R. B., Glaser, R. L. & Lis, J. T. Determinants of heat shock-induced chromosome puffing. *Cell* **40,** 805–817 (1985).
18. Boehm, A. K., Saunders, A., Werner, J. & Lis, J. T. Transcription factor and polymerase recruitment, modification, and movement on dhsp70 *in vivo* in the minutes following heat shock. *Mol. Cell. Biol.* **23,** 7628–7637 (2003).
19. Lee, C. *et al.* NELF and GAGA factor are linked to promoter-proximal pausing at many genes in *Drosophila*. *Mol. Cell. Biol.* **28,** 3290–3300 (2008).
20. Gilchrist, D. A. *et al.* NELF-mediated stalling of Pol II can enhance gene expression by blocking promoter-proximal nucleosome assembly. *Genes Dev.* **22,** 1921–1933 (2008).
21. Cai, W. *et al.* RNA polymerase II-mediated transcription at active loci does not require histone H3S10 phosphorylation in *Drosophila*. *Development* **135,** 2917–2925 (2008).
22. Lim, D. H., Kim, J., Kim, S., Carthew, R. W. & Lee, Y. S. Functional analysis of dicer-2 missense mutations in the siRNA pathway of *Drosophila*. *Biochem. Biophys. Res. Commun.* **371,** 525–530 (2008).
23. Kim, K., Lee, Y. S. & Carthew, R. W. Conversion of pre-RISC to holo-RISC by Ago2 during assembly of RNAi complexes. *RNA* **13,** 22–29 (2007).
24. Chambeyron, S. & Bickmore, W. A. Chromatin decondensation and nuclear reorganization of the *Hox*B locus upon induction of transcription. *Genes Dev.* **18,** 1119–1130 (2004).
25. Kim, D. H., Villeneuve, L. M., Morris, K. V. & Rossi, J. J. Argonaute-1 directs siRNA-mediated transcriptional gene silencing in human cells. *Nature Struct. Mol. Biol.* **13,** 793–797 (2006).
26. Kavi, H. H. & Birchler, J. A. Interaction of RNA polymerase II and the small RNA machinery affects heterochromatic silencing in *Drosophila*. *Epigenetics Chromatin* **2,** 15 (2009).
27. El-Shami, M. *et al.* Reiterated WG/GW motifs form functionally and evolutionarily conserved ARGONAUTE-binding platforms in RNAi-related components. *Genes Dev.* **21,** 2539–2544 (2007).
28. Ghildiyal, M. & Zamore, P. D. Small silencing RNAs: an expanding universe. *Nature Rev. Genet.* **10,** 94–108 (2009).
29. Hoskins, R. A. *et al.* Genome-wide analysis of promoter architecture in *Drosophila melanogaster*. *Genome Res.* **21,** 182–192 (2011).

Supplementary Information is linked to the online version of the paper at www.nature.com/nature.

Acknowledgements We are deeply grateful to P. Macino for discussions. We also thank R. Carthew, E. Lai, Q. Liu, R. Paro, Y. Sik Lee, and J. T. Kadonaga for reagents. This work was supported by grants from the following: the National Institutes of Health (GM47477) to D.S.G.; the Deutsche Forschungsgemeinschaft (SPP 1356) to A.B.; the Japan Society for the Promotion of Science (JSPS) through the 'Funding Program for Next Generation World-Leading Researchers' (NEXT Program) (a Grant-in-Aid for Scientific Research (A) No. 20241047) and the Council for Science and Technology Policy to P.C.; the NEXT Program (a Research Grant-in-Aid to the RIKEN OSC) to K.M., M.C.S. and H.S.; Core Research for Evolutional Science and Technology (CREST) from the Japan Science and Technology Agency to M.C.S.; Fondazione Telethon, the Giovanni Armenise Harvard Foundation, FIRB-MIUR, Associazione Italiana Ricerca Cancro (AIRC), the Human Frontier Science Program CDA and the EMBO Young investigator program to D.F.V.C.; Fondazione Telethon, AIRC and the EU FP6 Epigenome Network of Excellence to V.O. This work was also made possible with the contribution of the Italian Ministry of Foreign Affairs, 'Direzione Generale per la Promozione e la Cooperazione Culturale' to V.O. A.S. is supported by a JSPS fellowship (ID P09745). Sequencing was provided by the Genas service (RIKEN Omics Science Center).

Author Contributions F.M.C. and V.O. conceived the study. F.M.C. and A.B. performed the ChIP experiments. F.M.C. and K.M.P. carried out the chromatin fractionation assays and the western blotting. F.M.C. carried out the quantitative RT–PCR on S2 cells. K.M.P. and F.L.S. performed the quantitative RT–PCR on mutant larvae prepared by M.C.O. F.M.C. performed the co-immunoprecipitations and contributed reagents for the chromosome and permanganate footprinting experiments. M.C.O. performed the polytene chromosome experiments. G.D. and D.S.G. performed the permanganate footprinting experiments. A.M.B. performed the bioinformatic analysis. A.S. and P.C. performed the deep sequencing. K.M., H.S. and M.C.S. performed the purification of the AGO2-associated small RNAs. F.M.C., M.C.O., D.S.G., D.F.V.C. and V.O. designed the experiments and interpreted the results. F.M.C., D.S.G., D.F.V.C. and V.O. wrote the manuscript with the contribution of M.C.O., A.B. and A.M.B., as well as input from the other co-authors.

Author Information Sequence data have been deposited in the DNA Data Bank of Japan under accession code DRA000418. Reprints and permissions information is available at www.nature.com/reprints. The authors declare no competing financial interests. Readers are welcome to comment on the online version of this article at www.nature.com/nature. Correspondence and requests for materials should be addressed to V.O (vorlando@dti.telethon.it).

LETTER

doi:10.1038/nature10618

Structure of full-length *Drosophila* cryptochrome

Brian D. Zoltowski[1], Anand T. Vaidya[1], Deniz Top[2], Joanne Widom[1], Michael W. Young[2] & Brian R. Crane[1]

The cryptochrome/photolyase (CRY/PL) family of photoreceptors mediates adaptive responses to ultraviolet and blue light exposure in all kingdoms of life[1–5]. Whereas PLs function predominantly in DNA repair of cyclobutane pyrimidine dimers (CPDs) and 6-4 photolesions caused by ultraviolet radiation, CRYs transduce signals important for growth, development, magnetosensitivity and circadian clocks[1–5]. Despite these diverse functions, PLs/CRYs preserve a common structural fold, a dependence on flavin adenine dinucleotide (FAD) and an internal photoactivation mechanism[5,6]. However, members of the CRY/PL family differ in the substrates recognized (protein or DNA), photochemical reactions catalysed and involvement of an antenna cofactor. It is largely unknown how the animal CRYs that regulate circadian rhythms act on their substrates. CRYs contain a variable carboxy-terminal tail that appends the conserved PL homology domain (PHD) and is important for function[7–12]. Here, we report a 2.3-Å resolution crystal structure of *Drosophila* CRY with an intact C terminus. The C-terminal helix docks in the analogous groove that binds DNA substrates in PLs. Conserved Trp 536 juts into the CRY catalytic centre to mimic PL recognition of DNA photolesions. The FAD anionic semiquinone found in the crystals assumes a conformation to facilitate restructuring of the tail helix. These results help reconcile the diverse functions of the CRY/PL family by demonstrating how conserved protein architecture and photochemistry can be elaborated into a range of light-driven functions.

Drosophila CRY (dCRY), a type I cryptochrome[13,14], is the primary photoreceptor for entrainment of the fly circadian clock[1,3] and also elicits magnetosensitivity[4,5]. Type II animal CRYs are also key to circadian rhythms in mammals, but primarily participate in light-independent transcriptional repression[3,15]. dCRY usually regulates circadian function by targeting the timeless protein (TIM) for ubiquitin-mediated degradation in the presence of light[16,17]. Light also causes dCRY degradation, but on a longer timescale[7,16]. Both processes involve the E3-ubiquitin ligase jetlag (JET)[16–18] and the associated action spectra are similar[7,18–20]. The dCRY active photopigment is either FAD in the oxidized (FAD^{ox}) or anionic semiquinone state ($FAD^{\bullet-}$)[7,13,18,20,21]. Light promotes dCRY binding to TIM; but TIM degradation may require an additional light response[7,8,22]. The light-dependent interaction of dCRY with TIM involves the C-terminal tail of dCRY[7–10]. dCRY with the 19 or 20 C-terminal residues removed binds TIM both in the dark and light, but can still entrain the clock under low levels of light[7,8].

The structure of dCRY was determined to 2.3 Å resolution from crystals with an unusual form of non-merohedral twinning (see Supplementary Methods and Supplementary Figs 1–4). The asymmetric unit comprises a dCRY dimer, but the contacts between subunits are not extensive (Supplementary Fig. 5). The dCRY structure most resembles that of the *Drosophila* 6-4 PL (6-4 dPL, ref. 23) (Fig. 1a), but shows notable differences in loop structures, antenna cofactor binding site, FAD centre and importantly, the variable C-terminal extension. The additional 23 C-terminal residues form a short connection (residues 516–529) from the PHD to a 10-residue helical tail (residues 530–539) that inserts into what would be the active centre of the 6-4 photolyase (Fig. 1). The C-terminal tail (CTT) mimics the DNA substrates of PLs (6-4 and CPD lesions) and positions Trp 536 (of the FFW motif invariant in type I CRYs) analogously to the 6-4 photolesion (Figs 1, 2). FAD is positioned such that changes in its electronic state probably influence the extensive interactions between the binding pocket in dCRY and C-terminal residues 525–539 (Fig. 1d) and thus, FAD photochemistry may promote conformational changes at the CTT.

In cell culture, dCRY is less stable in light than in the dark and much less stable in both without the CTT (Δ)[7,10] or the CTT substituted with alanine residues (A10; Supplementary Fig. 6). Alanine substitution of the FFW motif reduced dCRY stability to a lesser extent in both the light and dark, whereas the W536A substitution alone had little effect (Supplementary Fig. 6a). For the Δ and A10 variants, where the CTT–PHD interaction is disrupted, TIM stabilizes the PHD equally in both light and dark (Supplementary Fig. 6b). In contrast, the FFW variant has a partially functional CTT interaction in the dark and the stabilizing effect of TIM occurs mostly in the light (Supplementary Fig. 6b). Thus, TIM provides interactions to the PHD in the light that compensate for those of the CTT in the dark. Because only the wild-type and W536A variant show enhanced dark against light stabilities with TIM (Supplementary Fig. 6b) a fully engaged CTT appears to stabilize the PHD to a greater extent than does TIM (Supplementary Fig. 6b). Phosphorylation may also regulate the CTT conformation and thereby dCRY stability. Mass-spectrometry and crystallography studies detected a phosphorylation site at Thr 518, which lies at the junction between the PHD and the C-terminal helix (Supplementary Fig. 7).

Structural differences among CRYs and 6-4 PL reflect recognition of a CTT instead of a DNA substrate and different modes of regulation. Sequestration of the dCRY tail helix within the PHD DNA binding groove is coupled to the position of three loop regions specific to Type I CRYs (Figs 1, 2 and Supplementary Fig. 8): (1) the phosphate-binding loop (residues 249–263), which coordinates a phosphate anion close to FAD in the structure of *Arabidopsis thalania* PL[5]; (2) the protrusion motif (residues 288–306), an extended surface loop adjacent to the phosphate binding loop; and (3) the C-terminal lid (residues 420–446), which packs against the dCRY C-terminal helix (Figs 2, 3). Compared to 6-4 PL, the dCRY phosphate-binding loop is altered by a two-turn extension of α8 that replaces the $\sim$90° kink between the α8/α9 junction (Fig. 2 and Supplementary Fig. 8). The dCRY α8 extension causes a 20-Å deviation from the PL structure that prevents approach of the phosphate-binding loop to FAD (Fig. 2). This removes a hydrogen bond from Lys 244 (at PL numbering) to the adenosine N7 that may stabilize a conserved site of Ser phosphorylation in Type II CRYs[6]. Although dCRY conserves this phosphorylation site (Ser 261) it is remote from the active centre and residues that would stabilize Ser phosphorylation in type II CRYs are not found in type I CRYs[6](Fig. 2 and Supplementary Fig. 9). In addition, several positively charged residues that bind the DNA phosphate backbone in 6-4 dPL (Lys 154, Lys 161, Lys 449, Arg 502, Arg 505)[23] are absent in dCRY.

The Ser-rich 'C-terminal lid' is conserved in sequence and structure by type I CRYs but comprises a different motif in type II CRYs and PLs (Fig. 2). In dCRY, the linker to the CTT binds between the C-terminal lid (residues 420–446) and the 154–160 loop, which extends down from the α/β domain (Supplementary Fig. 9). Given the close proximity of the C-terminal lid to where the CTT binds, this region may have a role

[1]Department of Chemistry and Chemical Biology, Cornell University, Ithaca, New York 14853, USA. [2]Laboratory of Genetics, The Rockefeller University, New York, New York 10065, USA.

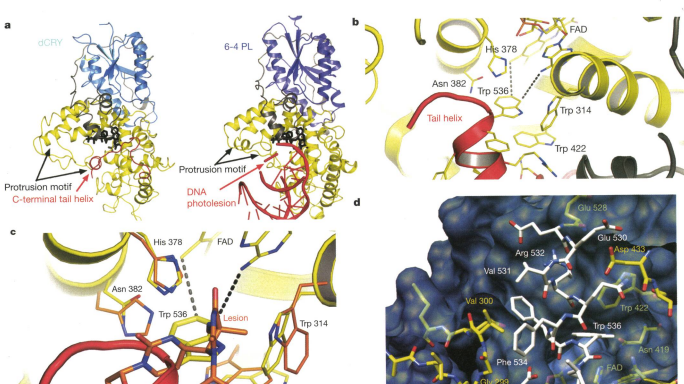

Figure 1 | dCRY resembles 6-4 PL with the C-terminal tail replacing the DNA substrate. a, Comparison of dCRY and 6-4 dPL. N-terminal α/β domain (blue) is coupled to the C-terminal helical domain (yellow) through a long linker (grey). In dCRY a C-terminal helix (red) docks to the PL DNA binding cleft besides the flavin (black). **b**, Close-up of C-terminal helix recognition groove. Trp 536 of the C-terminal helix (red) juts into what would be the 6-4 PL catalytic centre adjacent to FAD. **c**, Superposition of 6-4 photolyase and dCRY active site with bound pyrimidine dimer 'Dewar' lesion, which binds in a similar position relative to FAD and His 378 as Trp 536 in dCRY. **d**, Surface and chemical complementarity between the C-terminal helix (white) and the PHD (yellow) flavin pocket (blue).

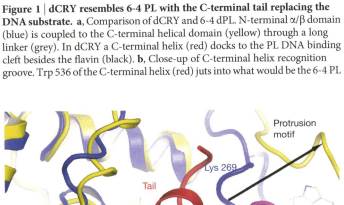

Figure 2 | Structural motifs that define Type I CRYs. Binding of the C-terminal tail into the dCRY active centre couples to structures of three loop regions unique to Type I CRYs. The protrusion motif, phosphate binding loop and C-terminal lid create a cavity to bind the CTT. Compared to 6-4 PL (blue), a β-strand shift in dCRY (yellow), displaces the YLP motif (Supplementary Fig. 9) 20 Å from the adenosine-interacting Lys of 6-4 PL. A six-residue insertion (magenta) in the phosphate loop leaves the C-term binding groove in an open conformation. dCRY has a two-turn extension of the α8 helix leading to the protrusion motif. The C-terminal linker (red) makes close contacts with an inserted Ser-rich loop: the C-terminal lid (residues 424–432).

in the recognition of targets, such as TIM or JET. Type II CRYs differ from type I CRYs and 6-4 PLs in the C-terminal lid by the introduction of three cysteine residues (Supplementary Fig. 9). The dCRY structure predicts that this cysteine-rich sequence binds near the active site of type II CRYs and may thereby serve a redox-related function (Fig. 2).

PLs use a pteridine-derived cofactor, either methenyl-trihydrofolate (MTHF), or a 8-hydroxy-deazaflavin (HDF), as a blue light antenna to sensitize the $FADH^{\bullet -}$ cofactor and thereby facilitate charge injection into pyrimidine dimers[2]. dCRY has been reported to copurify with small amounts of MTHF[21]. In contrast, we found no cofactors additional to FAD in dCRY samples purified from insect cells through chemical, spectral or crystallographic analyses. Isothermal calorimetry also indicated no binding of MTHF nor the HDF-analogue riboflavin to dCRY (Supplementary Fig. 10). Furthermore, residues that recognize the MTHF pterin moiety have very different character in dCRY than in *Escherichia coli* PL (Fig. 3a, b) and *Arabidopsis* CRY3 (Supplementary Fig. 11). Compared to 6-4 dPl, dCRY conserves a pocket, loop flexibility, and some HDF-interacting residues (for example, Phe 40, Leu 60), but others, particularly in the antenna recognition loop (residues 42–54) differ in dCRY (Fig. 3b and Supplementary Fig. 10). Thus, dCRY does not bind MTHF and is unlikely to bind HDF, unless a unique mode of recognition is used. Notably, most CRYs assume the FAD^{ox} or the $FAD^{\bullet -}$ state, but not the activated $FADH^{\bullet -}$ state required for DNA repair by PLs[24]. In the absence of an antenna cofactor dCRY can readily form $FAD^{\bullet -}$ (Supplementary Fig. 12), which is probably important as either the ground state, or photoproduct for light-regulation of the CTT[13,18,20,21].

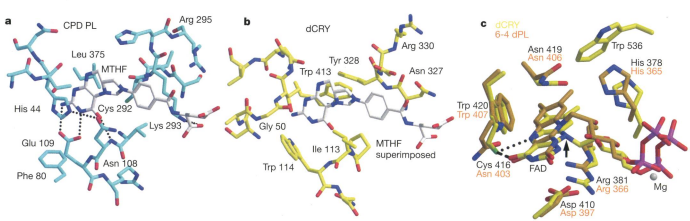

Figure 3 | Cofactor binding regions of dCRY. a, *E. coli* CPD PL binds MTHF as an antenna cofactor. **b**, In dCRY few of the residues that interact with MTFH in CPD PL are present, including the Glu residue that recognizes the pterin ring or otherwise contact MTHF (*E. coli* PL Glu 109 → dCRY Trp 114, Asn 108 → Ile 113, His 44 → Gly 50). Loop regions surrounding the cofactor in dCRY and 6-4 PL also have different structures and compositions (for example, 6-4 PL Ile 50 → dCRY Glu 45, Leu 51 → Ser 46, Leu 40 → Phe 42, Met 54 → Gly 50). **c**, Flavin centre of dCRY (yellow) compared to 6-4 PL (orange). dCRY Cys 416 replaces 6-4 PL Asn 403 and is in hydrogen bonding distance (dotted lines) of both N5 and O4 of FAD. The linkage between the ring and ribose is altered in dCRY by semiquinone formation (black arrow).

Upon light exposure dCRY rapidly converts to an anionic semiquinone $FAD^{\bullet-}$, which then decays back to the FAD^{ox} state in a manner dependent on oxygen[13,21,24]. In contrast, PLs typically form the neutral semiquinone $(FADH^{\bullet})$[24]. In PLs, an Asn residue is poised to hydrogen bond with the protonated flavin N5, but does not interact with the unprotonated flavin (Fig. 3c). In dCRY, Cys 416 at this same position is within hydrogen bonding distance of both unprotonated N5 and O4 (Fig. 3c). Thus, the negative charge that localizes on O4 and N5 in $FAD^{\bullet-}$ is stabilized by the neutral thiol. These interactions may prevent further proton transfer to $FAD^{\bullet-}$ and thereby disfavour conversion to the two-electron reduced state ($FADH^{-}$). Photoreduction of FAD_{ox} to $FAD^{\bullet-}$ depends upon stepwise electron transfer from the CRY/PL conserved Trp triad (Trp 342 → Trp 397 → Trp 420 → FAD^{*})[13,21,24]. For type I CRYs recombinantly expressed in insect cells, the Trp triad is required for photoreduction of FAD^{ox} to $FAD^{\bullet-}$, but not for light-induced degradation of CRY[13]. However, unlike other CRY/PLs, Trp 536 of the CTT provides an indole moiety as close to the flavin ring as Trp 420 (Fig. 4a). Thus, photo-oxidation of Trp 536 by FAD^{*} or $(FAD^{\bullet-})^{*}$ in type I CRYs could serve a role in photo- or magnetosensing[13,25].

The dCRY flavin shows distortions indicative of reduction (Fig. 3c), as is characteristic of flavoprotein crystals exposed to high X-ray doses[26,27]. Reduction increases the sp^3-character of N10 that leads to butterfly bending of the flavin and an expanded angle between the isoalloxazine ring and ribityl side chain[26,27]. $FAD^{\bullet-}$ probably forms in the crystal because low potential reductants cannot reduce dCRY beyond $FAD^{\bullet-}$ (ref. 18) and there is no further photoreduction, even on ps time scales[24]. Importantly, the reduced flavin conformation influences neighbouring residues that directly contact the tail helix (Fig. 3c). dCRY also conserves an active site His residue with PLs (His 378) that contacts Trp 536 (Figs 3c, 4b). In PL, the His 378 analogue protonates in the flavin semiquinone state[28]; a similar process in dCRY would further destabilize interactions between the CTT and active centre. Although crystal packing prevents CTT dissociation in the structure, the two crystallographically unique dCRY molecules display variation in tail helix binding mode, which includes displacement of Asp 539 from a buried pocket in only one molecule (Fig. 4b). These conformers indicate that the CTT is not tightly bound when the flavin is reduced. A recent study revealed that light excitation of dCRY in the $FAD^{\bullet-}$ state exposed two tryptic proteolysis sites at the dCRY C terminus: one at the end of the PHD domain and the other within the CTT[18]. Given the substantial structural alterations in FAD upon reduction, it is somewhat surprising that more modest and short-lived changes induced by photo-excitation of $FAD^{\bullet-}$ would be required to release the CTT. Nonetheless, the close association between the CTT and the flavin centre provides the proximity to mechanistically link tail restructuring to flavin electronic state. Notably, light still drives rhythms in flies containing dCRY with the CTT removed[7,8]. Thus,

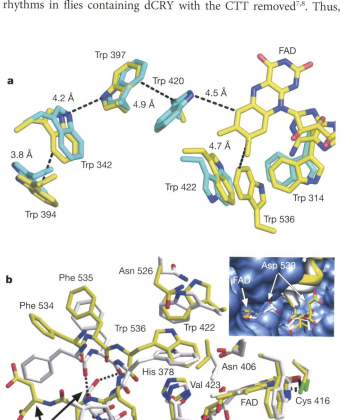

Figure 4 | Redox active groups and conformations in dCRY. a, Trp triad photoreduction pathway (Trp 420, Trp 397 and Trp 342) in dCRY (yellow) and *Drosophila* 6-4 photolyase (cyan). Trp 536 resides as close to FAD^{ox} as Trp 420. 6-4 dPL conserves all three Trp residues, and also contains surface residue Trp 394. Alternative electron transport pathways involving Trp 314, Trp 422 and Trp 536 are possible in dCRY. The Trp 422 indole flips relative to 6-4 dPL, but similar to CPD PLs. **b**, Conformational variation in the C-terminal peptide orientations of the two subunits (yellow and white) in the dCRY active centre. Asp 539 hydrogen bonds back to the CTT in one molecule (white), but displaces from the pocket in the other (inset).

although flavin-dependent change in CTT conformation gates formation of the proper target complex with TIM or JET, additional dCRY photochemistry may be required to send appropriate signals in these and other processes independent of TIM[4,25,29,30].

METHODS SUMMARY

dCRY amino acids 1–539 were cloned into pFastBac-HTa (Invitrogen) for Sf9 insect cell expression. Virus was selected and expanded (Kemp Biotechnologies) and protein was incubated at 27 °C for 72 h post infection. The 6×His-tagged protein was purified from 21 dCRY cultures via Ni-NTA (Qiagen) affinity chromatography. dCRY was eluted in buffer containing 100 mM imidazole, 50 mM HEPES pH 8, 150 mM NaCl, 2 mM DTT and 10% glycerol. The eluate was concentrated and run on a size-exclusion chromatography column (Superdex 200 GE Healthcare Life Sciences) in buffer containing 50 mM HEPES pH 8, 150 mM NaCl and 10% glycerol.

dCRY crystals were obtained using the hanging-drop method with equal volumes of well solution (18% PEG 4K, 150 mM magnesium acetate, and 100 mM Tris pH 8.5) and dCRY ($5\,mg\,ml^{-1}$). 2.3 Å resolution diffraction data were collected at the microbeam line ID-24E of the Advance Photon Light Source (APS) and corrected for non-merohedral twinning as described in the Supplementary Methods. Molecular replacement with PDB file 1TEZ gave initial phases. The structure was built in XtalView and refined in CNS.

dCRY cell culture studies were conducted with amino-terminally 3×Myc-tagged dCRY and 3×haemagglutinin (HA) C-terminally tagged ls-TIM (dTIM) cloned into pAc5.1/V5 (Invitrogen). S2 cells in Sneider's medium supplemented with 10% FBS were transfected with dCRY and either empty vector or dTIM plasmids. 24 h post-transfection the cell medium was refreshed and the cells divided into two populations. After 24 h cells were lysed under red light or after 1 h white-light treatment (~600 lx). Relative abundance of dCRY was then assayed via 6% SDS–PAGE immunostained with myc (SIGMA) and tubulin (SIGMA).

Full Methods and any associated references are available in the online version of the paper at www.nature.com/nature.

Received 24 March; accepted 5 October 2011.
Published online 13 November 2011.

1. Cashmore, A. R. Cryptochromes: enabling plants and animals to determine circadian time. *Cell* **114,** 537–543 (2003).
2. Sancar, A. Structure and function of DNA photolyase and cryptochrome blue-light photoreceptors. *Chem. Rev.* **103,** 2203–2238 (2003).
3. Partch, C. L. & Sancar, A. Photochemistry and photobiology of cryptochrome blue-light photopigments: the search for a photocycle. *Photochem. Photobiol.* **81,** 1291–1304 (2005).
4. Gegear, R. J., Casselman, A., Waddell, S. & Reppert, S. M. Cryptochrome mediates light-dependent magnetosensitivity in *Drosophila*. *Nature* **454,** 1014–1018 (2008).
5. Yoshii, T., Ahmad, M. & Helfrich-Forster, C. Cryptochrome mediates light-dependent magnetosensitivity of *Drosophila*'s circadian clock. *PLoS Biol.* **7,** e1000086 (2009).
6. Hitomi, K. *et al.* Functional motifs in the (6-4) photolyase crystal structure make a comparative framework for DNA repair photolyases and clock cryptochromes. *Proc. Natl Acad. Sci. USA* **106,** 6962–6967 (2009).
7. Busza, A., Emery-Le, M., Rosbash, M. & Emery, P. Roles of the two *Drosophila* CRYPTOCHROME structural domains in circadian photoreception. *Science* **304,** 1503–1506 (2004).
8. Dissel, S. *et al.* A constitutively active cryptochrome in *Drosophila melanogaster*. *Nature Neurosci.* **7,** 834–840 (2004).
9. Hemsley, M. J. *et al.* Linear motifs in the C-terminus of *D. melanogaster* cryptochrome. *Biochem. Biophys. Res. Commun.* **355,** 531–537 (2007).
10. Rosato, E. *et al.* Light-dependent interaction between *Drosophila* CRY and the clock protein PER mediated by the carboxy terminus of CRY. *Curr. Biol.* **11,** 909–917 (2001).
11. Partch, C. L., Clarkson, M. W., Ozgur, S., Lee, A. L. & Sancar, A. Role of structural plasticity in signal transduction by the cryptochrome blue-light photoreceptor. *Biochemistry* **44,** 3795–3805 (2005).
12. van der Schalie, E. A., Conte, F. E., Marz, K. E. & Green, C. B. Structure/function analysis of *Xenopus* cryptochromes 1 and 2 reveals differential nuclear localization mechanisms and functional domains important for interaction with and repression of CLOCK-BMAL1. *Mol. Cell. Biol.* **27,** 2120–2129 (2007).
13. Ozturk, N., Song, S. H., Selby, C. P. & Sancar, A. Animal type 1 cryptochromes. Analysis of the redox state of the flavin cofactor by site-directed mutagenesis. *J. Biol. Chem.* **283,** 3256–3263 (2008).
14. Yuan, Q., Metterville, D., Briscoe, A. D. & Reppert, S. M. Insect cryptochromes: gene duplication and loss define diverse ways to construct insect circadian clocks. *Mol. Biol. Evol.* **24,** 948–955 (2007).
15. Griffin, E. A. Jr, Staknis, D. & Weitz, C. J. Light-independent role of CRY1 and CRY2 in the mammalian circadian clock. *Science* **286,** 768–771 (1999).
16. Koh, K., Zheng, X. Z. & Sehgal, A. JETLAG resets the *Drosophila* circadian clock by promoting light-induced degradation of TIMELESS. *Science* **312,** 1809–1812 (2006).
17. Peschel, N., Chen, K. F., Szabo, G. & Stanewsky, R. Light-dependent interactions between the *Drosophila* circadian clock factors cryptochrome, jetlag, and timeless. *Curr. Biol.* **19,** 241–247 (2009).
18. Ozturk, N., Selby, C. P., Annayev, Y., Zhong, D. & Sancar, A. Reaction mechanism of *Drosophila* cryptochrome. *Proc. Natl Acad. Sci. USA* **108,** 516–521 (2011).
19. VanVickle-Chavez, S. J. & Van Gelder, R. N. Action spectrum of *Drosophila* cryptochrome. *J. Biol. Chem.* **282,** 10561–10566 (2007).
20. Hoang, N. *et al.* Human and *Drosophila* cryptochromes are light activated by flavin photoreduction in living cells. *PLoS Biol.* **6,** e160 (2008).
21. Berndt, A. *et al.* A novel photoreaction mechanism for the circadian blue light photoreceptor *Drosophila* cryptochrome. *J. Biol. Chem.* **282,** 13011–13021 (2007).
22. Ceriani, M. F. *et al.* Light-dependent sequestration of TIMELESS by CRYPTOCHROME. *Science* **285,** 553–556 (1999).
23. Maul, M. J. *et al.* Crystal structure and mechanism of a DNA (6-4) photolyase. *Angew. Chem. Int. Edn Engl.* **47,** 10076–10080 (2008).
24. Kao, Y. T. *et al.* Ultrafast dynamics and anionic active states of the flavin cofactor in cryptochrome and photolyase. *J. Am. Chem. Soc.* **130,** 7695–7701 (2008).
25. Gegear, R. J., Foley, L. E., Casselman, A. & Reppert, S. M. Animal cryptochromes mediate magnetoreception by an unconventional photochemical mechanism. *Nature* **463,** 804–807 (2010).
26. Senda, T., Senda, M., Kimura, S. & Ishida, T. Redox control of protein conformation in flavoproteins. *Antioxid. Redox Signal.* **11,** 1741–1766 (2009).
27. Rohr, A. K., Hersleth, H. P. & Andersson, K. K. Tracking flavin conformations in protein crystal structures with Raman spectroscopy and QM/MM calculations. *Angew. Chem. Int. Ed.* **49,** 2324–2327 (2010).
28. Schleicher, E. *et al.* Electron nuclear double resonance differentiates complementary roles for active site histidines in (6-4) photolyase. *J. Biol. Chem.* **282,** 4738–4747 (2007).
29. Tang, C. H. A., Hintergeger, E., Shang, Y. H. & Rosbash, M. Light-mediated TIM degradation within *Drosophila* pacemaker neurons (s-LNvs) is neither necessary nor sufficient for delay zone phase shifts. *Neuron* **66,** 378–385 (2010).
30. Fogle, K. J., Parson, K. G., Dahm, N. A. & Holmes, T. C. CRYPTOCHROME is a blue-light sensor that regulates neuronal firing rate. *Science* **331,** 1409–1413 (2011).

Supplementary Information is linked to the online version of the paper at www.nature.com/nature.

Acknowledgements This study was supported by NIH Grant GM079679 to B.R.C. and GM054339 to M.W.Y. We thank the NE-CAT at the Advanced Photon Source of Argonne Laboratories for access to data collection facilities. We are indebted to C. Kemp for insect cell expression of dCRY and C. Manahan, X. Xu and W. Horne for their help with the ITC experiments.

Author Contributions B.R.C., B.D.Z., A.T.V., D.T. and M.W.Y. designed the project. J.W. cloned, expressed and purified dCRY, B.D.Z. and A.T.V. purified and crystallized dCRY and collected diffraction data. B.D.Z. and B.R.C. determined the structure. D.T. and M.W.Y. performed CRY stability studies. A.T.V. performed ITC experiments. B.D.Z. and B.R.C. wrote the manuscript and all authors provided editorial input.

Author Information Atomic coordinates for the reported crystal structures have been deposited with the Protein Data Bank under accession code 3TVS. Reprints and permissions information is available at www.nature.com/reprints. The authors declare no competing financial interests. Readers are welcome to comment on the online version of this article at www.nature.com/nature. Correspondence and requests for materials should be addressed to B.R.C. (bc69@cornell.edu).

nature REVIEWS MOLECULAR CELL BIOLOGY

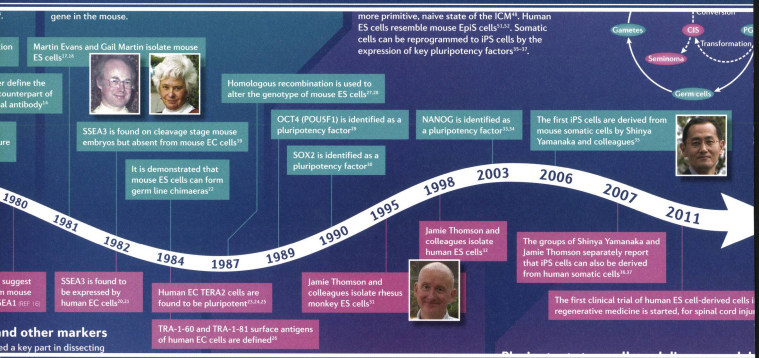
gene in the mouse.
more primitive, naive state of the ICM[44]. Human ES cells resemble mouse EpiS cells[53,57]. Somatic cells can be reprogrammed to iPS cells by the expression of key pluripotency factors[16–17].
Martin Evans and Gail Martin isolate mouse ES cells[37,38]
Homologous recombination is used to alter the genotype of mouse ES cells[27,28]
SSEA3 is found on cleavage stage mouse embryos but absent from mouse EC cells[39]
It is demonstrated that mouse ES cells can form germ line chimaeras[45]
OCT4 (POU5F1) is identified as a pluripotency factor[29]
SOX2 is identified as a pluripotency factor[30]
NANOG is identified as a pluripotency factor[53,54]
The first iPS cells are derived from mouse somatic cells by Shinya Yamanaka and colleagues[55]
Gametes
CIS
Transformation
Seminoma
Germ cells
1980
1981
1982
1984
1987
1989
1990
1995
1998
2003
2006
2007
2011
Jamie Thomson and colleagues isolate human ES cells[58]
The groups of Shinya Yamanaka and Jamie Thomson separately report that iPS cells can also be derived from human somatic cells[16,17]
SSEA3 is found to be expressed by human EC cells[39,43]
Human EC TERA2 cells are found to be pluripotent[52,54,93]
Jamie Thomson and colleagues isolate rhesus monkey ES cells[33]
TRA-1-60 and TRA-1-81 surface antigens of human EC cells are defined[26]
The first clinical trial of human ES cell-derived cells is regenerative medicine is started, for spinal cord injur

POSTER – From teratomas to embryonic stem cells: discovering pluripotency

This year marks the thirtieth anniversary since mouse embryonic stem (ES) cells were first isolated from blastocysts. This paved the way to the first targeted knockouts of genes in mice, which provided a crucial tool for studying mouse development and founded a new field of stem cell research. Today, researchers are able to generate induced pluripotent stem (iPS) cells from somatic cells, which might have important clinical applications.

This Poster by Peter W. Andrews and Paul J. Gokhale provides a timeline overview of the history of pluripotency, starting from early studies of teratocarcinomas in 1954, which preceded the isolation of mouse and human ES cells, and ending with the generation of iPS cells. In doing so, it highlights how our understanding of the pluripotent state has evolved over almost 60 years.

Access the poster free online!
www.nature.com/nrm/posters/discoveringpluripotency

Produced with support from

abcam® discover more

nature publishing group npg

nature REVIEWS GENETICS

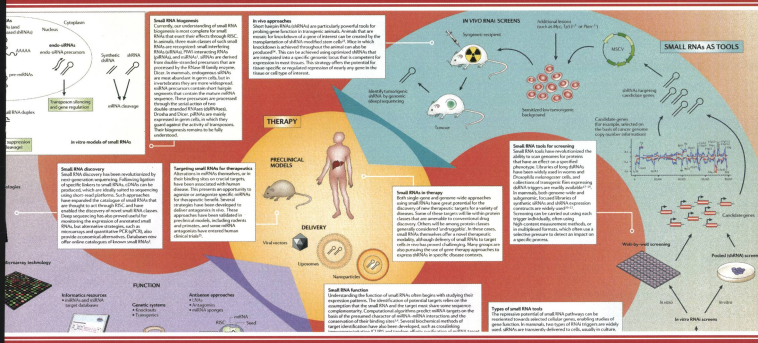
Small RNA biogenesis
Currently, our understanding of small RNA biogenesis comes from studies of miRNAs that exert their effects through RISC. In animals, three main classes of such small RNAs have been identified: miRNAs, siRNAs (siRNAs), PIWI-interacting RNAs (piRNAs), and snoRNA-derived RNAs (sdRNAs). sdRNAs are derived from double-stranded precursors that are processed by the RNase III family enzyme, Dicer. Although piRNA biogenesis is also an most abundant in germ cells, but in invertebrates they are more widespread. piRNAs are derived from single-stranded sequences that contain the mature miRNA sequence. These precursors are processed through the use of Dicer-1 (DCR-1), Drosha and Dicer. piRNAs are mainly expressed in germ cells, in which they guard against the activity of transposons. piRNA biogenesis remains to be fully understood.
In vivo approaches
Short hairpin RNAs (shRNAs) are particularly powerful tools for loss-of-function studies in mammals. shRNAs are RNAs that exert their effects through RISC. In animals, three main classes of such small RNAs have been identified: miRNAs, siRNAs (siRNAs), PIWI-interacting RNAs (piRNAs), and snoRNA-derived RNAs (sdRNAs). sdRNAs are derived from double-stranded precursors that are processed by the RNase III family enzyme, Dicer. Although piRNA biogenesis is also an most abundant in germ cells, but in invertebrates they are more widespread. piRNAs are derived from single-stranded sequences that contain the mature miRNA sequence. These precursors are processed through the use of Dicer-1 (DCR-1), Drosha and Dicer. piRNAs are mainly expressed in germ cells, in which they guard against the activity of transposons. piRNA biogenesis remains to be fully understood.
IN VIVO RNAi SCREENS
SMALL RNAs AS TOOLS
THERAPY
PRECLINICAL MODELS
DELIVERY
Viral vectors
Liposomes
Nanoparticles
Small RNA discovery
Small RNA discovery has been revolutionized by next-generation sequencing. Following ligation of 3′ and 5′ adapters to small RNAs (or their products), which are ideally suited to sequencing using short-read platforms. Such approaches have revealed many classes of small RNAs that are thought to act through RISC and have enabled the discovery of novel small RNA classes. Deep sequencing has also proved useful for monitoring the expression of annotated small RNAs. Microarrays, northern blotting, RNase protection assays and quantitative PCR (qPCR) also provide economical alternatives. Databases now offer online catalogues of known small RNAs.
Targeting small RNAs for therapeutics
Alterations in miRNAs themselves, or in their binding sites on coding targets, can contribute to the pathogenesis of disease. This presents an opportunity to agonize or antagonize specific miRNAs. Many different types of small RNA therapeutics have been developed to deliver antagonists in vivo. These approaches have been successful in pre-clinical models, including rodents and primates, and some miRNA antagonists have entered human clinical trials[1].
Small RNAs in therapy
Both single-gene and genome-wide approaches using small RNAs have great potential for the discovery of new therapeutic targets for a variety of diseases. Small RNAs can target many gene classes that are amenable to conventional drug discovery. Others will be among protein classes traditionally thought to be 'undruggable'. However, small RNAs themselves offer a novel therapeutic modality, although delivery of small RNAs to target cells in vivo has proved challenging. Many groups are also pursuing the use of gene therapy approaches to express shRNAs in specific disease contexts.
Small RNA tools for screening
Small RNA tools have revolutionized the ability to perform loss-of-function screens that have an effect on a specified phenotype. Libraries of long dsRNAs, which are processed into siRNAs in Drosophila melanogaster cells, and collections of transgenic flies expressing shRNAs in specific tissues, both of which are available, have proved powerful. Arrayed, focused libraries of synthetic siRNAs and shRNA-expression constructs are widely used[2,3,4]. Pooled screens, which are carried out using each trigger individually, offer more scope. High-content measurement methods, or selection for phenotypes, which often use a selective pressure to detect an impact on a specific process.
Small RNA function
Understanding the function of small RNAs often begins with studying their expression patterns. The identification of targets relies on the assumption that the small RNA and the target must share some sequence complementarity. Computational approaches have been developed on the basis of the presumed character of miRNA–mRNA interactions and the conservation of their binding sites[5,6]. Several biochemical methods of target identification have also been developed, such as cross-linking
Types of small RNA tools
The expression potential of small RNA pathways can be maximized towards selected cellular genes, enabling studies of mammalian biology and disease. shRNAs and siRNAs are most widely used. siRNAs are transiently delivered to cells, usually in cultures
Bioinformatics technology
FUNCTION
Informatics resources
• miRNAs and miRNA target databases
Genetic systems
• Knockouts
• Transgenics
Antisense approaches
• LNAs
• Antagomirs
• miRNA sponges
miRNA
RISC
Seed
Identify tumorigenic shRNA by genomic-scale sequencing
Tumour
Sensitized liver tumorigenic background
Additional lesions (such as Myc, Tp53−/− or Pten−/−)
MSCV
shRNAs targeting candidate genes
Candidate genes (for example, selected on the basis of their expression copy number alterations)
Candidate genes
Walk-by-well screening
Pooled shRNAs screen
In vitro
In vivo
In vitro RNAi screens

Poster – Tools for studying and using small RNAs: from pathways to functions to therapies

Authors: Kenneth Chang and Gregory J. Hannon

November 2011

This Poster illustrates the tools that have been developed to understand the functions of small RNAs and, conversely, the ways in which small RNAs can be harnessed as tools.

Access the poster **FREE** online!
www.nature.com/nrg/posters/small-RNA

COMING SOON:

RNA interference animation: an up-to-date, audiovisual overview of the RNAi pathway.

This Poster is freely available thanks to support from

Thermo SCIENTIFIC
Part of Thermo Fisher Scientific

nature publishing group npg

nature REVIEWS CANCER

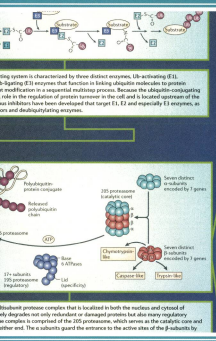
Activated
Substrate
Ub
1
2
3
Ub-activating enzyme (E1)
Ub-conjugating enzyme (E2)
Ub-protein ligase (E3)
Substrate
tting system is characterized by three distinct enzymes, Ub-activating (E1),
-ligating (E3) enzymes that function in linking ubiquitin molecules to protein
e modification in a sequential multistep process. Because the ubiquitin-conjugating
role in the regulation of protein turnover in the cell, and is located upstream of the
ase inhibitors have been developed that target E1, E2 and especially E3 enzymes, as
ors and deubiquitylating enzymes.
Polyubiquitin-protein conjugate
Released polyubiquitin chain
Seven distinct α subunits encoded by 7 genes
20S proteasome
Catalytic core
19S regulator
ATP
Seven distinct β subunits encoded by 7 genes
Chymotrypsin-like
Caspase-like
Trypsin-like
Base
6 ATPases
Lid
(specificity)
17+ subunits
19S proteasome
(regulatory)
Ubiquitin
Bisubunit protease complex that is localized in both the nucleus and cytosol of
ely-degrades not only redundant or damaged proteins but also many regulatory
e complex is comprised of the 20S proteasome, which serves as the catalytic core and
either end. The α subunits guard the entrance to the active sites of the β-subunits by

Interferon-γ-inducible form of the proteasome, is derived from replacement of the β1, β2, and β5 subunits with the immunoproteasome-specific β1i, β2i, and β5i subunits, respectively. This results in modified substrate specificity, altered proteolytic activity and a differential response to inhibitors. Increased expression of the immunoproteasome complex has been reported in multiple myeloma. PS-341 has been shown to preferably inhibit the immunoproteasome 20S activity (mainly by binding to the β1 subunit) resulting in increased apoptotic cell death in human haematopoietic cancer cells. Other PIBs that are being developed include PR-924, PR-957 and other β1 specific inhibitors.

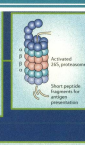

successfully in treating hematological malignancies (specifically multiple myeloma and mantle cell lymphoma), its effect on solid tumors has been less promising. This lack of efficacy in solid tumors may be due to the nature of reversible proteasome inhibition by bortezomib: its short duration of activity; and inherent or acquired resistance in tumor cells. The clinical use of bortezomib is also hampered by dose-limiting toxicities, such as peripheral neuropathy.

Table 1 | **Proteasome inhibitors as anticancer drugs in clinical development**

Proteasome inhibitor (developer)	Chemical structure	Structural class	Inhibition type	Inhibition profile	Development status	Types of cancers treated	Route of administration
Bortezomib (Millennium Pharmaceuticals)		Peptide boronic acid	Reversible	CTL, C-L and immuno-proteasome	Approved	Multiple myeloma, recurrent multiple myeloma, mantle cell lymphoma	Intravenous
Carfilzomib (Onyx Pharmaceuticals)		Peptide epoxyketone	Irreversible	CTL and immuno-proteasome	Phase II-III	Recurrent multiple myeloma, lymphoma, leukemia, disease and solid tumours	Intravenous
Marizomib (Nereus)		β-lactone-γ-lactam	Irreversible	CTL, C-L, TL and immuno-proteasome	Phase Ib	Recurrent multiple myeloma, solid tumors, lymphoma and brain leukemias	Intravenous
CEP-18770 (Cephalon)		Peptide boronic acid	Reversible	CTL	Phase I-III	Recurrent multiple myeloma, refractory drugs and solid tumors, lymphoblastic leukaemia and mantle cell lymphoma	Intravenous or oral
MLN-3709 (Millennium Pharmaceuticals)		Peptide boronic acid	Reversible	CTL	Phase I and II	Lymphoma and solid tumours	Intravenous or oral

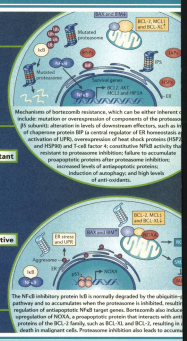
BAX or BAK
Mutated proteasome
BCL-2, MCL1 and BCL-XLT
Bcl-2
Bcl-XL
Mcl-1
Bax
Bak
Normal proteasome
BCL-2, MCL1 and BCL-XLT
NFκB
IκB
Mechanisms of bortezomib resistance, which can be either inherent o
include: mutation or overexpression of components of the proteaso
β5 subunit); alteration in levels of downstream effectors, such as in
of chaperone protein BiP (a central regulator of ER homeostasis a
activation of UPR), overexpression of heat shock proteins (HSP2
and HSP90) and T-cell factor 4 constitutive NFκB activity thro
resistant to proteasome inhibition; failure to accumulate
proapoptotic proteins after proteasome inhibition;
increased levels of antiapoptotic proteins;
induction of autophagy; and high levels
of anti-oxidants.
Resistant
Sensitive
ER stress and UPR
XBP-1(S) / HSP90
BCL-2, MCL1 and BCL-XLT
Aggresome
IκB
Bcl-xL
NOXA
The NFκB inhibitory protein IκB is normally degraded by the ubiquitin-
pathway and so accumulates when the proteasome is inhibited, result
regulation of downstream NFκB target genes. Bortezomib also induce
upregulation of NOXA, a BH3-only pro-apoptotic protein that interacts with pro-
proteins of the BCL-2 family, such as BCL-XL and BCL-2, leading to
death in malignant cells. Proteasome inhibition also leads to accumu

Poster – Proteasome inhibition and cancer therapy

Author: Q. Ping Dou

In recent years the ubiquitin-proteasome system has been identified as essential for maintaining a crucial balance between cell growth and death, the progression of human malignancies, and the development of drug resistance in cancer cells. Emerging evidence shows that targeting the ubiquitin-proteasome degradation pathway is a useful anticancer strategy. The approval of bortezomib by the US Food and Drug Administration (FDA) as the first proteasome inhibitor to be implemented in the treatment of malignant disease, either alone or in combination with other therapies, represents a substantial milestone in this field. Other novel proteasome inhibitors, such as marizomib and carfilzomib, have recently been developed and are being tested in clinical trials. These recent achievements and the development of new drugs that target the ubiquitin–proteasome pathway are highlighted in this poster.

Access the poster **FREE** online!
www.nature.com/nrc/posters/proteasome

This Poster is freely available thanks to sponsorship from

ONYX PHARMACEUTICALS

nature publishing group npg

CAREERS

TURNING POINT Geneticist works in academia while nurturing a non-profit group **p.403**

UNITED STATES Foreign-born US scholars are more prolific but less satisfied **p.403**

NATUREJOBS For the latest career listings and advice **www.naturejobs.com**

RESEARCH

Radical rethink

Student-initiated projects have the potential to change a lab's focus. But with freedom comes responsibility.

BY ROBERT FREDERICK

For the past three years, Jon Beckwith's lab has focused on studying *Mycobacterium smegmatis* as a model for tuberculosis. It has been a major shift in direction for Beckwith, a microbiologist at Harvard Medical School in Boston, Massachusetts, who spent the previous four decades using *Escherichia coli* to study fundamental problems of biology, including cell division, protein folding and membrane-protein structure. He is still surprised that he has ended up working on problems with direct medical significance. "It's a bit of a shock," says Beckwith. And he owes it all to a student.

Rachel Dutton was a PhD candidate in Beckwith's lab in 2006, when she first decided to study other bacteria. It wasn't so much that she was bored with *E. coli* as that she was interested in microbes about which little was known. "It took a while to convince Jon that it was an interesting project," recalls Dutton, who is now setting up her own microbial-diversity lab at Harvard. "We had many meetings where he would give me these looks." Dutton gained the support of Dana Boyd, a senior scientist in the lab, but she knew that Beckwith was questioning the value of her ideas. Eventually, however, he gave Dutton the freedom she was seeking. "If someone insists on doing something," says Beckwith, "I let them, unless I have really strong fundamental disagreements with what they're doing." Eventually, Dutton and Boyd's results convinced Beckwith to find funding for the project, which now occupies his entire lab.

Fledgling researchers can reap plentiful rewards from the freedom to pursue their own interests. They can learn important lessons about the responsibilities and pitfalls of independence. And successful projects might also lead to funding and publication opportunities for others in the home lab. But independence for students requires an open-minded principal investigator and a flexible funding source, and brings the risk of failure. Young scientists who are given research freedom need to know what they are getting into.

FLEXIBLE FOCUS

It is rare for a postgraduate project to completely change the focus of a lab as Dutton's did; but both students and mentors should embrace students' pursuit of tangential or parallel projects. Indeed, some researchers argue that it is crucial for those who want to run labs to carve their own niches. "You don't want to compete with your principal investigator for grants," says Maryrose Franko, senior programme officer for graduate science education at the Howard Hughes Medical Institute in Chevy Chase, Maryland. Instead, she says, "you want to set yourself apart" by branching out into new areas. Franko advises young scientists not to abandon their original projects. Instead, she says, they should volunteer to split their time between the mentor's project and their own. "They'll understand that you need those preliminary results," says Franko. "You need some research to take with you."

In some places, including the United States, students don't start their own projects as soon as they join the lab. "You first typically have to prove yourself in what the principal investigator needs to get done," says Zoe Fonseca-Kelly, an ophthalmology researcher at the Massachusetts Eye and Ear Infirmary in Boston. "After a certain amount of time you can develop your own projects, provided you can juggle your time." This usually happens between several months and a year into the PhD.

Students shouldn't get too discouraged if their mentor resists a proposed project, says Cynthia Fuhrmann, programme director for academic career development at the University of California, San Francisco. In 2008, Fuhrmann ▶

surveyed the university's graduate students and found that a significant proportion of them get disillusioned with academia around the time that they need to find their own projects, with almost half of those who reported being interested in academic research careers in their first year changing their minds by their third (C. N. Fuhrmann *et al. CBE Life Sci. Educ.* **10,** 239–249; 2011). The students who can be proactive and pursue a project that excites them — even if it deviates from the lab's focus and requires outside collaborators — are most likely to keep dreams of a professorship alive, says Fuhrmann.

PROCEED WITH CAUTION

Ideally, postdocs and graduate students should find out how much freedom to expect before they apply to work with a principal investigator (see *Nature* **470,** 129–131; 2011). They need to do their homework, says Cathee Johnson Phillips, executive director of the US National Postdoc Association in Washington DC. She advises that applicants consider the type of publications that come from the lab, and whether most of them were based on the principal investigator's research, or were prompted by lab members, graduate students or postdocs. But applicants should tread carefully — asking a potential employer about the flexibility of their research agenda can be taken as a criticism of their status or current work. "It's not an easy conversation to have," admits Phillips. Students and postdocs might also talk to lab members, or even to scientists working with other investigators in the same department.

Applicants could look for hints of flexibility in the investigator's own training, says Margaret Kiley, a social scientist at the Australian National University in Canberra, who studies how students learn to become researchers. "If you were socialized into the discipline and into the research, doing it in a particular way," says Kiley, "you are likely to replicate that yourself." Candidates should investigate the career or publication trajectory of their potential mentors, says Franko, as well as the grant portfolio of the potential mentor's own principal investigator before, during and after the mentor's stint as a protégé. But the "big thing", Franko emphasizes, "is communication ahead of time".

Robert Dooling, a psychology researcher at the University of Maryland in College Park, makes sure that he talks to students and postdocs both before and shortly after they join his lab. "Before you came," he tells them in the second chat, "we had a conversation about why you came and what you want to work on. There's flexibility to try out things that are unusual, but it's not an unbridled freedom to do whatever moves you in the moment." After that, Dooling shows them his successful grant applications and explains that all lab members have an obligation to help to keep the lab funded.

There are downsides to having a mentor who is open to letting students explore completely new research: projects could be too ambitious, or might not provide results, and so might drag on indefinitely. "I don't believe in eight-year PhD theses," says Karolin Luger, a structural biologist at Colorado State University in Fort Collins. Principal investigators "have a bit more experience, and so we know what it takes to graduate a student", she adds. Students "may be super-optimistic and say, 'Oh, I can have this done in three months', and we know it's going to be like a two-year project. They need to graduate."

VARIABLE FUNDING

Even for students whose mentors encourage freedom, money can be a constraint. Before totally changing his research programme, Beckwith needed to be convinced not only of the project's scientific rationale, but also of the likelihood that it would receive funding. To that end, Dutton and Boyd did a series of small, inexpensive experiments. "Each idea that she and Dana proposed, one after the other, turned out to be correct," says Beckwith. It took some time, but the results were so promising that Beckwith was able to secure the flexible funding that his lab needed to pursue the work further.

Strategic grant writing can help to give a lab's young scientists greater flexibility, suggests David Delpy, chief executive of the UK Engineering and Physical Sciences Research Council in Swindon. In grant applications, investigators could outline their grand research problems and several ways to seek solutions, from which young scientists can take their pick. Delpy cautions against extremely focused grant applications, which tend to quash creativity. "You can't define the outcome of your research at the outset," he says, "and you ought to follow up new ideas that come along that might be appropriate."

JUST ONE MORE EXPERIMENT

That extra, unplanned experiment often allows young researchers to find their own direction — and shows principal investigators that the researchers were right to take a radical departure. As a graduate student at Duke University in Durham, North Carolina, Jeremy Lenhardt did just one more experiment than was recommended by his supervisor, chemist Stephen Craig. It was a chance for Lenhardt to satisfy his scientific curiosity in his chosen field — mechanochemical coupling, the interplay between chemistry and materials. He had little in the way of a particular hypothesis, but he did have a hunch. "I want to try something," Lenhardt recalls thinking. The observations that he made led to several publications and, eventually, a postdoctoral position at Lawrence Livermore National Laboratory in Livermore, California, where he now works on superlightweight materials with energy applications.

Choosing that extra experiment means taking risks; to minimize them, graduate students and postdocs can conduct multiple experiments at the same time, advises Franko. Many postdocs in successful labs have four projects going on at once: one that is essential for the lab; one that is safe and will lead to publications; one that runs in parallel with or tangential to the general direction of the lab, and that the postdoc can take with them; and one that is risky. The risky project is often the one that leads to an independent research career, says Franko.

Nancy Schwartz, a biochemist at the University of Chicago in Illinois, gets even her graduate students to work on multiple projects. "If you say, 'Here, go do it', then you're treating them like technicians and they're not going to learn to be investigators," she says. But there should still be constraints on, and monitoring of, their work. "Often they fail," says Schwartz. "That's the only way you really learn to do science." ■

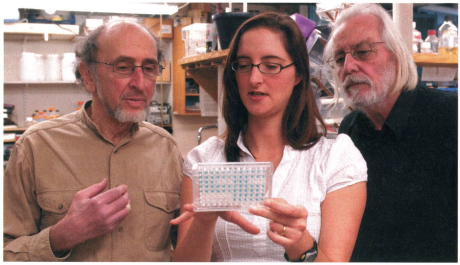

J. TOUSTER

Rachel Dutton quickly got senior scientist Dana Boyd (right) on board with her PhD project idea, which deviated from the lab's focus. But she had to convince her mentor, Jon Beckwith (left).

Robert Frederick *is a freelance writer based in North Carolina.*

TURNING POINT
Jimmy Lin

Jimmy Lin is a computational geneticist at Washington University in St Louis, Missouri, and founder of the Rare Genomics Institute (RGI), a non-profit group in Baltimore, Maryland. On 25 October, he was named as one of 25 fellows chosen to present an 'idea worth spreading' at the annual Technology Entertainment and Design (TED) conference, to be held in February and March in Long Beach, California. TED will help Lin to develop company strategies and brand recognition for the RGI.

At one point you were pursuing four degrees at once. Why?

I'm in the MD–PhD programme at Johns Hopkins University in Baltimore because I'm interested in scientific discovery as well as health. I finished the PhD two years ago, and am finishing my MD this year. As a computational biologist, last year I earned a master of science degree in health sciences focused on bioinformatics. I am also fascinated with the intersection of science and faith. Through my church, I'm pursuing a master's in religion, exploring how the concepts of philosophy apply to medicine and bioethics.

Given how busy you are, why did you start the RGI?

Combining foolish optimism with a passion for using science to help people, some friends and I started this group six months ago. Estimates suggest that there are between 20 million and 30 million children with rare diseases, many of whom are undiagnosed despite exhaustive testing. A lot of these patients have had medical problems since birth that are probably genetic, but we need genome sequences to identify any culprit genes. Our goal is to determine whether these patients have a genetic disorder, and to come up with a diagnosis.

How are you pursuing an academic career while promoting the RGI?

At Washington, I am writing a next-generation sequencing programme for the clinic. I will be creating a screen for cancer and other diseases, checking the more than 20,000 coding genes in the human genome. I have yet to decide whether to pursue either a residency or a tenure-track academic position. The university has been kind enough to let me spend time on the RGI as part of my duties there.

What do you expect from the TED fellowship?

We are using a grass-roots, crowdsourcing approach to fund-raising — empowering the public to help these kids. Individuals can go online and contribute; for example, US$50 will pay to sequence roughly 600 genes. But we need to spread the word. I'm not yet good at public relations, but I am good at applying for fellowships. I thought that TED would be a great way to put this need in front of a lot of people, potentially the world. I was overjoyed when I heard that I had been selected. The fellows each have to make a 4-minute video describing their idea, to be shared at the conference and online.

What do you hope to accomplish in those 240 seconds?

I'm working on telling a good story — how meeting these patients has changed my life. I want to give viewers a taste of the desperation that these people feel with nowhere else to turn. Then I want to make it clear that science can potentially help. I need to bring that connection to life. But connecting the public to science through a grass-roots funding mechanism is the big idea we want to propel.

Are you concerned about how to balance your academic and non-profit pursuits?

I'm conscious that spending time on patient advocacy decreases the amount I spend on my academic career, specifically publications. I've chosen this path in part because I have had the privilege of working for scientists who pursue their own passions. That has motivated me to pursue mine, to bring technology to patients. Some people create technologies; I want to make those technologies accessible. I'm fine with giving up aspects of an academic career if I can have more of an impact on kids' lives. ■

INTERVIEW BY VIRGINIA GEWIN

UNITED STATES

Foreigners more prolific

Foreign-born US scholars produce more publications than those born in the United States, but are less satisfied with their work lives, says a study in the *Journal of Higher Education* (D. Kim *et al. J. Higher Educ.* **82**, 720–747; 2011). Furthermore, foreign US faculty members who earned their undergraduate degrees in other countries are more productive than those who did so in the United States — but they are also less satisfied. The study gauged productivity on the basis of the number of research papers published over five years, using data from the US National Science Foundation's 2003 Survey of Doctorate Recipients. The authors speculate that only the "best and brightest" foreign scholars secure US faculty posts; or perhaps non-US scholars have better undergraduate training, especially in the sciences and maths.

UNITED KINGDOM

Jobs in animal research

The Institute for Animal Health in Pirbright, UK, is recruiting about 15 early-career researchers in fields such as animal virology and avian disease. On 29 November, the institute announced that it is to receive at least £80 million (US$125 million) from the UK government, to augment a £100-million development project launched last year. The plans call for a high-containment lab and facilities for research and translation of research into disease-control products. Michael Johnson, head of the Pirbright laboratory, says that more positions may arise in the next 2 years. The labs should be completed by 2016.

EUROPEAN UNION

Early-career boost

The European Commission's Horizon 2020 funding programme for 2014–20 will support about 110,000 research positions, the commission said on 30 November. The €80-billion (US$107-billion) scheme replaces final Framework Programme — FP7. It includes a 77% budget increase for the European Research Council (ERC) and a 21% increase for the Marie Curie Actions programme, which funds young researchers. Marie Curie Actions will raise the number of graduate students and postdocs it supports from 50,000 to 65,000. The ERC will fund some 9,500 principal investigators and 38,000 early-career researchers — almost twice as many scientists as under FP7.

naturejobs

European Head Office, London naturejobs@nature.com
The Macmillan Building, 4 Crinan Street, London N1 9XW, UK
Tel: +44 (0) 20 7843 4961 Fax: +44 (0) 20 7843 4996

European Manager:
Nils Moeller,+44 (0) 20 7843 4953 n.moeller@nature.com
Southwest UK/ReW:
Emma Hare, +44 (0) 20 7843 4944 e.hare@nature.com
Northeast UK/Ireland:
Matthew Ward, +44 (0) 20 7014 4059 m.ward@nature.com
France/Switzerland/Belgium:
Julie Aramburu, +44 (0) 20 7843 4994 j.aramburu@nature.com
Scandinavia/Spain/Portugal/Italy:
Megan Ball, +44 (0) 20 7843 4973 m.ball@nature.com
North Germany/The Netherlands/Eastern Europe:
Kristin Doelling +44 (0) 20 7843 4970 k.doelling@nature.com
South Germany/Austria:
Hildi Rowland, +44 (0) 20 7014 4084 h.rowland@nature.com
Natureevents:
Matthew Clare, +44 (0) 20 7014 4015 m.clare@nature.com
Business Development Manager, Middle East:
Jon Giuliani, +44 (0) 20 7843 4922 j.giuliani@nature.com

USA Head Office, New York naturejobs@us.nature.com
75 Varick Street, 9th Floor, New York, NY 10013-1917
Tel: +1 800 989 7716 Fax: +1 800 989 7103

US Sales Manager:
Ken Finnegan, +1 212 726 9248 k.finnegan@us.nature.com

Japan Head Office, Tokyo
Chiyoda Building, 2–37 Ichigayatamachi, Shinjuku-ku, Tokyo 162-0843
Tel: +81 3 3267 8751, Fax: +81 3 3267 8746

Asia-Pacific Sales & Business Development Manager:
Yuki Fujiwara, +81-3-3267-8765 y.fujiwara@natureasia.com
Business Development Manager, Greater China/Singapore:
Gloria To, +852 2811 7191 g.to@natureasia.com

India
3s, 4th Floor, DLF Corporate Park, Gurgaon, 122 002, India
Advertisement Sales:
Vikas Chawla, +91 1242881057 v.chawla@nature.com

---

www.cardiff.ac.uk/jobs

CARDIFF UNIVERSITY
PRIFYSGOL CAERDYDD

Research Assistant

Department of Surgery
Cardiff School of Medicine

You will join a multidisciplinary grouping including Biologists, Geneticists and Clinicians based at the School of Medicine. The position is funded by a Cancer Research Wales Grant and is focussed on investigating the mechanisms by which prostate cancers form osteoblastic metastasis in the bone.

You will undertake day to day research activity within the overall research programme using methodologies and analysis and will be expected to carry out any laboratory techniques necessary for the project.

You should have sufficient breadth or depth of specialist knowledge in molecular and cellular biology and cancer biology as well as previous research experience in cancer/cell biology. A first class or good second class degree in a relevant discipline or equivalent experience is essential.

This post is fixed-term for 3 years.

Salary: £24370 - £28251 per annum

To work for an employer that values and promotes equality of opportunity, visit www.cardiff.ac.uk/jobs telephone +44 (0)29 2087 9093 or email vacancies@cardiff.ac.uk for an application form quoting vacancy number 0652.

Closing date: 17:00GMT on 12 January 2012.

U219669R

MASARYK UNIVERSITY (http://www.muni.cz)

UNIVERSITAS MASARYKIANA BRUNENSIS

Postdoctoral Research Associates

We are currently expanding our research teams and seeking highly motivated and talented individuals for three year-fixed term positions in diverse areas. Young scientists who are interested in career at Masaryk University are encouraged to contact directly the individual team leaders listed below:

Petr Dvorak	Pluripotent Stem Cells, Growth Factor Signalling /pdvorak@med.muni.cz/
Lumir Krejci	Homologous Recombination and DNA Repair /lkrejci@chemi.muni.cz/
Stepanka Vanacova	RNA Quality Control in Development and Disease /vanacova@chemi.muni.cz/
Pavel Strnad	Molecular Gastroenterology and Hepatology /pavel_strnad@centrum.cz/
Jiri Friml	Developmental and Cell Biology in Plants /jiri.friml@psb.vib-ugent.be/
David Smajs	Treponemal Infections, Bacterial Genomics /dsmajs@med.muni.cz/
Ondrej Slaby	MicroRNAs in Solid Cancer /ondrej.slaby@ceitec.muni.cz/
Richard Stefl	Structural Biology, Transcription and RNA Processing /richard.stefl@ceitec.muni.cz/
Lukas Trantirek	Wnt Signalling, Cell Cycle Regulation /trant@paru.cas.cz/
Jiri Sponer	Computational Studies of RNA and DNA /sponer@ncbr.muni.cz/
Martin Zvonar	Hyperplasia, Factors of Muscle Cell Proliferation /zvonar@fsps.muni.cz/
Lubos Brim	Parameter Estimation in Computational Systems Biology /brim@fi.muni.cz/
Stjepan Uldrijan	Stress Response in Cancer Cells, Regulation of the p53 Pathway /uldrijan@med.muni.cz/
Petr Hlineny	Structural Graph Theory and Parameterized Algorithms /hlineny@fi.muni.cz/
Jaroslav Koca	Computational Chemistry of Biomolecules, Structural Bioinformatics and Chemoinformatics /jaroslav.koca@ceitec.muni.cz/
Michal Kozubek	Biomedical Image Analysis /kozubek@fi.muni.cz/
Jan Preisler	Bioanalytical Instrumentation, MALDI Mass Spectrometry, Capillary Electrophoresis /preisler@chemi.muni.cz/
Jiri Damborsky	Molecular Modelling, Computer-Assisted Protein Design /jiri@chemi.muni.cz/
Michaela Vorlickova	Quadruplexes in the Human Genome (mifi@ibp.cz)
Ivona Foltova	Self-Medical Behaviour in Orang-utan and Natural Anti-Parasites Compounds; Testing of Natural Anti-Parasitic Activity of Selected Plant Extracts /foltova@sci.muni.cz/
Pavel Zezula	Similarity Searching for Multi-modal Data Interpretation/Efficient Searching in Large Collections of Biometric Data /zezula@fi.muni.cz/
Radka Chaloupkova	Biophysical Methods for Protein-Ligand Interactions /radka@chemi.muni.cz/
Kamil Paruch	Medicinal Chemistry, Organic Synthesis /paruch@chemi.muni.cz/
Ivana Cerna	Formal Verification and Synthesis of Computer Systems /cerna@fi.muni.cz/
Radek Marek	Calculation of NMR Parameters in Transition-metal Complexes /rmarek@chemi.muni.cz/
Vladimir Sindelar	Supramolecular Organic Chemistry / sindelar@chemi.muni.cz/
Lenka Fajkusova	Inherited Disorders - Molecular Diagnostics and Functional Analysis (lfajkusova@fnbrno.cz)
Milan Konecny	Evaluation of Digital Cartographic Products for Crises Management /konecny@geogr.muni.cz/
Petr Vasina	Nanocomposite Coatings, PVD-PECVD, HIPIMS /vasina@physics.muni.cz/
Jiri Pinkas	Nonhydrolytic Sol-Gel and Molecular Building Blocks for Materials /jpinkas@chemi.muni.cz/
Mojmir Sob	Computational Materials Science – Magnetism in Extended Defects and Nanocomposites, Calculation of Phase Diagrams /sob@chemi.muni.cz/
Zbynek Prokop	Microfluidics in Enzyme Screening, Characterization and Evolution/Enzyme Kinetics on a Chip /zbynek@chemi.muni.cz/
Petr Klan	Pump-and-Probe and Laser Flash Spectroscopy of Organic Compounds /klan@sci.muni.cz/
Ludek Blaha	Environmental Toxicology, Endocrine Disruption /blaha@recetox.muni.cz/

The deadline for applications is **March 31, 2012**

W219633F

Lectureships in the Faculty of Life Sciences
£36,862 to £45,336 p.a.

The University of Manchester wishes to appoint Lecturers in the Faculty of Life Sciences to augment our current world leading expertise in biology. In particular we are seeking talented academics in the following areas:

Anatomy • Physiology • Pharmacology
Environmental Biology • Animal Evolution

Candidates should be well established with an inspiring view of the future of their field and of their contribution to it. For the Pharmacology position there will be an emphasis on design and delivery of teaching to undergraduate students across a number of popular programmes of study. The other positions will be expected to develop their own independent research programme in addition to contributing to teaching and other potential areas of activity.

The Faculty has a world leading profile in biology and a strong ethos of interdisciplinary working at the interfaces with medicine, the physical sciences and humanities, which provide an environment rich with opportunities for development and career progression.

To find out more about Manchester, the University and these roles, please visit **www.manchester.ac.uk/worldleadingminds/nature** where you are also able to submit an application. You will see named contacts who would be pleased to discuss our opportunities in more detail with you.

The closing date for applications is 27 January 2012.

The University will actively foster a culture of inclusion and diversity and will seek to achieve true equality of opportunity for all members of its community.

WORLD-LEADING MINDS ANSWERING THE WORLD'S BIGGEST QUESTIONS

THE FUTURE, MADE IN MANCHESTER

MANCHESTER 1824
The University of Manchester

U219681R

北京大学
PEKING UNIVERSITY

Faculty Positions in Systems and Synthetic Biology at Peking University

The Center for Quantitative Biology (CQB) at Peking University (PKU) invites applications for faculty positions at all ranks. We seek for creative individuals in all areas of quantitative biology, with emphases on systems and synthetic biology. As part of PKU's strategic initiative in enhancing interdisciplinary research, CQB is a newly established center dedicated to research and education at the interface between the traditionally more quantitative disciplines (such as mathematics, physical sciences, engineering, computer science) and the biological sciences. Faculty at CQB can also be associated with other schools and departments at Peking University and have the opportunity to join the Peking-Tsinghua Center for Life Sciences. We offer an internationally competitive start-up package. Peking University provides excellent interdisciplinary research environment and outstanding core research facilities.

Qualified candidates should hold a Ph.D. or an equivalent degree in relevant fields and must have an outstanding interdisciplinary research record. Application should include a CV, a research plan, and names of three references, and should be submitted electronically to the center director, Dr. Chao Tang (zhangzj@ctb.pku.edu.cn).

JP219382R

nature physics

Associate Editor

Nature Physics seeks an Associate Editor to join its editorial team.

Nature Physics is a prestigious journal covering all areas of research in physics. For more information about the journal, see our website (http://www.nature.com/nphys).

The ideal candidate will have completed a Ph.D. in a physics discipline, and postdoctoral experience is preferred (but not required). Key elements of the position include the selection of manuscripts for publication, as well as commissioning, editing and writing for the journal.

This is a demanding and intellectually stimulating role that calls for a keen interest in the practice and communication of science. The successful candidate will therefore be highly motivated and must possess excellent interpersonal skills.

The position will be based in our London office.

Applicants should upload a CV on the role **NPG/197/11** on Macmillan.com (including a brief account of their research and other relevant experience); a research highlight in *Nature Physics* style (200 words or fewer) on a recent relevant paper in the literature; and a brief cover letter explaining their interest in the post and their salary expectations.

Closing date – 19 December 2011

nature publishing group npg

IN219011RL

Max-Planck-Institut für Herz- und Lungenforschung
W.G. Kerckhoff-Institut

MAX-PLANCK-GESELLSCHAFT

The International Institute of Molecular and Cellular Biology (IIMCB), Warsaw, Poland and the Max Planck Institute for Heart and Lung Research (MPI-HLR), Bad Nauheim, Germany, invite applications for

two Research Groups

We seek talented, dynamic, independent, and motivated scientists early in his/her career to establish two research groups, one at IIMCB in Warsaw, the other at MPI-HLR in Bad Nauheim. Successful candidates will develop independent research programs using their own budgets, which will fund research positions, consumables, and equipment. The successful candidates will have outstanding scientific track records with clear evidence of leadership, and a strong interest in animal models of human diseases, particularly in zebrafish (for a position in Warsaw) or molecular mechanisms of cardiovascular diseases (for a position in Bad Nauheim).

Initial appointments of group leaders are for five years with the possibility of extension after international review. For more general information please see also: http://www.mpg.de/918399/MPRGL. The start date is negotiable.

IIMCB in Warsaw is one of the most modern country's research institutes in its field. The Institute's research topics cover the wide spectrum of protein structural biology, bioinformatics/computer modelling, protein and organellar biogenesis, neurobiology, cancer biology and cell biology. MPI-HLR in Bad Nauheim hosts 4 departments and several independent research groups and is committed to understand the mechanisms of cardiopulmonary development, diseases and regeneration at the molecular level. The environment of both institutes is international and the working language is English. Each of the institutes is equipped with state-of-the-art technology and excellent core facilities, mutually available for both groups. The institutes provide outstanding research opportunities for their scientists.

Applications should include:

- a cover letter explaining a reason for participation in this program,
- a Curriculum Vitae including a publication list,
- a statement of scientific achievements,
- a two page summary of applicant's future research plans,
- addresses of two academic referees
- two letters of reference
- copies of three applicant's most important papers

and be sent to **personal@mpi-bn.mpg.de**.

Deadline for application is **January 31, 2012**. Successful applicants should be prepared to join a selection symposium held on March 22 2012 in Bad Nauheim.

W219226R

Durham University

Shaped by the past, creating the future

Durham University is pleased to announce its 2012-13 Fellowship Scheme to attract the brightest Researchers in Europe and beyond. Applications are invited for;

3 ADDISON-WHEELER FELLOWSHIPS (REF: 1403)

14 JUNIOR RESEARCH FELLOWSHIPS (REF: 1390)

10 SENIOR RESEARCH FELLOWSHIPS

7 POLICY AND ENTERPRISE FELLOWSHIPS

For details on the Fellowships, how to apply and closing dates, please see www.dur.ac.uk\ias

U219579R

Visit
www.naturejobs.com
to seriously improve your career prospects.
nature jobs
making science work

VIB

VIB is a life sciences research institute, based in Flanders, Belgium. At VIB, more than 1,250 scientists from over 60 countries perform multidisciplinary basic research into the molecular foundations of life. Their work helps to understand why disease develops and how plants grow. VIB is an excellence-based entrepreneurial institute that focuses on translating basic scientific results into pharmaceutical, agricultural and industrial applications. VIB brings together the research capacities and complementary expertise of life sciences researchers at UGent, K.U.Leuven, University of Antwerp and Vrije Universiteit Brussel.

Two of the VIB departments located in Leuven (K.U.Leuven) are currently seeking new scientists at postdoctoral and group leader level.

VIB Vesalius Research Center, K.U.Leuven

Department Director: Peter Carmeliet

The Vesalius Research Center (VRC) has focused its research interests on unraveling the molecular basis of angiogenesis (i.e. the formation of blood vessels) and translating these genetic insights in therapeutic concepts - and, if possible, novel treatments. VRC is also studying in the neurovascular link in health and disease. Therefore, the VRC uses interdisciplinary functional genomic and genetic research strategies, from the bench to the bedside, and back again. www.vrc-lab.be

GROUP LEADERS

Oncology:
Applicants should have interest in cancer genetics and epigenetics, growth control, cellular signaling, tumor-stroma interactions, tumor inflammation, metabolism, hypoxia signaling, treatment and prevention.

Angiogenesis:
Interest in angiogenesis in development and disease. VRC seeks expertise in vascular development and vessel guidance in zebrafish and tumor angiogenesis.

Neuroscience:
Interest in molecular, cellular and/or pathological neuroscience, including neurodegeneration. Expertise in small animal models is an asset.

Candidates should have a Ph.D and/or M.D., with at least 3 years postdoctoral training, high quality research productivity, an outstanding publication record, and demonstrated success at securing research funding. Positions are guaranteed for 5 years, a generous start-up package with space, funding and resources to establish a high-quality, independent research program.

Please send cover letter, CV, outline of current & future research and contact details of 3 references to peter.carmeliet@vib-kuleuven.be

VIB Center for Biology of Disease, K.U.Leuven

Department Director: Bart De Strooper

Our department's mission is to perform frontline research, addressing significant questions and key issues relevant to major human health challenges. We focus on basic molecular and cellular mechanisms and use the power of modern genetics and genomics as well as molecular, cellular and developmental biology.
http://med.kuleuven.be/cme

POSTDOCTORAL SCIENTISTS

Following positions are currently available:

- Laboratory for the Research of Neurodegenerative Diseases - Bart De Strooper
  Project: research into the molecular and cellular biology of LRRK2 in Parkinson's disease
- Laboratory of Membrane Trafficking - Wim Annaert
  Project: research into the pathogenesis of Alzheimer's disease
- Laboratory of Molecular Pathogenesis of Leukemia - Jan Cools
  Project: research into leukemia genomes using next-generation sequencing
- Laboratory of Neuronal Communication - Patrik Verstreken
  Project: research into synaptic function and Parkinson's disease
- Laboratory of Glia Biology - Matthew Holt
  Project: development of transgenic tools for Astrocyte research
- Laboratory of Dystonia - Rose Goodchild
  Project: research into the pathophysiology of dystonia

Please send cover letter, CV and statement of research to diane.casteels@cme.vib-kuleuven.be All details can be found on www.vib.be and http://med.kuleuven.be/cme or via simple request to diane.casteels@cme.vib-kuleuven.be

Both departments are internationally visible centers of excellence, offering a stimulating environment by providing knowledge, expertise and training to the scientific community, students and medical industry.
Additionally VIB offers attractive salaries and ample social benefits.
Visit www.vib.be/jobs for an overview of job offers, including those for PhD students.

www.vib.be

KATHOLIEKE UNIVERSITEIT LEUVEN

W219642R

NATIONAL CANCER INSTITUTE

Department of Health and Human Services
National Institutes of Health
National Cancer Institute
Center for Cancer Research

Senior Tenure-Track or Tenure-Eligible Investigator Position in Structural Biology & Biophysics

The Structural Biophysics Laboratory (SBL), Center for Cancer Research (CCR), National Cancer Institute (NCI), National Institutes of Health (NIH), Department of Health and Human Services (DHHS) is seeking an outstanding tenure-track or tenure-eligible principal investigator to carry out original, independent, and innovative research in an area of Structural Biology or Biophysics integrated with molecular biology. This intramural position is similar to that of an associate (or higher) professor in academia.

Areas of emphasis include structural biology of biomacromolecular systems and/or characterization of dynamic assembly/function of macromolecular complexes that impact the biological processes relevant to cancer and/or AIDS. The incumbent will establish/continue a highly competitive and collaborative program, with an emphasis or utilization of NMR spectroscopy, including solid-state NMR. Applicants must have a Ph.D. or equivalent degree and have demonstrated expertise and a record of achievement.

The position is located at the NCI-Frederick, MD campus, which offers state-of-the-art facilities for NMR, SAXS and structural biology, collaborative opportunities with the Chemical Biology Laboratory and Molecular Targets Laboratory, as well as core facilities for biophysics, mass spectrometry; protein expression and proteomics; electron, optical and small animal imaging and other advanced technologies.

Consideration of applicants will begin February 16, 2012 and will continue until the position is filled. Salary is competitive and is commensurate with experience and full benefits (including retirement, health insurance, life insurance, and a Thrift Savings Plan). This position is not restricted to U.S. citizens.

To apply, please submit a cover letter, curriculum vitae, description of research plans (~ 5 pages), and have 3 letters of recommendation sent to: Ms. Deanna Dougherty, Administrative Officer, NCI-Frederick, PO Box B, Bldg. 578, Frederick, Maryland, 21702-1201, Tel. 301-846-5199, FAX 301-846-6053, E-mail: SBLsearch@mail.nih.gov. PDF files are encouraged.

This position is subject to a background investigation.
The NIH is dedicated to building a diverse community in its training and employment programs.

DHHS, NIH, and NCI are Equal Opportunity Employers

NATIONAL INSTITUTES OF HEALTH

NW219614R

ecetoc

EUROPEAN CENTRE FOR ECOTOXICOLOGY AND TOXICOLOGY OF CHEMICALS

ECETOC Secretary General

Founded in 1978, ECETOC is the foremost voice of chemical industry in Europe concerning health and environmental science. The activities of the association are dedicated to the development and promotion of top quality science in risk assessment of chemicals. To this end, a permanent secretariat coordinates the activities of industry experts in collaboration with government and academic scientists in task forces and workshops. The Secretary General is responsible for the execution of the strategy of the association, for the management of the secretariat and the work programmes adopted by the Scientific Committee. He/She is responsible to the board of management for the financial affairs of the association and to the assembly of members for the conduct of the science programme along with its promotion to external stakeholders in government, science and industry.

The ideal candidate would have excellent communication, collaboration and management skills, a higher degree qualification and experience that gives evidence of credibility of scientific accomplishments in areas which are relevant to the risk assessment of chemicals. Experience in a technical or government relations role in industry and/or the regulatory community would be an advantage, as would a working knowledge of the laws and regulations applicable to various types of chemicals in Europe (REACH, Pesticides, Biocides, Pharmaceuticals etc.). The candidate should have an innovative attitude that enables ECETOC to address current and future needs in a complex environment.

The position is based in Brussels and offers an attractive salary, benefits and relocation package. Applications should be accompanied by a C.V. giving full details of career history and be addressed to: Geneviève Gérits, ECETOC AISBL, 6 Avenue Edmond Van Nieuwenhuyse, 1160 Auderghem, Brussels, Belgium.
genevieve.gerits@ecetoc.org.

W219613R

STATE-OF-THE-ART LABORATORIES OVERLOOKING THE RED SEA

جامعة الملك عبدالله للعلوم والتقنية
King Abdullah University of Science and Technology

The complexity, diversity, and mystery of the Red Sea provide massive potential for breakthrough science. Located on the shores of the Red Sea, **King Abdullah University of Science and Technology** is leading fundamental and integrated research from the molecular level to the physical and chemical environment in which the whole ecosystem exists. The Red Sea is home to several different extreme environments such as deep brines and cold seeps, as well as warm deep-water and hypoxic layers. The Red Sea also contains the longest coral reef system in the world. With state-of -the-art facilities, the Red Sea Research Center (RSRC) is paving the way for leading-edge research into these ecosystems.

FACULTY POSITIONS

We seek creative and independent scientists with specific interests in Biological Oceanography, Marine Biology/Marine Ecology, and Genomics. Colleagues are invited to join our faculty at the **Assistant, Associate, or Full Professor** level with expertise in areas of:

- **Extreme Environments Biology**
- **Benthic Ecology**

MASTER'S PROGRAM

Undergraduate students interested in the University's Marine Science MSc program are also invited to apply. The general scholarship program of the University is the KAUST Fellowship and all students are evaluated for financial support under the KAUST Fellowship. When awarded, the scholarship supports students for the duration of their graduate studies. Benefits include:

- **Full tuition support**
- **Monthly living allowance ($20,000 annually)**
- **Housing**
- **Medical and dental coverage**
- **Relocation support**

Faculty and master's program applications should be sent to:
Marine.Science@kaust.edu.sa
Please include your CV, a cover letter, and two letters of reference.

King Abdullah University of Science and Technology is an international, graduate level university committed to advancing science and technology through transdisciplinary research, education, and innovation. The University's unique matrix structure supports both basic and goal-oriented research in the globally significant areas of energy, water, food, and environment to benefit Saudi Arabia and beyond.

www.kaust.edu.sa
rsrc.kaust.edu.sa

NW219604R

UCL

UCL Ear Institute

Professor of Auditory Science

Applications are invited for the position of Professor of Auditory Science at the UCL Ear Institute. The Institute provides state-of-the-art facilities and expertise in a wide range of disciplines related to hearing and deafness studies including genetics, molecular and cell biology, biophysics, systems and computational neuroscience, human performance and ENT medicine. In keeping with these broad research interests, an appointment can be made in any relevant field.

Experience in a similar academic position is essential with an outstanding track record of laboratory research. All necessary support will be made available to the appointee to incorporate his or her own research programme into the Institute. In addition, a critical feature of the Ear Institute's research strategy is to engage with industrial and other partners to develop our translational research agenda, and, to this end, the successful candidate will be expected to demonstrate the leadership qualities necessary to develop the Institute's research partnerships with industry.

The successful candidate will be expected to take up the post in sufficient time to participate in the Institute's return to the Research Excellence Framework in 2013.

The appointment will be full time on the UCL Professorial Grade. The salary range will be negotiable on the professorial scale but not less than £61,960 per annum, inclusive of London Allowance.

Informal enquiries may be made to Professor David McAlpine (tel: +44 (0)20 7679 8938; email: d.mcalpine@ucl.ac.uk).

For further details about the vacancy and how to apply online please go to http://www.ucl.ac.uk/hr/jobs/ and search on Reference Number 1218481.

Candidates unable to apply online should send their application materials to academic.services@ucl.ac.uk

Closing Date: 1st March 2012.

We particularly welcome female applicants and those from an ethnic minority, as they are under-represented within University College London at this level.

U219641R

SPINAL RESEARCH

Call for Proposals

Nathalie Rose Barr PhD Studentships

The International Spinal Research Trust is a UK-based medical research charity (no. 281325) with the sole purpose of funding research aimed at resolving the non - or partial functioning of the injured spinal cord.

We invite senior scientists (supervisors) at UK institutions to submit proposals for the support of PhD studentship projects. Studentships are open for science graduates or those with clinical qualifications.

Application forms are available on request, further information on our research strategy and other requirements can be found on our website.

Closing date for receipt of applications is Friday 17th February 2012.

www.spinal-research.org E-mail: research@spinal-research.org

U219224R

Follow *Naturejobs* on Twitter

For the latest career news: **twitter.com/naturejobs**
For all job listings: **twitter.com/naturejobs_feed**

twitter

A? Aalto University

Aalto University is a new university with over a century of experience. Created from a high-profile merger between three leading universities in Finland – the Helsinki University of Technology, the Helsinki School of Economics and the University of Art and Design Helsinki – Aalto University opens up new possibilities for strong multi-disciplinary education and research. The university's ambitious goal is to rank among the top universities in the world in its areas of specialization. At Aalto, there are 20,000 students and a staff of 4,500 including 340 professors.

Aalto University School of Chemical Technology invites applications for:

Tenure Track Position in Inorganic Materials Chemistry

The Department of Chemistry (**chemistry.aalto.fi/en**) invites candidates to apply for tenure track position preferably at the associate professor level in Inorganic Materials Chemistry. The department has strong tradition in new inorganic research, specifically in oxide materials. It is in the department's interest to make further investments in the research field to achieve real scientific breakthroughs. The focus of the professorship is development of novel functional inorganic materials.

A successful candidate will be expected to contribute to the existing research field and a commit to teaching. PhD in related field is required. Candidates must demonstrate distinction in published research, evidence of consistent extramural funding and strong international experience and collaboration.

The closing date for applications is January 20, 2012. To see the complete position description, please go to **aalto.fi/en/openpositions.**

aalto.fi

W219283R

---

nature

Subeditor, *Nature*

From astronomy to cell biology, particle physics to ecology — can you help explain why the latest developments in science matter? If you can make complex concepts accessible, can write headings and standfirsts that excite but don't resort to clichés, and can handle the English language with an eye for accuracy, we want to hear from you.

Nature, the international weekly journal of science, has a vacancy for a subeditor. You will handle copy written by our award-winning team of journalists and will be comfortable dealing with anything from general science news, to book reviews, to sophisticated primary research. You will be closely involved with the production process and will help ensure the smooth running of copy through the system.

You will need a good science degree, excellent literacy and word-processing skills and experience of subediting on a science-related magazine or journal. The ability to use InDesign and InCopy is desirable but not essential.

Nature Publishing Group (NPG) is a division of Macmillan Publishers Ltd, dedicated to serving the academic, professional scientific and medical communities. For further information please visit www.nature.com.

The position is based in our offices in central London.

Application is by uploading CV and covering letter, including a short paragraph stating why you would be suited to the job, to job reference number **NPG/199/11** on http://jobs.macmillan.com. Please include your current contact details, salary expectation, notice period (if applicable) and details of two referees.

All applicants must be able to demonstrate the right to live and work in the UK in order to be considered for the vacancy.

Closing Date: Wednesday 28th of December 2011

nature publishing group npg

IN219297R

The Novo Nordisk Foundation

Center for Protein Research

The Novo Nordisk Foundation Center for Protein Research has been established to promote basic and translational research on human proteins of medical relevance. Since the opening of the new dedicated laboratories in June 2009, the Center now comprises a wide range of expertise and skills within its research departments, with activities in the areas of disease systems biology, proteomics, high-throughput protein production and characterisation, chemical biology, disease biology, and protein therapeutics. Currently, ~130 staff members have been recruited and all essential research infrastructure has been established.

For additional information regarding the Center contact **contact@cpr.ku.dk** or see **www.cpr.ku.dk**

Chief Scientist in Protein Science & Technology

Professorship

Applications are invited for the post of a Chief Scientist/Professor in Protein Science and Technology with focus on protein families and signaling pathways. The position as Chief Scientist is available at the Facility for Protein Science and Technology at the Novo Nordisk Foundation Center for Protein Research (CPR), Faculty of Health Sciences at the University of Copenhagen.

The post entails research within the field of Protein Science and Technology (PST). Research areas of particular interest to the Center are e.g. human enzymes such as kinases or proteases, disease relevant signaling pathways, post translational modification dependent signaling, epigenetic regulation mechanisms and integral membrane protein function.

The appointee will buildup and lead the research within PST, be part of the Center Executive Management Team, work to set and implement long-term strategic objectives for PST and ensure that the activities within the PST are performed at the highest international level. The appointee will also be a key player regarding operations and strategic development of the Center overall.

Applications must be received by **16 January 2012, 14:00** local Danish time. This notice is an extract which **may not** be used as the basis for an application. The full text of the notice inviting applications for the associate professorship is available from www.cpr.ku.dk/jobs as well as www.ku.dk/stillinger or from the Faculty on tel. + 45 35 32 75 45.

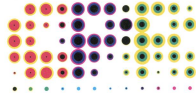

FACULTY OF HEALTH SCIENCES
UNIVERSITY OF COPENHAGEN

W219639R

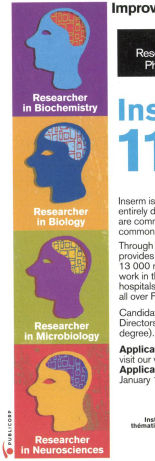

Improving human health requires…

Researcher in Public health, Researcher in Genetics, Researcher in Physiology and Physiopathology…

Inserm is recruiting: 119 researchers m/f dedicated to biomedical research

Inserm is the only French public research body entirely dedicated to human health. Its researchers are committed to studying all diseases, whether common or rare.

Through its diversity of approaches, Inserm provides a unique environment for researchers. 13 000 researchers, engineers and technicians work in the 321 Inserm laboratories housed in hospitals, universities and research campuses, all over France.

Candidates to Research Associates and Research Directors positions must have a PhD (or equivalent degree). There is no nationality restriction.

Application modalities:
visit our website : http//www.eva2.inserm.fr
Application deadline:
January 12th, 2012 - 4.00.pm (GMT+1)

Instituts thématiques **Inserm**
Institut national de la santé et de la recherche médicale

W219186R

Aalto University

Aalto University is a new multidisciplinary science and art community in the fields of technology and science, business and economics, and art and design. The University's cornerstones are its strengths in education and research.

Aalto University invites applications for:

Tenure Track or Tenured Position in Cognitive Neuroscience, Especially Affective and Social Neuroscience

The position is located in the Department of Biomedical Engineering and Computational Science (BECS) at Aalto University School of Science (**becs.tkk.fi/en/**), Finland.

The position is open to talented individuals who hold a doctorate and have excellent potential for a productive scientific career. The holder of the position should have a strong background in behavioral and cognitive science but also advanced skills in applying modern brain signal analysis and visualization methods, a good publication record, international scientific collaboration experience, and demonstrated ability to communicate effectively as a teacher. The focus area for research and teaching of the position is neural mechanisms of social interaction, especially under naturalistic conditions.

Please, consult **aalto.fi/en/openpositions** for a complete job advertisement and detailed application instructions. The closing date for sending applications is January 13th, 2012.

aalto.fi

W219185R

Albert-Ludwigs-Universität Freiburg

UNI FREIBURG

The German Consortium for Translational Cancer Research (DKTK) at Freiburg in conjunction with the cluster of excellence BIOSS II of the Albert-Ludwigs-University Freiburg, the University Hospital Freiburg and the Faculty of Medicine has an opening for a

Professorship (W 3) for Oncogenic Signaling in Hematologic Malignancies

for November 1, 2012. The professorship represents the subject in research and teaching. Applications from all areas of cancer research will be considered. Scientists with a research profile contributing to the understanding of the crosstalk between oncogenic signaling pathways are especially encouraged to apply. A focus on animal models is desired. The professorship will be part of the DKTK to be established at Freiburg as well as the cluster of excellence BIOSS II.

Applicants should have a final exam in Natural Sciences or Medicine, a MD or PhD degree, and a habilitation or an equivalent scientific qualification. Moreover, the new professor is expected to be well experienced in leading a research team, in competitive fundraising, in supervision of PhD students as well as in self-administration at universities. Teaching expertise is required.

The initial appointment will be for five years. After a successful evaluation, the position will be converted into a permanent (tenured) W3-Professorship.

The University of Freiburg is an equal opportunity employer. Applications of women are strongly encouraged. Handicapped candidates with equivalent qualifications will be given preference.

For application forms please contact the Dean of the Faculty of Medicine (E-mail: dekanat-professuren@uniklinik-freiburg.de). Completed applications along with all pertinent documents should be sent in written form and by E-Mail no later than January 15th, 2012 to the Dean of the Faculty of Medicine, Prof. Dr. Dr. h. c. Hubert E. Blum, University of Freiburg, D-79085 Freiburg im Breisgau, Germany (Phone: ++49-761 270-8465 or -7242; Fax: ++49-761 270-8467).

W21954R

The Institute for Genome Research at The University of Tokushima, Japan, seeks candidates for a permanent position of full professor in proteogenomics. Areas of interest include but are not restricted to the study of biomedical sciences in epigenomic and/or proteomic approaches.

Please view full details online at http://www.genome.tokushima-u.ac.jp.

Application should be received by January 31, 2012. The University of Tokushima is an equal opportunity employer.

JP21938OR

"The additional benefit of naturejobs.com is the cooperating portals [*Scientific American* and *Spektrum der Wissenschaft*] – these have generated a noticeable increase of interest in our offer."

Katarzyna Ginter, Jagiellonian University, Kraków, Poland

naturejobs

The James Hutton Institute

The James Hutton Institute is a brand ne international research centre based Scotland. The work we do is right at the top the global agenda and involves tackling som of the world's most challenging problem including the impact of climate change ar threats to food and water security.

Computational Biologist/ Bioinformatician

(Ref: TJHI 19/11) Salary up to £29,566

A Grade D (PostDoctoral) post exists within the James Hutton Institute for a Computation Biologist/Bioinformatician on a BBSRC / RESAS funded project that has an overall goal generating a draft sequence of the barley genome. The major duties of the post will be: t analysis of transcript sequences with a focus on differential expression, transcript divers and alternative splicing; the analysis of a deep diversity sequencing component of th project; the use of the diversity data for GWAS; the development and maintenance project webpages. Good writing, presentation and interpersonal skills are required, and PhD is essential.

Candidates should be familiar with modern principles of genomics / genetics ar demonstrated expertise in computational biology and genome scale bioinformatic He/she will join a larger team of scientists from The Genome Analysis Centre (TGAC), th European Bioinformatics Institute (EBI) and the International barley genomics communi that are focussed on ultimately generating a reference sequence of the barley genome.

Epidemiological Modeller

(Ref: TJHI 22/11) Salary up to £ 37,534

An Epidemiological Modeller is required to determine the effects of crop pests and disease on yield under climate change. This will help inform resistance and crop protection researc and climate change policy development. Assessments will need to integrate climate, cro growth and disease development models in the context of risk and uncertainty. Th post-holder will work closely with plant pathologists and other modellers.

Applicants must have a PhD or equivalent and experience in relevant modelling in biological context is essential.

Further particulars are available from www.hutton.ac.uk/careers To apply please send a covering letter & CV (including the names and addresses of 3 referees one of which must be your current or most recent employer) quoting the appropriate reference number to HR Office Dundee, Invergowrie, Dundee, DD2 5DA or vacancies@hutton.ac.uk Closing date: Tuesday, 3rd January 2012.

The Institute is an equal opportunities employer.

A Scottish Charity No: SC041796

INVESTOR IN PEOPLE

U21993R

Bringing jobseekers and recruiters together.

Academic • Industry • Government

Search now at **naturejobs.com**

naturejobs making science work

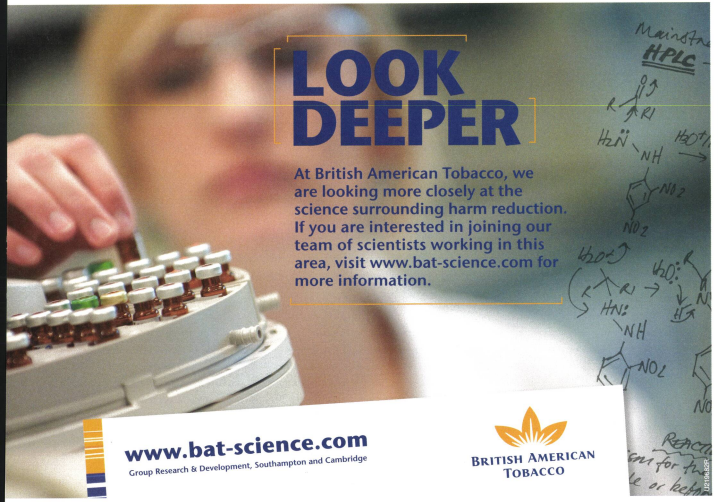
LOOK
DEEPER
At British American Tobacco, we are looking more closely at the science surrounding harm reduction. If you are interested in joining our team of scientists working in this area, visit www.bat-science.com for more information.
www.bat-science.com
Group Research & Development, Southampton and Cambridge
BRITISH AMERICAN TOBACCO

IN 2012
CNRS IS RECRUITING
330 PERMANENT RESEARCHERS
IN ALL SCIENTIFIC FIELDS

cnrs

- LIFE SCIENCES
- CHEMISTRY
- ENVIRONMENTAL SCIENCES AND SUSTAINABLE DEVELOPMENT
- HUMANITIES AND SOCIAL SCIENCES
- COMPUTER SCIENCE
- ENGINEERING
- MATHEMATICS
- PHYSICS
- NUCLEAR AND PARTICLE PHYSICS
- EARTH SCIENCES AND ASTRONOMY

Online registration at www.cnrs.fr from December 1, 2011

Registration deadline January 5, 2012

W217890R

Save time! Save your searches on **naturejobs.com** as a Job Alert email or RSS feed

nature jobs
making science work

HARVARD
School of Engineering and Applied Sciences

Faculty Positions in Environmental Science and Engineering at the Harvard University School of Engineering and Applied Sciences

The Harvard School of Engineering and Applied Sciences (SEAS) seeks applicants for positions at the tenure-track or tenured level in the field of Environmental Sciences and Engineering, with an expected start date of July 1, 2012.

The School of Engineering and Applied Sciences (SEAS) at Harvard University is embarking on a broad initiative within the area of Environmental Sciences and Engineering. Our goal is to expand and strengthen undergraduate and graduate education and research on problems that affect the environment, on scales from local to global and spanning basic and applied sciences and engineering. Highlighted topics include but are not limited to: environmental and energy science, technology, air and water quality, hydrology, natural hazard mitigation, atmospheric science, oceanography, glaciology, and climate science. A key aspect of our strategy in the development of teaching and research initiatives at Harvard has been the close relationship between SEAS and the other science departments at the University such as physics, chemistry and chemical biology, earth and planetary sciences, organismic and evolutionary biology, etc.

Candidates are required to have a PhD or an equivalent terminal degree, or to be able to certify that they will receive the degree within one year of the expected start date. In addition, we are seeking candidates of exceptional scientific and/or engineering talent who have demonstrated excellence in teaching and experimental, observational, theoretical, or computational research in one or more of these areas and who would be eager to participate in an expanding ESE undergraduate curriculum.

Applicants will apply on-line at http://academicpositions.harvard.edu/postings/3858. Required documents include a cover letter, curriculum vitae, copies of up to three representative papers, a research statement, a teaching statement, and names and contact information for at least three references. We encourage candidates to apply by January 31, 2012, but applications will be accepted until the positions are filled. Harvard University is an equal opportunity/affirmative action employer. Applications from women and underrepresented minority candidates are strongly encouraged.

NW219512R

自然出版集团上海公司 — 高薪诚聘中国业务主管

Country Head — China, Nature Publishing Group
Shanghai

As part of a major strategic move by Nature Publishing Group (NPG) into China, NPG, publisher of the international science journal *Nature*, seeks a Country Head to lead the group's future business and editorial activities in China.

Based in new offices in Shanghai, the Country Head will be part of a broader initiative by the Macmillan Group (to which NPG belongs) that aims to establish a strong presence for Macmillan in China, with particular emphasis on science and education.

This is a senior appointment with a reporting line to the Regional Managing Director of NPG, currently based in Tokyo, and to the Managing Director of Greater China for the Macmillan Group of Companies, based in Shanghai.

The Country Head will be responsible for leading NPG's activities on a broad range of fronts. Within the first half of 2012, four editors of the new online multidisciplinary science journal *Nature Communications* will be based in Shanghai (see below). This is the first time manuscript editors of a *Nature* journal will be based in China. This initiative is in response to the rapidly growing output of high-quality research from China and to the growing number of research articles from China in *Nature* publications (see http://www.natureasia.com/en/publishing-index/china/). The Country Head will be responsible for making this move successful by working with the *Nature Communications* team and networking with leading Chinese scientists in the best research institutions and laboratories throughout China, encouraging high-quality submissions from China not only to *Nature Communications* but to *Nature* and NPG journals as a whole.

The Country Head will also work with colleagues in Tokyo and Melbourne to continue the rapid expansion of the Asian Academic Journal programme of NPG in China, which will have expanded to seven journals by July 2012 — many of them open-access publications. The Country Head will also be responsible for expanding and developing the NPG's open-access publishing of research from China, both in terms of the publication of open-access research articles within existing NPG journals but also in the development of new open-access titles.

On a related front, the Country Head will also be responsible for developing scientific communication services with colleagues from Macmillan Scientific Communications (MSC) in Tokyo and London, aiming not only to assist scientists in their writing and presentation of research articles but also to help institutions in China promote their best research to the world through the creation of custom publications such as websites, newsletters and annual reports.

Furthermore, the Country Head will be responsible, along with colleagues in Tokyo and Hong Kong, for ensuring that our existing business in site license sales, sponsorship and advertising continues to grow in China.

Candidates must have at least five years experience in the science publishing industry and some firsthand knowledge of science in China. A doctoral degree in science is highly desired and postdoctoral experience would be an additional advantage. Fluency in English is essential and a working knowledge of Mandarin would be a plus.

A keen understanding of the rapidly evolving research sector in China, including its goals and challenges, is essential. The successful candidate will be able to think strategically with the necessary hands-on business development skills to translate NPG's strategy and vision for China into initiatives, partnerships and business models. Day-to-day management capability, including financial management and team development skills, are essential, together with superb skills in communication — both internally, within NPG and Macmillan, and with the external world, in particular with the highest levels of the scientific community and government in China.

The Country Head will need a global mindset that can identify and develop both local and global opportunities involving China, will have the maturity, credibility and skills to work with scientific institutions, government agencies and other key players in China's research communities, and will exhibit a collaborative style that encourages cooperation, innovation and a positive work environment.

This is a challenging and demanding senior position with a competitive salary and employment terms. Any offer of employment will be contingent on the necessary work permit for China, as applicable, being granted (NPG will provide reasonable assistance with the necessary application process in this respect).

Applicants should send their CV, a covering letter explaining their interest in the position and their salary expectations to recruitment@macmillan.co.uk. They should also include a brief document (maximum two pages) outlining their vision of how NPG can best develop its business and editorial activities in China. Please quote reference number NPG/179/11 in the subject header.

Closing Date: 6 January 2012

Editors of *Nature Communications* — China, Shanghai

NPG is also recruiting four Executive, Senior, Associate and Assistant Editor positions for *Nature Communications* to be based in Shanghai. For further details, please contact recruitment@macmillan.co.uk for further information.

Closing Date: 6 January 2012

nature publishing group

IN218064RL

NPG/179/11

Yale University
Faculty Position
in
Ecology and Evolutionary Biology

The Department of Ecology and Evolutionary Biology at Yale University invites applications for a tenure track faculty position at the junior level. We seek outstanding applicants working in any area of ecology and evolutionary biology and are particularly interested in applicants whose research has a strong focus in ecology. A record of outstanding achievement and a promising research program are more important than specific research area.

Application materials including a CV, three manuscripts or reprints, brief research and teaching statements and contact information for three evaluators should be submitted online at https://academicjobs online.org/ajo/Yale/EEB. The search will remain open until the position is filled. The review of applications will begin January 13, 2012.

Yale University is an Equal Opportunity/Affirmative Action Employer. Yale values diversity among its students, staff, and faculty and strongly welcomes applications from women and underrepresented minorities.

NW219728R

Founding Faculty Fellowship

The Skolkovo Institute of Science and Technology in collaboration with MIT

The Skolkovo Institute of Science and Technology (SkTech), a cooperative initiative with MIT, is proud to announce the creation of a limited number of Founding Faculty Fellowships. Faculty Fellows will participate in launching and shaping this new university in its crucial formative stages. SkTech is a startup university, to be located in the innovation zone called Skolkovo, outside of Moscow - sometimes called the "Russian Silicon Valley."

We seek candidates wishing to explore the function of universities, the creation of new research programs, the design of advanced educational environments and programs, and the interface between universities and industry that drives innovation.

Applicants must be permanent faculty members or senior administrative staff at major universities or senior staff from industrial or national research laboratories.

Faculty Fellows would be expected to spend at least half time with SkTech, working for a period of at least four months and up to one year, but individual time commitments are negotiable. English is the working language of SkTech and ability to speak Russian is a benefit. Levels of financial support commensurate with sabbaticals at western universities will be provided, as well as travel and living allowances.

Positions are available starting immediately and running through at least June 2013. Applications should be submitted to **https://ff-program.mit.edu/**. Questions on the goals and plans for the program can be directed to Professor **Michael Myagkov** at **myagkov@uoregon.edu**. Additional information can be found at the SkTech/MIT Initiative website: **http://web.mit.edu/sktech**.

SkTech is committed to diversity and equity, and all are invited to apply without regard for gender, race or national origin.

Massachusetts Institute of Technology

NW219454R

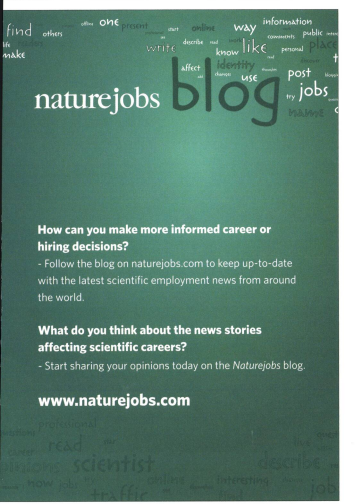

How can you make more informed career or hiring decisions?

- Follow the blog on naturejobs.com to keep up-to-date with the latest scientific employment news from around the world.

What do you think about the news stories affecting scientific careers?

- Start sharing your opinions today on the *Naturejobs* blog.

www.naturejobs.com

The University of Manchester

MANCHESTER 1824

Agency for Science, Technology and Research

Faculty of Life Sciences, University of Manchester with A*STAR Institutes, Singapore

Joint PhD Research Training Programme

The Faculty of Life Sciences, University of Manchester UK and the A*STAR Institutes Singapore are offering a number of prestigious international PhD studentships for outstanding applicants. The studentships will commence in September 2012 and be split between sites in Manchester and Singapore. Degrees will be awarded by the University of Manchester.

The Faculty of Life Sciences is an internationally leading Life Sciences facility; to find out more please visit www.ls.manchester.ac.uk/research

The participating A*STAR Institutes are:

- **Institute for Medical Biology**
- **Institute for Molecular and Cellular Biology**
- **Singapore Immunology Network**
- **Genome Institute of Singapore**
- **Bioinformatics Institute**

Projects will be available in the following areas:

- Cell adhesion and migration
- Cancer and epithelial cell biology
- Stem cells and developmental biology
- Genetic diseases
- Wound healing
- Cell biology
- Immunoregulation and inflammation biology
- Gene expression screening
- Genome architecture in mammalian cells
- Bioinformatics tools to predict protein interactions

For further information on the programme and how to apply, visit www.ls.manchester.ac.uk/phdprogrammes

Applicants should be from the UK/EU and have obtained (or be about to obtain) at least an upper second class Honours degree (or equivalent) in a Life Sciences area.

Initial closing date for first round of awards: Friday 13 January 2012.

The University will actively foster a culture of inclusion and diversity and will seek to achieve true equality of opportunity for all members of its community.

U219680R

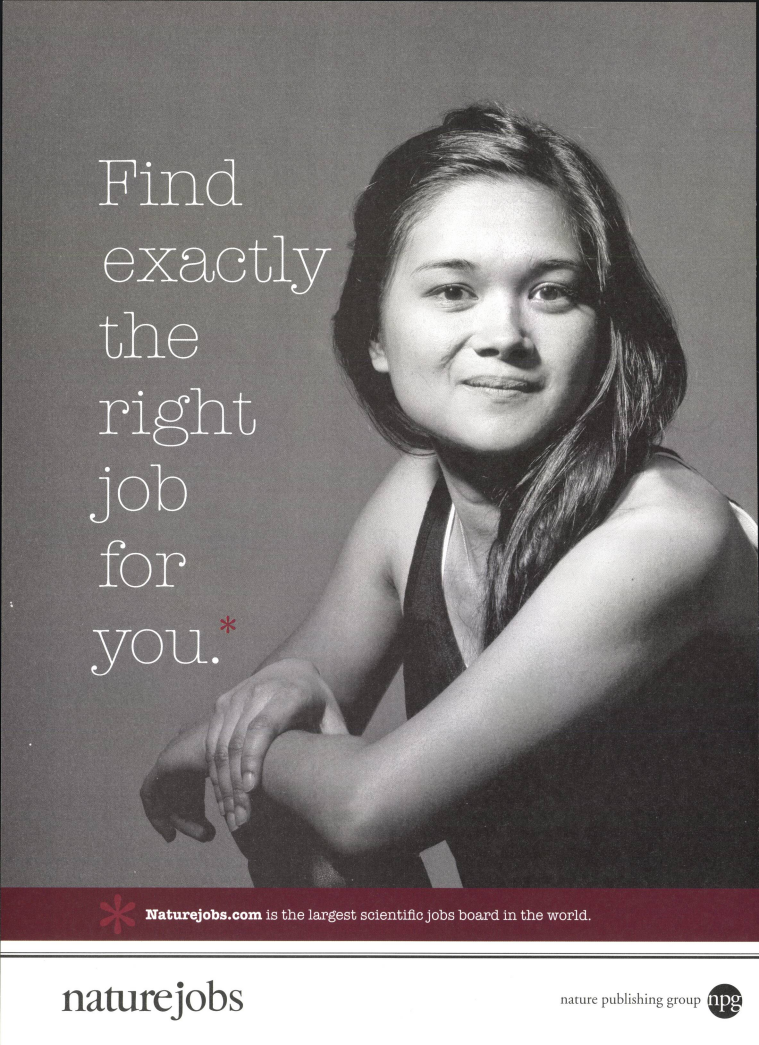
Find exactly the right job for you.*
*Naturejobs.com is the largest scientific jobs board in the world.
naturejobs
nature publishing group npg

Institute of Marine and Environmental Technology

UNIVERSITY SYSTEM OF MARYLAND

Director, Institute of Marine and Environmental Technology, University System of Maryland

The Institute of Marine and Environmental Technology (IMET) of the University System of Maryland seeks a Director. The IMET mission is to study and understand the biology of coastal marine biosystems, to ensure sustainable use of these marine biosystems, and use of marine-derived systems to improve human health (http://www.imet.usmd.edu/). IMET brings together faculty members from three major USM research institutions - the University of Maryland Baltimore, the University of Maryland Baltimore County, and the University of Maryland Center for Environmental Science - in a dedicated state-of-the art research facility located in Baltimore's Inner Harbor. The IMET Director will serve as Chief Scientific and Executive Officer with a mandate to expand IMET's basic and translational research effort in marine, environmental and biomedical science, to expand research programs that compliment existing research strengths and to build new research programs. The Director will be an eminent PhD scientist with outstanding research credentials, in an area suitable to lead the institute, and have demonstrated leadership credentials in an academic research setting. The Director will have a mandate to enhance the international stature of IMET and to bring additional grant, commercial and philanthropic support to IMET. Applicants should send a letter of interest, research statement, curriculum vitae and the names of three references to Christine Hiles, Institute of Marine and Environmental Technology, Columbus Center, 701 E. Pratt St, Baltimore, MD 21202, chiles@umbc.edu. To receive full consideration, applications should be submitted by February 15, 2012. Salary and benefits are competitive and dependent on qualifications.

The USM is an equal opportunity, affirmative action employer.

NW219649R

naturejobs
Attention Employers!
Stay up to date with deadlines and upcoming Naturejobs features:
Sign up for FREE employer e-alerts:
naturejobs.com/ealerts

UNIVERSITÄT BASEL

The Faculty of Medicine of the University of Basel, Switzerland, invites applications for a

Professor of Neurophysiology

The Medical Faculty of the University of Basel, Switzerland, invites applications for a faculty position in Neurophysiology. Candidates should hold an M.D. and/or a Ph.D. degree and are expected to have an outstanding research record in the field of neurophysiology. Candidates with experience in novel light microscopy and in vivo imaging techniques are especially encouraged to apply. The successful candidate will complement research activities in the "Focal Area Neurosciences" of the Department of Biomedicine (http://biomedizin.unibas.ch/home/) and is expected to collaborate with the neuroscience research groups at the University Hospital and the University. Basel has a high density of neuroscientists that cover a wide spectrum of neuroscience research, ranging from basic to clinical and applied research (http://www.neuronetwork.unibas.ch/index.html). Physiology teaching of medical students in German is required. The position provides access to core facilities, includes one post-doctoral position, one technician and secretarial assistance. Applications must be submitted in electronic form, should include a letter of motivation, a CV, a list of external research funding and a description of teaching experiences. A detailed outline of research interests should be part of the application.

Teaching language is German.

The University of Basel seeks to increase the proportion of women among the faculty members and therefore specifically encourages female candidates to apply.

For additional information: Prof. M. Sinnreich, Head of the Search Committee, Departments of Neurology and Biomedicine, University Hospital, Klingelbergstr. 50/70, 4056 Basel (Tel: +41 (0)61 265 2525).

Application deadline is 10.2.2012. Information about how to submit your application is available at: http://medizin.unibas.ch/ under Dekanat/Bewerbungen.

Please send your application only to bewerbungen-medizin@unibas.ch

UNI BASEL

W219489R

"Based on the huge response to our adverts in *Naturejobs* we have hired many excellent candidates annually. We highly appreciate the kind and professional support of the *Nature* team."

Karin Osibow,
Program Administrator,
Medical University of Graz, Austria

naturejobs

a nature conference

Nature Genetics and the *Journal of Investigative Dermatology* present:

Dermatogenetics

The conference will cover genetic variation, gene expression and cellular mechanisms in this shared area of exceptional interest to basic researchers, biopharma and translational medicine. Lectures and posters are invited in al areas of the field and sessions including: complex dermatological diseases, stem cells and skin cancer, development and regeneration, melanoma and pigmentation, monogenic skin disorders and epigenetics and gene expression.

February 9-12, 2012
JW Marriott Marquis Miami
Miami, FL, USA

KEYNOTE SPEAKERS:
Raphael Kopan
Fiona Watt

SPEAKERS:

Allan Balmain	**Andrzej Dlugosz**	**Anthony Oro**
Greg Barsh	**David Fisher**	**Dennis Roop**
Regina Betz	**Nick Hayward**	**Yardena Samuels**
David (Tim) Bishop	**Valerie Horsley**	**Julie Segre**
Natalia Botchkareva	**Birgitte Lane**	**Eli Sprecher**
Anne Bowcock	**Robert Lavker**	**Richard Spritz**
Pierre Coulombe	**Jianjun Liu**	**Xue Zhang**
James Elder	**Sarah Millar**	

ORGANIZERS:
Myles Axton (*Nature Genetics*, USA)
Angela Christiano (Columbia University, USA)
John McGrath (King's College London, UK)
Irwin McLean (University of Dundee, UK)

Artwork by: Daniel Kohn

For more information and to register, visit:
www.nature.com/natureconferences/dg2012

nature genetics

JOURNAL OF INVESTIGATIVE DERMATOLOGY

Announcing a Medical Research Funding Opportunity

The Kenneth Rainin Foundation 2012 Innovator Awards Program for Inflammatory Bowel Disease (IBD) Research

WHAT: $100,000 Grants for Transformative IBD Projects
WHERE: Apply Online via One-Page Letter of Inquiry
WHEN: January 15–February 15, 2012
WHY: Accelerate IBD Research to Find Causes and Cures

INTERDISCIPLINARY COLLABORATION IS STRONGLY ENCOURAGED.

The grant program is open to tenure track professors (or the equivalent) at all levels from any scientific discipline and from any non-profit research institution worldwide.

To learn more about our health grant award programs, please visit **KRFoundation.org/grants/health/**

Kenneth Rainin FOUNDATION

HEALTH · EDUCATION · ARTS

NW218866A

The Royal Society Pfizer Award 2012

Invitation to nominate

Registered Charity No. 207043

This prestigious international award, sponsored by Pfizer Inc, is designed to reward scientists at an early stage of their research career and to promote capacity building in the developing world. The 2012 award is open to any research scientist, based in Africa, making an innovative contribution to the biological sciences, including basic medical science that has led to a sustainable positive impact on Africa.

Up to £60,000 will be awarded as a grant, £5,000 will be given as a prize to the recipient.

To nominate, visit **royalsociety.org/pfizer-award**, call +44 (0)20 7451 2573 or email awards@royalsociety.org

Closing date: Monday 6 February 2012

EXCELLENCE IN SCIENCE

THE ROYAL SOCIETY

Pfizer

U219285A

cefic

LRI *The Long-range Research initiative*

LRI Innovative Science Award 2012

Are you a rebel thinker?
Do you have a good idea?
Make it come alive!

The European Chemical Industry Council (Cefic) in conjunction with SETAC, EUROTOX, ISES and Chemical Week is offering a **€100,000** award to support innovative, interdisciplinary research in the field of biologically-relevant exposure characterization.

The award will be presented to a Europe-based scientist with less than ten years post-doctoral experience.

Deadline for submissions: March 16, 2012

More details and application form:

www.cefic-lri.org/awards

W219687A

REPROGRAPHICS: CTT, London E17 6BU UK and **The Charlesworth Group**, Wakefield, UK.
PRINTED BY: William Gibbons & Sons Ltd, UK; **Publishers Press**, Lebanon Junction, Ky, USA and **Obun Printing Co. Inc**, Tokyo, Japan

EXTREMES

Living on the edge.

BY RACHEL SWIRSKY

So there I was, as near to the lava vents as I could get in a Bubble, with the robots droning on about extremophile lifeforms and whatever. Blank metal looks. Blank metal voices. "… Organisms that thrive in physically or geochemically extreme …" All the passengers and me, we're ignoring them, just staring down at the red and the burble, and I start to wonder, what if I took off my suit?

Fire hot, death bad, etc. etc.. Except that's all brain stem. Very twentieth.

We've all done that thing where we stick our hand on the stove and keep it there just for the XP, you know, to see how it feels. And it's riot, blistering agony, but then you've got through it, you've proved you're a real man or a real woman or a real tweener and they make you a new hand and that's that.

So wouldn't it be kinda sport? Just to dive? Char, burn, bubbling red and black, hot liquid ouch — but then they'd kick you into new skin and there you'd be. Only, like, with new experience cuz you've lived extremophile.

Would that be effer? That would be effer. Would that chat up any Fifi you want? That would chat up all the Fifis in the solar.

So I doff the suit, naked and already rocking from heat through the Bubble, push the emergency, klaxons going off all behind me, robots off to restrain the other passengers, the gasps, the shouting and me going free into the magma flow, me and hot, red rock and the little buggers that live in it.

Like I said — riot, blistering agony.

But I wake up, and I'm in the growing tank, swimming around all fetal, with my brain loaded into a proxy computer while I'm waiting for flesh to pile. And me, I'm sport. Sports rocket. I'd lived the lava vent. Held my hand to the stove, but 20 million times more X.

I'm expecting everyone to be like you are so rocket, so whoa, but no one's zinging, so I tap my direct and whoa but everyone's talking about me, but not me-me, because there's like another me, and it's still swimming down there in the lava, and how is that possible? It's taken less than a day for every trace of me-me — the one that's not lava-me — to disappear from the top link lists. I'm subterranean. I'm invisible. I'm replaced by lava-swimming me, and this weird link-up he's broadcasting that no one understands. Boom. It's everywhere.

I try to find out what's going on, but no one will zing, they're all directing this other me instead, so I have to go infoblip and it turns out no one's yessir, but …

They think it's got something to do with the plastic mods from when our greats took the sleep to this planet, when they were stitching into our gene code, in case we needed to have five legs or huge eyes or whatever, to cope with the new planet. And they tried to neg it all when we got here, but they left in strings for the medlinks and once you're that small on the micro, no one's 100 sure what everything does, like you ping one bit on and two off, and then you get sunburn-proof skin and everyone knows that, but later, it turns out that it makes everyone really like neon orange, too.

So somehow, the fluid, the plastic, the string, all pulled and twisted, and there's me, in the lava, *adapting* and sending back this sphincter-screech footage no one can decode, and no one will zing me cuz they're all zinging him.

And that's who I've been since. Me that's not the real me. No one even recognizes me, because me and him, first, we don't look at all the same, and also second, they don't expect to see him not being in lava.

Technically he's the A1 and I'm the clone, so my friends and family mostly are on him. He's famous, and I'm just A2. The robots made me because my rec said to do that if I was ever as good as dead, and they figured I was. They didn't know I'd still be all A1 in the lava, and even though I am, it's not like he thinks much like I do, much like any human does. It's not like he knows how to zing, or how to do anything but send footage nothing can translate.

I tried to make an infoblip on what it's like to melt in lava, but everyone's more interested in what it's like to *live* in lava, which I guess I twig, and besides, I get spam-waved a lot because he and I've got the same ID, and it looks like I'm forging.

So there's me. The most boring me out of 2. I'm thinking of going into deep ice, or out into vacuum, see if there's something special about my code, see if I can switch-change again. Might do it one, two, three times, if it works. Extreme-o-mes. Me-o-philes. But when I'm done, chill, I'm all bout nulling that good-as-dead rec. Gonna wink out, normal-me. No more A2. Just A1s on the edges, all alien and unknown. ■

Rachel Swirsky's *short fiction has been nominated for the Hugo, the Nebula and the Sturgeon among other awards. She holds a fiction MFA from the Iowa Writers Workshop. Visit http://www.rachelswirsky.com.*

➲ **NATURE.COM**
Follow Futures on Facebook at:
go.nature.com/mfoodm

JACEY

TrueMAB™ Monoclonal Antibodies

made against authentic protein antigens

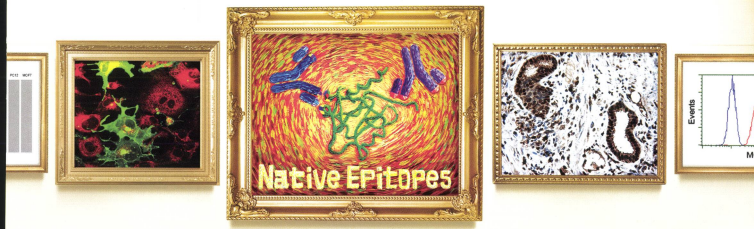

Most therapeutic and diagnostic antibodies are made against protein antigens. So, why compromise your research with antibodies made against short peptides?

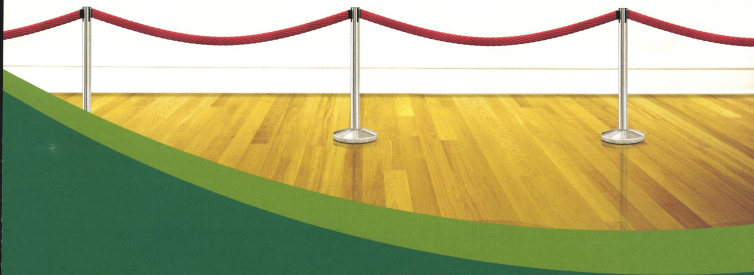

TrueMAB™ recognizing protein native epitopes

- Releasing over 200 TrueMAB™ monthly
- Extensive validation (IHC on 24 FFPE tissues, IF, Flow, IP, WB)
- Positive controls included

ORIGENE
Your Gene Company

origene.com/truemab

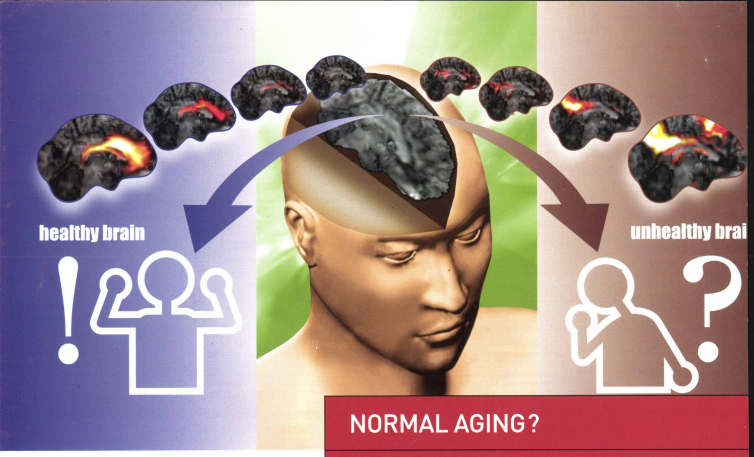

Using a massive brain PET database, Hamamatsu Photonics distinguishes Alzheimer's disease from normal aging.

Dementia is on the rise around the globe. Doctors hoping to maximize the effectiveness of treatments with early diagnosis and researchers scrambling to design drugs that address the causes or the symptoms are facing the same problem: How do you differentiate the normal aging processes from pathological conditions such as Alzheimer's disease?

Hamamatsu Photonics has pushed the quest for an objective, accurate diagnostic tool close to realization. Equipped with a unique database of over 6000 PET scans from normal individuals of various ages and both sexes, Hamamatsu Photonics' scientists have pieced together a detailed understanding of how the brain works and changes with time.

Based in that knowledge, the company carried out a study* comparing the brain activity of normal subjects and that of Alzheimer's disease patients using a Hamamatsu Photonics PET camera. The device picks up subtle differences in brain activity at distinct regions throughout the brain.

Hamamatsu Photonics converted that data into an easy scoring method that can discern quickly and simply between the groups and with unprecedented accuracy. The computer-aided diagnosis (CAD) was even able to predict which patients with mild cognitive impairment would progress to Alzheimer's disease, further expanding the treatment window.

As an objective and easy-to-use tool for CAD, it will suit both doctors and researchers. However, the main beneficiary will, of course, be patients and their families.

Main visual: PET brain scan images (color) overlay MRI images (gray) to provide a comprehensive view of the brain's health. The images on the left show brain changes associated with normal aging. The images on the right show the onset of dementia, one form of which is Alzheimer's disease. Orange-to-yellow coloring indicates regions with reduced glucose metabolism.

*Kakimoto A, et al. PLoS ONE 6(9): e25033. doi:10.1371/journal pone.0025033 (2011)

Hamamatsu Photonics' expertise with light has revealed an elegant solution to a complex problem.

HAMAMATSU

PHOTON IS OUR BUSINESS

For more information, visit our site at: http://jp.hamamatsu.com/en/rd/publication

HAMAMATSU PHOTONICS K. K.

325-6, Sunayama-cho, Naka-ku, Hamamatsu City, 430-8587 Japan Telephone: (81)53-452-2141, Fax: (81)53-456-7889 URL http://www.hamamatsu.com